

**PERFORMANCE AND CONSTRUCTABILITY
OF SILICA FUME BRIDGE DECK OVERLAYS**

By
**GERALD G. MILLER
DAVID DARWIN**

**A Report on Research Sponsored by
THE KANSAS DEPARTMENT OF TRANSPORTATION
K-TRAN PROJECT NO. KU-98-4**

**Structural Engineering and Engineering Materials
SM Report No. 57**

**UNIVERSITY OF KANSAS CENTER FOR RESEARCH, INC.
LAWRENCE, KANSAS
JANUARY 2000**

ABSTRACT

The effects of construction practices and material properties on the performance of concrete bridge decks are evaluated. Emphasis is placed on comparing bridge decks with silica fume and conventional concrete overlays and determining if the silica fume overlays commonly used on bridges in Kansas are performing at a level that justifies the extra cost and construction precautions. Forty continuous steel girder bridges, 20 with silica fume overlays, 16 with conventional overlays and 4 with monolithic bridge decks are included in the study. Field surveys were conducted to document cracking patterns and crack density and to obtain samples for chloride content and rapid chloride permeability (RCPT) analysis. Construction data was collected from construction documents, field books, and weather data logs. Information from the current study is combined with data from a 1995 study by Schmitt and Darwin. Twenty-seven variables are considered, covering bridge age, material properties, site conditions, construction procedures, design specifications, and traffic volume. Comparisons are made based on the properties of the upper surface and on the properties of the subdeck for bridges with overlays.

The study demonstrates that crack density increases with age for bridge decks with silica fume overlays. Younger decks with conventional overlays, however, exhibit increased cracking compared to older decks. The differences are attributed to differences in construction procedures. The limited number of silica fume and conventional overlay decks that are similar in age have similar crack densities, effective diffusion coefficient values, and chloride contents, both at and away from cracks. Chloride content increases with the age of the bridge deck, regardless of bridge deck type. Chloride content taken at crack locations at depths just above and below the transverse reinforcement exceeds the threshold level for corrosion in as little as 1000 days, regardless of bridge deck type. Increased paste contents in bridge subdecks result in cracking in decks with overlays, regardless of the quality of the overlay, and neither higher cement contents nor compressive strengths are beneficial

to the cracking performance of the concrete. Both fogging immediately after finishing and the application of precure material should be specified for conventional overlay and monolithic bridge decks, as they are now for silica fume overlay decks. Because of the relatively high number of silica fume overlay decks with ages under two years at the time of the study, these decks should be reexamined when they reach the age of the conventional overlay decks in the study.

Key Words: bridge decks, bridge construction, chloride content, concrete construction, concrete mix design, cracking, diffusion coefficient, durability, overlay, permeability, rapid chloride permeability test, reinforced concrete, shrinkage, silica fume

ACKNOWLEDGEMENTS

This report is based on research performed by Gerald G. Miller in partial fulfillment of the requirements for the MSCE degree from the University of Kansas. Funding for this research was provided by the Kansas Department of Transportation under K-TRAN Project No. KU-98-4.

Oversight of this project was provided by Dan Scherschligt of the Kansas Department of Transportation. Bridge deck construction data for the bridge surveys was provided by personnel from District I of KDOT. Personnel from the KDOT Bureau of Materials and Research provided traffic control for the bridge surveys, obtained concrete samples and performed rapid chloride permeability tests and chloride content tests, and obtained pavement profiles. The efforts of all those who participated are gratefully acknowledged, with special thanks to Dave Meggers, Craig Rutheford, Jim Bernica, Marc Catron, Bob Heinen, Greg Heinen, Robert Kennedy, John Mah, and Matt Sloyer from the KDOT Bureau of Materials and Research and David Reuter from the University of Kansas.

TABLE OF CONTENTS

	<u>Page</u>
ABSTRACT.....	ii
ACKNOWLEDGEMENTS	iv
LIST OF TABLES.....	ix
LIST OF FIGURES	xiii
CHAPTER 1: INTRODUCTION	1
1.1 General.....	1
1.2 Types of Cracking.....	1
1.2.1 Crack Classification Based on Causes of Cracking	1
1.2.2 Crack Classification Based on Orientation	3
1.3 Corrosion.....	4
1.4 Silica Fume	5
1.5 Rapid Chloride Permeability Test.....	6
1.6 Chloride Concentrations	9
1.7 Overlay Specifications	10
1.8 Previous Work	11
1.8.1 Cracking in Bridge Decks.....	13
1.8.2 Silica Fume in Bridge Decks	27
1.9 Object and Scope	30
CHAPTER 2: DATA COLLECTION	32
2.1 General.....	32
2.2 Selection of Bridges.....	32
2.3 Data Sources	34
2.4 On-Site Field Surveys.....	35
2.5 Rapid Chloride Permeability Test, Chloride Content, and Pavement Profile.....	36
2.5.1 Rapid Chloride Permeability.....	36
2.5.2 Chloride Content.....	37

2.5.3 Pavement Profile.....	37
2.6 Calculation of Crack Densities	38
2.7 Databases	40
CHAPTER 3: EVALUATION AND RESULTS.....	41
3.1 General.....	41
3.2 Inclusion of Data from Schmitt and Darwin.....	44
3.3 Bridge Age versus Crack Density.....	45
3.4 Rapid Chloride Permeability Test.....	46
3.5 Chloride Concentration and Effective Diffusion Coefficient	48
3.6 Effects of Material Properties	51
3.6.1 Slump	54
3.6.1.1 D_{eff} versus Slump.....	54
3.6.1.2 RCPT versus Slump.....	55
3.6.1.3 Crack Density versus Slump.....	55
3.6.2 Percent Volume of Water and Cementitious Material	56
3.6.2.1 D_{eff} versus Percent Volume of Water and Cementitious Materials	57
3.6.2.2 RCPT versus Percent Volume of Water and Cementitious Materials	57
3.6.2.3 Crack Density versus Percent Volume of Water and Cementitious Materials	58
3.6.3 Water Content	59
3.6.3.1 D_{eff} versus Water Content.....	59
3.6.3.2 RCPT versus Water Content.....	59
3.6.3.3 Crack Density versus Water Content.....	60
3.6.4 Cementitious Material Content.....	61
3.6.5 Water/Cementitious Material Ratio	62
3.6.5.1 D_{eff} versus Water/Cementitious Material Ratio	63
3.6.5.2 RCPT versus Water/Cementitious Material Ratio.....	63

3.6.5.5 Crack Density versus Water/Cementitious Material Ratio	63
3.6.6 Air Content.....	64
3.6.6.1 D_{eff} versus Air Content	64
3.6.6.2 RCPT versus Air Content	65
3.6.6.3 Crack Density versus Air Content	65
3.6.7 Compressive Strength	66
3.6.7.1 D_{eff} versus Compressive Strength.....	67
3.6.7.2 RCPT versus Compressive Strength.....	67
3.6.7.3 Crack Density versus Compressive Strength.....	67
3.7 Effects of Site Conditions	68
3.7.1 Average Air Temperature	69
3.7.2 Low Air Temperature	70
3.7.3 High Air Temperature.....	71
3.7.4 Daily Temperature Range	71
3.7.5 Relative Humidity	72
3.7.6 Average Wind Velocity	73
3.8 Effects of Finishing and Curing Procedures	74
3.9 Effects of Design Specifications	75
3.9.1 Structure Type.....	76
3.9.2 Deck Type.....	76
3.9.3 Deck Thickness.....	77
3.9.4 Top Cover	77
3.9.5 Transverse Reinforcing Bar Size	78
3.9.6 Transverse Reinforcing Bar Spacing	79
3.9.7 Girder End Condition.....	79
3.9.8 Span Length	80
3.9.9 Bridge Length	80
3.9.10 Span Type	81

3.9.11 Skew.....	81	
3.10 Effects of Traffic.....	82	
3.11 Pavement Profile.....	83	
CHAPTER 4: SUMMARY, CONCLUSIONS, AND RECOMMENDED		
IMPLEMENTATION PLAN		84
4.1 Summary	84	
4.2 Conclusions.....	84	
4.3 Recommended Implementation Plan	88	
4.4 Recommendations for Future Study	89	
REFERENCES	91	
ADDITIONAL BIBLIOGRAPHY	94	
APPENDIX A: BRIDGE DECK DATA AND CRACKING PATTERNS.....	237	
APPENDIX B: CRACK DENSITY CALCULATION PROGRAM		
LISTING	398	

LIST OF TABLES

<u>Table</u>	<u>Page</u>
3.1 Student's t-test for entire bridge crack density versus bridge age.....	98
3.2 Student's t-test entire bridge crack density versus date of construction.....	99
3.3 Student's t-test for coulomb results for individual placements versus deck type	100
3.4 Student's t-test for mean effective diffusion coefficient of individual placements versus deck type.....	101
3.5 Student's t-test for mean effective diffusion coefficient for individual placements versus concrete slump.....	102
3.6 Student's t-test for mean RCPT results for individual placements versus concrete slump	104
3.7 Student's t-test for mean crack density versus concrete slump	106
3.8 Student's t-test for mean effective diffusion coefficient for individual placements versus percent volume of water, cement, and silica fume	109
3.9 Student's t-test for mean RCPT results for individual placements versus percent volume of water, cement, and silica fume.....	110
3.10 Student's t-test for mean crack density for individual placements versus percent volume of water and cement and silica fume.....	111
3.11 Student's t-test for mean effective diffusion coefficient for individual placements versus water content	113
3.12 Student's t-test for mean RCPT results for individual placements versus water content.....	114
3.13 Student's t-test for mean crack density for individual placements versus water content.....	115
3.14 Student's t-test for mean crack density for individual placements versus cement content.....	117

3.15	Student's t-test for mean effective diffusion coefficient for individual placements versus water/cementitious material ratio	118
3.16	Student's t-test for mean RCPT results for individual placements versus water/cementitious material ratio	119
3.17	Student's t-test for mean crack density for individual placements versus water/cementitious material ratio	120
3.18	Student's t-test for mean effective diffusion coefficient for individual placements versus air content	122
3.19	Student's t-test for mean RCPT results for individual placements versus air content	123
3.20	Student's t-test for mean crack density for individual placements versus air content	124
3.21	Student's t-test for mean effective diffusion coefficient for individual placements versus compressive strength	126
3.22	Student's t-test for mean RCPT results for individual placements versus compressive strength	127
3.23	Student's t-test for mean crack density for individual placements versus compressive strength	128
3.24	Student's t-test for mean crack density for individual placements versus average air temperature.....	130
3.25	Student's t-test for mean crack density for individual placements versus low air temperature	132
3.26	Student's t-test for mean crack density for individual placements versus high air temperature	134
3.27	Student's t-test for mean crack density for individual placements versus daily temperature range	136
3.28	Student's t-test for mean crack density for individual placements versus relative humidity	138
3.29	Student's t-test for mean crack density for individual placements versus wind velocity.....	141

3.30	Student's t-test for mean crack density for individual silica fume overlay placements versus Special Provision Number	144
3.31	Student's t-test for mean crack density for entire bridge versus steel structure type.....	145
3.32	Student's t-test for mean crack density for entire bridge deck versus deck type	146
3.33	Student's t-test for mean crack density for entire bridge versus deck thickness.....	147
3.34	Student's t-test for mean crack density for entire bridge versus top cover.....	148
3.35	Student's t-test for mean crack density for entire bridge versus top transverse reinforcing bar size	149
3.36	Student's t-test for mean crack density for entire bridge versus top transverse bar spacing	150
3.37	Student's t-test for mean crack density for end sections versus girder end condition	151
3.38	Student's t-test for mean crack density for individual spans versus span length	152
3.39	Student's t-test for mean crack density for entire bridge versus bridge length.....	154
3.40	Student's t-test for mean crack density for individual spans versus span type	155
3.41	Student's t-test for mean crack density for entire bridge versus skew	157
3.42	Student's t-test for mean crack density for entire bridge versus traffic volume.....	159
3.43	Student's t-test for mean crack density for entire bridge versus load cycles.....	160
3.44	Student's t-test for mean crack density for entire bridge versus pavement roughness index	161

A.1	Crack densities and data for full bridge decks	238
A.2	Deck properties and crack densities for end sections	241
A.3	Crack density and mix design information for bridge deck placements.....	244
A.4	Cement and silica fume type information for bridge deck placements.....	252
A.5	Aggregate information for bridge deck placements.....	267
A.6	Field information for bridge deck placements	282
A.7	Site conditions.....	290
A.8	Crack densities and data for individual spans.....	298
A.9	RCPT and calculated diffusion coefficient results.....	303
A.10	Chloride concentration information.....	309
A.11	Pavement roughness index.....	354

LIST OF FIGURES

<u>Figure</u>	<u>Page</u>
3.1	Crack density of entire bridge decks for bridges evaluated in the current study and by Schmitt and Darwin (1995)..... 162
3.2	Correlation of crack density of entire bridge decks for bridges evaluated in the current study and by Schmitt and Darwin (1995)..... 163
3.3	Crack density of entire bridge deck versus bridge age for silica fume overlays (SFO), conventional overlays (CO), and monolithic (Mono) bridges in the current study..... 164
3.4	Crack density of entire bridge decks versus bridge age for silica fume (SFO) and conventional overlays (CO) evaluated in the current study and by Schmitt and Darwin (1995)..... 165
3.5	Crack density of entire bridge deck versus bridge age for silica fume overlays studied in the current study (SFO) and by Schmitt and Darwin (1995) (Schmitt SFO) 166
3.6	Crack density of entire bridge decks versus bridge age for silica fume overlays younger than 60 months evaluated in the current study (SFO) and by Schmitt and Darwin (1995) (Schmitt SFO) 167
3.7	Crack density of entire bridge decks versus bridge age for conventional overlays evaluated in the current study (CO) and by Schmitt and Darwin (1995) (Schmitt CO)..... 168
3.8	Crack density of entire bridge deck versus bridge age for conventional overlays younger than 60 months evaluated in the current study (CO) and by Schmitt and Darwin (1995) (Schmitt CO) 169
3.9	Crack density of entire bridge deck versus bridge age for monolithic bridge decks evaluated in the current study (Mono) and by Schmitt and Darwin (1995) (Schmitt Mono)..... 170
3.10	Mean crack density of entire bridge decks versus bridge age for silica fume overlays 171
3.11	Mean crack density of entire bridge decks versus bridge age for conventional overlays 171

3.12	Mean crack density of entire bridge decks versus bridge age for monolithic bridge decks.....	172
3.13	Mean crack density of entire bridge versus date of construction for silica fume overlay bridge decks.....	172
3.14	Mean crack density of entire bridge versus date of construction for conventional overlay bridge decks.....	173
3.15	Mean crack density of entire bridge versus date of construction for monolithic bridge decks.....	173
3.16	Mean RCPT test coulomb reading of individual placements versus deck type.....	174
3.17	Mean effective diffusion coefficient of individual placements grouped into age categories.....	174
3.18	Chloride content away from cracks at a mean depth of 9.5 mm versus placement age.....	175
3.19	Chloride content away from cracks at a mean depth of 28.6 mm versus placement age.....	176
3.20	Chloride content away from cracks at a mean depth of 47.6 mm versus placement age.....	177
3.21	Chloride content at cracks at a mean depth of 66.7 mm versus placement age.....	178
3.22	Chloride content at cracks at a mean depth of 85.7 mm versus placement age.....	179
3.23	Effective diffusion coefficient versus RCPT results.....	180
3.24	Mean effective diffusion coefficient of individual placements versus concrete slump for silica fume overlays.....	181
3.25	Mean effective diffusion coefficient of individual placements versus concrete slump for conventional overlays.....	181
3.26	Mean RCPT result of individual placements versus concrete slump for silica fume overlays.....	182

3.27	Mean RCPT result of individual placements versus concrete slump for conventional overlays.....	182
3.28	Mean crack density of individual placements versus concrete slump for silica fume overlays.....	183
3.29	Mean crack density of individual placements versus concrete slump for conventional overlays.....	183
3.30	Mean crack density of individual placements versus concrete slump for monolithic bridges.....	184
3.31	Mean crack density of bridge subdecks versus concrete slump	184
3.32	Mean effective diffusion coefficient of individual placements versus percent volume of water, cement, and silica fume for silica fume overlays	185
3.33	Mean effective diffusion coefficient of individual placements versus percent volume of water and cement for conventional overlays	185
3.34	Mean RCPT result of individual placements versus percent volume of water, cement, and silica fume for silica fume overlays	186
3.35	Mean RCPT result of individual placements versus percent volume of water and cement for conventional overlays	186
3.36	Mean crack density for individual placements versus percent volume of water, cement, and silica fume for silica fume overlays	187
3.37	Mean crack density for individual placements versus percent volume of water and cement for conventional overlays	187
3.38	Mean crack density for individual placements versus percent volume of water and cement for monolithic bridges	188
3.39	Mean crack density of bridge subdecks versus average percent volume of water and cement	188
3.40	Mean effective diffusion coefficient of individual placements versus water content for silica fume overlays	189

3.41	Mean effective diffusion coefficient of individual placements versus water content for conventional overlays	189
3.42	Mean RCPT result of individual placements versus water content for silica fume overlays	190
3.43	Mean RCPT result of individual placements versus water content for conventional overlays.....	190
3.44	Mean crack density for individual placements versus water content for silica fume overlays.....	191
3.45	Mean crack density for individual placements versus water content for conventional overlays.....	191
3.46	Mean crack density for individual placements versus water content for monolithic bridges	192
3.47	Mean crack density of bridge subdecks versus water content	192
3.48	Mean crack density of individual placements versus cement content for monolithic bridge decks	193
3.49	Mean crack density of bridge subdecks versus cement content	193
3.50	Mean effective diffusion coefficient of individual placements versus water/cementitious material ratio for silica fume overlays.....	194
3.51	Mean effective diffusion coefficient of individual placements versus water/cement ratio for conventional overlays.....	194
3.52	Mean RCPT result of individual placements versus water/cementitious material ratio for silica fume overlays.....	195
3.53	Mean RCPT result of individual placements versus water/cement ratio for conventional overlays	195
3.54	Mean crack density for individual placements versus water/cementitious material ratio for silica fume overlay bridge decks ..	196
3.55	Mean crack density for individual placements versus water/cement ratio for conventional overlay bridge decks.....	196

3.56	Mean crack density for individual placements versus water/cement ratio for monolithic bridge decks	197
3.57	Mean crack density of bridge subdecks versus water/cement ratio	197
3.58	Mean effective diffusion coefficient of individual placements versus air content for silica fume overlays.....	198
3.59	Mean effective diffusion coefficient of individual placements versus air content for conventional overlays	198
3.60	Mean RCPT result of individual placements versus air content for silica fume overlays	199
3.61	Mean RCPT result of individual placements versus air content for conventional overlays.....	199
3.62	Mean crack density for individual placements versus air content for silica fume overlay bridge decks	200
3.63	Mean crack density for individual placements versus air content for conventional overlay bridge decks	200
3.64	Mean crack density for individual placements versus air content for monolithic bridge decks	201
3.65	Mean crack density of bridge subdecks versus air content.....	201
3.66	Mean effective diffusion coefficient of individual placements versus compressive strength for silica fume overlays.....	202
3.67	Mean effective diffusion coefficient of individual placements versus compressive strength for conventional overlays.....	202
3.68	Mean RCPT result of individual placements versus compressive strength for silica fume overlays.....	203
3.69	Mean RCPT result of individual placements versus compressive strength for conventional overlays.....	203
3.70	Mean crack density for individual placements versus compressive strength for silica fume overlay bridge decks	204

3.71	Mean crack density for individual placements versus compressive strength for conventional overlay bridge decks	204
3.72	Mean crack density for individual placements versus compressive strength for monolithic bridge decks	205
3.73	Mean crack density of bridge subdecks versus compressive strength.....	205
3.74	Mean crack density for individual placements versus average air temperature for silica fume overlay bridge decks.....	206
3.75	Mean crack density for individual placements versus average air temperature for conventional overlay bridge decks.....	206
3.76	Mean crack density for individual placements versus average air temperature for monolithic bridge decks	207
3.77	Mean crack density of bridge subdecks versus average air temperature .	207
3.78	Mean crack density for individual placements versus low air temperature for silica fume overlay bridge decks.....	208
3.79	Mean crack density for individual placements versus low air temperature for conventional overlay bridge decks.....	208
3.80	Mean crack density for individual placements versus low air temperature for monolithic bridge decks	209
3.81	Mean crack density of bridge subdecks versus low air temperature	209
3.82	Mean crack density for individual placements versus high air temperature for silica fume overlay bridge decks.....	210
3.83	Mean crack density for individual placements versus high air temperature for conventional overlay bridge decks.....	210
3.84	Mean crack density for individual placements versus high air temperature for monolithic bridge decks	211
3.85	Mean crack density of bridge subdecks versus high air temperature	211
3.86	Mean crack density for individual placements versus daily temperature range for silica fume overlay bridge decks.....	212

3.87	Mean crack density for individual placements versus daily temperature range for conventional bridge decks.....	212
3.88	Mean crack density for individual placements versus daily temperature range for monolithic bridge decks	213
3.89	Mean crack density of bridge subdecks versus daily temperature range.	213
3.90	Mean crack density for individual placements versus relative humidity for silica fume overlay bridge decks	214
3.91	Mean crack density for individual placements versus relative humidity for conventional overlay bridge decks	214
3.92	Mean crack density for individual placements versus relative humidity for monolithic bridge decks.....	215
3.93	Mean crack density of bridge subdecks versus relative humidity	215
3.94	Mean crack density for individual placements versus wind velocity for silica fume overlay bridge decks.....	216
3.95	Mean crack density for individual placements versus wind velocity for conventional overlay bridge decks.....	216
3.96	Mean crack density for individual placements versus wind velocity for monolithic bridge decks	217
3.97	Mean crack density of bridge subdecks versus wind velocity.....	217
3.98	Mean crack density of individual placements versus silica fume overlay Special Provision revision number	218
3.99	Mean crack density for entire bridge versus structure type for silica fume overlay bridge decks.....	219
3.100	Mean crack density for entire bridge versus structure type for conventional overlay bridge decks.....	219
3.101	Mean crack density for entire bridge versus structure type for monolithic bridge decks.....	220
3.102	Mean crack density of entire bridge versus deck type.....	220

3.103	Mean crack density for entire bridge versus deck thickness for silica fume overlay bridge decks.....	221
3.104	Mean crack density for entire bridge versus deck thickness for conventional overlay bridge decks.....	221
3.105	Mean crack density for entire bridge versus deck thickness for monolithic bridge decks.....	222
3.106	Mean crack density for entire bridge versus top cover for monolithic bridge decks	222
3.107	Mean crack density for entire bridge versus top transverse reinforcing bar size for silica fume overlay bridge decks.....	223
3.108	Mean crack density for entire bridge versus top transverse reinforcing bar size for conventional overlay bridge decks.....	223
3.109	Mean crack density for entire bridge versus top transverse reinforcing bar size for monolithic bridge decks.....	224
3.110	Mean crack density for entire bridge versus top transverse bar spacing for silica fume overlay bridge decks.....	225
3.111	Mean crack density for entire bridge versus top transverse bar spacing for conventional overlay bridge decks.....	225
3.112	Mean crack density of end sections versus girder end condition for silica fume overlay bridge decks.....	226
3.113	Mean crack density of end sections versus girder end condition for conventional overlay bridge decks.....	226
3.114	Mean crack density of individual spans versus span length for silica fume overlay bridge decks.....	227
3.115	Mean crack density of individual spans versus span length for conventional overlay bridge decks.....	227
3.116	Mean crack density of individual spans versus span length for monolithic bridge decks.....	228
3.117	Mean crack density of entire bridge versus bridge length for silica fume overlay bridge decks.....	228

3.118	Mean crack density of entire bridge versus bridge length for conventional overlay bridge decks.....	229
3.119	Mean crack density of entire bridge versus bridge length for monolithic bridge decks.....	229
3.120	Mean crack density of individual spans versus span type for silica fume overlay bridge decks.....	230
3.121	Mean crack density of individual spans versus span type for conventional overlay bridge decks.....	230
3.122	Mean crack density of individual spans versus span type for monolithic bridge decks.....	231
3.123	Mean crack density of entire bridge versus skew for silica fume overlay bridge decks	231
3.124	Mean crack density of entire bridge versus skew for conventional overlay bridge decks	232
3.125	Mean crack density of entire bridge versus skew for monolithic bridge decks	232
3.126	Mean crack density of entire bridge versus traffic volume for silica fume overlay bridge decks.....	233
3.127	Mean crack density of entire bridge versus traffic volume for conventional overlay bridge decks.....	233
3.128	Mean crack density of entire bridge versus traffic volume for monolithic bridge decks.....	234
3.129	Mean crack density of entire bridge decks versus the total number of load cycles for silica fume overlays	234
3.130	Mean crack density of entire bridge decks versus the total number of load cycles for conventional overlays	235
3.131	Mean crack density of entire bridge decks versus the total number of load cycles for monolithic bridge decks.....	235

3.132	Mean pavement roughness index (PRI) of individual lanes versus deck type	236
A.1	Legend for Bridge Deck Cracking Patterns	357
A.2	Bridge Number 23-85 (Silica Fume Overlay)	358
A.3	Bridge Number 46-302 (Silica Fume Overlay)	359
A.4	Bridge Number 46-309 (Silica Fume Overlay)	360
A.5	Bridge Number 46-317, Unit 1 (Silica Fume Overlay)	361
A.6	Bridge Number 81-50, Unit 2 (Silica Fume Overlay)	362
A.7	Bridge Number 87-453 (Silica Fume Overlay)	363
A.8	Bridge Number 87-454 (Silica Fume Overlay)	364
A.9	Bridge Number 89-184 (Silica Fume Overlay)	365
A.10	Bridge Number 89-187 (Silica Fume Overlay)	366
A.11	Bridge Number 89-206 (Silica Fume Overlay)	367
A.12	Bridge Number 89-207 (Silica Fume Overlay)	368
A.13	Bridge Number 89-210 (Silica Fume Overlay)	369
A.14	Bridge Number 89-234 (Silica Fume Overlay)	370
A.15	Bridge Number 89-235 (Silica Fume Overlay)	371
A.16	Bridge Number 89-240 (Silica Fume Overlay)	372
A.17	Bridge Number 89-244 (Silica Fume Overlay)	373
A.18	Bridge Number 89-245 (Silica Fume Overlay)	374
A.19	Bridge Number 89-246 (Silica Fume Overlay)	375
A.20	Bridge Number 89-247 (Silica Fume Overlay)	376
A.21	Bridge Number 89-248 (Silica Fume Overlay)	377

A.22	Bridge Number 46-289 (Conventional Overlay)	378
A.23	Bridge Number 46-290 (Conventional Overlay)	379
A.24	Bridge Number 46-299 (Conventional Overlay)	380
A.25	Bridge Number 46-300 (Conventional Overlay)	381
A.26	Bridge Number 46-301 (Conventional Overlay)	382
A.27	Bridge Number 75-01 (Conventional Overlay)	383
A.28	Bridge Number 75-49 (Conventional Overlay)	384
A.29	Bridge Number 81-49 (Conventional Overlay)	385
A.30	Bridge Number 89-183 (Conventional Overlay)	386
A.31	Bridge Number 89-185 (Conventional Overlay)	387
A.32	Bridge Number 89-186 (Conventional Overlay)	388
A.33	Bridge Number 89-196 (Conventional Overlay)	389
A.34	Bridge Number 89-198 (Conventional Overlay)	390
A.35	Bridge Number 89-199 (Conventional Overlay)	391
A.36	Bridge Number 89-200 (Conventional Overlay)	392
A.37	Bridge Number 89-201 (Conventional Overlay)	393
A.38	Bridge Number 56-148 (Monolithic)	394
A.39	Bridge Number 70-107 (Monolithic)	395
A.40	Bridge Number 89-204 (Monolithic)	396
A.41	Bridge Number 89-208 (Monolithic)	397

CHAPTER 1

INTRODUCTION

1.1. GENERAL

Cracking in concrete bridge decks can be caused by a variety of reasons, ranging from settlement of the concrete over reinforcing steel to plastic shrinkage of the concrete. A predominant cause of cracking and premature deterioration in bridge decks is the corrosion of the reinforcing steel because of the penetration of chlorides from deicing chemicals in the concrete. A number of methods are or have been used to slow or stop the diffusion of chlorides through concrete to the reinforcing steel. One approach that has gained popularity in the United States and is being applied with increasing regularity in the state of Kansas is the use of silica-fume concrete overlays to decrease the permeability of the concrete. The reduction in permeability is intended to slow the diffusion of chlorides through the concrete and consequently delay the onset of corrosion in the reinforcing steel. Both the low diffusivity and good bonding qualities of silica-fume concrete make it ideal for use in concrete bridge decks. There are however, some concerns that the silica-fume concrete is more susceptible to both plastic shrinkage and drying shrinkage cracking.

1.2 TYPES OF CRACKING

Bridge deck cracking can be classified either by the causes of the cracking or by the orientation of the cracks with respect to the centerline of the bridge or roadway.

1.2.1 Crack Classification Based on Causes of Cracking

Cracking in concrete bridge decks results from a variety factors, in both the design and construction phases of the bridge decks. The factors that lead to bridge deck cracking are not fully understood, but specific types of cracking have been identified, such as plastic shrinkage cracking, subsidence cracking, thermal shrinkage

cracking, drying shrinkage cracking, flexural cracking, and cracking due to corrosion of reinforcing steel.

Plastic shrinkage cracking occurs when the surface evaporation rate exceeds the rate at which bleed water rises to the concrete surface. When the top layer of the concrete dries out because of the lack of surface water, it begins to shrink. However, the top layer is restrained by the lower layer of concrete that has not dried, because it is losing water at a slower rate. This difference in shrinkage creates tensile stresses in the concrete that has essentially zero strength at early age, causing cracks to develop. Several methods have been used to successfully avoid plastic shrinkage cracking during construction, including fogging, using evaporation retarders, erecting wind breaks, and the immediate application of curing compounds or wet burlap covered with plastic.

Subsidence cracking occurs due to the presence of reinforcing steel near the upper surface of a concrete slab. Fresh concrete subsides or settles after finishing and during bleeding. Reinforcing steel near the surface of the concrete provides resistance to the subsidence for the concrete directly above it. As the concrete on both sides of the reinforcing steel subsides, it pulls on the concrete directly above the reinforcing steel causing tensile stresses. Because the concrete has virtually no tensile strength at this early stage in its development cracks can form where the tensile stresses are greatest directly above the reinforcing steel. Subsidence cracking increases as concrete slump and bar size increase and as concrete cover decreases (Dakhil, Cady, and Carrier 1975).

Thermal shrinkage is due to the difference in deck and supporting beam temperatures. When concrete is curing, its temperature rises, and the concrete tends to expand. By the time the concrete has reached its peak temperature, it has also hardened. As the hardened concrete cools to ambient temperature, it begins to shrink, but the supporting beams or girders that are at ambient temperature provide resistance to the shrinkage, causing tensile stresses to form in the deck. If the difference between the peak concrete temperature and the temperature of the supporting

structure is great enough, cracks can form. (Babaei and Fouladgar 1997).

Drying shrinkage is similar to thermal shrinkage, because it occurs as the result of the resistance to shrinkage of the deck provided by the supporting beams or girders. After curing, hardened concrete dries and begins to shrink; however, the process is very slow and may take more than a year. Because the process is gradual, concrete creep helps to reduce the resulting tensile stresses. Therefore, the strain needed to cause cracking by drying shrinkage is about two and a half times the strain needed to cause cracking due to thermal shrinkage (Babaei and Fouladgar 1997).

Flexural cracking occurs in negative moment regions over internal supports in continuous concrete bridge decks resulting from dead and live loads on the bridge (Babaei and Fouladgar 1997).

When reinforcing steel corrodes, the corrosion products that form take up significantly more volume than the original steel. The increase in volume causes large pressures to be exerted on the concrete, causing it to crack.

1.2.2 Crack Classification Based on Orientation

In a study of bridge deck cracking, the Portland Cement Association (1970) classified cracks into six categories: transverse, longitudinal, diagonal, pattern, D, and random cracking.

Transverse cracking, perpendicular to the bridge centerline, is by far the most prevalent type found on bridge decks (PCA 1970). Transverse cracks occur both in new bridge decks, that have not been opened to traffic, and in older bridges. The cracks frequently occur directly over reinforcing steel. Transverse cracking can result from subsidence, thermal shrinkage, drying shrinkage, and flexure cracking.

Longitudinal cracking, parallel to the bridge centerline, occurs primarily in hollow and solid slab concrete bridges (PCA 1970). One of the most significant causes of longitudinal cracking is believed to be subsidence cracking that occurs over longitudinal reinforcing steel in the top of the slab or over void tubes.

Diagonal cracking, roughly parallel cracks forming an angle other than 90

degrees with the centerline of the roadway, occurs primarily on skewed bridges at the acute angled corners of abutments, but also occurs over single column piers of concrete box-girder, deck-girder, and hollow-slab bridges (PCA 1970). Diagonal cracking probably results from drying shrinkage or flexure cracking.

Pattern cracking is described as any size network of interconnected cracks. It tends to be shallow and is generally believed to result from both plastic and drying shrinkage (PCA 1970). In the PCA (1970) study, pattern cracking did not appear to have a significant effect on the performance of the bridge deck.

D cracking, a series of cracks in concrete near and roughly parallel to joints, edges, and structural members, is a result of deterioration at the base of concrete slabs due to destruction of aggregates by frost. It is not found on bridge decks (PCA 1970).

Random cracking is described as irregularly meandering cracks that have no form and do not fit another classification. It can be found on most bridge decks, but there is no clear relationship between random cracking and bridge deck characteristics (PCA 1970).

1.3 CORROSION

The use of deicing salts since the early 1960's has led to the increased deterioration of concrete bridge decks as a result of the corrosion of reinforcing steel (Weil 1988). It is a significant problem. Under normal conditions, the highly alkaline environment in concrete creates a tightly adhering film that passivates the steel, protecting it from corrosion. However, chloride ions, deposited as deicing salts, can diffuse through the concrete. If the chlorides reach a level of concentration high enough, called the chloride threshold level, they can penetrate the passivating layer and cause corrosion of the reinforcing steel if both oxygen and moisture are present (ACI Committee 222 1998). As described earlier, the corrosion products that form can then cause cracking of the concrete. Many factors influence the rate of the corrosion reaction and the protection provided to the reinforcing steel. However, the degree of corrosion protection for bridge decks is primarily determined by the

thickness of the reinforcing steel cover and the permeability of the concrete (ACI Committee 222 1998).

1.4 SILICA FUME

Silica fume is a pozzolanic material that is produced as a by-product during the production of silicon metal or ferrosilicon alloys in electric arc furnaces. It is approximately 100 times finer than portland cement. When it is used in concrete, it acts both as filler and as a cementitious material. The small silica fume particles fill spaces between cement particles and between the cement paste matrix and the aggregate particles (Whiting and Detwiler 1998). The silica fume also combines with calcium hydroxide (CH) to form additional calcium-silicate hydrate (CSH) through the pozzolanic reaction. Both these actions result in a denser, stronger, and less permeable material.

Silica fume is used to improve the durability, strength and bonding characteristics of concrete, but it is predominately used, in bridge decks to reduce the permeability of concrete. Significant testing has been performed to determine the resistance of silica fume concrete to chloride ion penetration, and it is generally agreed that silica-fume concretes show a reduction in permeability compared to conventional concretes. There is some concern, however, because the addition of silica fume to concrete reduces the pH of the pore solution, which could negatively affect the passivation of the reinforcing steel. However, the reduction in pH associated with the amounts of silica fume generally used in concretes is not large. The increase in electrical resistivity and the reduction in permeability to chloride are believed to be more significant than any reduction in the pH of the pore solution that might occur. It should be noted that the permeability of concrete depends in large part on the methods and length of time used for curing.

Although silica-fume concrete offers several advantages, several factors must be considered before using it. The addition of silica fume to concrete may increase the early age cracking of the concrete, and because silica fume has a very high surface

area, its addition results in an increased water demand, reduced bleed water and greater cohesiveness. The reduction in bleed water, results in the loss of surface water due to evaporation that is greater than the rate at which it is replaced by bleeding, which can lead to plastic shrinkage cracking.

To maintain the same degree of workability as conventional concrete, ACI Committee 234 recommends that the slump of the concrete be increased by about 50 mm (2 in.) above that used for conventional concrete. ACI Committee 234 recommends that water-reducing admixtures or high-range water-reducing admixtures be used to achieve the added slump at a reasonable w/cm.

1.5 RAPID CHLORIDE PERMEABILITY TEST

One test that has become both popular and routine for determining the ability of concrete to resist chloride ingress is ASTM C 1202 (AASHTO T277-93) "Electrical Indication of Concrete's ability to Resist Chloride Ion Penetration." It is frequently referred to as the Rapid Chloride Permeability Test (RCPT). The test has become popular because of its low cost and because it is relatively fast. It measures the total electrical charge in coulombs that passes through a concrete specimen during a standard time period. The charge passed is then related to chloride permeability, frequently with the use of a table that appears in both the ASTM and AASHTO standards. The table provides an indication of chloride ion penetrability for several ranges of charge passed, in coulombs. Chloride ion penetrability values are given as high, moderate, low, very low, and negligible. What is not clearly indicated in the standards is that the table is simply an example of results obtained from a very small group of specimens and that it is not intended to be used as a standard. Whiting and Mitchell (1992), the developers of the RCPT test, recommend, "that persons using this procedure prepare a set of concretes from local materials and use these to establish their own correlation between charge passed and known chloride permeability for their own particular materials."

It is important to note that this test only indirectly measures permeability. It is

actually a measure of the electrical conductance of concrete. Because the test measures electrical conductance, the addition of materials to the concrete that make the pore solution of the concrete less conductive will reduce the charge passed during the RCPT, regardless of how the addition of the material affects the pore structure and therefore permeability of the concrete.

This is one reason that recent studies have expressed concern over the use of the RCPT with silica fume concrete (Pfeifer, McDonald, and Krauss 1994, Shi, Stegemann, and Caldwell 1998). Pfeifer et al. (1994) reviewed 5 studies referenced in ASTM C 1202 and examined the correlation between the results of the RCPT and the results of AASHTO T 259, "Resistance of Concrete to Chloride Ion Penetration." Although the scope of ASTM C 1202 states that the RCPT is applicable only when a correlation for the concrete types being tested has been made between the RCPT and a long-term ponding test, such as AASHTO T 259, Pfeifer et al. (1994) found that, in numerous articles published both by American Concrete Institute (ACI) and ASTM, very few researchers had confirmed the correlation provided in the table in both ASTM C 1202 and AASHTO T 277. They concluded that many researchers used the results of RCPT to reach conclusions about permeability without confirming the correlation. After studying and evaluating the results of the 5 articles, they concluded that, "reliable and proper correlations do not exist between the six-hour rapid chloride permeability test results and the 90-day ponding test results when different studies are compared" (Pfeifer, McDonald, and Krauss 1994, p 46). They were especially concerned about the uses of the RCPT to specify concretes containing pozzolanic materials, such as silica fume and slag cements. They found that the charge passed by conventional concretes may decrease 5 to 10 times with the addition of 7 percent silica fume, but that actual chloride ingress as measured by the 90 day ponding test is only decreased by one to two times. In addition, silica fume concretes could show low values of "coulombs passed" despite being made with relatively high water-cement ratios (0.45 to 0.55), indicating that the RCPT can err in favor of poor quality concretes.

The permeability of concrete, an indication of how easily ions are transported through the concrete, depends on the physical pore structure of the concrete. The conductivity of concrete or its ability to pass an electric current depends not only on the physical pore structure of the concrete, but also on the pore solution or fluid in the pores. When Shi, Stegmann, and Caldwell (1998) examined the effect of supplementary cementing materials such as silica fume on the RCPT, they found that the addition of silica fume to concrete significantly reduces the conductivity of the pore solution. Because the RCPT measures the electrical conductivity of the concrete, it depends on both the pore structure of the concrete and the conductivity of the pore solution. Consequently, the addition of silica fume will cause the RCPT results to be much lower, regardless of physical pore structure or permeability of the concrete. They concluded that the RCPT should not be used to evaluate concretes with supplementary cementing materials, such as silica fume.

It should also be mentioned that the rapid chloride permeability test that was originally developed as an in situ device for field testing of concrete bridge decks (Whiting and Mitchell 1992, Whiting 1981). However, because of limitations in the field test, an alternative laboratory test (ASTM C 1202, AASHTO T 277) was developed. "It was not viewed as an accurate, standard laboratory test to determine the absolute permeability of a given concrete...Because the laboratory test was viewed as a fallback, it was not developed and tested nearly as thoroughly as the field method, and no systematic investigations were carried out on the many variables that might influence the test" (Whiting and Mitchell 1992). When the test was developed the effect of variables such as aggregate type and size, cement content and composition, density, and other factors were not studied. Whiting and Mitchell (1992) state that the precision of the RCPT needs to be improved and statistical acceptance schemes need to be developed for the test before it should be used with silica fume concretes.

1.6 CHLORIDE CONCENTRATIONS

It is well known that the transport of chloride ions in concrete is controlled by absorption, diffusion, and capillary action or wicking. “Except for the near-surface region of concrete, where capillary forces may be active under drying conditions, the predominant mechanism for transport of chloride ions in crack-free concrete is by ionic diffusion through the water-filled pore system” (Whiting and Mitchell 1992). Fick’s Second Law of Diffusion is commonly used to model the ingress of chlorides into concrete.

$$C(x, t, C_o, D_{eff}) = C_o \left[1 - \operatorname{erf} \left[\frac{x}{2\sqrt{tD_{eff}}} \right] \right] \quad (1.1)$$

where

x = depth

t = time

C_o = surface concentration

D_{eff} = effective diffusion coefficient

erf = error function

Although this equation generally fits chloride data well, it does have some limitations. Fick’s model makes several basic assumptions that are violated by concrete. First, it applies only to the diffusion process and does not consider other methods of chloride transport through concrete, such as sorption and wicking. Second, it assumes that the material in which diffusion is occurring is both permeable and homogenous. Concrete is indeed permeable, but it is not homogenous; there are aggregates, cracks, microcracks and interconnected pores within concrete that can affect the diffusion of chloride ions through the concrete. Third, the diffusion properties of the material cannot change with time or concentration of the diffusant. Concrete generally becomes less permeable as it ages and hydration proceeds. Fourth, the diffusant cannot react chemically or physically with the material through

which it is diffusing. Hydration products in cement are capable binding with chloride ions and preventing their diffusion. Finally, Fick's Second Law assumes the surface concentration of the ions being transported is constant over time. Chlorides are applied to bridges in the form of deicing salts, which are only applied during the winter months of the year and can be washed away by rains. However, despite the shortcomings of the equation, it does provide both useful and realistic information that can be used to judge the performance of concrete (Whiting and Detwiler 1998).

1.7 OVERLAY SPECIFICATIONS

Because bridges with both silica fume and conventional overlays are studied, it is important to understand the differences in the specifications used for the two overlay types. Although contractors may take greater precautions to avoid poor quality concrete than the minimum standards required by the specifications, the specifications serve as a general indication of the construction practices followed. The specifications are detailed documents that cover all aspects of the materials, equipment, and procedures to be used when placing overlay concrete. However, certain aspects, such as the mix design, finishing methods and curing practices are of particular interest, especially where the specifications differ for the two types of overlay. The following descriptions of specification requirements do not necessarily indicate the requirements of the most recent specifications, but rather the requirements of the specifications used for the bridges in this study.

The applicable silica fume overlay specifications (special provisions 90P-158-R3 and 90P-158-R4) had several requirements with regards to mix design, finishing, and curing of the concrete. They required Type II or Type I/II portland cement, a minimum cement content of 354 kg/m^3 (595 lb/yd^3), and a minimum silica fume content of 18 kg/m^3 (30 lb/yd^3), equal to 5 percent of the total cementitious material. The maximum water to cementitious material ratio was 0.40. The percent volume of air required was 6.0 plus or minus 2 percent. The maximum coarse aggregate size was 12.7 mm (1/2 in.), and the ratio of coarse aggregate to fine aggregate was 1:1 by

weight. The contractor could choose a target slump between 50.8 and 127 mm (2 and 5 inches), with a 25.4 mm (1 in.) tolerance for the chosen slump. Because of concern over plastic shrinkage cracking, fogging and/or application of a precure material was required. Initial curing with liquid membrane forming curing compound and final curing with wet burlap and polyethylene was required for at least seven days.

The conventional overlay (bridge deck wearing surface) specifications (section 720 of the standard specifications and special provisions 90P-95, 90P-95-R1, and 90P-95-R2) had several requirements with regards to mix design of the concrete, finishing and curing of the concrete. They required Type II or Type I/II portland cement, and a minimum cement content of 371 kg/m^3 (625 lb/yd^3). The maximum water to cementitious material ratio was 0.38, and the percent volume of air required was 6.0 plus or minus 2 percent. The maximum coarse aggregate size was 12.7 mm (1/2 in.), and the ratio of coarse aggregate to fine aggregate was 1:1 by weight. The maximum slump allowed was 19.1 mm (3/4 in.) Fogging was not required. Initial curing with liquid membrane forming curing compound and final curing with wet burlap and polyethylene was required for at least 72 hours.

The two oldest silica fume overlays studied, bridges 89-184 and 89-187, were constructed before the specifications for silica fume overlays were written. They were most likely constructed according to the conventional overlay specifications.

The current silica fume overlay specification (special provision 90M-158-R8) requires Type IP, Type II, or Type I/II portland cement, a minimum cement content of 346 kg/m^3 , and a minimum silica fume content of 26 kg/m^3 , 7 percent by weight of the cementitious material. The maximum water to cementitious material ratio is 0.37. The percent volume of air required is 6.5 plus or minus 1.5 percent. The maximum coarse aggregate size is 12.5 mm, and the ratio of coarse aggregate to fine aggregate is 1:1. The contractor can choose a target slump between 50 and 125 mm, with a tolerance of 25 percent or 18 mm, whichever is larger, for the chosen slump. Because of concern over plastic shrinkage cracking, fogging and application of precure material are required. Application of a liquid membrane forming curing

compound immediately behind the tining float is required. The required final cure is with wet burlap and polyethylene sheeting for at least seven days.

The current conventional overlay specification (special provision 90M-95-R4) requires Type IP, Type II, or Type I/II portland cement, and a minimum cement content of 370 kg/m^3 . The maximum water to cementitious material ratio is 0.38, and the percent volume of air required is 6.5 plus or minus 1.5 percent. The maximum coarse aggregate size is 12.5 mm, and the ratio of coarse aggregate to fine aggregate is 1:1 by weight. The contractor can choose a target slump between 50 and 125 mm, with a tolerance of 25 percent or 18 mm, whichever is larger, for the chosen slump. Application of a precure material is required. Application of liquid membrane forming curing compound immediately behind the tining float is required. The required final cure is with wet burlap and polyethylene sheeting for at least seven days.

1.8 PREVIOUS WORK

Numerous studies have been undertaken to study both cracking and the use of silica fume in bridge decks. It is useful to examine these previous studies, both to understand the previous work and to examine the conclusions of researchers. Studies relating to both bridge cracking in general and to the use of silica fume and its affect on cracking are reviewed.

Seven studies on bridge deck cracking are summarized. The first study examines the causes of bridge deck cracking in Kansas and served as a template for this study, in terms of collection of data and field surveying techniques. The second study was performed by the Portland Cement Association. It was one of the earliest studies to extensively examine the factors that affect bridge deck durability. The third study, by Dakhil, Cady, and Carrier (1975) examined the affects of concrete cover, concrete slump, and reinforcing bar size on cracking in concrete. The fourth study, by Poppe (1981), examined the effect of several construction practices and site conditions on bridge deck cracking. The fifth study was an extensive two part study

that examined both various construction practices and structural considerations (Cheng and Johnston 1985, Perfetti, Johnston, and Bingham 1985). The sixth is an extensive study performed for the National Cooperative Highway Research Program (Krauss and Rogalla 1996). A seventh study performed for the National Cooperative Highway Research Program (Whiting and Detwiler 1998) provides an extensive look at the use of silica fume in bridge decks.

1.8.1 Cracking in Bridge Decks

In 1995, Schmitt and Darwin completed a study of cracking in concrete bridge decks. The study was performed to find the probable causes of cracking, to determine the factors that contributed most to cracking, and to recommend alternate design and/or construction procedures to improve the performance of bridge decks.

The study consisted of on-site field surveys of 40 bridge decks in northeastern Kansas, and a detailed investigation of project files to examine construction procedures, design specifications, material properties, and environmental or site conditions. The scope of the study was limited to steel girder bridges, because it is generally acknowledged that they show the most severe cracking problems and because steel girder bridges account for a large percentage of bridges in Kansas. The study examined 37 composite and three non-composite bridge decks. It also examined both monolithic and two-layer bridge decks, two of which had silica fume overlays.

For the on-site field surveys the researchers marked all of the cracks on the bridge decks and then used a Fortran program to determine a crack density in meters of crack per square meter of bridge deck. Values of crack density were determined for each bridge deck, individual spans, individual placements and end sections of the bridge decks. The crack densities were then compared with bridge properties appropriate to those sections. For example, material properties of the bridge deck placements were compared with the crack densities for the individual placements.

From these observations, Schmitt and Darwin (1995, 1999) reached several conclusions in regard to monolithic, conventional two-layer, and silica fume two-layer decks. The deck type had only a small effect on the crack densities of the bridges studied. The mean crack density for the two layer bridges was only 6 percent greater than that for monolithic bridge decks. However, the effects of different material, structural, and environmental factors were analyzed separately for the different deck types and the trends found were not always the same for the different deck types. Schmitt and Darwin were also able to draw some conclusions based on design specifications.

Results for monolithic bridge decks showed several trends. Crack density increased as concrete slump, percent volume of water and cement, water content, cement content, and compressive strength increased. Crack density appeared to also increase with an increase in water/cement ratio, although this trend was established only for a small range of values. There was a decrease in cracking with increasing air content, which was especially significant at air contents greater than 6.0%. As the maximum daily air temperature and daily air temperature range on the day of concrete placement increased, cracking increased. Monolithic bridges with top cover of 64 mm (2.5 in.) showed less cracking than monolithic bridges with top cover of 76 mm (3.0 in.). However, a single concrete placement with a slump of 51 mm (2.0 in.) showed much greater cracking than the concrete placements with slumps of 64 or 76 mm (2.5 or 3.0 in.). Cracking appears to increase with bridge length, but the trend is not clearly defined. For monolithic bridge decks, there was almost no variation in the size of transverse reinforcing steel bars used, and the spacing between them, so no conclusion could be drawn with regard to transverse reinforcing steel.

Results for two-layer (overlay) bridges also showed several trends. Overlays placed with zero slump concrete showed consistently higher levels of cracking than overlays placed with slump greater than zero. As the average air temperature and daily air temperature range on the day of concrete placement increased, so did crack density. Cracking increased with increasing maximum daily air temperature, but the

trend was not as clearly defined it was for monolithic bridge decks. As placement length and bridge length increased, cracking in the overlay decks tended to increase, although the increase in cracking with bridge length is most likely a result of the increase in cracking with placement length, because most overlays were placed in sections that extended the entire length of the bridge. There also appeared to be an increase in cracking with increased skew. The crack densities of two layer bridges with No. 19 (No. 6) transverse reinforcing steel bars was greater than that of two layer bridges with either No. 16 (No. 5) bars or a combination of No. 13 and No. 16 (No. 4 and No. 5) bars. Crack densities were also greater in two layer bridges with a transverse reinforcing bar spacing greater than 150 mm (6 in.)

Only two bridges with silica fume overlays were included in the study, because of the limited application of the technique at the time of the study, but their analysis indicated that the use of silica fume could significantly increase cracking, if precautions were not taken to prevent plastic shrinkage cracking.

Certain results were established for all bridge types. There was increased cracking near the abutments for bridges with fix-ended girders compared to bridges with pin-ended girders. The magnitude of the cracking near the abutment increased for bridges with longer lengths of attachment along the abutments, especially when the length of attachment was greater than 14 m (45 ft). There also appeared to be an increase in cracking with an increase in the average annual daily traffic (AADT). The results showed that for both monolithic and two-layer bridges, the newer bridges (those constructed after 1988) showed increased cracking compared to older bridges.

Based on the results of the study, Schmitt and Darwin (1995) made three primary recommendations: (1) the volume of water and cement should not exceed 27.0 percent of the total volume of the concrete when generating mix designs for monolithic bridge decks and the subdecks of two-layer bridges, (2) the air content of concrete used for monolithic bridges should exceed 6.0 percent, and (3) concrete used for bridge deck overlays should not be placed with zero slump.

In addition to the three primary recommendations, Schmitt and Darwin (1995)

also mentioned several other items that should be taken into consideration. Designers should compare the advantages offered by fixed-end girders with the effects of increased cracking. The effects of high air temperatures on concrete should be considered when placing concrete, and proper precautions should be taken. For monolithic bridge decks, concrete slump should be limited to approximately 50 mm (2 in.). The use of shorter placement lengths should be considered, especially for bridge deck overlays. Consideration should also be given to limiting the size of transverse reinforcing steel to No. 13 or No. 16 mm (No. 4 or No. 5) bars spaced no further than 150 mm (6 in.) apart. When silica fume concrete is placed, fog sprays should be used to prevent plastic shrinkage cracking.

In 1961, the Portland Cement Association (1970) began an extensive study of bridge deck durability. One of the primary reasons for undertaking the study was the apparent connection between the increasing use of de-icing chemicals and the increased rate of deterioration of concrete bridge decks. The four primary objectives of the study were to determine the types and extent of bridge deck durability problems, to determine the causes of the various types of deterioration, to develop methods for improving the durability of future bridge decks, and to develop methods for slowing the deterioration of existing bridge decks. The research had 3 major parts: a detailed investigation of 70 bridge decks, a random survey of over 1000 bridges, and a theoretical study that computed the vibration characteristics of 46 of the bridges examined in the detailed investigation. All of the bridges examined were built between 1940 and 1960.

The primary purpose of the detailed investigation was to determine the causes of deterioration. The 70 bridges were selected to obtain a wide range of types and amounts of deterioration, ages, structure types, and locations. Representatives from state highway departments, the Bureau of Public Roads, and the Portland Cement Association, performed field inspections on each of the bridge decks, that included making sketches of the bridge decks with the locations and types of deterioration present. Types of deterioration recorded included scaling, various types of cracking,

surface spalling, popouts, and pitting. During the field inspections, concrete cores were collected from the bridge decks. The concrete cores were then examined in the laboratory to determine properties such as air content, the depth and width of cracks, chloride contents, and whether the cracks went through the aggregate particles or around them (an indication that cracking probably occurred when the concrete was still plastic). In addition to the field inspections and laboratory studies, the plans, specifications, and construction records were examined to determine any possible correlation with the observed deterioration.

The primary purpose of the random survey was to determine the types and amount of deterioration on bridge decks. The bridges surveyed were selected at random from the population of bridges in 8 states to get a representative sampling of all the bridge decks in the states. Portland Cement Association engineers and state highway department representatives used standard data sheets to classify the type and amount of deterioration on the bridge decks in accordance with the same definitions used in the detailed investigations.

The vibration characteristics of the bridges were calculated using a set of equations that had previously been shown to correlate well with actual bridge behavior. Once calculated, the vibration characteristics were interpreted only with respect to transverse cracking and surface spalling. The results of the theoretical study indicated that there was no correlation between transverse cracking or surface spalling and the vibration characteristics of the superstructure, regardless of the superstructure type.

Both the detailed investigations and the random survey classified cracking according to its directional trend into one of 6 categories: transverse, longitudinal, diagonal, pattern or map, D, and random. Results of the detailed investigation indicated that transverse and longitudinal cracking were the most prevalent and most significant because surface spalls were often associated with these two types of cracking. Several factors were found to contribute to transverse cracking in decks, but no single factor was more significant than the others. The detailed investigation

showed that the major factors contributing to transverse cracking in decks supported by steel girders are the restraint that the steel girders impose on both the short and long term shrinkage of the deck slab, and the tensile stress rise in the concrete caused by the top slab reinforcement. Both the field observations and the laboratory tests indicated that transverse cracks frequently occurred directly over reinforcing bars. Longitudinal cracks frequently formed directly over longitudinal reinforcement or void tubes in hollow slab bridges.

Based on the results of the study, the Portland Cement Association made several recommendations to improve bridge deck durability, especially in regard to cracking. The largest practical maximum size of coarse aggregate should be used to reduce paste content and thereby reduce concrete shrinkage. The maximum slump should be between 2 and 3 inches, because large slumps can cause segregation, increased bleeding, drying shrinkage, and therefore cracking tendency. Concrete cover over the top reinforcing steel should be at least 2 inches in areas where de-icing chemicals are used and at least 1.5 inches in areas where de-icing chemicals are not used. Curing should be started as soon as the concrete has hardened enough to prevent surface damage.

Because of the prevalence of cracking in bridge decks directly over reinforcing steel bars, Dakhil, Cady, and Carrier (1975) investigated the effect of the depth of concrete cover, concrete slump, and reinforcement bar size on the cracking tendency of concrete bridge decks. The study included a laboratory investigation of concrete specimens with varying depth of cover, concrete slump, and bar size, a photoelastic evaluation of gelatin models to determine the type and quantity of stress in the concrete specimens, and a corrosion study to evaluate how the formation of cracks affected the rate of corrosion activity.

A total of 108 concrete specimens were made using three different concrete slumps [51 mm (2 in.), 76 mm (3 in.) and 102 mm (4 in.)], four different depths of cover [19 mm (0.75 in.), 25 mm (1 in.), 38 mm (1.5 in.), and 51 mm (2 in.)], and three different reinforcing bar sizes [No. 13 (No. 4), No. 16 (No. 5), No. 19 (No. 6)].

The specimens were inspected and photographed 4 hours after concrete placement to determine the extent of cracking. The data indicated that both the occurrence and severity of cracking increased with increasing bar size, increasing slump, and decreasing cover. Depth of concrete cover was determined to be the single most important factor controlling the cracking tendency. Specimens with 51 mm (2 in.) cover resisted cracking in all cases except in combination with the largest bar size and highest slump. It should be noted that the effects of water reducers were not studied and higher slumps due to the use of water reducers may not exhibit the same behavior.

The photoelastic evaluation of gelatin models indicated that the skin stresses above the reinforcing steel bars are tensile and that the tensile stresses reach a maximum over the bars.

The specimens for the corrosion study contained No. 16 (No. 5) bars with 19 mm (0.75 in.) and 38 mm (1.5 in.) covers. The specimens were exposed to salt solutions, and the presence of active corrosion was determined by measuring the potential of the steel to a standard reference electrode. The most important result of the corrosion study was that corrosion was significantly greater in specimens that had cracks above the reinforcement.

In a study on concrete bridge deck durability, Poppe (1981) examined several variables including, bridge deck thickness, weather conditions at the time of placement, type of curing, volume of entrained air, use of shrinkage compensated cement, and reinforcing steel placement. To study the effects of the various variables, the construction of bridge decks with different designs, construction practices, and materials was observed.

To determine the performance of the bridge decks, crack surveys were performed. The results of the crack surveys were used to calculate a deck cracking index. The cracking index was calculated by dividing the bridge deck into a grid system and determining the average number of cracks per grid square. However, because large crack width was considered to be more harmful to bridge deck

performance than thin cracks, a weighted average was used that assigned a greater weight to wider cracks. The cracking index was then used as a quantitative indication of bridge deck performance.

Based on the results of the study, Poppe (1981) made several conclusions. Thicker bridge decks do not change cracking patterns, or eliminate cracking, but they do crack less than decks of the standard thickness [158.8 mm (6.25 in.)]. Adverse weather conditions, such as high wind, high heat, and low humidity, have a greater affect on increased bridge deck cracking than any of the construction practice variables studied. Both insufficient curing and late application of initial curing result in increased cracking. The use of curing compounds reduces cracking when high winds or low humidity occur during construction. The use of different amounts of entrained air in concrete had no effect on bridge deck cracking. Bridge decks with shrinkage compensating cement showed less cracking than those with Type II portland cement. Placement of reinforcing steel had a minimal affect on cracking.

North Carolina State University completed a two part study on transverse cracking in bridge decks in 1985 (Cheng and Johnston 1985, Perfetti, Johnston, and Bingham 1985). The first part of the study examined construction procedures, construction site conditions, and concrete properties. The second half of the study examined the superstructure type, the deck casting sequence employed at the time of construction, and the vibration characteristics at the time of construction. A total of 72 bridges constructed between 1972 and 1981 were evaluated. Twenty of the bridges were supported by prestressed concrete girders. The other 52 bridges were supported by steel girders. Thirty five of the bridges were simple spans, and the remaining 37 bridges were continuous span units. Data was collected for each bridge from a field survey, the final design plans, construction diaries, and material and test records. During the field survey, the number of major, and minor transverse cracks were recorded, and used to calculate "cracks per linear foot" of bridge deck (CLF), based on the following expression:

$$CLF = (MACR + (MICR/4))/LENGTH \quad (1.2)$$

where

MACR = major transverse cracks, those cracks that could be followed completely across the bridge deck surface, or that propagated from one edge of the deck up to the roadway centerline.

MICR = minor transverse cracks, those shorter transverse cracks that typically occurred close to the edge of the deck at the parapet joints or intersecting vertical drain pipes.

LENGTH = appropriate span of bridge length (ft)

The design plans were used to determine the superstructure type, girder type, girder spacing, girder size, and support conditions. The construction diaries were used to determine the order of the deck casting operation, and comments on construction progress. The material and test records were used to determine concrete cylinder strengths, and concrete mix design properties.

By comparing the data collected with the calculated CLF for each bridge, Cheng and Johnston were able to draw several conclusions. The transverse cracking problem was more significant in continuous girder bridges, both prestressed and steel, than in simple spans. The length of concrete placement did not significantly affect the rate of cracking observed. Low relative humidity, less than 60%, at the time of concrete placement caused increased transverse cracking. Low ambient temperatures at the time of concrete placement caused increased transverse cracking. Higher air contents in the mix design reduced transverse cracking. Other than air content, they found no significant correlation between mix design material factors and the amount of transverse cracking.

The second part of the study (Perfetti, Johnston, and Bingham 1985) examined the structural characteristics of the bridges. Perfetti et al. used the Nick-Ramiery and Veletsos procedure to calculate the vibration characteristics (natural

frequency and the dimensionless speed parameter that characterizes the dynamic response) of each bridge. The vibration characteristics were then compared with the CLF for each bridge. For simple steel spans, the fundamental natural frequency of the bridge decreased and the incidence of transverse cracking increased as span lengths increased. There was no correlation between span length and increased cracking for continuous steel units. When all structural types were considered, there was no consistent relationship between the vibration characteristics of the bridges and the incidence of cracking.

Perfetti et al. (1985) also used a finite element technique to analyze the bridges under dead and live load. For the dead load analysis, the maximum stress was calculated for conditions during the concrete placement and for the residual stresses in the deck after all concrete placement was completed. For the live load analysis, the stresses due to an HS20-44 lane loading were determined from a static analysis. They found no consistent relationship between the incidence of transverse cracking and the residual maximum stresses in the bridge deck after the completion of concrete placement. They found that transverse cracking increased as the calculated combined dead and live load stresses increased.

Krauss and Rogalla completed an extensive study of transverse cracking in newly constructed bridge decks in 1996. The study included a survey of 52 transportation agencies, a literature review, theoretical and finite element analysis of numerous bridge designs, field instrumentation of a deck replacement, and laboratory studies of the cracking tendency of different concretes. The project determined which factors most significantly affect bridge deck cracking based on structural design procedures, concrete material properties, and construction methods.

The survey of transportation agencies was used to determine what factors the agencies perceived to be most important in the control of cracking. Sixty two percent of the agencies considered early transverse cracking to be a problem. Although the results were diverse, the factors that elicited the most concern in regard to perceived causes of cracking were curing of the concrete and concrete material properties such

as drying shrinkage, plastic shrinkage, cement content, the use of retarders, and environmental conditions, such as temperature and relative humidity. Construction practices, other than curing, and design practices, other than deflections, were not generally considered to be major causes of cracking.

The literature review studied articles and papers that examined transverse cracking in bridge decks, and how cracking is related to corrosion of reinforcing steel, the visual appearance of the decks, and structural deterioration of concrete.

The field study consisted of instrumenting the Portland-Columbia Bridge between Pennsylvania and New Jersey to measure strains and temperatures in the bridge deck and girders. Environmental conditions were also monitored. Data was collected for several months, starting when the deck concrete was cast. The data collected could not be generalized to all bridges, but the data was useful in confirming the theoretical analysis.

The theoretical analysis involved the development of equations to “calculate stresses in a composite reinforced concrete bridge subjected to uniform and linear temperature and shrinkage conditions” (Krauss and Rogalla 1996). The behavior of the Portland-Columbia Bridge was used to confirm the accuracy of the equations. The equations were then used to examine more than 18,000 combinations of bridge geometry and material properties. The factors that affect shrinkage and thermal stresses were grouped into four categories: the concrete material, the geometry of the bridge, construction techniques, and the bridge environment. The concrete material properties had the greatest effect on shrinkage stresses. The shrinkage stresses were generally linearly proportional to the shrinkage of the concrete, so that any changes in the concrete material properties that reduced its shrinkage also directly reduced shrinkage stresses.

Krauss and Rogalla developed a restrained ring test to determine cracking tendency and used it to evaluate 39 different concrete mixtures. The effects of water-cement ratio, cement content, aggregate size and type, superplasticizer, silica fume, set accelerators and retarders, air entrainment, evaporation rate, curing, and

shrinkage-compensating cement were examined.

Based on the results of the entire study, conclusions were drawn, and recommendations were made with respect to design, material properties, and construction practices to reduce bridge deck cracking. Design factors include girder type, deck thickness, concrete cover, reinforcing bar size, type and alignment, quantity of reinforcement, skew, and traffic volume. Concrete material property factors include modulus of elasticity of the concrete, concrete strength, cement content, water content, water-cement ratio, aggregate and cement paste content, aggregate size and shape, cement type, use of silica fume, use of water reducers, use of set retarders and accelerators, slump, and air content. Construction practice factors include weather and time of placement, temperature, wind speed, placement sequence, finishing, vibration of fresh concrete, construction loads, traffic induced vibrations, and curing

The literature review indicated that cracking was more common on steel girder structures, continuous structures were more susceptible to cracking than simple spans. Higher temperature variations and, therefore, greater thermal stresses occur with steel girders. Both the literature review and theoretical analysis suggested that thicker decks are less susceptible to cracking. However, the analysis also showed that the size of spans and girders can affect the relationship between cracking and deck thickness. Reinforcing bar cover between 38 and 76 mm (1.5 and 3 in.) was recommended. It was also mentioned that a minimum cover of 50 mm (2 in.) is needed to avoid settlement cracks and is recommended for corrosion protection. Reduction of reinforcing bar size and decreasing spacing (necessary to maintain the same reinforcement ratio) reduced stress concentrations and the width of cracks. Although the literature review indicated that epoxy-coated reinforcement caused wider cracks, it also caused fewer cracks and performed better in corrosive conditions, consequently improving deck performance. Krauss and Rogalla recommended that bridges subject to deicing chemicals should contain some form of corrosion resistant reinforcement, such as epoxy-coated bars. Offsetting top and

bottom bars reduced the chances of full depth cracking, which usually occurred when the top and bottom bars were aligned. Both the analysis and the literature review indicated that the skew of bridge decks did not significantly affect transverse cracking. The literature review indicated that some researchers found an increase in cracking on bridges with higher traffic volumes, not all researchers agreed that traffic volume affected cracking in bridge decks.

The restrained ring tests showed that concrete modulus of elasticity and creep have a more significant affect on thermal and shrinkage stresses in concrete than any other material properties. A reduction in the modulus of elasticity and an increase in creep of the concrete reduce the risk of transverse deck cracking. This can be accomplished by using lower strength concrete and decreasing its paste content. The restrained ring tests showed that free shrinkage was directly proportional to paste volume; therefore, decreasing the paste volume, decreased shrinkage and consequently cracking. Although a slight relationship between lower water-cement ratios and increased cracking was found, the affect of cement content was not evaluated separately. The restrained ring tests showed that concretes with high cement contents and low water-cement ratios were more likely to crack than concretes with low cement contents and high water cement ratios. Therefore, Krauss and Rogalla recommended that bridge deck concrete should have 28 day compressive strength between 21 and 28 MPa (3000 and 4000 psi) to reduce cracking. They also recommended, not only low cement contents, but also that transportation agencies should specify a maximum cement content. The restrained ring tests showed no correlation between water content and cracking tendency. However, Krauss and Rogalla believe that, although concrete with higher water content and therefore higher paste content shrinks more than concrete with a lower water content, it may not crack sooner because it also has higher creep. To achieve a higher aggregate content, and therefore lower paste volume, it was also recommended that the largest permissible aggregate size be used, in accordance with ACI guidelines. Crushed aggregate reduced cracking better than rounded aggregate in the restrained ring tests. Krauss

and Rogalla found that the lower heats of hydration developed when Type II cements were used led to reduced cracking. The restrained ring tests indicated that adding silica fume to concrete increased the risk and/or severity of deck cracking. The results also indicated that water reducers could help delay cracking. Although, concrete specimens with accelerators cracked slightly sooner than concrete without accelerators during restrained ring tests, Krauss and Rogalla state that accelerators have minimal effects on cracking. Results on the effects of retarders were scattered and inconclusive, but Krauss and Rogalla recommend that precautions should be taken to avoid plastic shrinkage cracking when retarders are used. Although slump did not appear to affect deck cracking, it was recommended that a slump of at least 75 mm (3 in.) be used so that adequate compaction can be achieved. Restrained ring test specimens with entrained air did not show a cracking tendency significantly different from that of specimens without entrained air.

The report recommends that decks should be cast in cool, but not cold weather to reduce cracking. High humidity and low evaporation rates reduce cracking. Wind breaks and immediate water fogging were recommended in cases where the evaporation rate exceeds $1 \text{ kg/m}^2/\text{hr}$ ($0.2 \text{ lb/ft}^2/\text{hr}$). It was found that, although the use of a placing sequence to avoid negative bending and tensile stresses is important, negative bending stresses are not a primary cause of early bridge deck cracking. The findings indicate that concrete should be thoroughly vibrated, and mechanically screeded, and then floated after early bleeding. Effective vibration reduced voids and cracking. Construction loads can cause cracking by overloading the deck at an early age, but they are generally not a significant cause of transverse bridge deck cracking. Traffic-induced vibrations were not large enough to cause cracking in early age concrete. The research showed that curing is both a major cause of concern with transportation agencies and has a significant effect on transverse cracking in bridge decks. The optimum curing recommended for bridge decks includes the use of windbreaks when evaporation rates are excessive, fogging to cool the concrete during placement and finishing, misting or use of a monomolecular film immediately after

screeding, applying curing compound in two directions after bleed water diminishes but before the surface is dry, moist curing with wet burlap after the concrete can resist indentation, for at least 7 days, using a curing membrane after wet curing, and grooving with a diamond saw, instead of tining so that wet curing with burlap can begin sooner.

1.8.2 Silica Fume in Bridge Decks

In 1998, Whiting and Detwiler completed a report investigating the use of silica fume in concrete bridge decks. The study had several objectives: (1) to investigate the effects of the different forms and amounts of silica fume used in the concrete, (2) to examine the mix design parameters that most affect the behavior of silica fume concrete, (3) to produce information regarding the ability of silica fume concrete to reduce the diffusion of chloride ions, (4) to evaluate the tendency of silica fume concrete to crack, as well as methods to reduce cracking, (5) to analyze how well silica fume concrete overlays bond to deck concrete, and (6) to determine the optimum mix design parameters for the desired overlay performance.

The research included preparing both "full depth" concrete mixtures that contained 368 kg/m^3 (620 lb/yd^3) of cementitious material and "overlay" mixtures that contained 415 kg/m^3 (700 lb/yd^3) of cementitious material. Mix designs for both cementitious material contents were prepared with a practical range of water-cementitious material ratios (w/cm) and silica fume contents. The w/cm ratio was varied from 0.35 to 0.45 for the "full depth" mixtures and from 0.30 to 0.40 for the "overlay" mixtures. Silica fume content was varied from 0 to a 12 percent replacement by weight of cement. Specimens were tested to determine drying shrinkage, cracking tendency, chloride ion diffusivity, compressive strength, elastic modulus, strength of bond to the concrete substrate, and the coefficient of thermal expansion. The "full depth" mixtures were cured for 7 days, while the "overlay" mixtures were cured for 3 days, before testing began. The test results for drying shrinkage, cracking tendency, chloride ion diffusivity, compressive strength, elastic

modulus, strength of bond to the concrete substrate, and the coefficient of thermal expansion were then analyzed with respect to both w/cm ratio and silica fume content.

Drying shrinkage was measured on beam specimens over a period of 64 weeks at regular time intervals. The results showed that the “overlay” mixtures showed a greater degree of drying shrinkage than the “full depth” mixtures, especially at later ages. Two reasons were suggested for this behavior: (1) the “overlay” mixtures had higher paste contents, and (2) the “overlay” mixtures were only cured for 3 days compared to 7 days for the “full depth” mixtures. Although the “overlay” mixtures had lower w/cm ratios and exhibited greater drying shrinking, when the “full depth” and “overlay” mixtures were evaluated separately, the results showed that the mix designs with lower w/cm ratios exhibited less drying shrinkage. The tests also indicated that at fixed w/cm ratios, the changes in drying shrinkage are only sensitive to silica fume content at the extremes of the w/cm ratios used, especially at the lower extreme. The “full depth” mixtures exhibited minimal change in shrinkage with changing silica fume contents at the midpoint of the w/cm ratio range.

Cracking tendency was measured with the restrained ring test developed by Krauss and Rogalla (1996). When Krauss and Rogalla developed the test, they found good correlation between cracking in concrete bridge decks and cracking in the ring test specimens. “Full depth” mixtures were tested for different values of w/cm ratios, silica fume content, and curing time. When the specimens were moist cured for only 1 day, there was a significant increase in cracking with increasing silica fume content. After 7 days of moist curing, the difference in cracking tendency with increasing silica fume content was no longer evident. The results supported the generally held belief that silica fume concrete is more sensitive to moist curing times than conventional concrete. The w/cm ratio had no significant effect on cracking tendency as a function of curing time.

Chloride ion diffusivity specimens were subjected to 180 days of ponding, in accordance with AASHTO T259 “Resistance of Concrete to Chloride Ion

Penetration,” with the exception that the “overlay” mixtures were only moist cured for 3 days and the “full depth” mixtures were only moist cured for 7 days compared to the 14 days in the standard. After ponding, the specimens were milled in 1 mm (0.04 in.) layers that were tested for chloride content. The apparent diffusion coefficient was then calculated using a least-squares regression fit to Fick’s second law of diffusion. The results showed a dramatic overall decrease in diffusivity as silica fume content increased. However, for silica fume contents greater than 6 percent, a greater amount of silica fume was required to cause a given change in diffusivity than at silica fume contents lower than 6 percent. Whiting and Detwiler (1998) comment with regards to chloride diffusivity that, because “silica fume is expensive, a point of diminishing returns may be reached as one adds silica fume over about 6 percent.”

Compressive strength tests showed increases of up to 10 MPa when increasing the silica fume content of the concrete from 0 to 6 percent. However, when silica fume content was increased from 6 to 12 percent, there was little or no increase in compressive strength. It should also be noted that the highest compressive strength test results were obtained at the lowest w/cm ratio regardless of the silica fume content.

Modulus of elasticity in compression was measured on the specimens that were tested for compressive strength at 28 and 90 days of age. The modulus of elasticity increased as the silica fume content increased. As might be expected because of the approximate square root relationship between the modulus of elasticity and compressive strength, there was less spread in the data for modulus of elasticity than there was for compressive strength. “For example, at 28 days, the difference in strength between mixtures having the highest and lowest compressive strengths was 52 percent of the mean strength, while the range in modulus for the same set of mixtures was only 22 percent of the mean modulus.” Whiting and Detwiler (1998) concluded that it is unlikely that the small increases in elastic modulus would lead to an increased brittleness of the silica fume concrete compared to the conventional

concretes.

The bond strength of overlay concretes to the concrete substrate was tested using a pull-off bond procedure described in ACI 503R-93. The specimens were mixed and cast at 35 °C (95 °F) to simulate hot-weather conditions, which lead to frequent problems with overlay placements. Although the results indicated that the highest bond strengths occurred with silica fume contents of 6 percent and greater, the differences in the test results were statistically insignificant.

Coefficient of thermal expansion tests showed small differences, of less than $1 \times 10^{-6} \text{ } ^\circ\text{C}^{-1}$ between the smallest and largest values, for the “full depth” mixtures, as silica fume content varied. The results for the “overlay” mixtures showed a slight decrease in the coefficient of thermal expansion with increased silica fume contents, but the resulting coefficients were within the expected range for conventional concretes. Whiting and Detwiler (1998) concluded that the addition of silica fume to concrete has a minimal effect on the coefficient of thermal expansion.

Although the study did not specifically address field practices, based on the results of the investigation, a minimum cure time of 7 days was recommended. The study also suggested that silica fume levels between 6 and 8 percent will yield optimum results with respect to both cost and performance for highway agency projects that use silica fume concrete.

1.9 OBJECT AND SCOPE

In this study, factors that contribute to cracking, and concrete permeability in bridge decks are examined. The goal is to determine how construction practices and material properties correlate with the performance of the bridge decks. It is also desired to gage the performance of bridge decks with silica fume overlays relative to bridges with conventional concrete overlays and to determine if the silica fume overlays commonly used on bridges in Kansas are performing at a level that justifies the extra cost and construction precautions. Forty bridges, 20 with silica fume overlays, 16 with non-silica fume concrete overlays, and 4 monolithic bridges, were

evaluated.

Field surveys were performed on each bridge. The field surveys consisted of making detailed sketches of the observed cracking patterns on scale drawings of the bridge decks. A computer program was used to calculate crack densities for each of the bridge decks based on the completed sketches. Concrete samples were taken from each concrete placement to determine chloride content at five different depths and for rapid chloride permeability testing. Plans and construction diaries were examined to determine the material properties of the concrete used, environmental conditions at the time of placement, and age. The information taken from the construction documents and determined from the concrete sample testing is compared to the crack density data, calculated effective diffusion coefficients, and rapid chloride permeability test results to identify the principal factors that contribute to the cracking of the bridge decks and to evaluate the performance of the bridge decks.

CHAPTER 2

DATA COLLECTION

2.1 GENERAL

To determine the factors that contributed to performance of the 40 concrete bridge decks evaluated in this study, design and construction data were collected and compared to the cracking observed on each deck. Data on the material properties of the concrete was also compared with the results of the rapid chloride permeability test and calculated diffusion coefficients. Previous work by Schmitt and Darwin (1995, 1999) shows that several variables play an important role in crack formation on bridge decks. Based on the earlier work several variables were considered in this study. Data on design specifications, construction methods, site conditions, and material properties were collected from project files, field books, bridge plans, and weather data logs. Field surveys were performed to determine the extent of cracking, the permeability and chloride content of the concrete, and the roughness of each of the bridge decks in the study.

Most, but not all, of the data pertinent to this study were available in KDOT records. The type of curing materials was infrequently mentioned in bridge logs, and the times of placement and removal were rarely mentioned. Concrete temperatures at the time of placement were, on occasion, available in field books, but not often enough to make use of the information. Daily high and low temperatures were recorded in many daily logs, but wind speeds and relative humidity were not recorded and only available through the Kansas State University Weather Data Library.

2.2 SELECTION OF BRIDGES

A total of 40 steel girder bridges, predominantly in northeast Kansas, were selected for evaluation from eight counties: 1 from Douglas; 8 from Johnson; 1 from Lyon; 1 from Osage; 2 from Pottowatomie; 2 from Riley; 2 from Sedgwick; and 25 from Shawnee. Steel girder bridges were chosen because it is generally

acknowledged that cracking is more severe on steel girder bridges and because steel girder bridges account for a large percentage of the bridges built in Kansas. Additionally, Schmitt and Darwin (1995, 1999) surveyed steel girder bridges, and by comparing results for the same type of bridges, the possibility existed of incorporating data from the earlier report.

Bridges built between 1990 and 1998 were selected for evaluation. Because field books and other construction data are often discarded or otherwise difficult to obtain after 5 years, emphasis by necessity was placed on bridges built after 1993. The lack of long-term construction records, noted earlier by Schmitt and Darwin (1995), represents a weakness in the ability of an agency such as KDOT, to improve its construction procedures based on field experience.

Twenty bridges with silica fume overlays and 20 bridges without silica fume overlays were selected. The 20 bridges that did not have silica fume overlays included 16 bridges with conventional concrete overlays and 4 monolithic bridges. The bridges without silica fume were used to gage the performance of the silica fume overlays. Of the 40 bridges evaluated in this study, 2 with silica fume overlays, 6 with conventional overlays and 3 with monolithic decks had been evaluated earlier by Schmitt and Darwin (1995, 1999).

The first step in the selection of the bridges was to find the project files that contained information on the bridges in either the Construction Management System (CMS) database or the field books. The project files were necessary to be able to examine factors such as mix design, construction dates, and the width, length and location of concrete placements. Second, it was necessary to select bridges that could be safely inspected. Third, in the selection process, it was considered desirable to match the percentage of sample bridges of each structure type to the percentage of bridges in the state of Kansas of that structure type. However, this proved unfeasible because of the limitations set by the first two conditions. Four types of bridge structures were evaluated: 11 (27.5%) SMCC (steel beam, composite continuous), 26 (65%) SWCC (steel welded plate girder, composite continuous), 2 (5%) SWCH

(steel welded plate girder, composite continuous and haunched), and 1 (2.5%) WWCH (weathering steel welded plate girder, composite continuous and haunched). Schmitt and Darwin (1995) found that in the state of Kansas the percentages of structure types for steel composite girder bridges were 39 percent SMCC, 31 percent SWCC, and 11 percent SWCH. Nine other structure types accounted for the remaining 19 percent, with no single type accounting for more than 4 percent of the total. Although, the percentages of structure type in this study did not match the statewide percentages, it was not considered to heavily impact the results because Schmitt and Darwin (1995) found that type of composite bridge had little or no effect on bridge deck cracking.

2.3 DATA SOURCES

Information on the bridges surveyed was collected from a variety of sources. The plans for the bridges came from the KDOT Bureau of Design in Topeka. Information collected from the plans included bridge length, width, number of spans, span length, bridge skew, deck thickness, top cover thickness, thickness of the overlays, and reinforcing bar spacing. The location of the bridge and AADT were found in the KDOT Bridge Log. The older project files, which were available in the KDOT District 1 office, contained material test reports that contained information on the mix design, air content, slump, and cylinder strength of the concrete. Field books and construction diaries provided information on both placement dates and locations. They sometimes included daily temperature highs and lows and concrete temperatures. For newer bridges, material test reports, daily air content and slump reports, mix design, and daily diaries were available almost exclusively through the CMS database, at KDOT area offices. Background information on bridges that had been included in the work by Schmitt and Darwin (1995) was available from the earlier report. Additional weather information, such as relative humidity, average wind speed and daily high and lows (when not listed in daily journals), was obtained from the Weather Data Library at Kansas State University.

2.4 ON-SITE FIELD SURVEYS

An on-site inspection was performed for each of the 40 bridges selected. The field inspection consisted of several steps. First, scale drawings of the bridge were made from the plans. Second, once traffic control was setup, the bridge deck was inspected to determine its general condition. Third, cracks in the bridge deck were marked with lumber crayon. Fourth, the cracks were plotted on the scale drawing of the bridge deck. The fifth step included taking cores for rapid chloride permeability testing and concrete samples for chloride content testing. The fifth step generally occurred concurrently with the third and fourth steps and was performed by the KDOT Bureau of Materials and Research. The sixth step involved examining the underside of the deck for cracking. In detail, the steps proceeded as follows:

Before going to each bridge, a scale drawing of the bridge deck was created on engineering paper at a scale of 1 inch equal to 10 feet (the plans were all in customary units). The drawing indicated compass directions and the dimensions and boundaries of the bridge deck.

Once on site at the bridge, personnel from the KDOT Bureau of Materials and Research provided traffic control. Generally one lane of traffic was closed and that lane was completely surveyed before moving to the next lane. After traffic control was established, the bridge was stationed in 5-foot increments, marking the total distance from the end of the bridge to each station. Once the bridge was stationed, the inspection team walked the length of the bridge in the closed lane looking for cracks. When cracks were located, lumber crayon was used to draw on top of the crack or immediately adjacent to it, so that cracks could easily be seen, located, and measured when making the scale drawings. Spalls, regions of scaling and small repair areas were noted, but were not included in the sketches.

As the inspection teams moved along the bridge and finished marking cracks, the cracks were marked on the scale drawing. The crack locations were measured from the nearest station marking. The crack lengths were then measured or estimated based on the length of nearby cracks of known length and added to the scale drawing.

Once a portion of the deck was marked and mapped, the samples for the rapid chloride permeability test and chloride content were taken by technicians from the KDOT Bureau of Materials and Research. Three, 100 mm (4 in.) diameter concrete cores were taken from each concrete placement on the deck. Samples for chloride content were taken at 6 locations from each placement, 3 on cracks and 3 away from cracks. At each location, powdered samples were obtained with a vacuum drill in 5 depth increments of 19 mm (3/4 in.) each: 0-19 mm (0-3/4 in.), 19-38 mm (3/4-1.5 in.), 38-57 mm. (1.5-2.25 in.), 57-76 mm (2.25-3in.), and 76-95 mm (3-3.75 in.).

Finally, the underside of each deck was inspected for cracks, which could be easily identified by white efflorescence along their edges.

2.5 RAPID CHLORIDE PERMEABILITY TEST, CHLORIDE CONTENT, AND PAVEMENT PROFILE

2.5.1 Rapid Chloride Permeability

The KDOT Bureau of Materials and Research performed the rapid chloride permeability tests (RCPT), the chloride content evaluation, and the pavement profiling. The rapid chloride permeability test determines the electrical conductance of concrete, which is used to provide an indication of the permeability of the concrete to chloride ions. The test involves passing an electrical charge through a concrete cylinder and determining the total charge in coulombs that passes through the cylinder and was performed in accordance with ASTM C 1202 "Standard Test Method for Electrical Indication of Concrete's Ability to Resist Chloride Ion Penetration," with the exception that the cores were not 51 mm (2 in.) thick. The concrete cores were cut approximately 38 mm (1.5 in.) thick and the exact thicknesses were recorded. The cores were not cut to the standard 51 mm (2 in.) thickness because silica fume overlays are only 38 mm (1.5 in.) thick. The final readings from the RCPT test were then linearly scaled to arrive at results approximately equivalent to a standard 51 mm (2 in.) thick cylinder.

2.5.2 Chloride Content

Chloride content was determined using a silver nitrate titration process similar to that described in ASTM C 1218. The samples for testing are placed in a small plastic cup and include the filter paper used in the vacuum drill when the sample is obtained. The procedure is as follows: (1) Place a 400 ml beaker onto a top loading balance and tare the balance. (2) Retrieve the filter paper from the sample cup and using scissors, cut the filter paper into at least 3 pieces, placing the pieces into the beaker. (3) Add the remaining material from the sample cup into the beaker. (4) Note and record to +/- 0.02 grams the mass of the sample. (5) Add approximately 150 ml of distilled water to the beaker. (6) Place a lid onto the beaker and place the beaker onto a hot plate on a high heat setting. Allow the solution to come to a boil and boil for approximately 20 minutes. (7) Remove the beaker from the hot plate and allow it to cool near room temperature. (8) Once cool, vacuum filter the solution through No. 1 Whatman filter paper in a 2 piece Buchner filter funnel into a 500 ml vacuum flask. Clean and rinse the beaker with hot distilled water. (9) Pour the filtrate in the vacuum flask into a 250 ml plastic Mettler titration beaker. Rinse the flask 3 times with distilled water pouring the rinse into the plastic beaker. (10) Add 5 ml of concentrated nitric acid to the beaker. Then add distilled water to the beaker until the total volume is approximately 300 ml. (11) Titrate the sample on the Mettler DL70 Automatic Titrator using a chloride ion specific electrode in combination with a silver/silver chloride reference electrode and 1.0 N standardized silver nitrate titrant solution. Chloride content (kg/m^3) is then calculated by dividing the product of the volume of the silver nitrate titrant (ml), the normal concentration of titrant (mmol/ml), and a constant [$81.27 \text{ kg}\cdot\text{g}/(\text{m}^3\cdot\text{mmol})$] by the difference between the mass of the concrete sample and filter paper (g) and the mass of filter paper (g).

2.5.3 Pavement Profile

The pavement profiles were performed according to Kansas Test Method KT-54 "Determination of Pavement Profile with the Profilograph." The primary

apparatus used in the test is a California type 7.6 m profilograph with pointer. It is a rolling straight edge, that measures vertical deviations from a moving 7.6 m reference plane. The pavement profile is graphically recorded on a profilogram with scales of 300:1 longitudinally and 1:1 vertically.

The test is run by moving the profilograph at walking speed (approximately 5 km/h) along an appropriate path for each section of pavement (1 meter inside from the lane edge or construction joint). The pointer is used to maintain the required trace path. As the profilograph moves forward, both the longitudinal and vertical displacement of the profile wheel are measured and recorded on recording paper. The vertical displacement includes both rises and drops. The roughness of the profiled pavement is then determined by summing the vertical rises and dividing the result by the length over which the recording was made. This yields a profile roughness index (PRI) in mm/km (in./mi) that indicates the vertical deviation from the surface over a unit distance and is used to evaluate the roughness of the entire path that was measured.

2.6 CALCULATION OF CRACK DENSITIES

It was necessary to calculate the crack densities of the bridges to obtain quantitative values to compare the performance of the bridge decks. In the earlier study, Schmitt and Darwin (1995,1999) used a FORTRAN program to evaluate the crack densities of bridges. Because the code was available, it was possible to recreate the earlier FORTRAN program and make necessary changes. The program was useful because it could be used to calculate crack densities for a bridge deck more rapidly and consistently than doing the equivalent work by hand. It could also calculate separate crack densities for the entire bridge, individual placements and individual spans; and determine crack densities for cracks with specific angles with respect to the bridge axis.

The program operates essentially by identifying cracks as groups of "dark" pixels and then determining the distance and angle between the endpoints of the

cracks. The process of using the program to create crack densities involved several steps. First, the scale drawings of the bridge were photocopied onto white paper to provide a clean image for scanning. The images were then converted to digital TIFF images using an HP scanner and scanning software. The images were scanned at 100 dpi as grayscale images with 256 shades of gray. Once the picture was in digital format, all of the boundary lines and other markings that did not represent cracks were removed with Paint Shop Pro 5, an image editing software program. A single dark line was added from the top of the page to the top left corner of the bridge to indicate the starting point for the FORTRAN program. Because the program calculates the length of a crack by the distance between its endpoints, any cracks that were bent or intersecting needed to be separated into cracks that were essentially straight so that the program could accurately determine the length of the cracks. This was accomplished by removing individual "dark pixels" to separate bent cracks into two or more approximately straight cracks. After the TIFF image was configured, the image was then converted to ASCII using two programs created by Associate Professor John Gauch at the University of Kansas. The ASCII file represents each pixel of the image file with a number indicating its level of darkness (0 for black and 255 for white). Miscellaneous information at the beginning and end of the converted ASCII file needed to be removed to get a file that consisted of only the pixel gray levels.

Once the ASCII file was prepared, the FORTRAN program was run. The program operated by grouping pixels darker than a gray level of 200. These "dark" pixels represented cracks on the bridge deck. The program then determined distances between the endpoints of the pixel groups. Finally, the crack density, in linear meters of crack per square meter of bridge deck, was calculated based on the total length of cracks and the area of the chosen portion of the deck. A listing of the crack measurement program, as modified for this study, appears in Appendix B.

2.7 DATABASES

Several databases were created to help analyze the data. Because crack densities were calculated for entire bridge decks, individual placements, and individual spans, information was separated into categories with data relevant to these three divisions. The first database included information on design specifications relevant to the entire bridge, such as structure type, deck type, number of spans, traffic volume, bridge length, age, deck thickness, top cover thickness, overlay thickness, reinforcing bar size and spacing, and girder end condition. The second database contained information relevant to the individual placements. This included mix design information, weather data, material test results, permeabilities, and chloride contents. The third database contained variables relevant to individual spans including span length and span type (interior/exterior).

CHAPTER 3

EVALUATION AND RESULTS

3.1 GENERAL

Bridge deck performance is evaluated based on crack density, the rapid chloride permeability test (RCPT), and the effective diffusion coefficient (D_{eff}). Crack densities are determined for the entire bridge deck, individual placements, individual spans, and end sections. Charge passed in coulombs during the RCPT test and D_{eff} are determined for individual concrete placements. The effects of variables related to bridge design specifications, construction site conditions, and material properties of the concrete are analyzed by comparing those variables with crack densities for the appropriate section of bridge deck. In addition, the effects of material properties are compared with the RCPT results and the D_{eff} determined for the appropriate concrete placements.

The variables were first plotted against the appropriate crack density, RCPT result, and/or D_{eff} . These plots generally show a large amount of scatter, because of the combined effects of the many factors that affect these measures of deck performance. To better visualize the trends in the data, further analysis is performed using bar charts.

The bar charts, starting with Fig. 3.10, follow a standard format. Each bar or category represents a range of values of the variable under consideration and is defined by the midpoint of that range. The size of the range is equal to the difference between the midpoints of consecutive categories. Deviations from this format are noted in the text.

Because sample sizes are often small and the differences between the means of different categories are frequently small, the Student's t-test is used to provide guidance in determining whether the means of two groups are statistically different from each other. The t-test is frequently used for hypothesis testing when only small samples are available and the true population standard deviations are not known.

In using the t-test, a decision can be made by testing the null hypothesis that the measured means of two samples, X_1 and X_2 , represent populations with means, μ_1 and μ_2 , that are equal. A value, t , is calculated that takes into account the difference in the means of the two groups, the size, and standard deviation of each group. To test the statistical significance of the result, a “level of significance” (α) is chosen. An α of 0.05, which is commonly used, indicates that there is a 5 percent chance that the test would indicate a statistically significant difference between means even if there were none [a 5 percent chance of rejecting the null hypothesis ($\mu_1 = \mu_2$) when it is true]. Larger values of α make it easier to reject the null hypothesis and conclude that X_1 and X_2 represent populations with real differences in their means μ_1 and μ_2 .

Once the t value has been calculated and α has been chosen, the value of t is compared with a value determined from the Student’s t -distribution for that level of significance. If the calculated t value is greater than the t -distribution value, then the null hypothesis ($\mu_1 = \mu_2$) is rejected at that level of significance. When the null hypothesis is rejected the two sample means may be regarded as being significantly different (“Y” in Tables 3.1 - 3.43). If the null hypothesis is not rejected (“N” in Tables 3.1 - 3.43) then the two sample means being compared may be treated as being not significantly different at that particular α . In the current analysis a two sided test is used, meaning that the null hypothesis ($\mu_1 = \mu_2$) is compared against two hypotheses, $\mu_1 > \mu_2$ and $\mu_1 < \mu_2$, each of which have a level of significance $\alpha/2$.

Because of the small samples sizes used for the bar chart categories and the generally small differences in values between samples, the differences are not always statistically significant. However, trends in the data can still be distinguished, even if the differences are not statistically significant.

The data collected from the bridge decks is divided into three categories: silica fume overlays (SFO), conventional overlays (CO), and monolithic bridge decks (Mono). This is done, in part, because of the significant differences in materials, construction procedures and age ranges of the three groups. However, it is also done so that the effect of the variables on silica fume overlays can be evaluated separately

and the trends in the data for silica fume overlays can be compared to the trends in the data for both conventional overlays and monolithic bridge decks.

Analysis of the effects of material properties and site conditions includes a fourth category, bridge subdecks. This is done because the performance of a bridge subdeck can have a significant effect on the performance of the deck overlay. Cracks in the subdeck can “reflect” into the overlay and reduce overlay performance. Because the bridge subdecks could not be directly observed, crack densities determined for the section of the bridge deck above the overlay are used. In all but 6 cases, the entire bridge deck crack density is used to represent the crack density of the subdeck, because the bridge subdeck was placed on one day and is treated as one placement. In 3 of the remaining 6 cases (bridges 46-289, 46-290, and 75-49), the bridge subdeck was placed on 2 separate days, but the location of each placement is not known. Therefore, the entire bridge deck crack density is used for both subdeck placements. In the remaining 3 cases (bridges 46-317, 81-50, and 89-245), the crack density determined for the section of deck directly above the subdeck placement is used.

Two of the silica fume bridges (89-184 and 89-187) are included in evaluation of bridge age, construction date, and deck type versus crack density, but are not included in the analysis of other variables. Construction of these two bridges was finished in 1990, much earlier than the other bridges with silica fume overlays in this study. Not only do these two bridges show significantly higher crack densities than other silica fume bridges in the current study, but they were also constructed according to different specifications. The overlay thickness for these two bridges is 57 mm (2.25 in.). However, all other silica fume overlays in this study have 38 mm (1.5 in.) thick overlays. Although there is no record of the finishing procedures used on these two bridges in the daily journals and/or project files, the bridge deck wearing surface specification in use at the time they were constructed did not require fogging. The specifications for all other silica fume overlay bridges in this study require, as a minimum, either fogging or application of a precure material.

3.2 INCLUSION OF DATA FROM SCHMITT AND DARWIN

The earlier study by Schmitt and Darwin (1995) used similar methods to evaluate 40 bridges in Kansas. It was considered desirable to be able to use the bridge data from the earlier study to increase the sample size. However, because the survey methods used can be subjective, it was necessary to establish a comparison between bridges from the current and earlier study, to determine if data from the earlier study could reasonably be included.

The current study examined 11 bridges that had also been examined in the earlier study. The crack densities determined for these 11 bridges are compared and a reasonable correlation is found. The scatter in the data is not considered excessive and the data from Schmitt and Darwin (1995) is included with the data from the current study when possible. Fig. 3.1 shows a bridge by bridge comparison of crack densities. Fig. 3.2 shows a plot of the crack densities from the current study versus the crack densities from Schmitt and Darwin (1995). The crack densities from the current study are greater for 6 of the 11 bridges. Of the remaining 5 bridges, the crack densities for 4 of them differ from Schmitt and Darwin (1995) by 0.05 m/m^2 or less. In general, crack densities from the current study are nearly equivalent or greater than those determined by Schmitt and Darwin, but greater values of crack density are considered reasonable because of the increased age of the bridges.

Bridges 89-184 and 89-187, the silica fume overlay bridges with significantly higher crack densities than the other silica fume overlay bridges in this study, were also part of the study by Schmitt and Darwin, but for reasons mentioned, the data from those two bridges is only included in the analysis of bridge age, construction date, and deck type versus crack density.

The current study only includes 4 monolithic bridge decks. Therefore, it does not add a significant amount of data to that from Schmitt and Darwin (1995). Because Schmitt and Darwin (1995) did not collect samples for analysis of RCPT or chloride content, there is not enough data on monolithic bridges to evaluate trends with respect to RCPT or D_{eff} .

3.3 BRIDGE AGE VERSUS CRACK DENSITY

Bridge age is equal to the interval between the date of concrete placement and the date the bridge was surveyed. The silica fume overlay bridges evaluated in the current study are, with 2 exceptions (bridges 89-184 and 89-187), all younger than the conventional overlay bridges evaluated. The silica fume overlay bridges, except for bridges 89-184 and 89-187, range in age from 4 to 33 months, while the conventional overlays range in age from 36 to 97 (Fig. 3.3). This difference in age limits the direct comparison of silica fume overlay bridge decks with conventional overlay and monolithic bridge decks. When the data from Schmitt and Darwin (1995) are included, there are more conventional overlay bridges in the same age range as the silica fume overlay bridges, but the silica fume bridges are still younger than most of the conventional overlay bridges (Fig. 3.4).

Although there is scatter in the data, plots of crack density versus bridge age exhibit a trend of increased crack density with age for silica fume overlay bridges (Figs. 3.5 and 3.6). Conventional overlay bridges do not exhibit a clear trend, but crack density appears to be generally lower for older bridges (Fig. 3.7 and 3.8). Monolithic bridges do not exhibit a discernible trend (Fig. 3.9).

The bar charts for crack density versus bridge age for silica fume overlays very clearly show the trend towards increased crack density with increased age (Fig. 3.10). The crack density for bridges in between 20 and 40 months old, 0.42, is nearly double that of the crack density for the bridges between 0 and 20 months old, 0.19. Although bridges older than 40 months have a crack density, 1.00 m/m^2 , significantly higher than all other silica fume overlay bridges, only 3 bridges are represented by the category. Because the 3 oldest bridges were built to different material and construction specifications, they are probably not an accurate representation of the future performance of the younger silica fume overlay bridges. The differences between all age categories are statistically significant for $\alpha = 0.05$ (Table 3.1).

For both conventional overlays and monolithic bridges, older bridges show

slightly lower crack densities than younger bridges (Figs. 3.11 and 3.12). Although counter intuitive, this trend was also observed by Schmitt and Darwin (1995), who stated that the trend most likely reflected changes that had occurred over the years in construction procedures, material properties, and design specifications. Thirty-month old (20 to 40 month old) silica fume overlay bridges exhibited a crack density, 0.42 m/m^2 , almost equal that for 90-month old (60 to 120 month old) conventional overlays, 0.43 m/m^2 , and 30-month old (0 to 60 month old) monolithic bridge decks, 0.39 m/m^2 . Although it is difficult to make accurate predictions, if the silica fume overlay bridges continue to follow their current trend, it is likely that their performance, in terms of crack density, will not be any better than that of conventional overlays, or monolithic bridge decks.

It is also useful to examine crack density versus the construction date of the bridges, even though the age of the bridge at the time it was surveyed is not taken into account. Fig. 3.13 shows that the most recently constructed silica fume bridges, between 1997 and 1998, have the lowest cracking. For conventional overlays, bridge decks constructed between 1993 and 1995 have higher crack densities, 0.77 m/m^2 , than all earlier constructed bridge decks, and more than double the crack density, 0.28 m/m^2 , of conventional overlay bridge decks constructed between 1985 and 1987 (Fig. 3.14). Monolithic bridge decks show the same pattern as conventional overlay bridges. Monolithic bridges constructed between 1989 and 1993 have a crack density, 0.47 m/m^2 , more than twice the crack density, 0.19 m/m^2 , of monolithic bridge decks constructed between 1984 and 1987 (Fig. 3.15). All the differences between categories based on date of construction are statistically significant (Table 3.2). The trends in crack density with construction date probably indicate that changes have occurred that reduce the performance in the more recently constructed conventional overlay and monolithic bridge decks.

3.4 RAPID CHLORIDE PERMEABILITY TEST

Coulomb readings from the rapid chloride permeability test were taken after

the first half hour and at the end of six hours. As discussed in Chapter 1, the addition of silica fume to concrete appears to cause spurious readings, because the test measures the electrical conductivity/resistivity of the concrete and not actually its permeability to chloride ions. Pfeifer et al. (1994) suggest that concrete resistivity can be determined by simply using the initial AC resistivity reading after the power supply is activated. They also state that changes in current after the initial reading are probably due to changes in the temperature of the concrete.

To avoid the effects of both temperature rise, and changes in resistance of the concrete with time, the coulomb reading recorded during the first 30 minutes of the test is multiplied by 12 and used in this study in place of the coulomb reading for the full 6 hour test.

A low coulomb reading indicates that the concrete has a low electrical conductivity. This is typically interpreted to mean that the concrete has a higher resistance to chloride penetration. However, certain factors can cause the test results to be very low without necessarily increasing the resistance of the concrete to chloride penetration (as discussed in Chapter 1). Consequently, although silica fume overlays have lower RCPT values than either conventional overlay or monolithic bridge decks, as shown in Fig. 3.16, comparisons with the concretes used in conventional overlays or monolithic bridge decks that do not contain silica fume, may not be valid.

As discussed in Chapter 1, several researchers (Pfeifer et al. 1994, Shi et al. 1998) object to the use of the RCPT test to compare concretes with and without silica fume. Whiting and Mitchell (1992), the developers of the RCPT test, expressed concern over the use of the RCPT without developing a correlation between charge passed and known chloride permeability for the particular materials being tested, especially for silica fume concretes.

The average RCPT results for the three bridge decks types, taken after 6 hours, vary from 1371 coulombs, for silica fume overlays, to 3596 coulombs for monolithic bridge decks (Fig. 3.16). The RCPT results, based on the readings taken

after 30 minutes, are lower and vary less than the readings taken after 6 hours, varying from 1082 coulombs, for silica fume overlays, to 2457 coulombs, for monolithic bridge decks. The RCPT results for conventional overlays, for both cases, are approximately halfway between the values for silica fume overlays and monolithic bridge decks.

3.5 CHLORIDE CONCENTRATION AND EFFECTIVE DIFFUSION COEFFICIENT

Although Fick's Second Law of Diffusion [Eq. (1.1)] is not an exact model for the transport of chloride ions in concrete, it does provide a useful method for comparing the relative concrete permeabilities based on the measured chloride ion concentrations. The chloride concentrations of the samples taken from crack free areas of the bridge decks are used to calculate an effective diffusion coefficient (D_{eff}) and surface chloride concentration (C_0) for each concrete placement using a least-squares curve fitting technique. The midpoints of the depth increments for the chloride samples [9.5 mm (0.375 in.), 28.6 mm (1.125 in.), 47.6 mm (1.875 in.), 66.7 mm (2.625 in.), and 85.7 mm (3.375 in.)] are used as the depth x in Eq. (1.1). The ages of the bridge decks are used as the total time t . The minimization solver in Microsoft Excel 97 is used to determine the values of D_{eff} and C_0 that minimize the squared difference between the actual chloride concentrations and the chloride concentrations predicted by Fick's Second Law.

Because bridge deck concrete can contain chlorides that occur because the aggregates, the water, or admixtures contain chlorides, a base level chloride content for each bridge is subtracted from the chloride concentrations for that bridge before solving for D_{eff} and C_0 . The base level chlorides are estimated for each placement by observing the chloride contents at all depths and locations for that placement. Values that do not differ significantly (more than 0.05 kg/m^3) from the chloride concentration at the deepest level are considered to be base level chlorides. To determine the base level chloride used for each placement, the chloride concentrations considered to be

base level for that placement are averaged. Base level chloride contents generally range between 0.20 and 0.40 kg/m³.

A lower D_{eff} indicates slower diffusion of chlorides or a higher resistance to chloride penetration and, therefore, better performance. The values of C_0 and D_{eff} for each placement can be found in Table A.9. The chloride concentrations at all locations and depths, for all placements, can be found in Table A.10.

Relatively new bridge decks that had not been exposed to more than one winter rarely had chloride contents above the base level at depths below the 28.6 mm (1.125 in.) sample. Although Fick's equation takes the age of the bridge deck into account, there is concern that the D_{eff} and C_0 are not as accurate for the younger bridges as for the older bridges, because the total time variable is relatively small. The mean effective diffusion coefficients (D_{eff}) for silica fume overlays and conventional overlays were compared for bridges in different age ranges (all bridges, age greater than 500 days, age between 500 and 1500 days, and age between 900 and 1500 days) in Fig. 3.17. The only case in which there is a statistically significant difference between the D_{eff} for silica fume and conventional overlays is when all bridges are considered (Table 3.4). This is due to the fact that the values of mean D_{eff} for the older age ranges are close and because the number of bridge placements in the sample becomes smaller as the age range is narrowed. When all of the bridges are considered, the mean D_{eff} is significantly higher for silica fume overlays than for conventional overlays. However, when bridges younger than 500 days are discounted, the silica fume overlays show values comparable to those for the conventional overlays. The mean value of D_{eff} for silica fume overlays older than 500 days (0.115 mm²/day) is slightly higher than that for conventional overlays (0.101 mm²/day), but the difference is not statistically significant. For decks between 500 and 1500 days old, the mean D_{eff} for silica fume overlays (0.115 mm²/day) is smaller than that for conventional overlays (0.153 mm²/day). For bridge decks between 900 and 1500 days old, the mean D_{eff} is lower for silica fume overlays (0.124 mm²/day) than conventional overlays (0.153 mm²/day), but the difference between

the mean values of D_{eff} is smaller than for bridge decks between 500 and 1500 days old.

The age range between 500 and 1500 days includes both silica fume and conventional overlays and provides the most accurate comparisons of mean D_{eff} for the two bridge deck types. The analysis indicates that silica fume overlays, in the best case, have a mean value of D_{eff} only slightly lower than that for conventional overlays. Overall, the silica fume overlays do not appear to provide significantly higher resistance to chloride penetration and may actually perform worse than the conventional overlays.

Based on the analysis of the mean D_{eff} for bridges in the different age ranges and because the D_{eff} are considered to be more accurate when the bridges younger than 500 days are disregarded, only bridges older than 500 days are used to compare the effects of different material properties on D_{eff} . This does not eliminate any bridge decks with conventional overlays from the analysis (35), but it does remove several bridge decks with silica fume overlays from the analysis (leaving 19).

Figs. 3.18, 3.19, and 3.20 show chloride content of locations away from cracks, at mean depths of 9.5 mm (0.375 in.), 28.6 mm (1.125 in.), and 47.6 mm (1.875 in.), plotted against the age of the bridge deck placement. All bridges in the current study are included in the plots. There is a clear trend, regardless of bridge deck type, towards increased chloride content with age. In the figures, "Old SFO" refers to bridges 89-184 and 89-187, the two silica fume overlay bridges built at an earlier date, to different specifications than the other silica fume overlay bridges evaluated in the study. The chloride contents of bridges 89-184 and 89-187 fall within the range of chloride contents for conventional overlay placements of the same age, indicating that their resistance to chloride penetration is not significantly higher than the conventional overlays.

Figs. 3.21 and 3.22 show chloride contents taken at cracks at mean depths of 66.7 mm (2.625 in.), and 85.7 mm (3.375 in.) plotted against the age of the bridge deck placements. Transverse reinforcing steel is placed at a depth of 76 mm (3.0 in.).

Thus, the samples shown in these figures represent the concrete just above and at the level of the reinforcement, respectively. Although certain factors affect the chloride threshold level for the corrosion of steel it is generally believed to be between 0.60 and 0.90 kg/m³ (1.0 and 1.5 lb/yd³). McDonald et al. (1998) used a value of 0.74 kg/m³ (1.25 lb/yd³) for black reinforcing steel. They found that the chloride threshold level for damaged epoxy-coated bars is similar to that of black bars. Figs. 3.21 and 3.22 not only show a nearly linear increase in chloride content with age, regardless of bridge deck type, but they also show that chloride contents at cracks, exceed chloride threshold levels in as little as 1000 days (2.7 years) for all deck types. This indicates that even concretes with high resistance to chloride penetration will not perform well if there is a high level of cracking.

D_{eff} is compared with the RCPT results for each bridge deck placement, but there is no clear correlation (Fig. 3.23). However, as will be discussed in the next section, D_{eff} and RCPT results show the same trends for certain material properties. For percent volume of water, cement and silica fume, water content, and water to cementitious materials ratio, the trends for D_{eff} and RCPT are nearly identical. It is possible that the quality of construction affects both properties of the concrete in a similar manner.

3.6 EFFECTS OF MATERIAL PROPERTIES

The material properties analyzed include concrete slump, percent volume of water and cementitious materials, water content, cement content, water/cementitious material ratio, air content, and compressive strength. The bridges are divided into four groups for analysis of the material properties: silica fume overlays, conventional overlays, monolithic bridge decks, and bridge subdecks. Material properties for all bridge deck and subdeck placements are compared with RCPT values, effective diffusion coefficients, and crack density for the appropriate section of deck.

The analysis of the effects of material properties on RCPT results, effective diffusion coefficient, and crack density for silica fume overlays includes all silica

fume overlays in the current study, except those of bridges 89-184 and 89-187, for reasons mentioned earlier. The analysis of the effects of material properties on RCPT results does not include bridges 89-184 and 89-187, monolithic bridges, or bridges from the study by Schmitt and Darwin (1995, 1999).

The analysis of the effects of the material properties on effective diffusion coefficient includes only bridges from the current study older than 500 days, but does not include monolithic bridges, or bridges 89-184 and 89-187. Bridges younger than 500 days are not used because of the assumed lower accuracy of the effective diffusion coefficients, as discussed earlier. Bridges from the study by Schmitt and Darwin (1995, 1999) are not included because effective diffusion coefficients are not available for those bridges. The analysis of crack density includes all bridges in the current study and all relevant bridges evaluated by Schmitt and Darwin (1995, 1999), except bridges 89-184 and 89-187.

The analysis of the effects of material properties includes 38 silica fume overlay placements, 58 conventional overlay placements, 36 monolithic bridge deck placements, and 50 subdeck placements. Because D_{eff} and RCPT data was not collected by Schmitt and Darwin (1995, 1999), only 35 conventional overlay placements are analyzed with respect to D_{eff} and RCPT values. The analysis of D_{eff} with respect to silica fume overlays includes only 19 silica fume overlay placements, because bridges younger than 500 days are not analyzed, but all 38 silica fume overlay placements are analyzed with respect to RCPT values. Because information on material properties of the concrete placements was not always available, not all the concrete placements are included in the analyses of the various factors.

Detailed analyses of the effects of material properties are presented in the balance of this section. The key observations from these analyses can be summarized as follows:

For silica fume overlays, there is no apparent correlation between D_{eff} and concrete slump. RCPT values tend to increase as slump increases, and crack density increases significantly for slumps greater than 90 mm (3.5 in.).

D_{eff} , RCPT values, and crack density decrease as the (1) percent volume of water, cement and silica fume, (2) water content, and (3) water/cementitious material ratio increase, observations that are counter to the expected trends. This may be due to the fact that only two mix designs are represented in the data for silica fume overlays, resulting in only two categories, with identical populations. Thus, comparisons based on these three parameters really represent comparisons based on all properties of the two distinct groups of bridges and may not accurately represent the effects of these three parameters. D_{eff} and crack density increase as air content increases, but no trend for air content with respect to RCPT values is apparent. D_{eff} increases with increasing compressive strength. RCPT values and crack density tend to decrease as compressive strength increases.

For conventional overlays, there is no apparent correlation between D_{eff} , RCPT values, or crack density and concrete slump. D_{eff} and RCPT values exhibit no trend with respect to percent volume of water and cement, or water content. RCPT values tend to increase as water/cement ratios increase. Crack density decreases as percent volume of water and cement, water content, and water/cement ratio increase. D_{eff} remains nearly constant for air contents between 4.375 and 5.875 and then increases for 6.625 percent air. RCPT values tend to increase as air content increases, but there is no trend for crack density with respect to air content. No trend is apparent between D_{eff} and compressive strength. RCPT values decrease and crack density increases as compressive strength increases.

For monolithic bridge decks, crack density increases as slump increases. Crack density also increases as percent volume of water and cement, water content, cement content, and water/cement ratio increase. Crack density is nearly constant for air contents between 4.875 and 5.625, but drops significantly for 6.375 percent air. Crack density increases as compressive strength increases.

For bridge subdecks, there is a slight trend towards higher levels of cracking as slump increases. Crack density increases as percent volume of water and cement, water content, and cement content increase. There is no significant change in crack density with respect to water/cement ratio. Crack density increases as air content and compressive strength increase.

It is important to recognize that because of the limited variation in cement content in the mix designs of silica fume and conventional overlays, the comparisons for percent volume of water and cementitious material, water content, and water-cementitious material ratio always compare the same bridges (with the exception of three conventional overlays that change categories for water content comparisons). Although silica fume and conventional overlays exhibit counter-intuitive trends for these material properties, the comparisons are not necessarily of the material properties, but rather the individual bridges. The results are not unbiased and may be dominated by unknown construction procedures.

3.6.1 Slump

For silica fume overlays, concrete slump varies from 19 to 127 mm (0.75 to 5.0 in.), with categories ranging from 26 to greater than 90 mm (1.0 to > 3.5 in.). For conventional overlays, concrete slump varies from 0 to 160 mm (0 to 6.25 in.), with categories ranging from 0 to 19 mm (0 to 0.75 in.). For monolithic bridge decks, concrete slump and categories for mean crack density both range from 38 to 76 mm (1.25 to 3.0 in.). For bridge subdecks, concrete slump varies from 6 to 160 mm (0.25 to 6.25 in.), with categories ranging from 38 to 76 mm (1.25 to 3.0 in.).

3.6.1.1 D_{eff} versus Slump

Mean effective diffusion coefficient (D_{eff}) for individual placements is shown as a function of concrete slump for silica fume and conventional overlays in Figs. 3.24 and 3.25. One silica fume overlay is outside the range of concrete slumps

analyzed. Therefore, only 18 silica fume overlay placements are included in the analysis. Because of missing data, only 25 conventional overlay placements are included in the analysis.

Neither silica fume overlays nor conventional overlays show a trend for effective diffusion coefficient with respect to slump. The D_{eff} does not appear to be sensitive to concrete slump.

3.6.1.2 RCPT versus Slump

Mean RCPT values for individual placements are shown as a function of concrete slump for silica fume and conventional overlays in Figs. 3.26 and 3.27. One silica fume overlay is outside the range of concrete slumps analyzed, therefore, only 37 silica fume overlay placements are included in the analysis. Because of missing data, only 25 conventional overlay placements are included in the analysis.

For silica fume overlays, the RCPT values tend to increase as slump increases (Fig. 3.26), but the differences in means are generally not statistically significant (Table 3.6). The RCPT results for conventional overlays exhibit no clear trend (Fig. 3.27). The mean value is lowest for a slump of 19 mm (0.75 in.).

3.6.1.3 Crack Density versus Slump

Mean crack density for individual placements is shown as a function of concrete slump for silica fume overlays, conventional overlays, and monolithic bridge decks in Figs. 3.28, 3.29, and 3.30. Mean crack density for bridge subdecks is shown as a function of concrete slump in Fig. 3.31. One silica fume overlay is outside the range of concrete slumps analyzed. Therefore, only 37 silica fume overlay placements are included in the analysis. Because of missing data, only 25 conventional overlay placements, 34 monolithic bridge deck placements, and 48 bridge subdecks are included in the analysis.

For silica fume overlays, no trend is apparent, except that the highest mean crack densities are obtained for the highest slump category [> 90 mm (> 3.5 in.)], an

observation that is statistically significant (Table 3.7).

For conventional overlays, there is also no clear trend for levels of crack density as a function of slump (Fig. 3.29). The highest levels of crack density are for zero slump concretes and the lowest levels of crack density are for 3 mm (0.125 in.) slump concrete. Schmitt and Darwin (1995, 1999) found that the crack densities for zero slump concrete were nearly three times greater than densities at any other slump and that the lowest levels of cracking were obtained at a slump of 13 mm (0.50 in.). The differences in the levels of cracking based on the combined sample are not as large as those found by Schmitt and Darwin (1995, 1999), but they demonstrate that using zero slump concrete may lead to increased cracking.

For monolithic bridge decks, there is a clear trend towards increased cracking as concrete slump increases (Fig. 3.30).

For bridge subdecks, there is a slight trend towards higher levels of cracking as slump increases (Fig. 3.31). The values of crack density for 64 and 76 mm (2.5 and 3.0 in.), 0.49 and 0.46 m/m^2 , respectively, are higher than the crack densities for 38 and 51 mm (1.5 and 2.0 in.), 0.38 and 0.45 m/m^2 , respectively. Although the trend is not statistically significant (Table 3.7) and the levels of cracking are not as great as those seen for monolithic bridge decks, it is the same as that for monolithic bridge decks. The similarity of the trends indicates that reflective cracking from subdecks may be a significant factor in the performance of bridge decks.

The results for monolithic bridge decks and subdecks are consistent with research by the Portland Cement Association (1970) and Dakhil et al. (1975). Krauss and Rogalla (1996) found no correlation between concrete slump and shrinkage cracking.

3.6.2 Percent Volume of Water and Cementitious Material

Water and cementitious materials are the constituents of the cement paste component of concrete; for concrete types other than the silica fume overlays, the cementitious material consists only of cement. For silica fume overlays, the values

for volume of water and cementitious materials are 26.0 and 26.8 percent as a percentage of concrete volume. For conventional overlays, the values for volume of water and cement are 25.1, 25.9, and 26.6 percent. For monolithic bridge decks, the volume of water and cement ranges from 26.0 to 29.0 percent, and for bridge subdecks, the volume of water and cement ranges from 26.0 to 30.0 percent.

3.6.2.1 D_{eff} versus Percent Volume of Water and Cementitious Material

Mean D_{eff} for individual placements is shown as a function of percent volume of water and cementitious material for silica fume overlays and conventional overlays in Figs. 3.32 and 3.33. For silica fume overlays, the mean D_{eff} is lower for 26.8 percent than it is for 26.0 percent (Fig. 3.32). For conventional overlays, there is no clear trend (Fig. 3.33). The mean D_{eff} is lowest at 25.9 percent and highest at 26.6 percent. None of the differences in mean D_{eff} , however, are statistically significant at $\alpha = 0.05$ (Table 3.8).

3.6.2.2 RCPT versus Percent Volume of Water and Cementitious Material

Mean RCPT values for individual placements are shown as a function of the percent volume of water and cementitious materials for silica fume overlays and conventional overlays in Figs. 3.34 and 3.35. For silica fume overlays, the RCPT value is lower for 26.8 percent than it is for 26.0 percent (Fig. 3.34). These differences are statistically significant in spite of the small differences in the cement paste volumes. For conventional overlays, the lowest mean RCPT values are obtained at 25.9 percent and the mean RCPT values for 26.6 percent are significantly higher than those for either 25.1 or 25.9 percent (Fig. 3.35) (Table 3.9).

Although no direct correlation is found between the D_{eff} and the RCPT results (Fig. 3.23), both properties show the same trends with respect to percent volume of water and cementitious material (Fig. 3.32, 3.33, 3.34, and 3.35).

3.6.2.3 Crack Density versus Percent Volume of Water and Cementitious Materials

Mean crack density for individual placements is shown as a function of the percent volume of water and cementitious materials for silica fume overlays, conventional overlays, and monolithic bridge decks in Figs. 3.36, 3.37, and 3.38. Mean crack density for bridge subdecks is shown as a function of the percent volume of water and cementitious materials for bridge subdecks in Fig. 3.39. For silica fume overlays, the level of cracking is lower for 26.8 percent than for 26.0 percent (Fig. 3.36), but the difference is not statistically significant (Table 3.10). For conventional overlays, there is a clear trend towards a lower level of cracking with increased percent volume of water and cement (Fig. 3.37). For monolithic bridge decks, the level of cracking at both 28 and 29 percent is almost four times greater than it is at 26 and 27 percent (Fig. 3.38). For bridge subdecks, the level of cracking increases as the volume of water and cement increases.

The volume of water and cementitious materials in the initial mix provides a close approximation of the paste volume of concrete. Because paste is the component of concrete that shrinks, a larger paste volume is expected to cause greater levels of shrinkage cracking. The study by the Portland Cement Association (1970) recommended reducing paste content to reduce shrinkage cracking. Krauss and Rogalla (1996) found that paste content was directly proportional to free shrinkage, and that decreasing paste volume decreased shrinkage and consequently cracking. Both the silica fume and conventional overlays show trends contrary to this research. However, the range of values of percent volume of water, cement, and silica fume is relatively small for silica fume and conventional overlays (26.0 to 26.8%, and 25.1 to 26.6%, respectively) compared to the range of values for monolithic bridge decks and subdecks (26 to 29%, and 26 to 30%, respectively) and may not be an accurate representation of the trend that would be observed with a greater range of values. The trends for both monolithic bridge decks and subdecks show increased cracking with increased paste volume, in agreement with previous research. It is clear, based on the

results in Fig. 3.39, that increased paste contents in bridge subdecks will cause cracking in decks with overlays, regardless of the quality of the overlay.

3.6.3 Water Content

For silica fume overlays, the water content values are 141 kg/m^3 (238 lb/yd^3) and 148 kg/m^3 (250 lb/yd^3). For conventional overlays, the water content values are 133 kg/m^3 (224 lb/yd^3), 139 kg/m^3 (235 lb/yd^3), and 145 kg/m^3 (245 lb/yd^3). For monolithic bridge decks the water content ranges from 147 kg/m^3 (248 lb/yd^3) to 165 kg/m^3 (278 lb/yd^3). For bridge subdecks, the water content ranges from 147 kg/m^3 (248 lb/yd^3) to 174 kg/m^3 (293 lb/yd^3). Because there is minimal variation in cement content, the trends for water content do not vary significantly from the trends for percent volume of water and cementitious materials.

3.6.3.1 D_{eff} versus Water Content

Mean D_{eff} for individual placements is shown as a function of water content for silica fume and conventional overlays in Figs. 3.40 and 3.41. For silica fume overlays, the mean D_{eff} is lower for 148 kg/m^3 (250 lb/yd^3) than it is for 141 kg/m^3 (238 lb/yd^3) (Fig. 3.40). For conventional overlays there is no clear trend (Fig. 3.41). The mean D_{eff} is greatest at 145 kg/m^3 (245 lb/yd^3), but not significantly greater than it is at 133 kg/m^3 (224 lb/yd^3). The differences in mean D_{eff} are not statistically significant at $\alpha = 0.05$ (Table 3.11) for either silica fume or conventional overlays.

3.6.3.2 RCPT versus Water Content

Mean RCPT values for individual placements are shown as a function of water content for silica fume overlays and conventional overlays in Figs. 3.42 and 3.43. For silica fume overlays, the RCPT result for 141 kg/m^3 (238 lb/yd^3) is almost twice the value for 148 kg/m^3 (250 lb/yd^3) (Fig. 3.42). The results are statistically significant at $\alpha = 0.05$. For conventional overlays, the lowest mean RCPT result is obtained at 139 kg/m^3 (234 lb/yd^3) (Fig. 3.43). The value at 145 kg/m^3 (245 lb/yd^3) is

significantly greater than that for the other categories (Table 3.12).

The trends for D_{eff} and RCPT results are the same, indicating once again that there is some degree of correlation between the two properties.

3.6.3.3 Crack Density versus Water Content

Mean crack density for individual placements is shown as a function of water content for silica fume overlays, conventional overlays, and monolithic bridge decks in Figs. 3.44, 3.45, and 3.46. Mean crack density for bridge subdecks is shown as a function of the water content in Fig. 3.47. For silica fume overlays, the level of cracking is lower for 148 kg/m^3 (250 lb/yd^3) than for 141 kg/m^3 (238 lb/yd^3) (Fig. 3.44). However, the difference in the two values, 0.08 m/m^2 , is small and not statistically significant (Table 3.13). For conventional overlays, there is a clear trend towards a lower level of cracking with increased water content (Fig. 3.45). The crack density for a water content of 133 kg/m^3 (225 lb/yd^3) is nearly twice that of a water content of 145 kg/m^3 (245 lb/yd^3); the difference is statistically significant (Table 3.13). For monolithic bridge decks, there is a clear trend towards increased cracking with increased water content (Fig. 3.46) with statistically significant differences between the means of all categories (Table 3.13). For bridge subdecks, the differences in level of cracking are not statistically significant (Table 3.13), but there is a clear trend towards increased cracking with increased water content (Fig. 3.47).

As discussed in section 3.6.2.3, the paste volume of concrete depends on both the water and cementitious material content. However, because there was little variation in cement content for the concrete placements studied, a higher water content also indicates a higher paste content. Both silica fume and conventional overlays show trends towards decreased cracking with increased water content, which contradicts previous research. In restrained ring tests, Krauss and Rogalla (1996) found a direct correlation between increased paste content and increased shrinkage. However, they did not find a clear correlation between water content and cracking

tendency. They suggested that, although concretes with higher water contents and therefore higher paste content shrink more than concretes with lower water contents, the higher water content may increase the creep of the concrete and delay cracking. Both monolithic bridges and bridge subdecks showed trends towards increased cracking with increased water content. Because the trend for monolithic bridge decks and bridge subdecks agrees with previous research, that recommends reducing paste content, it can be concluded that the performance of subdeck concrete may control the performance of overlay concrete.

3.6.4 Cementitious Material Content

Cementitious material content did not vary significantly for silica fume or conventional overlays. For silica fume overlays, cementitious material contents range only from 370 kg/m^3 (623 lb/yd^3) to 371 kg/m^3 (625 lb/yd^3). The cementitious material content of all conventional overlays is 371 kg/m^3 (625 lb/yd^3). Therefore, the effects of cementitious material content on D_{eff} , RCPT results, and cracking are not evaluated for silica fume or conventional overlays.

For monolithic bridge decks, cement contents include 357 kg/m^3 (602 lb/yd^3), 359 kg/m^3 (605 lb/yd^3), 379 kg/m^3 (639 lb/yd^3), and 390 kg/m^3 (657 lb/yd^3). The difference between 357 kg/m^3 (602 lb/yd^3) and 359 kg/m^3 (605 lb/yd^3) is negligible. Therefore, the two cement contents were grouped together. Although there are two data points for 390 kg/m^3 (657 lb/yd^3) of cement, they represent only one bridge, one surveyed both in the current study and by Schmitt and Darwin (1995, 1999). Therefore, the data for a cementitious material content of 390 kg/m^3 (657 lb/yd^3) is neglected.

For bridge subdecks, cement contents vary from 357 kg/m^3 (602 lb/yd^3) to 413 kg/m^3 (696 lb/yd^3). Only one bridge has a cement content of 390 kg/m^3 (657 lb/yd^3). Therefore, it is grouped with bridges with a cement content of 379 kg/m^3 (639 lb/yd^3). Although, four subdecks have cement contents of 413 kg/m^3 (696 lb/yd^3), they represent a single bridge.

The mean crack densities for monolithic decks and subdecks are shown as a function of the cement content in Figs. 3.48 and 3.49. Monolithic bridge decks with higher cement contents show significantly greater levels of cracking (Table 3.14). The crack density for a cement content of 379 kg/m^3 (639 lb/yd^3) is nearly four times greater than that for cement contents of 357 and 359 kg/m^3 (602 and 605 lb/yd^3) (Fig. 3.48). Although the differences in mean crack density for bridge subdecks are not statistically significant at $\alpha = 0.05$ (Table 3.14), the level of cracking increases as cement content increases (Fig. 3.49), and the increase in crack density between concretes with cement contents of 357 and 359 kg/m^3 (602 and 605 lb/yd^3) and 413 kg/m^3 (696 lb/yd^3) is statistically significant at $\alpha = 0.1$ (Table 3.14).

The trend towards increased cracking with increasing cement content, observed for both monolithic bridge decks and bridge subdecks, agrees with the findings of Krauss and Rogalla (1996). They found that high cement content concretes with low water-cement ratios were more likely to crack than low cement content concretes with high water-cement ratios.

The similarity in trends between monolithic bridge decks and bridge subdecks again indicates that the performance of bridge subdecks plays a significant role in the performance of the bridge deck overlays.

3.6.5 Water/Cementitious Material Ratio

Only the silica fume overlays contain cementitious materials other than cement. For concrete types other than the silica fume overlays, the cementitious materials consists only of cement. For silica fume overlays, the water/cementitious material ratios are 0.38 and 0.40. For conventional overlays, the water/cement ratios vary from 0.36 to 0.40. For monolithic bridge decks and bridge subdecks, the water/cement ratios vary from 0.40 to 0.44. Because there is minimal variation in cement content, the trends for water/cementitious material ratios vary little from the trends for percent volume of water and cementitious materials.

3.6.5.1 D_{eff} versus Water-Cementitious Material Ratio

Mean D_{eff} for individual placements is shown as a function of the water/cementitious material ratio for silica fume overlays and conventional overlays in Figs. 3.50 and 3.51. For silica fume overlays, the mean D_{eff} is lower for 0.40 than it is for 0.38 (Fig. 3.50). However, the difference is not statistically significant at $\alpha = 0.05$ (Table 3.15). For conventional overlays, there is no clear trend (Fig. 3.51). The mean D_{eff} is highest at 0.40 but not significantly higher than it is at 0.36, and the differences are not statistically significant at $\alpha = 0.05$.

3.6.5.2 RCPT versus Water/Cementitious Material Ratio

Mean RCPT values for individual placements are shown as a function of the water/cementitious material ratio for silica fume overlays and conventional overlays in Figs. 3.52 and 3.53. For silica fume overlays, the RCPT values are significantly lower for 0.40 than it is for 0.38 (Fig. 3.52) (Table 3.16). For conventional overlays, the general trend is an increase in the RCPT value with statistically significant increases from water/cement ratios of 0.36 and 0.38 to water/cement ratio of 0.40 (Fig. 3.53) (Table 3.16).

The trends for D_{eff} and RCPT results are once again the same, indicating that there is some degree of correlation between the D_{eff} and RCPT values for both silica fume and conventional overlays.

3.6.5.3 Crack Density versus Water/Cementitious Material Ratio

Mean crack density for individual placements is shown as a function of the water-cementitious materials ratio for silica fume overlays, conventional overlays, and monolithic bridge decks in Figs. 3.54, 3.55, and 3.56. Mean crack density for bridge subdecks is shown as a function of the water/cementitious material ratio in Fig. 3.57. For silica fume overlays, the level of cracking is lower for 0.40 than for 0.38 (Fig. 3.54). But the difference, 0.08m/m^2 is small and not statistically significant (Table 3.17). For conventional overlays, there is a clear trend towards a lower level

of cracking with increasing water/cement ratio (Fig. 3.55). For monolithic bridge decks, the level of cracking increases as the water/cement ratio increases (Fig. 3.56). No trend is apparent for bridge subdecks. The level of cracking does not change significantly with changes in water/cement ratio (Fig. 3.57) (Table 3.17).

Although both silica fume and conventional overlays with higher water-cementitious materials ratios appear to perform better than those with lower water-cementitious materials ratios, the range of values for water/cementitious material ratio is small. It may not be accurate to draw conclusions for such a small range of values. In addition, water/cementitious material ratio alone should not be strongly correlated to cracking due to shrinkage. Higher water/cementitious material ratios (especially in an overlay) may result in less cracking due to a lower modulus of elasticity and greater tendency to creep.

3.6.6 Air Content

For silica fume overlays, air content varies from 3.5 to 7.25 percent, and the categories range from 4.5 to 6.5 percent. For conventional overlays, air content varies from 2 to 7.1 percent, and the categories range from 4.375 to 6.625 percent. For monolithic bridge decks, air content varies from 4.5 to 6.5 percent, and the categories range from 4.875 to 6.375 percent. For bridge subdecks, air content varies from 2.25 to 7.5 percent, with the categories ranging from 4.125 to 6.375 percent.

3.6.6.1 D_{eff} versus Air Content

Mean D_{eff} for individual placements is shown as a function of air content for silica fume and conventional overlays in Figs. 3.58 and 3.59. One silica fume overlay is outside the range of air contents analyzed. Therefore, only 18 silica fume overlay placements are included in the analysis. Because of missing data, only 24 conventional overlay placements are included in the analysis.

For silica fume overlays, D_{eff} increases slightly as air content increases (Fig. 3.58). For conventional overlays, D_{eff} remains nearly constant for air contents

between 4.375 and 5.875 percent and then increases for 6.625 percent air (Fig. 3.59). The differences in mean D_{eff} for both silica fume and conventional overlays are not statistically significant for either type of overlay (Table 3.18).

3.6.6.2 RCPT versus Air Content

Mean RCPT values for individual placements are shown as a function of air content for silica fume and conventional overlays in Figs. 3.60 and 3.61. Three silica fume overlays are outside the range of air contents analyzed and data is missing for one silica fume overlay placement. Therefore, only 34 silica fume overlay placements are included in the analysis. Because of missing data, only 24 conventional overlay placements are included in the analysis.

For silica fume overlays, there is no trend with respect to air content (Fig. 3.60). For conventional overlays, there is a general increase in coulombs passed as air content increases (Fig. 3.61); the RCPT values increase only slightly as air content increases from 4.375 to 5.875 percent, but increase about 50 percent for a 6.625 percent air content. The differences in mean RCPT values, however, are not statistically significant for either type of overlay (Table 3.18).

3.6.6.3 Crack Density versus Air Content

Mean crack density for individual placements is shown as a function of air content for silica fume overlays, conventional overlays, and monolithic bridge decks in Figs. 3.62, 3.63, and 3.64. Mean crack density for bridge subdecks is shown as a function of air content in Fig. 3.65. Three silica fume overlays are outside the range of air contents analyzed and data is missing for one silica fume overlay placement. Therefore, only 34 silica fume overlay placements are included in the analysis. Because of missing data, only 24 conventional overlay placements, 34 monolithic bridge deck placements, and 47 subdeck placements are included in the analysis.

For silica fume overlays, the level of cracking increases slightly with increasing air content (Fig. 3.62). The increase in level of cracking is small and not

statistically significant (Table 3.20). For conventional overlays, the level of cracking does not vary significantly with air content and no trend is apparent (Fig. 3.63) (Table 3.20). For monolithic bridge decks the level of cracking is nearly constant for 4.875 and 5.625 percent air, but the level drops by more than half for 6.375 percent air (Fig. 3.64); the difference is statistically significant. For bridge subdecks, the level of cracking increases about 50 percent for an increase in air content from 4.125 to 6.375 percent (Fig 3.65), but the differences are not statistically significant (Table 3.20).

Schmitt and Darwin (1995,1999) found reduced levels of cracking at higher air contents for monolithic bridge decks, and recommended a minimum air content of 6.0 percent for monolithic bridge decks. They did not find any correlation between cracking and air content for conventional overlays. Cheng and Johnston (1985) also found that higher air contents in concrete mix designs reduced transverse cracking. Poppe (1981) showed air content to have a neutral effect. Krauss and Rogalla (1996) found that concretes without entrained air did not show cracking tendencies significantly different than that for concretes with entrained air. In the current study, the only case in which there are statistically significant differences in mean level of cracking is for monolithic bridge decks.

3.6.7 Compressive Strength

For silica fume overlays, compressive strength varies from 36 to 62 MPa (5200 to 9000 psi). Categories range from 38 MPa (5500 psi) to 59 MPa (8500 psi). For conventional overlays, compressive strength varies from 34 to 57 MPa (4900 to 8200 psi), with categories ranging from 38 MPa (5500 psi) to 52 MPa (7500 psi). For monolithic bridge decks, compressive strength varies from 29 to 51 MPa (4200 to 7400 psi), with categories ranging from 31 to 45 MPa (4500 to 6500 psi), and for bridge subdecks, compressive strength varies from 29 to 52 MPa (4200 to 7500 psi), with categories ranging from 31 to 52 MPa (4500 to 7500 psi).

3.6.7.1 D_{eff} versus Compressive Strength

Mean D_{eff} for individual placements is shown as a function of compressive strength for silica fume and conventional overlays in Figs. 3.66 and 3.67. Because of missing data, only 12 silica fume overlay placements, and 18 conventional overlay placements are included in the analysis.

For silica fume overlays, D_{eff} increases as compressive strength increases (Fig. 3.66). For conventional overlays, D_{eff} varies only slightly with changes in compressive strength (Fig. 3.67). In neither case are the changes statistically significant (Table 3.21).

3.6.7.2 RCPT versus Compressive Strength

Mean RCPT values for individual placements are shown as a function of compressive strength for silica fume and conventional overlays in Figs. 3.68 and 3.69. Because of missing data, only 22 silica fume overlay placements, and 18 conventional overlay placements are included in the analysis.

In both cases there is a general trend towards lower RCPT values with increasing compressive strength such a trend is expected, but the current results are statistically significant only for the silica fume overlays at $\alpha = 0.10$.

3.6.7.3 Crack Density versus Compressive Strength

Mean crack density for individual placements is shown as a function of compressive strength for silica fume overlays, conventional overlays, and monolithic bridge decks in Figs. 3.70, 3.71, and 3.72. Mean crack density for bridge subdecks is shown as a function of compressive strength in Fig. 3.73. Because of missing data, only 22 silica fume overlay placements, 39 conventional overlay placements, 32 monolithic bridge deck placements, and 37 bridge subdeck placements are included in the analysis.

For silica fume overlays, there is a drop in cracking with increasing compressive strength (Fig. 3.70), but the changes are not statistically significant at

$\alpha = 0.05$ (Table 3.23). In the other three cases, to varying degrees, the level of cracking increases as the compressive strength increases (Figs. 3.71, 3.72, and 3.73). These trends are statistically significant at $\alpha = 0.05$ only for monolithic decks (Fig. 3.72) (Table 3.23).

Schmitt and Darwin (1995, 1999) found the same trend for monolithic bridge decks and suggested that the trend towards increased cracking with increased compressive strength reflected the increased cement content associated with higher compressive strengths. Krauss and Rogalla (1996) found that concretes with high cement contents and low water-cement ratios were more likely to crack than concretes with low cement contents and high water-cement ratios. They recommended not only using low cement contents, but also that specifications include maximum cement contents. Based on the results, it is reasonable to conclude that increased compressive strengths are not beneficial to the cracking performance of bridge deck concretes.

3.7 EFFECTS OF SITE CONDITIONS

Site conditions for the date of concrete placement analyzed include average air temperature, low air temperature, high air temperature, daily temperature range, relative humidity, and average wind velocity. Air temperature, relative humidity, and wind speed all play a role in the rate of evaporation of water on the concretes surface. The rate of evaporation is also very sensitive to concrete temperature. Unfortunately concrete temperatures were not recorded in the daily journals or project files. The information was unavailable and evaporation rates could not be calculated, and are, therefore, not analyzed. Site conditions can serve as an indication of the rate of evaporation, but without concrete temperature the data is incomplete and trends in the data may not accurately reflect rates of evaporation.

Because high levels of evaporation can lead to plastic shrinkage cracking, site conditions are compared with crack densities. Concrete placements are divided into 4 categories: silica fume overlays, conventional overlays, monolithic bridge decks, and

bridge subdecks. The site conditions are not believed to play a significant role in the chloride permeability of concrete and are, therefore, not compared with D_{eff} or RCPT results.

Detailed analyses of the effects of site conditions are presented in the balance of this section. The effects of site conditions varied significantly and few correlations are found in the data. The key observations from these analyses, some of which are counter to expected behavior, can be summarized as follows. However the observations followed by a (Y) are statistically significant at $\alpha = 0.05$.

For silica fume overlays, crack density increases as the temperature range increases. Crack density decreases as relative humidity increases (Y).

For conventional overlays crack density increases as the average air temperature, daily low air temperature, daily high air temperature (Y), and temperature range increase. Conventional overlays show decreased levels of cracking as wind velocity increases (Y).

For monolithic overlays, the level of cracking is constant for average air temperatures of 5 and 15 °C and drops slightly for 25 °C. Monolithic overlays show increased levels of cracking as the daily high temperature, and the daily temperature range increase.

For bridge subdecks crack density increases as low air temperature increases. Crack density decreases as the daily air temperature increases.

3.7.1 Average Air Temperature

Mean crack density for individual placements is shown as a function of average daily air temperature for the date of concrete placement for silica fume overlays, conventional overlays, and monolithic bridges in Figs. 3.74, 3.75, and 3.76. The mean crack density of bridge subdecks is shown as a function of average daily air temperature for the date of concrete placement in Fig. 3.77. The average air temperature ranges from 3 to 29 °C for silica fume overlays, from 5 to 30 °C for conventional overlays, from 2 to 30 °C for monolithic bridge decks, and from 3 to

31 °C for bridge subdecks. Average air temperature categories range from 5 to 25 °C.

Overall, there is no clear relationship between average temperature and crack density, and the differences observed (Figs. 3.74 - 3.77) (Table 3.24) are not statistically significant. The clearest trend is observed for conventional overlays, for which crack density increases as the average air temperature increases (Fig. 3.75). For monolithic bridge decks, the level of cracking is constant for 5 and 15 °C and drops slightly for 25 °C (Fig. 3.76).

Cheng and Johnston (1985) found that, for continuous steel girder bridges, cracking tended to increase as average temperatures decreased, especially below 7 °C. Poppe (1981) found that high heat lead to increased cracking. Schmitt and Darwin (1995) found no trend for monolithic bridge decks, but found that cracking increased as average air temperature increased for conventional overlays. The analysis of conventional overlays in the current study, which include the data for conventional overlays obtained by Schmitt and Darwin (1995), does not contradict the trend found by Schmitt and Darwin. The increase in cracking with higher average temperatures probably reflects increased cracking with higher rates of evaporation.

3.7.2 Low Air Temperature

Mean crack density for individual placements is shown as a function of minimum daily air temperature for the date of concrete placement for silica fume overlays, conventional overlays, and monolithic bridges in Figs. 3.78, 3.79, and 3.80. Mean crack density for bridge subdecks is shown as a function of minimum daily air temperature for the date of concrete placement in Fig. 3.81.

The low air temperature ranges from -4 to 24 °C for silica fume overlays, from -3 to 24 °C for conventional overlays, from -3 to 23 °C for monolithic bridge decks, and from -7 to 24 °C for bridge subdecks. The minimum air temperature categories range from 0 to 20 °C.

For silica fume overlays and monolithic bridge decks, there is no trend between the level of cracking and the low air temperature (Figs. 3.78 and 3.80). For

conventional overlays and bridge subdecks, crack density increases as the low air temperature increases (Figs. 3.79 and 3.81). The level of cracking is nearly constant at 10 and 20 °C for conventional overlays (Fig. 3.79). None of the differences in mean crack density for a given deck type are statistically significant at $\alpha = 0.05$ (Table 3.25).

3.7.3 High Air Temperature

Mean crack density for individual placements is shown as a function of maximum daily air temperature for the date of concrete placement for silica fume overlays, conventional overlays, and monolithic bridges in Figs. 3.82, 3.83, and 3.84. Mean crack density for bridge subdecks is shown as a function of maximum daily air temperature for the date of concrete placement in Fig. 3.85.

The maximum daily air temperature varies from 7 to 34 °C for silica fume overlays, from 9 to 37 °C for conventional overlays, from 6 to 36 °C for monolithic bridge decks, and from 12 to 39 °C for bridge subdecks. For silica fume overlays, conventional overlays, and bridge subdecks, the maximum air temperature categories range from 15 to 35 °C. For monolithic bridge decks, the categories range from 5 to 35 °C.

For silica fume overlays and bridge subdecks, no trend between crack density and high air temperature is apparent (Figs. 3.82 and 3.85). For conventional overlays and monolithic bridge decks, the level of cracking generally increases as the maximum daily air temperature increases (Figs. 3.83 and 3.84). In each case, however, the crack density at 35 °C is slightly lower than the crack density at 25 °C.

3.7.4 Daily Temperature Range

Mean crack density for individual placements is shown as a function of daily air temperature range for the date of concrete placement for silica fume overlays, conventional overlays, and monolithic bridges in Figs. 3.86, 3.87, and 3.88. Mean crack density for bridge subdecks is shown as a function of daily air temperature

range for the date of concrete placement in Fig. 3.89.

The daily air temperature range varies between 4 and 24 °C for silica fume overlays, between 3 and 24 °C for conventional overlays, between 2 and 22 °C for monolithic bridge decks, and between 4 and 20°C for bridge subdecks. The daily air temperature range categories range from 4 to 20 °C.

Crack density increases with the daily temperature range for silica fume overlays, conventional overlays, and monolithic bridge decks (Figs. 3.86 - 3.88). Crack density drops with increasing daily air temperature range for bridge subdecks (Fig. 3.89). While the trends appear clear in each case, the trends are not statistically significant at $\alpha = 0.05$ (Table 3.27).

3.7.5 Relative Humidity

Mean crack density for individual placements is shown as a function of average daily relative humidity for the date of concrete placement for silica fume overlays, conventional overlays, and monolithic bridges in Figs. 3.90, 3.91, and 3.92. Mean crack density for bridge subdecks is shown as a function of average daily relative humidity for the date of concrete placement in Fig. 3.93.

Relative humidity varies from 15 to 94 percent for silica fume overlays, from 30 to 125 percent for conventional overlays, from 43 to 92 percent for monolithic bridge decks, and from 37 to 90 percent for bridge subdecks. The average daily relative humidity categories range from 35 to 75 percent for silica fume overlays, from 45 to 75 percent for conventional overlays, and from 45 to 85 percent for monolithic bridge decks, and bridge subdecks.

For silica fume overlays, the level of cracking generally tends to decrease as the relative humidity increases (Fig. 3.90). The trend is statistically significant. For conventional overlays, the level of cracking is almost constant. The greatest level of cracking occurs for the 55 percent relative humidity category (Fig. 3.91). For monolithic bridge decks, the level of cracking does not vary significantly, and no trend is apparent (Fig. 3.92) (Table 3.28). For bridge subdecks, there is no apparent

trend in the level of cracking with change in relative humidity, although the greatest level of cracking occurs at an 85 percent relative humidity (Fig. 3.93), but this category contains only two subdecks.

The findings for silica fume overlays agree with the findings of Cheng and Johnson (1985), who found a correlation between low humidity and increased levels of cracking, and with the findings of Krauss and Rogalla (1996), who found that high humidity and low evaporation rates reduced cracking. No clear trends are apparent for conventional overlays, monolithic bridge decks, or bridge subdecks.

3.7.6 Average Wind Velocity

Mean crack density for individual placements is shown as a function of average wind speed for the date of concrete placement for silica fume overlays, conventional overlays, and monolithic bridges in Figs. 3.94, 3.95, and 3.96. Mean crack density for bridge subdecks is shown as a function of average wind speed for the date of concrete placement for in Fig. 3.97.

Wind velocity varies from 2.7 to 36.2 km/h (1.7 to 22.5 mi/h) for silica fume overlays, from 2.1 to 29.5 km/h (1.3 to 18.3 mi/h) for conventional overlays, from 1.3 to 25.8 km/h (0.8 to 16.0 mi/h) for monolithic bridge decks, and from 3.2 to 36.2 km/h (2.0 to 22.5 mi/h) for bridge subdecks. The average wind velocity categories for silica fume overlays, conventional overlays, and bridge subdecks range from 2.5 to 22.5 km/h (1.5 to 14.0 mi/h). The average wind velocity categories for monolithic bridge decks range from 7.5 to 22.5 km/h (4.6 to 14.0 mi/h).

For silica fume overlays and monolithic bridge decks, crack density is nearly constant with respect to wind velocity (Figs. 3.94 and 3.96). For conventional overlays, there is a general trend towards *lower* levels of cracking with increasing wind velocity (Fig. 3.95). For bridge subdecks, crack density is nearly constant for average wind velocities between 2.5 and 17.5 km/h (1.5 and 10.9 mi/h), but drops substantially for the three subdecks in the highest wind velocity category, 22.5 km/h (14.0 mi/h) (Fig. 3.97) (Table 3.29).

Greater wind velocities lead to higher rates of evaporation, which in turn can cause problems with plastic shrinkage cracking. Poppe (1981) observed increased levels of cracking for decks subjected to high wind velocities. Krauss and Rogalla (1996) recommend wind breaks for cases in which the evaporation rates exceed $1 \text{ kg/m}^2/\text{hr}$ ($0.2 \text{ lb/ft}^2/\text{hr}$). The results for silica fume overlays, monolithic bridge decks, and bridge subdecks show no trend, while the results for conventional overlays show lower levels of cracking as wind velocity increases, all of which contradict Poppe (1981). This contradiction may be due to the fact that although higher wind speeds generally contribute to higher rates of evaporation, high wind velocities are not the only contributing factor and do not necessarily indicate excessive rates of evaporation.

3.8 EFFECTS OF FINISHING AND CURING PROCEDURES

Methods used for finishing and curing, as well as the length of time for curing, were not regularly recorded. Occasionally, daily journals described the curing process, but not frequently enough to provide adequate information for analysis. It would be extremely useful for future studies, if this information were recorded.

The Special Provisions for silica fume overlays provide the minimum requirements for overlay construction, including finishing and curing. For many of the silica fume overlays, mix design information includes information on which revision of the silica fume overlays special provision was in effect for that bridge. Assumptions on the revision number in effect for other silica fume bridges are made on a chronological basis. A bridge deck constructed after one bridge and before another bridge both of which are known to have used Revision 3 of the silica fume overlay Special Provision is assumed to also have used Revision 3.

Bridges 89-184 and 89-187 were constructed before the Special Provision for silica fume overlays was written and are, therefore, assumed to have been constructed under the bridge deck wearing surface specifications, which did not require the use of fogging or precure material during and after finishing. All other silica fume overlay

bridges were, apparently, constructed under Revision 3 or 4 of the Special Provision. Revision 3 required the use of fogging and/or precure material during and after finishing. Revision 4 required the use of both fogging and precure material during and after finishing. The mean crack density of entire bridge decks for silica fume overlays from the current study is shown as a function of the silica fume special provision revision number in Fig. 3.98. The bridges constructed under Revision 4 exhibit, on average, 36 percent less cracking than those constructed under Revision 3, and 77 percent less than those constructed without a silica fume overlay Special Provision. It is important to realize that the lower levels of cracking are also associated with younger bridges and it is, therefore, difficult to separate the effects of different revisions of the special provision from the effects of bridge age.

3.9 EFFECTS OF DESIGN SPECIFICATIONS

Design considerations include both the bridge deck and the structure type. Three structure types are examined: SMCC (steel beam, composite continuous), SWCC (steel welded plate girder, composite continuous), and SWCH (steel welded plate girder, composite continuous and haunched). Because of differences in age between silica fume overlays and other bridge decks, it is difficult to make accurate comparisons between the two. However, when all silica fume overlays are included, the mean crack density for silica fume overlays (0.41 m/m^2) is greater than that for monolithic bridge decks (0.36 m/m^2) and only 0.05 m/m^2 less than that for conventional overlays (0.46 m/m^2). When the older silica fume overlays, bridges 89-184 and 89-187, are excluded the average crack density (0.30 m/m^2) is lower than that observed for conventional overlays or monolithic decks.

Detailed analyses of the effects of design specifications are presented in the balance of this section. In addition to the observations on the effects of deck type, it is observed that crack density is significantly higher for the end sections of fixed-end girders than for pinned-end girders and that crack density increases as bar size and bar spacing increase. Crack density does not appear to depend on the steel structure type,

bridge or span length, span type (interior or exterior), or skew.

3.9.1 Structure Type

Mean crack density for entire bridge decks is shown as a function of structure type for silica fume overlays, conventional overlays, and monolithic bridge decks in Figs. 3.99, 3.100, and 3.101. For silica fume overlays, SWCH structures exhibit a much higher level of cracking than the other two structure types (Fig. 3.99), but only two SWCH bridges are included in the study. For conventional overlays, SWCH structures show the lowest level of cracking and SWCC structures show the highest level of cracking (Fig. 3.100). For monolithic bridge decks, the single SWCH bridge shows significantly higher levels of cracking than observed for the other two structure types (Fig. 3.101), while SWCC bridges show the least level of cracking. In general, structure type appears to have very little effect on bridge deck cracking.

3.9.2 Deck Type

Mean crack density for entire bridge decks is shown as a function of bridge deck type in Fig. 3.102. The three bridge deck types examined are silica fume overlays (SFO), conventional overlays (CO), and monolithic bridge decks (Mono). For all bridge decks, from both the current study and the study by Schmitt and Darwin (1995), monolithic bridge decks have the lowest overall level of cracking (0.36 m/m^2) and conventional overlays have the highest level of cracking (0.46 m/m^2). The silica fume overlay average a crack density of 0.41 m/m^2 . When bridges 89-184 and 89-187, the bridges with older silica fume overlays with very high levels of cracking, are excluded from the data set, the silica fume overlays exhibit the lowest level of cracking (0.30 m/m^2). Based on the student's t-test, none of the differences is statistically significant (Table 3.32).

It is important to realize that the ages of the silica fume overlay decks, with the two exceptions, are much younger than those of the conventional overlays. If the level of cracking for the silica fume overlays continues to increase with age, when the

silica fume overlays are in the same age range as the conventional overlays studied, their level of cracking may well exceed that of the conventional overlays.

3.9.3 Deck Thickness

Mean crack density for entire bridge decks is shown as a function of deck thickness for silica fume overlays, conventional overlays, and monolithic bridge decks in Figs. 3.103, 3.104, and 3.105. Deck thickness varies from 216 mm (8.5 in.) to 229 mm (9.0 in.) for silica fume and conventional overlays, and from 203 mm (8.0 in.) to 229 mm (9.0 in.) for monolithic bridge decks.

For silica fume overlays, thicker decks show levels of cracking nearly twice that of thinner decks (Fig. 3.103). For conventional overlays, thicker decks exhibit lower levels of cracking (Fig. 3.104). For monolithic bridge decks, there is no trend (Fig. 3.105). For all three deck types the differences observed for different deck thicknesses are not statistically significant (Table 3.33), which is not surprising considering the small difference in deck thicknesses considered.

Poppe (1981) found that cracking tends to decrease with increases in deck thickness. However, the bridge decks that Poppe studied included a greater range in deck thickness and bridge decks [158.8 mm (6.25 in.)] thinner than the thinnest [177.8 mm (7.0 in.)] bridge deck in the current study.

3.9.4 Top Cover

Mean crack density for entire bridge decks is shown as a function of concrete cover over the top reinforcing steel for monolithic bridge decks in Fig. 3.106. Because all silica fume and conventional overlays have a cover of 76 mm (3.0 in.), no evaluation of the effect of cover is possible for those decks. Monolithic bridge decks with a top cover of 64 mm (2.5 in.) have a lower level of cracking than those with a top cover of 76 mm (3.0 in.), but the differences are statistically significant only at $\alpha = 0.20$ (Table 3.34). Higher levels of cracking for increased bar cover contradict the findings of Dakhil, Cady, and Carrier (1975), who found that the severity of

settlement cracking decreases with increasing bar cover. However, higher cover may result in wider cracks, which increases the probability of seeing and recording the cracks.

3.9.5 Transverse Reinforcing Bar Size

Mean crack density for entire bridge decks is shown as a function of transverse reinforcing bar size for silica fume overlays, conventional overlays, and monolithic bridge decks in Figs. 3.107, 3.108, and 3.109. Silica fume overlay decks include bar sizes No. 5 (16 mm), No. 6 (19 mm) and No. 5 and No. 6 (16 and 19 mm) combined.

In silica fume overlays, all three size categories of transverse reinforcement show approximately equal levels of cracking (Fig. 3.107) with no statistically significant differences between them (Table 3.35).

Conventional overlays include bar sizes No. 4 and No. 5 (13 and 16 mm) combined, No. 5 (16 mm) and No. 6 (19 mm). The level cracking increases as size of the transverse reinforcing bars increases (Fig. 3.108).

Monolithic bridge decks included bar sizes No. 4 (13 mm), No. 4 and No. 5 (13 and 16 mm) combined, No. 5 (16 mm), and No. 6 (19 mm). However, No. 4 (13 mm) and No. 6 (19 mm) are each only represented by one bridge deck and are, therefore, not included in the analysis. In the monolithic bridge decks analyzed, the level of cracking is lower for bridge decks with only No. 5 (16 mm) bars than it is for bridge decks with No. 4 and No. 5 (13 and 16 mm) bars (Fig. 3.109). However, the differences are not statistically significant (Table 3.35).

Dakhil, Cady, and Carrier (1975) found that severity of cracking increased with increasing bar size, when comparing results for No. 5, No. 8, and No. 11 bars. Although the data for monolithic overlays contradicts these findings, if one bridge with a relatively high crack density of 0.84 m/m^2 is removed from the category for No. 4 and No. 5 (13 and 16 mm) bars, the mean crack density for that category becomes 0.26 m/m^2 almost equal to the crack density of 0.27 m/m^2 for No. 5 (16 mm)

bars. Under any circumstances, the differences in bar size in the bridge decks surveyed are substantially less than used by Dakhil, Cady, and Carrier (1975).

3.9.6 Transverse Reinforcing Bar Spacing

Mean crack density for entire bridge decks is shown as a function of transverse reinforcing bar spacing for silica fume and conventional overlays in Figs. 3.110 and 3.111. For silica fume overlays, bar spacing varies from 102 to 229 mm (4.0 to 9.0 in.), while for conventional overlays, bar spacing varies from 140 to 305 mm (5.5 to 12.0 in.). All monolithic bridge decks, except one, had a transverse reinforcing bar spacing of 153 mm (6 in.) and are not analyzed further. Bar spacing is divided into two categories: less than or equal to 153 mm (6 in.), and greater than 153 mm (6 in.). For silica fume overlays, the level of cracking is nearly equal for both categories of transverse reinforcing bar spacing (Fig. 3.110). For conventional overlays, the crack density for transverse reinforcing bar spacings greater than 153 mm (6 in.) is double that for transverse reinforcing bar spacing less than or equal to 153 mm (6 in.) (Fig. 3.111), a result that is statistically significant at $\alpha = 0.002$. In general, a greater transverse bar spacing tends toward increased levels of cracking.

3.9.7 Girder End Condition

To evaluate the effect of the girder end condition on crack density, densities for the first and last 3 m (10 ft) of each bridge deck are calculated. Mean crack density for end sections is shown as a function of girder end condition for silica fume and conventional overlays in Figs. 3.112, and 3.113. Girder ends are either fixed (F) or pinned (P). For both silica fume and conventional overlays, the level of cracking for fixed end conditions is nearly three times greater than that for pinned conditions. Because only two monolithic bridges have a pinned end condition, the effect of girder end condition is not evaluated for monolithic bridge decks.

3.9.8 Span Length

Mean crack density for individual spans is shown as a function of span length for silica fume overlays, conventional overlays, and monolithic bridge decks in Figs. 3.114, 3.115, and 3.116. For silica fume overlays, span length ranges from 6.1 to 61.6 m (20 to 202 ft) and span length categories range from 15 to 55 m (49 to 180 ft). Crack density decreases as the span length increases from 15 to 35 m (49 to 115 ft), and increases as the span length increases from 35 to 55 m (115 to 180 ft). The greatest crack density occurs for span lengths of 15 m (49 ft) (Fig. 3.114).

For conventional overlays, span length ranges from 12.2 to 48.8 m (40 to 160 ft) and span lengths categories range from 15 to 45 m (49 to 148 ft). There is a slight trend towards lower levels of cracking with increasing span length. However, the differences are not statistically significant (Fig. 3.115) (Table 3.38).

For monolithic bridge decks, span length ranges from 11.3 to 36.6 m (37 to 120 ft) and the span length categories range from 15 to 35 m (49 to 115 ft). The level of cracking is slightly higher at 25 m (82 ft) span length, but the differences in crack density are small and statistically insignificant (Fig. 3.116) (Table 3.38).

In general, span length does not significantly affect the level of cracking on concrete bridge decks.

3.9.9 Bridge Length

Mean crack density for entire bridge decks is shown as a function of bridge length for silica fume overlays, conventional overlays, and monolithic bridge decks in Figs. 3.117, 3.118, 3.119. Bridge length categories range from 50 to 130 m (164 to 427 ft) for all deck types. For silica fume overlays, bridge length ranges from 60.4 to 432.2 m (198 to 1388.5 ft). Crack density is greatest for 90 m (295 ft) bridge lengths and least for 50 m (164 ft) bridge lengths (Fig. 3.117).

For conventional overlays, bridge length ranges from 40.4 to 134.1 m (132.5 to 439.8 ft). The level of cracking increases as bridge length increases (Fig. 3.118), but the differences are not statistically significant (Table 3.39).

For monolithic bridge decks, bridge length ranges from 37.2 to 303.5 m (122.0 to 995.7 ft). The level of cracking is nearly constant for all bridge lengths, although slightly greater at 90 m (295 ft) bridge lengths.

In general, bridge length does not appear to have a significant affect on the level of cracking.

3.9.10 Span Type

Mean crack density for individual spans is shown as a function of span type for silica fume overlays, conventional overlays, and monolithic bridge decks in Figs. 3.120, 3.121, and 3.122. Span type is divided into three categories: fixed connection end spans, pinned connection end spans, and interior spans.

For silica fume overlays, the level of cracking is lowest for pinned connection end spans (Fig. 3.120). The level of cracking for fixed connection end spans and interior spans differs by only 0.02 m/m^2 . For conventional overlays the level of cracking is the same for fixed connection end spans and interior spans and only 0.02 m/m^2 greater for pinned connection end spans (Fig. 3.121). For monolithic bridge decks, the level of cracking for fixed connection end spans is only 0.02 m/m^2 less than that for interior spans (Fig. 3.122). The level of cracking is much less for pinned connection end spans, but only 2 bridges are represented. The differences between crack density for pinned connection end spans, and other spans for silica fume overlays and monolithic bridge decks are statistically significant only at $\alpha = 0.20$ (Table 3.40).

The type of span appears, at best, to have a small effect on crack density.

3.9.11 Skew

The mean crack density of entire bridge decks is shown as a function of deck skew for silica fume overlays, conventional overlays, and monolithic bridge decks in Figs. 3.123, 3.124, and 3.125. Skew is defined as the acute angle between the centerline of the abutment and a line normal to the centerline of the roadway. In no

case does bridge skew appear to affect the level of cracking in bridge decks.

3.10 EFFECTS OF TRAFFIC

Mean crack density for entire bridge decks is shown as a function of the average annual daily traffic (AADT) for silica fume overlays, conventional overlays, and monolithic bridge decks in Figs. 3.126, 3.127, and 3.128. AADT ranges from 0 to 14705 for silica fume overlays, from 245 to 19570 for conventional overlays, and from 0 to 13725 for monolithic bridge decks. Categories of 2500, 7500, and 12500 are used for silica fume and conventional overlays. Categories of 1000, 3000, and 5000 are used for monolithic bridge decks. AADT does not take the age of a bridge into account, only the amount of daily traffic. For silica fume overlays, crack density decreases as traffic volume increases (Fig. 3.126). However, silica fume overlays with higher traffic volumes are younger bridges and only 2 bridges represent a mean AADT of 12500. For conventional overlays, crack density increases as the AADT increases (Fig. 3.127). For monolithic bridge decks, crack density at 1000 AADT is less than 40 percent of the crack density at 3000 or 5000 AADT. In no case, are the differences in crack density statistically significant at $\alpha = 0.05$.

Mean crack density for entire bridge decks is shown as a function of the total number of load cycles that a bridge had been subjected to over its lifetime for silica fume overlays, conventional overlays, and monolithic bridge decks in Figs. 3.129, 3.130, and 3.131. The number of load cycles a bridge has experienced takes into account the age of a bridge and, therefore, should be a more accurate measurement of the effect of traffic on the level of cracking. Total load cycles range from 1.53×10^5 to 7.69×10^6 for silica fume overlays, from 3.64×10^5 to 4.89×10^7 for conventional overlays, and from 6.30×10^5 to 3.44×10^7 for monolithic bridge decks. Categories range from 1.0×10^6 to 7.0×10^6 for silica fume overlays, from 0.5×10^6 to 4.5×10^6 , from 1.5×10^6 to greater than 10×10^6 for monolithic bridge decks.

For silica fume overlays, the level of cracking increases as the number of load cycles increases (Fig. 3.129), as it does for monolithic bridges (Fig. 3.131). For

conventional overlays, there is no clear trend between the number of load cycles and the level of cracking (Fig. 3.130), although for load cycles greater than 2.5×10^6 , the level of cracking increases as the number of load cycles increases. The effect of load cycles on cracking is especially difficult to ascertain for conventional overlay bridges because of the observation (Section 3.3) that younger conventional overlay bridges tend to crack more than older conventional overlay bridges.

Generally, it appears that bridges subjected to a greater number of load cycles show greater levels of cracking, but it is not clear whether the difference is due to loading or time.

3.11 PAVEMENT PROFILE

Because of concerns that silica fume overlays are providing excessively rough driving surfaces, pavement profiles were determined for the driving lanes of the bridges studied. Fig. 3.132 compares mean pavement roughness index (PRI) of individual driving lanes as a function of deck type. The mean PRI does not vary significantly (the total range is only 685 to 698 mm/km), regardless of bridge deck type (Table 3.44).

CHAPTER 4
SUMMARY, CONCLUSIONS, AND
RECOMMENDED IMPLEMENTATION PLAN

4.1 SUMMARY

The purpose of this study was to determine how construction practices and material properties correlate with the performance of concrete bridge decks, to gage the performance of bridge decks with silica fume overlays relative to bridges with conventional concrete overlays, and to determine if the silica fume overlays commonly used on bridges in Kansas are performing at a level that justifies the extra cost and construction precautions. Forty continuous steel girder bridges, primarily from northeast Kansas (thirty-eight from KDOT District 1, and two from KDOT District 5) were evaluated. The study included three deck types: silica fume overlays (20 bridges), conventional overlays (16 bridges), and monolithic bridge decks (4 bridges). Field surveys were conducted to document the cracking patterns and crack density for each bridge and to take samples for chloride content analysis and rapid chloride permeability (RCPT) tests. Information for each bridge was collected from construction documents, field books, and weather data logs. The information was combined with data from the earlier study by Schmitt and Darwin (1995) and compared to the observed levels of cracking, effective diffusion coefficients, and rapid chloride permeability test results. Twenty-seven variables were considered, covering bridge age, material properties, site conditions, construction procedures, design specifications, and traffic volume. Comparisons are made based on the properties of the upper surface and on the properties of the subdeck for bridges with overlays.

4.2 CONCLUSIONS

The following conclusions are based on the investigation and analysis described in this report. Conclusions relative to “subdecks” address crack density in

bridges with overlays as affected by the material properties or construction conditions of the subdecks. Conclusions relative to “overlay bridge decks” address deck properties as affected by the material properties or construction conditions of the overlays themselves:

1. For the 11 bridges included in both the current study and the earlier study by Schmitt and Darwin (1995), the crack densities obtained in the two studies show close agreement. The crack densities in the current study are, generally, similar or greater than those obtained by Schmitt and Darwin.
2. Crack density increases with age for bridge decks with silica fume overlays.
3. The newest silica fume overlay decks, constructed in 1997 and 1998, have lower crack densities than the older silica fume overlay decks. It is not clear if the reduced crack density is due to improved construction procedures or low age.
4. The most recent conventional overlays, constructed between 1993 and 1995, have higher crack densities than conventional overlays constructed earlier.
5. Monolithic bridge decks constructed between 1989 and 1993 have higher crack densities than monolithic bridges constructed between 1984 and 1987.
6. Crack densities are generally similar for conventional and silica fume overlay decks. If silica fume overlays follow their current trend of increased cracking with age, they will not perform better than the conventional overlays, when they are of equivalent age.
7. Effective diffusion coefficients for silica fume and conventional overlay bridge decks between 500 and 1500 days old do not differ significantly.
8. Silica fume overlay bridge decks have much lower RCPT values than either conventional overlay or monolithic bridge decks. However, this may be a result of the effect of silica fume on the pore solution of the concrete, and does not necessarily reflect lower chloride permeability.

9. Chloride content increases with the age of the bridge deck, regardless of bridge deck type. Silica fume and conventional overlay decks in the same age range, have similar chloride contents.
10. Chloride content taken at crack locations at mean depths of 66.7 mm (2.625 in.) and 85.7 mm (3.375 in.) (just above and below the transverse reinforcement, respectively), exceeds the threshold level for corrosion in as little as 1000 days (2.7 years), regardless of bridge deck type. Silica fume and conventional overlay decks in the same age range exhibit similar chloride contents.
11. For silica fume and conventional overlay decks, there is no correlation between D_{eff} and concrete slump.
12. For silica fume overlay decks, there is no correlation between RCPT values and concrete slump.
13. For bridge decks with silica fume overlays, the highest mean crack densities are observed for concrete slumps greater than 90 mm (3.5 in.).
14. For bridge decks with conventional overlays, the highest crack densities are observed for concretes with zero slump.
15. For monolithic bridge decks and bridge subdecks, crack density increases as concrete slump, percent volume of water and cement, water content, and cement content increase. In general, increased paste contents in bridge subdecks result in cracking in decks with overlays, regardless of the quality of the overlay.
16. For monolithic bridge decks, crack density increases as the water-cement ratio increases.
17. For silica fume overlays, D_{eff} increases slightly as air content increases.
18. For conventional overlay decks, RCPT values increase as air content increases.
19. For conventional overlay decks, there is no correlation between crack density and air content.

20. For monolithic bridge decks, crack density is significantly lower for air contents above 6 percent.
21. For conventional overlays, monolithic bridge decks, and bridge subdecks, the level of cracking increases as the compressive strength increases. In general, increased compressive strengths are not beneficial to the cracking performance of bridge deck concrete.
22. For conventional overlays, crack density increases as the average air temperature for the date of concrete placement increases.
23. For conventional overlays and bridge subdecks, crack density increases as the low air temperature for the date of concrete placement increases.
24. For conventional overlays and monolithic bridge decks, crack density increases as the maximum air temperature for the date of concrete placement increases.
25. For silica fume overlays, conventional overlays, and monolithic bridge decks, crack density increases as the daily air temperature range for the date of concrete placement increases.
26. For silica fume overlays, the crack density decreases as the relative humidity increases.
27. For silica fume overlays, the use of both fogging and precure material during and after finishing decreases the crack density.
28. In general, the steel structure type appears to have no effect on bridge deck cracking.
29. In general, a greater transverse bar size and spacing tends to increase levels of cracking.
30. For both silica fume and conventional overlays decks, the crack density for fixed end girders is nearly three times greater than that for pinned end girders.
31. In general, bridge length, span length, span type (interior and exterior), and bridge skew do not appear to affect crack density.

32. Generally, it appears that bridges subjected to a greater number of load cycles show greater levels of cracking, but it is not clear whether the difference is due to loading or time.
33. The mean pavement roughness index (PRI) is nearly identical for the monolithic, conventional overlay, and silica fume overlay bridges surveyed.

4.3 RECOMMENDED IMPLEMENTATION PLAN

Based on the results of this study, several recommendations are made. First, because the silica fume overlay bridges in the current study are younger than the conventional overlay and monolithic bridge decks included in the study, it is difficult to compare the different bridge deck types. The small number of silica fume and conventional overlay decks that are in the same age range have similar crack densities, D_{eff} values, and chloride contents, both at and away from cracks. If these observations are correct, they indicate that silica fume overlays provide no advantage over conventional overlay decks. This conclusion, however, is premature due to the young age of the majority of silica fume overlay decks in the study. As a result, the silica fume overlay decks should be reexamined when they are all in the same age range as the conventional overlay decks included in the study. This would provide data on changes in crack density and chloride content to more accurately compare the performance of silica fume overlays to conventional overlays.

Second, construction records should be maintained for the lifetime of each bridge. As noted earlier, the lack of long-term construction records represents a weakness in the ability to improve construction procedures based on field experience. Either the Construction Management System (CMS) database should be maintained in an easily accessible format or another database should be developed to include information from the CMS database, such as concrete mix design, materials used in the mix design, dates of bridge deck concrete placement (both subdeck and overlay), results of field tests (air content and slump), and results of compressive strength tests. In addition, information on the concrete temperature at the time of placement, daily

maximum and minimum air temperature, wind speed, relative humidity, and rate of evaporation on the date of concrete placement, detailed descriptions of finishing and curing procedures, including the length of curing, should be included in the database. The current special provisions for silica fume overlays require contractors to measure air temperature and relative humidity on the bridge deck, and to either measure or estimate concrete temperatures and wind speed on the bridge deck. Because contractors are already required to determine these values, it should not be difficult to obtain this information. Because of its importance, concrete temperature should be measured rather than estimated.

Third, a maximum cementitious material content and/or compressive strength should be included in the provisions for both subdeck and overlay concrete. Although an analysis of the effect of cement content on overlay concrete is not possible based on the current database, the results for both monolithic bridge decks and bridge subdecks, indicate that neither higher cement contents nor compressive strengths are beneficial to the cracking performance of the concrete.

Fourth, the use of both fogging immediately after finishing and precure material should be expanded to cover conventional overlay and monolithic decks, as well as silica fume overlay decks. Fogging and precure materials that do not affect bond should also be used for bridge subdecks.

4.4 RECOMMENDATIONS FOR FUTURE STUDY

As stated in Section 4.3, due to the age disparity between silica fume and conventional overlay decks, it is recommended that silica fume overlay decks be reexamined when they are in the same age range as the conventional overlay decks included in this study.

It would be beneficial to determine the correlation between the charge passed during the rapid chloride permeability test and known chloride permeabilities for the types of concrete used in bridge decks. The determination of such a correlation is recommended both by Whiting (the developer of the test) (1992) and in the

ASTM/AASHTO standard (ASTM C 1202 and AASHTO T 277). Further testing should be conducted to determine if the RCPT provides reasonable results for silica fume concrete.

It would also be beneficial to study the correlation between effective diffusion coefficients (D_{eff}) and the time to corrosion of reinforcing steel in concrete bridge decks.

REFERENCES

AASHTO T 259-80. (1980). "Resistance of Concrete to Chloride Ion Penetration," *1995 Standard Specifications for Transportation Materials and Methods of Sampling and Testing*, Part II Tests, American Association of State Highway and Transportation Officials, Washington, D.C., pp. 648-649

AASHTO T 277-93. (1993). "Electrical Indication of Concrete's Ability to Resist Chloride," *1995 Standard Specifications for Transportation Materials and Methods of Sampling and Testing*, Part II Tests, American Association of State Highway and Transportation Officials, Washington, D.C., pp. 721-726

ACI Committee 222, (1996). "Corrosion of Metals in Concrete (ACI 222R-96)," *Manual of Concrete Practice*, Part 1, American Concrete Institute, Farmington Hills, MI, 30 pp.

ACI Committee 234, (1996). "Guide for the Use of Silica Fume in Concrete (ACI 234R-96)," *Manual of Concrete Practice*, Part 1, American Concrete Institute, Farmington Hills, MI, 51 pp.

ASTM C 1202-97. (1997). "Electrical Indication of Concrete's Ability to Resist Chloride Ion Penetration," *1999 Annual Book of ASTM Standards*, Vol. 4.02, American Society for Testing and Materials, West Conshohocken, PA, 1999, pp. 618-623

Babaei, K. and Fouladgar, A.M. (1997). "Solutions to Concrete Bridge Deck Cracking," *Concrete International*, Vol.15, No.7, July, pp. 34-37.

Cheng, Timothy Tung-Hai, and Johnston, David W. (1985). "Incidence Assessment of Transverse Cracking in Concrete Bridge Decks: Construction and Material Considerations," *Report No. FHWA/NC/85-002 Vol. 1*, North Carolina State University, Raleigh, Department of Civil Engineering, 232 pp.

Dakhil, Fadh H.; Cady, Philip D.; and Carrier, Roger E. (1975). "Cracking of Fresh Concrete as Related to Reinforcement," *ACI Journal, Proc.* Vol. 72, No. 8, Aug., pp. 421-428.

Durability of Concrete Bridge Decks-A Cooperative Study, Final Report, (1970). the state highway departments of California, Illinois, Kansas, Michigan, Minnesota, Missouri, New Jersey, Ohio, Texas, and Virginia; the Bureau of Public Roads; and Portland Cement Association, 35 pp.

Kansas Department of Transportation (1990) *Standard Specifications for State Road and Bridge Construction*, Topeka, KS, 1154 pp.

Kansas Department of Transportation (1994) *Special Provision to the Standard Specifications Edition of 1990*, 90P-158-R3, Topeka, KS, 10 pp.

Kansas Department of Transportation (1995) *Special Provision to the Standard Specifications Edition of 1990*, 90P-158-R4, Topeka, KS, 12 pp.

Kansas Department of Transportation (1998) *Special Provision to the Standard Specifications Edition of 1990*, 90M-95-R4, Topeka, KS, 9 pp.

Kansas Department of Transportation (1999) *Special Provision to the Standard Specifications Edition of 1990*, 90M-158-R8, Topeka, KS, 14 pp.

Krauss, Paul D., and Rogalla, Ernest A. (1996). "Transverse Cracking in Newly Constructed Bridge Decks," *National Cooperative Highway Research Program Report 380*, Transportation Research Board, Washington, D.C.,

Perfetti, Gregory R.; Johnston, David W.; and Bingham, William L. (1985). "Incidence Assessment of Transverse Cracking in Concrete Bridge Decks: Structural Considerations," *Report No. FHWA/NC/88002 Vol. 2*, North Carolina State University, Raleigh, Dept. of Civil Engineering, 201 pp.

Pfeifer, Donald W.; McDonald, David B.; and Krauss, Paul D. (1994). "The Rapid Chloride Permeability Test and Its Correlation to the 90-Day Chloride Ponding Test," *PCI Journal*, Vol. 39 No. 1, Jan.-Feb., pp. 38-47.

Poppe, John B. (1981). "Factors Affecting the Durability of Concrete Bridge Decks: Summary Final Report," *Report No. FHWA/CA/SD-81/2*, California Department of Transportation, Division of Transportation Facilities Design, Sacramento, CA, 61 pp.

Schmitt, Tony R., and Darwin, David (1995). "Cracking in Concrete Bridge Decks," *SM Report No. 39*, The University of Kansas Center for Research, Inc., Lawrence, Kansas, 151 pp.

Schmitt, Tony R., and Darwin, David (1999). "Effect of Material Properties on Cracking in Bridge Decks," *Journal of Bridge Engineering*, ASCE, Feb., Vol. 4, No. 1, pp. 8-13.

Shi, Caijun; Stegmann, Julia A.; and Caldwell Robert J. (1998). "Effect of Supplementary Cementing Materials on the Specific Conductivity of Pore Solution and Its Implications on the Rapid Chloride Permeability Test (AASHTO T 277 and ASTM C 1202) Results," *ACI Materials Journal*, Vol. 95, No. 4, July-Aug., pp. 389-394.

Whiting, David (1981). "Rapid Determination of the Chloride Permeability of Concrete," *Report No. FHWA/RD-81/119*, Federal Highway Administration, Washington, D.C., 176 pp.

Whiting, David, and Mitchell, Terry M. (1992). "History of the Rapid Chloride Permeability Test," *Transportation Research Record*, Transportation Research Board, Washington, D.C., No. 1335, pp. 55-62.

Whiting, D., and Detwiler, R. (1998). "Silica Fume Concrete for Bridge Decks," *National Cooperative Highway Research Program Report 410*, Transportation Research Board, Washington, D.C., 18 pp.

ADDITIONAL BIBLIOGRAPHY

ACI Committee 201, (1992), "Guide for Making a Condition Survey of Concrete in Service (ACI 201.1R-92)," *Manual of Concrete Practice*, Part 1, American Concrete Institute, Farmington Hills, MI, 16 pp.

ACI Committee 212, (1991), "Chemical Admixtures for Concrete, (ACI 212.3R-91)," *Manual of Concrete Practice*, Part 1, American Concrete Institute, Farmington Hills, MI, 31 pp.

ACI Committee 224, (1990), "Control of Cracking in Concrete Structures (ACI 224R-90)," *Manual of Concrete Practice*, Part 3, American Concrete Institute, Farmington Hills, MI, 43 pp.

ACI Committee 224, (1992), "Cracking of Concrete Members in Direct Tension, (ACI 224.2R-92)," *Manual of Concrete Practice*, Part 3, American Concrete Institute, Farmington Hills, MI, 12 pp.

ACI Committee 304, (1989), "Guide for Measuring, Mixing, Transporting, and Placing Concrete (ACI 304R-89) Reapproved 1997," *Manual of Concrete Practice*, Part 2, American Concrete Institute, Farmington Hills, MI, 49 pp.

ACI Committee 305, (1991), "Hot Weather Concreting (ACI 305R-91)," *Manual of Concrete Practice*, Part 2, American Concrete Institute, Farmington Hills, MI, 20 pp.

ACI Committee 306, (1988), "Cold Weather Concreting (ACI 306R-88)," *Manual of Concrete Practice*, Part 2, American Concrete Institute, Farmington Hills, MI, 23 pp.

ACI Committee 308, (1992), "Standard Practice for Curing Concrete (ACI 308-92) Reapproved 1997," *Manual of Concrete Practice*, Part 1, American Concrete Institute, Farmington Hills, MI, 11 pp.

ACI Committee 309, (1996), "Guide for Consolidation of Concrete (ACI 309R-96)," *Manual of Concrete Practice*, Part 2, American Concrete Institute, Farmington Hills, MI, 39 pp.

ACI Committee 345, (1991), "Guide for Concrete Highway Bridge Deck Construction (ACI 345R-91)," *Manual of Concrete Practice*, Part 4, American Concrete Institute, Farmington Hills, MI, 38 pp.

Berke, N.S. (1988). "Microsilica and Concrete Durability," *Transportation Research Record*, Transportation Research Board, Washington, D.C., No. 1204, pp. 21-26.

- Bunke, Dennis (1988). "ODOT Experience with Silica-Fume Concrete," *Transportation Research Record*, Transportation Research Board, Washington, D.C., No. 1204, pp. 27-35.
- Darwin, David, and Salamizavareh, Shahin (1993). "Bond Strength of Grouted Reinforcing Bars," *SM Report* No. 32, The University of Kansas Center for Research Inc., Lawrence, Kansas, 139 pp.
- Detwiler, Rachel J.; Kojundic, Tony; and Fidjestøl, Per (1997). "Evaluation of Bridge Deck Overlays," *Concrete International*, ACI, Vol. 19, No. 8, Aug., pp. 43-45.
- Fitch, Michael G., and Abdulshafi, Osama A. (1998). "Field and Laboratory Evaluation of Silica Fume Modified Concrete Bridge Deck Overlays in Ohio," *Transportation Research Record*, Transportation Research Board, Washington, D.C., No. 1610, pp. 20-27.
- Freund, John E. (1999). *Mathematical Statistics*. Prentice Hall, Upper Saddle River, New Jersey, 624 pp.
- Gjørv, Odd E. (1995). "Effect of Condensed Silica Fume on Steel Corrosion in Concrete," *ACI Materials Journal*, ACI, Vol. 92, No.6, Nov.-Dec., pp. 591-598.
- Halvorsen, Grant T. (1993). "Bridge Deck Overlays," *Concrete Construction*, Vol. 30, No. 6, June, pp. 415-419
- Halvorsen, Grant T. (1993). "Concrete Cover," *Concrete Construction*, Vol. 38, No. 6, June, pp. 427-429.
- Halvorsen, Grant T. (1993). "Troubleshooting Concrete Cracking During Construction," *Concrete Construction*, Vol. 38, No. 10, Oct., pp. 700-710.
- Haque, M.N. (1998). "Give it a Week: 7 Days Initial Curing," *Concrete International*, Vol. 20, No. 9, Sept., pp. 45-48.
- Hernon, Peter (1991). *Statistics: A Component of the Research Process*. Ablex Publishing Corporation, Norwood, New Jersey, 198 pp.
- Holland, Terrence C. (1988). "Practical Considerations for Using Silica Fume in Field Concrete," *Transportation Research Record*, Transportation Research Board, Washington, D.C., No. 1204, pp. 1-7.

Ketcham, Kirk W.; Romero, Francisco A.; Darwin, David; Gong, Shanglong; Abou-Zeid, Mohamed Nagib; and Martin, Jeffrey L. (1993). "Automated Crack Identification for Cement Paste," *SM Report* No. 34, The University of Kansas Center for Research Inc., Lawrence, KS, 75 pp.

Kurtis, Kimberly E., and Mehta, Kumar (1997). "A Critical Review of Deterioration of Concrete Due to Corrosion of Reinforcing Steel," *Proceedings, CANMET/ACI Fourth International Conference on the Durability of Concrete*, Sydney, Australia, ed. Malhotra, V.M., SP-170-27, ACI, Farmington Hills, Michigan, pp. 535-554.

Lundy, James R., and Sujjavanich, Suvimol (1997). "Latex and Microsilica Modified Concrete Bridge Deck Overlays in Oregon," *Report* Department of Civil, Construction and Environmental Engineering Oregon State University, Corvallis, OR, 24 pp.

Luther, Mark D. (1993). "Silica Fume (Microsilica) Concrete in Bridge," *Concrete International*, Vol. 15, No. 4, April, pp. 29-33.

Luther, Mark D. "Silica-Fume (Microsilica) Concrete in Bridges in the United States," *Transportation Research Record*, Transportation Research Board, Washington, D.C., No. 1204, pp. 11-20.

Malhotra, V.M. (1993). "Fly Ash, Slag, Silica Fume and Rice-Husk Ash in Concrete: A Review," *Concrete International*, Vol. 15, No. 4, April, pp. 23-28.

McDonald, D.B.; Krauss, P.D.; and Rogalla, E.A. (1995). "Early Age Transverse Deck Cracking," *Concrete International*, Vol. 17, No. 5, May, pp. 49-51

McDonald, D.B.; Pfeifer, D.W.; and Sherman, M.R. (1998). "Corrosion Evaluation of Epoxy-Coated Metallic-Clad and Solid Metallic Reinforcing Bars in Concrete," Publication No. FHWA-RD-98-153, *Federal Highway Administration*, McLean, VA, 127 pp.

McGrath, Patrick F., and Hooton, Doug R. (1999). "Re-evaluation of the AASHTO T259 90-day Salt Ponding Test," *Cement and Concrete Research*, Pergamon, Special Issue: Papers Presented at the *Engineering Foundation International Conference on Advances in Cement and Concrete*, Banff, Alberta, Canada, July 5-10, pp. 1239-1248.

Ozyildirim, Celik (1988). "Experimental Installation of a Concrete Bridge-Deck Overlay Containing Silica Fume," *Transportation Research Record*, Transportation Research Board, Washington, D.C., No. 1204, pp. 36-41.

Ozyildirim, C. (1992) "Concrete Bridge-Deck Overlays Containing Silica Fume," *Proceedings, CANMET/ACI Fourth International Conference on the Use of Fly Ash, Silica Fume, Slag, and Natural Pozzolans*, Istanbul, Turkey, ed. V.M. Malhotra, SP-132-69, American Concrete Institute, Detroit, pp. 1287-1303.

Perenchi, William F. (1993). "Queries on Concrete: Cracks in Deck Slabs," *Concrete International*, Vol. 15, No. 2, Feb., pp. 87-88.

Rocole, Larry (1993). "Silica-fume Concrete Proves to be an Economical Alternative," *Concrete Construction*, Vol. 30, No. 6, June, pp. 441-442.

Rogalla, E.A.; Krauss, P.D.; and McDonald, D.B. (1995). "Reducing Transverse Cracking in New Concrete Bridge Decks." *Concrete Construction*, Vol. 40, No. 9, Sep., pp. 735-738.

Thomas, M.D.A.; Cail, K.; and Hooton, R.D. (1998). "Development and Field Applications of Silica Fume Concrete in Canada: a Retrospective," *Canadian Journal of Civil Engineering*, National Research Council of Canada, Vol. 25, No. 3, June, pp. 391-400.

Weil, Thomas G. (1988). "Addressing Parking Garage Corrosion with Silica Fume," *Transportation Research Record*, Transportation Research Board, Washington, D.C., No. 1204, pp. 8-10.

Whiting, D. and Dzedzic, W. (1989). "Chloride Permeabilities of Rigid Concrete Bridge Deck Overlays," *Transportation Research Record*, Transportation Research Board, Washington, D.C., No. 1234, pp. 24-29.

Whiting, David. (1991) "Effect of Rigid Overlays on Corrosion Rate of Reinforcing Steel in Concrete Bridge Decks," *Construction Technology Laboratories, Inc.*, Skokie, IL, 39 pp.

Zemajtis, Jerzy; Weyers, Richard E.; and Sprinkel, Michael M. (1998). "Corrosion Protection Service Life of Low-Permeable Concretes and Low-Permeable Concrete with a Corrosion Inhibitor," *Transportation Research Record*, Transportation Research Board, Washington, D.C., No. 1642, pp. 51-59.

Table 3.1: Student's t-test for entire bridge crack density versus bridge age

		Confidence Interval		80%	90%	95%	98%				
Silica Fume Overlays		t calc	α :	t table							
Age (months)				0.2	0.1	0.05	0.02				
10	30	2.4872		1.33338	Y	1.73961	Y	2.10982	Y	2.56694	N
10	>40	7.5065		1.38303	Y	1.83311	Y	2.26216	Y	2.82143	Y
30	>40	4.6275		1.35622	Y	1.78229	Y	2.17881	Y	2.68099	Y
Conventional Overlays		t calc	α :	0.2	0.1	0.05	0.02				
30	90	1.6589		1.30774	Y	1.69236	N	2.03452	N	2.44479	N
Monolithic Bridge Decks		t calc	α :	0.2	0.1	0.05	0.02				
30	90	0.9300		1.33676	N	1.74588	N	2.1199	N	2.58349	N

Key:

t calc = calculated value of t; t table = value from Student's t-distribution for the given value of α

α = level of significance

Y = statistically significant difference, i.e. null hypothesis rejected

N = not statistically significant difference, i.e. null hypothesis not rejected

Table 3.2: Student's t-test entire bridge crack density versus date of construction

		Confidence Interval		80%	90%	95%	98%			
Silica Fume Overlays				t table						
Date of Construction	t calc	α :	0.2	0.1	0.05	0.02				
1990-1991 1995-1996	4.7142		1.35622	Y	1.78229	Y	2.17881	Y	2.68099	Y
1990-1991 1997-1998	6.9104		1.37218	Y	1.81246	Y	2.22814	Y	2.76377	Y
1995-1996 1997-1998	2.2229		1.33676	Y	1.74588	Y	2.1199	Y	2.58349	N
Conventional Overlays										
Date of Construction	t calc	α :	0.2	0.1	0.05	0.02				
1985-1987 1990-1992	3.3817		1.3137	Y	1.70329	Y	2.05183	Y	2.47266	Y
1985-1987 1993-1995	3.9101		1.41492	Y	1.89458	Y	2.36462	Y	2.99795	Y
1990-1992 1993-1995	2.6122		1.31784	Y	1.71088	Y	2.0639	Y	2.49216	Y
Monolithic Bridge Decks										
Date of Construction	t calc	α :	0.2	0.1	0.05	0.02				
1984-1987 1989-1993	2.4993		1.34503	Y	1.76131	Y	2.14479	Y	2.62449	N

Key:

t calc = calculated value of t; t table = value from Student's t-distribution for the given value of α

α = level of significance

Y = statistically significant difference, i.e. null hypothesis rejected

N = not statistically significant difference, i.e. null hypothesis not rejected

Table 3.3: Student's t-test for coulomb results for individual placements versus deck type

Test Result (Coulombs)		Confidence Interval		80%	90%	95%	98%				
		t calc	α :	t table 0.2	0.1	0.05	0.02				
SFO	CO	4.0629		1.29359	Y	1.6666	Y	1.99394	Y	2.38002	Y
SFO	Mono	4.9546		1.30308	Y	1.68385	Y	2.02107	Y	2.42326	Y
CO	Mono	1.9376		1.30485	Y	1.68709	Y	2.02619	N	2.43144	N
30 min x 12 result											
Test Result (Coulombs)		t calc	α :	0.2	0.1	0.05	0.02				
SFO	CO	4.5821		1.29359	Y	1.6666	Y	1.99394	Y	2.38002	Y
SFO	Mono	4.5542		1.30308	Y	1.68385	Y	2.02107	Y	2.42326	Y
CO	Mono	3.1178		1.30485	Y	1.68709	Y	2.02619	Y	2.43144	Y

Key:

t calc = calculated value of t; t table = value from Student's t-distribution for the given value of α

α = level of significance

Y = statistically significant difference, i.e. null hypothesis rejected

N = not statistically significant difference, i.e. null hypothesis not rejected

SFO = silica fume overlay; CO = conventional overlay; Mono = Monolithic Bridge Deck

Table 3.4: Student's t-test for mean effective diffusion coefficient of individual placements versus deck type

		Confidence Interval		80%	90%	95%	98%				
All Bridges		t calc	α :	t table							
Deck Type				0.2	0.1	0.05	0.02				
SFO	CO	3.3817		1.29394	Y	1.66724	Y	1.99494	Y	2.38161	Y
Age > 500 days		t calc	α :	0.2	0.1	0.05	0.02				
SFO	CO	0.7958		1.29804	N	1.67469	N	2.00665	N	2.40023	N
Age 500 - 1500 days		t calc	α :	0.2	0.1	0.05	0.02				
SFO	CO	1.4839		1.31635	Y	1.70814	N	2.05954	N	2.4851	N
Age 900-1500 days		t calc	α :	0.2	0.1	0.05	0.02				
SFO	CO	0.9465		1.35017	N	1.77093	N	2.16037	N	2.6503	N

Key:

t calc = calculated value of t; t table = value from Student's t-distribution for the given value of α

α = level of significance

Y = statistically significant difference, i.e. null hypothesis rejected

N = not statistically significant difference, i.e. null hypothesis not rejected

SFO = silica fume overlay; CO = conventional overlay

Table 3.5: Student's t-test for mean effective diffusion coefficient for individual placements versus concrete slump

Silica Fume Overlays Slump (mm)		Confidence Interval		80%	90%	95%	98%				
		t calc	α :	t table 0.2	0.1	0.05	0.02				
38	51	0.5650		1.43976	N	1.94318	N	2.44691	N	3.14267	N
38	64	1.7638		1.47588	Y	2.01505	N	2.57058	N	3.36493	N
38	76	0.5569		1.53321	N	2.13185	N	2.77645	N	3.74694	N
38	>90	0.4416		1.63775	N	2.35336	N	3.18245	N	4.54071	N
51	64	1.3017		1.41492	N	1.89458	N	2.36462	N	2.99795	N
51	76	0.9600		1.43976	N	1.94318	N	2.44691	N	3.14267	N
51	>90	0.0246		1.41492	N	1.89458	N	2.36462	N	2.99795	N
64	76	1.7786		1.47588	Y	2.01505	N	2.57058	N	3.36493	N
64	>90	1.0019		1.43976	N	1.94318	N	2.44691	N	3.14267	N
76	>90	0.7629		1.47588	N	2.01505	N	2.57058	N	3.36493	N

Table 3.5 (cont.): Student's t-test for mean effective diffusion coefficient for individual placements versus concrete slump

Conventional Overlays		t calc	α :	0.2		0.1		0.05		0.02	
Slump (mm)											
0	6	1.0823		1.36343	N	1.79588	N	2.20099	N	2.71808	N
0	13	0.1771		1.34503	N	1.76131	N	2.14479	N	2.62449	N
0	19	0.0445		1.39682	N	1.85955	N	2.30601	N	2.89647	N
6	13	0.8204		1.35017	N	1.77093	N	2.16037	N	2.6503	N
6	19	1.1094		1.41492	N	1.89458	N	2.36462	N	2.99795	N
13	19	0.1759		1.37218	N	1.81246	N	2.22814	N	2.76377	N

Key:

t calc = calculated value of t; t table = value from Student's t-distribution for the given value of α

α = level of significance

Y = statistically significant difference, i.e. null hypothesis rejected

N = not statistically significant difference, i.e. null hypothesis not rejected

Table 3.6: Student's t-test for mean RCPT results for individual placements versus concrete slump

Silica Fume Overlays Slump (mm)		Confidence Interval		80%	90%	95%	98%				
		t calc	α :	t table 0.2	0.1	0.05	0.02				
26	38	0.6692		1.47588	N	2.01505	N	2.57058	N	3.36493	N
26	51	0.9349		1.35017	N	1.77093	N	2.16037	N	2.6503	N
26	64	1.1573		1.43976	N	1.94318	N	2.44691	N	3.14267	N
26	76	2.4400		1.41492	Y	1.89458	Y	2.36462	Y	2.99795	N
26	>90	1.3583		1.53321	N	2.13185	N	2.77645	N	3.74694	N
38	51	0.9557		1.33676	N	1.74588	N	2.1199	N	2.58349	N
38	64	0.6693		1.38303	N	1.83311	N	2.26216	N	2.82143	N
38	76	2.4433		1.37218	Y	1.81246	Y	2.22814	Y	2.76377	N
38	>90	1.9169		1.41492	Y	1.89458	Y	2.36462	N	2.99795	N
51	64	0.5913		1.33338	N	1.73961	N	2.10982	N	2.56694	N
51	76	0.6322		1.33039	N	1.73406	N	2.10092	N	2.55238	N
51	>90	1.5560		1.34061	Y	1.75305	N	2.13145	N	2.60248	N
64	76	1.8314		1.36343	Y	1.79588	Y	2.20099	N	2.71808	N
64	>90	1.8196		1.39682	Y	1.85955	N	2.30601	N	2.89647	N
76	>90	1.1763		1.38303	N	1.83311	N	2.26216	N	2.82143	N

Table 3.6 (cont.): Student's t-test for mean RCPT results for individual placements versus concrete slump

Conventional Overlays		t calc	α :	0.2		0.1		0.05		0.02	
Slump (mm)											
0	6	0.7617		1.36343	N	1.79588	N	2.20099	N	2.71808	N
0	13	0.3769		1.34503	N	1.76131	N	2.14479	N	2.62449	N
0	19	2.0215		1.39682	Y	1.85955	Y	2.30601	N	2.89647	N
6	13	0.6155		1.35017	N	1.77093	N	2.16037	N	2.6503	N
6	19	2.0450		1.41492	Y	1.89458	Y	2.36462	N	2.99795	N
13	19	1.9296		1.37218	Y	1.81246	Y	2.22814	N	2.76377	N

Key:

t calc = calculated value of t; t table = value from Student's t-distribution for the given value of α

α = level of significance

Y = statistically significant difference, i.e. null hypothesis rejected

N = not statistically significant difference, i.e. null hypothesis not rejected

Table 3.7: Student's t-test for mean crack density versus concrete slump

Silica Fume Overlays Slump (mm)		Confidence Interval		80%		90%		95%		98%	
		t calc	α :	0.2		0.1		0.05		0.02	
26	38	0.7181		1.47588	N	2.01505	N	2.57058	N	3.36493	N
26	51	0.2796		1.35017	N	1.77093	N	2.16037	N	2.6503	N
26	64	0.1716		1.43976	N	1.94318	N	2.44691	N	3.14267	N
26	76	0.5864		1.41492	N	1.89458	N	2.36462	N	2.99795	N
26	>90	2.0040		1.53321	Y	2.13185	N	2.77645	N	3.74694	N
38	51	0.9284		1.33676	N	1.74588	N	2.1199	N	2.58349	N
38	64	1.4255		1.38303	Y	1.83311	N	2.26216	N	2.82143	N
38	76	0.1647		1.37218	N	1.81246	N	2.22814	N	2.76377	N
38	>90	0.9878		1.41492	N	1.89458	N	2.36462	N	2.99795	N
51	64	0.7268		1.33338	N	1.73961	N	2.10982	N	2.56694	N
51	76	0.7558		1.33039	N	1.73406	N	2.10092	N	2.55238	N
51	>90	2.2167		1.34061	Y	1.75305	Y	2.13145	Y	2.60248	N
64	76	1.1997		1.36343	N	1.79588	N	2.20099	N	2.71808	N
64	>90	3.3624		1.39682	Y	1.85955	Y	2.30601	Y	2.89647	Y
76	>90	1.1180		1.38303	N	1.83311	N	2.26216	N	2.82143	N

Table 3.7 (cont.): Student's t-test for mean crack density versus concrete slump

Conventional Overlays		t calc	α:	0.2		0.1		0.05		0.02	
Slump (mm)											
0	3	5.0128		1.35017	Y	1.77093	Y	2.16037	Y	2.6503	Y
0	6	2.8231		1.31497	Y	1.70562	Y	2.05553	Y	2.47863	Y
0	13	0.9138		1.32124	N	1.71714	N	2.07388	N	2.50832	N
0	19	1.6506		1.33039	Y	1.73406	N	2.10092	N	2.55238	N
3	6	1.2575		1.34061	N	1.75305	N	2.13145	N	2.60248	N
3	13	2.0033		1.36343	Y	1.79588	Y	2.20099	N	2.71808	N
3	19	1.0889		1.41492	N	1.89458	N	2.36462	N	2.99795	N
6	13	1.4335		1.31784	Y	1.71088	N	2.0639	N	2.49216	N
6	19	0.3549		1.32534	N	1.72472	N	2.08596	N	2.52798	N
13	19	0.6999		1.33676	N	1.74588	N	2.1199	N	2.58349	N

Monolithic Bridge Decks		t calc	α:	0.2		0.1		0.05		0.02	
Slump (mm)											
38	51	0.7481		1.31784	N	1.71088	N	2.0639	N	2.49216	N
38	64	1.8593		1.38303	Y	1.83311	Y	2.26216	N	2.82143	N
38	76	3.7754		1.47588	Y	2.01505	Y	2.57058	Y	3.36493	Y
51	64	1.0094		1.31635	N	1.70814	N	2.05954	N	2.4851	N
51	76	1.7403		1.32319	Y	1.72074	Y	2.07961	N	2.51765	N
64	76	1.3262		1.43976	N	1.94318	N	2.44691	N	3.14267	N

Table 3.7 (cont.): Student's t-test for mean crack density versus concrete slump

Bridge Subdecks		t calc	α :	0.2		0.1		0.05		0.02	
Slump (mm)											
38	51	0.4480		1.31946	N	1.71387	N	2.06865	N	2.49987	N
38	64	1.1846		1.32773	N	1.72913	N	2.09302	N	2.53948	N
38	76	0.5017		1.39682	N	1.85955	N	2.30601	N	2.89647	N
51	64	0.4706		1.30551	N	1.6883	N	2.02809	N	2.4345	N
51	76	0.0899		1.31635	N	1.70814	N	2.05954	N	2.4851	N
64	76	0.2600		1.32319	N	1.72074	N	2.07961	N	2.51765	N

Key:

t calc = calculated value of t; t table = value from Student's t-distribution for the given value of α

α = level of significance

Y = statistically significant difference, i.e. null hypothesis rejected

N = not statistically significant difference, i.e. null hypothesis not rejected

Table 3.8: Student's t-test for mean effective diffusion coefficient for individual placements versus percent volume of water, cement, and silica fume

Silica Fume Overlays (% Volume)		Confidence Interval		80%	90%	95%	98%				
		t calc	α :	t table 0.2	0.1	0.05	0.02				
26.0	26.8	1.3356		1.31635	Y	1.70814	N	2.05954	N	2.4851	N
Conventional Overlays (% Volume)		t calc	α :	0.2	0.1	0.05	0.02				
25.1	25.9	1.9058		1.31143	Y	1.69913	Y	2.04523	N	2.46202	N
25.1	26.6	0.9341		1.31497	N	1.70562	N	2.05553	N	2.47863	N
25.9	26.6	2.1472		1.38303	Y	1.83311	Y	2.26216	N	2.82143	N

Key:

t calc = calculated value of t; t table = value from Student's t-distribution for the given value of α

α = level of significance

Y = statistically significant difference, i.e. null hypothesis rejected

N = not statistically significant difference, i.e. null hypothesis not rejected

Table 3.9: Student's t-test for mean RCPT results for individual placements versus percent volume of water, cement, and silica fume

Silica Fume Overlays (% Volume)		Confidence Interval		80%	90%	95%	98%				
		t calc	α :	t table 0.2	0.1	0.05	0.02				
26.0	26.8	3.3296		1.30551	Y	1.6883	Y	2.02809	Y	2.4345	Y
Conventional Overlays (% Volume)		t calc	α :	0.2	0.1	0.05	0.02				
				0.2	0.1	0.05	0.02				
25.1	25.9	0.9726		1.31143	N	1.69913	N	2.04523	N	2.46202	N
25.1	26.6	3.3343		1.31497	Y	1.70562	Y	2.05553	Y	2.47863	Y
25.9	26.6	2.8686		1.38303	Y	1.83311	Y	2.26216	Y	2.82143	Y

Key:

t calc = calculated value of t; t table = value from Student's t-distribution for the given value of α

α = level of significance

Y = statistically significant difference, i.e. null hypothesis rejected

N = not statistically significant difference, i.e. null hypothesis not rejected

Table 3.10 : Student's t-test for mean crack density for individual placements versus percent volume of water and cement and silica fume

Silica Fume Overlays (% Volume)		Confidence Interval		80%		90%		95%		98%	
		t calc	α :	t table 0.2	0.1	0.05	0.02				
26.0	26.8	0.7874		1.30551	N	1.6883	N	2.02809	N	2.4345	N
Conventional Overlays (% Volume)		t calc	α :	0.2	0.1	0.05	0.02				
25.1	26.0	2.1665		1.29944	Y	1.67722	Y	2.01063	Y	2.40658	N
25.1	26.6	3.1340		1.30308	Y	1.68385	Y	2.02107	Y	2.42326	Y
26.0	26.6	0.7371		1.32124	N	1.71714	N	2.07388	N	2.50832	N
Monolithic Bridge Decks (% Volume)		t calc	α :	0.2	0.1	0.05	0.02				
26	27	0.6830		1.31784	N	1.71088	N	2.0639	N	2.49216	N
26	28	2.8661		1.37218	Y	1.81246	Y	2.22814	Y	2.76377	Y
26	29	7.0408		1.35622	Y	1.78229	Y	2.17881	Y	2.68099	Y
27	28	4.0786		1.32534	Y	1.72472	Y	2.08596	Y	2.52798	Y
27	29	7.1526		1.32124	Y	1.71714	Y	2.07388	Y	2.50832	Y
28	29	0.0488		1.39682	N	1.85955	N	2.30601	N	2.89647	N

Table 3.10 (cont.): Student's t-test for mean crack density for individual placements versus percent volume of water and cement and silica fume

Bridge Subdecks (% Volume)		t calc	α :	0.2	0.1	0.05	0.02
26	27	0.5121		1.30551 N	1.6883 N	2.02809 N	2.4345 N
26	28	0.9739		1.53321 N	2.13185 N	2.77645 N	3.74694 N
26	29	2.1760		1.53321 Y	2.13185 Y	2.77645 N	3.74694 N
26	30	9.9721		1.53321 Y	2.13185 Y	2.77645 Y	3.74694 Y
27	28	0.1801		1.30423 N	1.68595 N	2.02439 N	2.42857 N
27	29	1.5894		1.30423 Y	1.68595 N	2.02439 N	2.42857 N
27	30	1.7433		1.30423 Y	1.68595 Y	2.02439 N	2.42857 N
28	29	1.5554		1.43976 Y	1.94318 N	2.44691 N	3.14267 N
28	30	2.5763		1.43976 Y	1.94318 Y	2.44691 Y	3.14267 N
29	30	0.1701		1.43976 N	1.94318 N	2.44691 N	3.14267 N

Key:

t calc = calculated value of t; t table = value from Student's t-distribution for the given value of α

α = level of significance

Y = statistically significant difference, i.e. null hypothesis rejected

N = not statistically significant difference, i.e. null hypothesis not rejected

Table 3.11: Student's t-test for mean effective diffusion coefficient for individual placements versus water content

		Confidence Interval		80%	90%	95%	98%				
Silica Fume Overlays		t calc	α :	t table							
Water (kg/m ³)				0.2	0.1	0.05	0.02				
141	148	1.3532		1.33338	Y	1.73961	N	2.10982	N	2.56694	N
Conventional Overlays		t calc	α :	0.2	0.1	0.05	0.02				
Water (kg/m ³)											
133	139	1.9058		1.31143	Y	1.69913	Y	2.04523	N	2.46202	N
133	145	0.9341		1.31497	N	1.70562	N	2.05553	N	2.47863	N
139	145	2.1472		1.38303	Y	1.83311	Y	2.26216	N	2.82143	N

Key:

t calc = calculated value of t; t table = value from Student's t-distribution for the given value of α

α = level of significance

Y = statistically significant difference, i.e. null hypothesis rejected

N = not statistically significant difference, i.e. null hypothesis not rejected

Table 3.12: Student's t-test for mean RCPT results for individual placements versus water content

Silica Fume Overlays		Confidence Interval		80%		90%		95%		98%	
		t calc	α :	t table							
Water (kg/m ³)				0.2		0.1		0.05		0.02	
141	148	3.3296		1.30551	Y	1.6883	Y	2.02809	Y	2.4345	Y
Conventional Overlays											
Water (kg/m ³)		t calc	α :	0.2		0.1		0.05		0.02	
133	139	0.9726		1.31143	N	1.69913	N	2.04523	N	2.46202	N
133	145	3.3343		1.31497	Y	1.70562	Y	2.05553	Y	2.47863	Y
139	145	2.8686		1.38303	Y	1.83311	Y	2.26216	Y	2.82143	Y

Key:

t calc = calculated value of t; t table = value from Student's t-distribution for the given value of α

α = level of significance

Y = statistically significant difference, i.e. null hypothesis rejected

N = not statistically significant difference, i.e. null hypothesis not rejected

Table 3.13: Student's t-test for mean crack density for individual placements versus water content

		Confidence Interval		80%	90%	95%	98%				
Silica Fume Overlays		t calc	α :	t table							
Water (kg/m ³)				0.2	0.1	0.05	0.02				
141.0	148.0	0.7874		1.30551	N	1.6883	N	2.02809	N	2.4345	N
Conventional Overlays		t calc	α :	0.2	0.1	0.05	0.02				
Water (kg/m ³)											
133	139	1.2376		1.30065	N	1.67943	N	2.0141	N	2.41212	N
133	145	4.3679		1.30155	Y	1.68107	Y	2.01669	Y	2.41625	Y
139	145	2.0458		1.32124	Y	1.71714	Y	2.07388	N	2.50832	N
Monolithic Bridge Decks		t calc	α :	0.2	0.1	0.05	0.02				
Water (kg/m ³)											
147	156	2.1403		1.31784	Y	1.71088	Y	2.0639	Y	2.49216	N
147	165	5000000		1.37218	Y	1.81246	Y	2.22814	Y	2.76377	Y
156	165	2.3978		1.35622	Y	1.78229	Y	2.17881	Y	2.68099	N

Table 3.13 (cont.): Student's t-test for mean crack density for individual placements versus water content

Bridge Subdecks		t calc	α :	0.2		0.1		0.05		0.02	
Water (kg/m ³)											
147	156	0.5914		1.30485	N	1.68709	N	2.02619	N	2.43144	N
147	165	1.3489		1.38303	N	1.83311	N	2.26216	N	2.82143	N
147	174	6.2727		1.88562	Y	2.91999	Y	4.30266	Y	6.96455	N
156	165	1.0980		1.30109	N	1.68023	N	2.01537	N	2.41414	N
156	174	1.1043		1.30485	N	1.68709	N	2.02619	N	2.43144	N
165	174	0.6548		1.38303	N	1.83311	N	2.26216	N	2.82143	N

Key:

t calc = calculated value of t; t table = value from Student's t-distribution for the given value of α

α = level of significance

Y = statistically significant difference, i.e. null hypothesis rejected

N = not statistically significant difference, i.e. null hypothesis not rejected

Table 3.14: Student's t-test for mean crack density for individual placements versus cement content

Monolithic Bridge Decks		Confidence Interval		80% t table		90%		95%		98%	
Cement (kg/m³)		t calc	α:	0.2	0.1	0.05	0.02				
357&359	379	6.2585		1.30857	Y	1.69389	Y	2.03693	Y	2.44868	Y
Bridge Subdecks		t calc	α:	0.2	0.1	0.05	0.02				
357&359	379&390	1.2789		1.30109	N	1.68023	N	2.01537	N	2.41414	N
357&359	413	1.8097		1.30308	Y	1.68385	Y	2.02107	N	2.42326	N
379&390	413	1.1401		1.37218	N	1.81246	N	2.22814	N	2.76377	N

Key:

t calc = calculated value of t; t table = value from Student's t-distribution for the given value of α

α = level of significance

Y = statistically significant difference, i.e. null hypothesis rejected

N = not statistically significant difference, i.e. null hypothesis not rejected

Table 3.15: Student's t-test for mean effective diffusion coefficient for individual placements versus water/cementitious material ratio

Silica Fume Overlays (w/cm)		Confidence Interval		80%	90%	95%	98%				
		t calc	α :	t table 0.2	0.1	0.05	0.02				
0.38	0.40	1.3532		1.33338	Y	1.73961	N	2.10982	N	2.56694	N
Conventional Overlays (w/cm)		t calc	α :	0.2	0.1	0.05	0.02				
				0.2	0.1	0.05	0.02				
0.36	0.38	1.9058		1.31143	Y	1.69913	Y	2.04523	N	2.46202	N
0.36	0.40	0.9341		1.31497	N	1.70562	N	2.05553	N	2.47863	N
0.38	0.40	2.1472		1.38303	Y	1.83311	Y	2.26216	N	2.82143	N

Key:

t calc = calculated value of t; t table = value from Student's t-distribution for the given value of α

α = level of significance

Y = statistically significant difference, i.e. null hypothesis rejected

N = not statistically significant difference, i.e. null hypothesis not rejected

w/cm = water to cementitious material ratio

Table 3.16: Student's t-test for mean RCPT results for individual placements versus water/cementitious material ratio

Silica Fume Overlays (w/cm)		Confidence Interval		80%		90%		95%		98%	
		t calc	α :	t table 0.2	0.1	0.05	0.02				
0.38	0.40	3.3296		1.30551	Y	1.6883	Y	2.02809	Y	2.4345	Y
Conventional Overlays (w/cm)		t calc	α :	0.2	0.1	0.05	0.02				
0.36	0.38	0.9726		1.31143	N	1.69913	N	2.04523	N	2.46202	N
0.36	0.40	3.3343		1.31497	Y	1.70562	Y	2.05553	Y	2.47863	Y
0.38	0.40	2.8686		1.38303	Y	1.83311	Y	2.26216	Y	2.82143	Y

Key:

t calc = calculated value of t; t table = value from Student's t-distribution for the given value of α

α = level of significance

Y = statistically significant difference, i.e. null hypothesis rejected

N = not statistically significant difference, i.e. null hypothesis not rejected

w/cm = water to cementitious material ratio

Table 3.17: Student's t-test for mean crack density for individual placements versus water/cementitious material ratio

		Confidence Interval		80%	90%	95%	98%				
Silica Fume Overlays		t calc	α :	t table							
(w/cm)				0.2	0.1	0.05	0.02				
0.38	0.40	0.7874		1.30551	N	1.6883	N	2.02809	N	2.4345	N
Conventional Overlays		t calc	α :	0.2	0.1	0.05	0.02				
(w/cm)											
0.36	0.38	2.1665		1.29944	Y	1.67722	Y	2.01063	Y	2.40658	N
0.36	0.40	3.1340		1.30308	Y	1.68385	Y	2.02107	Y	2.42326	Y
0.38	0.40	0.7371		1.32124	N	1.71714	N	2.07388	N	2.50832	N
Monolithic Bridge Decks		t calc	α :	0.2	0.1	0.05	0.02				
(w/cm)											
0.42	0.44	0.2394		1.30774	N	1.69236	N	2.03452	N	2.44479	N

Table 3.17 (cont.): Student's t-test for mean crack density for individual placements versus water/cementitious material ratio

Bridge Subdecks		t calc	α:	0.2		0.1		0.05		0.02	
(w/cm)											
0.40	0.42	0.4534		1.38303	N	1.83311	N	2.26216	N	2.82143	N
0.40	0.44	0.5491		1.30203	N	1.68195	N	2.01808	N	2.41847	N
0.42	0.44	1.0797		1.30155	N	1.68107	N	2.01669	N	2.41625	N

Key:

t calc = calculated value of t; t table = value from Student's t-distribution for the given value of α

α = level of significance

Y = statistically significant difference, i.e. null hypothesis rejected

N = not statistically significant difference, i.e. null hypothesis not rejected

w/cm = water to cementitious material ratio

Table 3.18: Student's t-test for mean effective diffusion coefficient for individual placements versus air content

Silica Fume Overlays		Confidence Interval			80%		90%		95%		98%	
		Air (%)	t calc	α :	t table		t table		t table		t table	
Air (%)		t calc	α :	0.2		0.1		0.05		0.02		
4.5	5.5	0.5691		1.35017	N	1.77093	N	2.16037	N	2.6503	N	
4.5	6.5	1.2616		1.41492	N	1.89458	N	2.36462	N	2.99795	N	
5.5	6.5	0.6799		1.37218	N	1.81246	N	2.22814	N	2.76377	N	
Conventional Overlays		t calc	α :	0.2		0.1		0.05		0.02		
Air (%)		t calc	α :	0.2		0.1		0.05		0.02		
4.375	5.125	0.0519		1.38303	N	1.83311	N	2.26216	N	2.82143	N	
4.375	5.875	0.3819		1.35622	N	1.78229	N	2.17881	N	2.68099	N	
4.375	6.625	1.5464		1.47588	Y	2.01505	N	2.57058	N	3.36493	N	
5.125	5.875	0.5661		1.34061	N	1.75305	N	2.13145	N	2.60248	N	
5.125	6.625	2.0992		1.39682	Y	1.85955	Y	2.30601	N	2.89647	N	
5.875	6.625	1.5927		1.36343	Y	1.79588	N	2.20099	N	2.71808	N	

Key:

t calc = calculated value of t; t table = value from Student's t-distribution for the given value of α

α = level of significance

Y = statistically significant difference, i.e. null hypothesis rejected

N = not statistically significant difference, i.e. null hypothesis not rejected

Table 3.19: Student's t-test for mean RCPT results for individual placements versus air content

		Confidence Interval		80%	90%	95%	98%
Silica Fume Overlays				t table			
Air (%)		t calc	α :	0.2	0.1	0.05	0.02
4.5	5.5	0.5402		1.31497 N	1.70562 N	2.05553 N	2.47863 N
4.5	6.5	1.2145		1.35017 N	1.77093 N	2.16037 N	2.6503 N
5.5	6.5	1.1909		1.31946 N	1.71387 N	2.06865 N	2.49987 N
Conventional Overlays							
Air (%)		t calc	α :	0.2	0.1	0.05	0.02
4.375	5.125	0.3972		1.38303 N	1.83311 N	2.26216 N	2.82143 N
4.375	5.875	0.1959		1.35622 N	1.78229 N	2.17881 N	2.68099 N
4.375	6.625	1.1562		1.47588 N	2.01505 N	2.57058 N	3.36493 N
5.125	5.875	0.0560		1.34061 N	1.75305 N	2.13145 N	2.60248 N
5.125	6.625	1.4806		1.39682 Y	1.85955 N	2.30601 N	2.89647 N
5.875	6.625	1.5520		1.36343 Y	1.79588 N	2.20099 N	2.71808 N

Key:

t calc = calculated value of t; t table = value from Student's t-distribution for the given value of α

α = level of significance

Y = statistically significant difference, i.e. null hypothesis rejected

N = not statistically significant difference, i.e. null hypothesis not rejected

Table 3.20: Student's t-test for mean crack density for individual placements versus air content

			Confidence Interval		80%		90%		95%		98%	
Silica Fume Overlays			t calc	α :	t table							
Air (%)					0.2	0.1	0.05	0.02				
4.5	5.5		0.2599		1.31497	N	1.70562	N	2.05553	N	2.47863	N
4.5	6.5		0.5607		1.34061	N	1.75305	N	2.13145	N	2.60248	N
5.5	6.5		0.5507		1.33039	N	1.73406	N	2.10092	N	2.55238	N
Conventional Overlays			t calc	α :	0.2	0.1	0.05	0.02				
Air (%)												
4.375	5.125		0.7143		1.32319	N	1.72074	N	2.07961	N	2.51765	N
4.375	5.875		0.0237		1.31784	N	1.71088	N	2.0639	N	2.49216	N
4.375	6.625		0.1708		1.39682	N	1.85955	N	2.30601	N	2.89647	N
5.125	5.875		1.0400		1.30774	N	1.69236	N	2.03452	N	2.44479	N
5.125	6.625		0.3700		1.33338	N	1.73961	N	2.10982	N	2.56694	N
5.875	6.625		0.2157		1.32534	N	1.72472	N	2.08596	N	2.52798	N
Monolithic Bridge Decks			t calc	α :	0.2	0.1	0.05	0.02				
Air (%)												
4.875	5.625		0.1247		1.33039	N	1.73406	N	2.10092	N	2.55238	N
4.875	6.375		2.2806		1.32319	Y	1.72074	Y	2.07961	Y	2.51765	N
5.625	6.375		3.3312		1.31946	Y	1.71387	Y	2.06865	Y	2.49987	Y

Table 3.20 (cont.): Student's t-test for mean crack density versus air content

Bridge Subdecks											
Air (%)		t calc	α:	0.2		0.1		0.05		0.02	
4.125	4.875	0.5859		1.32534	N	1.72472	N	2.08596	N	2.52798	N
4.125	5.625	1.0371		1.31635	N	1.70814	N	2.05954	N	2.4851	N
4.125	6.375	1.2851		1.33676	N	1.74588	N	2.1199	N	2.58349	N
4.875	5.625	0.2886		1.3137	N	1.70329	N	2.05183	N	2.47266	N
4.875	6.375	0.7506		1.33039	N	1.73406	N	2.10092	N	2.55238	N
5.625	6.375	0.7083		1.31946	N	1.71387	N	2.06865	N	2.49987	N

Key:

t calc = calculated value of t; t table = value from Student's t-distribution for the given value of α

α = level of significance

Y = statistically significant difference, i.e. null hypothesis rejected

N = not statistically significant difference, i.e. null hypothesis not rejected

Table 3.21: Student's t-test for mean effective diffusion coefficient for individual placements versus compressive strength

Silica Fume Overlays		Confidence Interval		80%		90%		95%		98%	
		t calc	α :	t table							
Strength (MPa)				0.2		0.1		0.05		0.02	
38	45	0.5068		1.47588	N	2.01505	N	2.57058	N	3.36493	N
38	52	1.6519		1.47588	Y	2.01505	N	2.57058	N	3.36493	N
45	52	1.2702		1.39682	N	1.85955	N	2.30601	N	2.89647	N
Conventional Overlays											
Strength (MPa)		t calc	α :	0.2		0.1		0.05		0.02	
38	45	0.9041		1.35622	N	1.78229	N	2.17881	N	2.68099	N
38	52	0.1732		1.39682	N	1.85955	N	2.30601	N	2.89647	N
45	52	1.2068		1.37218	N	1.81246	N	2.22814	N	2.76377	N

Key:

t calc = calculated value of t; t table = value from Student's t-distribution for the given value of α

α = level of significance

Y = statistically significant difference, i.e. null hypothesis rejected

N = not statistically significant difference, i.e. null hypothesis not rejected

Table 3.22: Student's t-test for mean RCPT results for individual placements versus compressive strength

		Confidence Interval		80%	90%	95%	98%				
Silica Fume Overlays				t table							
Strength (MPa)		t calc	α :	0.2	0.1	0.05	0.02				
38	45	1.9533		1.39682	Y	1.85955	Y	2.30601	N	2.89647	N
38	52	1.3624		1.38303	N	1.83311	N	2.26216	N	2.82143	N
38	59	1.9436		1.41492	Y	1.89458	Y	2.36462	N	2.99795	N
45	52	1.9789		1.36343	Y	1.79588	Y	2.20099	N	2.71808	N
45	59	0.2684		1.38303	N	1.83311	N	2.26216	N	2.82143	N
52	59	2.7477		1.37218	Y	1.81246	Y	2.22814	Y	2.76377	N
Conventional Overlays											
Strength (MPa)		t calc	α :	0.2	0.1	0.05	0.02				
38	45	1.1911		1.36343	N	1.79588	N	2.20099	N	2.71808	N
38	52	1.2340		1.38303	N	1.83311	N	2.26216	N	2.82143	N
45	52	0.5954		1.37218	N	1.81246	N	2.22814	N	2.76377	N

Key:

t calc = calculated value of t; t table = value from Student's t-distribution for the given value of α

α = level of significance

Y = statistically significant difference, i.e. null hypothesis rejected

N = not statistically significant difference, i.e. null hypothesis not rejected

Table 3.23: Student's t-test for mean crack density for individual placements versus compressive strength

		Confidence Interval		80%		90%		95%		98%	
Silica Fume Overlays				t table							
Strength (MPa)		t calc	α :	0.2	0.1	0.05	0.02				
38	45	1.9580		1.39682	Y	1.85955	Y	2.30601	N	2.89647	N
38	52	1.2155		1.38303	N	1.83311	N	2.26216	N	2.82143	N
38	59	1.4342		1.41492	Y	1.89458	N	2.36462	N	2.99795	N
45	52	0.5306		1.36343	N	1.79588	N	2.20099	N	2.71808	N
45	59	0.0855		1.38303	N	1.83311	N	2.26216	N	2.82143	N
52	59	0.4885		1.37218	N	1.81246	N	2.22814	N	2.76377	N
Conventional Overlays											
Strength (MPa)		t calc	α :	0.2	0.1	0.05	0.02				
38	45	0.6980		1.30946	N	1.69552	N	2.03951	N	2.45283	N
38	52	1.2048		1.34061	N	1.75305	N	2.13145	N	2.60248	N
45	52	0.6460		1.31497	N	1.70562	N	2.05553	N	2.47863	N
Monolithic Bridge Decks											
Strength (MPa)		t calc	α :	0.2	0.1	0.05	0.02				
31	38	1.3297		1.33338	N	1.73961	N	2.10982	N	2.56694	N
31	45	2.5699		1.33039	Y	1.73406	Y	2.10092	Y	2.55238	Y
38	45	1.8697		1.31946	Y	1.71387	Y	2.06865	N	2.49987	N

Table 3.23 (cont.): Student's t-test for mean crack density for individual placements versus compressive strength

Bridge Subdecks		t calc	α :	0.2		0.1		0.05		0.02	
Strength (MPa)											
31	38	0.7186		1.34061	N	1.75305	N	2.13145	N	2.60248	N
31	45	1.4095		1.32773	Y	1.72913	N	2.09302	N	2.53948	N
31	52	0.4163		1.38303	N	1.83311	N	2.26216	N	2.82143	N
38	45	2.6049		1.31784	Y	1.71088	Y	2.0639	Y	2.49216	Y
38	52	1.1031		1.34503	N	1.76131	N	2.14479	N	2.62449	N
45	52	0.7567		1.33039	N	1.73406	N	2.10092	N	2.55238	N

Key:

t calc = calculated value of t; t table = value from Student's t-distribution for the given value of α

α = level of significance

Y = statistically significant difference, i.e. null hypothesis rejected

N = not statistically significant difference, i.e. null hypothesis not rejected

Table 3.24: Student's t-test for mean crack density for individual placements versus average air temperature

		Confidence Interval		80%		90%		95%		98%	
Silica Fume Overlays				t table							
Avg. Air Temp. (C)		t calc	α :	0.2		0.1		0.05		0.02	
5	15	0.5242		1.31946	N	1.71387	N	2.06865	N	2.49987	N
5	25	0.0522		1.32124	N	1.71714	N	2.07388	N	2.50832	N
15	25	0.6100		1.31635	N	1.70814	N	2.05954	N	2.4851	N
Conventional Overlays											
Avg. Air Temp. (C)		t calc	α :	0.2		0.1		0.05		0.02	
5	15	1.0293		1.32124	N	1.71714	N	2.07388	N	2.50832	N
5	21-30	1.3986		1.29871	Y	1.67591	N	2.00856	N	2.40327	N
15	21-30	0.9736		1.29492	N	1.66901	N	1.99773	N	2.38604	N
Monolithic Bridge Decks											
Avg. Air Temp. (C)		t calc	α :	0.2		0.1		0.05		0.02	
5	15	0.0696		1.31253	N	1.70113	N	2.04841	N	2.46714	N
5	25	0.7828		1.33338	N	1.73961	N	2.10982	N	2.56694	N
15	25	0.4933		1.32773	N	1.72913	N	2.09302	N	2.53948	N

Table 3.24 (cont.): Student's t-test for mean crack density for individual placements versus average air temperature

Bridge Subdecks		t calc	α :	0.2		0.1		0.05		0.02	
Avg. Air Temp. (C)											
5	15	0.6903		1.33338	N	1.73961	N	2.10982	N	2.56694	N
5	25	0.3392		1.30695	N	1.69092	N	2.03224	N	2.44115	N
15	25	0.5947		1.30254	N	1.68288	N	2.01954	N	2.4208	N

Key:

t calc = calculated value of t; t table = value from Student's t-distribution for the given value of α

α = level of significance

Y = statistically significant difference, i.e. null hypothesis rejected

N = not statistically significant difference, i.e. null hypothesis not rejected

Table 3.25: Student's t-test for mean crack density for individual placements versus low air temperature

		Confidence Interval		80%	90%	95%	98%				
Silica Fume Overlays		t calc	α :	t table							
Low Air Temp. (C)				0.2	0.1	0.05	0.02				
0	10	0.4963		1.3137	N	1.70329	N	2.05183	N	2.47266	N
0	20	1.3944		1.33676	Y	1.74588	N	2.1199	N	2.58349	N
10	20	1.9195		1.3137	Y	1.70329	Y	2.05183	N	2.47266	N
Conventional Overlays		t calc	α :	0.2	0.1	0.05	0.02				
0	10	1.2886		1.30774	N	1.69236	N	2.03452	N	2.44479	N
0	20	1.0759		1.30423	N	1.68595	N	2.02439	N	2.42857	N
10	20	0.2458		1.29471	N	1.66864	N	1.99714	N	2.3851	N

Table 3.25 (cont.): Student's t-test for mean crack density for individual placements versus low air temperature

Monolithic Bridge										
Decks										
Low Air Temp. (C)		t calc	α:	0.2	0.1	0.05	0.02			
0	10	0.7736		1.3137 N	1.70329 N	2.05183 N	2.47266 N			
0	20	0.6784		1.32124 N	1.71714 N	2.07388 N	2.50832 N			
10	20	0.9370		1.34061 N	1.75305 N	2.13145 N	2.60248 N			

Bridge Subdecks										
Low Air Temp. (C)		t calc	α:	0.2	0.1	0.05	0.02			
0	10	0.5750		1.31946 N	1.71387 N	2.06865 N	2.49987 N			
0	20	1.0985		1.31784 N	1.71088 N	2.0639 N	2.49216 N			
10	20	0.8849		1.30155 N	1.68107 N	2.01669 N	2.41625 N			

Key:

t calc = calculated value of t; t table = value from Student's t-distribution for the given value of α

α = level of significance

Y = statistically significant difference, i.e. null hypothesis rejected

N = not statistically significant difference, i.e. null hypothesis not rejected

Table 3.26: Student's t-test for mean crack density for individual placements versus high air temperature

		Confidence Interval		80%	90%	95%	98%				
Silica Fume Overlays				t table							
High Air Temp. (C)		t calc	α :	0.2	0.1	0.05	0.02				
15	25	1.3903		1.31497	Y	1.70562	N	2.05553	N	2.47863	N
15	35	0.1196		1.32773	N	1.72913	N	2.09302	N	2.53948	N
25	35	1.1641		1.31946	N	1.71387	N	2.06865	N	2.49987	N
Conventional Overlays											
High Air Temp. (C)		t calc	α :	0.2	0.1	0.05	0.02				
15	25	2.9946		1.30551	Y	1.6883	Y	2.02809	Y	2.4345	Y
15	35	2.3147		1.30308	Y	1.68385	Y	2.02107	Y	2.42326	N
25	35	0.7334		1.29632	N	1.67155	N	2.00172	N	2.39238	N
Monolithic Bridge Decks											
High Air Temp. (C)		t calc	α :	0.2	0.1	0.05	0.02				
5	15	1.0309		1.33039	N	1.73406	N	2.10092	N	2.55238	N
5	25	0.9388		1.35622	N	1.78229	N	2.17881	N	2.68099	N
5	35	1.2074		1.41492	N	1.89458	N	2.36462	N	2.99795	N
15	25	0.5178		1.31784	N	1.71088	N	2.0639	N	2.49216	N
15	35	0.4000		1.32773	N	1.72913	N	2.09302	N	2.53948	N
25	35	0.0653		1.35017	N	1.77093	N	2.16037	N	2.6503	N

Table 3.26 cont.: Student's t-test for mean crack density for individual placements versus high air temperature

Bridge Subdecks		t calc	α :	0.2		0.1		0.05		0.02	
High Air Temp. (C)											
15	25	0.3511		1.31143	N	1.69913	N	2.04523	N	2.46202	N
15	35	0.1300		1.31635	N	1.70814	N	2.05954	N	2.4851	N
25	35	0.5903		1.30308	N	1.68385	N	2.02107	N	2.42326	N

Key:

t calc = calculated value of t; t table = value from Student's t-distribution for the given value of α

α = level of significance

Y = statistically significant difference, i.e. null hypothesis rejected

N = not statistically significant difference, i.e. null hypothesis not rejected

Table 3.27: Student's t-test for mean crack density for individual placements versus daily temperature range

		Confidence Interval		80%	90%	95%	98%				
Silica Fume Overlays		t calc	α :	t table							
Temp. Range (C)				0.2	0.1	0.05	0.02				
4	12	1.0331		1.3137	N	1.70329	N	2.05183	N	2.47266	N
4	20	1.4048		1.35622	Y	1.78229	N	2.17881	N	2.68099	N
12	20	0.7256		1.30946	N	1.69552	N	2.03951	N	2.45283	N
Conventional Overlays		t calc	α :	0.2	0.1	0.05	0.02				
4	12	0.5700		1.29773	N	1.67412	N	2.00575	N	2.39879	N
4	20	0.9314		1.31635	N	1.70814	N	2.05954	N	2.4851	N
12	20	0.5143		1.29632	N	1.67155	N	2.00172	N	2.39238	N
Monolithic Bridge Decks		t calc	α :	0.2	0.1	0.05	0.02				
4	12	0.6497		1.31946	N	1.71387	N	2.06865	N	2.49987	N
4	20	0.8389		1.36343	N	1.79588	N	2.20099	N	2.71808	N
12	20	1.0779		1.31042	N	1.69726	N	2.04227	N	2.45726	N

Table 3.27 (cont.): Student's t-test for mean crack density for individual placements versus daily temperature range

Bridge Subdecks		t calc	α :	0.2		0.1		0.05		0.02	
Temp.	Range (C)										
4	12	1.3768		1.30364	Y	1.68488	N	2.02269	N	2.42584	N
4	20	1.5697		1.33676	Y	1.74588	N	2.1199	N	2.58349	N
12	20	0.5915		1.30364	N	1.68488	N	2.02269	N	2.42584	N

Key:

t calc = calculated value of t; t table = value from Student's t-distribution for the given value of α

α = level of significance

Y = statistically significant difference, i.e. null hypothesis rejected

N = not statistically significant difference, i.e. null hypothesis not rejected

Table 3.28: Student's t-test for mean crack density for individual placements versus relative humidity

Silica Fume Overlays		Confidence Interval		80%		90%		95%		98%		
		R.H. (%)	t calc	α :	t table 0.2		0.1		0.05		0.02	
35	45	0.1915			1.39682	N	1.85955	N	2.30601	N	2.89647	N
35	55	1.4456			1.38303	Y	1.83311	N	2.26216	N	2.82143	N
35	65	1.3708			1.35622	Y	1.78229	N	2.17881	N	2.68099	N
35	75	1.9314			1.39682	Y	1.85955	Y	2.30601	N	2.89647	N
45	55	2.1001			1.36343	Y	1.79588	Y	2.20099	N	2.71808	N
45	65	1.8061			1.34503	Y	1.76131	Y	2.14479	N	2.62449	N
45	75	3.1366			1.37218	Y	1.81246	Y	2.22814	Y	2.76377	Y
55	65	0.3223			1.34061	N	1.75305	N	2.13145	N	2.60248	N
55	75	0.7591			1.36343	N	1.79588	N	2.20099	N	2.71808	N
65	75	1.1171			1.34503	N	1.76131	N	2.14479	N	2.62449	N
Conventional Overlays												
R.H. (%)		t calc	α :	0.2		0.1		0.05		0.02		
45	55	0.9190			1.36343	N	1.79588	N	2.20099	N	2.71808	N
45	65	0.5375			1.30857	N	1.69389	N	2.03693	N	2.44868	N
45	75	0.4614			1.33338	N	1.73961	N	2.10982	N	2.56694	N
55	65	0.9512			1.30485	N	1.68709	N	2.02619	N	2.43144	N
55	75	1.0285			1.32124	N	1.71714	N	2.07388	N	2.50832	N
65	75	0.1869			1.30155	N	1.68107	N	2.01669	N	2.41625	N

Table 3.28 (cont.): Student's t-test for mean crack density for individual placements versus relative humidity

Monolithic Bridge											
Decks											
R.H. (%)		t calc	α:	0.2	0.1	0.05	0.02				
45	55	0.2743		1.39682	N	1.85955	N	2.30601	N	2.89647	N
45	65	0.3010		1.33676	N	1.74588	N	2.1199	N	2.58349	N
45	75	0.0528		1.34503	N	1.76131	N	2.14479	N	2.62449	N
45	85	0.4411		1.38303	N	1.83311	N	2.26216	N	2.82143	N
55	65	0.0131		1.35622	N	1.78229	N	2.17881	N	2.68099	N
55	75	0.4385		1.37218	N	1.81246	N	2.22814	N	2.76377	N
55	85	0.7539		1.47588	N	2.01505	N	2.57058	N	3.36493	N
65	75	0.4149		1.33039	N	1.73406	N	2.10092	N	2.55238	N
65	85	0.6689		1.35017	N	1.77093	N	2.16037	N	2.6503	N
75	85	0.5350		1.36343	N	1.79588	N	2.20099	N	2.71808	N

Table 3.28 (cont.): Student's t-test for mean crack density for individual placements versus relative humidity

Bridge Subdecks		t calc	α :	0.2		0.1		0.05		0.02	
R.H. (%)											
45	55	1.3694		1.43976	N	1.94318	N	2.44691	N	3.14267	N
45	65	0.9670		1.32319	N	1.72074	N	2.07961	N	2.51765	N
45	75	0.5510		1.33338	N	1.73961	N	2.10982	N	2.56694	N
45	85	3.1372		1.47588	Y	2.01505	Y	2.57058	Y	3.36493	N
55	65	0.7116		1.32773	N	1.72913	N	2.09302	N	2.53948	N
55	75	0.8969		1.34061	N	1.75305	N	2.13145	N	2.60248	N
55	85	1.5816		1.63775	N	2.35336	N	3.18245	N	4.54071	N
65	75	0.4738		1.31042	N	1.69726	N	2.04227	N	2.45726	N
65	85	2.2595		1.33039	Y	1.73406	Y	2.10092	Y	2.55238	N
75	85	2.2613		1.34503	Y	1.76131	Y	2.14479	Y	2.62449	N

Key:

t calc = calculated value of t; t table = value from Student's t-distribution for the given value of α

α = level of significance

Y = statistically significant difference, i.e. null hypothesis rejected

N = not statistically significant difference, i.e. null hypothesis not rejected

Table 3.29: Student's t-test for mean crack density for individual placements versus wind velocity

Silica Fume Overlays		Confidence Interval		80%		90%		95%		98%	
		Wind Vel. (km/hr)	t calc	α :	t table 0.2		0.1		0.05		0.02
2.5	7.5	0.0834		1.38303	N	1.83311	N	2.26216	N	2.82143	N
2.5	12.5	0.6686		1.35017	N	1.77093	N	2.16037	N	2.6503	N
2.5	17.5	0.4052		1.34503	N	1.76131	N	2.14479	N	2.62449	N
2.5	22.5	0.4070		1.47588	N	2.01505	N	2.57058	N	3.36493	N
7.5	12.5	0.4709		1.34503	N	1.76131	N	2.14479	N	2.62449	N
7.5	17.5	0.4710		1.34061	N	1.75305	N	2.13145	N	2.60248	N
7.5	22.5	0.2526		1.43976	N	1.94318	N	2.44691	N	3.14267	N
12.5	17.5	1.4913		1.32773	Y	1.72913	N	2.09302	N	2.53948	N
12.5	22.5	0.0279		1.37218	N	1.81246	N	2.22814	N	2.76377	N
17.5	22.5	0.9071		1.36343	N	1.79588	N	2.20099	N	2.71808	N

Table 3.29 (cont.): Student's t-test for mean crack density for individual placements versus wind velocity

Conventional Overlays		t calc	α:	0.2		0.1		0.05		0.02	
Wind Vel. (km/hr)											
2.5	7.5	1.1865		1.34061	N	1.75305	N	2.13145	N	2.60248	N
2.5	12.5	0.6593		1.31143	N	1.69913	N	2.04523	N	2.46202	N
2.5	17.5	1.4179		1.33676	Y	1.74588	N	2.1199	N	2.58349	N
2.5	22.5	3.2614		1.47588	Y	2.01505	Y	2.57058	Y	3.36493	N
7.5	12.5	0.4615		1.30423	N	1.68595	N	2.02439	N	2.42857	N
7.5	17.5	0.6721		1.31635	N	1.70814	N	2.05954	N	2.4851	N
7.5	22.5	2.0126		1.34503	Y	1.76131	Y	2.14479	N	2.62449	N
12.5	17.5	1.1215		1.30364	N	1.68488	N	2.02269	N	2.42584	N
12.5	22.5	1.7507		1.31253	Y	1.70113	Y	2.04841	N	2.46714	N
17.5	22.5	1.2265		1.34061	N	1.75305	N	2.13145	N	2.60248	N
Monolithic Bridge Decks		t calc	α:	0.2		0.1		0.05		0.02	
Wind Vel. (km/hr)											
7.5	12.5	0.5710		1.33676	N	1.74588	N	2.1199	N	2.58349	N
7.5	17.5	0.1174		1.34061	N	1.75305	N	2.13145	N	2.60248	N
7.5	22.5	0.1897		1.39682	N	1.85955	N	2.30601	N	2.89647	N
12.5	17.5	0.9081		1.32319	N	1.72074	N	2.07961	N	2.51765	N
12.5	22.5	0.7862		1.34503	N	1.76131	N	2.14479	N	2.62449	N
17.5	22.5	0.1420		1.35017	N	1.77093	N	2.16037	N	2.6503	N

Table 3.29 (cont.): Student's t-test for mean crack density for individual placements versus wind velocity

Bridge Subdecks		t calc	α :	0.2		0.1		0.05		0.02	
Wind Vel. (km/hr)											
2.5	7.5	0.4484		1.34503	N	1.76131	N	2.14479	N	2.62449	N
2.5	12.5	0.4137		1.33039	N	1.73406	N	2.10092	N	2.55238	N
2.5	17.5	0.0943		1.37218	N	1.81246	N	2.22814	N	2.76377	N
2.5	22.5	2.4061		1.47588	Y	2.01505	Y	2.57058	N	3.36493	N
7.5	12.5	0.0220		1.31497	N	1.70562	N	2.05553	N	2.47863	N
7.5	17.5	0.8025		1.33039	N	1.73406	N	2.10092	N	2.55238	N
7.5	22.5	3.0253		1.35017	Y	1.77093	Y	2.16037	Y	2.6503	Y
12.5	17.5	0.7254		1.32124	N	1.71714	N	2.07388	N	2.50832	N
12.5	22.5	2.4146		1.33338	Y	1.73961	Y	2.10982	Y	2.56694	N
17.5	22.5	4.0035		1.38303	Y	1.83311	Y	2.26216	Y	2.82143	Y

Key:

t calc = calculated value of t; t table = value from Student's t-distribution for the given value of α

α = level of significance

Y = statistically significant difference, i.e. null hypothesis rejected

N = not statistically significant difference, i.e. null hypothesis not rejected

Table 3.30: Student's t-test for mean crack density for individual silica fume overlay placements versus Special Provision Number

Silica Fume Overlays Special Prov. (SP R)		Confidence Interval		80%		90%		95%		98%	
		t calc	α :	t table 0.2		t table 0.1		t table 0.05		t table 0.02	
No SP	SP R3	0.5637		1.32534	N	1.72472	N	2.08596	N	2.52798	N
No SP	SP R4	1.3334		1.32124	Y	1.71714	N	2.07388	N	2.50832	N
SP R3	SP R4	2.7931		1.30551	Y	1.6883	Y	2.02809	Y	2.4345	Y

Key:

t calc = calculated value of t; t table = value from Student's t-distribution for the given value of α

α = level of significance

Y = statistically significant difference, i.e. null hypothesis rejected

N = not statistically significant difference, i.e. null hypothesis not rejected

No SP = No Special Provision used; SP R3 = Special Provision revision 3; SP R4 = Special Provision revision 4

Table 3.31: Student's t-test for mean crack density for entire bridge versus steel structure type

		Confidence Interval		80%		90%		95%		98%	
Silica Fume Overlays		t calc	α :	t table							
Structure Type				0.2	0.1	0.05	0.02				
SMCC	SWCC	0.2297		1.34503	N	1.76131	N	2.14479	N	2.62449	N
SMCC	SWCH	0.9884		1.53321	N	2.13185	N	2.77645	N	3.74694	N
SWCC	SWCH	1.0735		1.35622	N	1.78229	N	2.17881	N	2.68099	N
Conventional Overlays											
Structure Type		t calc	α :	0.2	0.1	0.05	0.02				
SMCC	SWCC	1.8044		1.31143	Y	1.69913	Y	2.04523	N	2.46202	N
SMCC	SWCH	0.8743		1.34503	N	1.76131	N	2.14479	N	2.62449	N
SWCC	SWCH	3.4858		1.31946	Y	1.71387	Y	2.06865	Y	2.49987	Y
Monolithic Bridge Decks											
Structure Type		t calc	α :	0.2	0.1	0.05	0.02				
SMCC	SWCC	0.5200		1.33676	N	1.74588	N	2.1199	N	2.58349	N

Key:

t calc = calculated value of t; t table = value from Student's t-distribution for the given value of α

α = level of significance; Y = statistically significant difference, i.e. null hypothesis rejected

N = not statistically significant difference, i.e. null hypothesis not rejected

SMCC = steel beam, composite continuous; SWCC = steel welded plate girder, composite continuous

SWCH = steel welded plate girder, composite continuous and haunched

Table 3.32: Student's t-test for mean crack density for entire bridge deck versus deck type

Deck Types		Confidence Interval		80%		90%		95%		98%	
		t calc	α :	t table 0.2		0.1		0.05		0.02	
SFO all	SFO	1.2908		1.30423	N	1.68595	N	2.02439	N	2.42857	N
SFO all	CO	0.8324		1.29685	N	1.67252	N	2.00324	N	2.3948	N
SFO all	Mono	0.5856		1.30364	N	1.68488	N	2.02269	N	2.42584	N
SFO	CO	0.5756		1.29804	N	1.67469	N	2.00665	N	2.40023	N
SFO	Mono	0.7155		1.30621	N	1.68957	N	2.03011	N	2.43772	N
CO	Mono	0.2088		1.29773	N	1.67412	N	2.00575	N	2.39879	N

Key:

t calc = calculated value of t; t table = value from Student's t-distribution for the given value of α

α = level of significance

Y = statistically significant difference, i.e. null hypothesis rejected

N = not statistically significant difference, i.e. null hypothesis not rejected

SFO all = all silica fume overlays included; SFO = all silica fume overlays, except bridges 89-184 and 89-187

CO = conventional overlays; Mono = Monolithic Bridge Decks

Table 3.33: Student's t-test for mean crack density for entire bridge versus deck thickness

		Confidence Interval		80%	90%	95%	98%				
Silica Fume Overlays		t calc	α :	t table							
Thickness (mm)				0.2	0.1	0.05	0.02				
216	226	1.6530		1.34061	Y	1.75305	N	2.13145	N	2.60248	N
Conventional Overlays		t calc	α :	0.2	0.1	0.05	0.02				
216	229	1.8159		1.31042	Y	1.69726	Y	2.04227	N	2.45726	N
Monolithic Bridge Decks		t calc	α :	0.2	0.1	0.05	0.02				
203	210&216	0.8588		1.39682	N	1.85955	N	2.30601	N	2.89647	N
203	222&229	0.4272		1.43976	N	1.94318	N	2.44691	N	3.14267	N
210&216	222&229	0.3104		1.39682	N	1.85955	N	2.30601	N	2.89647	N

Key:

t calc = calculated value of t; t table = value from Student's t-distribution for the given value of α

α = level of significance

Y = statistically significant difference, i.e. null hypothesis rejected

N = not statistically significant difference, i.e. null hypothesis not rejected

Table 3.34: Student's t-test for mean crack density for entire bridge versus top cover

Monolithic Bridge		Confidence Interval		80%	90%	95%	98%			
Decks										
Top Cover (mm)	t calc	α :	0.2	0.1	0.05	0.02				
64	75	1.6421	1.35017	Y	1.77093	N	2.16037	N	2.6503	N

Key:

t calc = calculated value of t; t table = value from Student's t-distribution for the given value of α

α = level of significance

Y = statistically significant difference, i.e. null hypothesis rejected

N = not statistically significant difference, i.e. null hypothesis not rejected

Table 3.35: Student's t-test for mean crack density for entire bridge versus top transverse reinforcing bar size

		Confidence Interval		80%		90%		95%		98%	
Silica Fume Overlays		t calc	α :	t table							
Bar Size				0.2	0.1	0.05	0.02				
5	6	0.4606		1.38303	N	1.83311	N	2.26216	N	2.82143	N
5	5,6	0.2386		1.39682	N	1.85955	N	2.30601	N	2.89647	N
6	5,6	0.3381		1.38303	N	1.83311	N	2.26216	N	2.82143	N
Conventional Overlays											
Bar Size		t calc	α :	0.2	0.1	0.05	0.02				
4,5	5	0.0727		1.33039	N	1.73406	N	2.10092	N	2.55238	N
4,5	6	3.4033		1.32773	Y	1.72913	Y	2.09302	Y	2.53948	Y
5	6	3.0459		1.31635	Y	1.70814	Y	2.05954	Y	2.4851	Y
Monolithic Bridge Decks											
Bar Size		t calc	α :	0.2	0.1	0.05	0.02				
4,5	5	0.9138		1.36343	N	1.79588	N	2.20099	N	2.71808	N

Key:

t calc = calculated value of t; t table = value from Student's t-distribution for the given value of α

α = level of significance

Y = statistically significant difference, i.e. null hypothesis rejected

N = not statistically significant difference, i.e. null hypothesis not rejected

Table 3.36: Student's t-test for mean crack density for entire bridge versus top transverse bar spacing

Silica Fume Overlays		Confidence Interval		80%	90%	95%	98%				
		t calc	α :	t table							
Spacing (mm)				0.2	0.1	0.05	0.02				
<=153	>153	0.2817		1.34061	N	1.75305	N	2.13145	N	2.60248	N
Conventional Overlays		t calc	α :	0.2	0.1	0.05	0.02				
Spacing (mm)											
<=153	>153	3.6796		1.30946	Y	1.69552	Y	2.03951	Y	2.45283	Y

Key:

t calc = calculated value of t; t table = value from Student's t-distribution for the given value of α

α = level of significance

Y = statistically significant difference, i.e. null hypothesis rejected

N = not statistically significant difference, i.e. null hypothesis not rejected

Table 3.37: Student's t-test for mean crack density for end sections versus girder end condition

		Confidence Interval		80%	90%	95%	98%				
Silica Fume Overlays		t calc	α :	t table							
End Condition				0.2	0.1	0.05	0.02				
F	P	2.4713		1.33676	Y	1.74588	Y	2.1199	Y	2.58349	N
Conventional Overlays		t calc	α :	0.2	0.1	0.05	0.02				
F	P	3.8560		1.30946	Y	1.69552	Y	2.03951	Y	2.45283	Y

Key:

t calc = calculated value of t; t table = value from Student's t-distribution for the given value of α

α = level of significance

Y = statistically significant difference, i.e. null hypothesis rejected

N = not statistically significant difference, i.e. null hypothesis not rejected

F = fixed end condition

P = pinned end condition

Table 3.38: Student's t-test for mean crack density for individual spans versus span length

Silica Fume Overlays		Confidence Interval		80%		90%		95%		98%		
		Span Length (m)	t calc	α :	t table 0.2		0.1		0.05		0.02	
15	25	0.9288			1.30857	N	1.69389	N	2.03693	N	2.44868	N
15	35	2.0261			1.30254	Y	1.68288	Y	2.01954	Y	2.4208	N
15	45	0.8411			1.32319	N	1.72074	N	2.07961	N	2.51765	N
15	55	0.4100			1.32773	N	1.72913	N	2.09302	N	2.53948	N
25	35	1.0129			1.30254	N	1.68288	N	2.01954	N	2.4208	N
25	45	0.2571			1.32319	N	1.72074	N	2.07961	N	2.51765	N
25	55	0.1269			1.32773	N	1.72913	N	2.09302	N	2.53948	N
35	45	0.4124			1.31042	N	1.69726	N	2.04227	N	2.45726	N
35	55	0.7501			1.31253	N	1.70113	N	2.04841	N	2.46714	N
45	55	0.2702			1.39682	N	1.85955	N	2.30601	N	2.89647	N
Conventional Overlays												
Span Length (m)		t calc	α :	0.2		0.1		0.05		0.02		
15	25	0.9699			1.29053	N	1.66105	N	1.98525	N	2.36624	N
15	35	1.0734			1.30023	N	1.67866	N	2.01289	N	2.41019	N
15	45	1.3581			1.29713	Y	1.67303	N	2.00404	N	2.39608	N
25	35	0.6524			1.29558	N	1.67022	N	1.99962	N	2.38904	N
25	45	0.7699			1.29376	N	1.66692	N	1.99444	N	2.3808	N
35	45	0.1981			1.32319	N	1.72074	N	2.07961	N	2.51765	N

Table 3.38 (cont.): Student's t-test for mean crack density for individual spans versus span length

Monolithic Bridge		t calc	α:	0.2		0.1		0.05		0.02	
Decks											
Span Length (m)											
15	25	0.7204		1.30254	N	1.68288	N	2.01954	N	2.4208	N
15	35	0.4305		1.31946	N	1.71387	N	2.06865	N	2.49987	N
25	35	0.9198		1.30423	N	1.68595	N	2.02439	N	2.42857	N

Key:

t calc = calculated value of t; t table = value from Student's t-distribution for the given value of α

α = level of significance

Y = statistically significant difference, i.e. null hypothesis rejected

N = not statistically significant difference, i.e. null hypothesis not rejected

Table 3.39: Student's t-test for mean crack density for entire bridge versus bridge length

		Confidence Interval		80%	90%	95%	98%				
Silica Fume Overlays		t calc	α :	t table							
Bridge Length (m)				0.2	0.1	0.05	0.02				
50	90	1.9113		1.41492	Y	1.89458	Y	2.36462	N	2.99795	N
50	130	1.7398		1.43976	Y	1.94318	N	2.44691	N	3.14267	N
90	130	0.9541		1.36343	N	1.79588	N	2.20099	N	2.71808	N
Conventional Overlays		t calc	α :	0.2	0.1	0.05	0.02				
50	90	1.0991		1.31042	N	1.69726	N	2.04227	N	2.45726	N
50	130	0.9865		1.33676	N	1.74588	N	2.1199	N	2.58349	N
90	130	0.4422		1.32534	N	1.72472	N	2.08596	N	2.52798	N
Monolithic Bridge Decks		t calc	α :	0.2	0.1	0.05	0.02				
50	90	0.2050		1.35622	N	1.78229	N	2.17881	N	2.68099	N
50	130	0.0081		1.47588	N	2.01505	N	2.57058	N	3.36493	N
90	130	0.2017		1.35017	N	1.77093	N	2.16037	N	2.6503	N

Key:

t calc = calculated value of t; t table = value from Student's t-distribution for the given value of α
 α = level of significance; Y = statistically significant difference, i.e. null hypothesis rejected
 N = not statistically significant difference, i.e. null hypothesis not rejected

Table 3.40: Student's t-test for mean crack density for individual spans versus span type

		Confidence Interval		80%	90%	95%	98%				
Silica Fume Overlays		t calc	α :	t table							
Span Type				0.2	0.1	0.05	0.02				
End (F)	End (P)	1.6147		1.30857	Y	1.69389	N	2.03693	N	2.44868	N
End (F)	Interior	0.1739		1.29837	N	1.67528	N	2.00758	N	2.40172	N
End (P)	Interior	1.5473		1.29907	Y	1.67655	N	2.00957	N	2.40489	N
Conventional Overlays		t calc	α :	0.2	0.1	0.05	0.02				
Span Type											
End (F)	End (P)	0.1915		1.29413	N	1.66757	N	1.99547	N	2.38245	N
End (F)	Interior	0.0465		1.29062	N	1.66123	N	1.98552	N	2.36667	N
End (P)	Interior	0.0000		1.29413	N	1.66757	N	1.99547	N	2.38245	N

Table 3.40 (cont.): Student's t-test for mean crack density for individual spans versus span type

Monolithic Bridge											
Decks											
Span Type		t calc	α:	0.2	0.1	0.05	0.02				
End (F)	End (P)	1.6331		1.31143	Y	1.69913	N	2.04523	N	2.46202	N
End (F)	Interior	0.4598		1.29871	N	1.67591	N	2.00856	N	2.40327	N
End (P)	Interior	1.4991		1.31946	Y	1.71387	N	2.06865	N	2.49987	N

Key:

t calc = calculated value of t; t table = value from Student's t-distribution for the given value of α

α = level of significance

Y = statistically significant difference, i.e. null hypothesis rejected

N = not statistically significant difference, i.e. null hypothesis not rejected

End (F) = end span, fixed end condition

End (P) = end span, pinned end condition

Interior = Interior span

Table 3.41: Student's t-test for mean crack density for entire bridge versus skew

Silica Fume Overlays		Confidence Interval		80%		90%		95%		98%		
		Skew (deg)	t calc	α :	t table 0.2	N	0.1	N	0.05	N	0.02	N
0	10	0.2834			1.39682	N	1.85955	N	2.30601	N	2.89647	N
0	30	0.3946			1.43976	N	1.94318	N	2.44691	N	3.14267	N
0	50	0.4492			1.41492	N	1.89458	N	2.36462	N	2.99795	N
10	30	0.1717			1.43976	N	1.94318	N	2.44691	N	3.14267	N
10	50	0.1967			1.41492	N	1.89458	N	2.36462	N	2.99795	N
30	50	0.0160			1.47588	N	2.01505	N	2.57058	N	3.36493	N

Conventional Overlays		Confidence Interval		80%		90%		95%		98%		
Skew (deg)	t calc	α :	0.2	N	0.1	N	0.05	N	0.02	N		
0	10	0.5022			1.35017	N	1.77093	N	2.16037	N	2.6503	N
0	30	0.0944			1.33676	N	1.74588	N	2.1199	N	2.58349	N
0	50	1.5511			1.34061	Y	1.75305	N	2.13145	N	2.60248	N
10	30	0.4924			1.33338	N	1.73961	N	2.10982	N	2.56694	N
10	50	0.7126			1.33676	N	1.74588	N	2.1199	N	2.58349	N
30	50	1.5665			1.32773	Y	1.72913	N	2.09302	N	2.53948	N

Table 3.41 (cont.): Student's t-test for mean crack density for entire bridge versus skew

Monolithic Bridge		t calc	α:	0.2		0.1		0.05		0.02	
Decks											
Skew (deg)											
0	30	0.6472		1.35017	N	1.77093	N	2.16037	N	2.6503	N
0	50	0.8500		1.35017	N	1.77093	N	2.16037	N	2.6503	N
30	50	0.9403		1.43976	N	1.94318	N	2.44691	N	3.14267	N

Key:

t calc = calculated value of t; t table = value from Student's t-distribution for the given value of α

α = level of significance

Y = statistically significant difference, i.e. null hypothesis rejected

N = not statistically significant difference, i.e. null hypothesis not rejected

Table 3.42: Student's t-test for mean crack density for entire bridge versus traffic volume

		Confidence Interval			80%	90%	95%	98%			
Silica Fume Overlays		t calc	α :	t table							
AADT				0.2	0.1	0.05	0.02				
2500	7500	0.6536		1.34503	N	1.76131	N	2.14479	N	2.62449	N
2500	12500	2.5420		1.39682	Y	1.85955	Y	2.30601	Y	2.89647	N
7500	12500	1.6157		1.47588	Y	2.01505	N	2.57058	N	3.36493	N
Conventional Overlays		t calc	α :	0.2	0.1	0.05	0.02				
AADT											
2500	7500	0.7479		1.31946	N	1.71387	N	2.06865	N	2.49987	N
2500	12500	1.2383		1.35622	N	1.78229	N	2.17881	N	2.68099	N
7500	12500	0.6689		1.31635	N	1.70814	N	2.05954	N	2.4851	N
Monolithic Bridge Decks		t calc	α :	0.2	0.1	0.05	0.02				
AADT											
1000	3000	3.9609		1.35017	Y	1.77093	Y	2.16037	Y	2.6503	Y
1000	5000	1.7375		1.38303	Y	1.83311	N	2.26216	N	2.82143	N
3000	5000	0.2365		1.43976	N	1.94318	N	2.44691	N	3.14267	N

Key:

t calc = calculated value of t; t table = value from Student's t-distribution for the given value of α
 α = level of significance; Y = statistically significant difference, i.e. null hypothesis rejected
 N = not statistically significant difference, i.e. null hypothesis not rejected

Table 3.43: Student's t-test for mean crack density for entire bridge versus load cycles

		Confidence Interval		80%		90%		95%		98%	
Silica Fume Overlays		t calc	α :	t table							
Load Cycles				0.2		0.1		0.05		0.02	
1x10 ⁶	3x10 ⁶	0.9092		1.35622	N	1.78229	N	2.17881	N	2.68099	N
1x10 ⁶	5x10 ⁶	1.0897		1.53321	N	2.13185	N	2.77645	N	3.74694	N
1x10 ⁶	7x10 ⁶	0.8407		1.53321	N	2.13185	N	2.77645	N	3.74694	N
3x10 ⁶	5x10 ⁶	0.0177		1.37218	N	1.81246	N	2.22814	N	2.76377	N
3x10 ⁶	7x10 ⁶	0.3363		1.37218	N	1.81246	N	2.22814	N	2.76377	N
5x10 ⁶	7x10 ⁶	0.2063		1.88562	N	2.91999	N	4.30266	N	6.96455	N
Conventional Overlays											
Load Cycles		t calc	α :	0.2		0.1		0.05		0.02	
0.5x10 ⁶	1.5x10 ⁶	0.9587		1.31635	N	1.70814	N	2.05954	N	2.4851	N
0.5x10 ⁶	2.5x10 ⁶	0.8263		1.36343	N	1.79588	N	2.20099	N	2.71808	N
0.5x10 ⁶	3.5x10 ⁶	0.3797		1.35017	N	1.77093	N	2.16037	N	2.6503	N
0.5x10 ⁶	4.5x10 ⁶	1.3746		1.35622	Y	1.78229	N	2.17881	N	2.68099	N
1.5x10 ⁶	2.5x10 ⁶	0.4767		1.33676	N	1.74588	N	2.1199	N	2.58349	N
1.5x10 ⁶	3.5x10 ⁶	1.2361		1.33039	N	1.73406	N	2.10092	N	2.55238	N
1.5x10 ⁶	4.5x10 ⁶	2.3532		1.33338	Y	1.73961	Y	2.10982	Y	2.56694	N
2.5x10 ⁶	3.5x10 ⁶	1.4125		1.53321	N	2.13185	N	2.77645	N	3.74694	N
2.5x10 ⁶	4.5x10 ⁶	2.4044		1.63775	Y	2.35336	Y	3.18245	N	4.54071	N
3.5x10 ⁶	4.5x10 ⁶	2.3534		1.47588	Y	2.01505	Y	2.57058	N	3.36493	N

Table 3.43 (cont.): Student's t-test for mean crack density for entire bridge versus load cycles

Monolithic Bridge Decks		t calc	α:	0.2		0.1		0.05		0.02	
Load Cycles											
1.5x10 ⁶	4.5x10 ⁶	1.5954		1.36343	Y	1.79588	N	2.20099	N	2.71808	N
1.5x10 ⁶	>10x10 ⁶	1.9587		1.36343	Y	1.79588	Y	2.20099	N	2.71808	N
4.5x10 ⁶	>10x10 ⁶	0.4642		1.43976	N	1.94318	N	2.44691	N	3.14267	N

Table 3.44: Student's t-test for mean crack density for entire bridge versus pavement roughness index

Deck Type		t calc	α:	Confidence Interval		80%		90%		95%		98%	
				t table									
				0.2	0.1	0.05	0.02						
SFO	CO	0.3691		1.29432	N	1.66792	N	1.99601	N	2.3833	N		
SFO	Mono	0.1055		1.30364	N	1.68488	N	2.02269	N	2.42584	N		
CO	Mono	0.0000		1.30423	N	1.68595	N	2.02439	N	2.42857	N		

Key:

t calc = calculated value of t; t table = value from Student's t-distribution for the given value of α

α = level of significance

Y = statistically significant difference, i.e. null hypothesis rejected

N = not statistically significant difference, i.e. null hypothesis not rejected

SFO = silica fume overlays; CO = conventional overlays; Mono = Monolithic Bridge Decks

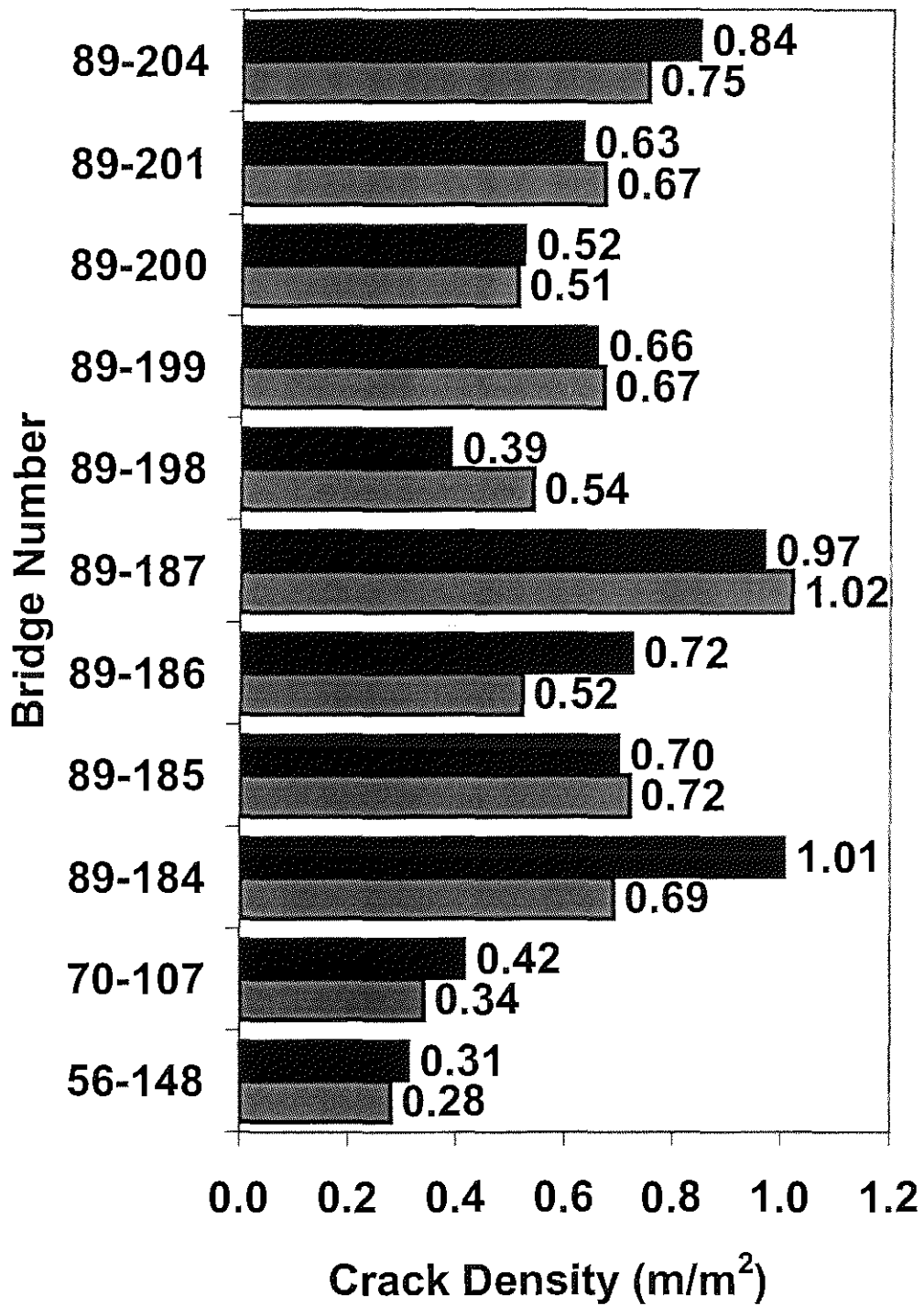


Fig. 3.1: Crack density of entire bridge decks for bridges evaluated in the current study and by Schmitt and Darwin (1995)

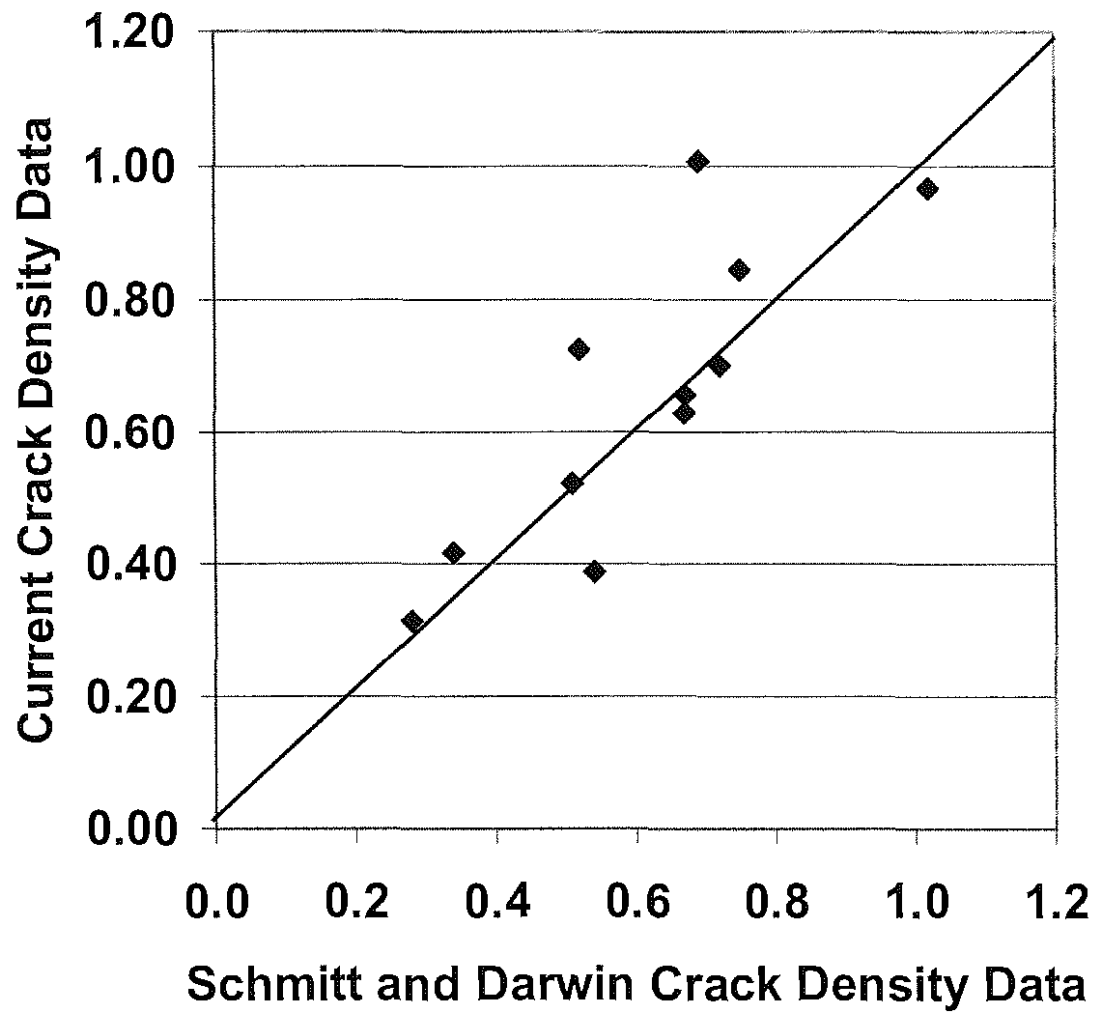


Fig. 3.2: Correlation of crack density of entire bridge decks for bridges evaluated in the current study and by Schmitt and Darwin (1995)

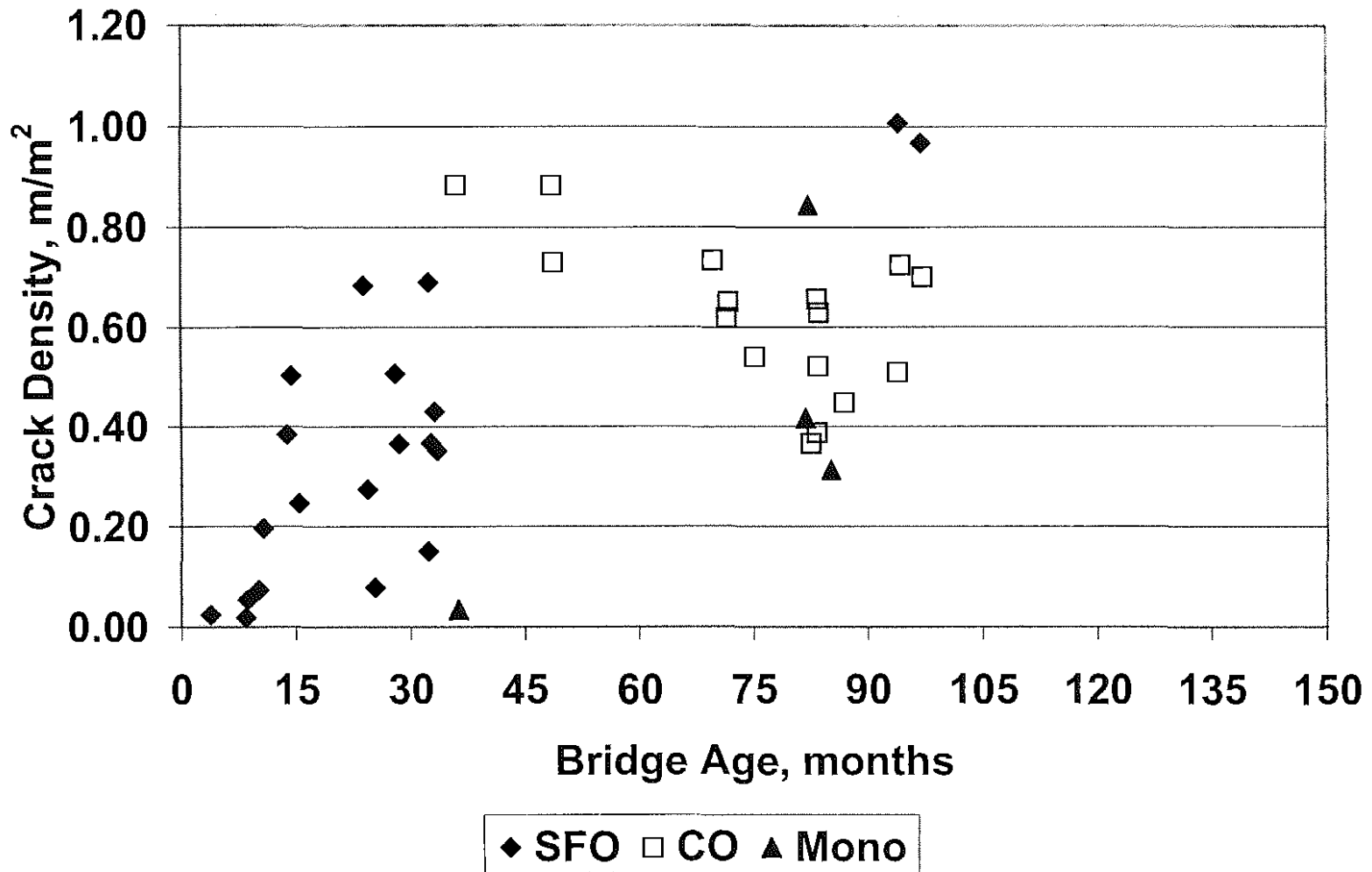


Fig. 3.3: Crack density of entire bridge deck versus bridge age for silica fume overlays (SFO), conventional overlays (CO) and monolithic (Mono) bridges in the current study

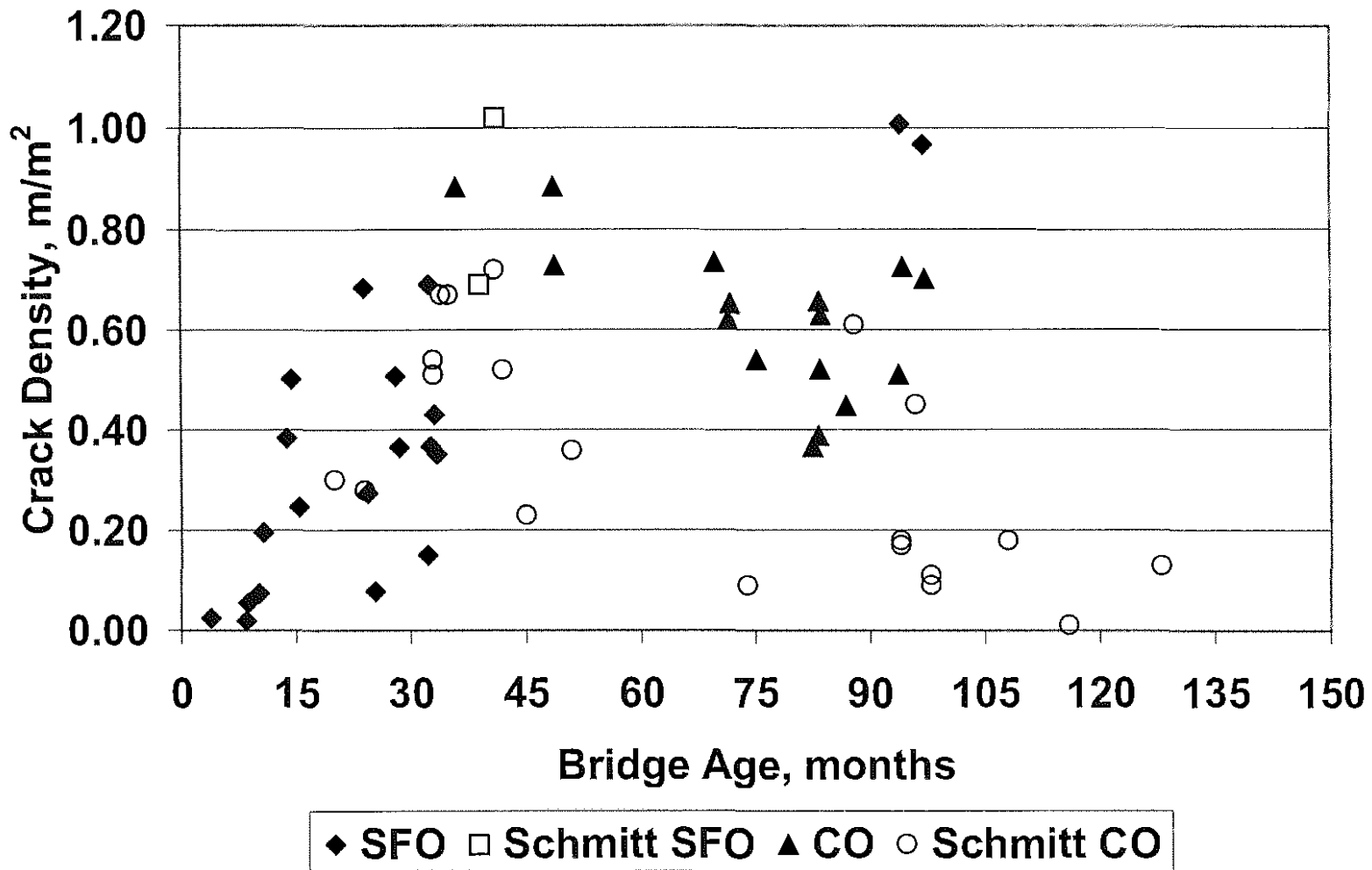


Fig. 3.4: Crack density of entire bridge deck versus bridge age for silica fume (SFO) and conventional overlays (CO) evaluated in the current study and by Schmitt and Darwin (1995)

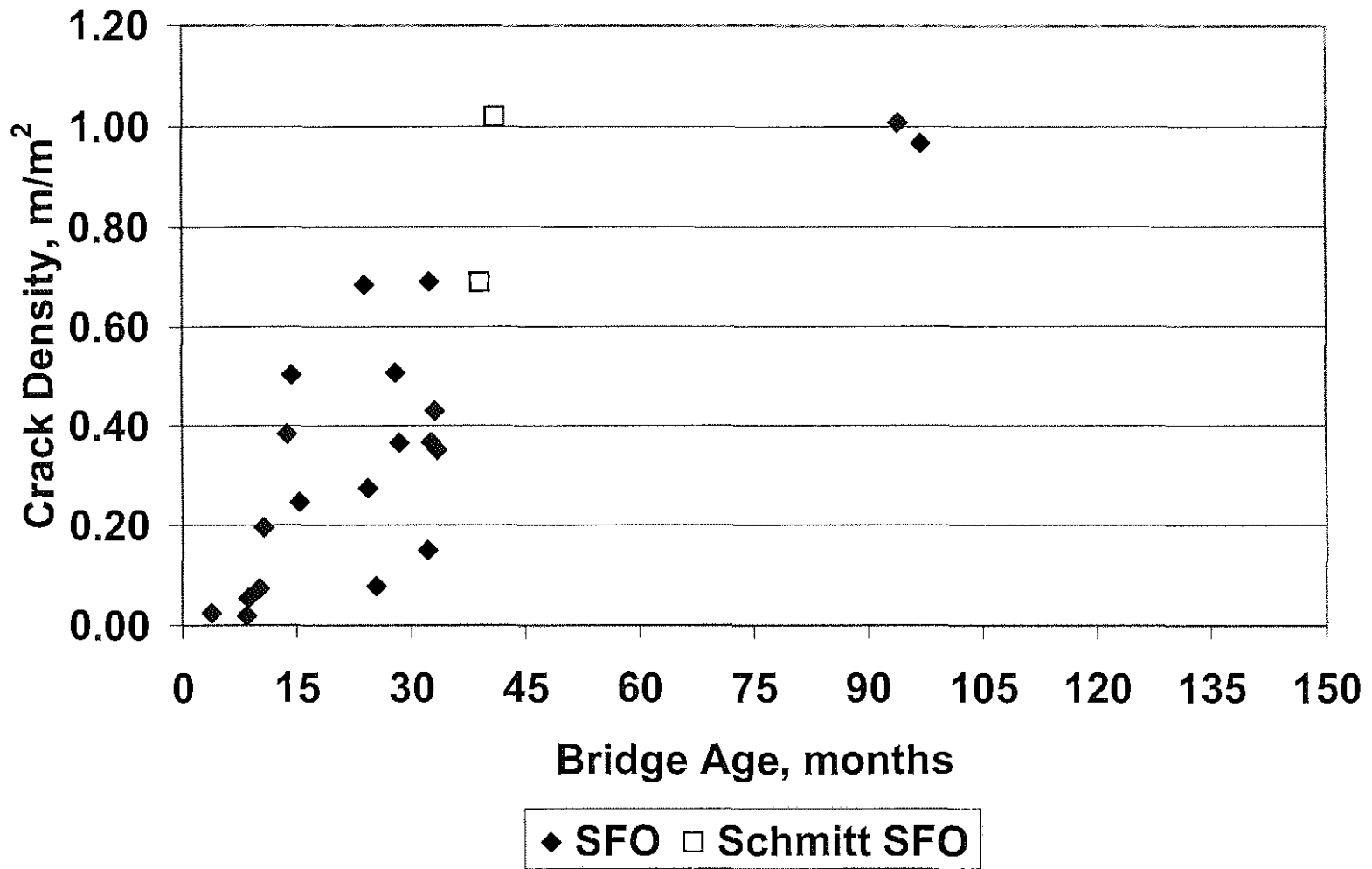


Fig. 3.5: Crack Density of entire bridge deck versus bridge age for silica fume overlays studied in the current study (SFO) and by Schmitt and Darwin (1995) (Schmitt SFO)

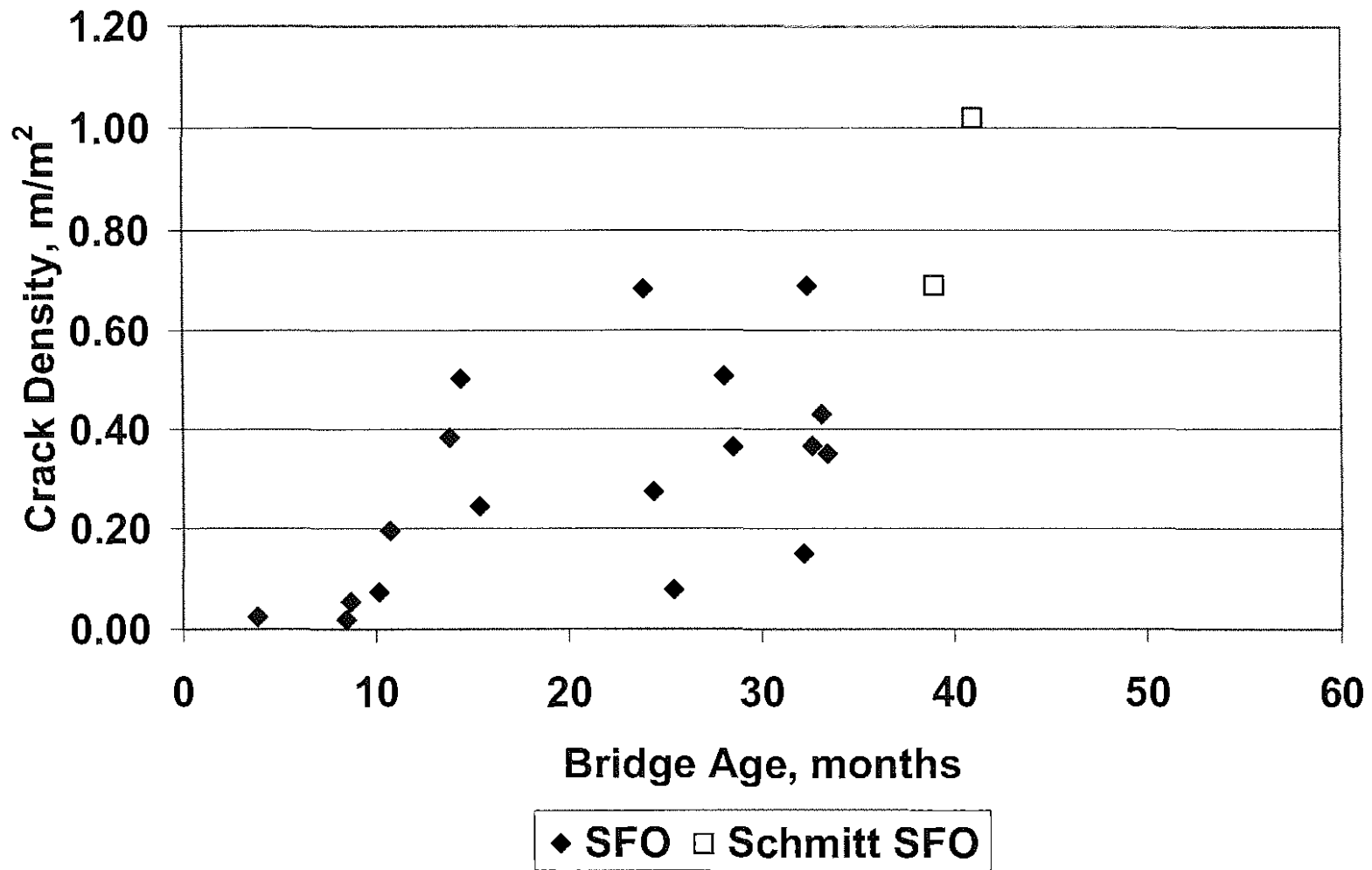


Fig. 3.6: Crack Density of entire bridge deck versus bridge age for silica fume overlays younger than 60 months evaluated in the current study (SFO) and by Schmitt and Darwin (1995) (Schmitt SFO)

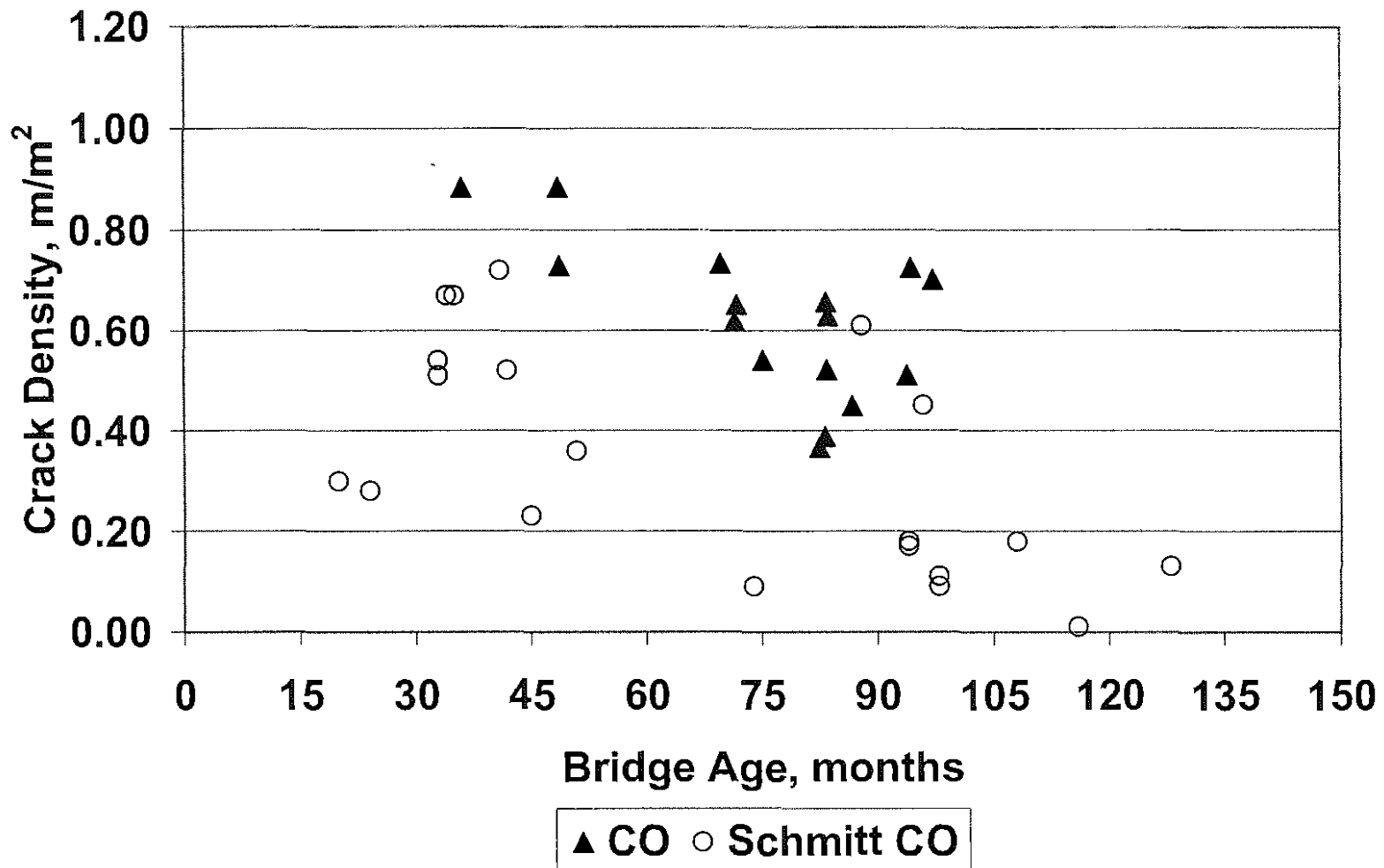


Fig. 3.7: Crack density of entire bridge deck versus bridge age for conventional overlays evaluated in the current study (CO) and by Schmitt and Darwin (1995) (Schmitt CO)

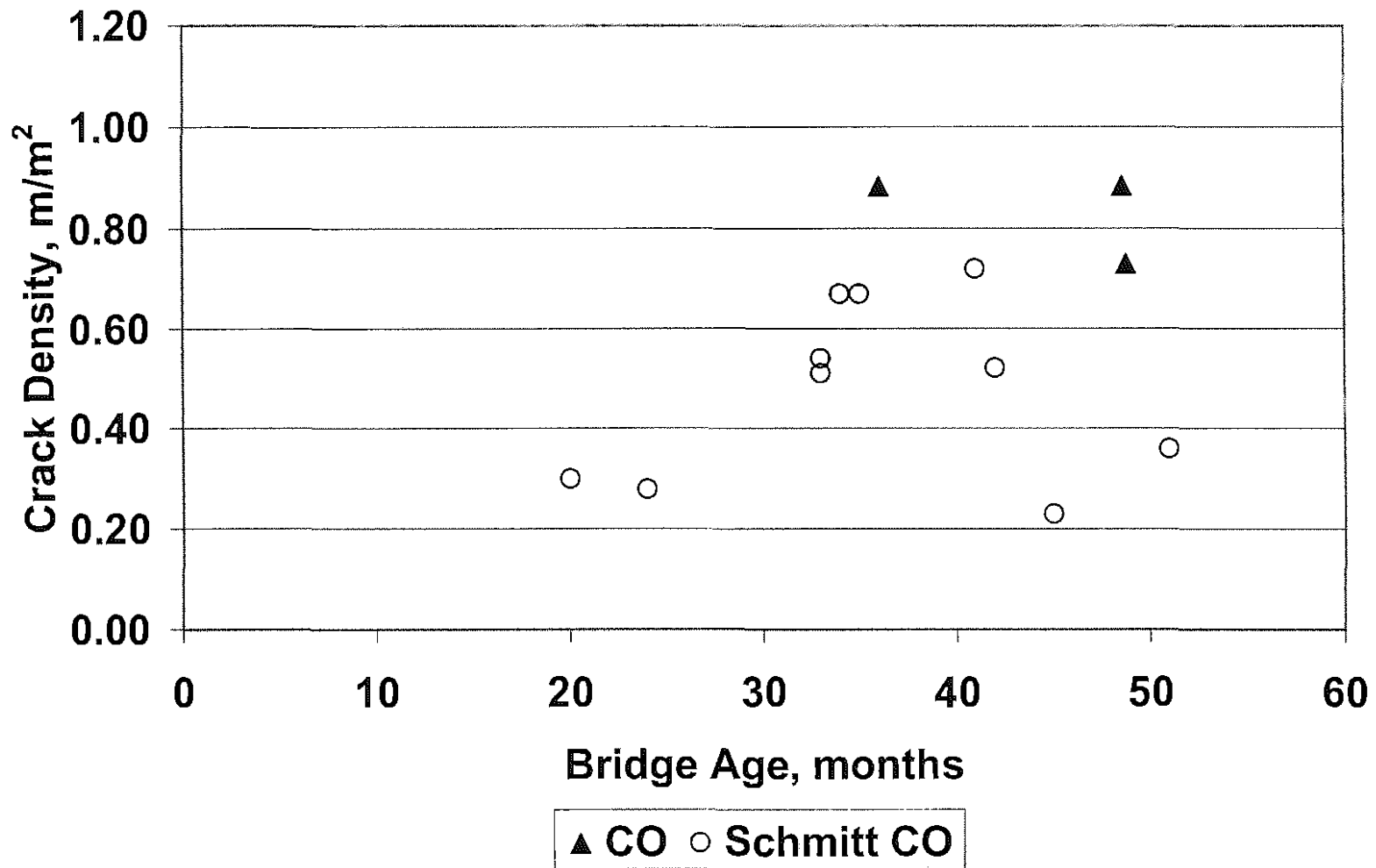


Fig. 3.8: Crack density of entire bridge deck versus bridge age for conventional overlays younger than 60 months evaluated in the current study (CO) and by Schmitt and Darwin (1995) (Schmitt CO)

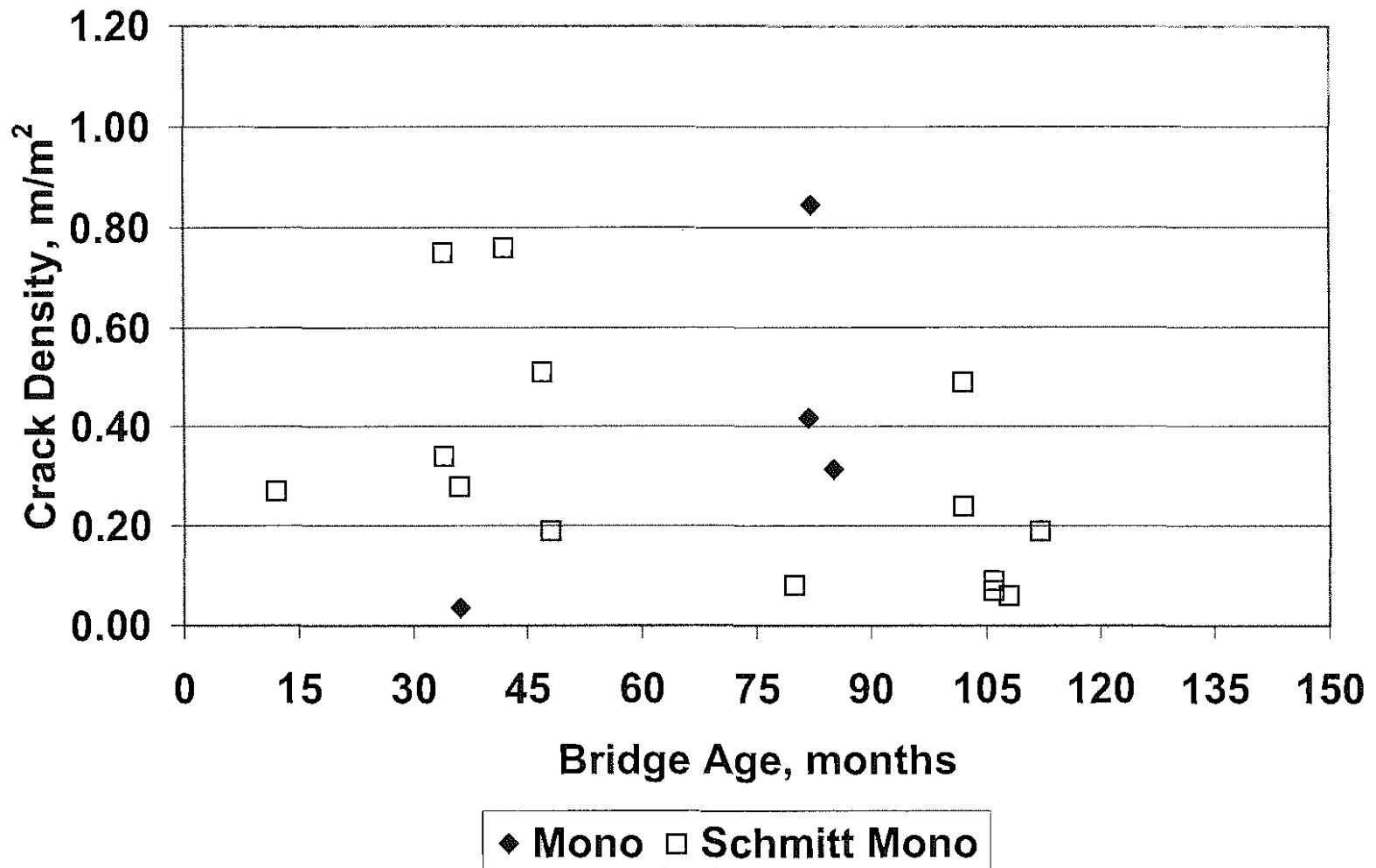


Fig. 3.9: Crack density of entire bridge deck versus bridge age for monolithic bridge decks evaluated in the current study (Mono) and by Schmitt and Darwin (1995) (Schmitt Mono)

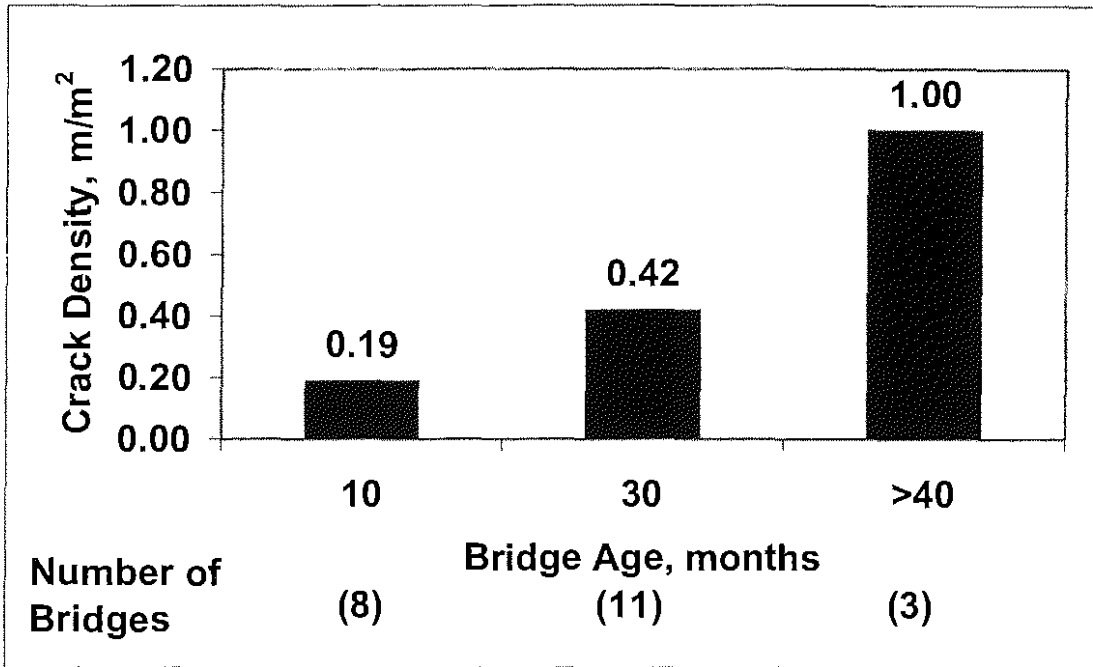


Figure 3.10 : Mean Crack Density of entire bridge decks versus bridge age for silica fume overlays

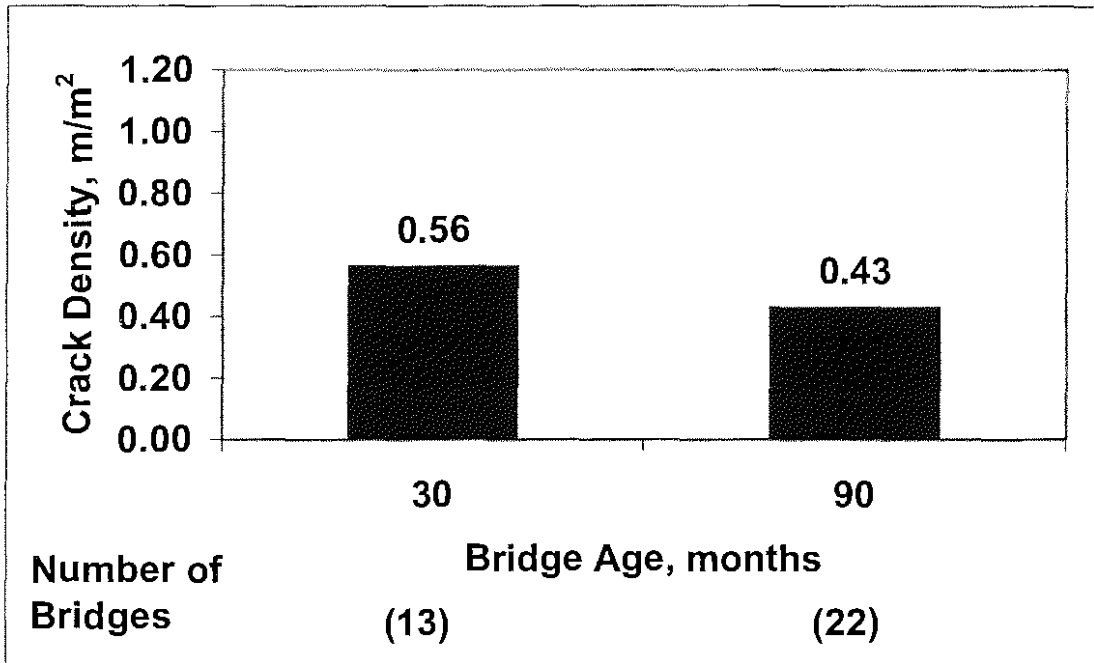


Figure 3.11 : Mean Crack Density of entire bridge decks versus bridge age for conventional overlays

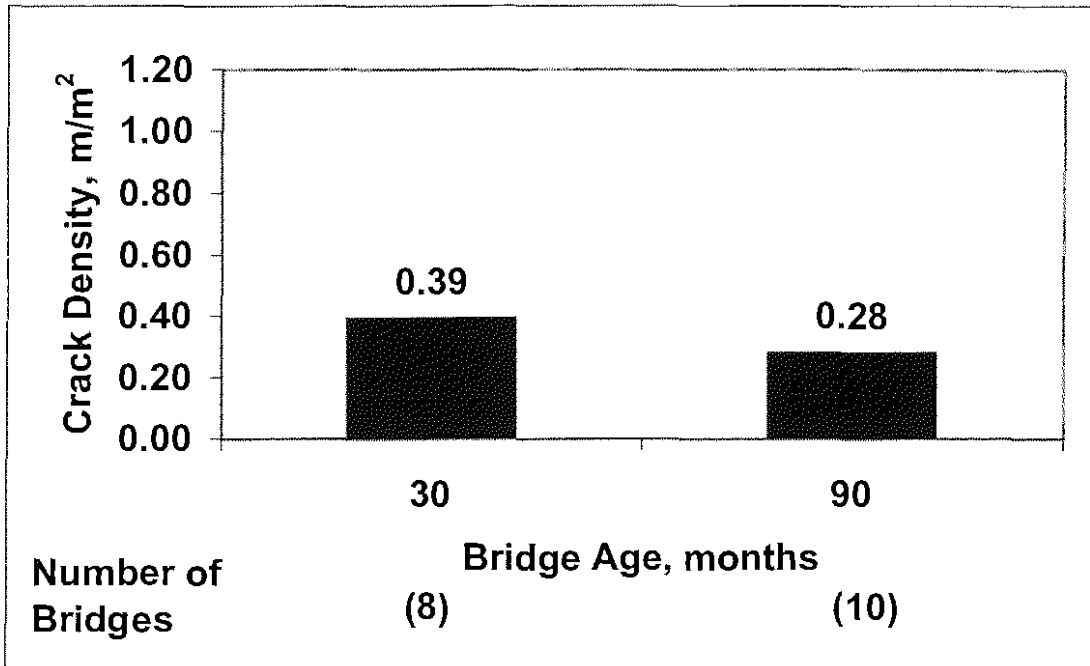


Figure 3.12 : Mean Crack Density of entire bridge decks versus bridge age for monolithic bridge decks

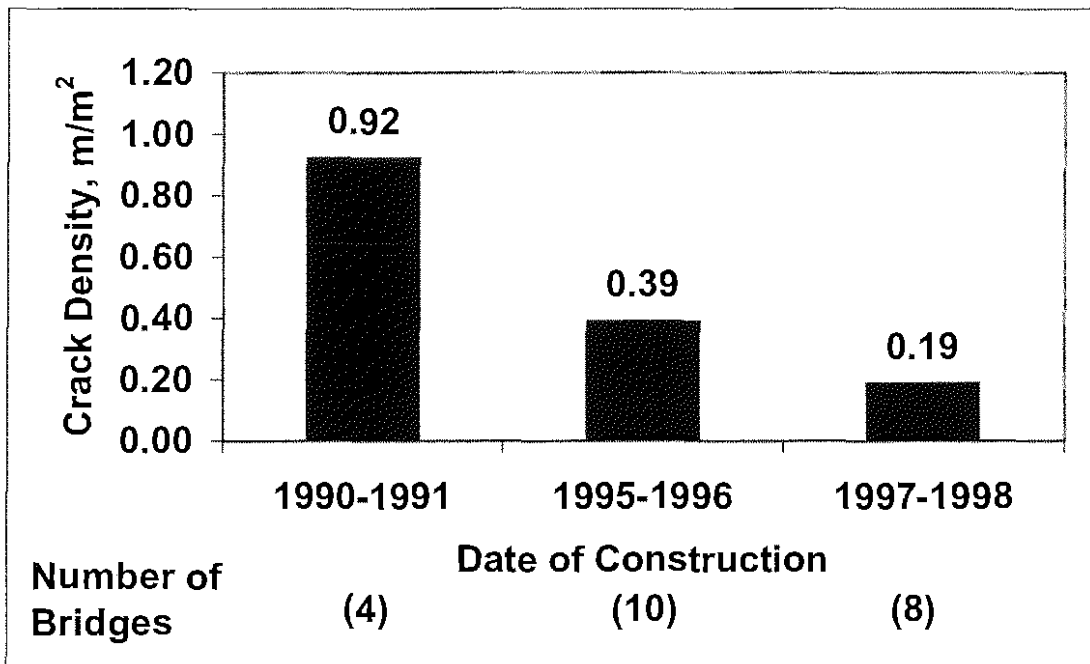


Figure 3.13 : Mean crack density of entire bridge versus date of construction for silica fume overlay bridge decks

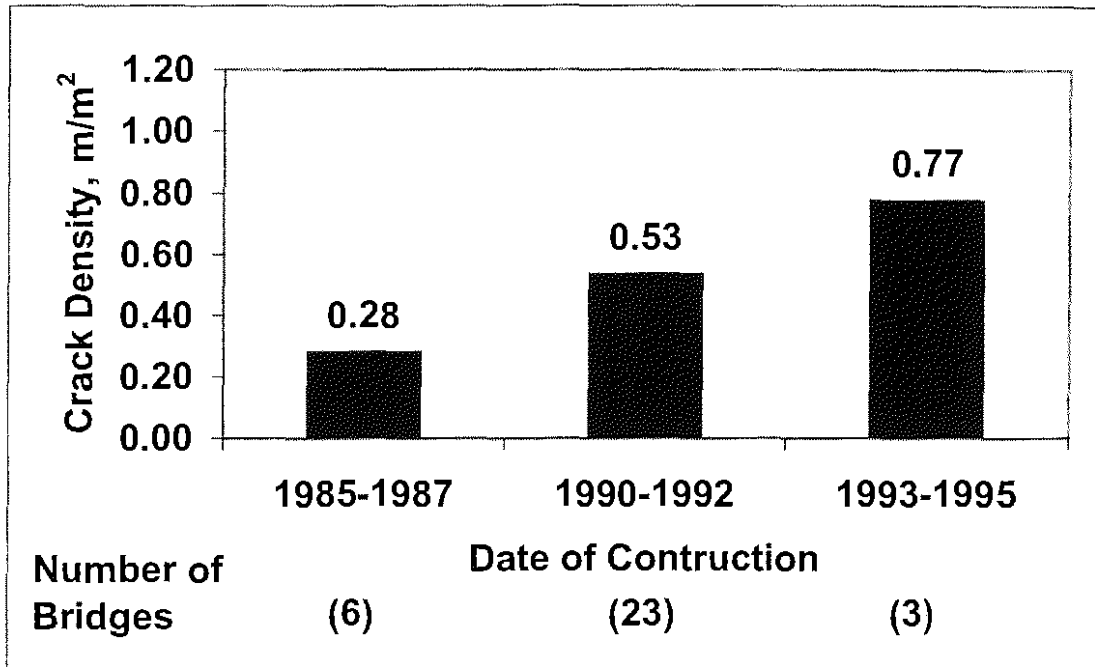


Figure 3.14 : Mean crack density of entire bridge versus date of construction for conventional overlay bridge decks

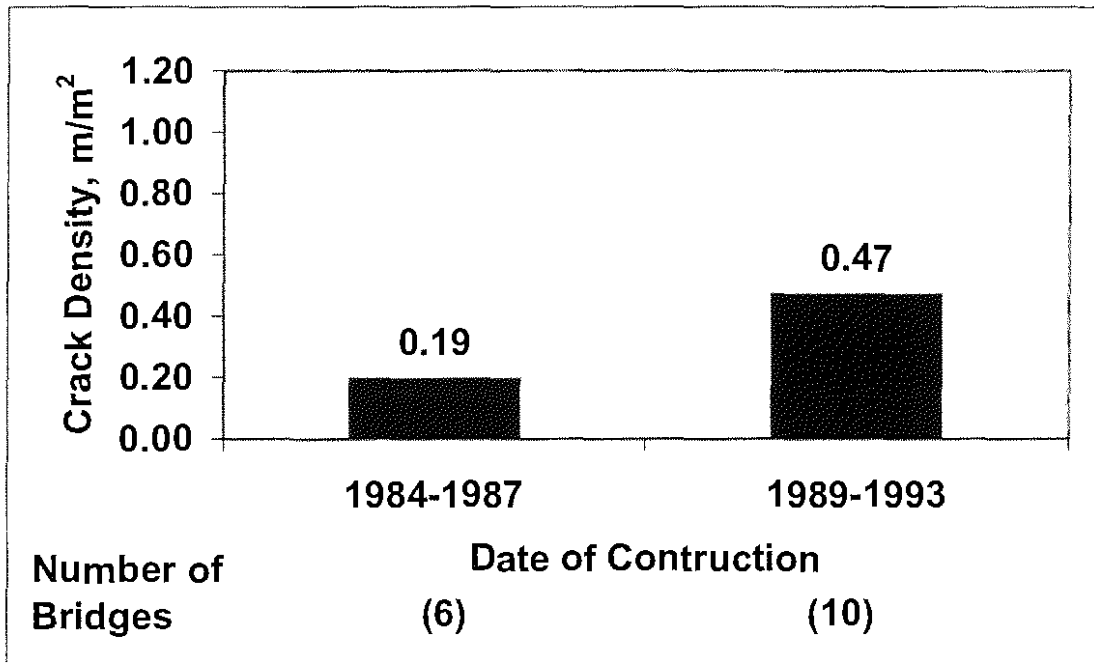


Figure 3.15 : Mean crack density of entire bridge versus date of construction for monolithic bridge decks

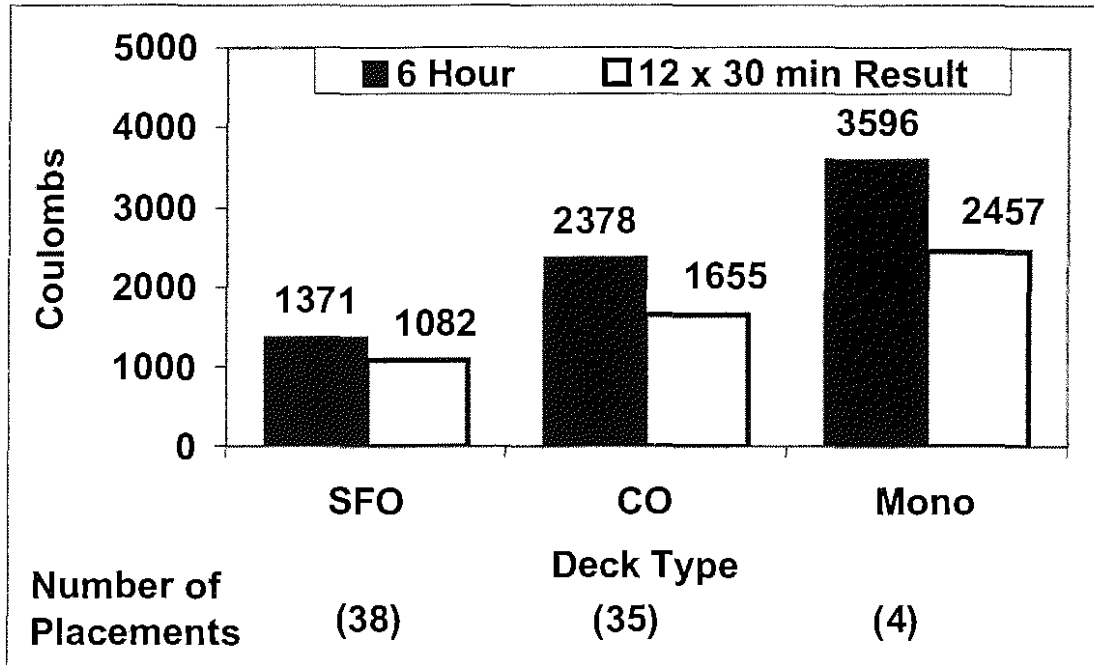


Figure 3.16 : Mean RCPT coulomb reading of individual placements versus deck type. Deck types are silica fume overlay (SFO), conventional overlay (CO), and Monolithic bridge decks (Mono).

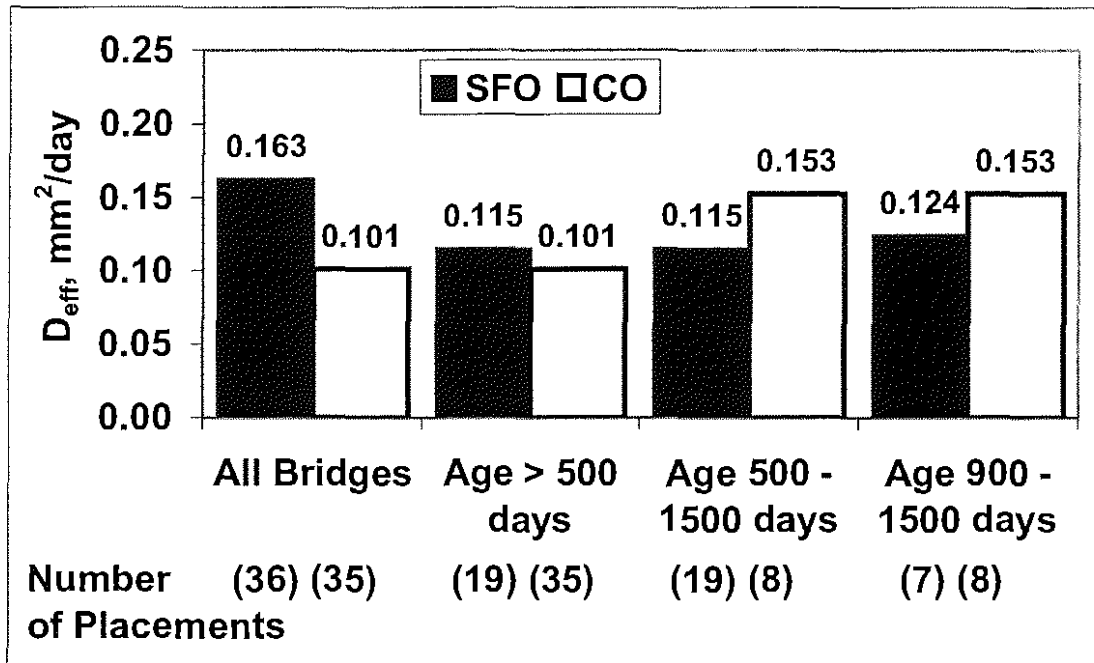


Figure 3.17: Mean effective diffusion coefficient of individual placements grouped into age categories. Deck types are silica fume overlay (SFO) and conventional overlay (CO).

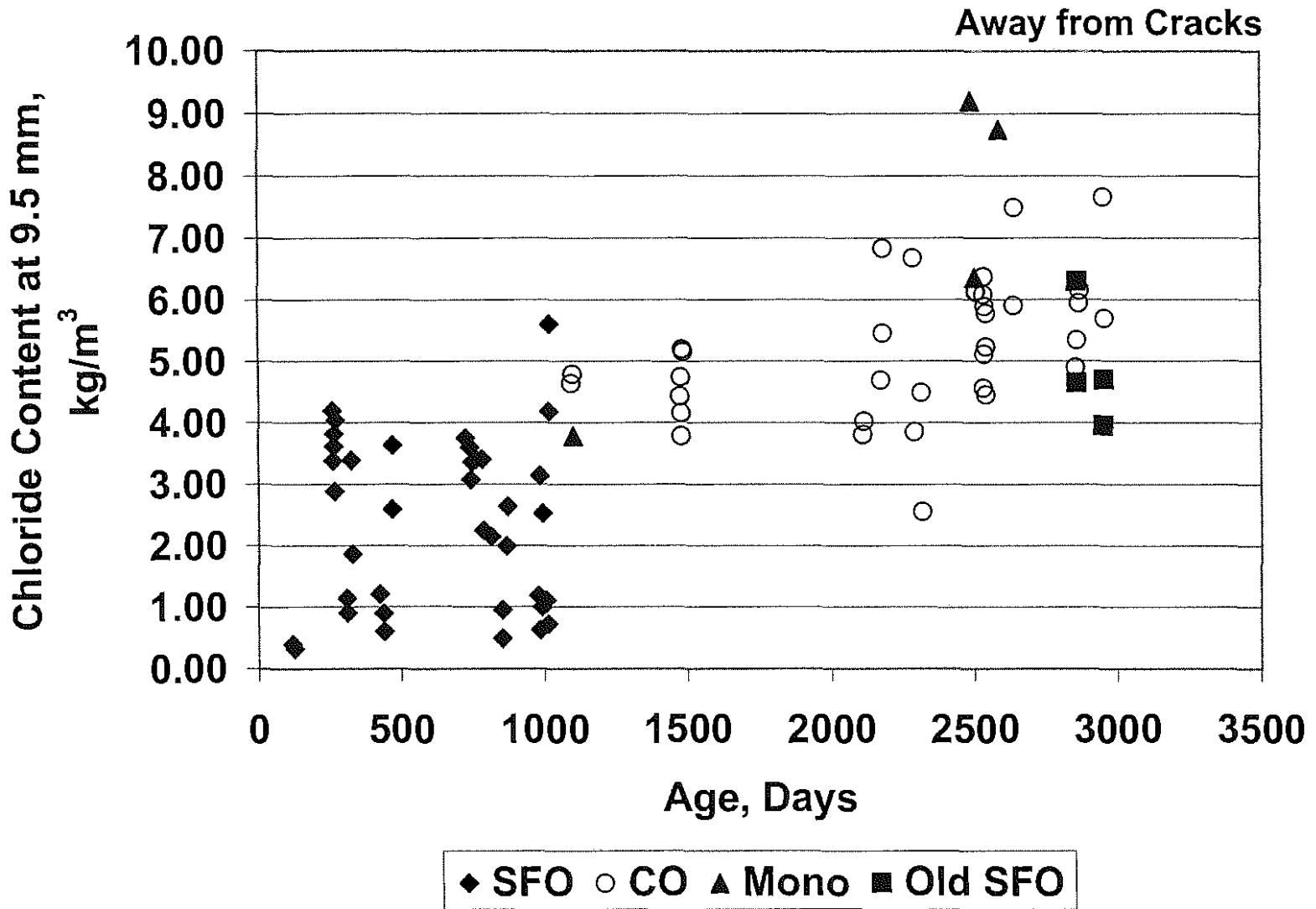


Fig. 3.18: Chloride content away from cracks at a mean depth of 9.5 mm versus placement age. Categories are silica fume overlays (SFO), conventional overlays (CO), monolithic bridge decks (Mono), bridges 89-184 and 89-187 (Old SFO)

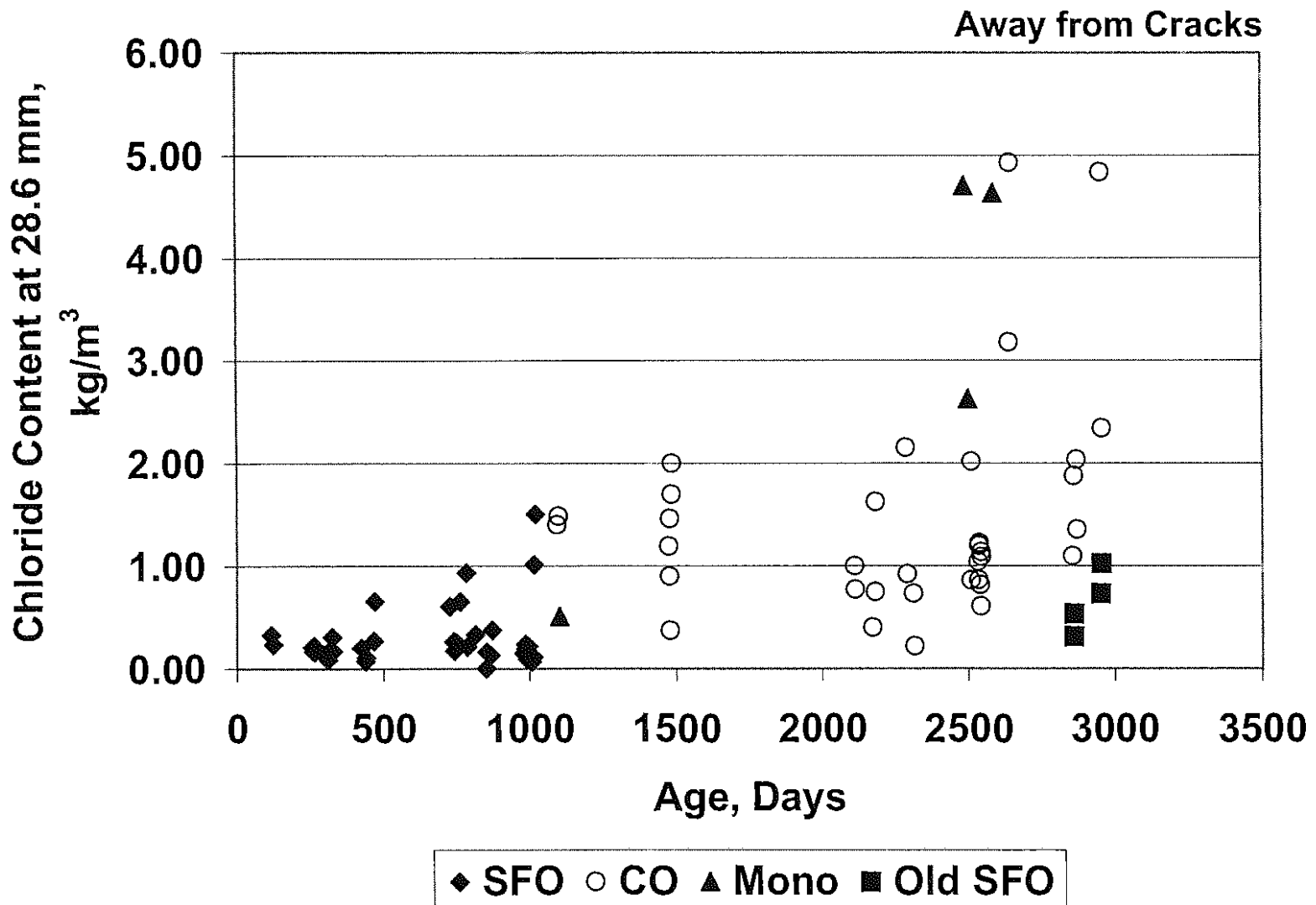


Fig. 3.19: Chloride content away from cracks at a mean depth of 28.6 mm versus placement age. Categories are silica fume overlays (SFO), conventional overlays (CO), monolithic bridge decks (Mono), and bridges 89-184 and 89-187 (Old SFO).

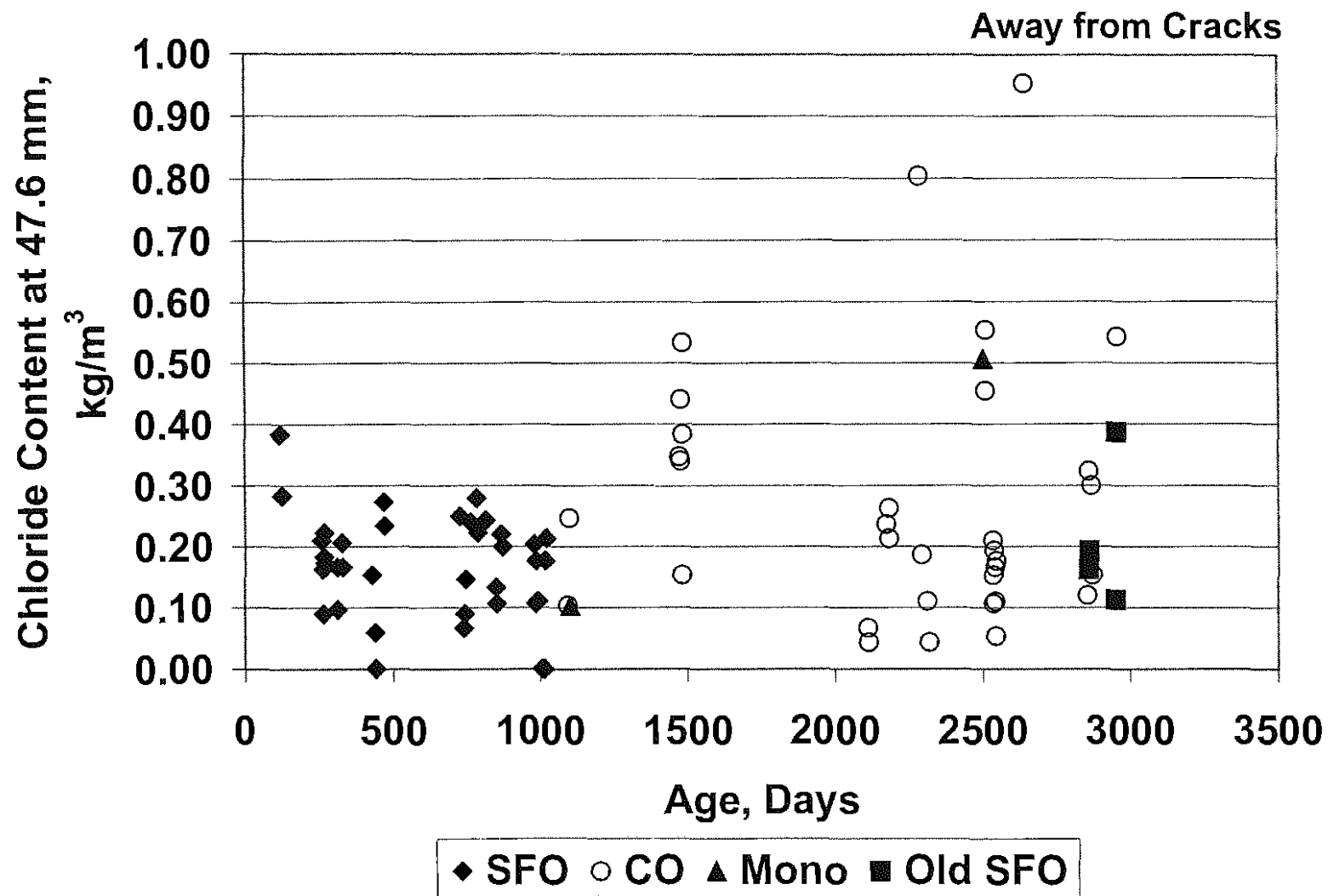


Fig. 3.20: Chloride content away from cracks at a mean depth of 47.6 mm versus placement age. Only chloride contents less than 1.0 kg/m³ are included. Silica fume overlay (SFO). Conventional overlay (CO). Monolithic (Mono).

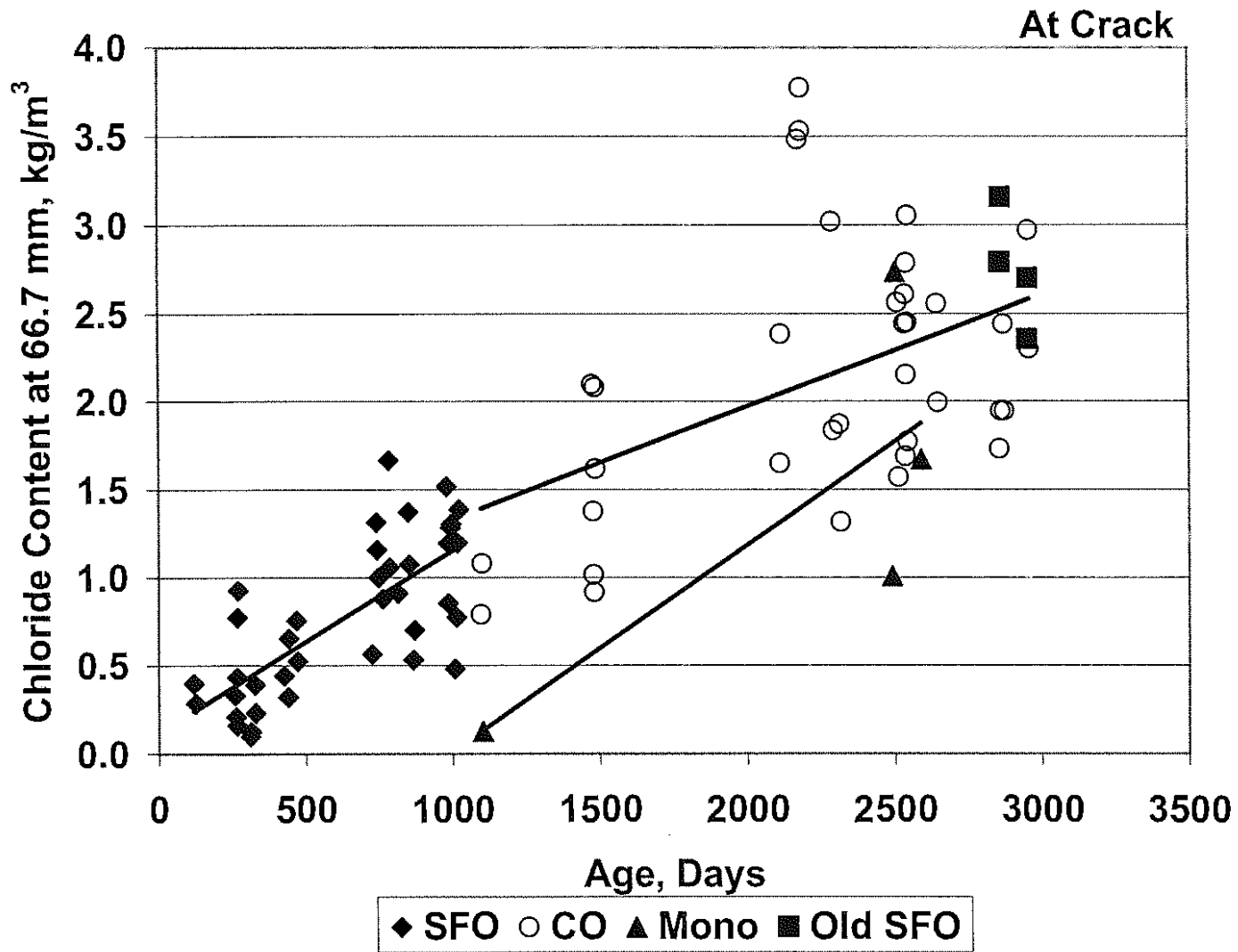
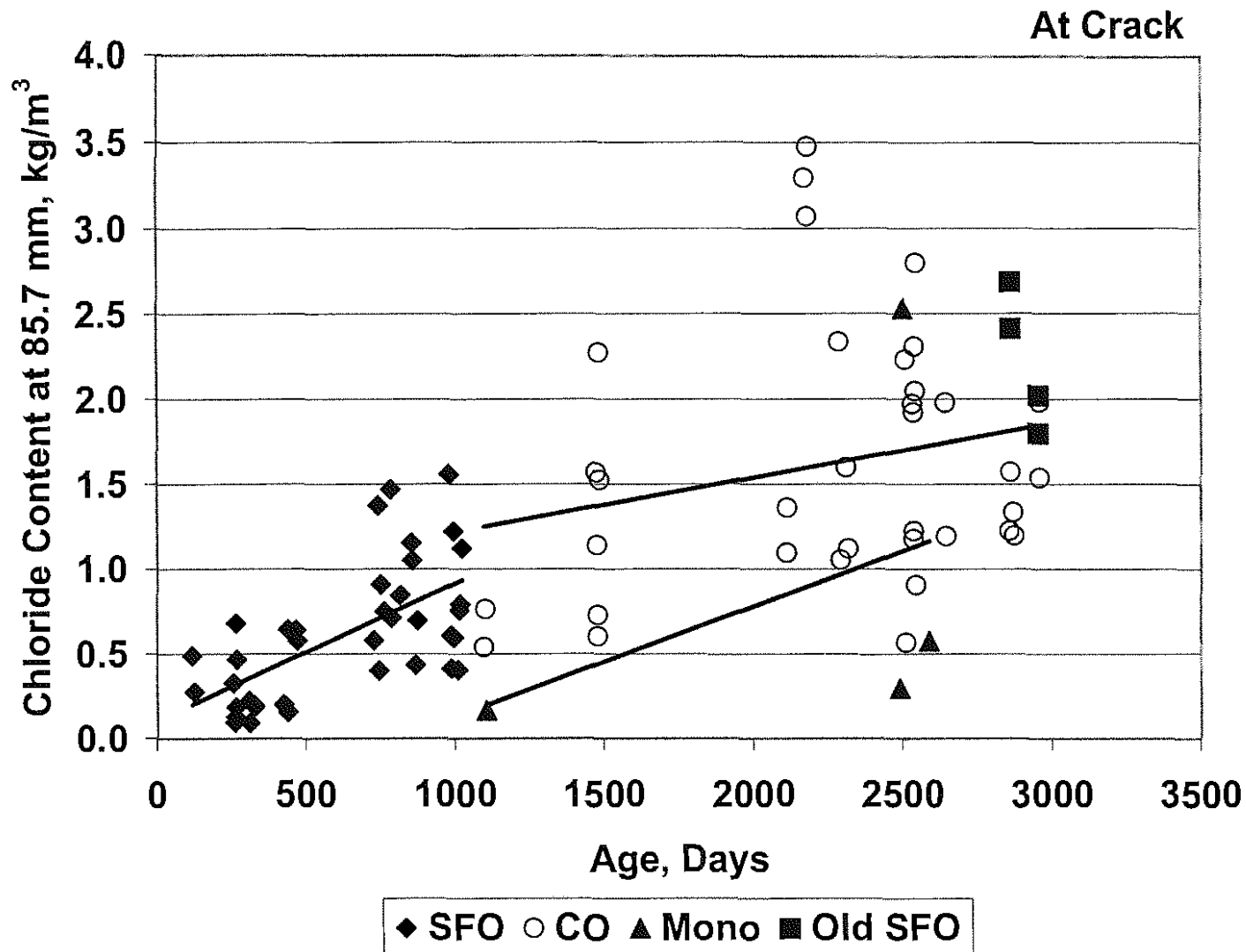


Fig. 3.21: chloride content at cracks at a mean depth of 66.7 mm versus placement age. Categories are silica fume overlays (SFO), conventional overlays (CO), monolithic bridge decks (Mono), and bridges 89-184 and 89-187 (Old SFO)



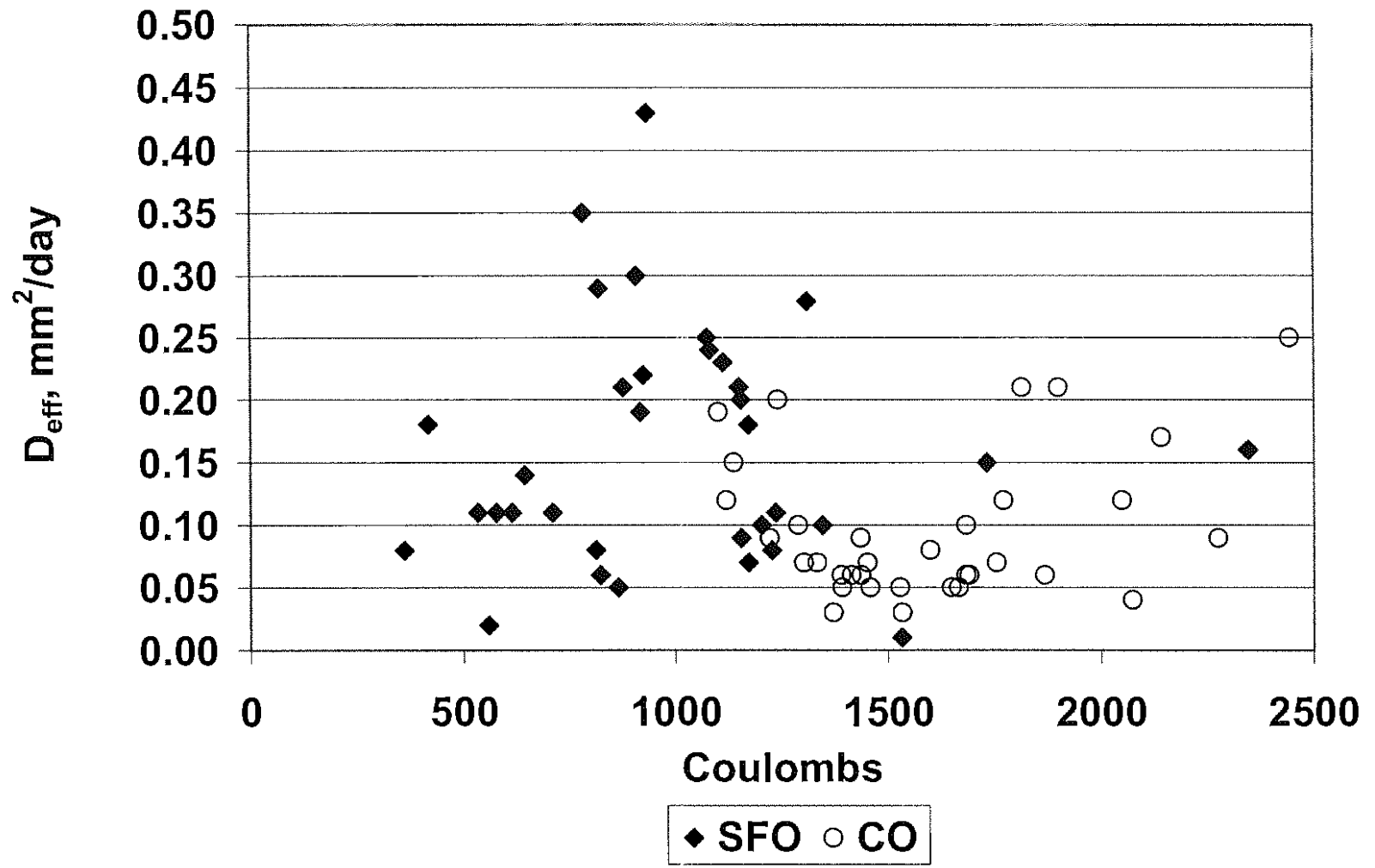


Fig. 3.23: Effective diffusion coefficient versus RCPT results

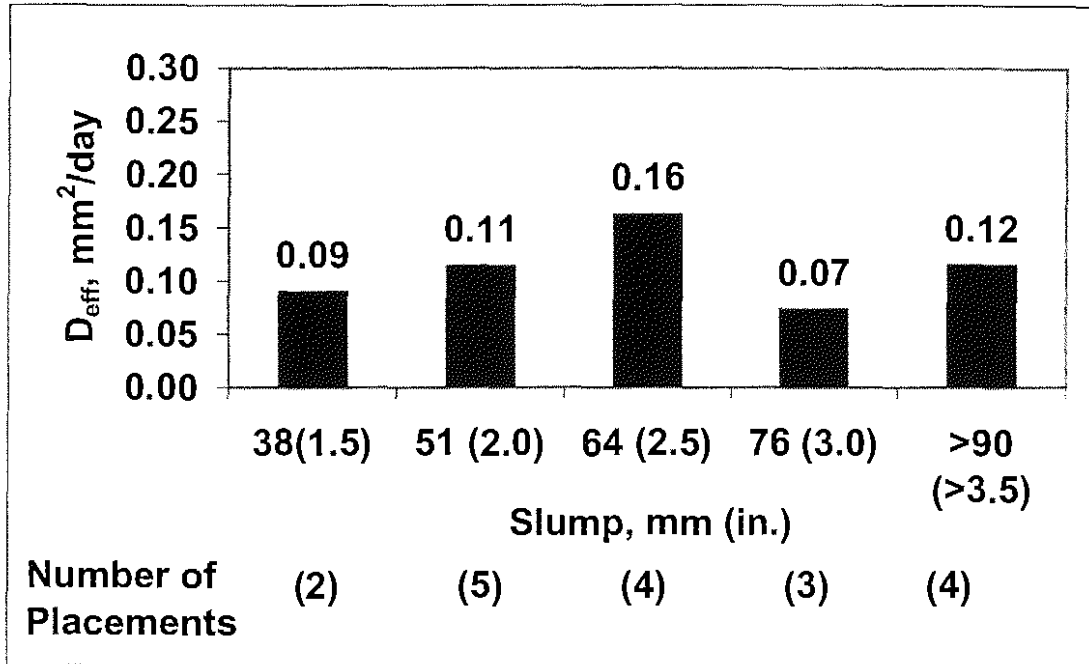


Figure 3.24: Mean effective diffusion coefficient of individual placements versus concrete slump for silica fume overlays

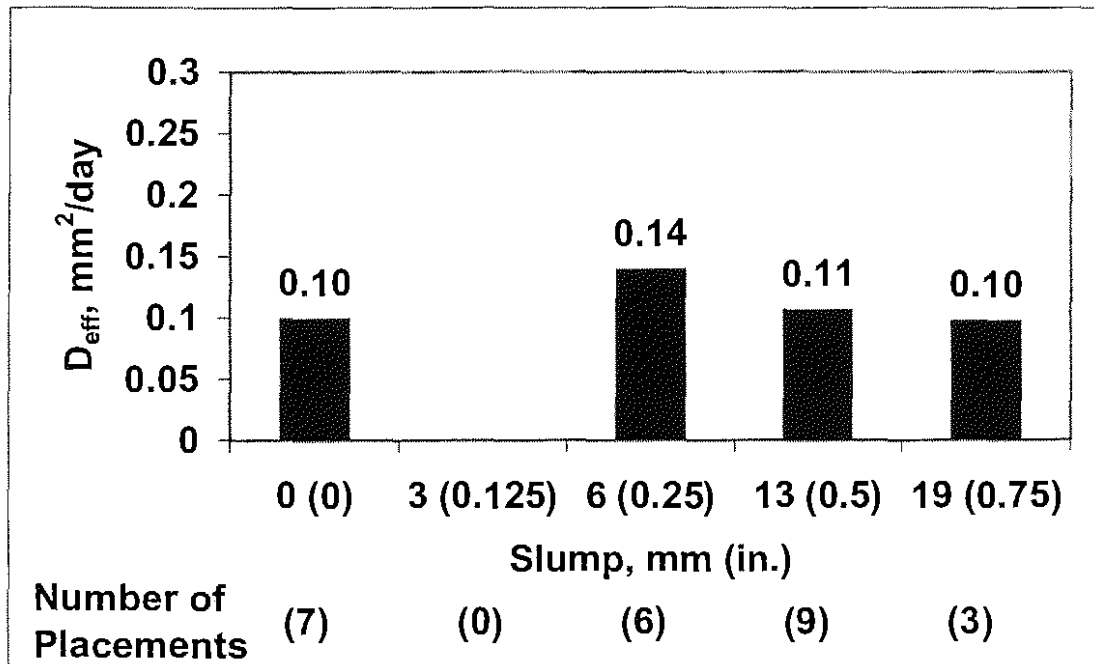


Figure 3.25: Mean effective diffusion coefficient of individual placements versus concrete slump for conventional overlays

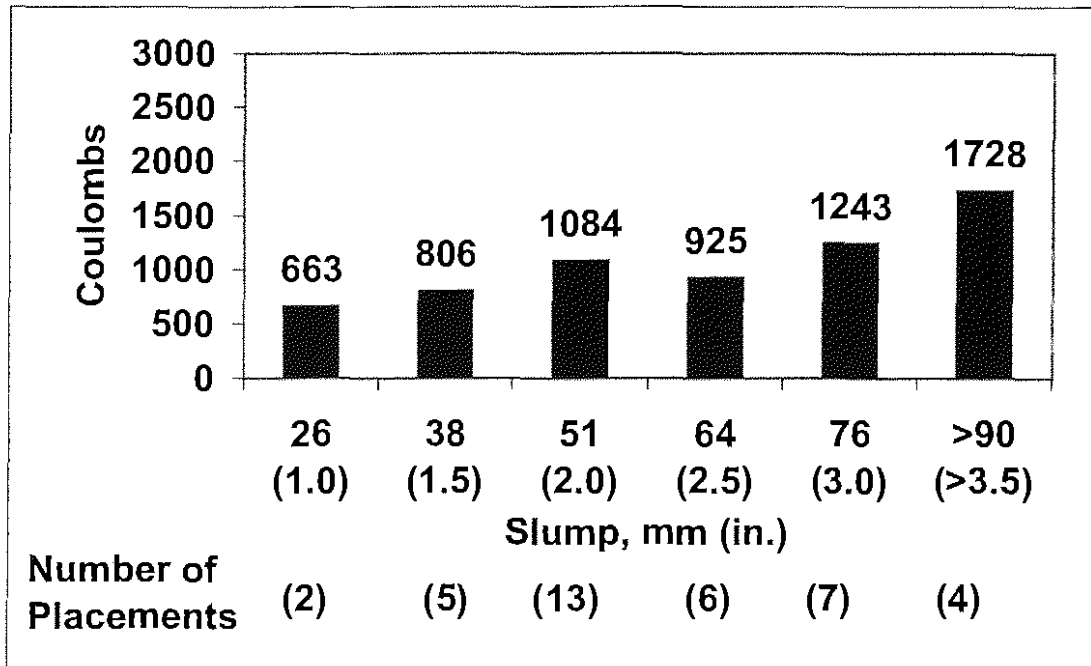


Figure 3.26: Mean RCPT result of individual placements versus concrete slump for silica fume overlays

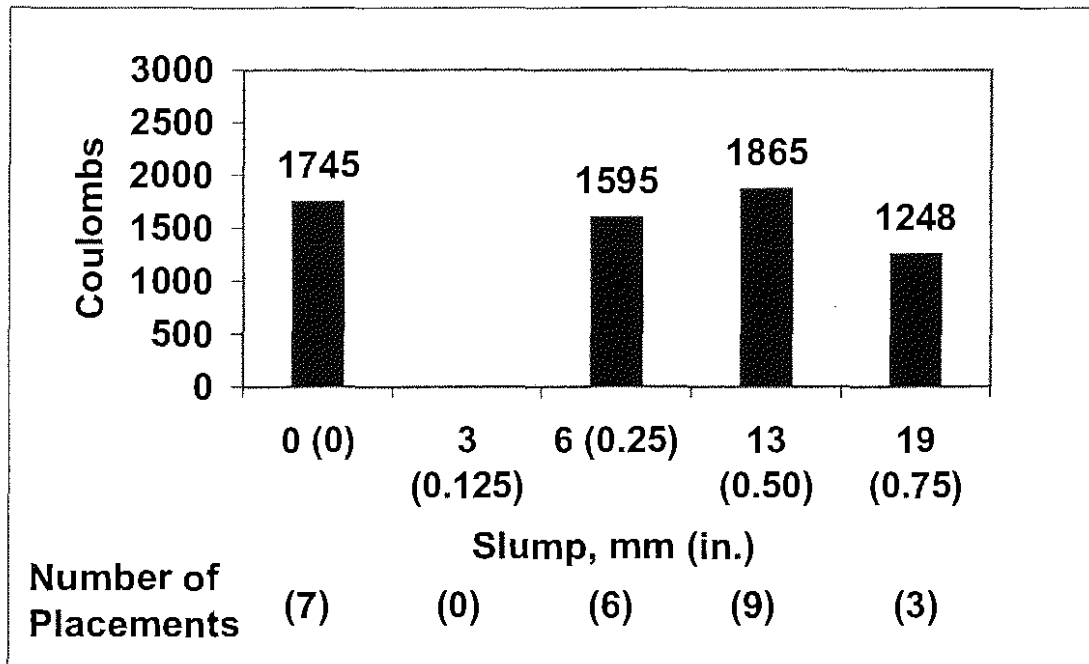


Figure 3.27: Mean RCPT result of individual placements versus concrete slump for conventional overlays

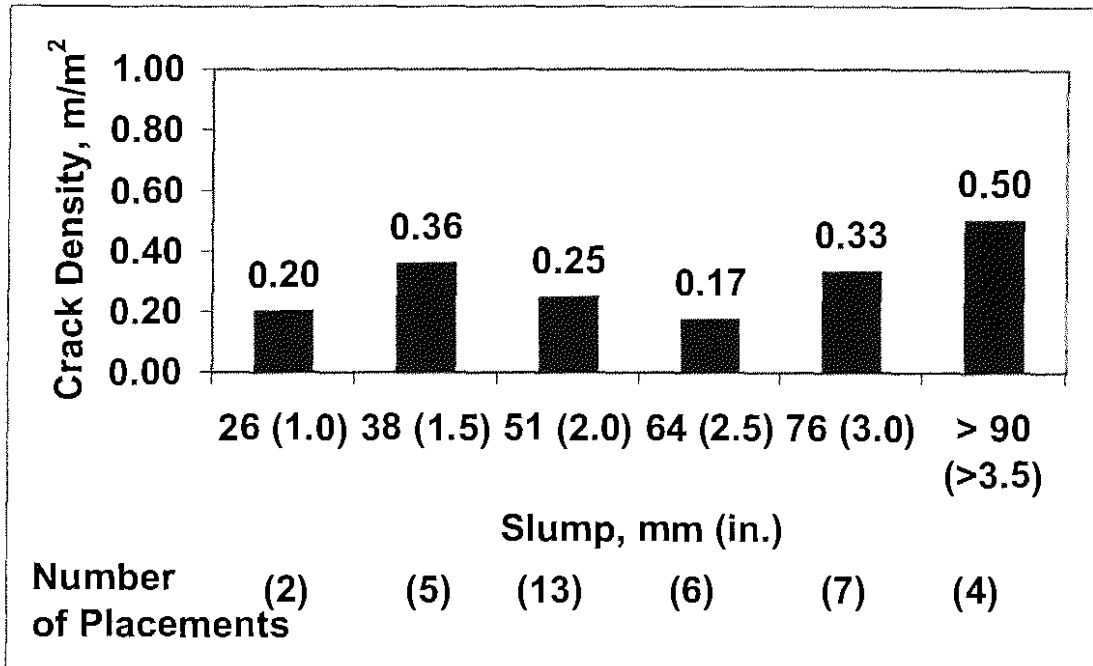


Figure 3.28: Mean crack density of individual placements versus concrete slump for silica fume overlays

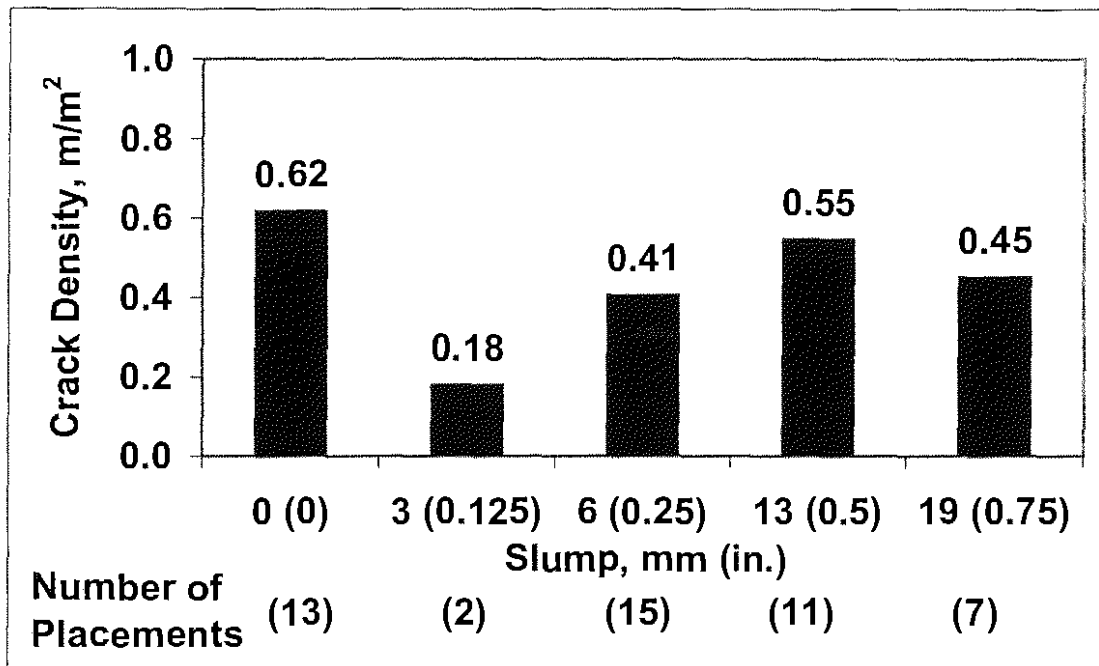


Figure 3.29: Mean crack density of individual placements versus concrete slump for conventional overlays

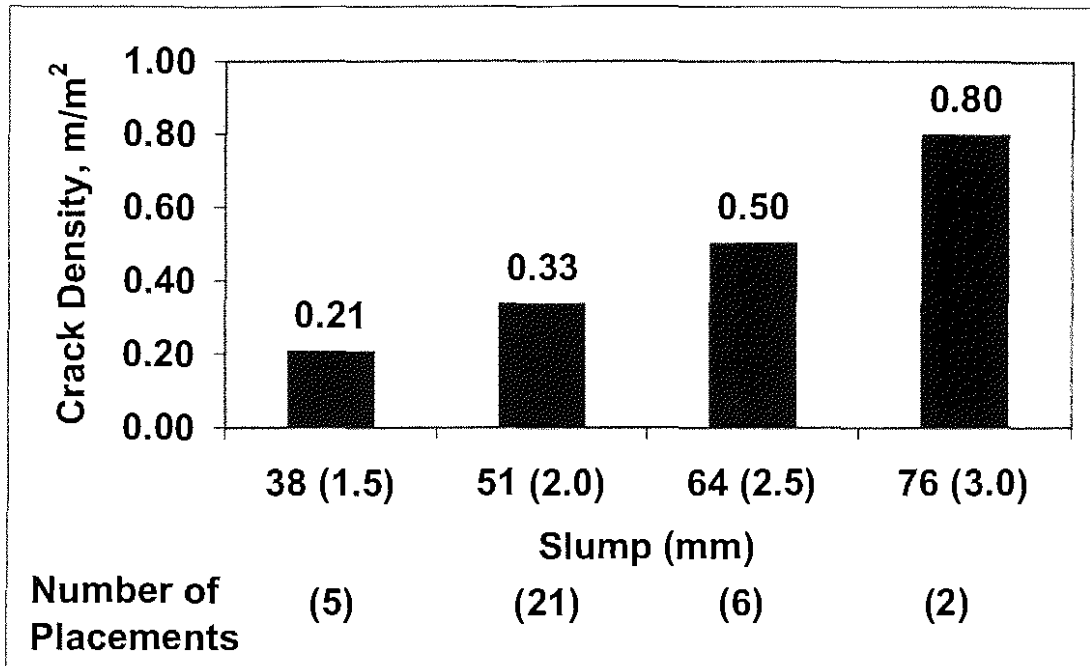


Figure 3.30: Mean crack density of individual placements versus concrete slump for monolithic bridges

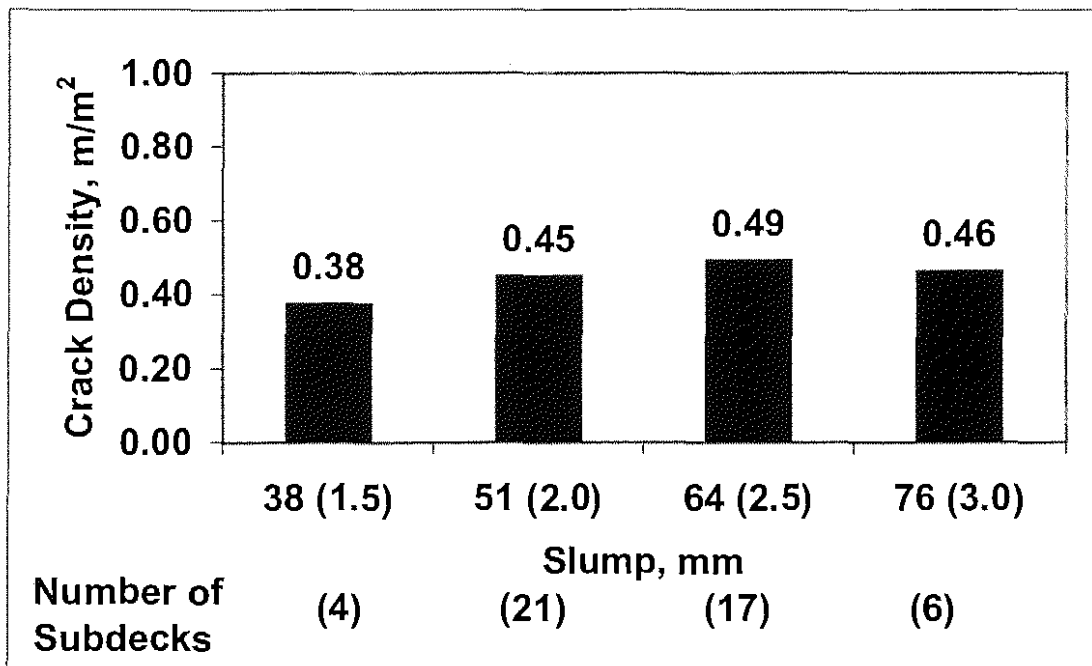


Figure 3.31: Mean crack density of bridge subdecks versus concrete slump

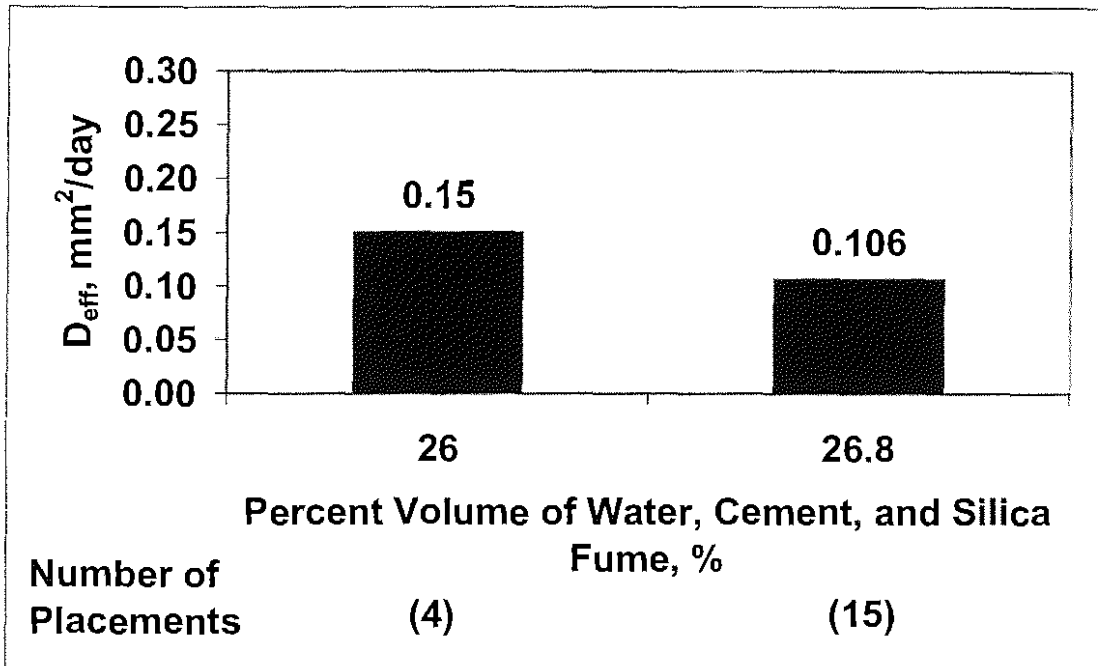


Figure 3.32: Mean effective diffusion coefficient of individual placements versus percent volume of water, cement, and silica fume for silica fume overlays

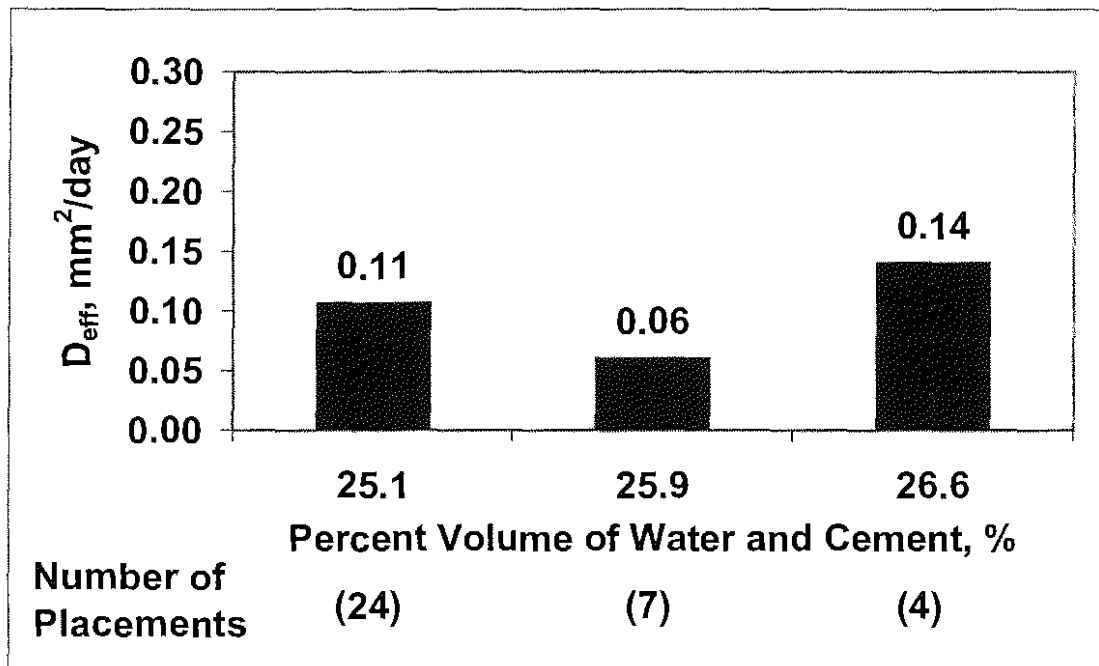


Figure 3.33: Mean effective diffusion coefficient of individual placements versus percent volume of water and cement for conventional overlays

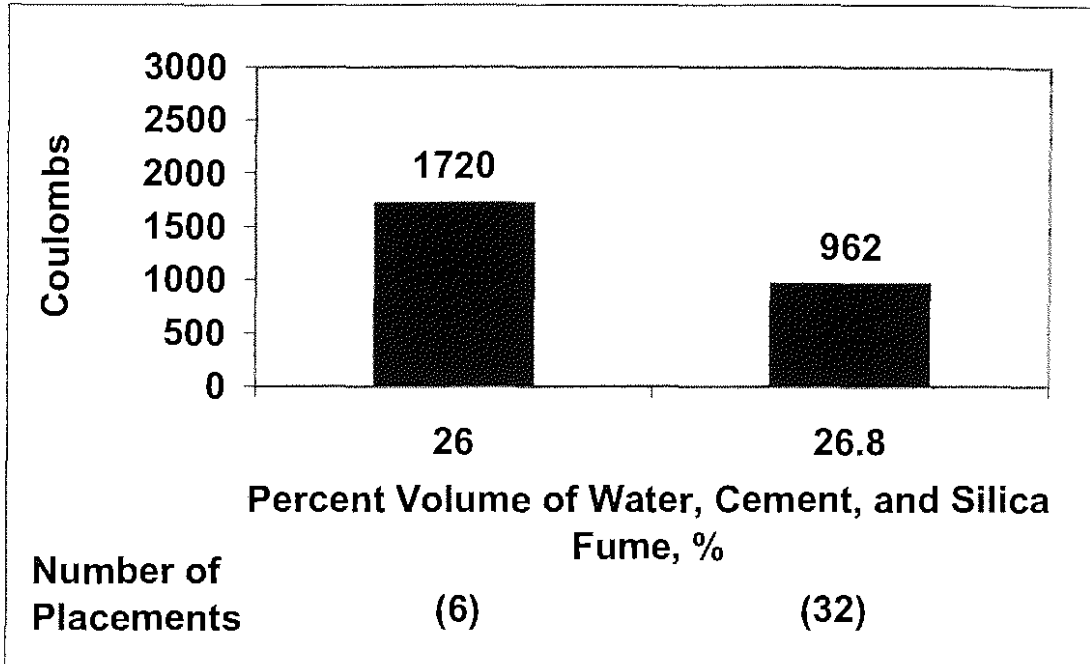


Figure 3.34: Mean RCPT result of individual placements versus percent volume of water, cement, and silica fume for silica fume overlays

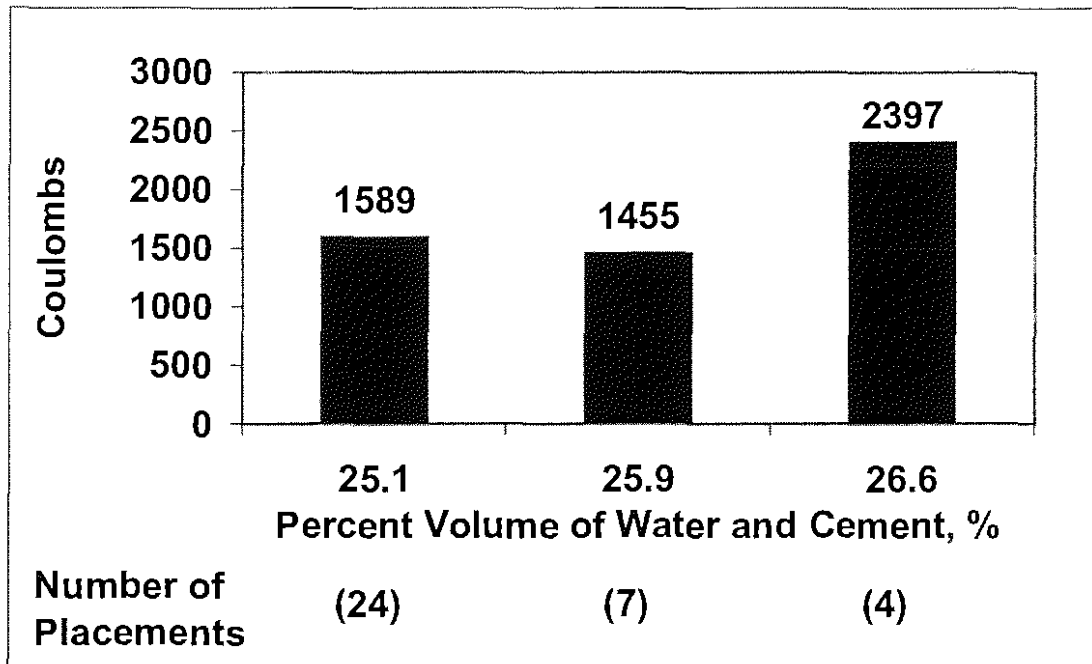


Figure 3.35: Mean RCPT result of individual placements versus percent volume of water and cement for conventional overlays

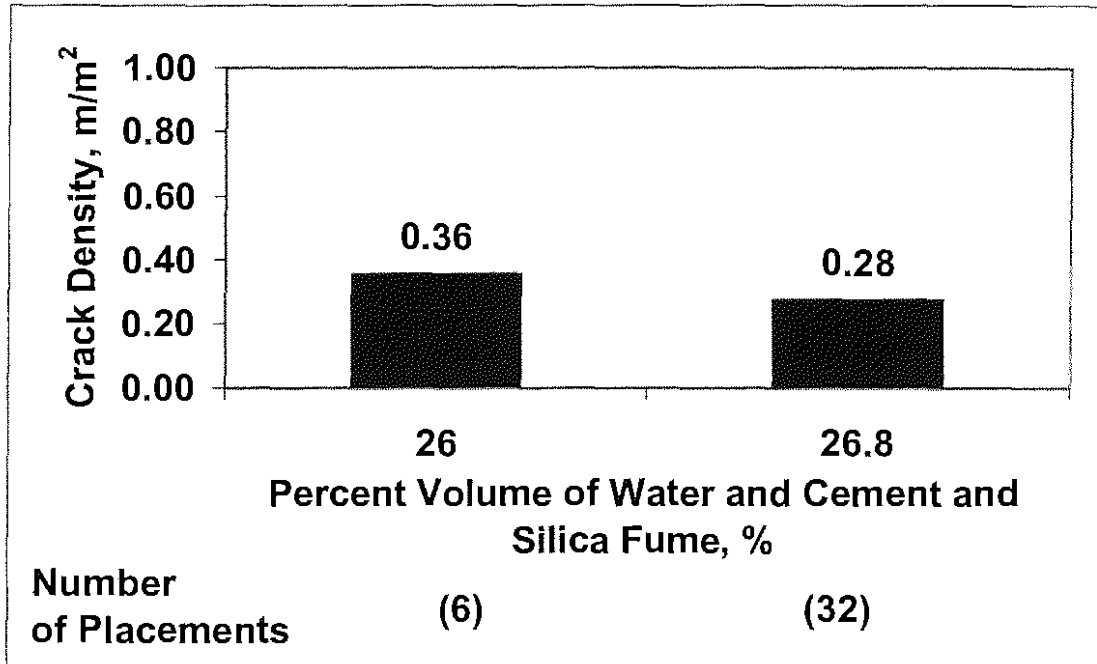


Figure 3.36: Mean crack density for individual placements versus percent volume of water, cement, and silica fume for silica fume overlays

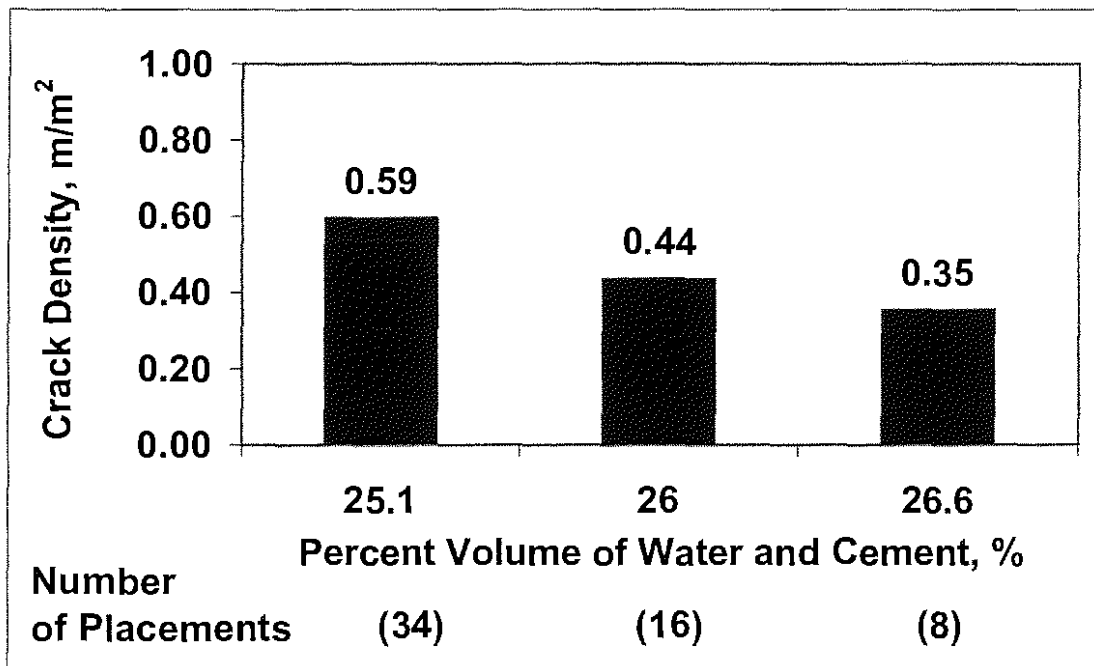


Figure 3.37: Mean crack density for individual placements versus percent volume of water and cement for conventional overlays

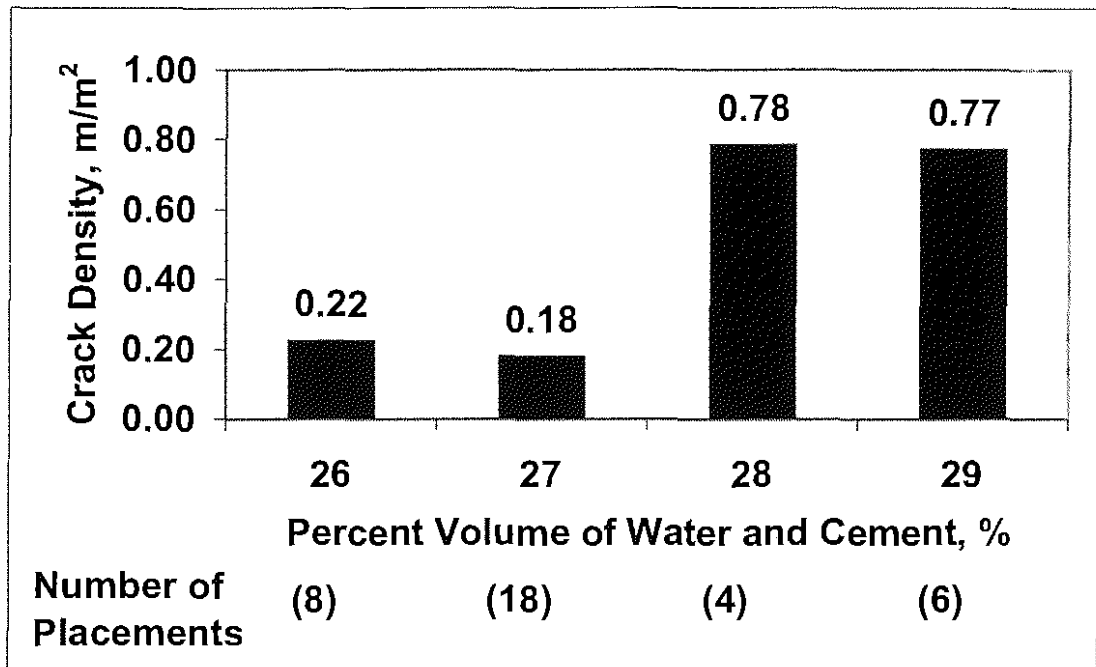


Figure 3.38: Mean crack density for individual placements versus percent volume of water and cement for monolithic bridges

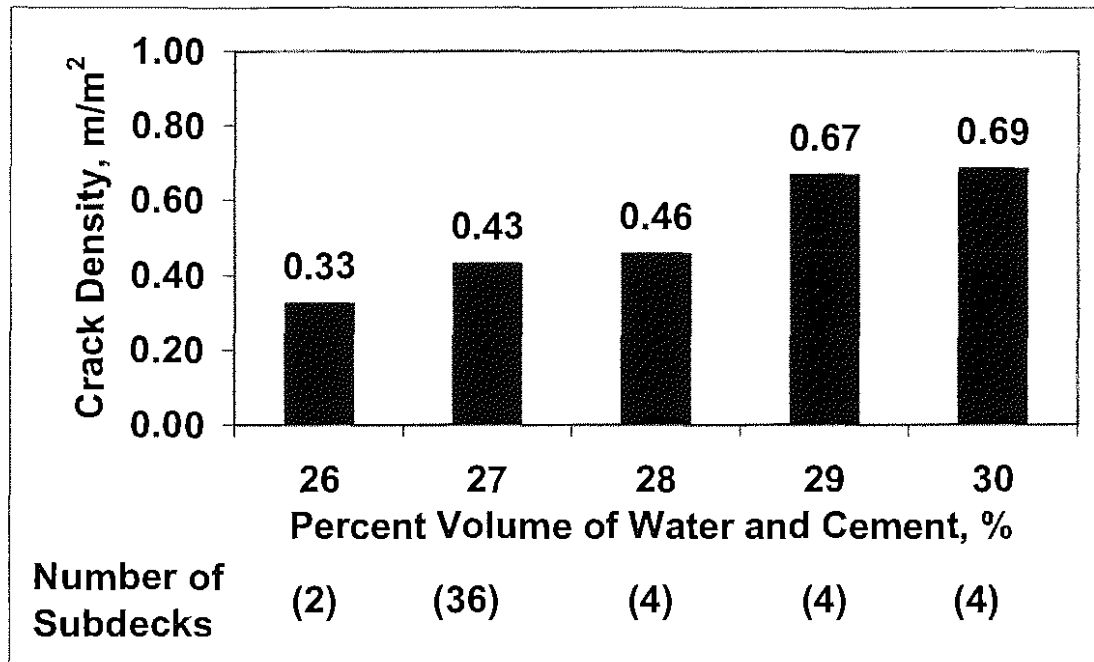


Figure 3.39: Mean crack density of bridge subdecks versus average percent volume of water and cement

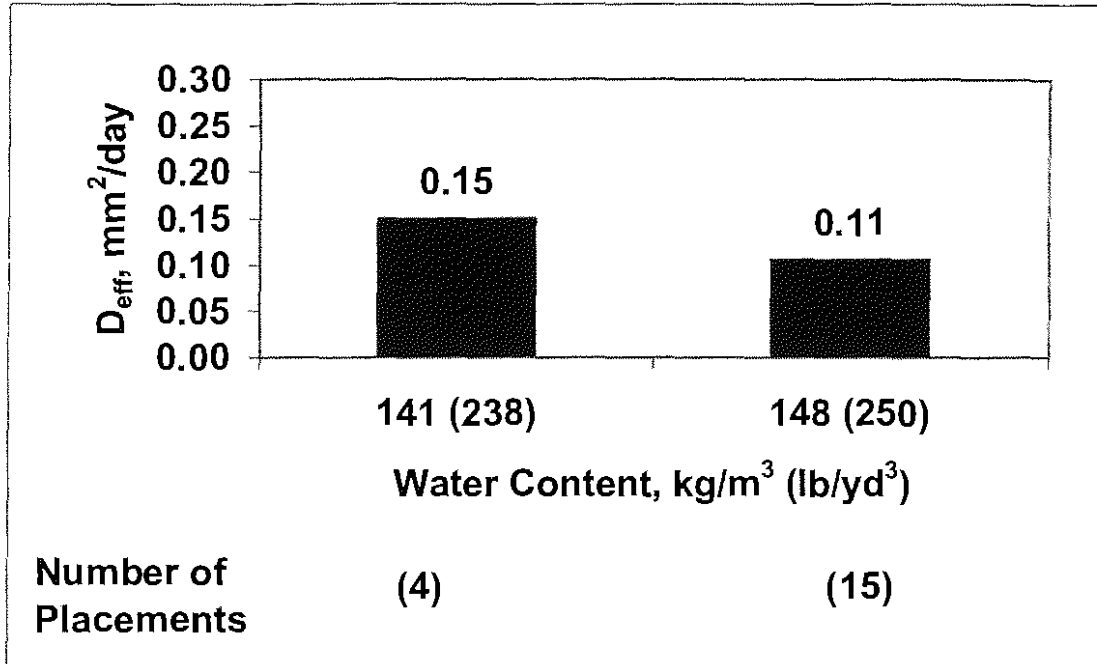


Figure 3.40: Mean effective diffusion coefficient of individual placements versus water content for silica fume overlays

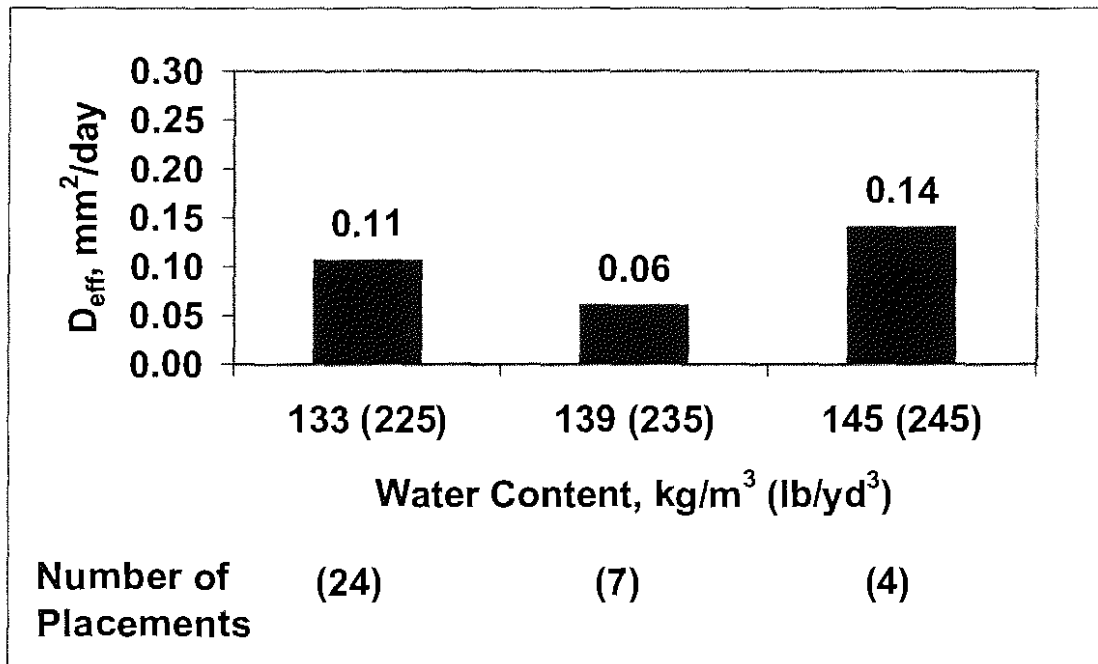


Figure 3.41: Mean effective diffusion coefficient of individual placements versus water content for conventional overlays

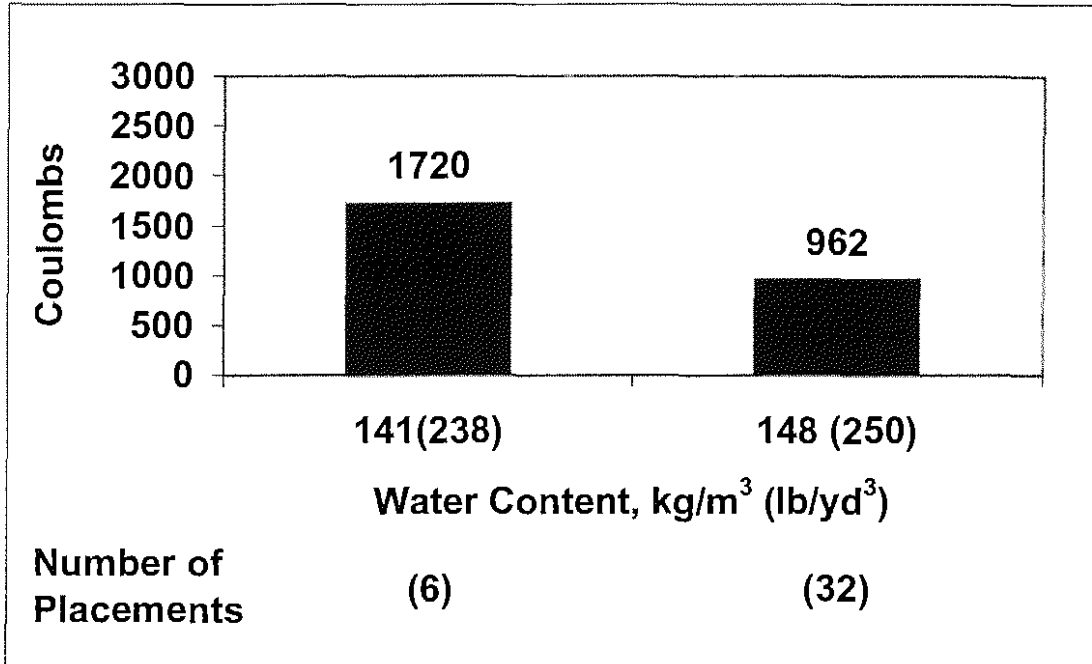


Figure 3.42: Mean RCPT result of individual placements versus water content for silica fume overlays

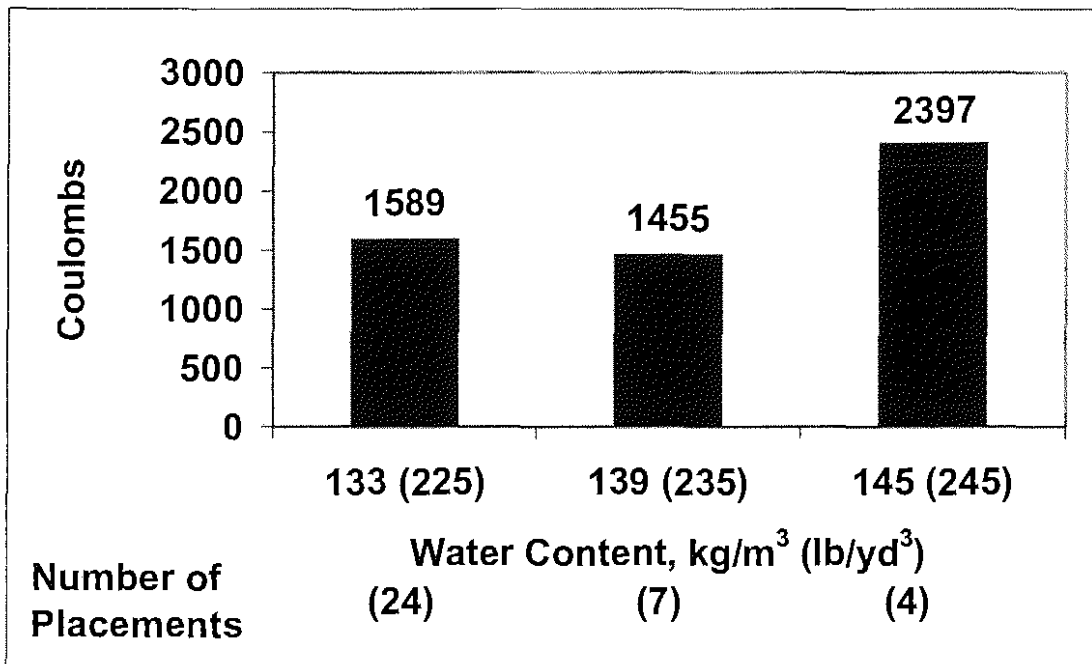


Figure 3.43: Mean RCPT result of individual placements versus water content for conventional overlays

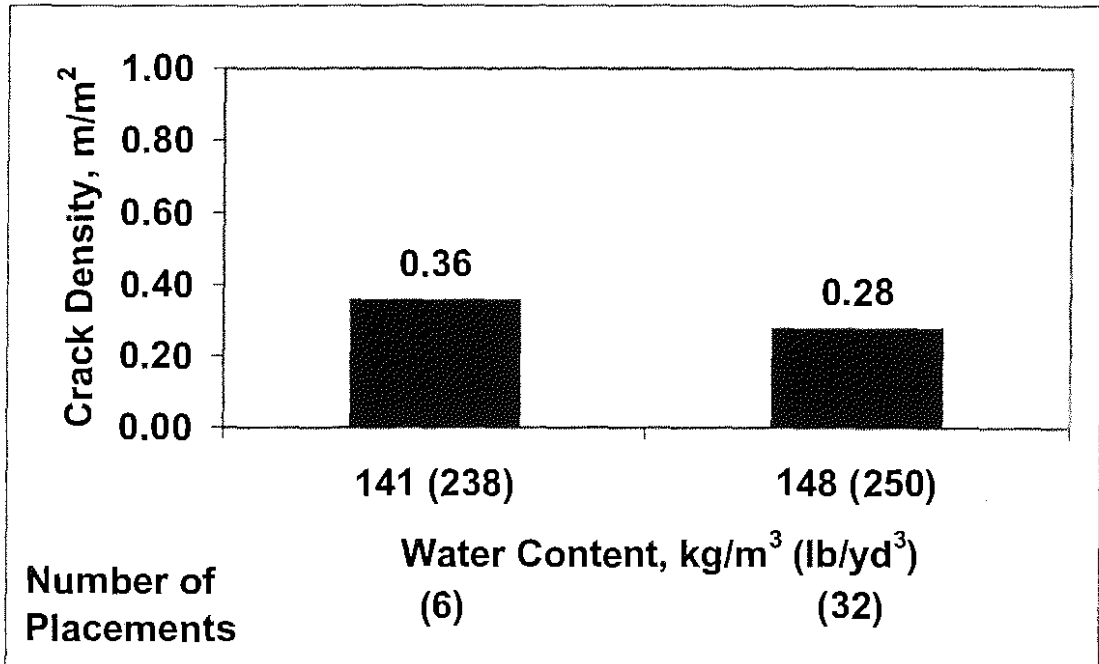


Figure 3.44: Mean crack density for individual placements versus water content for silica fume overlays

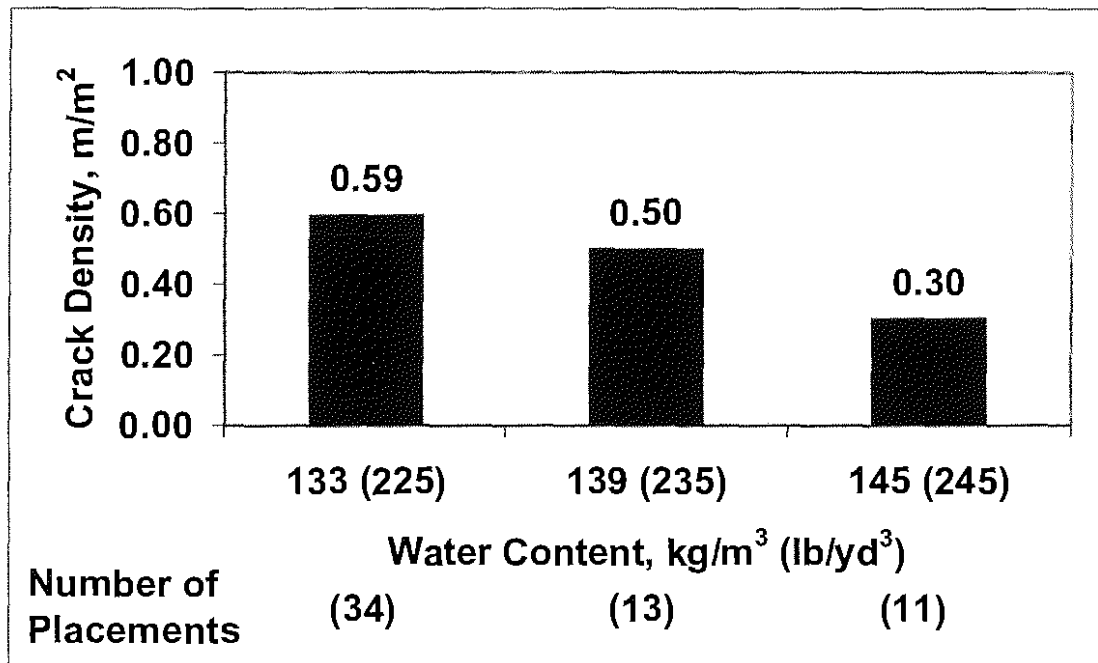


Figure 3.45: Mean crack density for individual placements versus water content for conventional overlays

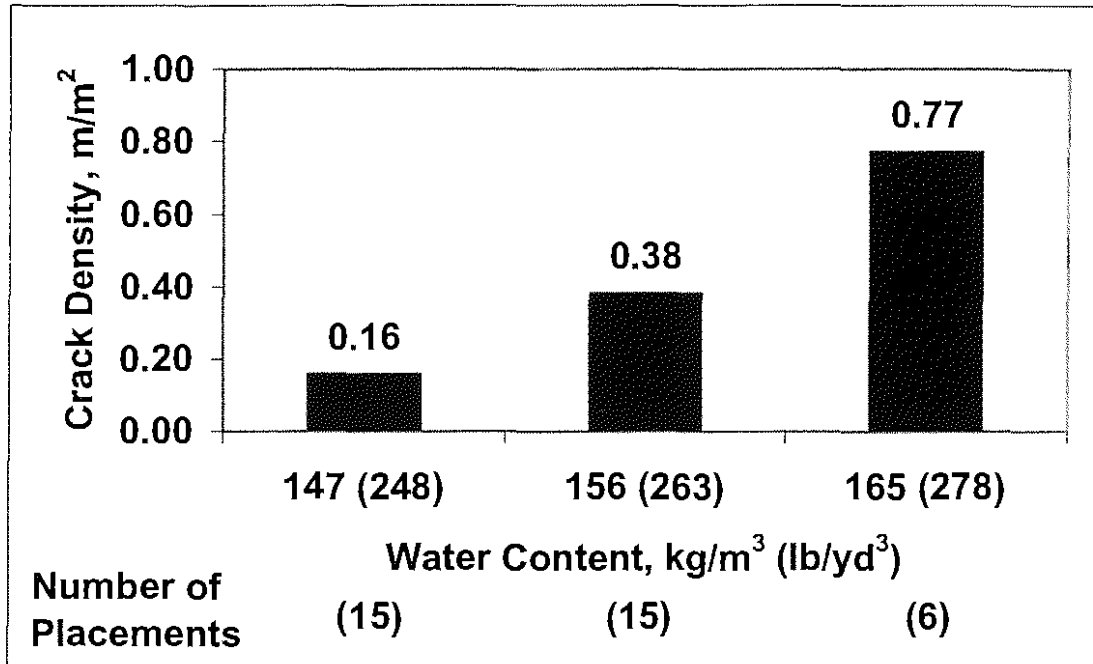


Figure 3.46: Mean crack density for individual placements versus water content for monolithic bridges

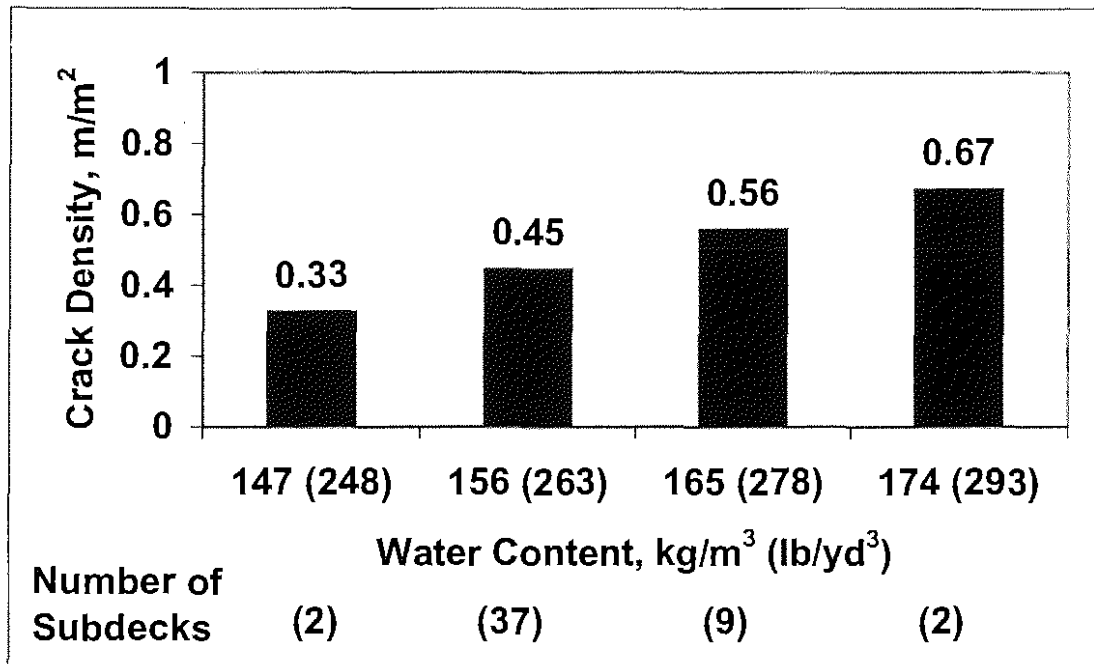


Figure 3.47: Mean crack density of bridge subdecks versus water content

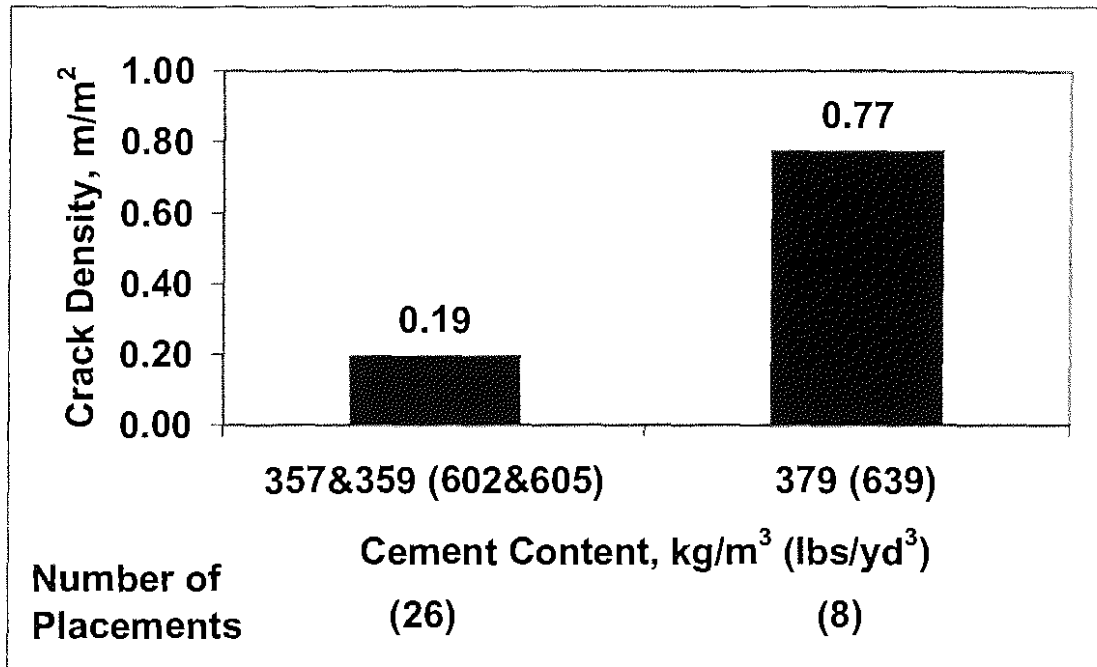


Figure 3.48: Mean crack density of individual placements versus cement content for monolithic bridge decks

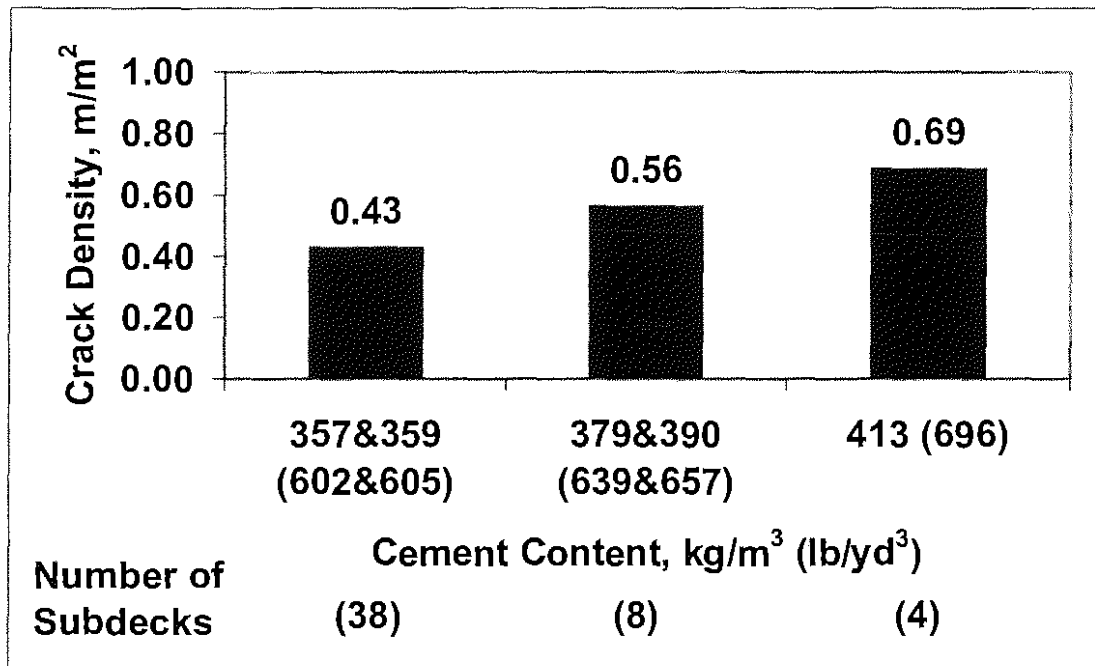


Figure 3.49: Mean crack density of bridge subdecks versus cement content

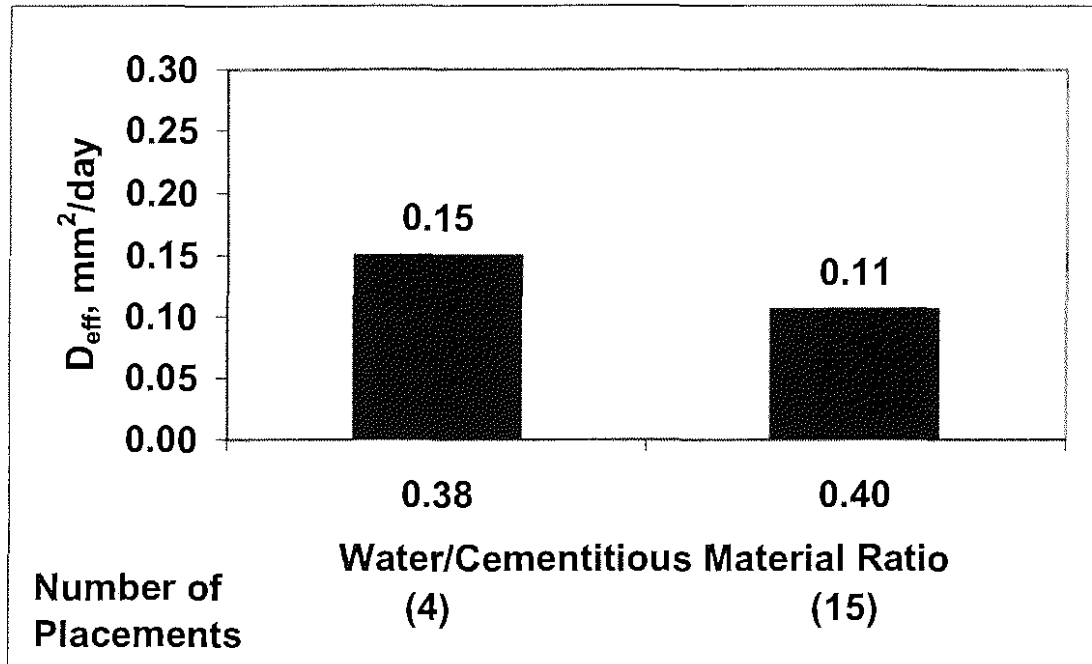


Figure 3.50 : Mean effective diffusion coefficient of individual placements versus water/cementitious material ratio for silica fume overlays

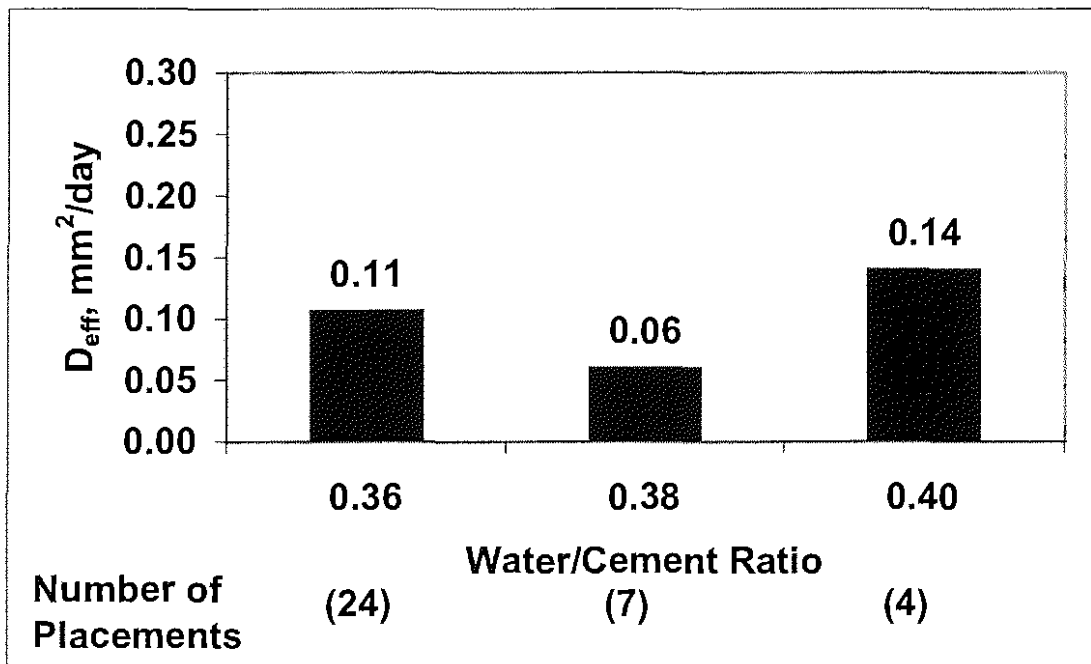


Figure 3.51 : Mean effective diffusion coefficient of individual placements versus water/cement ratio for conventional overlays

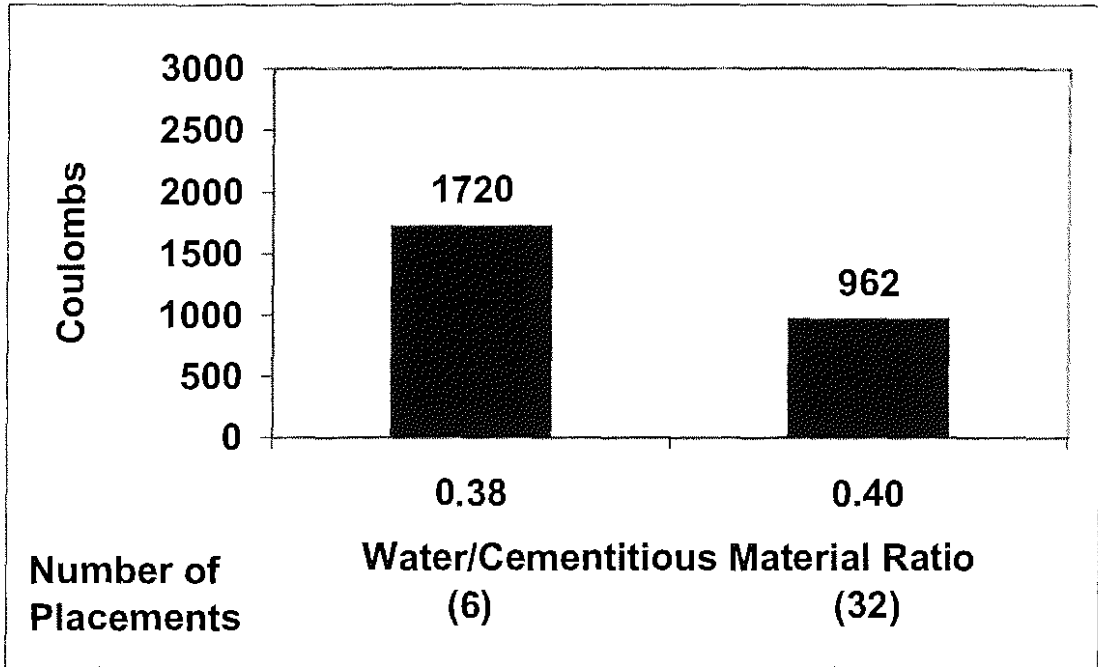


Figure 3.52: Mean RCPT result of individual placements versus water/cementitious material ratio for silica fume overlays

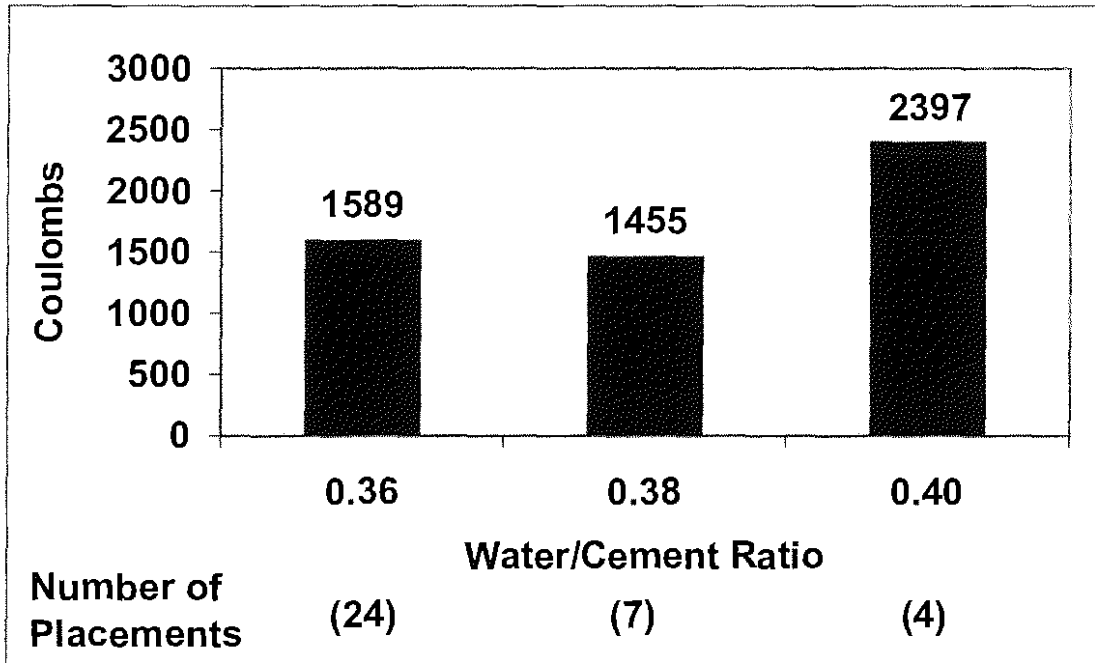


Figure 3.53: Mean RCPT result of individual placements versus water/cement ratio for conventional overlays

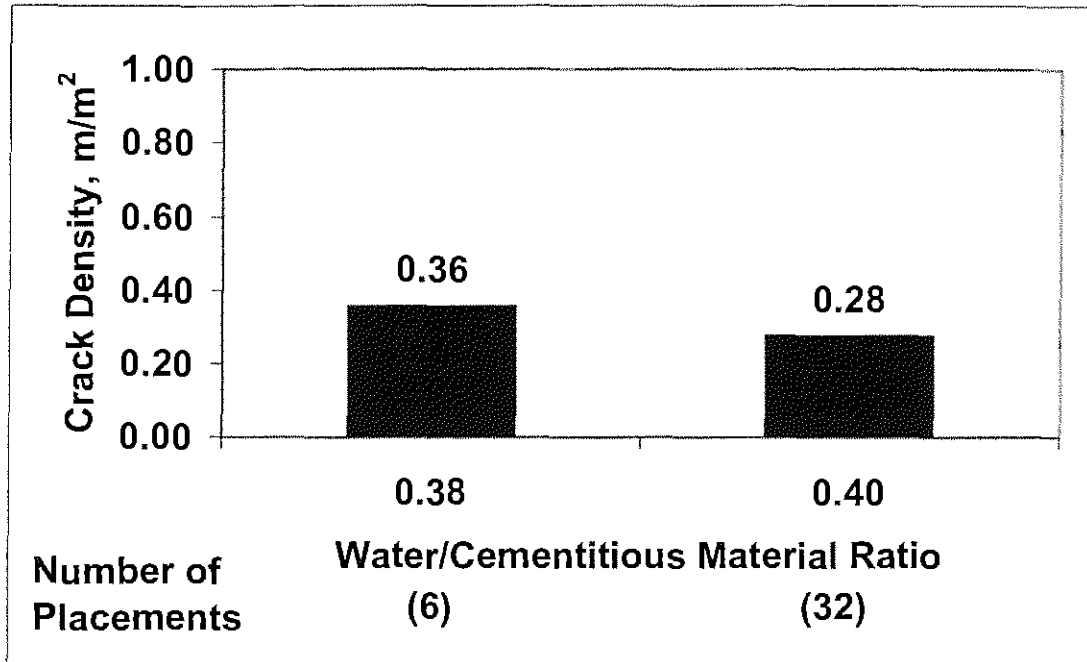


Figure 3.54: Mean crack density for individual placements versus water/cementitious material ratio for silica fume overlay bridge decks

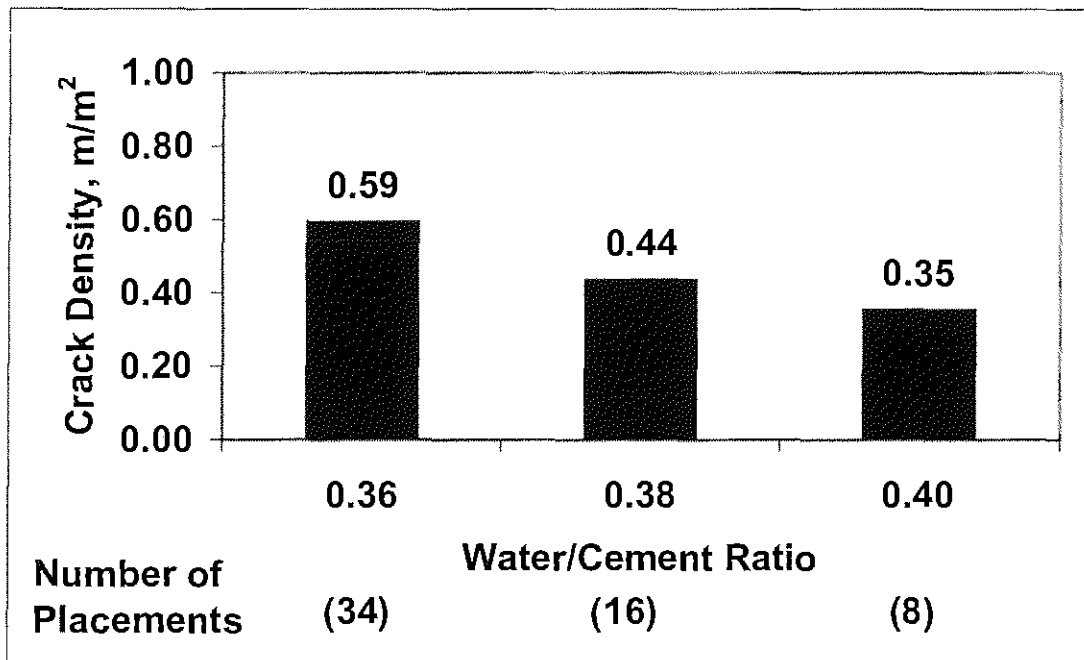


Figure 3.55: Mean crack density for individual placements versus water/cement ratio for conventional overlay bridge decks

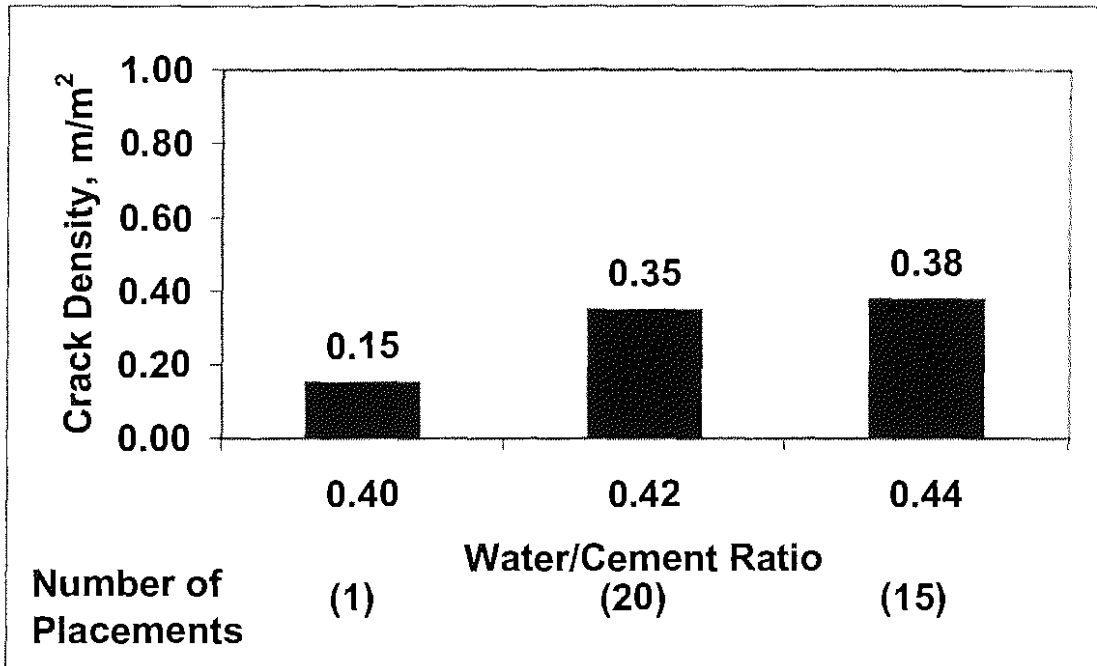


Figure 3.56: Mean crack density for individual placements versus water/cement ratio for monolithic bridge decks

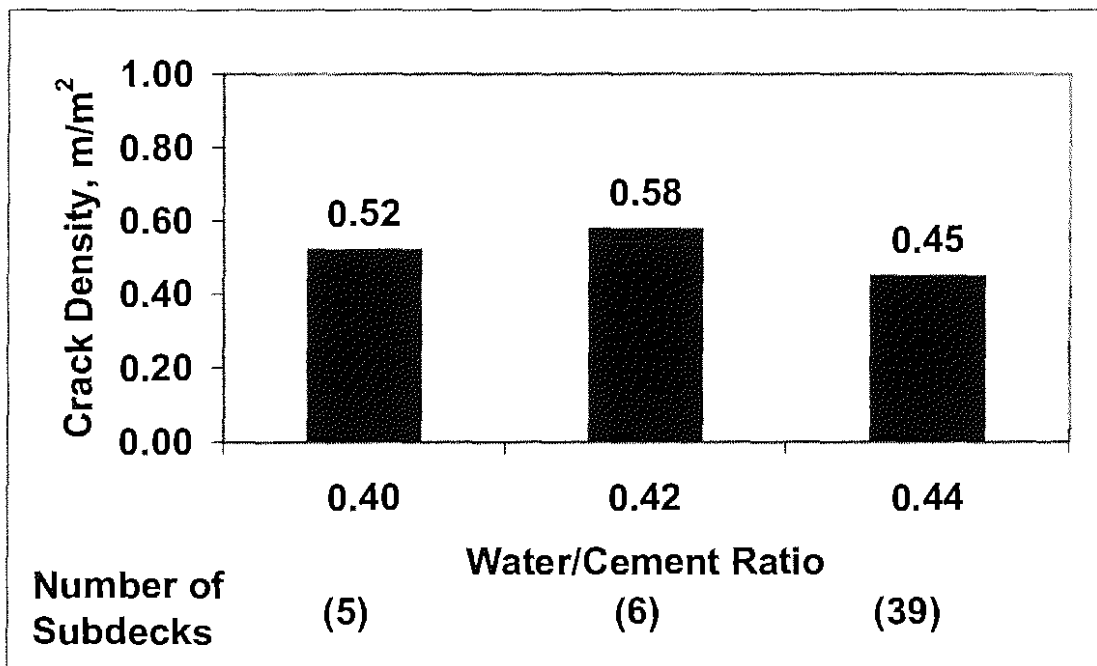


Figure 3.57: Mean crack density of bridge subdecks versus water/cement ratio

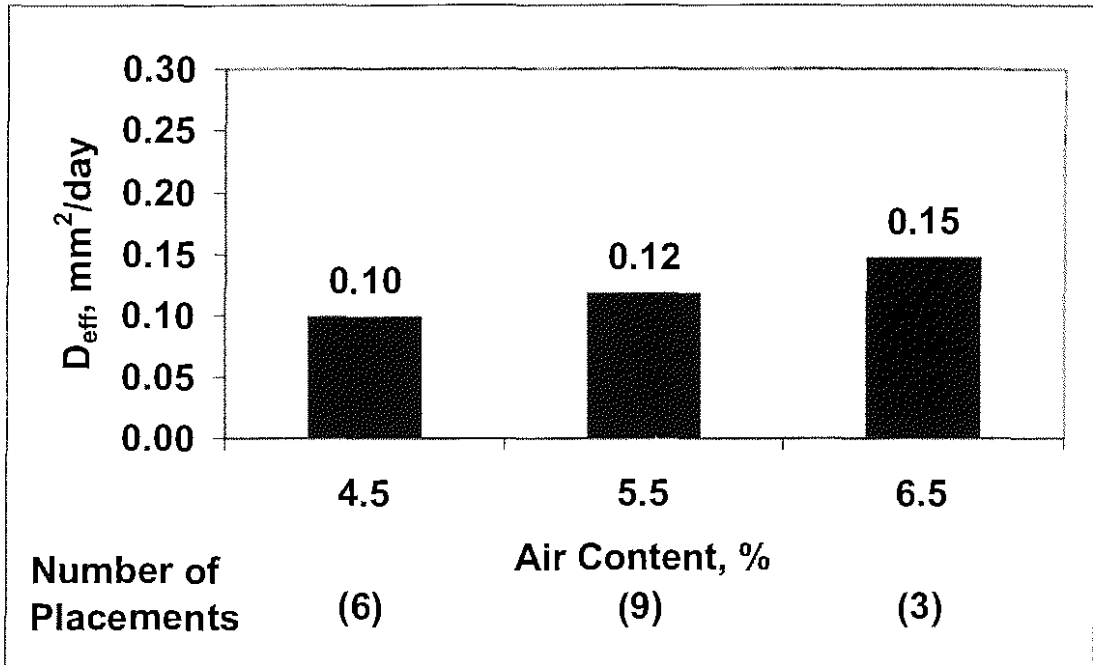


Figure 3.58: Mean effective diffusion coefficient of individual placements versus air content for silica fume overlays

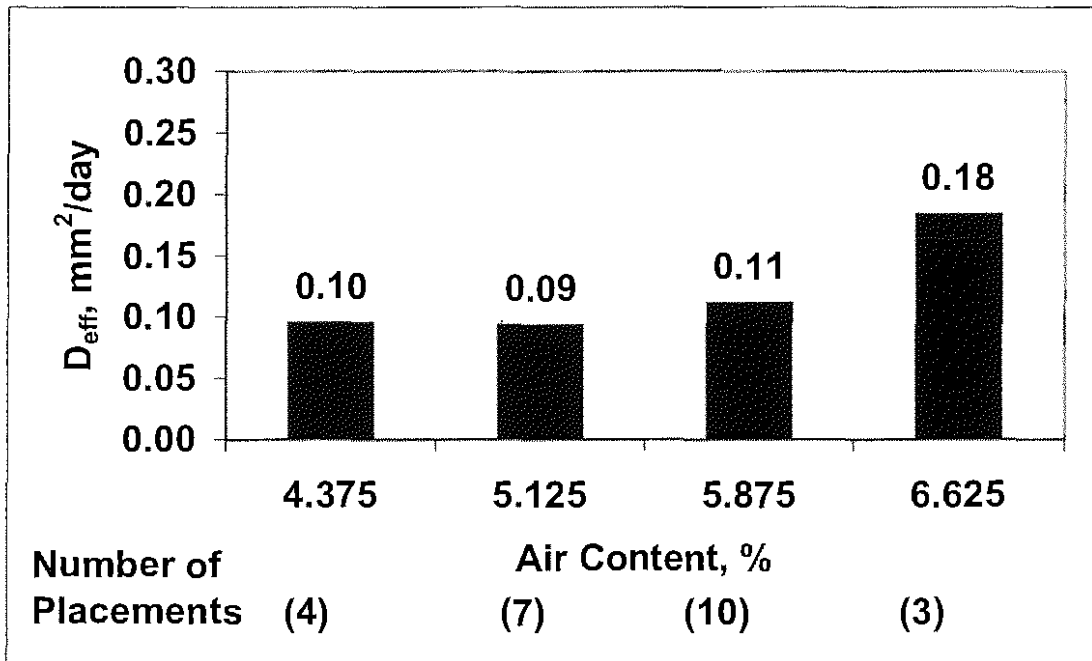


Figure 3.59: Mean effective diffusion coefficient of individual placements versus air content for conventional overlays

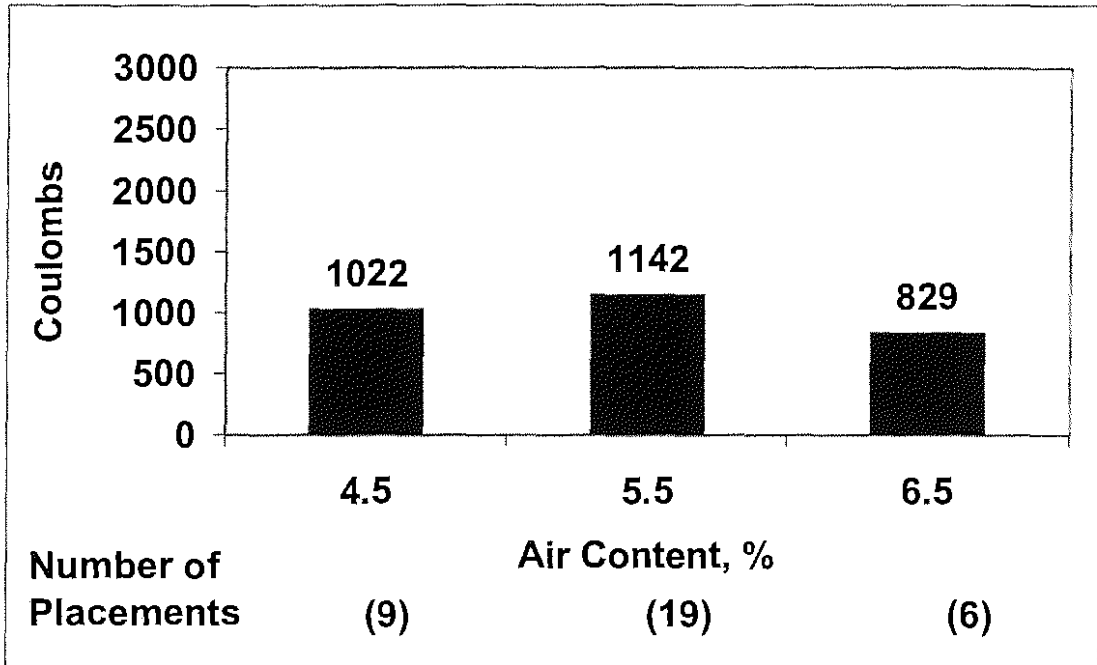


Figure 3.60: Mean RCPT result of individual placements versus air content for silica fume overlays

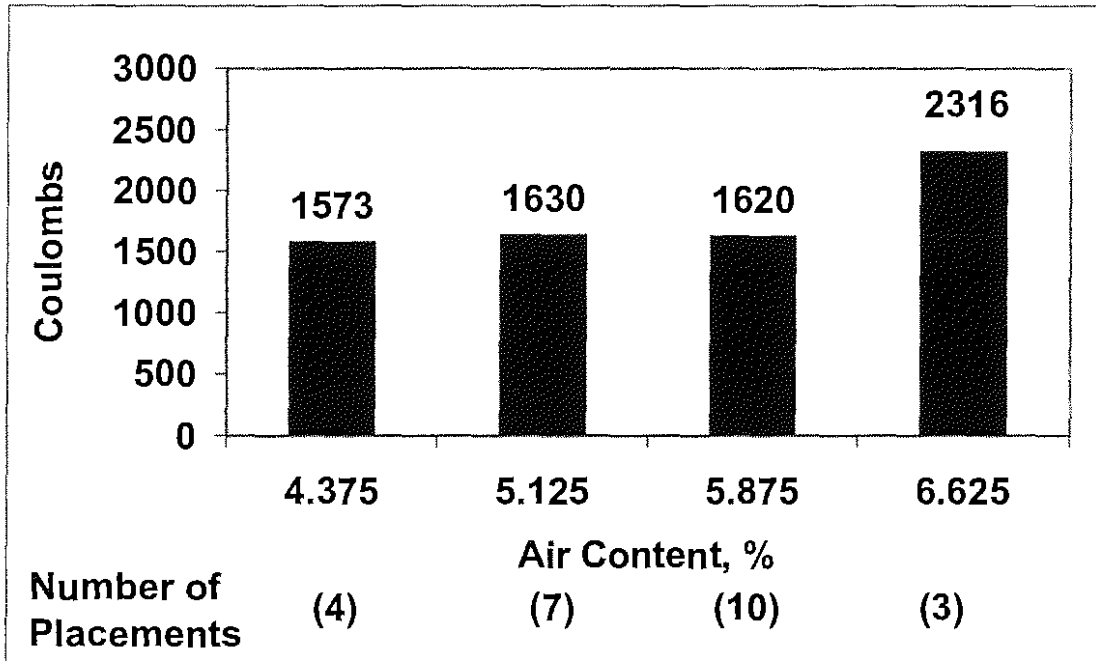


Figure 3.61: Mean RCPT result of individual placements versus air content for conventional overlays

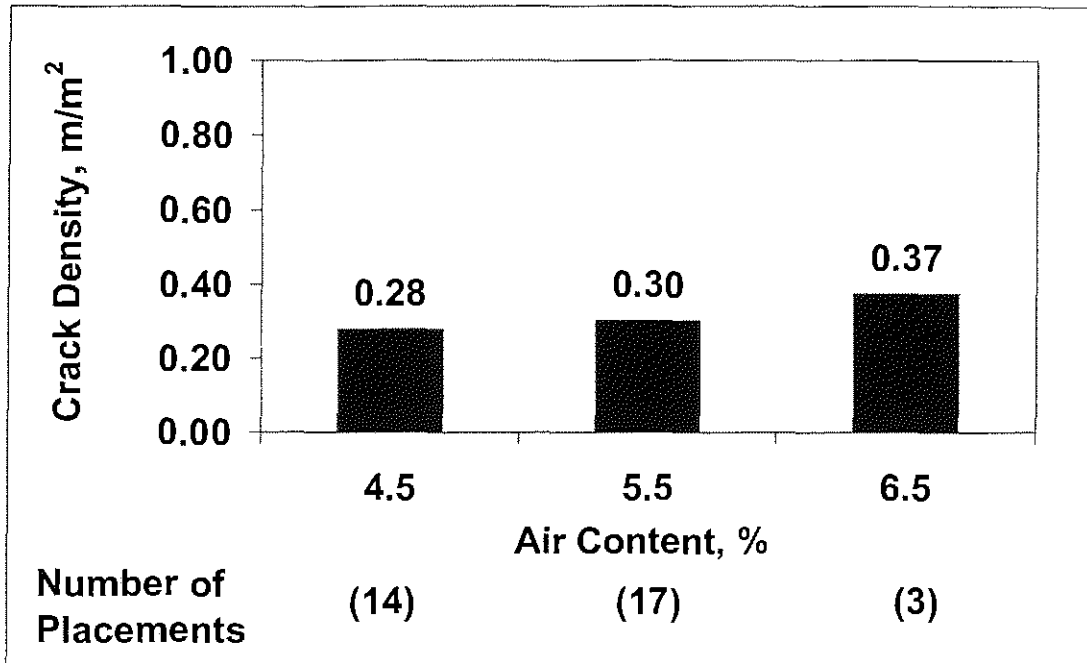


Figure 3.62: Mean crack density for individual placements versus air content for silica fume overlay bridge decks

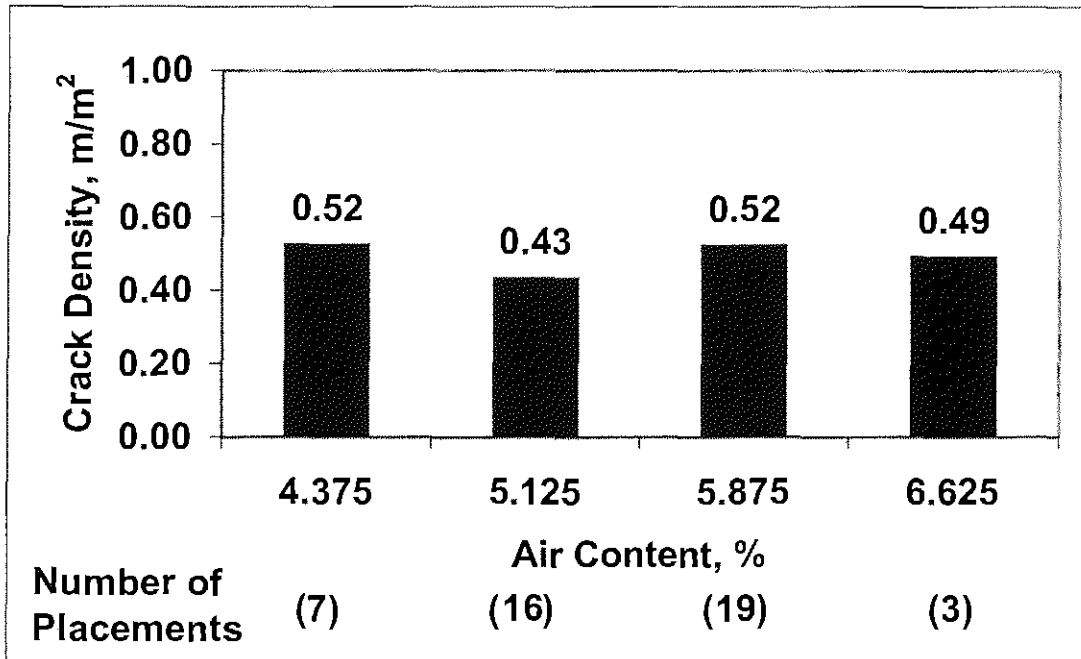


Figure 3.63: Mean crack density for individual placements versus air content for conventional overlay bridge decks

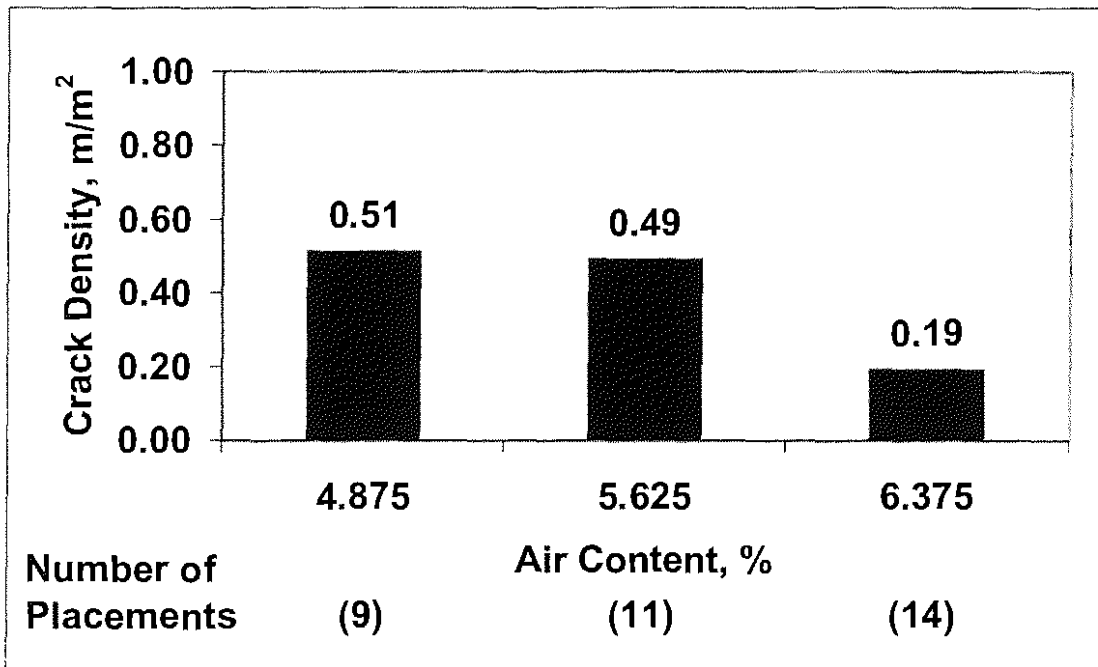


Figure 3.64: Mean crack density for individual placements versus air content for monolithic bridge decks

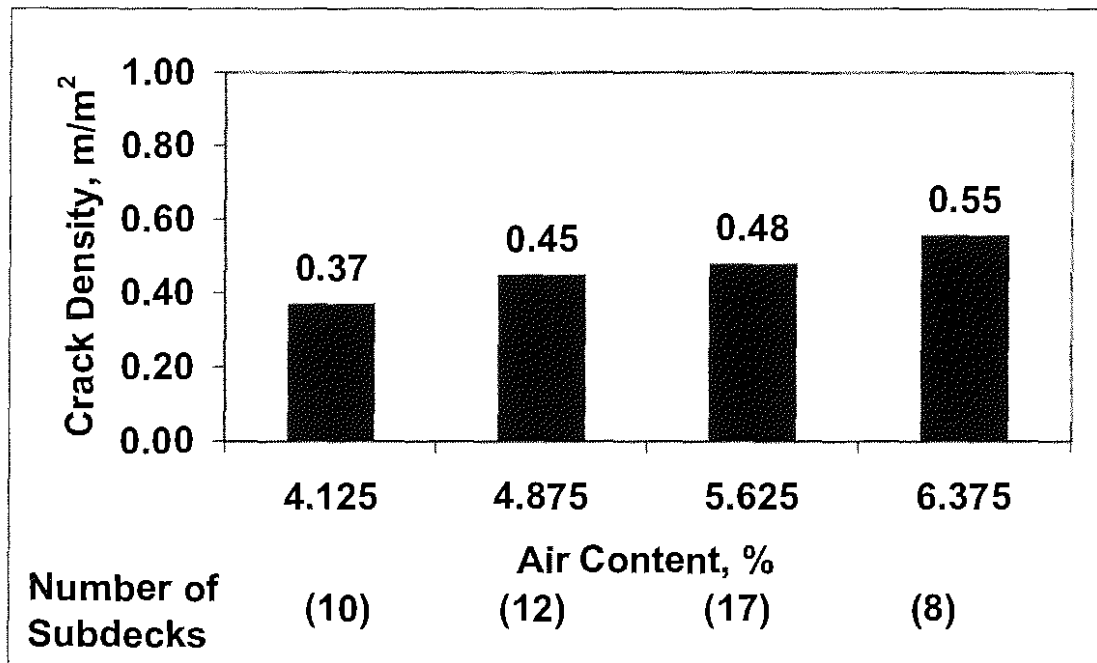


Figure 3.65: Mean crack density of bridge subdecks versus air content

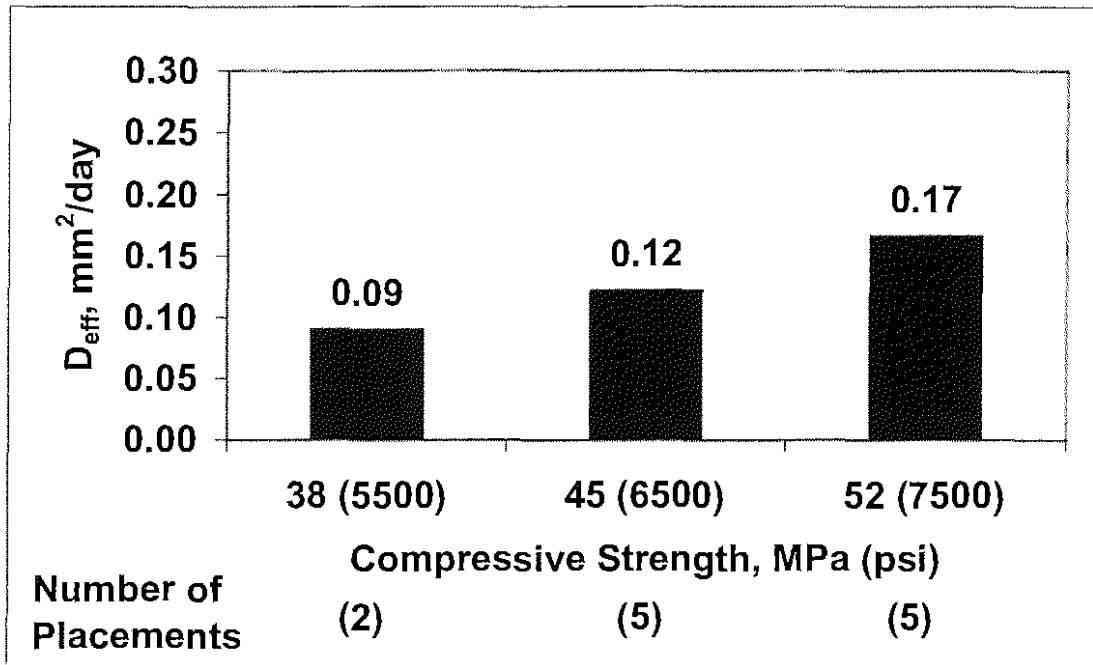


Figure 3.66: Mean effective diffusion coefficient of individual placements versus compressive strength for silica fume overlays

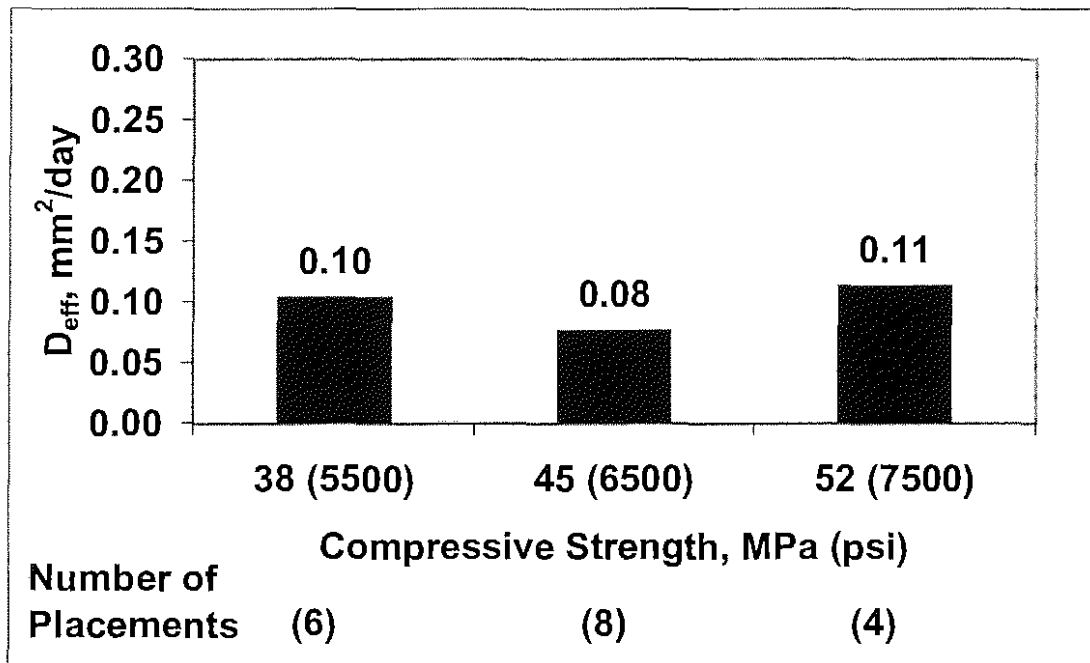


Figure 3.67: Mean effective diffusion coefficient of individual placements versus compressive strength for conventional overlays

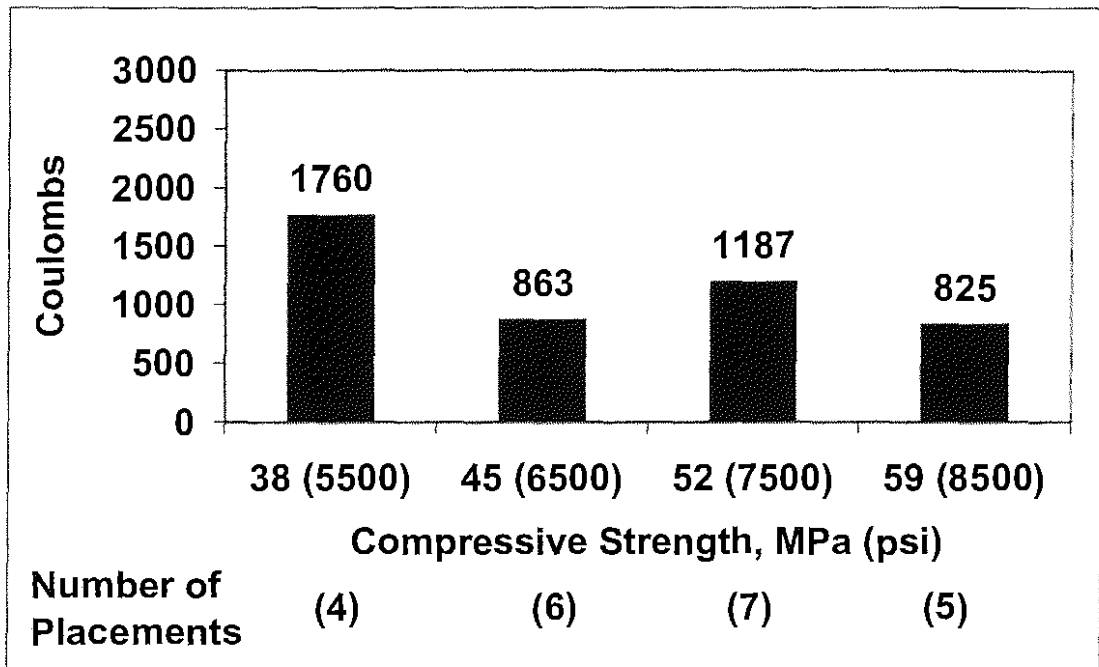


Figure 3.68: Mean RCPT result of individual placements versus compressive strength for silica fume overlays

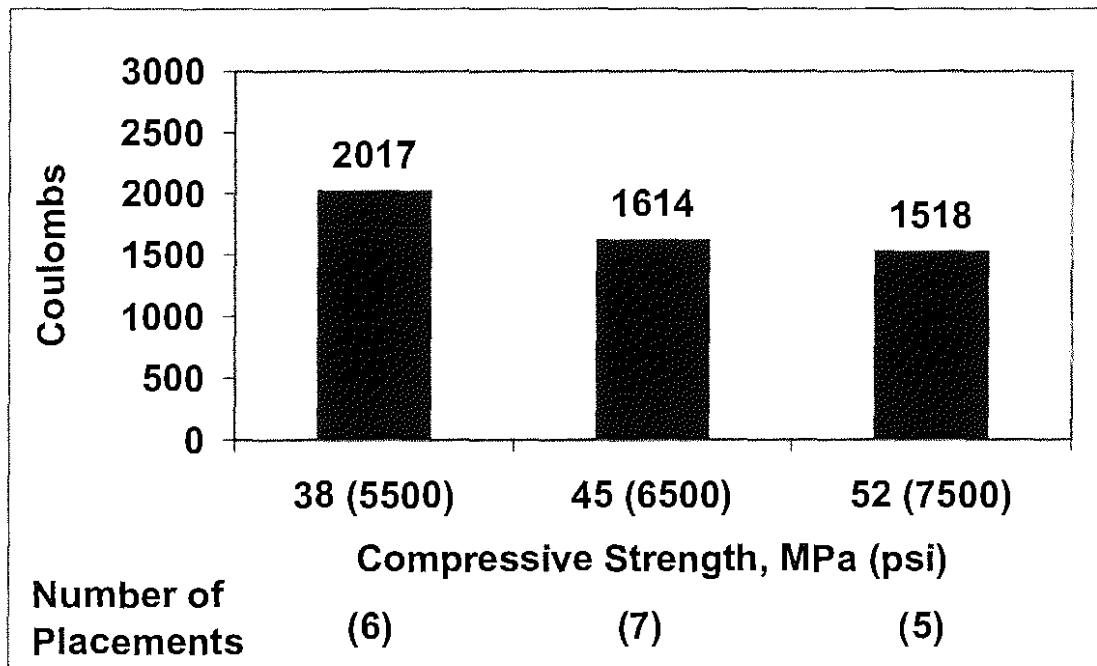


Figure 3.69: Mean RCPT result of individual placements versus compressive strength for conventional overlays

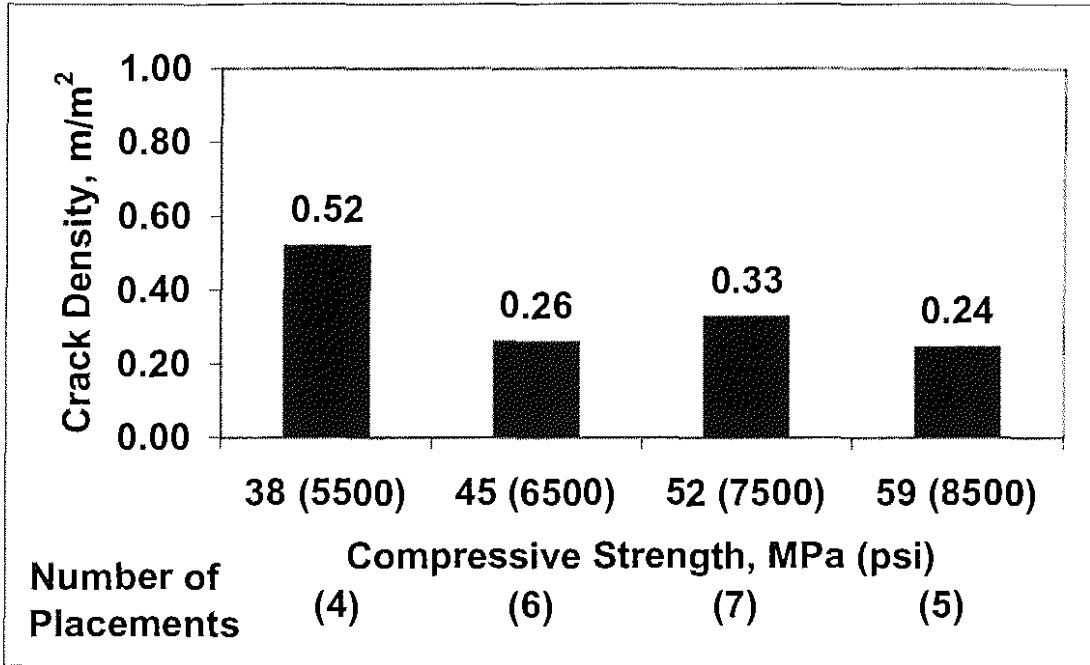


Figure 3.70: Mean crack density for individual placements versus compressive strength for silica fume overlay bridge decks

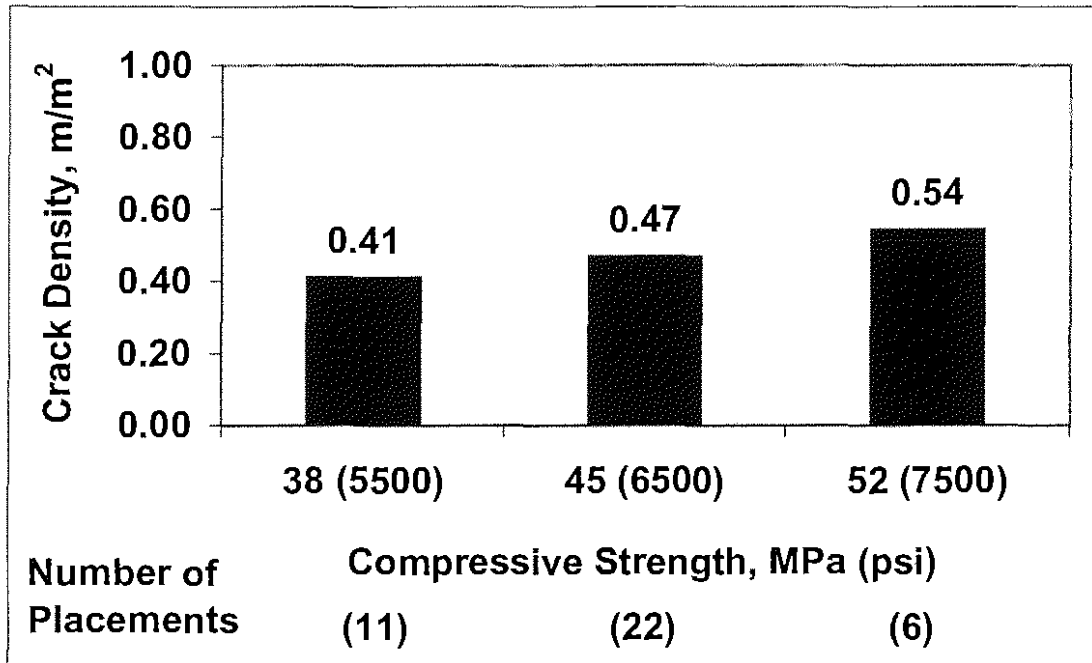


Figure 3.71: Mean crack density for individual placements versus compressive strength for conventional overlay bridge decks

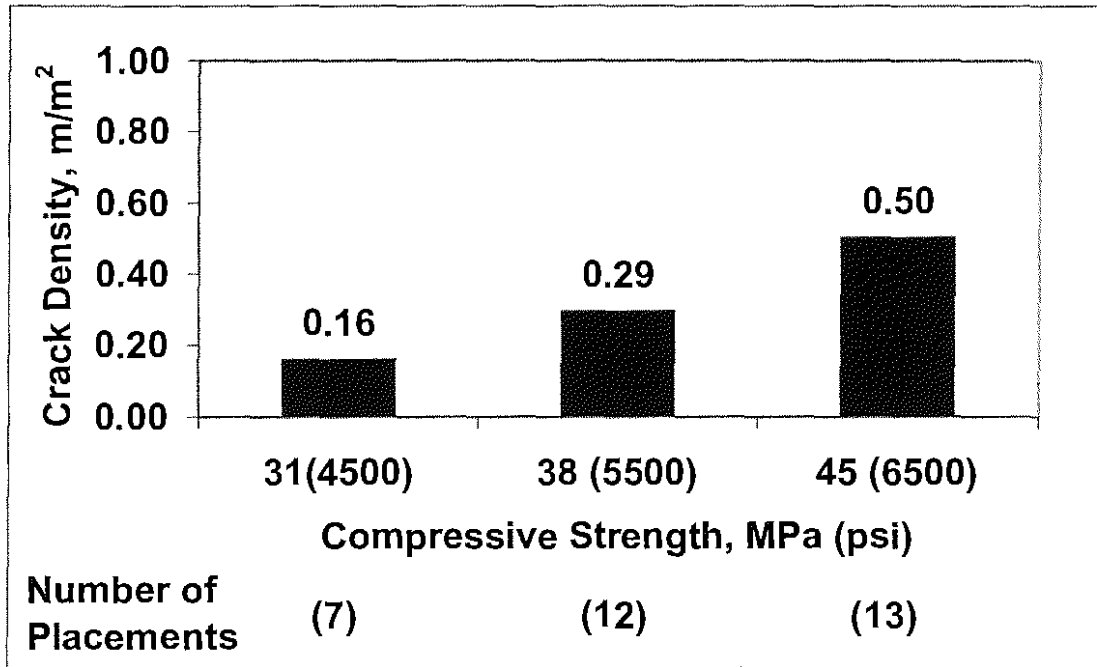


Figure 3.72: Mean crack density for individual placements versus compressive strength for monolithic bridge decks

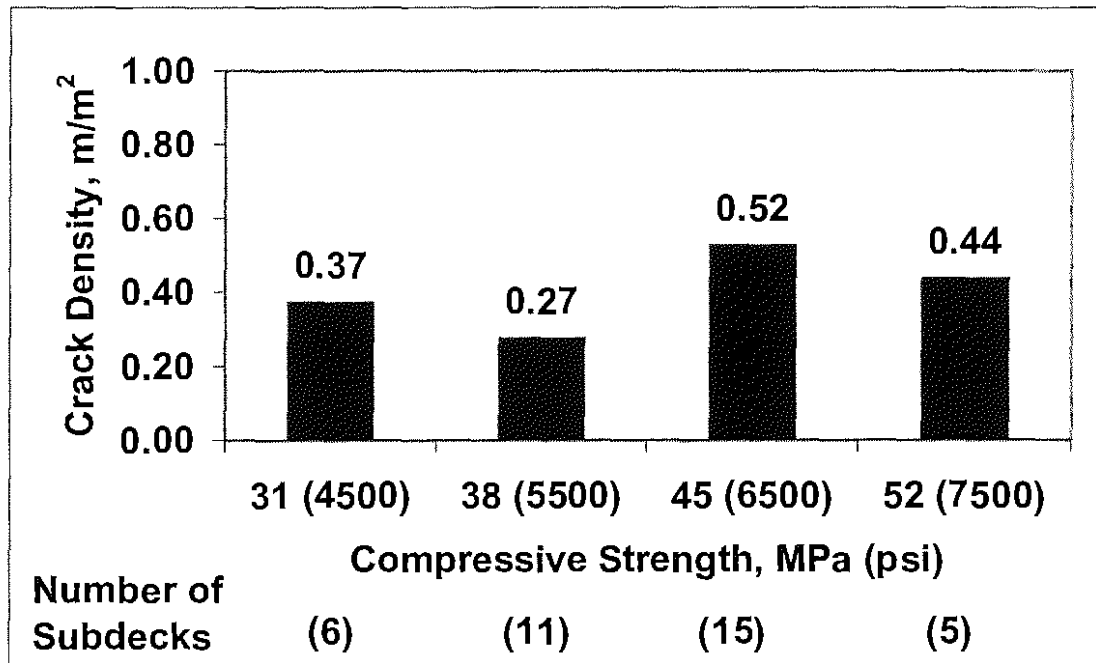


Figure 3.73: Mean crack density of bridge subdecks versus compressive strength

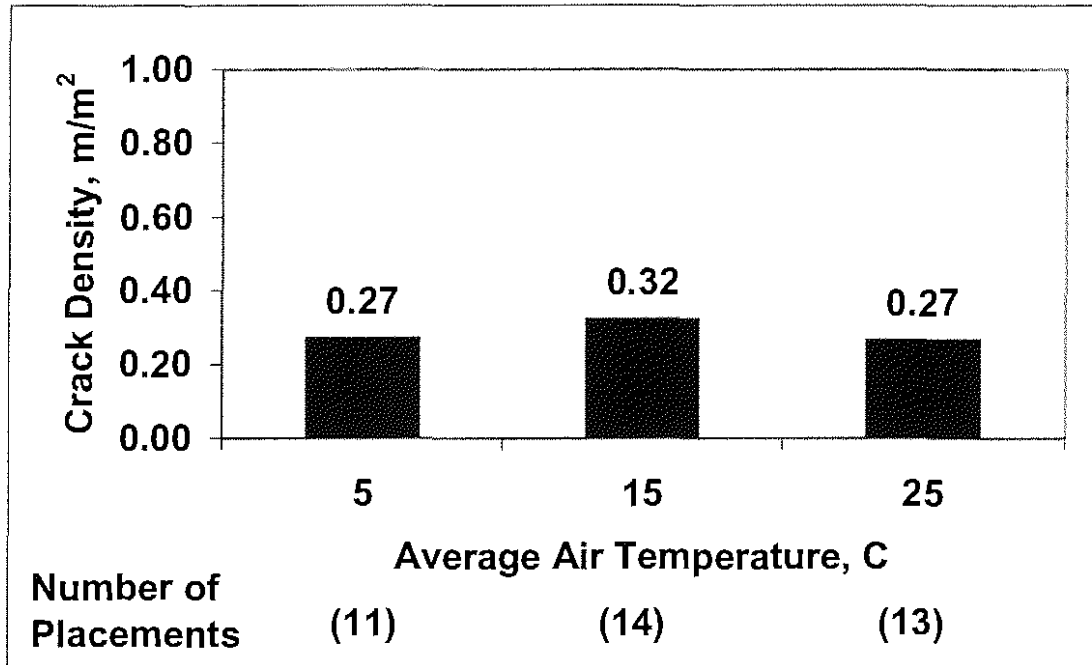


Figure 3.74: Mean crack density for individual placements versus average air temperature for silica fume overlay bridge decks

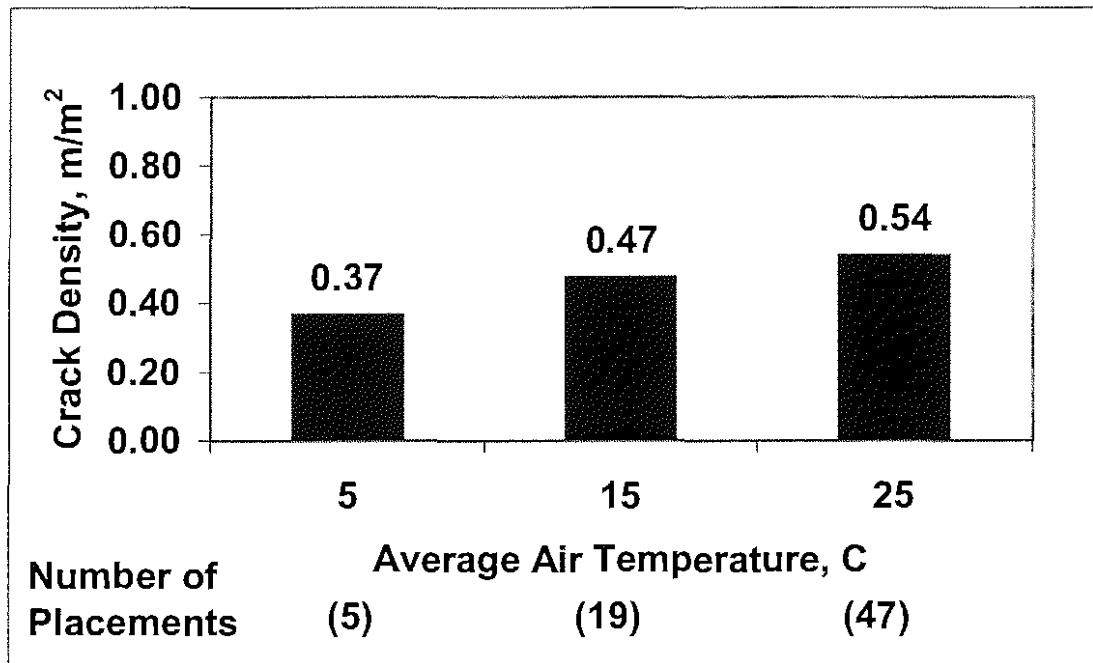


Figure 3.75: Mean crack density for individual placements versus average air temperature for conventional overlay bridge decks

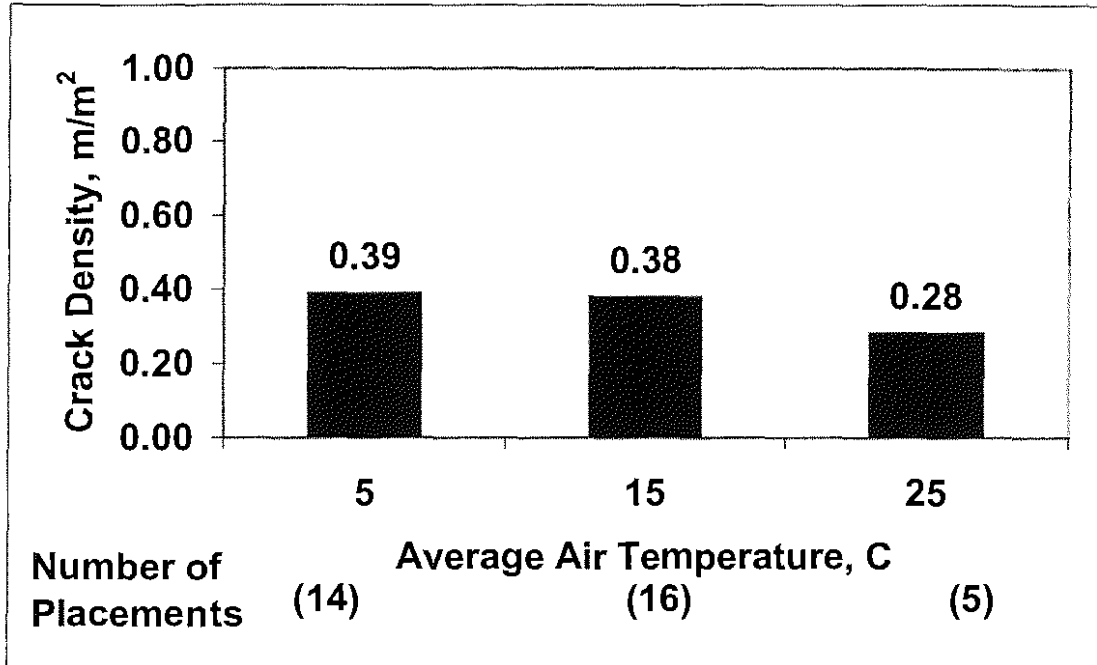


Figure 3.76: Mean crack density for individual placements versus average air temperature for monolithic bridge decks

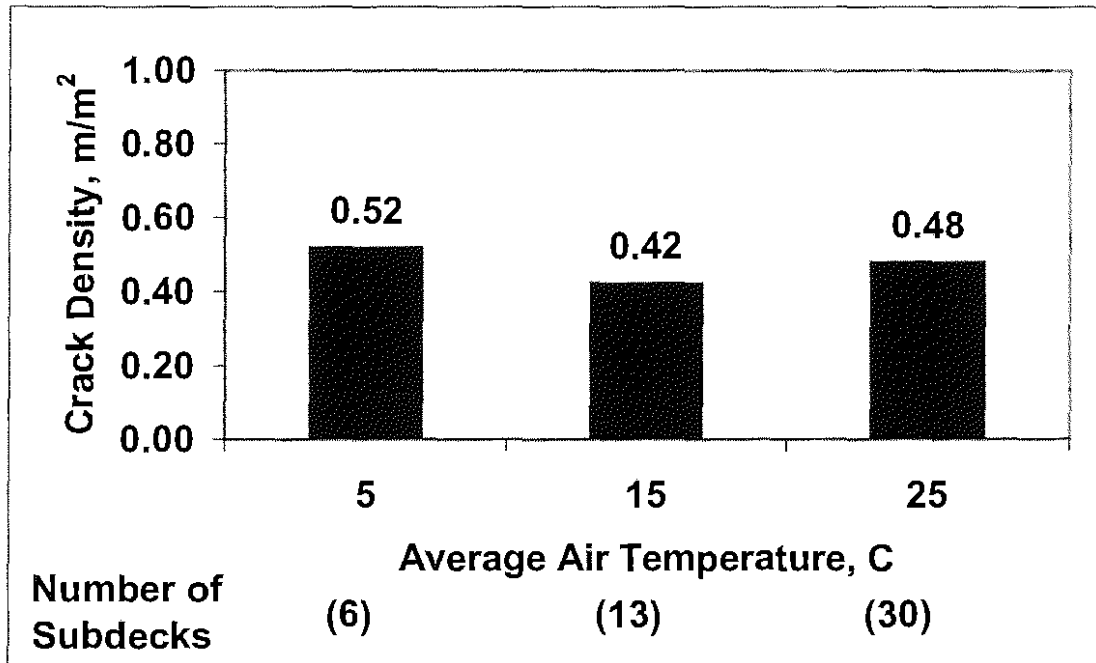


Figure 3.77: Mean crack density of bridge subdecks versus average air temperature

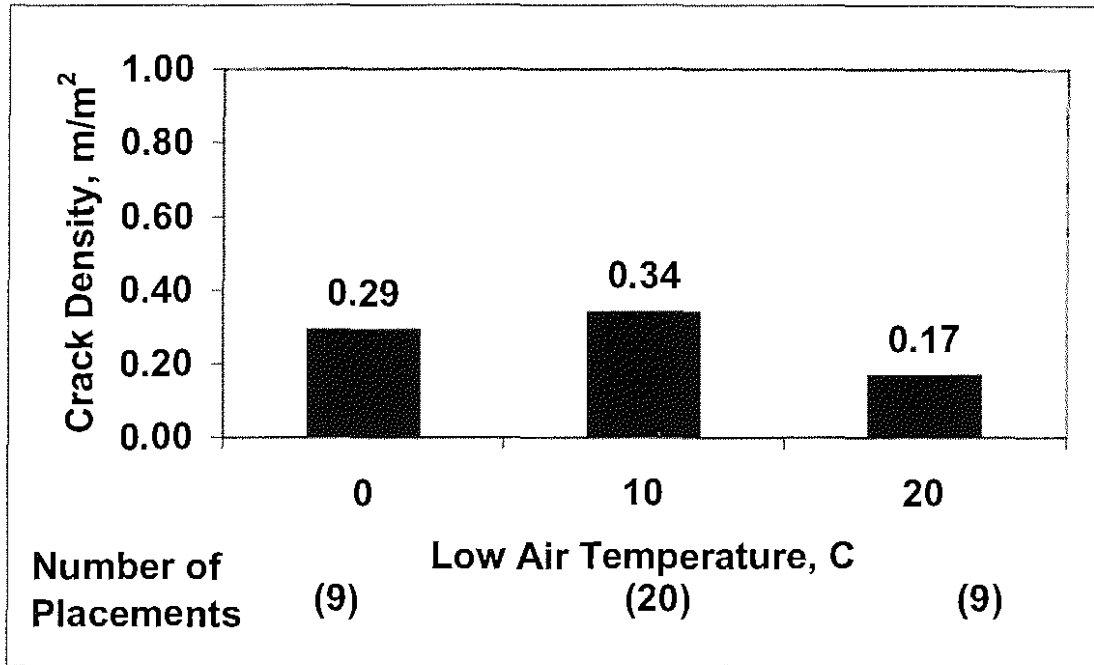


Figure 3.78: Mean crack density for individual placements versus low air temperature for silica fume overlay bridge decks

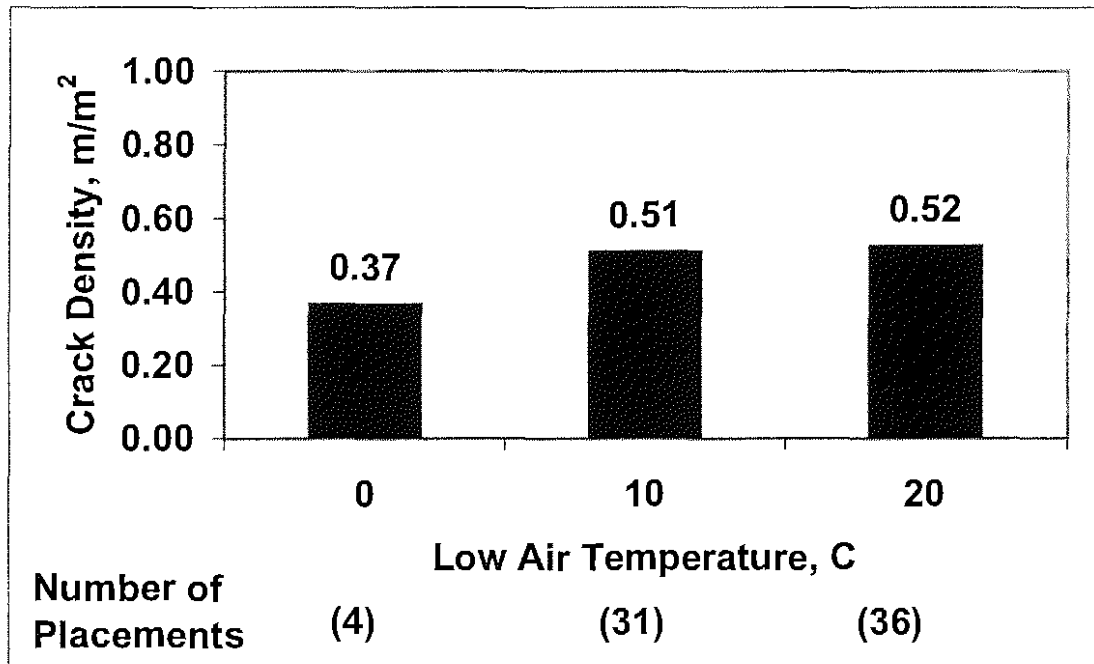


Figure 3.79: Mean crack density for individual placements versus low air temperature for conventional overlay bridge decks

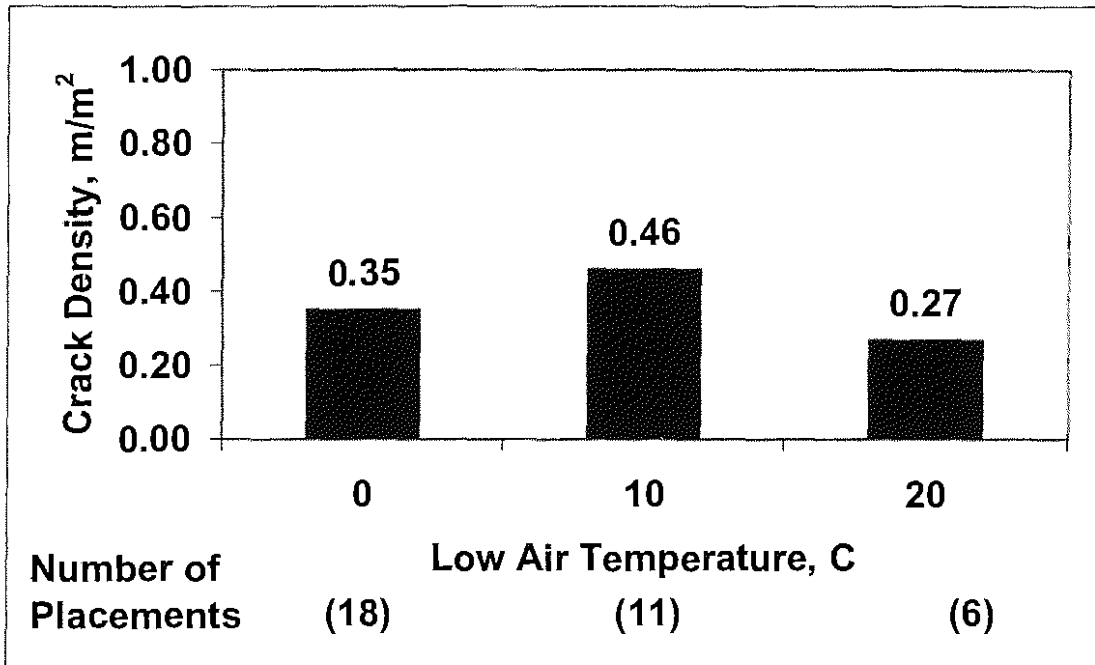


Figure 3.80: Mean crack density for individual placements versus low air temperature for monolithic bridge decks

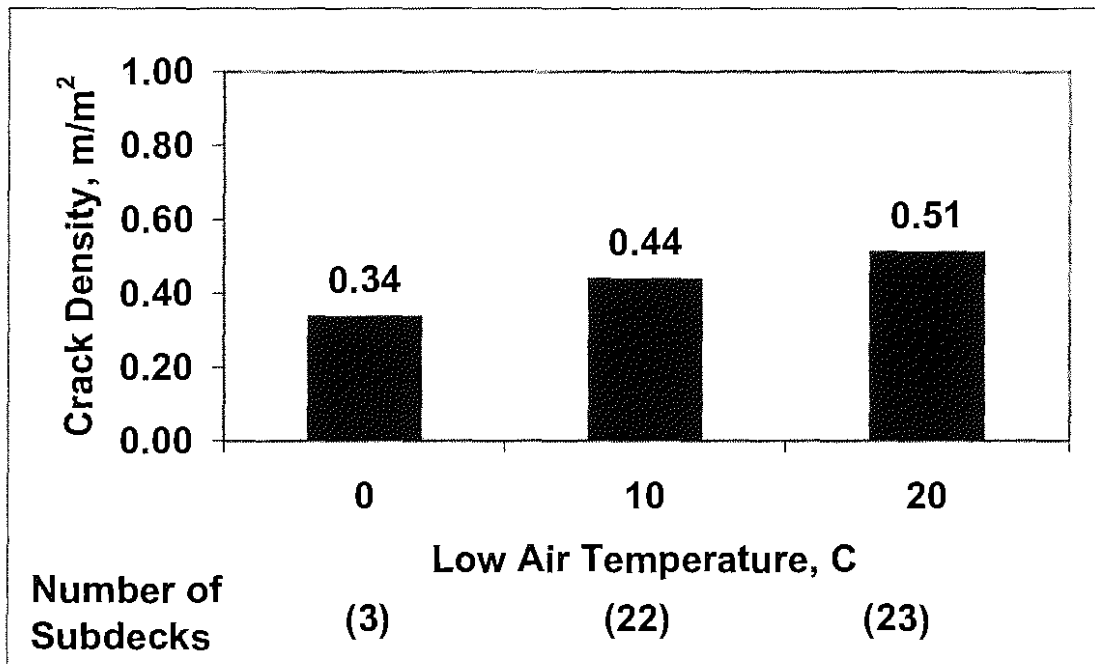


Figure 3.81: Mean crack density of bridge subdecks versus low air temperature

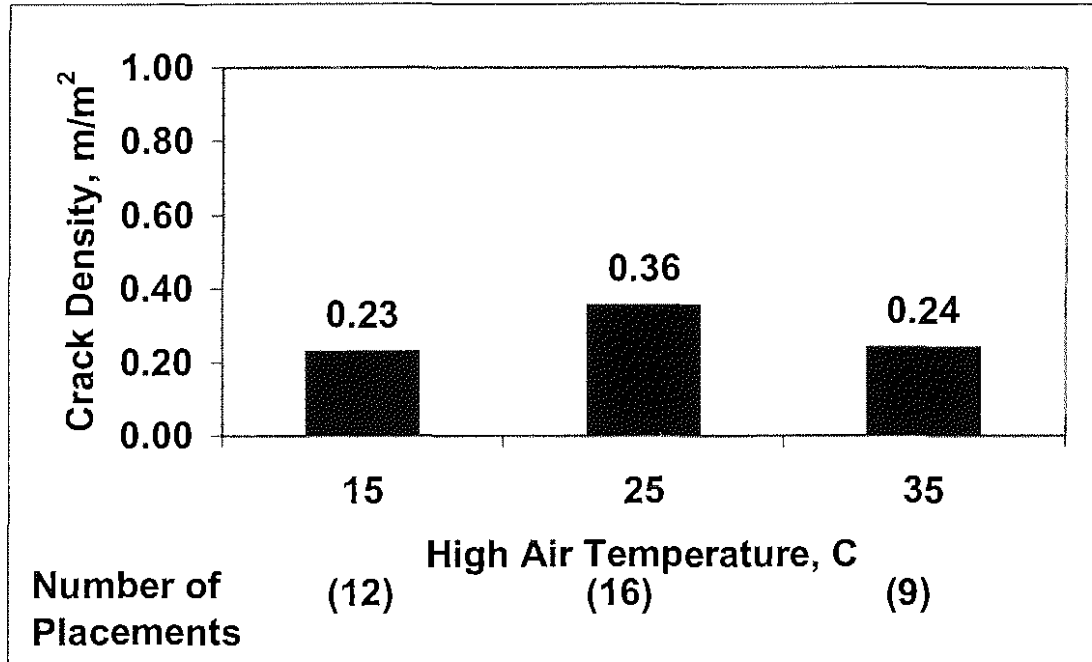


Figure 3.82: Mean crack density for individual placements versus high air temperature for silica fume overlay bridge decks

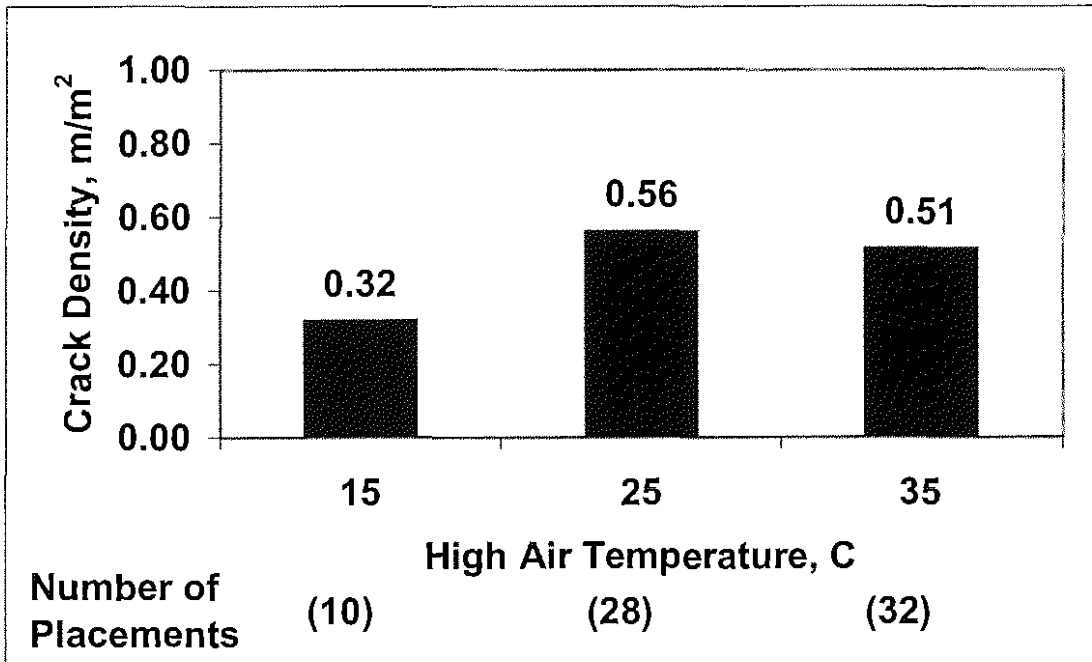


Figure 3.83: Mean crack density for individual placements versus high air temperature for conventional overlay bridge decks

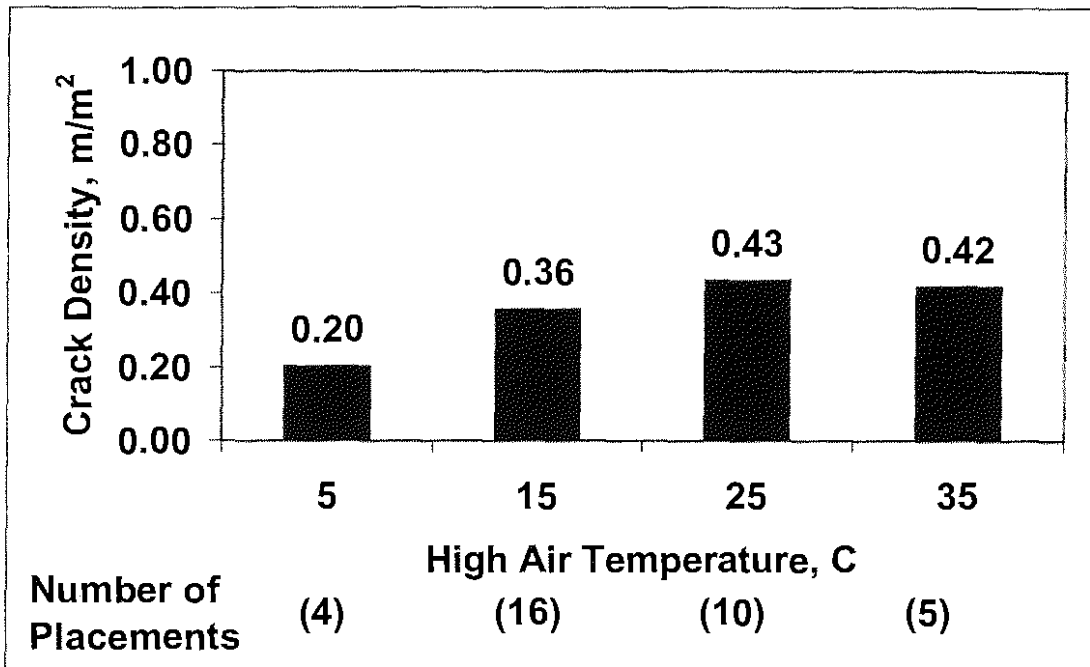


Figure 3.84: Mean crack density for individual placements versus high air temperature for monolithic bridge decks

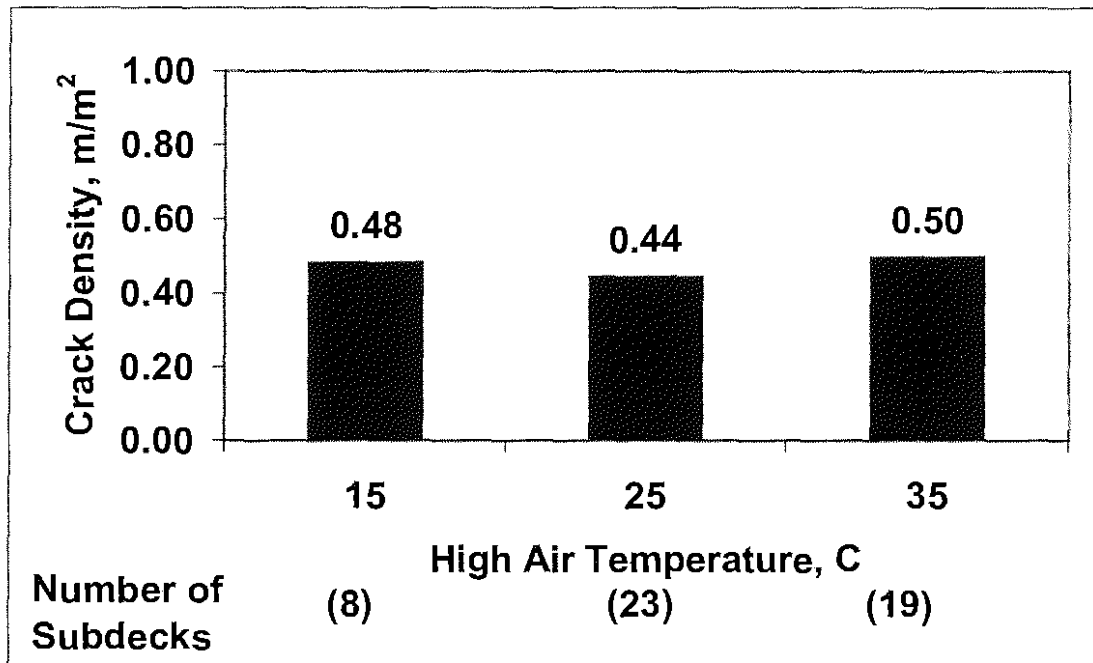


Figure 3.85: Mean crack density of bridge subdecks versus high air temperature

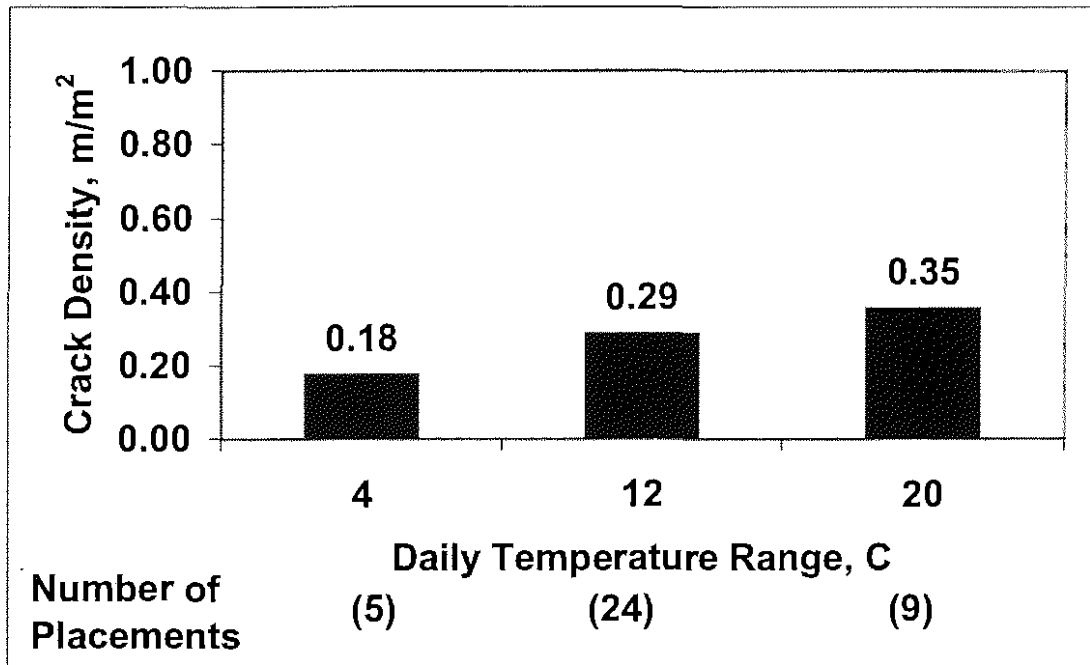


Figure 3.86: Mean crack density for individual placements versus daily temperature range for silica fume overlay bridge decks

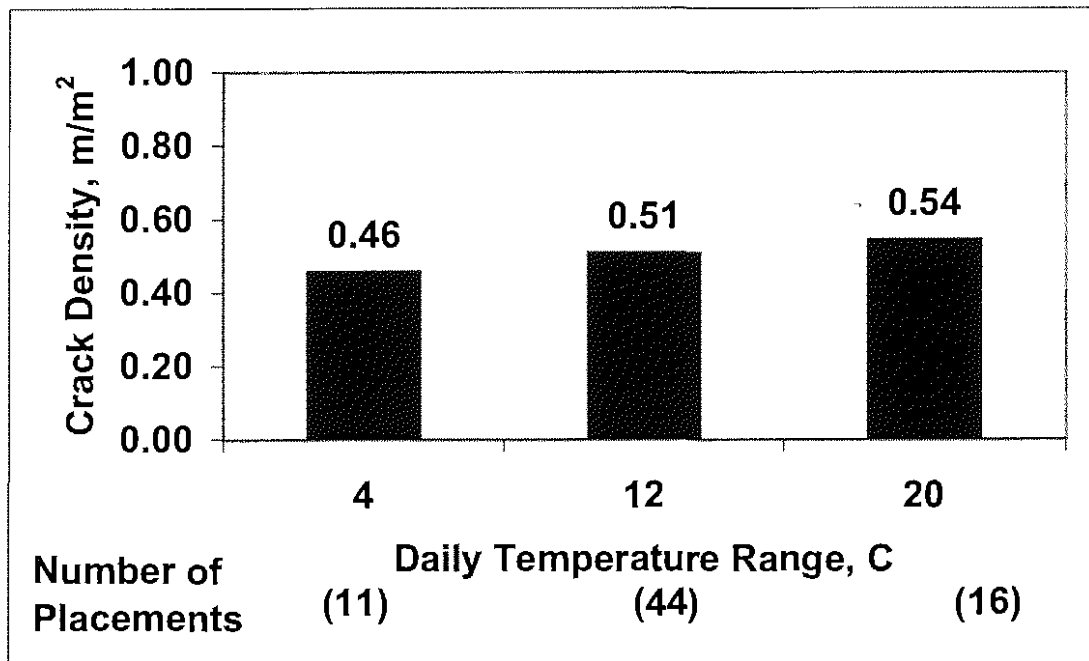


Figure 3.87: Mean crack density for individual placements versus daily temperature range for conventional bridge decks

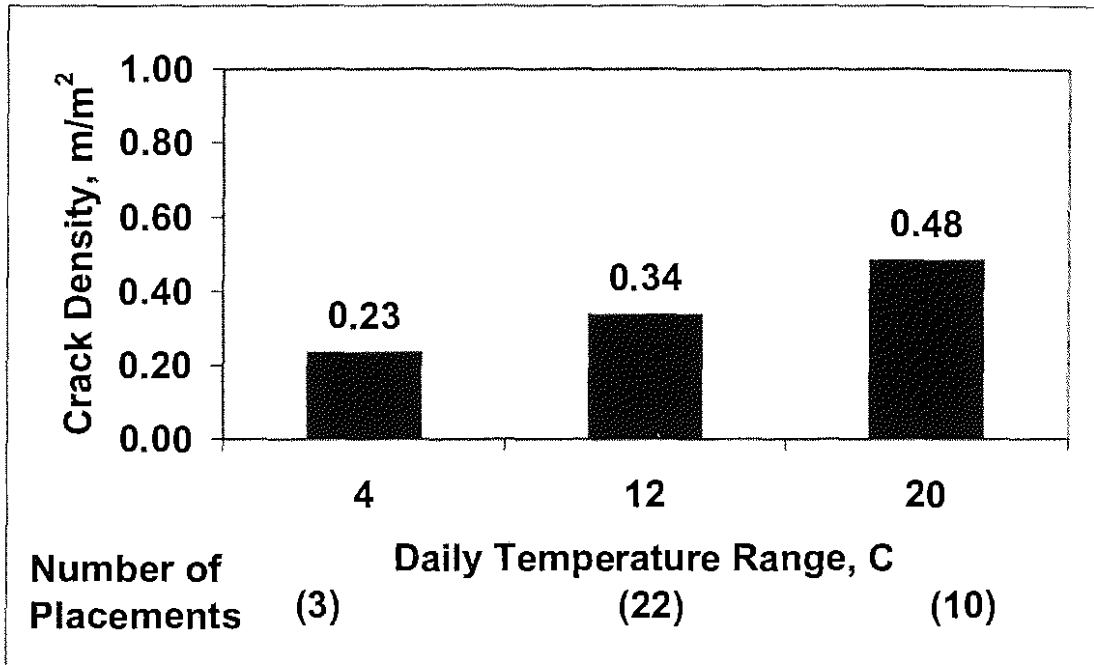


Figure 3.88: Mean crack density for individual placements versus daily temperature range for monolithic bridge decks

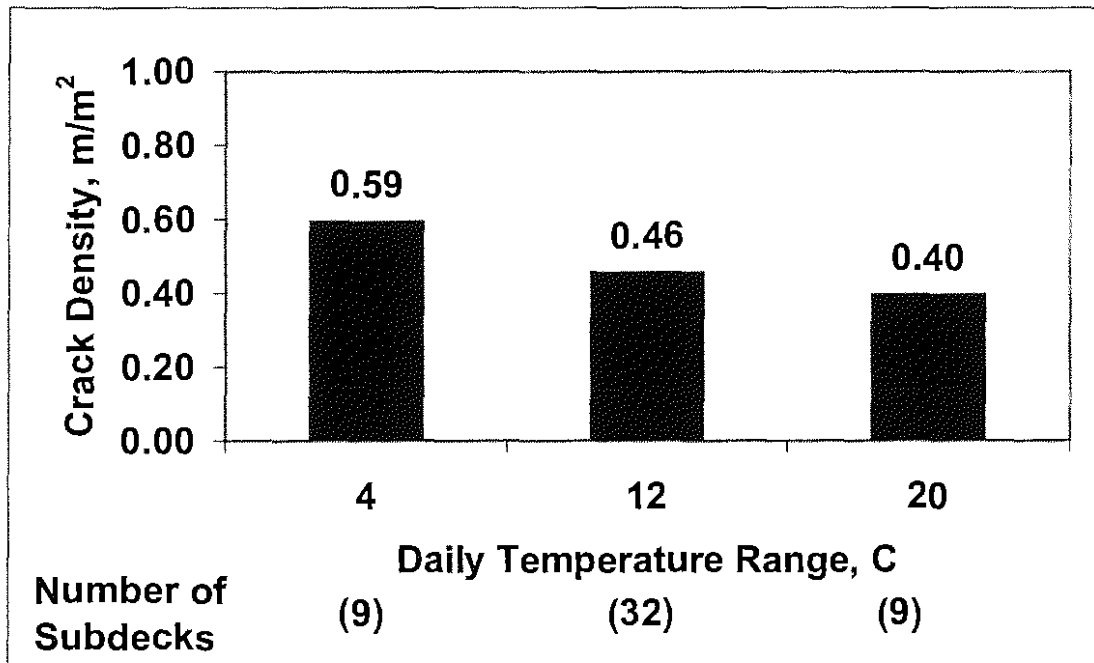


Figure 3.89: Mean crack density of bridge subdecks versus daily temperature range

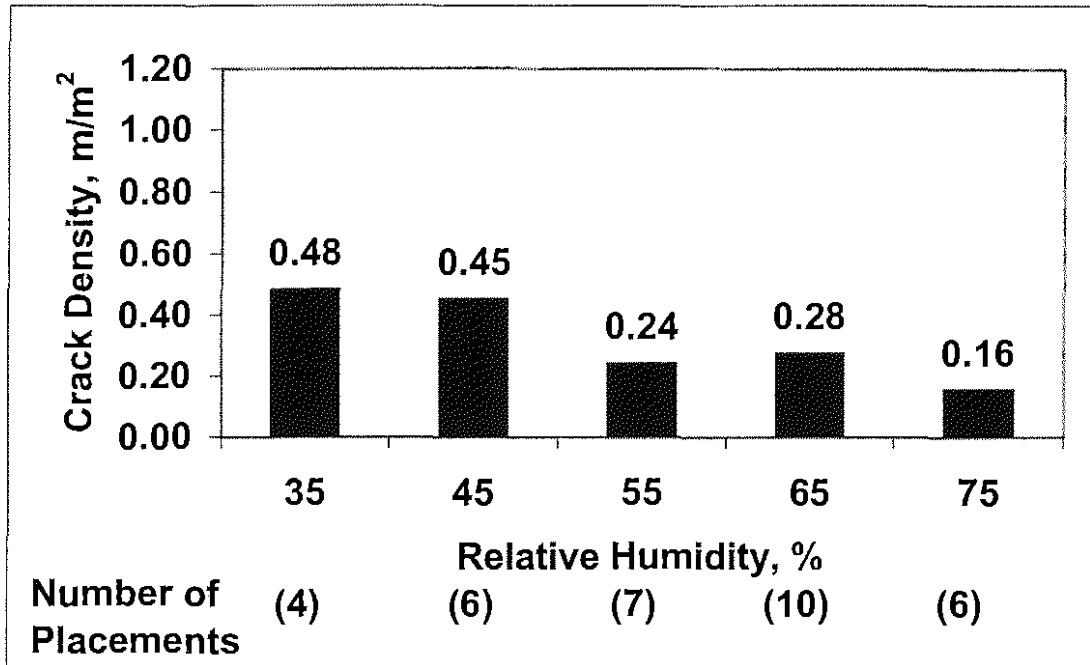


Figure 3.90: Mean crack density for individual placements versus relative humidity for silica fume overlay bridge decks

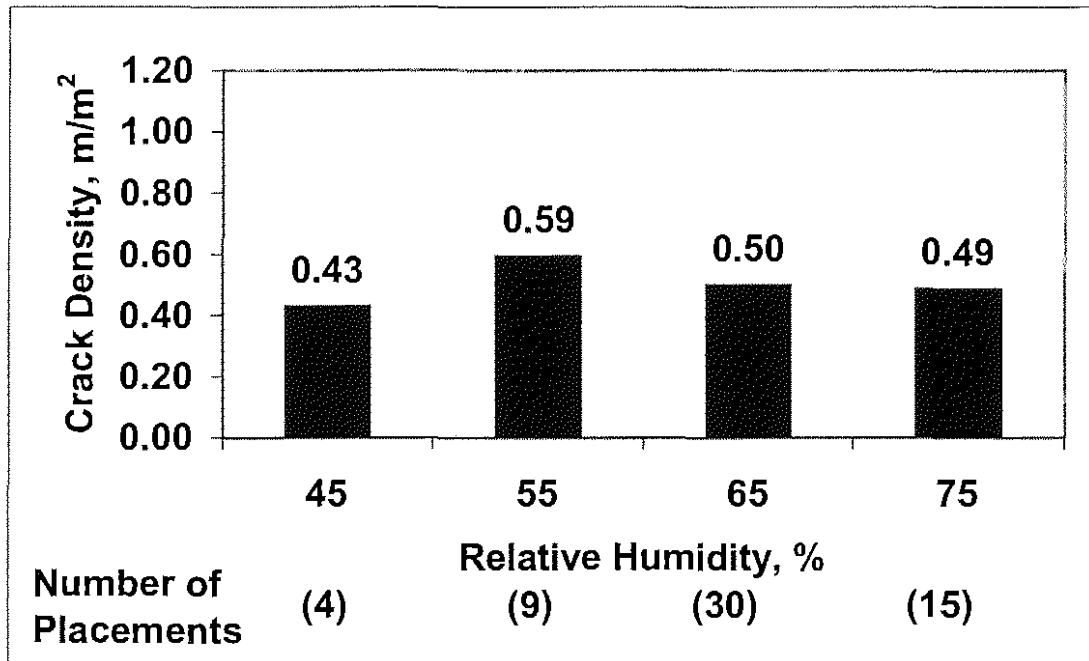


Figure 3.91: Mean crack density for individual placements versus relative humidity for conventional overlay bridge decks

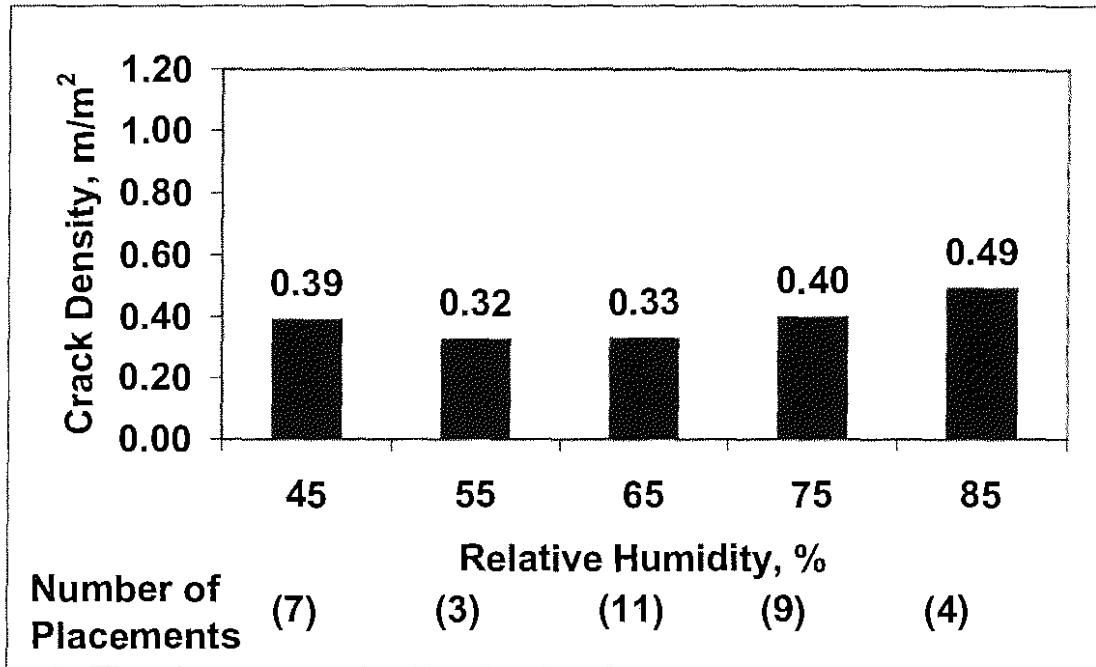


Figure 3.92: Mean crack density for individual placements versus relative humidity for monolithic bridge decks

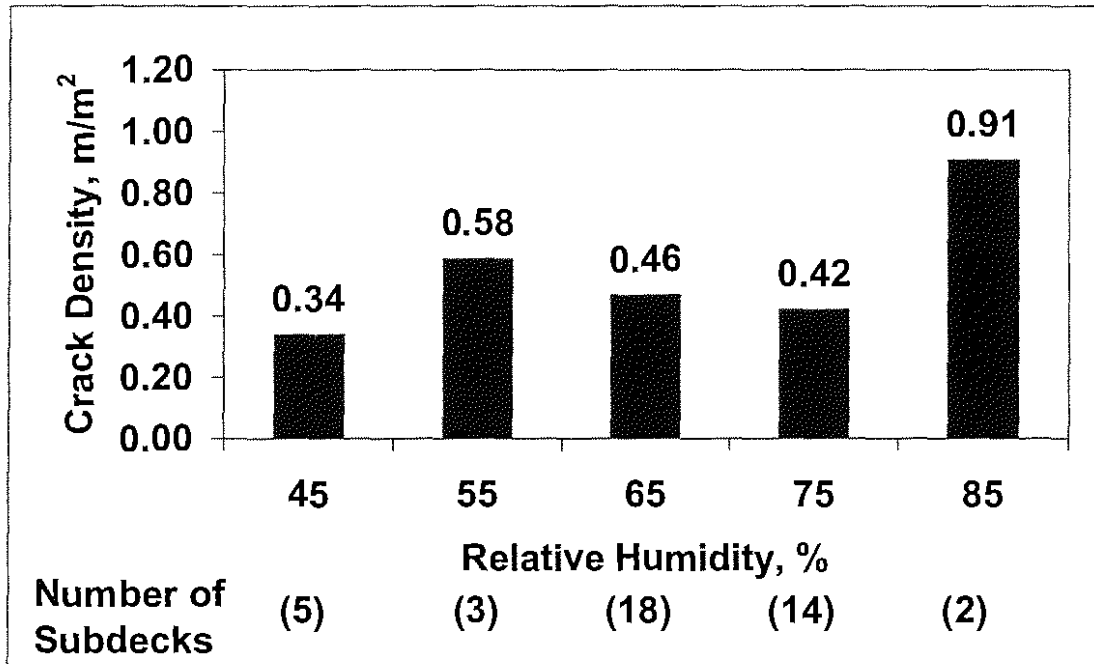


Figure 3.93: Mean crack density of bridge subdecks versus relative humidity

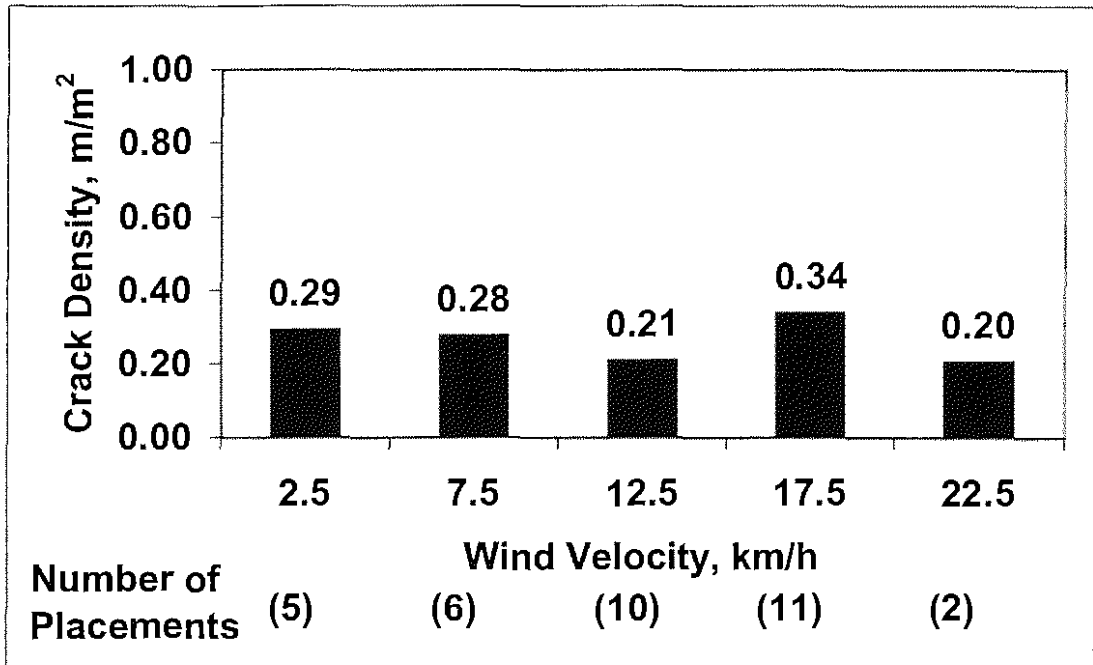


Figure 3.94: Mean crack density for individual placements versus wind velocity for silica fume overlay bridge decks

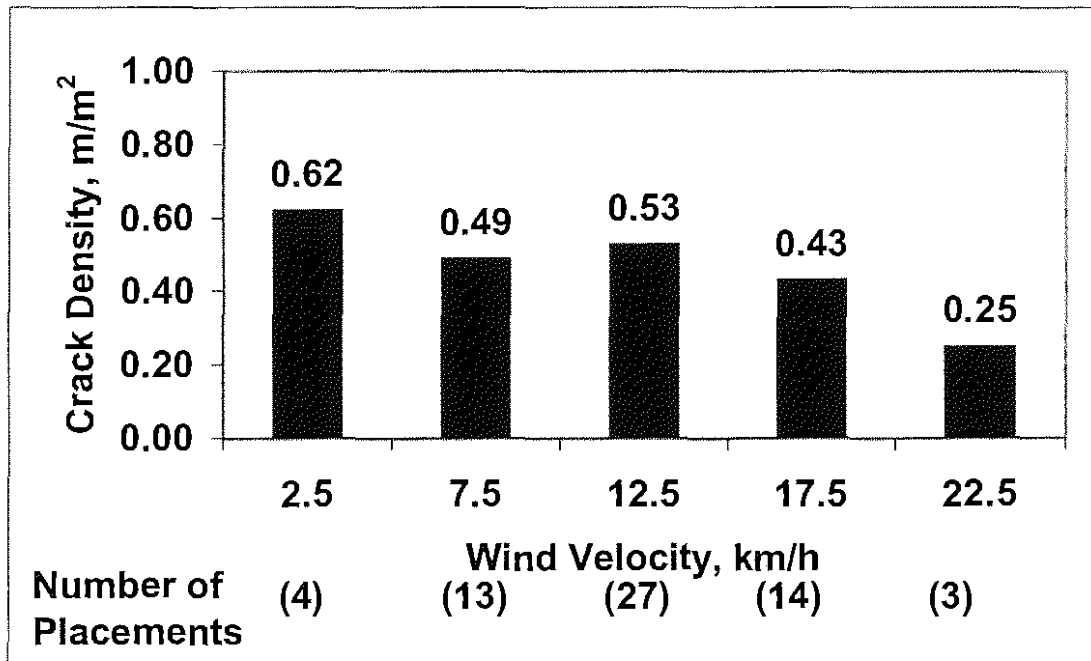


Figure 3.95: Mean crack density for individual placements versus wind velocity for conventional overlay bridge decks

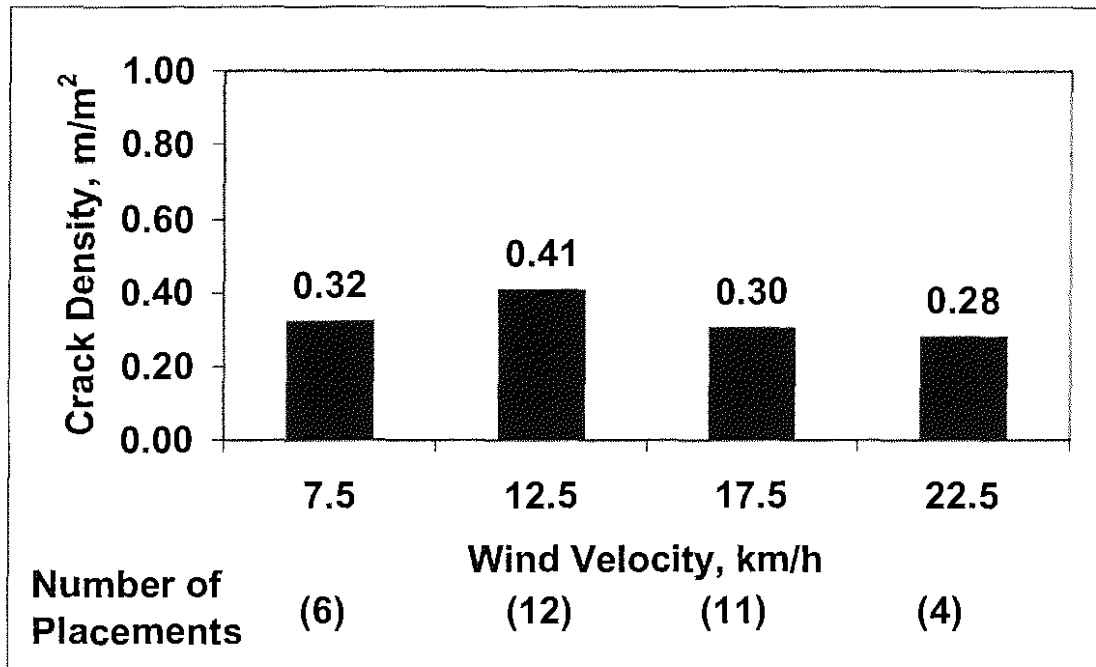


Figure 3.96: Mean crack density for individual placements versus wind velocity for monolithic bridge decks

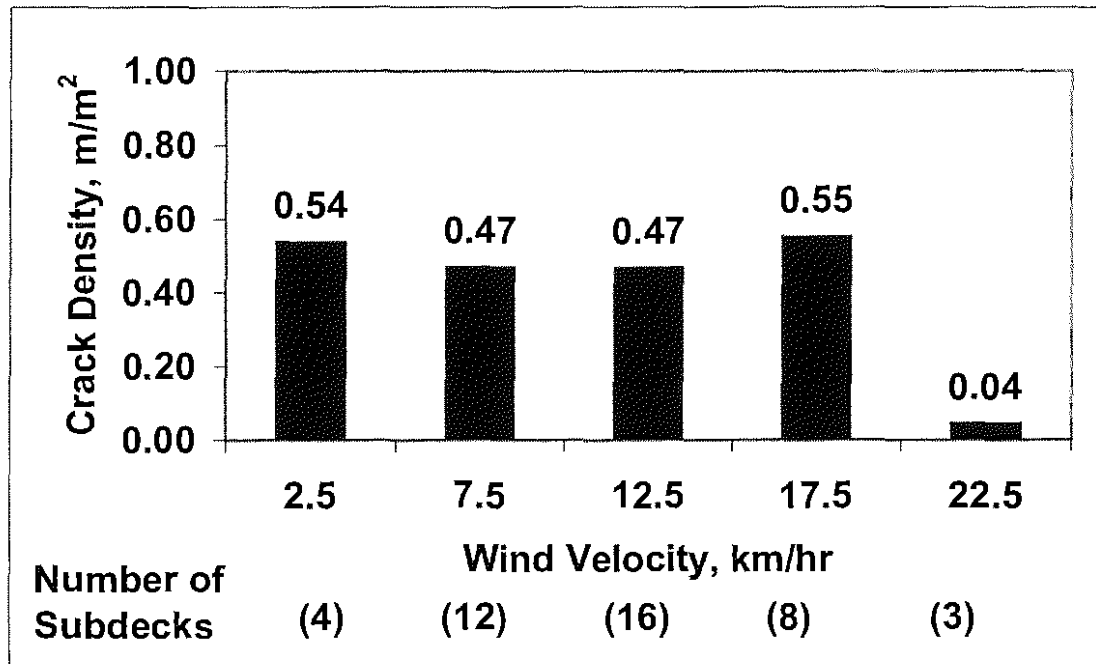


Figure 3.97: Mean crack density of bridge subdecks versus wind velocity

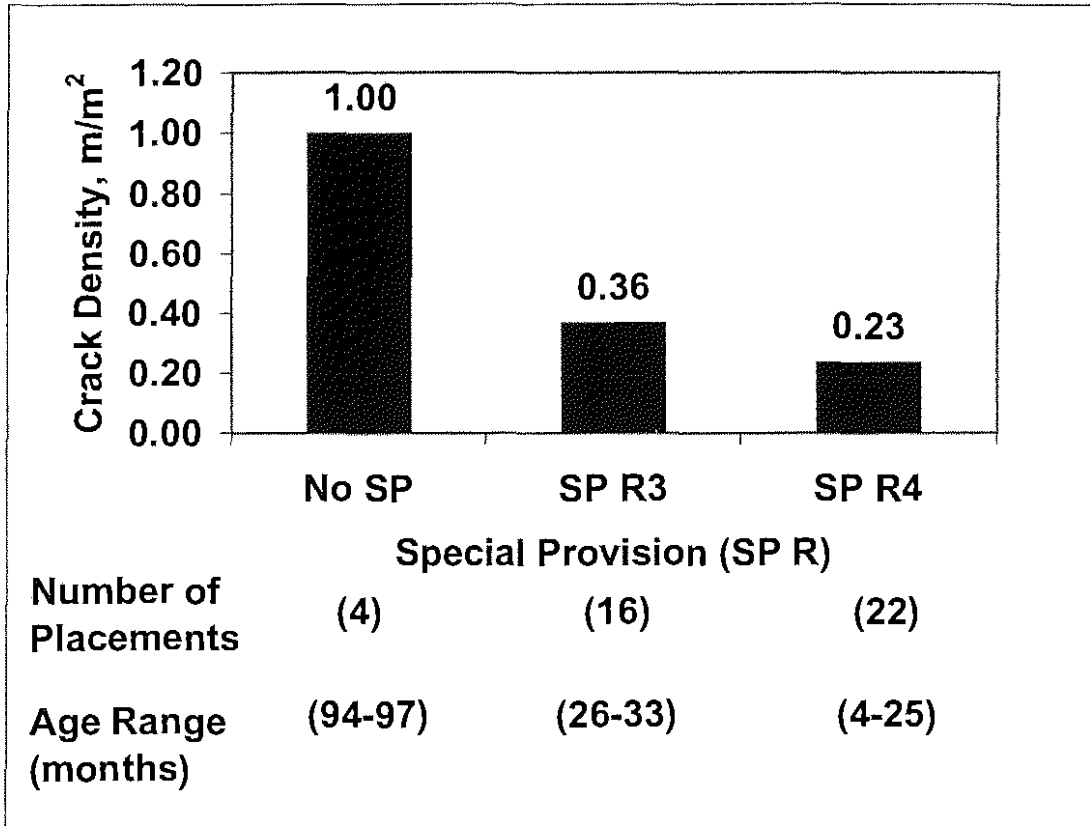


Figure 3.98: Mean crack density of individual placements versus silica fume overlay Special Provision revision number

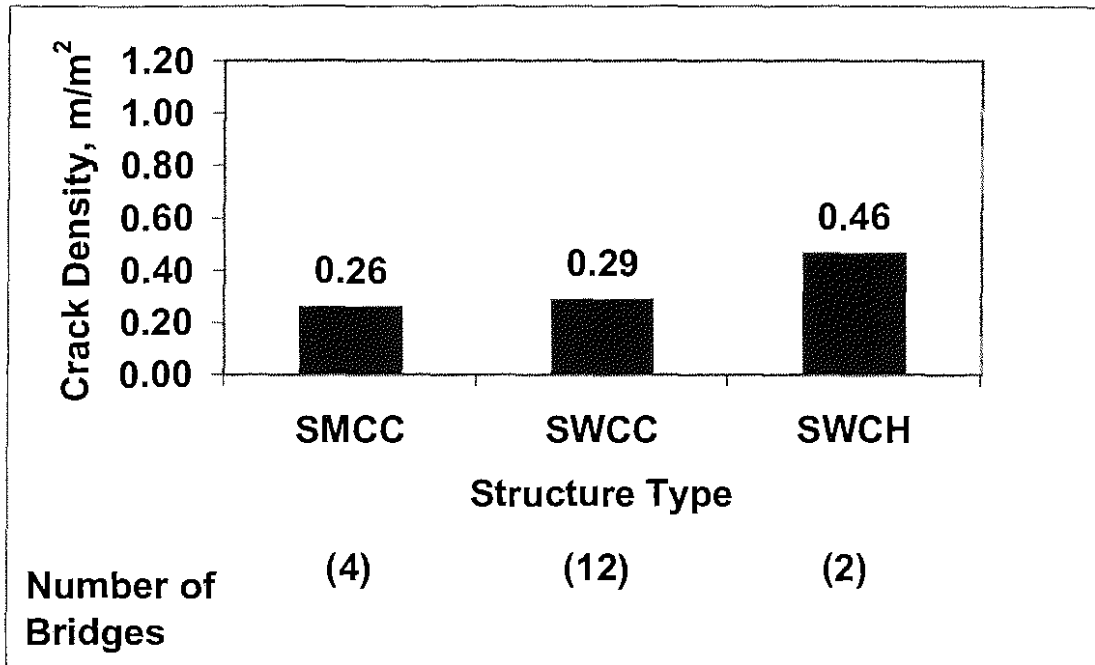


Figure 3.99: Mean crack density for entire bridge versus structure type for silica fume overlay bridge decks. Steel beam, composite continuous (SMCC); Steel welded plate girder, composite continuous (SWCC); Steel welded plate girder, composite continuous and haunched (SWCH)

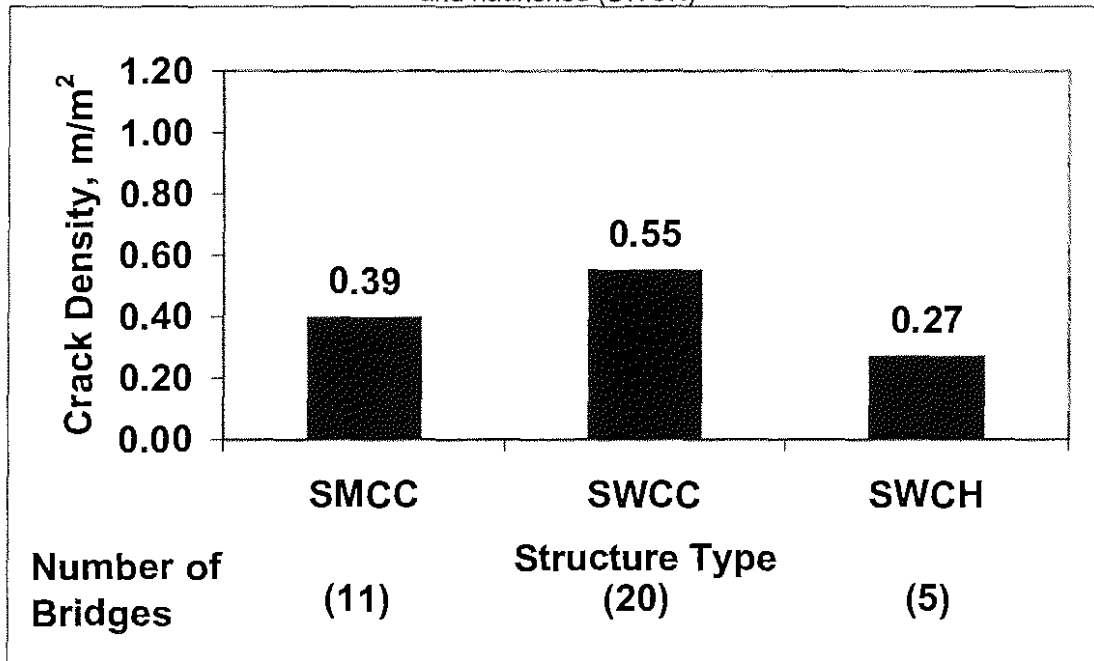


Figure 3.100 : Mean crack density for entire bridge versus structure type for conventional overlay bridge decks. Steel beam, composite continuous (SMCC); Steel welded plate girder, composite continuous (SWCC); Steel welded plate girder, composite continuous and haunched (SWCH)

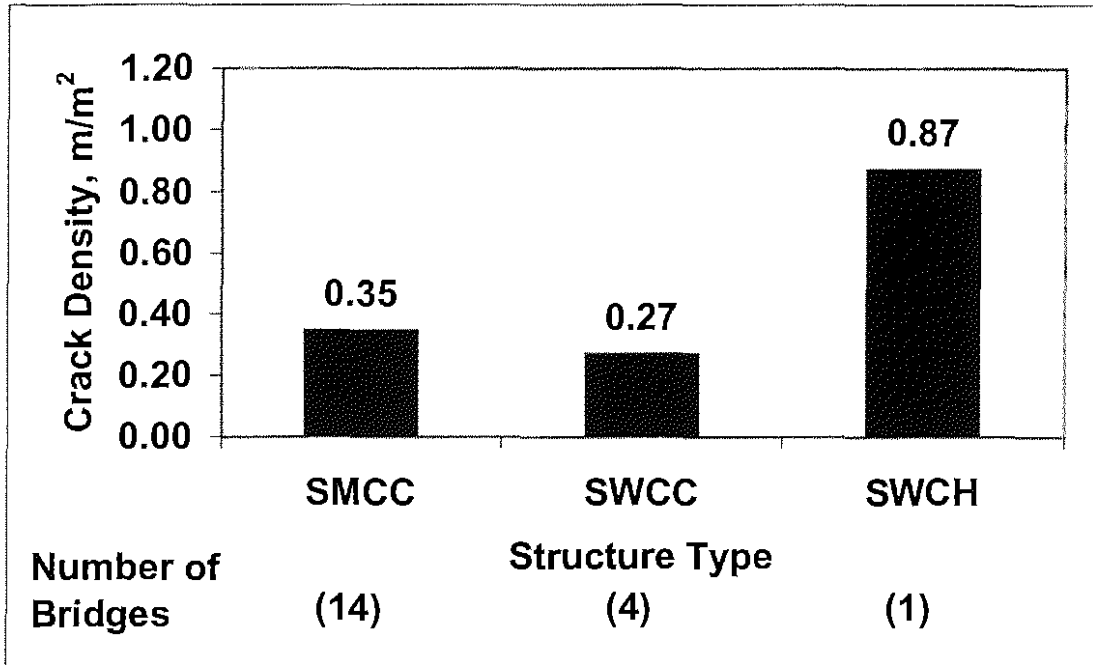


Figure 3.101: Mean crack density for entire bridge versus structure type for monolithic bridge decks. Steel beam, composite continuous (SMCC); Steel welded plate girder, composite continuous (SWCC); Steel welded plate girder, composite continuous and haunched (SWCH)

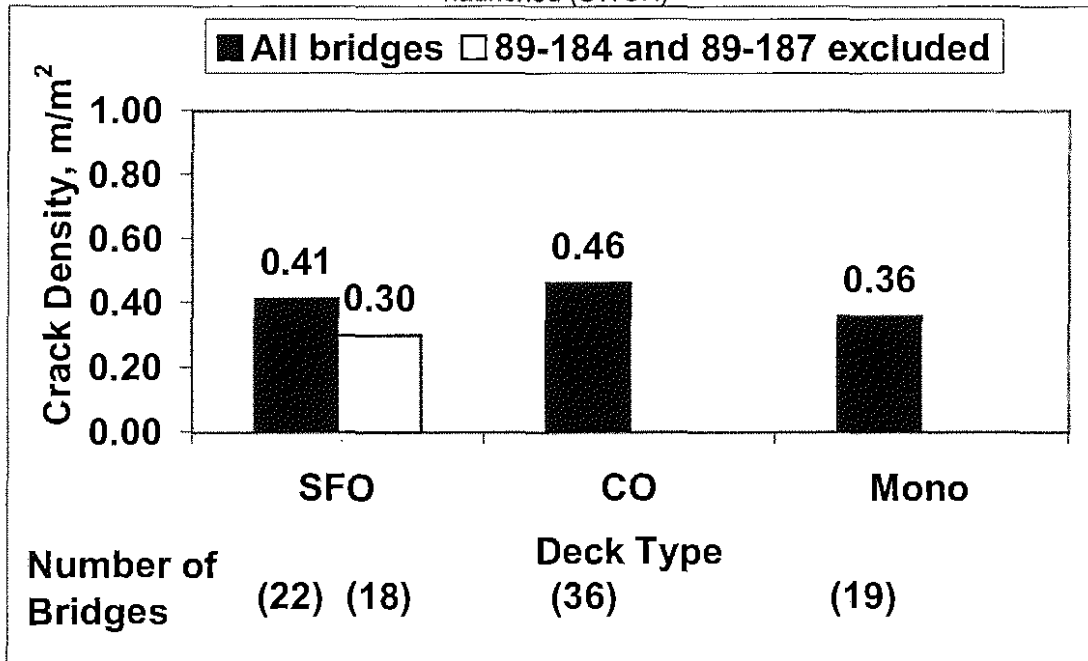


Figure 3.102: Mean crack density of entire bridge versus deck type. Silica fume overlay (SFO); Conventional Overlay (CO); Monolithic Bridge Deck (Mono)

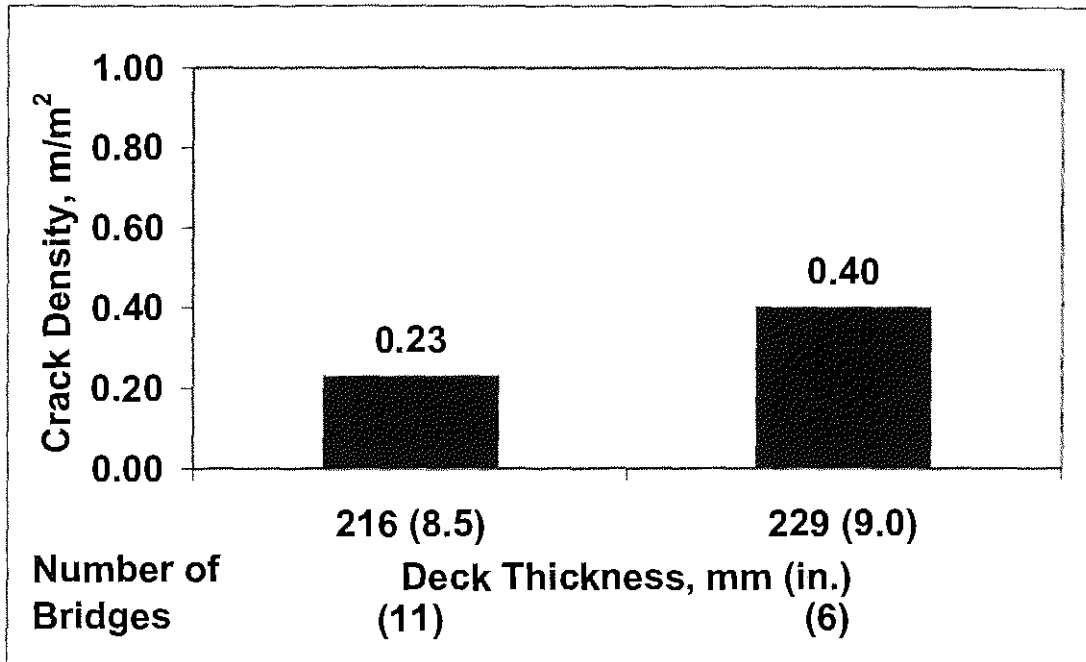


Figure 3.103: Mean crack density for entire bridge versus deck thickness for silica fume overlay bridge decks

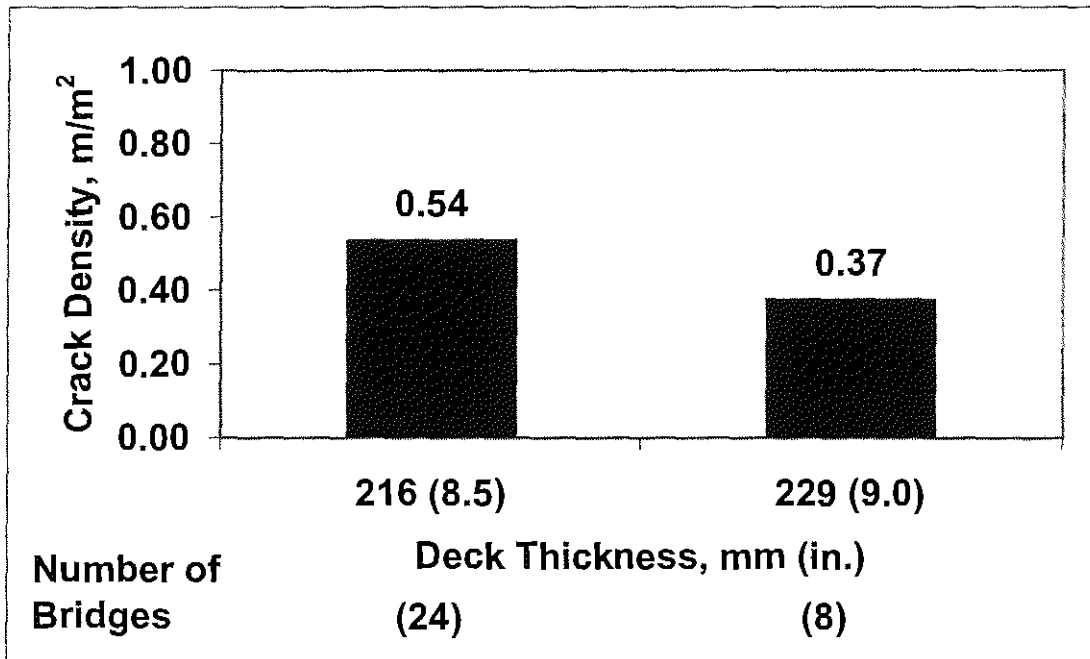


Figure 3.104: Mean crack density for entire bridge versus deck thickness for conventional overlay bridge decks

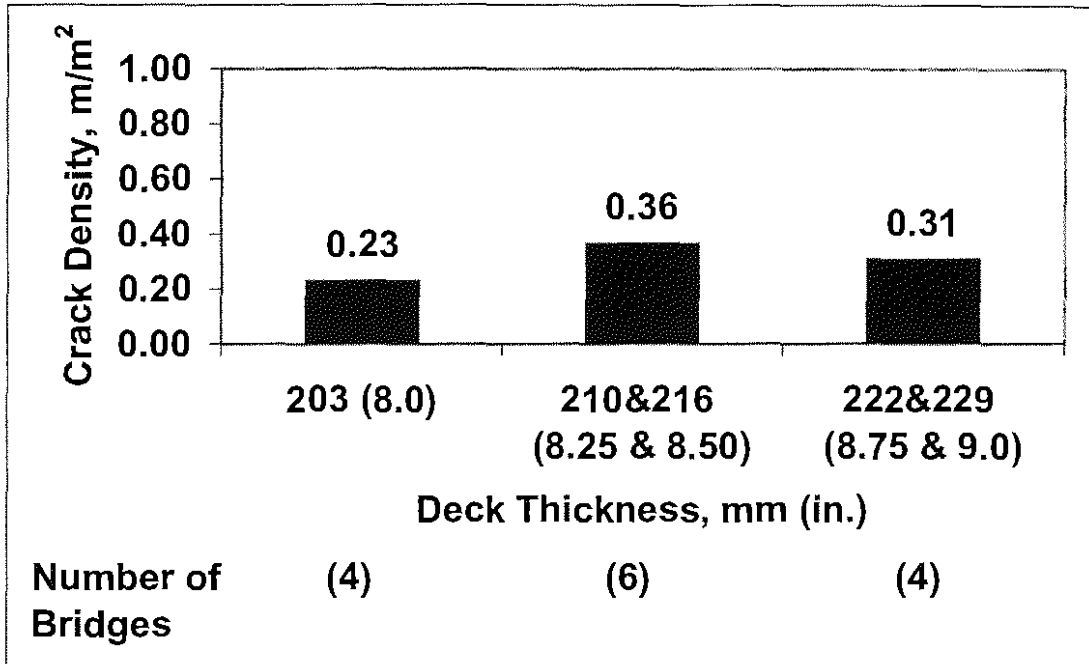


Figure 3.105: Mean crack density for entire bridge versus deck thickness for monolithic bridge decks

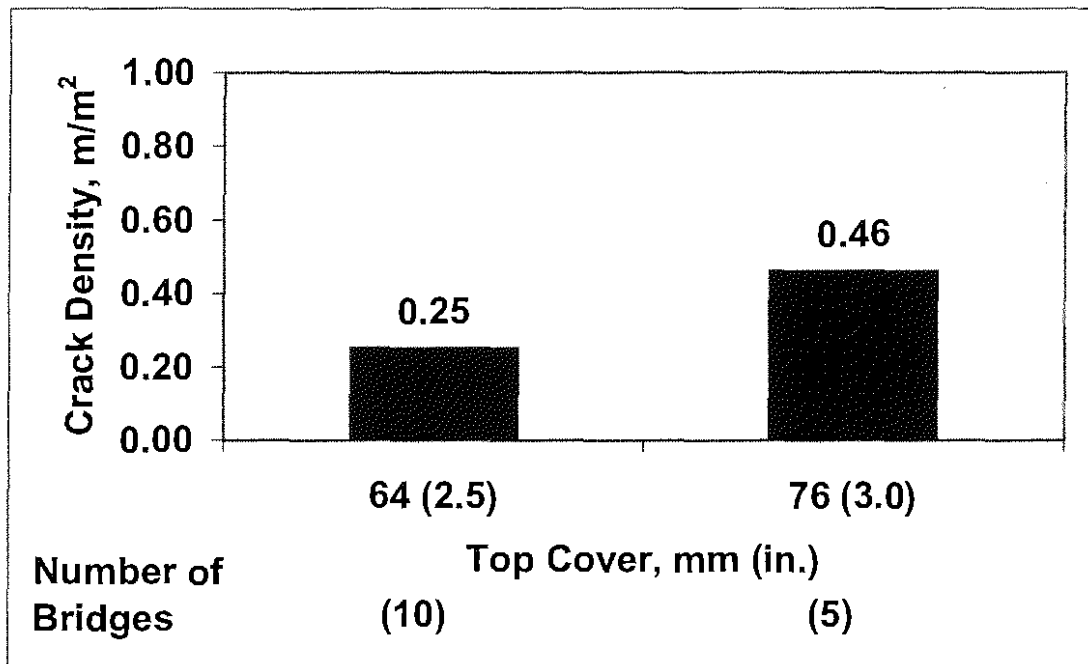


Figure 3.106: Mean crack density for entire bridge versus top cover for monolithic bridge decks

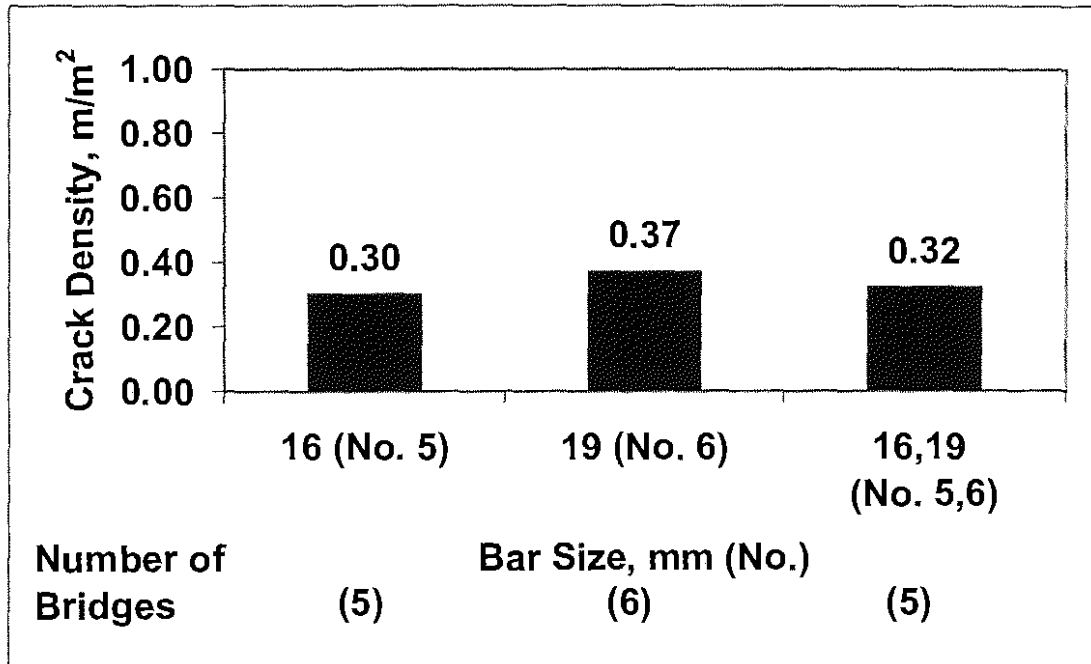


Figure 3.107: Mean crack density for entire bridge versus top transverse reinforcing bar size for silica fume overlay bridge decks

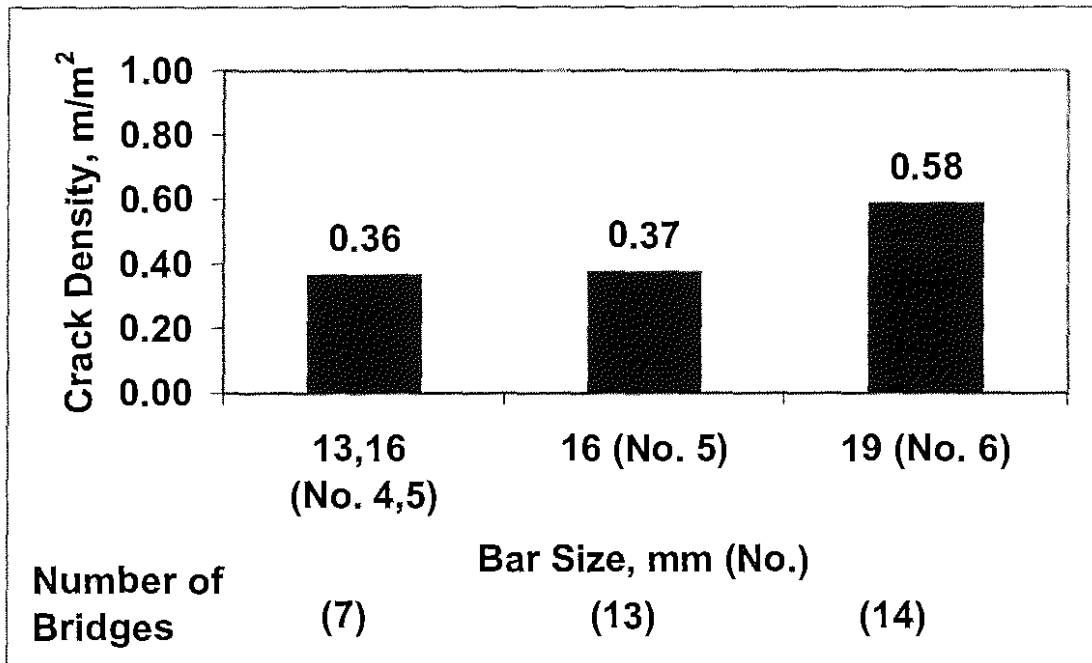


Figure 3.108: Mean crack density for entire bridge versus top transverse reinforcing bar size for conventional overlay bridge decks

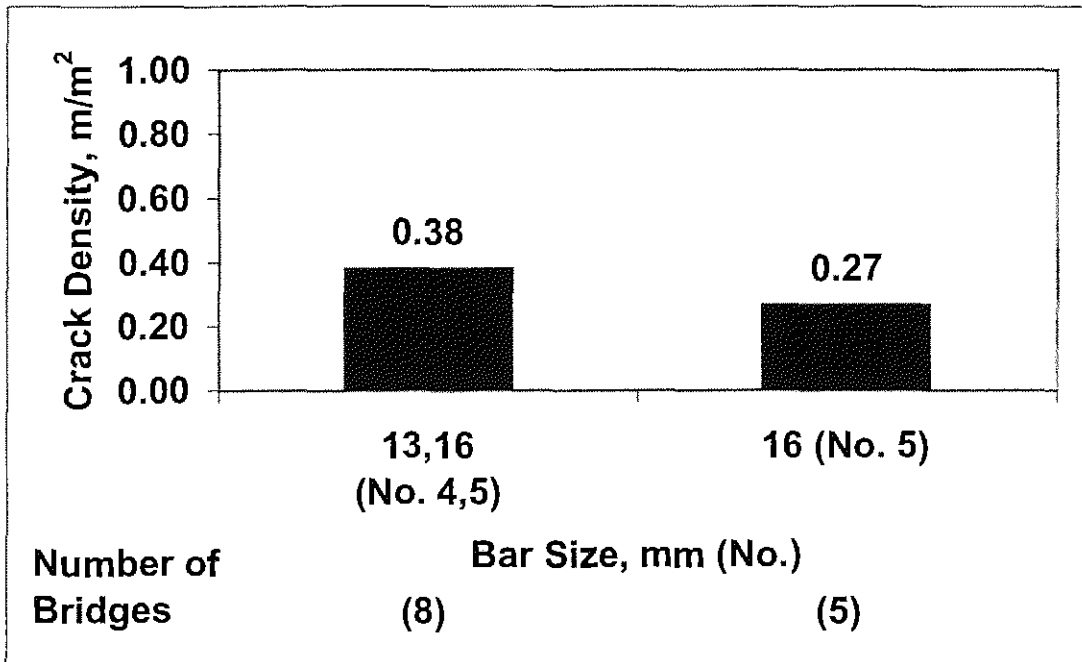


Figure 3.109: Mean crack density for entire bridge versus top transverse reinforcing bar size for monolithic bridge decks

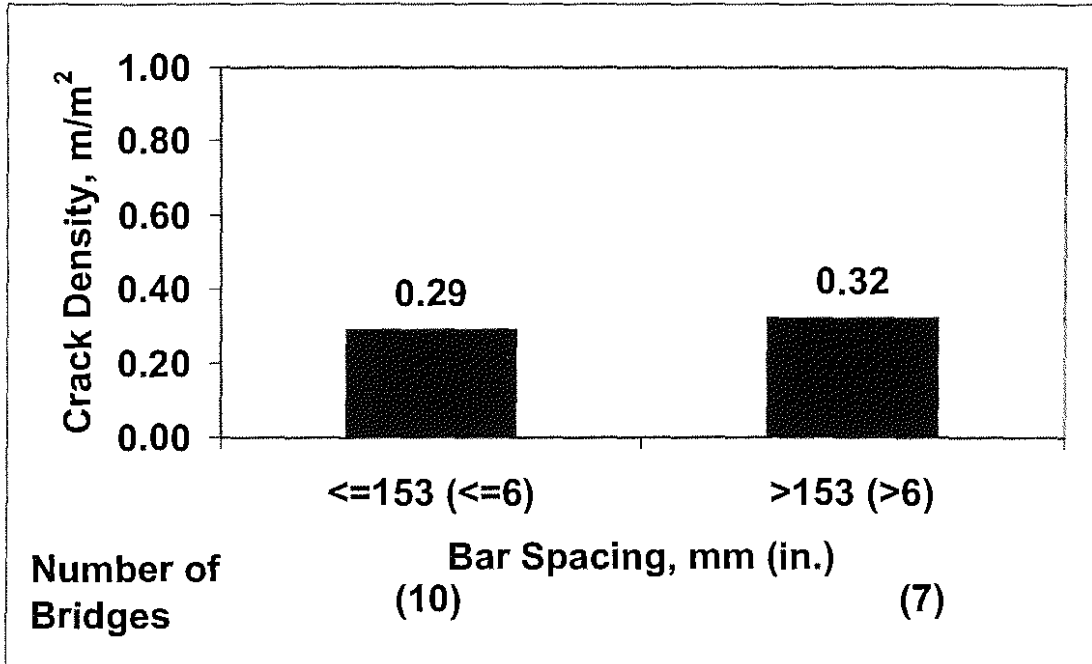


Figure 3.110: Mean crack density for entire bridge versus top transverse bar spacing for silica fume overlay bridge decks

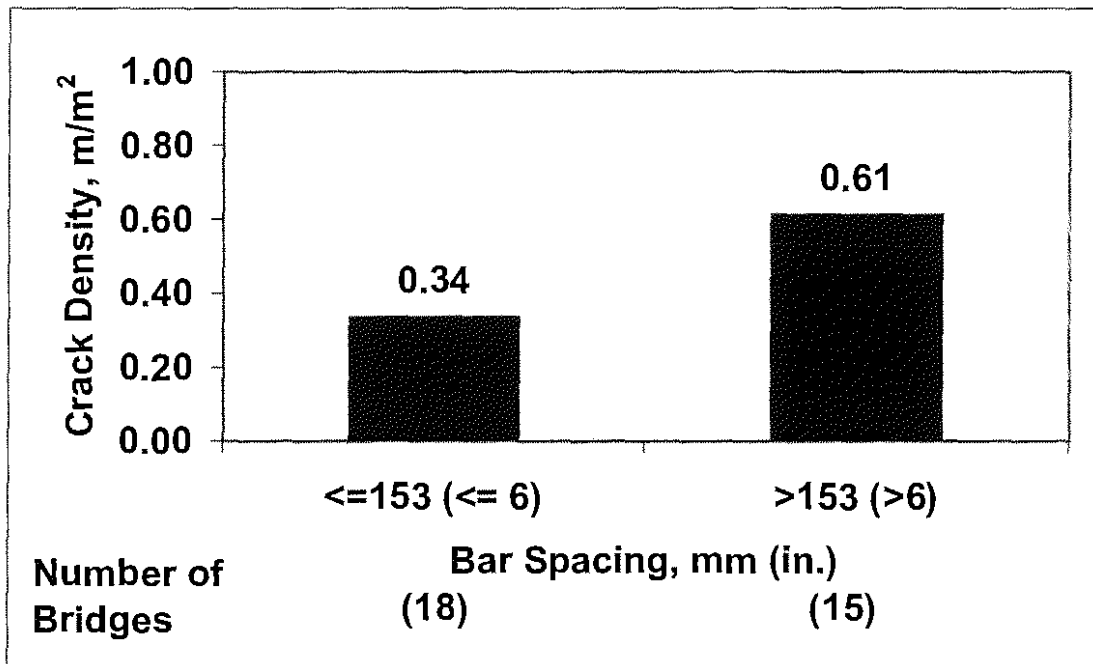


Figure 3.111: Mean crack density for entire bridge versus top transverse bar spacing for conventional overlay bridge decks

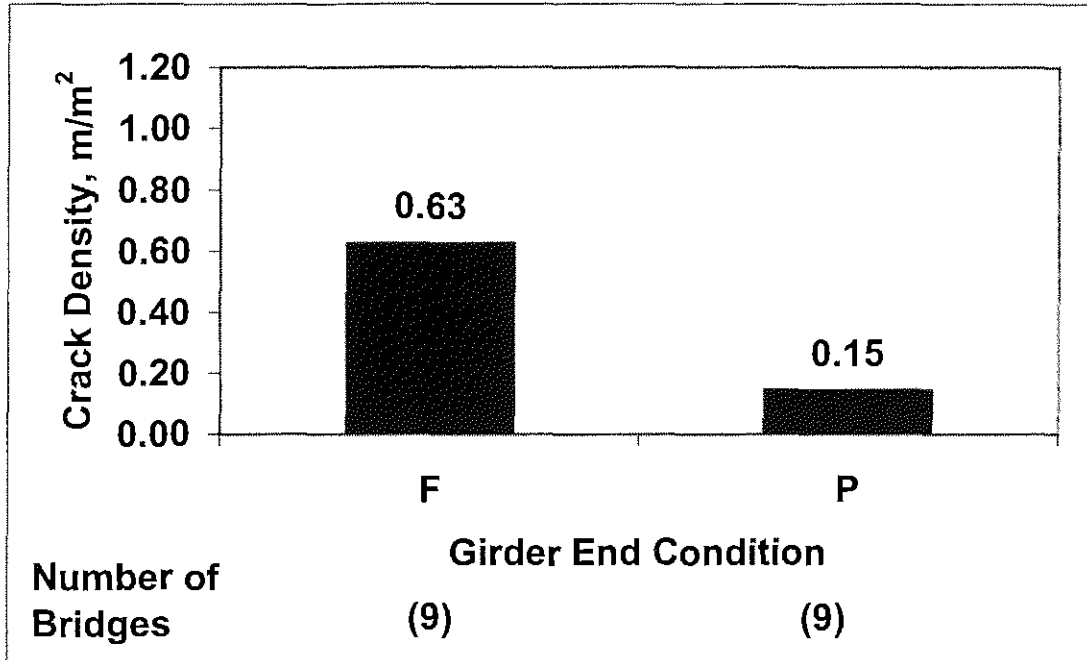


Figure 3.112 : Mean crack density of end sections versus girder end condition for silica fume overlay bridge decks

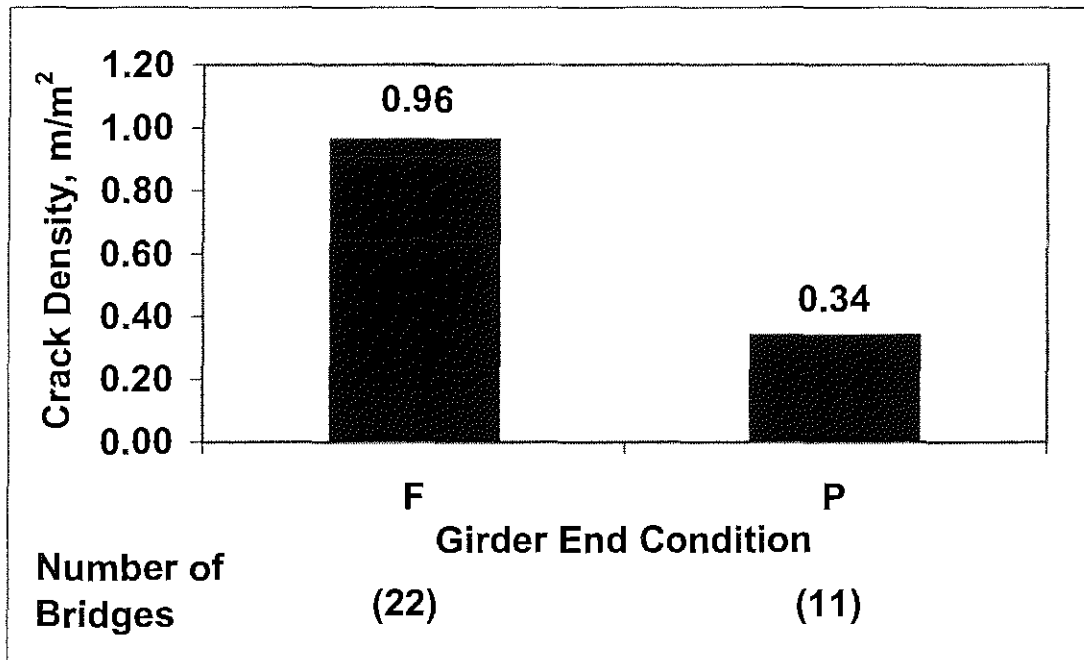


Figure 3.113: Mean crack density of end sections versus girder end condition for conventional overlay bridge decks

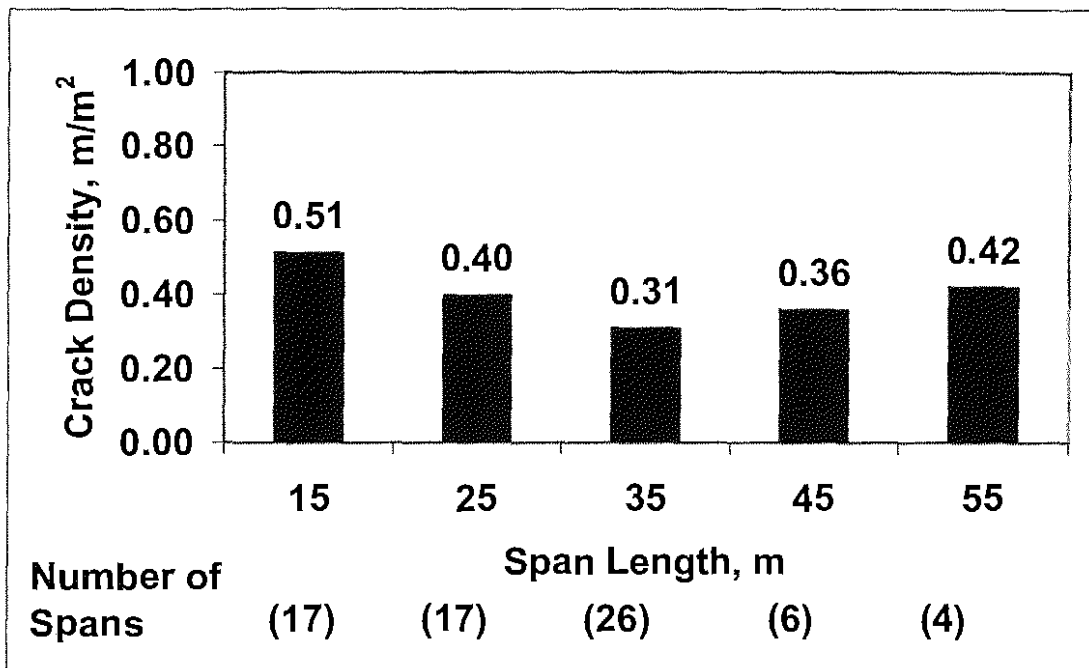


Figure 3.114: Mean crack density of individual spans versus span length for silica fume overlay bridge decks

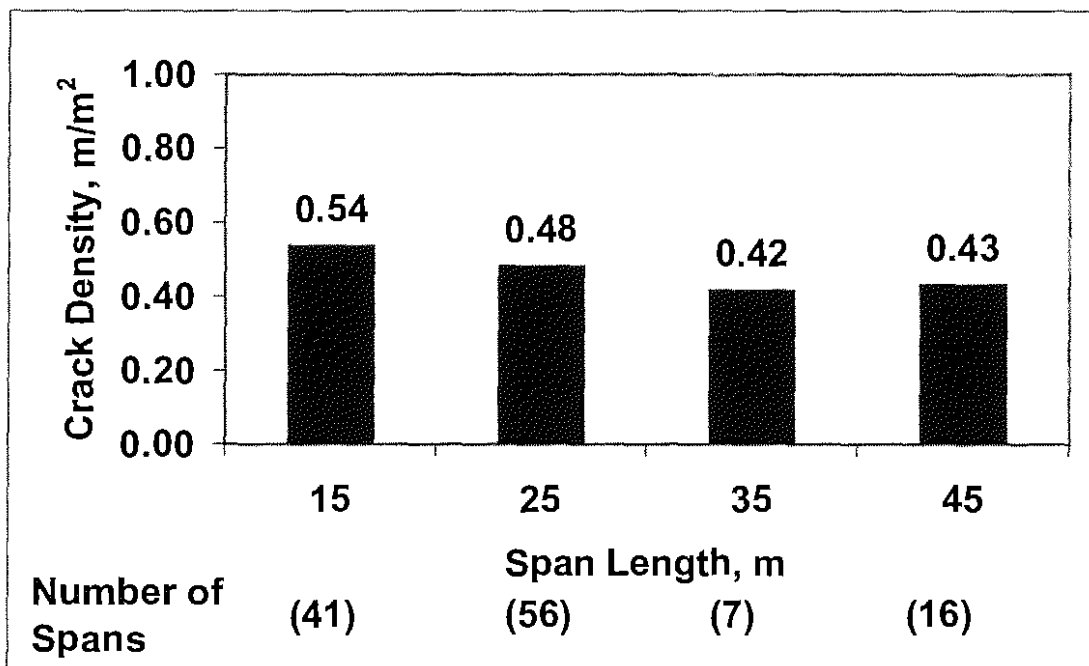


Figure 3.115: Mean crack density of individual spans versus span length for conventional overlay bridge decks

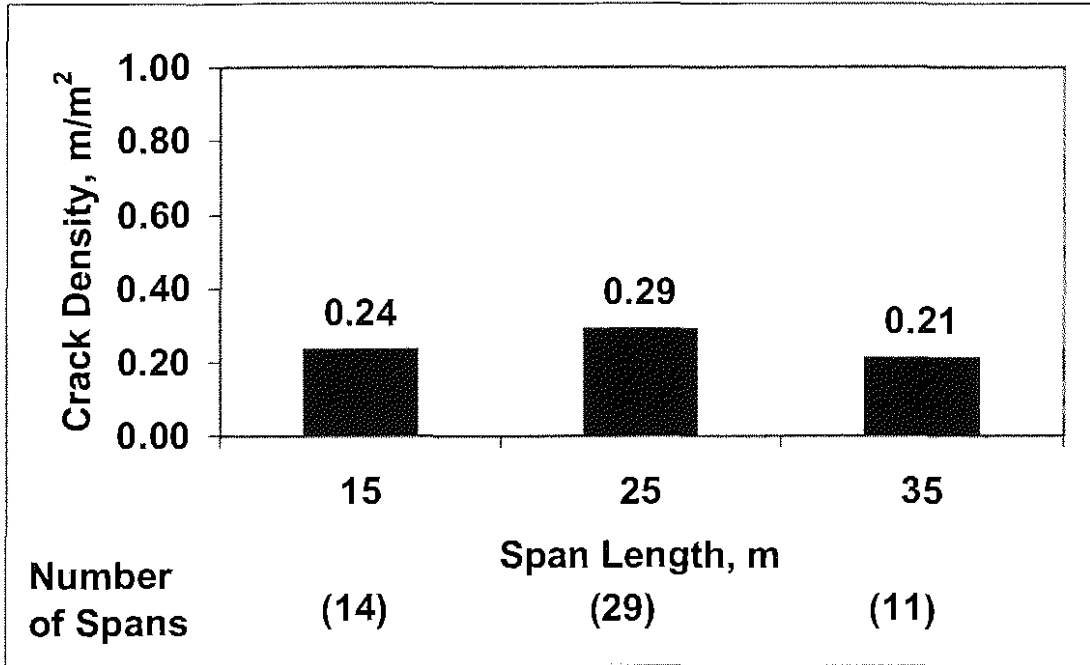


Figure 3.116: Mean crack density of individual spans versus span length for monolithic bridge decks

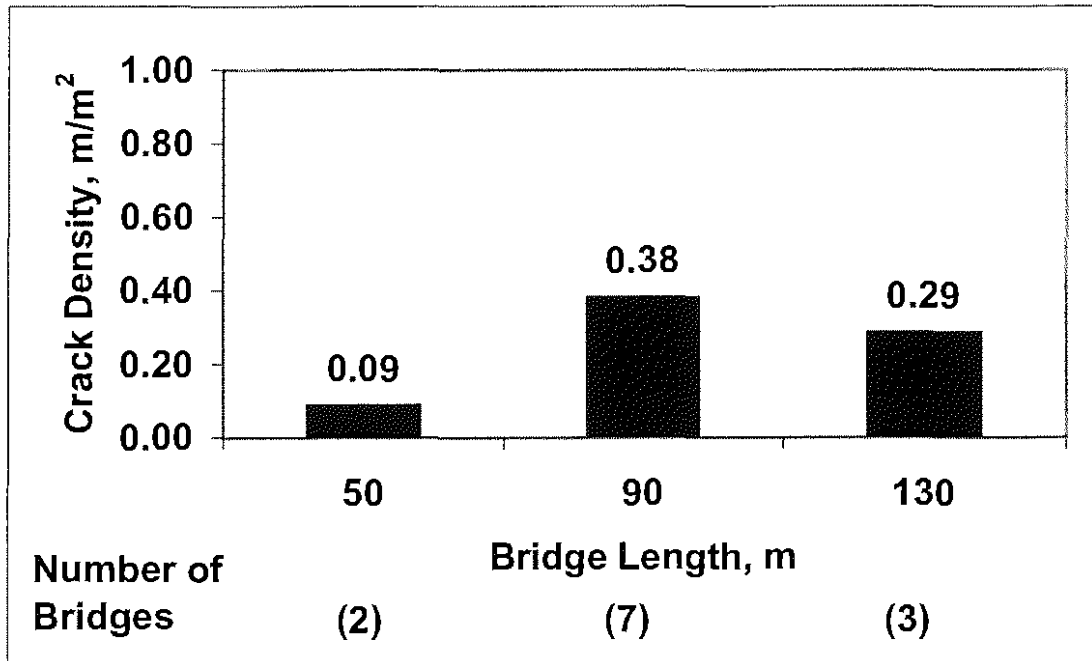


Figure 3.117: Mean crack density of entire bridge versus bridge length for silica fume overlay bridge decks

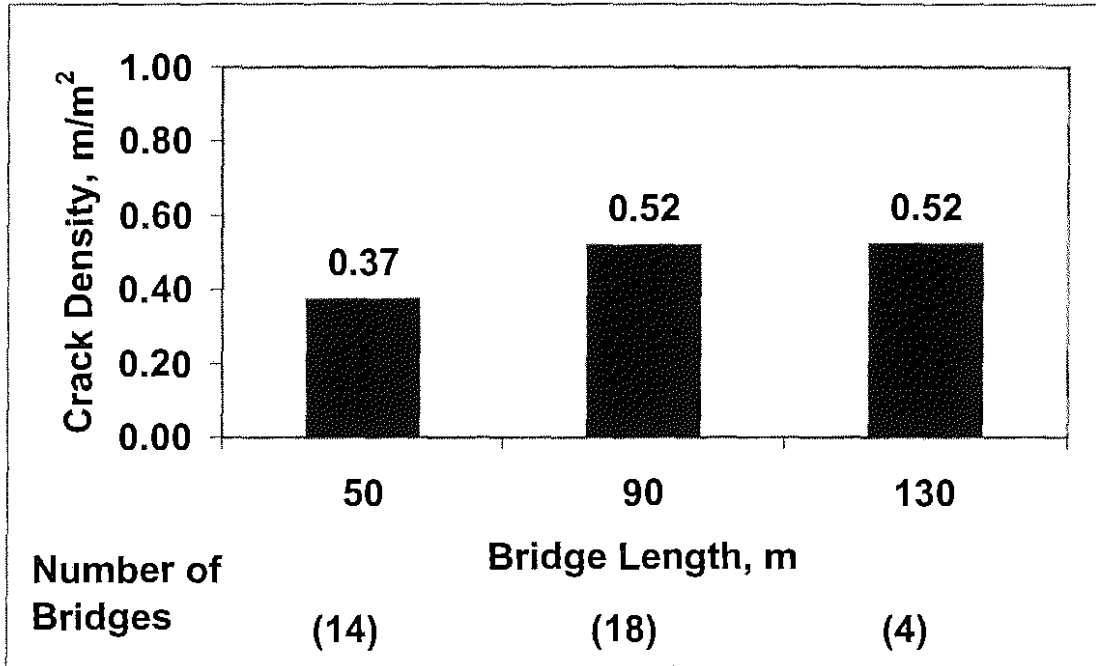


Figure 3.118: Mean crack density of entire bridge versus bridge length for conventional overlay bridge decks

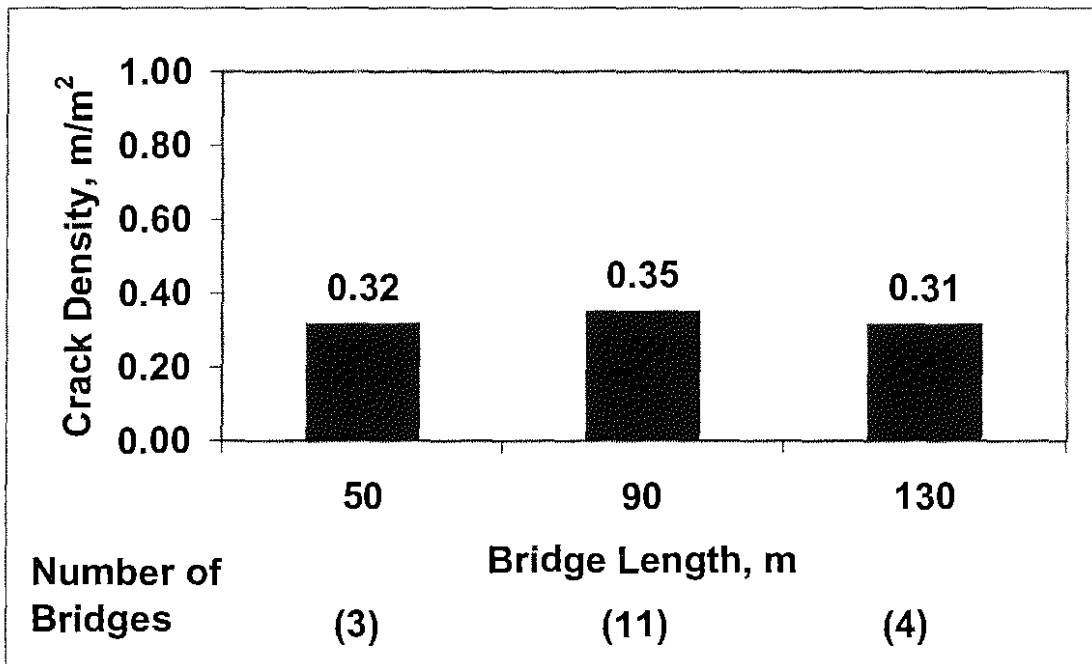


Figure 3.119: Mean crack density of entire bridge versus bridge length for monolithic bridge decks

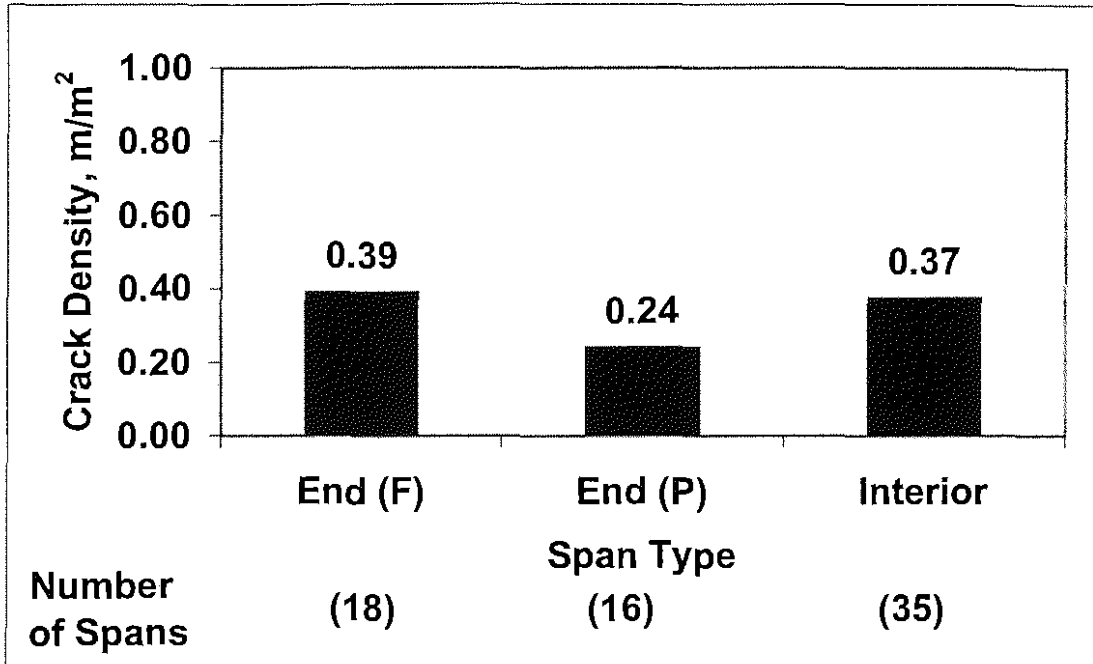


Figure 3.120: Mean crack density of individual spans versus span type for silica fume overlay bridge decks. Categories are fixed connection end spans [End (F)], pinned connection end spans [End(P)], and interior spans (interior).

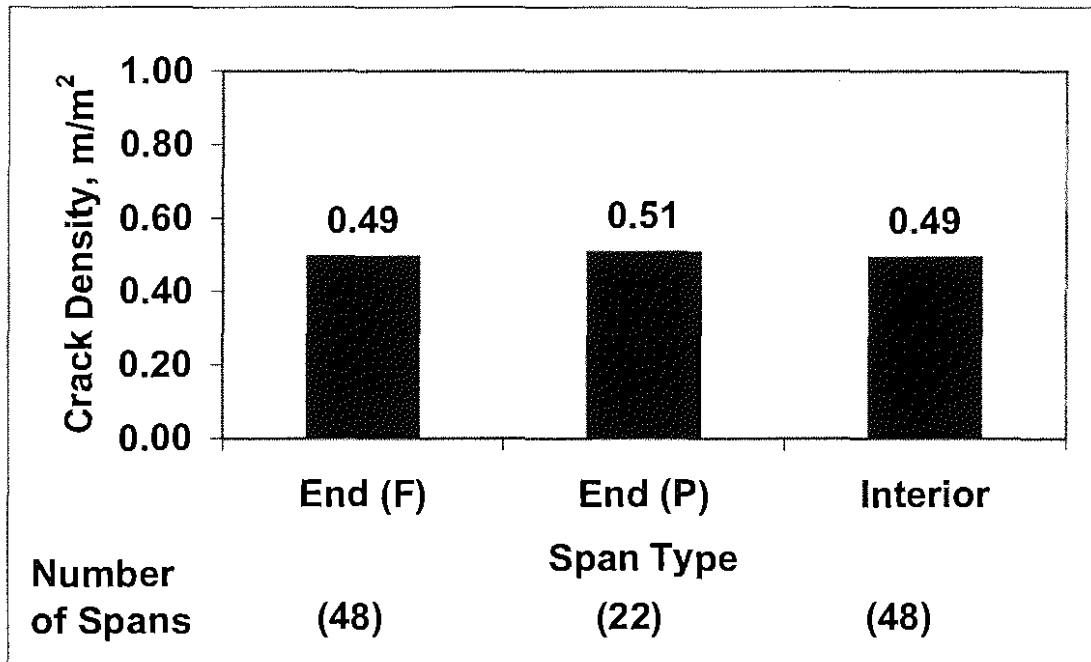


Figure 3.121: Mean crack density of individual spans versus span type for conventional overlay bridge decks. Categories are fixed connection end spans [End (F)], pinned connection end spans [End(P)], and interior spans (interior).

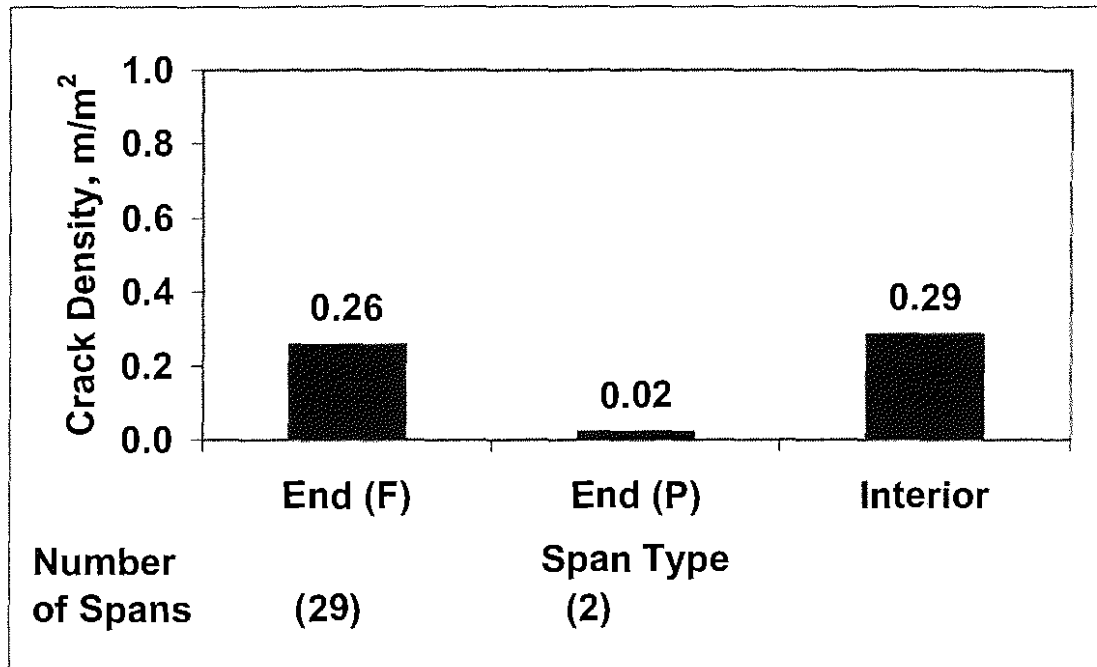


Figure 3.122: Mean crack density of individual spans versus span type for monolithic bridge decks. Categories are fixed connection end spans [End (F)], pinned connection end spans [End(P)], and interior spans (interior).

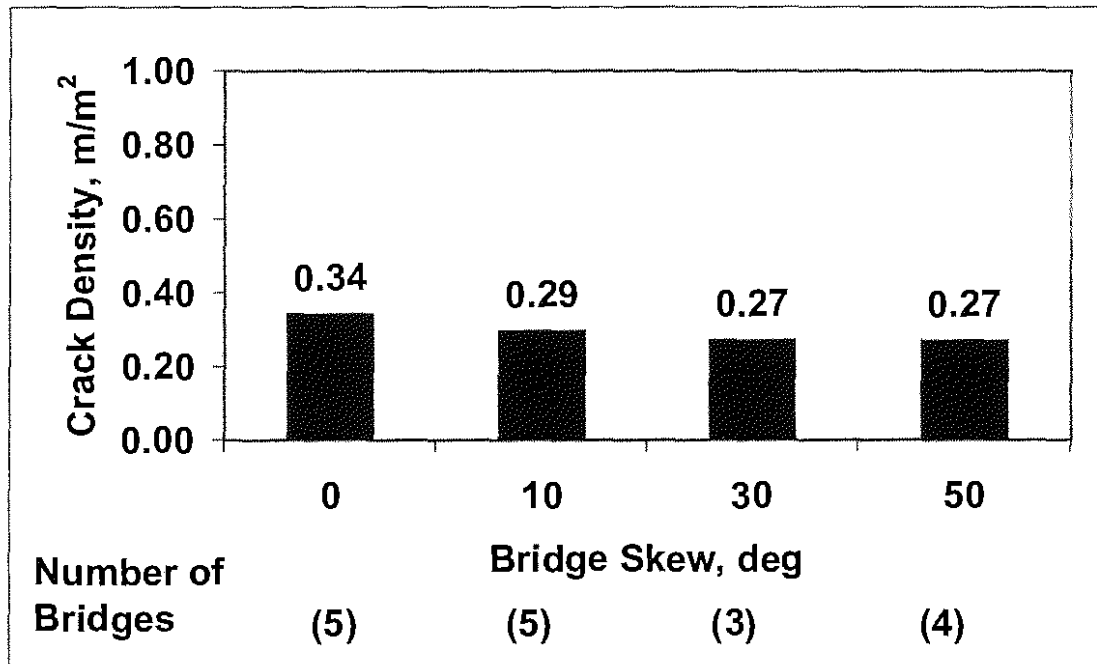


Figure 3.123: Mean crack density of entire bridge versus skew for silica fume overlay bridge decks. The zero category (0) includes only bridges with a zero degree skew.

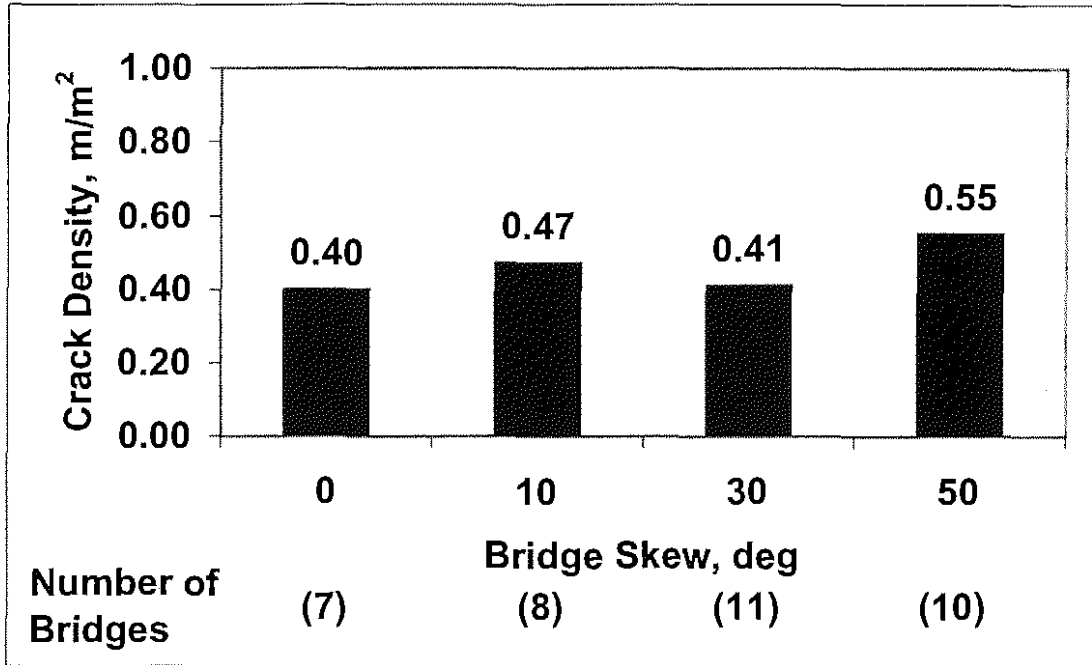


Figure 3.124: Mean crack density of entire bridge versus skew for conventional overlay bridge decks. The zero category (0) includes only bridges with a zero degree skew.

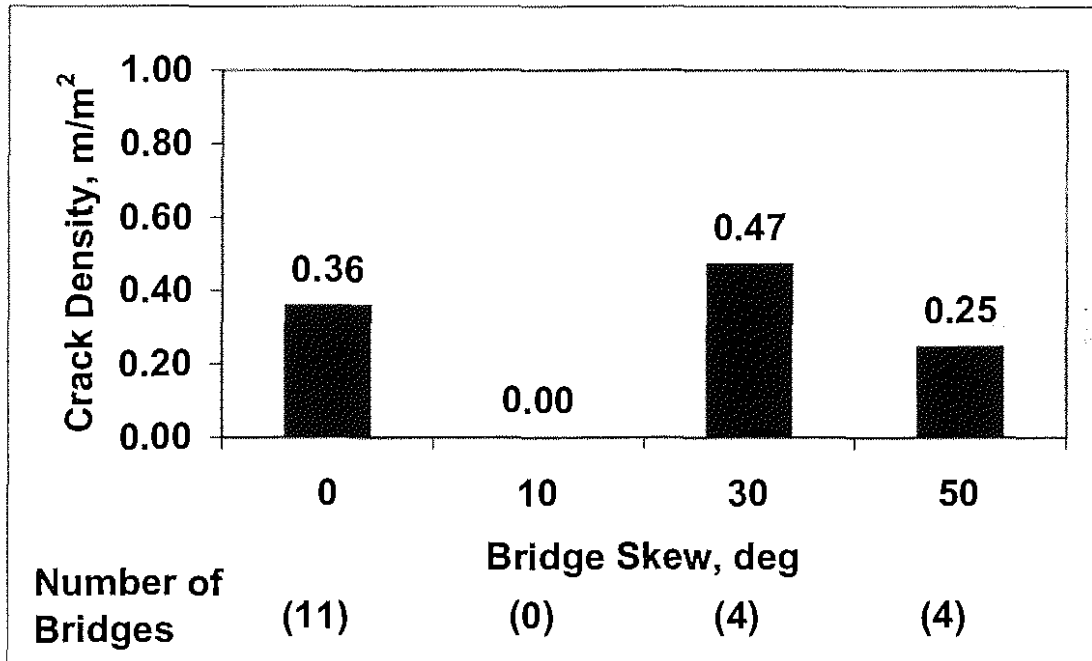


Figure 3.125: Mean crack density of entire bridge versus skew for monolithic bridge decks. The zero category (0) includes only bridges with a zero degree skew.

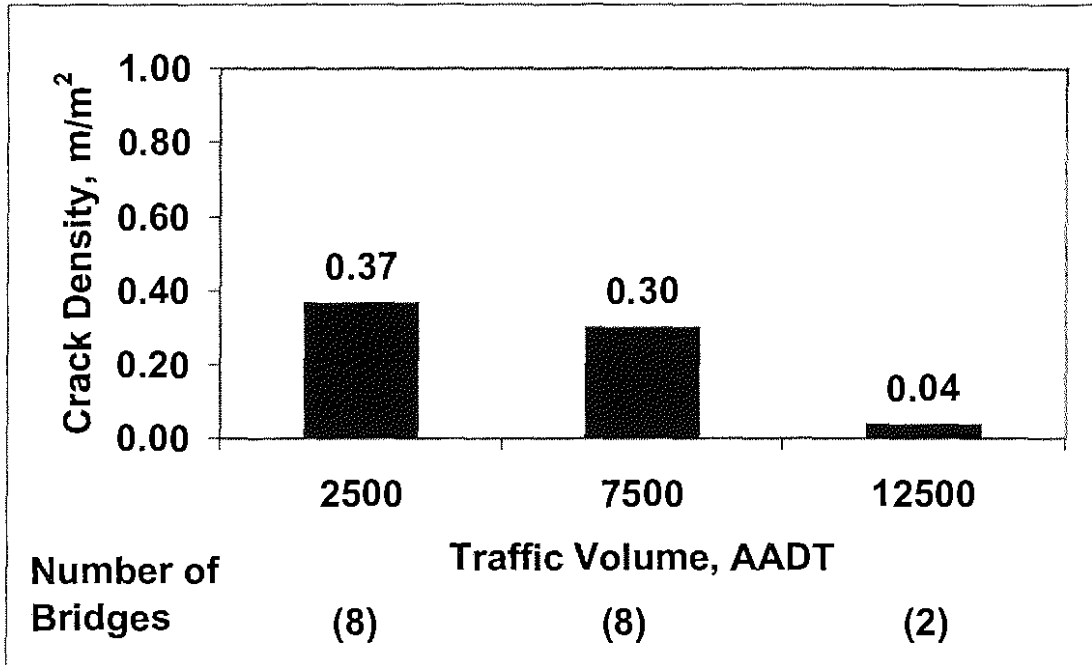


Figure 3.126: Mean crack density of entire bridge versus traffic volume for silica fume overlay bridge decks

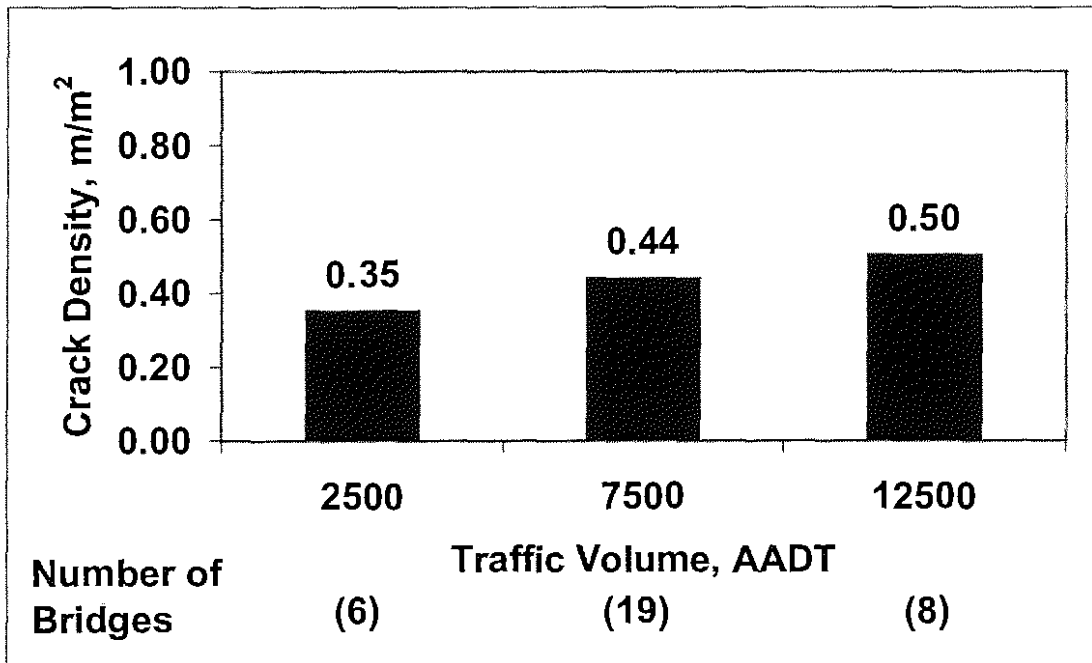


Figure 3.127: Mean crack density of entire bridge versus traffic volume for conventional overlay bridge decks

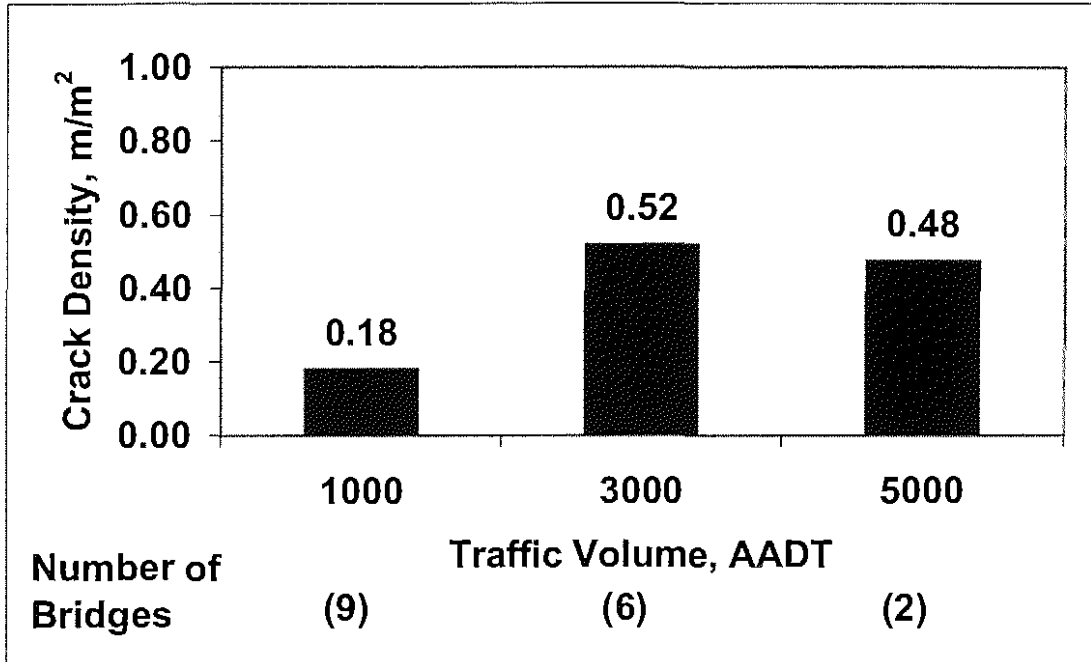


Figure 3.128: Mean crack density of entire bridge versus traffic volume for monolithic bridge decks

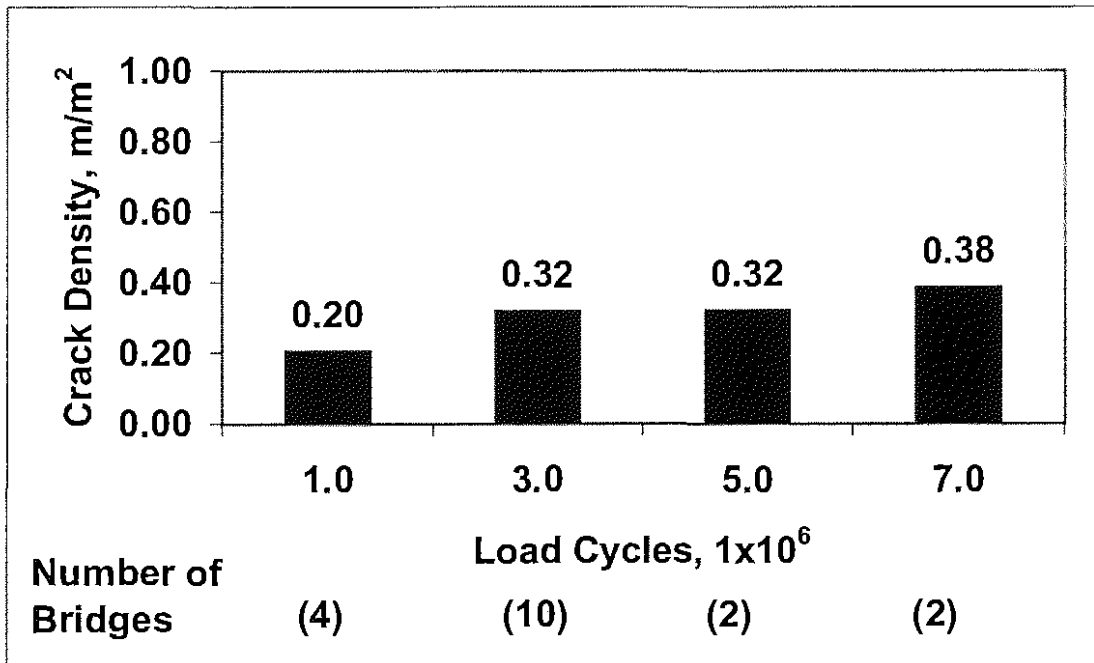


Fig. 3.129: Mean crack density of entire bridge decks versus the total number of load cycles for silica fume overlays

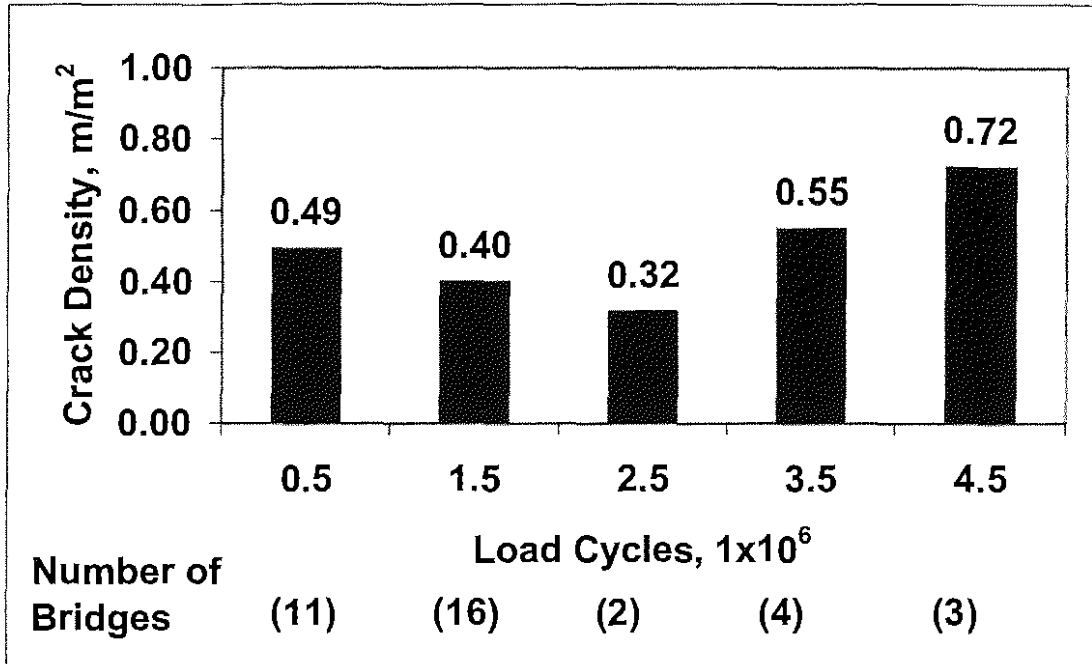


Fig. 3.130: Mean crack density of entire bridge decks versus the total number of load cycles for conventional overlays

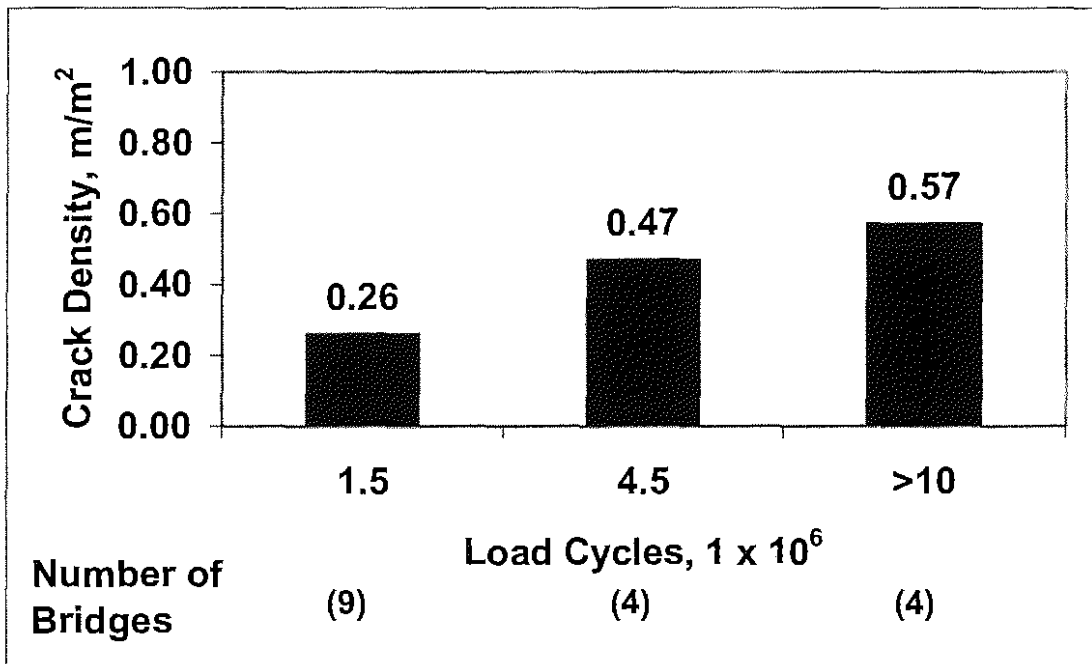


Fig. 3.131: Mean crack density of entire bridge decks versus the total number of load cycles for monolithic bridge decks

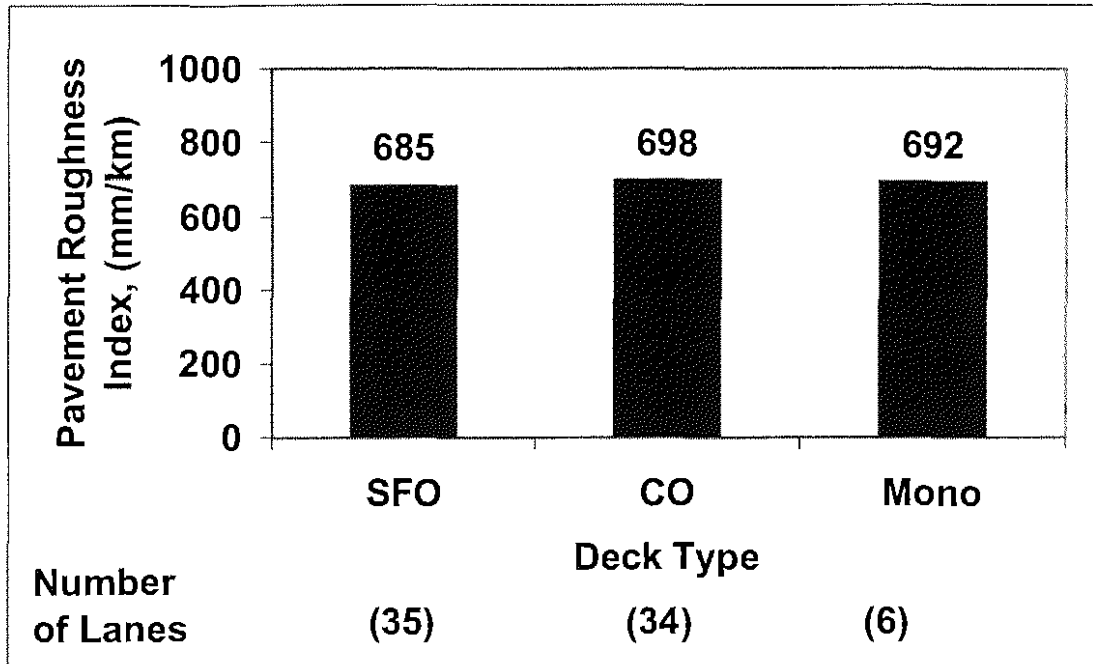


Figure 3.132: Mean pavement roughness index (PRI) of individual lanes versus deck type. Silica fume overlay (SFO); Conventional Overlay (CO); Monolithic Bridge Decks (Mono)

Table A.1: (continued)

Bridge Number	Crack Density (m/m ²)	Structure Type	Deck Type	Bridge Skew (deg.)	Traffic Volume (AADT)	Total Length		Bridge Age (months)
						(ft)	(m)	
89-247	0.50	SWCC	SFO	19	6898	257.4	78.5	14
89-248	0.02	SMCC	SFO	10	5520	198.0	60.4	4
Conventional Overlay Bridges								
46-289	0.65	SWCC	CO	50	8735	439.8	134.1	72
46-290	0.62	SWCC	CO	50	8735	439.8	134.1	72
46-299	0.88	SMCC	CO	17	6200	212.3	64.7	49
46-300	0.71	SMCC	CO	17	6200	212.3	64.7	36
46-301	0.73	SWCC	CO	0	245	292.5	89.2	49
75-1	0.37	SWCC	CO	0	6060	419.5	127.9	83
75-49	0.45	SWCH	CO	0	6060	419.5	127.9	87
81-49	0.73	SWCC	CO	15	19570	266.6	81.3	70
89-183	0.51	SWCC	CO	15	6410	313.2	95.5	94
89-185	0.70	SWCC	CO	41	16540	261.3	79.6	97
89-186	0.72	SMCC	CO	22	16540	213.3	65.0	94
89-196	0.54	SWCC	CO	5	9815	162.5	49.5	75
89-198	0.39	SWCC	CO	53	13725	347.5	105.9	83
89-199	0.66	SWCC	CO	53	13725	347.5	105.9	83
89-200	0.52	SWCC	CO	34	13700	321.0	97.8	84

Table A.1: (continued)

Bridge Number	Crack Density (m/m ²)	Structure Type	Deck Type	Bridge Skew (deg.)	Traffic Volume (AADT)	Total Length		Bridge Age (months)
						(ft)	(m)	
89-201	0.63	SWCC	CO	34	13700	321.0	97.8	84
Monolithic Bridges								
56-148	0.31	SMCC	Mono	0	820	246.5	75.1	85
70-107	0.42	SMCC	Mono	0	2225	202.5	61.7	82
89-204	0.84	SMCC	Mono	38	13725	231.0	70.4	82
89-208	0.03	SWCC	Mono	0	0	367.3	112.0	36

Table A.2: Deck Properties and Crack Densities for End Sections

Bridge Number	Total Deck Thickness		Overlay Thickness		Top Cover		Transverse Steel			Angle of Rebar (deg.)	Girder End Condition	End Section Crack Density	
	(in.)	(mm)	(in.)	(mm)	(in.)	(mm)	Size (No.)	Spacing (in.)	(mm)			(end 1)	(end 2)
Silica Fume Overlay Bridges													
23-85	8.50	216	1.50	38	3.0	76	5	6.00	152	0	F	0.34	0.27
46-302	8.75	222	1.50	38	3.0	76	5	6.00	152	0	F	0.32	0.58
46-309	8.50	216	1.50	38	3.0	76	5	6.00	152	0	F	0.26	0.61
46-317	8.50	216	1.50	38	3.0	76	5	6.00	152	0	P	0.00	0.00
81-50	8.50	216	1.50	38	3.0	76	6	8.00	203	0	P	0.41	0.76
87-453	9.00	229	1.50	38	3.0	76	6	8.00	203	0	F	0.30	1.61
87-454	9.00	229	1.50	38	3.0	76	6	8.00	203	0	F	0.89	2.32
89-184	8.50	216	2.25	57	3.0	76	5	7.00	178	0	F	1.46	1.92
89-187	8.50	216	2.25	57	3.0	76	4,5	6.50	165	0	F	1.85	1.57
89-206	9.00	229	1.50	38	3.0	76	5,6	6.00	152	0	P	0.32	0.00
89-207	9.00	229	1.50	38	3.0	76	5,6	6.00	152	0	P	0.12	0.03
89-210	8.50	216	1.50	38	3.0	76	5,6	6.00	152	0	F	0.01	0.19
89-234	9.00	229	1.50	38	3.0	76	5,6	6.00	152	0	F	0.63	0.52
89-235	9.00	229	1.50	38	3.0	76	5,6	6.00	152	0	F	2.43	0.00
89-240	8.50	216	1.50	38	3.0	76	5	6.00	152	0	P	0.13	0.17
89-244	8.50	216	1.50	38	3.0	76	6	8.00	203	0	P	0.00	0.00
89-245	8.50	216	1.50	38	3.0	76	4,6	4.00	102	0	P	0.00	0.00

Table A.2: (continued)

Bridge Number	Total Deck Thickness		Overlay Thickness		Top Cover		Transverse Steel			Angle of Rebar (deg.)	Girder End Condition	End Section Crack Density	
	(in.)	(mm)	(in.)	(mm)	(in.)	(mm)	Size (No.)	Spacing (in.)	(mm)			(end 1)	(end 2)
89-246	8.50	216	1.50	38	3.0	76	6	9.00	229	0	P	0.00	0.00
89-247	8.50	216	1.50	38	3.0	76	6	9.00	229	0	P	0.31	0.02
89-248	8.50	216	1.50	38	3.0	76	4,5	6.50	165	0	F	0.00	0.00
Conventional Overlay Bridges													
46-289	8.50	216	2.25	57	3.0	76	6	8.00	203	0	P	0.50	0.13
46-290	8.50	216	2.25	57	3.0	76	5	6.00	152	0	P	0.46	0.17
46-299	9.00	229	2.25	57	3.0	76	6	6.00	152	0	P	0.33	0.93
46-300	9.00	229	2.25	57	3.0	76	6	6.00	152	0	P	0.33	0.40
46-301	9.00	229	2.25	57	3.0	76	5	5.00	127	0	F	0.00	0.01
75-1	8.50	216	2.25	57	3.0	76	6	5.00	127	0	P	0.30	0.12
75-49	8.50	216	2.25	57	3.0	76	6	6.00	152	0	F	0.76	0.92
81-49	8.50	216	2.25	57	3.0	76	5	12.00	305	15	F	0.98	0.88
89-183	8.50	216	2.25	57	3.0	76	4,5	6.00	152	15	F	1.30	1.10
89-185	8.50	216	2.25	57	3.0	76	5	7.00	178	0	F	1.43	1.99
89-186	8.50	216	2.25	57	3.0	76	4,5	6.50	165	0	F	1.09	1.23
89-196	8.50	216	2.25	57	3.0	76	6	8.00	203	0	F	1.06	1.47
89-198	8.50	216	2.25	57	3.0	76	6	8.00	203	0	P	0.40	0.19

Table A.2: (continued)

Bridge Number	Total Deck Thickness		Overlay Thickness		Top Cover		Transverse Steel			Angle of Rebar (deg.)	Girder End Condition	End Section Crack Density	
	(in.)	(mm)	(in.)	(mm)	(in.)	(mm)	Size (No.)	Spacing (in.)	(mm)			(end 1)	(end 2)
89-199	8.50	216	2.25	57	3.0	76	6	8.00	203	0	P	0.24	0.56
89-200	8.50	216	2.25	57	3.0	76	6	8.00	203	0	F	1.64	1.48
89-201	8.50	216	2.25	57	3.0	76	6	8.00	203	0	F	1.80	1.59
Monolithic Bridges													
56-148	8.25	210	0.00	0	2.50	64	5	6.00	152	0	F	0.63	0.30
70-107	8.00	203	0.00	0	2.50	64	4,5	6.00	152	0	F	0.53	0.56
89-204	8.50	216	0.00	0	3.00	76	4,5	6.00	152	0	F	0.72	0.64
89-208	8.75	222	0.00	0	2.50	64	5,6	6.00	152	0	F	0.02	0.04

Table A.3: Crack Density and Mix Design Information for Bridge Deck Placements

Bridge Number	Portion Placed	Date of Placement	Crack Density (m/m ²)	Water Content		Cement Content		SF Content		W/CM Ratio	Volume of W+C+SF (%)	Types of Admixtures
				(lb/yd ³)	(kg/m ³)	(lb/yd ³)	(kg/m ³)	(lb/yd ³)	(kg/m ³)			
Silica Fume Overlay Bridges												
23-85	Subdeck	11/06/95	---	265	157	602	357	0	0	0.44	27.07	AEA
23-85	East 1/2 SFO	03/29/96	0.37	250	148	595	353	30	18	0.40	26.86	AEA
23-85	West 1/2 SFO	04/03/96	0.37	250	148	595	353	30	18	0.40	26.86	AEA
46-302	Subdeck	11/14/95	---	265	157	602	357	0	0	0.44	27.07	AEA
46-302	Lt. 1/2 SFO	04/09/96	0.43	250	148	595	353	30	18	0.40	26.86	AEA, Type A
46-302	Rt. 1/2 SFO	04/11/96	0.56	250	148	595	353	30	18	0.40	26.86	AEA, Type A
46-309	Subdeck	09/26/95	---	265	157	602	357	0	0	0.44	27.07	AEA
46-309	Rt. 1/2 SFO	10/20/95	0.32	250	148	595	353	30	18	0.40	26.86	AEA, Type A
46-309	Lt. 1/2 SFO	10/24/95	0.38	250	148	595	353	30	18	0.40	26.86	AEA, Type A
46-317	Subdeck Sec. 2	04/11/96	---	265	157	602	357	0	0	0.44	27.07	AEA
46-317	Subdeck Sec. 1	04/26/96	---	265	157	602	357	0	0	0.44	27.07	AEA
46-317	SFO 12'	06/28/96	0.07	238	141	595	353	30	18	0.38	26.15	AEA, Prokrete-N
46-317	SFO 16'	07/01/96	0.08	238	141	595	353	30	18	0.38	26.15	AEA, Prokrete-N
81-50	Subdeck Rt. 36+38 to Ab. #2	08/31/95	---	292	173	696	413	0	0	0.42	30.45	AEA, Type D
81-50	Subdeck Rt. 34+69 to 36+38	09/13/95	---	292	173	696	413	0	0	0.42	30.45	AEA, Type D
81-50	Subdeck Rt. 30+06 to 34+69	09/26/95	---	278	165	696	413	0	0	0.40	29.61	AEA, Type D
81-50	Subdeck Rt. Ab. #1 to 30+06	10/02/95	---	278	165	696	413	0	0	0.40	29.61	AEA, Type D
81-50	Subdeck Lt. 36+38 to Ab. #2	10/06/95	---	278	165	696	413	0	0	0.40	29.61	AEA, Type D

Table A.3: (continued)

Bridge Number	Portion Placed	Date of Placement	Crack Density (m/m ²)	Water Content		Cement Content		SF Content		W/CM Ratio	Volume of W+C+SF (%)	Types of Admixtures
				(lb/yd ³)	(kg/m ³)	(lb/yd ³)	(kg/m ³)	(lb/yd ³)	(kg/m ³)			
81-50	Subdeck Lt. 34+69 to 36+38	10/11/95	---	278	165	696	413	0	0	0.40	29.61	AEA, Type D
81-50	Subdeck Lt. 30+06 to 34+69	10/18/95	---	278	165	696	413	0	0	0.40	29.61	AEA, Type D
81-50	Subdeck Lt. Ab. #1 to 30+06	10/21/95	---	278	165	696	413	0	0	0.40	29.61	AEA, Type D
81-50	SFO Rt. Unit #1	11/15/95	---	249	148	594	352	30	18	0.40	26.78	AEA, Type A, Type F
81-50	SFO Lt. Unit #1	11/18/95	---	249	148	594	352	30	18	0.40	26.78	AEA, Type A, Type F
81-50	SFO Rt. Unit #2	11/21/95	0.67	249	148	594	352	30	18	0.40	26.78	AEA, Type A, Type F
81-50	SFO Lt. Unit #2	11/30/95	0.70	249	148	594	352	30	18	0.40	26.78	AEA, Type A, Type F
87-453	Subdeck	05/22/97	---	262	155	639	379	0	0	0.41	27.59	AEA
87-453	North 22'	06/30/97	0.19	237	141	593	352	30	18	0.38	26.05	AEA, Type F
87-453	South 18'	07/03/97	0.32	237	141	593	352	30	18	0.38	26.05	AEA, Type F
87-454	Subdeck	08/01/96	---	262	155	639	379	0	0	0.41	27.59	AEA
87-454	Left of CL	09/10/96	0.66	237	141	593	352	30	18	0.38	26.05	AEA, Type F
87-454	Right of CL	10/16/96	0.82	237	141	593	352	30	18	0.38	26.05	AEA, Type F
89-184	Subdeck	09/13/90	---	265	157	602	357	0	0	0.44	27.07	---
89-184	Inside	09/26/90	0.94	225	133	578	343	47	28	0.36	25.51	WR
89-184	Outside	09/28/90	1.06	225	133	578	343	47	28	0.36	25.51	WR
89-187	Subdeck	05/31/90	---	265	157	602	357	0	0	0.44	27.07	---
89-187	Inside	06/26/90	1.21	238	141	594	352	31	18	0.38	26.16	WR
89-187	Outside	06/28/90	0.79	238	141	594	352	31	18	0.38	26.16	WR

Table A.3: (continued)

Bridge Number	Portion Placed	Date of Placement	Crack Density (m/m ²)	Water Content		Cement Content		SF Content		W/CM Ratio	Volume of W+C+SF (%)	Types of Admixtures
				(lb/yd ³)	(kg/m ³)	(lb/yd ³)	(kg/m ³)	(lb/yd ³)	(kg/m ³)			
89-206	Subdeck	07/19/95	---	271	161	602	357	0	0	0.45	27.43	AEA
89-206	Right	10/04/95	0.58	250	148	595	353	30	18	0.40	26.86	AEA, Type F, Type A
89-206	Left	10/10/95	0.27	250	148	595	353	30	18	0.40	26.86	AEA, Type F, Type A
89-207	Subdeck	08/29/95	---	271	161	602	357	0	0	0.45	27.43	AEA
89-207	Left	10/24/95	0.33	250	148	595	353	30	18	0.40	26.86	AEA, Type F, Type A
89-207	Right	04/19/96	0.39	250	148	595	353	30	18	0.40	26.86	AEA, Type F, Type A
89-210	Subdeck	09/15/95	---	271	161	602	357	0	0	0.45	27.43	AEA
89-210	Right	10/12/95	0.17	249	148	593	352	30	18	0.40	26.76	AEA, Type F, Type A
89-210	Left	10/18/95	0.15	249	148	593	352	30	18	0.40	26.76	AEA, Type F, Type A
89-234	Subdeck	05/16/96	---	241	143	602	357	0	0	0.40	25.65	AEA
89-234	SFO South 20'	06/20/96	0.17	249	148	594	352	30	18	0.40	26.78	AEA
89-234	SFO North 18'	06/25/96	0.23	249	148	594	352	30	18	0.40	26.78	AEA
89-234	SFO Center 12'	06/28/96	0.51	249	148	594	352	30	18	0.40	26.78	AEA
89-235	Subdeck	03/21/97	---	253	150	602	357	0	0	0.42	26.36	AEA
89-235	SFO Left 20'	04/29/97	---	249	148	594	352	30	18	0.40	26.78	AEA
89-235	SFO Right 18'	05/01/97	0.38	249	148	594	352	30	18	0.40	26.78	AEA
89-235	SFO Center 12'	05/06/97	---	249	148	594	352	30	18	0.40	26.78	AEA
89-240	Subdeck	07/02/97	---	265	157	602	357	0	0	0.44	27.07	AEA
89-240	Rt. 22' SFO	08/05/97	0.01	250	148	595	353	30	18	0.40	26.86	AEA, Type F

Table A.3: (continued)

Bridge Number	Portion Placed	Date of Placement	Crack Density (m/m ²)	Water Content		Cement Content		SF Content		W/CM Ratio	Volume of W+C+SF (%)	Types of Admixtures
				(lb/yd ³)	(kg/m ³)	(lb/yd ³)	(kg/m ³)	(lb/yd ³)	(kg/m ³)			
89-240	Lt. 22' SFO	08/07/97	0.41	250	148	595	353	30	18	0.40	26.86	AEA, Type F
89-244	Subdeck	08/21/97	---	265	157	602	357	0	0	0.44	27.07	AEA
89-244	SFO Rt.	10/17/97	0.03	249	148	594	352	30	18	0.40	26.78	AEA, Type F
89-244	SFO Lt.	10/21/97	0.00	249	148	594	352	30	18	0.40	26.78	AEA, Type F
89-245	Subdeck Unit #1	09/26/97	---	265	157	602	357	0	0	0.44	27.07	AEA
89-245	Subdeck Unit #2	10/02/97	---	265	157	602	357	0	0	0.44	27.07	AEA
89-245	Lt. 1/2 Unit 2 SFO	10/20/97	0.03	249	148	594	352	30	18	0.40	26.78	AEA, Type F
89-245	Lt. 1/2 Unit 1 SFO	10/22/97	0.03	249	148	594	352	30	18	0.40	26.78	AEA, Type F
89-245	Rt. 1/2 Unit 2 SFO	10/23/97	0.05	249	148	594	352	30	18	0.40	26.78	AEA, Type F
89-245	Rt. 1/2 Unit 1 SFO	10/24/97	0.09	249	148	594	352	30	18	0.40	26.78	AEA, Type F
89-246	Subdeck	08/27/97	---	265	157	602	357	0	0	0.44	27.07	AEA
89-246	East 1/2 SFO	09/08/97	0.08	249	148	594	352	30	18	0.40	26.78	AEA, Type F
89-246	West 1/2 SFO	09/10/97	0.06	249	148	594	352	30	18	0.40	26.78	AEA, Type F
89-247	Subdeck	04/24/97	---	265	157	602	357	0	0	0.44	27.07	AEA
89-247	Lt. 13' SFO	05/05/97	0.47	249	148	594	352	30	18	0.40	26.78	AEA, Type F
89-247	Rt. 26' SFO	05/07/97	0.52	249	148	594	352	30	18	0.40	26.78	AEA, Type F
89-248	Subdeck	04/06/98	---	265	157	602	357	0	0	0.44	27.07	AEA
89-248	Westbound Lane	04/24/98	0.02	249	148	594	352	30	18	0.40	26.78	AEA, Type F
89-248	Eastbound Lane	05/01/98	0.03	249	148	594	352	30	18	0.40	26.78	AEA, Type F

Table A.3: (continued)

Bridge Number	Portion Placed	Date of Placement	Crack Density (m/m ²)	Water Content		Cement Content		SF Content		W/CM Ratio	Volume of W+C+SF (%)	Types of Admixtures
				(lb/yd ³)	(kg/m ³)	(lb/yd ³)	(kg/m ³)	(lb/yd ³)	(kg/m ³)			
Conventional Overlay Bridges												
46-289	Subdeck	08/06/92	---	265	157	602	357	0	0	0.44	27.07	AEA
46-289	Subdeck	08/18/92	---	265	157	602	357	0	0	0.44	27.07	AEA
46-289	Inside 24'	09/02/92	0.66	238	141	625	371	0	0	0.38	25.90	AEA
46-289	Outside 20'	09/11/92	0.64	238	141	625	371	0	0	0.38	25.90	AEA
46-290	Subdeck	08/04/92	---	265	157	602	357	0	0	0.44	27.07	AEA
46-290	Subdeck	08/11/92	---	265	157	602	357	0	0	0.44	27.07	AEA
46-290	Inside 24'	09/08/92	0.66	238	141	625	371	0	0	0.38	25.90	AEA
46-290	Outside 10'	09/15/92	0.53	238	141	625	371	0	0	0.38	25.90	AEA
46-299	Subdeck	06/30/94	---	265	157	602	357	0	0	0.44	27.07	AEA
46-299	Rt. of CL 22'	07/28/94	0.69	225	133	625	371	0	0	0.36	25.13	AEA
46-299	Lt. of CL 18'	07/30/94	1.12	225	133	625	371	0	0	0.36	25.13	AEA
46-300	Subdeck	06/12/95	---	265	157	602	357	0	0	0.44	27.07	AEA
46-300	BDWS 18' Rt. of CL	08/10/95	0.98	225	133	625	371	0	0	0.36	25.13	AEA
46-300	BDWS 22' Lt. of CL	08/14/95	0.49	225	133	625	371	0	0	0.36	25.13	AEA
46-301	Subdeck	06/10/94	---	265	157	602	357	0	0	0.44	27.07	AEA
46-301	BDWS Rt. CL 24'	08/03/94	0.98	225	133	625	371	0	0	0.36	25.13	AEA

Table A.3: (continued)

Bridge Number	Portion Placed	Date of Placement	Crack Density (m/m ²)	Water Content		Cement Content		SF Content		W/CM Ratio	Volume of W+C+SF (%)	Types of Admixtures
				(lb/yd ³)	(kg/m ³)	(lb/yd ³)	(kg/m ³)	(lb/yd ³)	(kg/m ³)			
46-301	BDWS Lt. CL 24' to 38'	08/03/94	0.92	225	133	625	371	0	0	0.36	25.13	AEA
46-301	BDWS Rt. CL 24' to 38'	08/05/94	0.43	225	133	625	371	0	0	0.36	25.13	AEA
46-301	BDWS Lt. CL 24'	08/06/94	0.57	225	133	625	371	0	0	0.36	25.13	AEA
75-1	Subdeck	09/30/91	---	281	167	639	379	0	0	0.44	28.72	AEA, Type D
75-1	BDWS Lt of CL	10/17/91	0.35	250	148	625	371	0	0	0.40	26.62	AEA
75-1	BDWS Rt of CL	10/19/91	0.39	250	148	625	371	0	0	0.40	26.62	AEA
75-49	Subdeck	05/09/91	---	268	159	639	379	0	0	0.42	27.95	AEA
75-49	Subdeck	05/17/91	---	268	159	639	379	0	0	0.42	27.95	AEA
75-49	Eastbound	06/04/91	0.41	250	148	625	371	0	0	0.40	26.62	AEA
75-49	Westbound	06/07/91	0.49	250	148	625	371	0	0	0.40	26.62	AEA
81-49	Subdeck Rt. of CL	03/12/92	---	281	167	639	379	0	0	0.44	28.72	AEA
81-49	BDWS Rt. 22'	04/08/92	0.58	238	141	625	371	0	0	0.38	25.90	AEA
81-49	BDWS 12' Rt of CL	04/13/92	0.80	238	141	625	371	0	0	0.38	25.90	AEA
81-49	Subdeck Lt. of CL	10/07/92	---	281	167	639	379	0	0	0.44	28.72	AEA
81-49	BDWS Lt. 22'	10/21/92	0.71	238	141	625	371	0	0	0.38	25.90	AEA
81-49	BDWS 12' Lt. of CL	10/23/92	1.01	238	141	625	371	0	0	0.38	25.90	AEA
89-183	Subdeck	08/17/90	---	265	157	602	357	0	0	0.44	27.07	---
89-183	BDWS Rt. Side	09/21/90	0.44	225	133	625	371	0	0	0.36	25.13	---

Table A.3: (continued)

Bridge Number	Portion Placed	Date of Placement	Crack Density (m/m ²)	Water Content		Cement Content		SF Content		W/CM Ratio	Volume of W+C+SF (%)	Types of Admixtures
				(lb/yd ³)	(kg/m ³)	(lb/yd ³)	(kg/m ³)	(lb/yd ³)	(kg/m ³)			
89-183	BDWS Lt. Side	09/25/90	0.58	225	133	625	371	0	0	0.36	25.13	---
89-185	Subdeck	06/12/90	---	265	157	602	357	0	0	0.44	27.07	---
89-185	Outside	06/21/90	0.81	225	133	625	371	0	0	0.36	25.13	None
89-185	Inside	06/23/90	0.57	225	133	625	371	0	0	0.36	25.13	---
89-186	Subdeck	08/30/90	---	265	157	602	357	0	0	0.44	27.07	---
89-186	Inside	09/14/90	0.69	225	133	625	371	0	0	0.36	25.13	---
89-186	Outside	09/17/90	0.75	225	133	625	371	0	0	0.36	25.13	None
89-196	Subdeck	10/17/91	---	265	157	602	357	0	0	0.44	27.07	AEA
89-196	BDWS Rt. Side	05/01/92	0.66	225	133	625	371	0	0	0.36	25.13	AEA
89-196	BDWS Lt. Side	05/05/92	0.40	225	133	625	371	0	0	0.36	25.13	AEA
89-198	Subdeck	08/07/91	---	265	157	602	357	0	0	0.44	27.07	AEA
89-198	Left	08/24/91	0.36	225	133	625	371	0	0	0.36	25.13	None
89-198	Right	08/27/91	0.41	225	133	625	371	0	0	0.36	25.13	---
89-199	Subdeck	08/14/91	---	265	157	602	357	0	0	0.44	27.07	AEA
89-199	Left	08/26/91	0.75	225	133	625	371	0	0	0.36	25.13	None
89-199	Right	08/28/91	0.54	225	133	625	371	0	0	0.36	25.13	None
89-200	Subdeck	08/02/91	---	265	157	602	357	0	0	0.44	27.07	AEA
89-200	Right	08/17/91	0.67	225	133	625	371	0	0	0.36	25.13	None
89-200	Left	08/20/91	0.44	225	133	625	371	0	0	0.36	25.13	None
89-201	Subdeck	08/09/91	---	265	157	602	357	0	0	0.44	27.07	AEA
89-201	Right	08/19/91	0.66	225	133	625	371	0	0	0.36	25.13	None

Table A.3: (continued)

Bridge Number	Portion Placed	Date of Placement	Crack Density (m/m ²)	Water Content		Cement Content		SF Content		W/CM Ratio	Volume of W+C+SF (%)	Types of Admixtures
				(lb/yd ³)	(kg/m ³)	(lb/yd ³)	(kg/m ³)	(lb/yd ³)	(kg/m ³)			
89-201	Left	08/21/91	0.59	225	133	625	371	0	0	0.36	25.13	None

Monolithic Bridges

56-148	Deck	07/18/91	0.31	266	158	605	359	0	0	0.44	27.19	Retarder
70-107	Deck	10/25/91	0.42	266	158	605	359	0	0	0.44	27.19	None
89-204	Deck	10/03/91	0.84	276	164	658	390	0	0	0.42	28.78	None
89-208	Deck	06/15/95	0.03	265	157	602	357	0	0	0.44	27.07	AEA

Key

SFO = Silica fume overlay

BDWS = Bridge deck wearing surface, i.e. conventional overlay

CL = centerline

Rt. = Right

Lt. = Left

AEA = air entraining agent

WR = water reducer

Table A.4: Cement and Silica Fume Type Information for Bridge Deck Placements

Bridge Number	Date of Placement	Portion Placed	Cement Type	Cement Producer	Cement spg	SF Prod	Misc.
---------------	-------------------	----------------	-------------	-----------------	------------	---------	-------

Silica Fume Overlay Bridges

23-85	11/06/95	Subdeck	---	---	---	---	---
23-85	03/29/96	East 1/2 SFO	---	---	---	---	SP 90P-158-R3
23-85	04/03/96	West 1/2 SFO	---	---	---	---	SP 90P-158-R3
46-302	11/14/95	Subdeck	II	Lafarge, Fredonia, KS	3.20	---	---
46-302	04/09/96	Lt. 1/2 SFO	II	Lafarge, Sugar Creek	3.20	WR Grace Silica Fume	SF spg = 2.2
46-302	04/11/96	Rt. 1/2 SFO	II	Lafarge, Sugar Creek	3.20	WR Grace Silica Fume	SF spg = 2.2
46-309	09/26/95	Subdeck	II	Lafarge, Fredonia, KS	3.20	---	---
46-309	10/20/95	Rt. 1/2 SFO	II	Lafarge, Sugar Creek	3.20	WR Grace Silica Fume	SF spg = 2.2

Table A.4: (continued)

Bridge Number	Date of Placement	Portion Placed	Cement Type	Cement Producer	Cement spg	SF Prod	Misc.
46-309	10/24/95	Lt. 1/2 SFO	II	Lafarge, Sugar Creek	3.20	WR Grace Silica Fume	SF spg = 2.2
46-317	04/11/96	Subdeck Sec. 2	II	Lafarge, Fredonia, KS	---	---	---
46-317	04/26/96	Subdeck Sec. 1	II	Lafarge, Fredonia, KS	---	---	---
46-317	06/28/96	SFO 12'	II	Lafarge, Fredonia, KS	---	Master Builders SF	---
46-317	07/01/96	SFO 16'	II	Lafarge, Fredonia, KS	---	Master Builders SF	---
81-50	08/31/95	Subdeck Rt. 36+38 to Ab. #2	I/II	Monarch Cement, Humboldt KS	3.15	---	---
81-50	09/13/95	Subdeck Rt. 34+69 to 36+38	I/II	Monarch Cement, Humboldt KS	3.15	---	---
81-50	09/26/95	Subdeck Rt. 30+06 to 34+69	I/II	Monarch Cement, Humboldt KS	3.15	---	---
81-50	10/02/95	Subdeck Rt. Ab. #1 to 30+06	I/II	Monarch Cement, Humboldt KS	3.15	---	---
81-50	10/06/95	Subdeck Lt. 36+38 to Ab. #2	I/II	Monarch Cement, Humboldt KS	3.15	---	---

Table A.4: (continued)

Bridge Number	Date of Placement	Portion Placed	Cement Type	Cement Producer	Cement spg	SF Prod	Misc.
81-50	10/11/95	Subdeck Lt. 34+69 to 36+38	I/II	Monarch Cement, Humboldt KS	3.15	---	---
81-50	10/18/95	Subdeck Lt. 30+06 to 34+69	I/II	Monarch Cement, Humboldt KS	3.15	---	---
81-50	10/21/95	Sudeck Lt. Ab. #1 to 30+06	I/II	Monarch Cement, Humboldt KS	3.15	---	---
81-50	11/15/95	SFO Rt. Unit #1	I/II	Lone Star, Pryor, OK	3.15	WR Grace Silica Fume	---
81-50	11/18/95	SFO Lt. Unit #1	I/II	Lone Star, Pryor, OK	3.15	WR Grace Silica Fume	---
81-50	11/21/95	SFO Rt. Unit #2	I/II	Lone Star, Pryor, OK	3.15	WR Grace Silica Fume	---
81-50	11/30/95	SFO Lt. Unit #2	I/II	Lone Star, Pryor, OK	3.15	WR Grace Silica Fume	---
87-453	05/22/97	Subdeck	I/II	Ash Grove, Chanute	3.17	---	---
87-453	06/30/97	North 22'	I/II	Ash Grove, Chanute	3.17	WR Grace- Force 10000D	---
87-453	07/03/97	South 18'	I/II	Ash Grove, Chanute	3.17	WR Grace- Force 10000D	---

Table A.4: (continued)

Bridge Number	Date of Placement	Portion Placed	Cement Type	Cement Producer	Cement spg	SF Prod	Misc.
87-454	08/01/96	Subdeck	I/II	Ash Grove, Chanute	3.17	---	---
87-454	09/10/96	Left of CL	I/II	Ash Grove, Chanute	3.17	WR Grace- Force 10000D	---
87-454	10/16/96	Right of CL	I/II	Ash Grove, Chanute	3.17	WR Grace- Force 10000D	---
89-184	09/13/90	Subdeck	---	---	---	---	---
89-184	09/26/90	Inside	---	---	---	---	---
89-184	09/28/90	Outside	---	---	---	---	---
89-187	05/31/90	Subdeck	---	---	---	---	---
89-187	06/26/90	Inside	---	---	---	---	---
89-187	06/28/90	Outside	---	---	---	---	---
89-206	07/19/95	Subdeck	I/II	Lone Star, Pryor, OK	3.15	---	---

Table A.4: (continued)

Bridge Number	Date of Placement	Portion Placed	Cement Type	Cement Producer	Cement spg	SF Prod	Misc.
89-206	10/04/95	Right	I/II	Lone Star, Pryor, OK	3.15	WR Grace-Force 10000D	SP 90P-158-R3
89-206	10/10/95	Left	I/II	Lone Star, Pryor, OK	3.15	WR Grace-Force 10000D	SP 90P-158-R3
89-207	08/29/95	Subdeck	I/II	Lone Star, Pryor, OK	3.15	---	---
89-207	10/24/95	Left	I/II	Lone Star, Pryor, OK	3.15	WR Grace-Force 10000D	SP 90P-158-R3
89-207	04/19/96	Right	I/II	Lone Star, Pryor, OK	3.15	WR Grace-Force 10000D	SP 90P-158-R3
89-210	09/15/95	Subdeck	I/II	Lone Star, Pryor, OK	3.15	---	---
89-210	10/12/95	Right	I/II	Lone Star, Pryor, OK	3.15	WR Grace-Force 10000D	SP 90P-158-R3
89-210	10/18/95	Left	I/II	Lone Star, Pryor, OK	3.15	WR Grace-Force 10000D	SP 90P-158-R3
89-234	05/16/96	Subdeck	IP	Ash Grove, Chanute	3.00	---	---
89-234	06/20/96	SFO South 20'	I/II	Monarch Cement, Humboldt KS	3.15	WR Grace-Force 10000D	SP 90P-158-R4

Table A.4: (continued)

Bridge Number	Date of Placement	Portion Placed	Cement Type	Cement Producer	Cement spg	SF Prod	Misc.
89-234	06/25/96	SFO North 18'	I/II	Monarch Cement, Humboldt KS	3.15	WR Grace- Force 10000D	SP 90P-158-R4
89-234	06/28/96	SFO Center 12'	I/II	Monarch Cement, Humboldt KS	3.15	WR Grace- Force 10000D	SP 90P-158-R4
89-235	03/21/97	Subdeck	I/II	Ash Grove, Chanute	3.15	---	---
89-235	04/29/97	SFO Left 20'	I/II	Monarch Cement, Humboldt KS	3.15	WR Grace- Force 10000D	SP 90P-158-R4
89-235	05/01/97	SFO Right 18'	I/II	Monarch Cement, Humboldt KS	3.15	WR Grace- Force 10000D	SP 90P-158-R4
89-235	05/06/97	SFO Center 12'	I/II	Monarch Cement, Humboldt KS	3.15	WR Grace- Force 10000D	SP 90P-158-R4
89-240	07/02/97	Subdeck	I/II	Monarch Cement, Humboldt KS	3.15	---	---
89-240	08/05/97	Rt. 22' SFO	I/II	Monarch Cement, Humboldt KS	3.15	WR Grace- Force 10000D	SP 90P-158-R4
89-240	08/07/97	Lt. 22' SFO	I/II	Monarch Cement, Humboldt KS	3.15	WR Grace- Force 10000D	SP 90P-158-R4
89-244	08/21/97	Subdeck	I/II	Monarch Cement, Humboldt KS	3.15	None	---

Table A.4: (continued)

Bridge Number	Date of Placement	Portion Placed	Cement Type	Cement Producer	Cement spg	SF Prod	Misc.
89-244	10/17/97	SFO Rt.	I/II	Monarch Cement, Humboldt KS	3.15	WR Grace- Force 10000D	SP 90P-158-R4
89-244	10/21/97	SFO Lt.	I/II	Monarch Cement, Humboldt KS	3.15	WR Grace- Force 10000D	SP 90P-158-R4
89-245	09/26/97	Subdeck Unit #1	I/II	Monarch Cement, Humboldt KS	3.15	---	---
89-245	10/02/97	Subdeck Unit #2	I/II	Monarch Cement, Humboldt KS	3.15	---	---
89-245	10/20/97	Lt. 1/2 Unit 2 SFO	I/II	Monarch Cement, Humboldt KS	3.15	WR Grace- Force 10000D	SP 90P-158-R4
89-245	10/22/97	Lt. 1/2 Unit 1 SFO	I/II	Monarch Cement, Humboldt KS	3.15	WR Grace- Force 10000D	SP 90P-158-R4
89-245	10/23/97	Rt. 1/2 Unit 2 SFO	I/II	Monarch Cement, Humboldt KS	3.15	WR Grace- Force 10000D	SP 90P-158-R4
89-245	10/24/97	Rt. 1/2 Unit 1 SFO	I/II	Monarch Cement, Humboldt KS	3.15	WR Grace- Force 10000D	SP 90P-158-R4
89-246	08/27/97	Subdeck	I/II	Monarch Cement, Humboldt KS	3.15	---	---
89-246	09/08/97	East 1/2 SFO	I/II	Monarch Cement, Humboldt KS	3.15	WR Grace- Force 10000D	SP 90P-158-R4

Table A.4: (continued)

Bridge Number	Date of Placement	Portion Placed	Cement Type	Cement Producer	Cement spg	SF Prod	Misc.
89-246	09/10/97	West 1/2 SFO	I/II	Monarch Cement, Humboldt KS	3.15	WR Grace- Force 10000D	SP 90P-158-R4
89-247	04/24/97	Subdeck	I/II	Monarch Cement, Humboldt KS	3.15	---	---
89-247	05/05/97	Lt. 13' SFO	I/II	Monarch Cement, Humboldt KS	3.15	WR Grace- Force 10000D	SP 90P-158-R4
89-247	05/07/97	Rt. 26' SFO	I/II	Monarch Cement, Humboldt KS	3.15	WR Grace- Force 10000D	SP 90P-158-R4
89-248	04/06/98	Subdeck	I/II	Monarch Cement, Humboldt KS	3.15	---	---
89-248	04/24/98	Westbound Lane	I/II	Monarch Cement, Humboldt KS	3.15	WR Grace- Force 10000D	SP 90P-158-R4
89-248	05/01/98	Eastbound Lane	I/II	Monarch Cement, Humboldt KS	3.15	WR Grace- Force 10000D	SP 90P-158-R4

259

Conventional Overlay Bridges

46-289	08/06/92	Subdeck	---	---	---	---	---
--------	----------	---------	-----	-----	-----	-----	-----

Table A.4: (continued)

Bridge Number	Date of Placement	Portion Placed	Cement Type	Cement Producer	Cement spg	SF Prod	Misc.
46-289	08/18/92	Subdeck	---	---	---	---	---
46-289	09/02/92	Inside 24'	II	Lafarge	3.20	---	SP 90P-95-R1
46-289	09/11/92	Outside 20'	II	Lafarge	3.20	---	SP 90P-95-R1
46-290	08/04/92	Subdeck	---	---	---	---	---
46-290	08/11/92	Subdeck	---	---	---	---	---
46-290	09/08/92	Inside 24'	II	Lafarge	3.20	---	SP 90P-95-R1
46-290	09/15/92	Outside 10'	II	Lafarge	3.20	---	SP 90P-95-R1
46-299	06/30/94	Subdeck	---	---	---	---	---
46-299	07/28/94	Rt. Of CL 22'	II	Lafarge, Sugar Creek	3.20	---	---
46-299	07/30/94	Lt. Of CL 18'	II	Lafarge, Sugar Creek	3.20	---	---

Table A.4: (continued)

Bridge Number	Date of Placement	Portion Placed	Cement Type	Cement Producer	Cement spg	SF Prod	Misc.
46-300	06/12/95	Subdeck	---	---	---	---	---
46-300	08/10/95	BDWS 18' Rt. of CL	II	Lafarge, Sugar Creek	3.20	---	---
46-300	08/14/95	BDWS 22' Lt. of CL	II	Lafarge, Sugar Creek	3.20	---	---
46-301	06/10/94	Subdeck	---	---	---	---	---
46-301	08/03/94	BDWS Rt. CL 24'	II	Lafarge, Sugar Creek	3.20	---	---
46-301	08/03/94	BDWS Lt. CL 24' to 38'	II	Lafarge, Sugar Creek	3.20	---	---
46-301	08/05/94	BDWS Rt. CL 24' to 38'	II	Lafarge, Sugar Creek	3.20	---	---
46-301	08/06/94	BDWS Lt. CL 24'	II	Lafarge, Sugar Creek	3.20	---	---
75-1	09/30/91	Subdeck	I/II	Monarch Cement, Humboldt KS	---	---	---
75-1	10/17/91	BDWS Lt. of CL	I/II	Heartland, Indepence, KS	---	---	---

Table A.4: (continued)

Bridge Number	Date of Placement	Portion Placed	Cement Type	Cement Producer	Cement spg	SF Prod	Misc.
75-1	10/19/91	BDWS Rt. of CL	I/II	Heartland, Independence, KS	---	---	---
75-49	05/09/91	Subdeck	I/II	Monarch Cement, Humboldt KS	---	---	---
75-49	05/17/91	Subdeck	I/II	Monarch Cement, Humboldt KS	---	---	---
75-49	06/04/91	Eastbound	I/II	Heartland, Independence, KS	---	---	---
75-49	06/07/91	Westbound	I/II	Heartland, Independence, KS	---	---	---
81-49	03/12/92	Subdeck Rt. of CL	I/II	Lone Star, Pryor, OK	---	---	---
81-49	04/08/92	BDWS Rt. 22'	I/II	Monarch Cement, Humboldt KS	---	---	---
81-49	04/13/92	BDWS 12' Rt of CL	I/II	Monarch Cement, Humboldt KS	---	---	---
81-49	10/07/92	Subdeck Lt. of CL	I/II	Lone Star, Pryor, OK	---	---	---
81-49	10/21/92	BDWS Lt. 22'	I/II	Monarch Cement, Humboldt KS	---	---	---

Table A.4: (continued)

Bridge Number	Date of Placement	Portion Placed	Cement Type	Cement Producer	Cement spg	SF Prod	Misc.
81-49	10/23/92	BDWS 12' Lt. of CL	I/II	Monarch Cement, Humboldt KS	---	---	---
89-183	08/17/90	Subdeck	---	---	---	---	---
89-183	09/21/90	BDWS Rt. Side	---	---	---	---	---
89-183	09/25/90	BDWS Lt. Side	---	---	---	---	---
89-185	06/12/90	Subdeck	---	---	---	---	---
89-185	06/21/90	Outside	---	---	---	---	---
89-185	06/23/90	Inside	---	---	---	---	---
89-186	08/30/90	Subdeck	---	---	---	---	---
89-186	09/14/90	Inside	---	---	---	---	---
89-186	09/17/90	Outside	---	---	---	---	---

Table A.4: (continued)

Bridge Number	Date of Placement	Portion Placed	Cement Type	Cement Producer	Cement spg	SF Prod	Misc.
89-196	10/17/91	Subdeck	---	---	---	---	---
89-196	05/01/92	BDWS Rt. Side	---	---	---	---	SP 90P-95
89-196	05/05/92	BDWS Lt. Side	---	---	---	---	SP 90P-95
89-198	08/07/91	Subdeck	II	Lafarge, Fredonia, KS	---	---	---
89-198	08/24/91	Left	II	Monarch Cement, Humboldt KS	---	---	---
89-198	08/27/91	Right	II	Monarch Cement, Humboldt KS	---	---	---
89-199	08/14/91	Subdeck	II	Lafarge, Fredonia, KS	---	---	---
89-199	08/26/91	Left	II	Monarch Cement, Humboldt KS	---	---	---
89-199	08/28/91	Right	II	Monarch Cement, Humboldt KS	---	---	---
89-200	08/02/91	Subdeck	II	Lafarge, Fredonia, KS	---	---	---

Table A.4: (continued)

Bridge Number	Date of Placement	Portion Placed	Cement Type	Cement Producer	Cement spg	SF Prod	Misc.
89-200	08/17/91	Right	II	Monarch Cement, Humboldt KS	---	---	---
89-200	08/20/91	Left	II	Monarch Cement, Humboldt KS	---	---	---
89-201	08/09/91	Subdeck	II	Lafarge, Fredonia, KS	---	---	---
89-201	08/19/91	Right	II	Monarch Cement, Humboldt KS	---	---	---
89-201	08/21/91	Left	II	Monarch Cement, Humboldt KS	---	---	---
Monolithic Bridges							
56-148	07/18/91	Deck	---	---	---	---	---
70-107	10/25/91	Deck	---	---	---	---	---
89-204	10/03/91	Deck	---	---	---	---	---

Table A.4: (continued)

Bridge Number	Date of Placement	Portion Placed	Cement Type	Cement Producer	Cement spg	SF Prod	Misc.
89-208	06/15/95	Deck	I/II	Lone Star, Pryor, OK	3.15	---	---

Key

SFO = Silica fume overlay

BDWS = Bridge deck wearing surface, i.e. conventional overlay

CL = centerline

Rt. = Right

Lt. = Left

Table A.5: Aggregate Information for Bridge Deck Placements

Bridge Number	Date of Placement	CA (lb/yd ³)	CA Name	CA Prod. Name	CA spg	FA (lb/yd ³)	FA Name	FA Prod. Name	FA spg
Silica Fume Overlay Bridges									
23-85	11/06/95	---	---	---	---	---	---	---	---
23-85	03/29/96	---	---	---	---	---	---	---	---
23-85	04/03/96	---	---	---	---	---	---	---	---
46-302	11/14/95	1484	Crushed Limestone	Inland Quarry Bingham	2.64	1484	Natural Sand	Holliday Sand, MO	2.61
46-302	04/09/96	1470	Chat	Sand/Gravel Bingham Sand/	2.57	1470	Natural Sand	Holliday Sand, MO	2.61
46-302	04/11/96	1470	Chat	Gravel, OK	2.57	1470	Natural Sand	Holliday Sand, MO	2.61
46-309	09/26/95	1484	Crushed Limestone	Inland Quarry Bingham Sand/	2.64	1484	Natural Sand	Holliday Sand, MO	2.61
46-309	10/20/95	1470	Chat	Gravel, OK	2.57	1470	Natural Sand	Holliday Sand, MO	2.61

Table A.5:(continued)

Bridge Number	Date of Placement	CA (lb/yd ³)	CA Name	CA Prod. Name	CA spg	FA (lb/yd ³)	FA Name	FA Prod. Name	FA spg
46-309	10/24/95	1470	Chat	Bingham Sand/ Gravel, OK	2.57	1470	Natural Sand	Holliday Sand, MO	2.61
46-317	04/11/96	---	---	Inland Quarry	2.63	---	---	Holliday Sand, MO	2.61
46-317	04/26/96	---	---	Inland Quarry	2.63	---	---	Holliday Sand, MO	2.61
46-317	06/28/96	1489	Chat	Bingham Sand/ Gravel, OK	2.58	1489	Natural Sand	Holliday Sand, MO	2.61
46-317	07/01/96	1489	Chat	Bingham Sand/ Gravel, OK	2.58	1489	Natural Sand	Holliday Sand, MO	2.61
81-50	08/31/95	0	---	---	---	2794	Total	Blue River Sand	2.61
81-50	09/13/95	0	---	---	---	2794	Total	Blue River Sand	2.61
81-50	09/26/95	0	---	---	---	2830	Total	Blue River Sand	2.61
81-50	10/02/95	0	---	---	---	2830	Total	Blue River Sand	2.61
81-50	10/06/95	0	---	---	---	2830	Total	Blue River Sand	2.61

Table A.5:(continued)

Bridge Number	Date of Placement	CA (lb/yd ³)	CA Name	CA Prod. Name	CA spg	FA (lb/yd ³)	FA Name	FA Prod. Name	FA spg
81-50	10/11/95	0	---	---	---	2830	Total	Blue River Sand	2.61
81-50	10/18/95	0	---	---	---	2830	Total	Blue River Sand	2.61
81-50	10/21/95	0	---	---	---	2830	Total	Blue River Sand	2.61
81-50	11/15/95	1484	Sandstone	Couch Materials	2.63	1484	Natural Sand	Concrete Co. Midwest	2.60
81-50	11/18/95	1484	Sandstone	Couch Materials	2.63	1484	Natural Sand	Concrete Co. Midwest	2.60
81-50	11/21/95	1484	Sandstone	Couch Materials	2.63	1484	Natural Sand	Concrete Co. Midwest	2.60
81-50	11/30/95	1484	Sandstone	Couch Materials	2.63	1484	Natural Sand	Concrete Co. Midwest	2.60
87-453	05/22/97	867	Crushed Limestone	Dolese Stone Co., OK	2.68	2022	Basic SSG for MA-1	Ritchie Sand	2.60
87-453	06/30/97	1494	Chat	Bingham Sand/Gravel, OK	2.60	1494	Natural Sand	Ritchie Sand	2.60
87-453	07/03/97	1494	Chat	Bingham Sand/Gravel, OK	2.60	1494	Natural Sand	Ritchie Sand	2.60

Table A.5:(continued)

Bridge Number	Date of Placement	CA (lb/yd ³)	CA Name	CA Prod. Name	CA spg	FA (lb/yd ³)	FA Name	FA Prod. Name	FA spg
87-454	08/01/96	867	Crushed Limestone	Dolese Stone Co., OK	2.68	2022	Basic SSG for MA-1	Ritchie Sand	2.60
87-454	09/10/96	1494	Chat	Bingham Sand/Gravel, OK	2.60	1494	Natural Sand	Ritchie Sand	2.60
87-454	10/16/96	1494	Chat	Bingham Sand/Gravel, OK	2.60	1494	Natural Sand	Ritchie Sand	2.60
89-184	09/13/90	---	---	---	---	---	---	---	---
89-184	09/26/90	---	---	---	---	---	---	---	---
89-184	09/28/90	---	---	---	---	---	---	---	---
89-187	05/31/90	---	---	---	---	---	---	---	---
89-187	06/26/90	---	---	---	---	---	---	---	---
89-187	06/28/90	---	---	---	---	---	---	---	---
89-206	07/19/95	1458	Durable Clay	Fogle Quarry	2.60	1458	Natural Sand	Meier's Sand Co.	2.60

Table A.5:(continued)

Bridge Number	Date of Placement	CA (lb/yd ³)	CA Name	CA Prod. Name	CA spg	FA (lb/yd ³)	FA Name	FA Prod. Name	FA spg
89-206	10/04/95	1447	Chat	Bingham Sand/ Gravel, OK	2.49	1447	Natural Sand	Meier's Sand Co.	2.61
89-206	10/10/95	1447	Chat	Bingham Sand/ Gravel, OK	2.49	1447	Natural Sand	Meier's Sand Co.	2.61
89-207	08/29/95	1458	Durable Clay	Fogle Quarry	2.60	1458	Natural Sand	Meier's Sand Co.	2.60
89-207	10/24/95	1447	Chat	Bingham Sand/ Gravel, OK	2.49	1447	Natural Sand	Meier's Sand Co.	2.61
89-207	04/19/96	1447	Chat	Bingham Sand/ Gravel, OK	2.49	1447	Natural Sand	Meier's Sand Co.	2.61
89-210	09/15/95	1458	Durable Clay	Fogle Quarry	2.60	1458	Natural Sand	Meier's Sand Co.	2.60
89-210	10/12/95	1447	Chat	Bingham Sand/ Gravel, OK	2.49	1447	Natural Sand	Meier's Sand Co.	2.61
89-210	10/18/95	1447	Chat	Bingham Sand/ Gravel, OK	2.49	1447	Natural Sand	Meier's Sand Co.	2.61
89-234	05/16/96	1485	Durable Clay	Fogle Quarry	2.60	1485	Natural Sand	Builders Sand Kansas Sand	2.60
89-234	06/20/96	1473	Chat	Bingham Sand/ Gravel, OK	2.58	1473	Natural Sand	(West Location)	2.61

Table A.5:(continued)

Bridge Number	Date of Placement	CA (lb/yd ³)	CA Name	CA Prod. Name	CA spg	FA (lb/yd ³)	FA Name	FA Prod. Name	FA spg
89-234	06/25/96	1473	Chat	Bingham Sand/ Gravel, OK	2.58	1473	Natural Sand	Kansas Sand (West Location)	2.61
89-234	06/28/96	1473	Chat	Bingham Sand/ Gravel, OK	2.58	1473	Natural Sand	Kansas Sand (West Location)	2.61
89-235	03/21/97	1499	Durable Clay	Fogle Quarry	2.66	1499	Natural Sand	Builders Sand	2.60
89-235	04/29/97	1473	Chat	Bingham Sand/ Gravel, OK	2.58	1473	Natural Sand	Kansas Sand (West Location)	2.61
89-235	05/01/97	1473	Chat	Bingham Sand/ Gravel, OK	2.58	1473	Natural Sand	Kansas Sand (West Location)	2.61
89-235	05/06/97	1473	Chat	Bingham Sand/ Gravel, OK	2.58	1473	Natural Sand	Kansas Sand (West Location)	2.61
89-240	07/02/97	1483	Durable Clay	Fogle Quarry	2.66	1483	Natural Sand	Kansas Sand (West Location)	2.60
89-240	08/05/97	1473	Chat	Bingham Sand/ Gravel, OK	2.58	1473	Natural Sand	Kansas Sand (West Location)	2.61
89-240	08/07/97	1473	Chat	Bingham Sand/ Gravel, OK	2.58	1473	Natural Sand	Kansas Sand (West Location)	2.61
89-244	08/21/97	1474	Crushed Limestone	Inland Quarry	2.63	1474	Natural Sand	Kansas Sand (West Location)	2.60

Table A.5:(continued)

Bridge Number	Date of Placement	CA (lb/yd ³)	CA Name	CA Prod. Name	CA spg	FA (lb/yd ³)	FA Name	FA Prod. Name	FA spg
89-244	10/17/97	1473	Chat	Bingham Sand/ Gravel, OK	2.58	1473	Natural Sand	Kansas Sand (West Location)	2.61
89-244	10/21/97	1473	Chat	Bingham Sand/ Gravel, OK	2.58	1473	Natural Sand	Kansas Sand (West Location)	2.61
89-245	09/26/97	1474	Crushed Limestone	Inland Quarry	2.63	1474	Natural Sand	Kansas Sand (West Location)	2.60
89-245	10/02/97	1474	Crushed Limestone	Inland Quarry	2.63	1474	Natural Sand	Kansas Sand (West Location)	2.60
89-245	10/20/97	1473	Chat	Bingham Sand/ Gravel, OK	2.58	1473	Natural Sand	Kansas Sand (West Location)	2.61
89-245	10/22/97	1473	Chat	Bingham Sand/ Gravel, OK	2.58	1473	Natural Sand	Kansas Sand (West Location)	2.61
89-245	10/23/97	1473	Chat	Bingham Sand/ Gravel, OK	2.58	1473	Natural Sand	Kansas Sand (West Location)	2.61
89-245	10/24/97	1473	Chat	Bingham Sand/ Gravel, OK	2.58	1473	Natural Sand	Kansas Sand (West Location)	2.61
89-246	08/27/97	1474	Crushed Limestone	Inland Quarry	2.63	1474	Natural Sand	Kansas Sand (West Location)	2.60
89-246	09/08/97	1473	Chat	Bingham Sand/ Gravel, OK	2.58	1473	Natural Sand	Kansas Sand (West Location)	2.61

Table A.5:(continued)

Bridge Number	Date of Placement	CA (lb/yd ³)	CA Name	CA Prod. Name	CA spg	FA (lb/yd ³)	FA Name	FA Prod. Name	FA spg
89-246	09/10/97	1473	Chat	Bingham Sand/ Gravel, OK	2.58	1473	Natural Sand	Kansas Sand (West Location)	2.61
89-247	04/24/97	1483	Durable Clay	Fogle Quarry	2.66	1483	Natural Sand	Kansas Sand (West Location)	2.60
89-247	05/05/97	1473	Chat	Bingham Sand/ Gravel, OK	2.58	1473	Natural Sand	Kansas Sand (West Location)	2.61
89-247	05/07/97	1473	Chat	Bingham Sand/ Gravel, OK	2.58	1473	Natural Sand	Kansas Sand (West Location)	2.61
89-248	04/06/98	1474	Crushed Limestone	Inland Quarry	2.63	1474	Natural Sand	Kansas Sand (West Location)	2.60
89-248	04/24/98	1473	Chat	Bingham Sand/ Gravel, OK	2.58	1473	Natural Sand	Kansas Sand (West Location)	2.61
89-248	05/01/98	1473	Chat	Bingham Sand/ Gravel, OK	2.58	1473	Natural Sand	Kansas Sand (West Location)	2.61

Conventional Overlay Bridges

46-289	08/06/92	---	---	---	---	---	---	---	---
--------	----------	-----	-----	-----	-----	-----	-----	-----	-----

Table A.5:(continued)

Bridge Number	Date of Placement	CA (lb/yd ³)	CA Name	CA Prod. Name	CA spg	FA (lb/yd ³)	FA Name	FA Prod. Name	FA spg
46-289	08/18/92	---	---	---	---	---	---	---	---
46-289	09/02/92	1492	---	---	2.58	1492	---	---	2.61
46-289	09/11/92	1492	---	---	2.58	1492	---	---	2.61
46-290	08/04/92	---	---	---	---	---	---	---	---
46-290	08/11/92	---	---	---	---	---	---	---	---
46-290	09/08/92	1492	---	---	2.58	1492	---	---	2.61
46-290	09/15/92	1492	---	---	2.58	1492	---	---	2.61
46-299	06/30/94	---	---	---	---	---	---	---	---
46-299	07/28/94	1509	Chat	Bingham Sand/ Gravel, OK	2.58	1509	Natural Sand	Holliday Sand, MO	2.61
46-299	07/30/94	1509	Chat	Bingham Sand/ Gravel, OK	2.58	1509	Natural Sand	Holliday Sand, MO	2.61

Table A.5:(continued)

Bridge Number	Date of Placement	CA (lb/yd ³)	CA Name	CA Prod. Name	CA spg	FA (lb/yd ³)	FA Name	FA Prod. Name	FA spg
46-300	06/12/95	---	---	---	---	---	---	---	---
46-300	08/10/95	1509	Chat	Bingham Sand/ Gravel, OK	2.58	1509	Natural Sand	Holliday Sand, MO	2.61
46-300	08/14/95	1509	Chat	Bingham Sand/ Gravel, OK	2.58	1509	Natural Sand	Holliday Sand, MO	2.61
46-301	06/10/94	---	---	---	---	---	---	---	---
46-301	08/03/94	1509	Chat	Bingham Sand/ Gravel, OK	2.58	1509	Natural Sand	Holliday Sand, MO	2.61
46-301	08/03/94	1509	Chat	Bingham Sand/ Gravel, OK	2.58	1509	Natural Sand	Holliday Sand, MO	2.61
46-301	08/05/94	1509	Chat	Bingham Sand/ Gravel, OK	2.58	1509	Natural Sand	Holliday Sand, MO	2.61
46-301	08/06/94	1509	Chat	Bingham Sand/ Gravel, OK	2.58	1509	Natural Sand	Holliday Sand, MO	2.61
75-1	09/30/91	941	---	---	---	1912	---	---	---
75-1	10/17/91	1491	---	---	---	1491	---	---	---

Table A.5:(continued)

Bridge Number	Date of Placement	CA (lb/yd ³)	CA Name	CA Prod. Name	CA spg	FA (lb/yd ³)	FA Name	FA Prod. Name	FA spg
75-1	10/19/91	1491	---	---	---	1491	---	---	---
75-49	05/09/91	952	---	---	---	1934	---	---	---
75-49	05/17/91	952	---	---	---	1934	---	---	---
75-49	06/04/91	1491	---	---	---	1491	---	---	---
75-49	06/07/91	1491	---	---	---	1491	---	---	---
81-49	03/12/92	952	---	---	---	1934	---	---	---
81-49	04/08/92	1491	---	---	---	1491	---	---	---
81-49	04/13/92	1491	---	---	---	1491	---	---	---
81-49	10/07/92	952	---	---	---	1934	---	---	---
81-49	10/21/92	1491	---	---	---	1491	---	---	---

Table A.5:(continued)

Bridge Number	Date of Placement	CA (lb/yd ³)	CA Name	CA Prod. Name	CA spg	FA (lb/yd ³)	FA Name	FA Prod. Name	FA spg
81-49	10/23/92	1491	---	---	---	1491	---	---	---
89-183	08/17/90	---	---	---	---	---	---	---	---
89-183	09/21/90	---	---	---	---	---	---	---	---
89-183	09/25/90	---	---	---	---	---	---	---	---
89-185	06/12/90	---	---	---	---	---	---	---	---
89-185	06/21/90	---	---	---	---	---	---	---	---
89-185	06/23/90	---	---	---	---	---	---	---	---
89-186	08/30/90	---	---	---	---	---	---	---	---
89-186	09/14/90	---	---	---	---	---	---	---	---
89-186	09/17/90	---	---	---	---	---	---	---	---

Table A.5:(continued)

Bridge Number	Date of Placement	CA (lb/yd ³)	CA Name	CA Prod. Name	CA spg	FA (lb/yd ³)	FA Name	FA Prod. Name	FA spg
89-196	10/17/91	---	---	---	---	---	---	---	---
89-196	05/01/92	1509	---	---	---	1509	---	---	---
89-196	05/05/92	1509	---	---	---	1509	---	---	---
89-198	08/07/91	1484	---	---	---	1484	---	---	---
89-198	08/24/91	1496	---	---	---	1496	---	---	---
89-198	08/27/91	1496	---	---	---	1496	---	---	---
89-199	08/14/91	1484	---	---	---	1484	---	---	---
89-199	08/26/91	1496	---	---	---	1496	---	---	---
89-199	08/28/91	1496	---	---	---	1496	---	---	---
89-200	08/02/91	1484	---	---	---	1484	---	---	---

Table A.5:(continued)

Bridge Number	Date of Placement	CA (lb/yd ³)	CA Name	CA Prod. Name	CA spg	FA (lb/yd ³)	FA Name	FA Prod. Name	FA spg
89-200	08/17/91	1496	---	---	---	1496	---	---	---
89-200	08/20/91	1496	---	---	---	1496	---	---	---
89-201	08/09/91	1484	---	---	---	1484	---	---	---
89-201	08/19/91	1496	---	---	---	1496	---	---	---
89-201	08/21/91	1496	---	---	---	1496	---	---	---
Monolithic Bridges									
56-148	07/18/91	---	---	---	---	---	---	---	---
70-107	10/25/91	---	---	---	---	---	---	---	---
89-204	10/03/91	---	---	---	---	---	---	---	---

Table A.5:(continued)

Bridge Number	Date of Placement	CA (lb/yd ³)	CA Name	CA Prod. Name	CA spg	FA (lb/yd ³)	FA Name	FA Prod. Name	FA spg
89-208	06/15/95	1466	Durable Clay	Fogle Quarry	2.60	1466	Natural Sand	Meier's Sand Co.	2.60

Table A.6: Field Information for Bridge Deck Placements

Bridge Number	Portion Placed	Date of Placement	Survey Date	Average Slump		Compressive Strength		Air Content (%)	Curing Materials
				(in.)	(mm)	(psi)	(MPa)		
Silica Fume Overlay Bridges									
23-85	Subdeck	11/06/95	---	2.50	64	---	---	6.25	---
23-85	East 1/2 SFO	03/29/96	08/18/98	5.00	127	---	---	7.25	---
23-85	West 1/2 SFO	04/03/96	08/18/98	3.00	76	---	---	5.00	---
46-302	Subdeck	11/14/95	---	3.00	76	---	---	5.00	white cure, burlap, white poly
46-302	Lt. 1/2 SFO	04/09/96	08/11/98	4.00	102	7320	50	4.50	clear cure, burlap, white poly
46-302	Rt. 1/2 SFO	04/11/96	08/11/98	3.75	95	5660	39	4.50	clear cure, burlap, white poly
46-309	Subdeck	09/26/95	---	2.50	64	5940	41	5.80	white cure, burlap, white poly
46-309	Rt. 1/2 SFO	10/20/95	08/06/98	2.25	57	7480	52	6.30	clear cure, burlap, white poly
46-309	Lt. 1/2 SFO	10/24/95	08/06/98	2.50	64	7720	53	5.70	clear cure, burlap, white poly
46-317	Subdeck Sec. 2	04/11/96	---	0.25	6	6960	48	4.10	---
46-317	Subdeck Sec. 1	04/26/96	---	3.00	76	5330	37	5.00	---
46-317	Subdeck Pier 5 to Ab.	06/10/96	---	2.00	51	5240	36	6.00	---
46-317	SFO 12'	06/28/96	08/24/98	3.50	89	6270	43	4.00	---
46-317	SFO 16'	07/01/96	08/24/98	2.50	64	6720	46	5.00	---
81-50	Subdeck Rt.36+38 to Ab. #2	08/31/95	---	2.75	70	6170	43	6.50	---
81-50	Subdeck Rt. 34+69 to 36+38	09/13/95	---	2.00	51	6530	45	5.70	---

Table A.6: (continued)

Bridge Number	Portion Placed	Date of Placement	Survey Date	Average Slump		Compressive Strength		Air Content (%)	Curing Materials
				(in.)	(mm)	(psi)	(MPa)		
81-50	Subdeck Rt. 30+06 to 34+69	09/26/95	---	2.00	51	6920	48	6.50	---
81-50	Subdeck Rt. Ab. #1 to 30+06	10/02/95	---	2.00	51	7520	52	5.80	---
81-50	Subdeck Lt. 36+38 to Ab. #2	10/06/95	---	2.50	64	7100	49	6.50	---
81-50	Subdeck Lt. 34+69 to 36+38	10/11/95	---	1.50	38	6060	42	6.00	---
81-50	Subdeck Lt. 30+06 to 34+69	10/18/95	---	1.75	44	7520	52	5.20	---
81-50	Subdeck Lt. Ab. #1 to 30+06	10/21/95	---	2.00	51	7120	49	5.80	---
81-50	SFO Rt. Unit #1	11/15/95	---	1.25	32	8400	58	4.00	---
81-50	SFO Lt. Unit #1	11/18/95	---	1.75	44	---	---	5.70	---
81-50	SFO Rt. Unit #2	11/21/95	08/12/98	2.00	51	5840	40	5.20	---
81-50	SFO Lt. Unit #2	11/30/95	08/12/98	1.25	32	8660	60	4.30	---
87-453	Subdeck	05/22/97	---	2.50	64	5870	40	4.30	---
87-453	North 22'	06/30/97	10/14/98	2.00	51	5270	36	5.70	---
87-453	South 18'	07/03/97	10/14/98	2.00	51	6710	46	3.50	---
87-454	Subdeck	08/01/96	---	3.00	76	4840	33	5.00	---
87-454	Left of CL	09/10/96	10/13/98	5.00	127	5230	36	5.50	---
87-454	Right of CL	10/16/96	10/13/98	3.00	76	7510	52	4.50	---
89-184	Subdeck	09/13/90	---	2.00	51	---	---	6.30	---
89-184	Inside	09/26/90	07/27/98	1.50	38	7060	49	6.40	---

Table A.6: (continued)

Bridge Number	Portion Placed	Date of Placement	Survey Date	Average Slump		Compressive Strength		Air Content (%)	Curing Materials
				(in.)	(mm)	(psi)	(MPa)		
89-184	Outside	09/28/90	07/27/98	---	---	---	---	---	---
89-187	Subdeck	05/31/90	---	2.00	51	---	---	5.00	curing compound, poly
89-187	Inside	06/26/90	07/28/98	2.25	57	6240	43	6.00	---
89-187	Outside	06/28/90	07/28/98	---	---	---	---	---	---
89-206	Subdeck	07/19/95	---	2.25	57	6220	43	6.00	---
89-206	Right	10/04/95	07/14/98	2.00	51	6790	47	6.00	---
89-206	Left	10/10/95	07/14/98	2.00	51	---	---	5.70	---
89-207	Subdeck	08/29/95	---	1.75	44	4650	32	6.00	---
89-207	Left	10/24/95	07/13/98	2.50	64	6170	43	6.70	---
89-207	Right	04/19/96	07/13/98	0.75	19	---	---	5.30	---
89-210	Subdeck	09/15/95	---	2.00	51	5020	35	5.25	---
89-210	Right	10/12/95	06/24/98	1.75	44	6260	43	5.70	---
89-210	Left	10/18/95	06/24/98	---	---	---	---	---	---
89-234	Subdeck	05/16/96	---	3.00	76	5000	34	7.50	---
89-234	SFO South 20'	06/20/96	07/09/98	2.00	51	---	---	5.40	Fug. Dye, burlap, white poly
89-234	SFO North 18'	06/25/96	07/09/98	2.75	70	7210	50	5.00	Fug. Dye, burlap, white poly
89-234	SFO Center 12'	06/28/96	07/09/98	1.75	44	---	---	4.60	Fug. Dye, burlap, white poly
89-235	Subdeck	03/21/97	---	2.00	51	6450	44	4.00	---

Table A.6: (continued)

Bridge Number	Portion Placed	Date of Placement	Survey Date	Average Slump		Compressive Strength		Air Content (%)	Curing Materials
				(in.)	(mm)	(psi)	(MPa)		
89-235	SFO Left 20'	04/29/97	---	1.50	38	---	---	6.30	---
89-235	SFO Right 18'	05/01/97	07/01/98	1.75	44	---	---	5.50	---
89-235	SFO Center 12'	05/06/97	---	2.25	57	---	---	4.30	---
89-240	Subdeck	07/02/97	---	2.00	51	4410	30	6.00	---
89-240	Rt. 22' SFO	08/05/97	06/29/98	0.75	19	8710	60	5.00	---
89-240	Lt. 22' SFO	08/07/97	06/29/98	3.00	76	---	---	5.60	---
89-244	Subdeck	08/21/97	---	2.75	70	5440	38	5.50	---
89-244	SFO Rt.	10/17/97	07/06/98	2.00	51	---	---	5.00	---
89-244	SFO Lt.	10/21/97	07/06/98	2.50	64	8170	56	4.70	---
89-245	Subdeck Unit #1	09/26/97	---	2.75	70	4990	34	4.50	---
89-245	Subdeck Unit #2	10/02/97	---	2.25	57	---	---	6.10	---
89-245	Lt. 1/2 Unit 2 SFO	10/20/97	07/16/98	1.75	44	9050	62	4.60	---
89-245	Lt. 1/2 Unit 1 SFO	10/22/97	07/16/98	2.00	51	---	---	4.50	---
89-245	Rt. 1/2 Unit 2 SFO	10/23/97	07/16/98	2.00	51	---	---	5.10	---
89-245	Rt. 1/2 Unit 1 SFO	10/24/97	07/16/98	2.00	51	---	---	5.40	---
89-246	Subdeck	08/27/97	---	1.75	44	5720	39	4.00	---
89-246	East 1/2 SFO	09/08/97	07/17/98	3.00	76	7820	54	6.00	---
89-246	West 1/2 SFO	09/10/97	07/17/98	3.00	76	---	---	5.10	---

Table A.6: (continued)

Bridge Number	Portion Placed	Date of Placement	Survey Date	Average Slump		Compressive Strength		Air Content (%)	Curing Materials
				(in.)	(mm)	(psi)	(MPa)		
89-247	Subdeck	04/24/97	---	2.00	51	6510	45	4.50	---
89-247	Lt. 13' SFO	05/05/97	07/20/98	2.00	51	8140	56	6.30	---
89-247	Rt. 26' SFO	05/07/97	07/20/98	3.00	76	---	---	5.20	---
89-248	Subdeck	04/06/98	---	2.25	57	5150	36	5.00	---
89-248	Westbound Lane	04/24/98	08/27/98	2.75	70	---	---	7.20	---
89-248	Eastbound Lane	05/01/98	08/27/98	2.00	51	7900	54	6.00	---

Conventional Overlay Bridges

46-289	Subdeck	08/06/92	---	2.25	57	---	---	5.00	---
46-289	Subdeck	08/18/92	---	2.50	64	4280	30	4.50	---
46-289	Inside 24'	09/02/92	08/25/98	0.50	13	5510	38	4.60	---
46-289	Outside 20'	09/11/92	08/25/98	0.50	13	---	---	5.80	---
46-290	Subdeck	08/04/92	---	2.25	57	---	---	6.20	---
46-290	Subdeck	08/11/92	---	2.50	64	---	---	4.50	---
46-290	Inside 24'	09/08/92	08/31/98	0.25	6	5900	41	5.80	---
46-290	Outside 10'	09/15/92	08/31/98	0.50	13	4900	34	6.20	---
46-299	Subdeck	06/30/94	---	2.25	57	6250	431	4.50	---
46-299	Rt. of CL 22'	07/28/94	08/17/98	1.00	25	6030	42	4.00	---

Table A.6: (continued)

Bridge Number	Portion Placed	Date of Placement	Survey Date	Average Slump		Compressive Strength		Air Content (%)	Curing Materials
				(in.)	(mm)	(psi)	(MPa)		
46-299	Lt. of CL 18'	07/30/94	08/17/98	0.50	13	---	---	6.00	---
46-300	Subdeck	06/12/95	---	6.30	160	---	---	2.25	---
46-300	BDWS 18' Rt. of CL	08/10/95	08/14/98	0.25	6	7050	49	4.00	---
46-300	BDWS 22' Lt. of CL	08/14/95	08/14/98	0.25	6	---	---	5.50	---
46-301	Subdeck	06/10/94	---	2.50	64	5060	35	5.50	---
46-301	BDWS Rt. CL 24'	08/03/94	08/20/98	6.30	160	---	---	2.00	---
46-301	BDWS Lt. CL 24' to 38'	08/03/94	08/28/98	6.30	160	---	---	2.00	---
46-301	BDWS Rt. CL 24' to 38'	08/05/94	08/28/98	0.25	6	7040	49	6.00	---
46-301	BDWS Lt. CL 24'	08/06/94	08/20/98	0.75	19	---	---	6.50	---
75-1	Subdeck	09/30/91	---	1.50	38	7450	51	5.80	curing compound, burlap, poly
75-1	BDWS Lt. of CL	10/17/91	09/02/98	0.25	6	6190	43	6.00	burlap, poly, fug. dye
75-1	BDWS Rt. of CL	10/19/91	09/02/98	0.50	13	5710	39	6.00	burlap, poly, fug. dye
75-49	Subdeck	05/09/91	---	2.25	57	7360	51	5.60	curing compound, burlap, white poly
75-49	Subdeck	05/17/91	---	2.50	64	---	---	5.70	curing compound, burlap, white poly
75-49	Eastbound	06/04/91	09/01/98	0.50	13	5220	36	6.50	burlap, poly, fug. dye
75-49	Westbound	06/07/91	09/01/98	0.50	13	---	---	6.60	burlap, poly, fug. dye
81-49	Subdeck Rt. of CL	03/12/92	---	2.50	64	6080	42	5.50	---
81-49	BDWS Rt. 22'	04/08/92	08/13/98	0.50	13	7290	50	5.50	---

Table A.6: (continued)

Bridge Number	Portion Placed	Date of Placement	Survey Date	Average Slump		Compressive Strength		Air Content (%)	Curing Materials
				(in.)	(mm)	(psi)	(MPa)		
81-49	BDWS 12' Rt of CL	04/13/92	08/13/98	---	---	---	---	---	---
81-49	Subdeck Lt. of CL	10/07/92	---	2.50	64	5800	40	5.80	---
81-49	BDWS Lt. 22'	10/21/92	08/05/98	0.75	19	7020	48	4.60	---
81-49	BDWS 12' Lt. of CL	10/23/92	08/05/98	0.75	19	---	---	5.00	---
89-183	Subdeck	08/17/90	---	2.25	57	---	---	5.20	---
89-183	BDWS Rt. Side	09/21/90	07/22/98	---	---	---	---	---	---
89-183	BDWS Lt. Side	09/25/90	07/22/98	---	---	---	---	---	---
89-185	Subdeck	06/12/90	---	2.25	57	---	---	6.40	---
89-185	Outside	06/21/90	07/28/98	0.00	0	6670	46	6.00	---
89-185	Inside	06/23/90	07/28/98	0.00	0	---	---	6.20	---
89-186	Subdeck	08/30/90	---	2.00	51	---	---	5.30	---
89-186	Inside	09/14/90	07/27/98	0.50	13	---	---	7.10	---
89-186	Outside	09/17/90	07/27/98	0.25	6	6410	44	5.70	---
89-196	Subdeck	10/17/91	---	2.50	64	5580	38	7.50	---
89-196	BDWS Rt. Side	05/01/92	08/10/98	0.00	0	5920	41	6.00	curing compound, white poly
89-196	BDWS Lt. Side	05/05/92	08/10/98	0.50	13	5910	41	5.00	curing compound, white poly
89-198	Subdeck	08/07/91	---	3.00	76	6200	43	5.00	white cure, poly
89-198	Left	08/24/91	08/04/98	0.00	0	7140	49	5.00	---

Table A.6: (continued)

Bridge Number	Portion Placed	Date of Placement	Survey Date	Average Slump		Compressive Strength		Air Content (%)	Curing Materials
				(in.)	(mm)	(psi)	(MPa)		
89-198	Right	08/27/91	08/04/98	---	---	---	---	---	---
89-199	Subdeck	08/14/91	---	2.50	64	6320	44	5.70	white cure, poly
89-199	Left	08/26/91	08/07/98	0.00	0	6920	48	4.80	---
89-199	Right	08/28/91	08/07/98	---	---	---	---	---	---
89-200	Subdeck	08/02/91	---	2.75	70	6890	48	5.00	white cure, poly
89-200	Right	08/17/91	08/04/98	0.00	0	6570	45	4.80	---
89-200	Left	08/20/91	08/04/98	---	---	---	---	---	---
89-201	Subdeck	08/09/91	---	2.25	57	7550	52	4.30	white cure, poly
89-201	Right	08/19/91	08/07/98	0.00	0	6820	47	---	---
89-201	Left	08/21/91	08/07/98	---	---	---	---	---	---
Monolithic Bridges									
56-148	Deck	07/18/91	08/19/98	2.58	66	6170	43	6.50	---
70-107	Deck	10/25/91	08/19/98	2.15	55	6820	47	5.40	burlap, poly
89-204	Deck	10/03/91	08/10/98	3.00	76	6370	44	5.20	---
89-208	Deck	06/15/95	06/22/98	2.25	57	7430	51	5.00	---

Table A.7: Site Conditions

Bridge Number	Portion Placed	Date	Air Temperature								Average Daily		Average
			Low		High		Range		Average		Wind Speed		R.H.
			(F)	(C)	(F)	(C)	(F)	(C)	(F)	(C)	(mph)	(km/hr)	(%)
Silica Fume Overlay Bridges													
23-85	Subdeck	11/06/95	43	6	55	13	12	7	49	9	---	---	---
23-85	East 1/2 SFO	03/29/96	38	3	50	10	12	7	44	7	---	---	---
23-85	West 1/2 SFO	04/03/96	56	13	77	25	21	12	67	19	---	---	---
46-302	Subdeck	11/14/95	28	-2	55	13	27	15	42	5	9.5	15.3	70.0
46-302	Lt. 1/2 SFO	04/09/96	39	4	60	16	21	12	50	10	11.3	18.2	52.0
46-302	Rt. 1/2 SFO	04/11/96	57	14	86	30	29	16	72	22	22.5	36.2	41.0
46-309	Subdeck	09/26/95	50	10	75	24	25	14	63	17	10.6	17.1	62.0
46-309	Rt. 1/2 SFO	10/20/95	43	6	57	14	14	8	50	10	18.6	29.9	45.0
46-309	Lt. 1/2 SFO	10/24/95	36	2	61	16	25	14	49	9	10.6	17.1	46.0
46-317	Subdeck Sec. 2	04/11/96	57	14	86	30	29	16	72	22	22.5	36.2	41.0
46-317	Subdeck Sec. 1	04/26/96	39	4	70	21	31	17	55	13	14.4	23.2	38.0
46-317	Subdeck Pier 5 to Ab.	06/10/96	60	16	74	23	14	8	67	19	6.5	10.5	74.0
46-317	SFO 12'	06/28/96	73	23	89	32	16	9	81	27	11.7	18.8	74.0
46-317	SFO 16'	07/01/96	74	23	89	32	15	8	82	28	2.8	4.5	86.0
81-50	Subdeck Rt.36+38 to Ab. #2	08/31/95	70	21	86	30	16	9	78	26	5.0	8.1	74.0
81-50	Subdeck Rt. 34+69 to 36+38	09/13/95	59	15	88	31	29	16	74	23	2.8	4.5	66.0
81-50	Subdeck Rt. 30+06 to 34+69	09/26/95	50	10	79	26	29	16	65	18	4.5	7.2	66.0

Table A.7: (continued)

Bridge Number	Portion Placed	Date	Air Temperature								Average Daily		Average R.H. (%)
			Low		High		Range		Average		Wind Speed		
			(F)	(C)	(F)	(C)	(F)	(C)	(F)	(C)	(mph)	(km/hr)	
81-50	Subdeck Rt. Ab. #1 to 30+06	10/02/95	52	11	66	19	14	8	59	15	2.0	3.2	82.0
81-50	Subdeck Lt. 36+38 to Ab. #2	10/06/95	44	7	57	14	13	7	51	10	9.0	14.5	74.0
81-50	Subdeck Lt. 34+69 to 36+38	10/11/95	52	11	87	31	35	19	70	21	3.7	6.0	66.0
81-50	Subdeck Lt. 30+06 to 34+69	10/18/95	48	9	84	29	36	20	66	19	5.3	8.5	52.0
81-50	Subdeck Lt. Ab. #1 to 30+06	10/21/95	29	-2	63	17	34	19	46	8	2.8	4.5	56.0
81-50	SFO Rt. Unit #1	11/15/95	30	-1	45	7	15	8	38	3	5.5	8.9	94.0
81-50	SFO Lt. Unit #1	11/18/95	25	-4	68	20	43	24	47	8	4.8	7.7	67.0
81-50	SFO Rt. Unit #2	11/21/95	25	-4	53	12	28	16	39	4	2.9	4.7	45.0
81-50	SFO Lt. Unit #2	11/30/95	42	6	75	24	33	18	59	15	6.9	11.1	36.0
87-453	Subdeck	05/22/97	51	11	68	20	17	9	60	15	9.2	14.8	71.0
87-453	North 22'	06/30/97	65	18	93	34	28	16	79	26	8.3	13.4	75.0
87-453	South 18'	07/03/97	58	14	86	30	28	16	72	22	10.4	16.7	60.0
87-454	Subdeck	08/01/96	67	19	89	32	22	12	78	26	7.5	12.1	71.0
87-454	Left of CL	09/10/96	53	12	89	32	36	20	71	22	5.1	8.2	70.0
87-454	Right of CL	10/16/96	55	13	81	27	26	14	68	20	5.7	9.2	34.0
89-184	Subdeck	09/13/90	63	17	89	32	26	14	76	24	7.5	12.1	70.6
89-184	Inside	09/26/90	48	9	96	36	48	27	72	22	3.1	5.0	62.0
89-184	Outside	09/28/90	58	14	82	28	24	13	70	21	7.4	11.9	68.0

Table A.7: (continued)

Bridge Number	Portion Placed	Date	Air Temperature								Average Daily		Average
			Low		High		Range		Average		Wind Speed		R.H.
			(F)	(C)	(F)	(C)	(F)	(C)	(F)	(C)	(mph)	(km/hr)	(%)
89-187	Subdeck	05/31/90	59	15	70	21	11	6	65	18	9.0	14.5	88.5
89-187	Inside	06/26/90	70	21	93	34	23	13	82	28	8.4	13.5	78.0
89-187	Outside	06/28/90	76	24	93	34	17	9	85	29	18.1	29.1	72.0
89-206	Subdeck	07/19/95	69	21	92	33	23	13	81	27	8.7	14.0	67.5
89-206	Right	10/04/95	47	8	78	26	31	17	63	17	11.9	19.2	55.9
89-206	Left	10/10/95	44	7	82	28	38	21	63	17	1.7	2.7	67.4
89-207	Subdeck	08/29/95	68	20	98	37	30	17	83	28	5.8	9.3	60.4
89-207	Left	10/24/95	36	2	61	16	25	14	49	9	8.0	12.9	46.9
89-207	Right	04/19/96	48	9	81	27	33	18	65	18	15.3	24.6	35.0
89-210	Subdeck	09/15/95	59	15	83	28	24	13	71	22	6.8	10.9	70.1
89-210	Right	10/12/95	62	17	88	31	26	14	75	24	11.5	18.5	54.9
89-210	Left	10/18/95	46	8	83	28	37	21	65	18	7.4	11.9	54.9
89-234	Subdeck	05/16/96	68	20	85	29	17	9	77	25	10.7	17.2	75.9
89-234	SFO south 20'	06/20/96	68	20	92	33	24	13	80	27	8.6	13.8	69.6
89-234	SFO Norht 18'	06/25/96	71	22	89	32	18	10	80	27	9.4	15.1	67.5
89-234	SFO Center 12'	06/28/96	76	24	94	34	18	10	85	29	10.3	16.6	66.4
89-235	Subdeck	03/21/97	22	-6	54	12	32	18	38	3	6.2	10.0	46.3
89-235	SFO Left 20'	04/29/97	44	7	76	24	32	18	60	16	9.3	15.0	51.0

Table A.7: (continued)

Bridge Number	Portion Placed	Date	Air Temperature								Average Daily		Average
			Low		High		Range		Average		Wind Speed		R.H.
			(F)	(C)	(F)	(C)	(F)	(C)	(F)	(C)	(mph)	(km/hr)	(%)
89-235	SFO Right 18'	05/01/97	34	1	65	18	31	17	50	10	8.4	13.5	69.9
89-235	SFO Center 12'	05/06/97	44	7	75	24	31	17	60	15	8.2	13.2	56.5
89-240	Subdeck	07/02/97	64	18	89	32	25	14	77	25	7.3	11.8	46.1
89-240	Rt. 22' SFO	08/05/97	65	18	84	29	19	11	75	24	6.8	10.9	62.3
89-240	Lt. 22' SFO	08/07/97	55	13	84	29	29	16	70	21	3.0	4.8	62.5
89-244	Subdeck	08/21/97	58	14	82	28	24	13	70	21	2.7	4.3	77.8
89-244	SFO Rt.	10/17/97	37	3	63	17	26	14	50	10	2.6	4.2	73.3
89-244	SFO Lt.	10/21/97	36	2	57	14	21	12	47	8	5.2	8.4	59.9
89-245	Subdeck Unit #1	09/26/97	50	10	82	28	32	18	66	19	3.9	6.3	74.0
89-245	Subdeck Unit #2	10/02/97	59	15	89	32	30	17	74	23	8.7	14.0	60.3
89-245	Lt. 1/2 Unit 2 SFO	10/20/97	40	4	56	13	16	9	48	9	6.8	10.9	66.0
89-245	Lt. 1/2 Unit 1 SFO	10/22/97	43	6	58	14	15	8	51	10	8.2	13.2	51.0
89-245	Rt. 1/2 Unit 2 SFO	10/23/97	44	7	61	16	17	9	53	11	9.6	15.5	79.0
89-245	Lt. 1/2 Unit 1 SFO	10/24/97	50	10	57	14	7	4	54	12	7.8	12.6	92.0
89-246	Subdeck	08/27/97	64	18	90	32	26	14	77	25	5.7	9.2	67.4
89-246	East 1/2 SFO	09/08/97	63	17	90	32	27	15	77	25	4.6	7.4	74.9
89-246	West 1/2 SFO	09/10/97	51	11	78	26	27	15	65	18	5.5	8.9	65.0
89-247	Subdeck	04/24/97	45	7	62	17	17	9	54	12	8.0	12.9	56.1

Table A.7: (continued)

Bridge Number	Portion Placed	Date	Air Temperature								Average Daily		Average
			Low		High		Range		Average		Wind Speed		R.H.
			(F)	(C)	(F)	(C)	(F)	(C)	(F)	(C)	(mph)	(km/hr)	(%)
89-247	Lt. 13' SFO	05/05/97	51	11	77	25	26	14	64	18	9.9	15.9	46.5
89-247	Rt. 26' SFO	05/07/97	58	14	78	26	20	11	68	20	12.4	20.0	72.0
89-248	Subdeck	04/06/98	47	8	76	24	29	16	62	16	12.8	20.6	66.3
89-248	Westbound Lane	04/24/98	44	7	80	27	36	20	62	17	13.7	22.1	15.0
89-248	Eastbound Lane	05/01/98	44	7	76	24	32	18	60	16	5.2	8.4	34.0

Conventional Overlay Bridges

46-289	Subdeck	08/06/92	65	18	80	27	15	8	73	23	---	---	---
46-289	Subdeck	08/18/92	63	17	85	29	22	12	74	23	---	---	---
46-289	Inside 24'	09/02/92	63	17	83	28	20	11	73	23	---	---	---
46-289	Outside 20'	09/11/92	50	10	75	24	25	14	63	17	---	---	---
46-290	Subdeck	08/04/92	62	17	79	26	17	9	71	21	---	---	---
46-290	Subdeck	08/11/92	65	18	84	29	19	11	75	24	---	---	---
46-290	Inside 24'	09/08/92	52	11	78	26	26	14	65	18	---	---	---
46-290	Outside 10'	09/15/92	70	21	88	31	18	10	79	26	---	---	---
46-299	Subdeck	06/30/94	68	20	91	33	23	13	80	26	11.2	18.0	52.0
46-299	Rt. of CL 22'	07/28/94	57	14	83	28	26	14	70	21	6.9	11.1	52.0

Table A.7: (continued)

Bridge Number	Portion Placed	Date	Air Temperature								Average Daily		Average
			Low		High		Range		Average		Wind Speed		R.H.
			(F)	(C)	(F)	(C)	(F)	(C)	(F)	(C)	(mph)	(km/hr)	(%)
46-299	Lt. of CL 18'	07/30/94	62	17	86	30	24	13	74	23	7.9	12.7	52.0
46-300	Subdeck	06/12/95	57	14	77	25	20	11	67	19	8.2	13.2	49.0
46-300	BDWS 18' Rt. of CL	08/10/95	72	22	92	33	20	11	82	28	9.5	15.3	59.0
46-300	BDWS 22' Lt. of CL	08/14/95	75	24	92	33	17	9	84	29	8.4	13.5	70.0
46-301	Subdeck	06/10/94	64	18	77	25	13	7	71	21	2.8	4.5	67.0
46-301	BDWS Rt. CL 24'	08/03/94	72	22	87	31	15	8	80	26	---	---	---
46-301	BDWS Lt. CL 24' to 38'	08/03/94	72	22	87	31	15	8	80	26	---	---	---
46-301	BDWS Rt. CL 24' to 38'	08/05/94	59	15	75	24	16	9	67	19	---	---	---
46-301	BDWS Lt. CL 24'	08/06/94	56	13	79	26	23	13	68	20	---	---	---
75-1	Subdeck	09/30/91	57	14	83	28	26	14	70	21	4.6	7.4	51.0
75-1	BDWS Lt. of CL	10/17/91	59	15	92	33	33	18	76	24	6.9	11.1	30.0
75-1	BDWS Rt. of CL	10/19/91	27	-3	59	15	32	18	43	6	2.0	3.2	48.0
75-49	Subdeck	05/09/91	56	13	81	27	25	14	69	20	5.3	8.5	79.0
75-49	Subdeck	05/17/91	56	13	79	26	23	13	68	20	3.9	6.3	77.0
75-49	Eastbound	06/04/91	64	18	87	31	23	13	76	24	4.1	6.6	76.0
75-49	Westbound	06/07/91	57	14	81	27	24	13	69	21	5.0	8.1	72.0
81-49	Subdeck Rt. of CL	03/12/92	20	-7	54	12	34	19	37	3	2.4	3.9	67.0
81-49	BDWS Rt. 22'	04/08/92	46	8	64	18	18	10	55	13	2.3	3.7	64.0

Table A.7: (continued)

Bridge Number	Portion Placed	Date	Air Temperature								Average Daily		Average
			Low		High		Range		Average		Wind Speed		R.H.
			(F)	(C)	(F)	(C)	(F)	(C)	(F)	(C)	(mph)	(km/hr)	(%)
81-49	BDWS 12' Rt of CL	04/13/92	35	2	48	9	13	7	42	5	1.3	2.1	50.0
81-49	Subdeck Lt. of CL	10/07/92	53	12	80	27	27	15	67	19	3.7	6.0	69.0
81-49	BDWS Lt. 22'	10/21/92	44	7	78	26	34	19	61	16	2.1	3.4	64.0
81-49	BDWS 12' Lt. of CL	10/23/92	64	18	83	28	19	11	74	23	7.7	12.4	66.0
89-183	Subdeck	08/17/90	76	24	91	33	15	8	84	29	12.3	19.8	69.1
89-183	BDWS Rt. Side	09/21/90	52	11	78	26	26	14	65	18	12.3	19.8	59.5
89-183	BDWS Lt. Side	09/25/90	49	9	92	33	43	24	71	21	6.4	10.3	60.9
89-185	Subdeck	06/12/90	76	24	91	33	15	8	84	29	18.3	29.5	68.5
89-185	Outside	06/21/90	67	19	89	32	22	12	78	26	8.8	14.2	77.0
89-185	Inside	06/23/90	59	15	84	29	25	14	72	22	8.6	13.8	65.0
89-186	Subdeck	08/30/90	64	18	93	34	29	16	79	26	4.8	7.7	63.5
89-186	Inside	09/14/90	53	12	83	28	30	17	68	20	10.6	17.1	57.0
89-186	Outside	09/17/90	54	12	71	22	17	9	63	17	12.1	19.5	75.0
89-196	Subdeck	10/17/91	58	14	90	32	32	18	74	23	12.0	19.3	39.5
89-196	BDWS Rt. Side	05/01/92	63	17	86	30	23	13	75	24	15.9	25.6	68.4
89-196	BDWS Lt. Side	05/05/92	42	6	65	18	23	13	54	12	9.8	15.8	53.4
89-198	Subdeck	08/07/91	73	23	97	36	24	13	85	29	8.1	13.0	60.6
89-198	Left	08/24/91	65	18	95	35	30	17	80	27	5.5	8.9	75.0

Table A.7: (continued)

Bridge Number	Portion Placed	Date	Air Temperature								Average Daily		Average
			Low		High		Range		Average		Wind Speed		R.H.
			(F)	(C)	(F)	(C)	(F)	(C)	(F)	(C)	(mph)	(km/hr)	(%)
89-198	Right	08/27/91	66	19	94	34	28	16	80	27	7.2	11.6	67.0
89-199	Subdeck	08/14/91	56	13	91	33	35	19	74	23	5.2	8.4	67.1
89-199	Left	08/26/91	65	18	95	35	30	17	80	27	5.2	8.4	61.0
89-199	Right	08/28/91	68	20	94	34	26	14	81	27	7.1	11.4	71.0
89-200	Subdeck	08/02/91	73	23	102	39	29	16	88	31	12.1	19.5	36.8
89-200	Right	08/17/91	62	17	90	32	28	16	76	24	8.1	13.0	63.0
89-200	Left	08/20/91	51	11	85	29	34	19	68	20	4.6	7.4	67.0
89-201	Subdeck	08/09/91	67	19	74	23	7	4	71	21	9.3	15.0	78.4
89-201	Right	08/19/91	56	13	85	29	29	16	71	21	6.5	10.5	63.0
89-201	Left	08/21/91	56	13	94	34	38	21	75	24	5.2	8.4	66.0
Monolithic Bridges													
56-148	Deck	07/17/91	74	23	97	36	23	13	86	30	8.0	12.9	47.1
70-107	Deck	10/25/91	36	2	57	14	21	12	47	8	7.6	12.2	75.0
89-204	Deck	10/03/91	56	13	77	25	21	12	67	19	10.6	17.1	90.0
89-208	Deck	06/15/95	68	20	89	32	21	12	79	26	13.0	20.9	64.6

Table A.8: Crack Densities and Data for Individual Spans

Bridge Number	Span Type	Span Location	Crack Density (m/m ²)	Span Length	
				(ft)	(m)
Silica Fume Overlay Bridges					
23-85	End	South	0.46	124	37.8
23-85	End	North	0.27	124	37.8
46-302	End	South	0.41	61	18.6
46-302	Int.	S. Center	0.57	85	25.9
46-302	Int.	N. Center	0.50	85	25.9
46-302	End	North	0.48	61	18.6
46-309	End	South	0.40	51	15.5
46-309	Int.	S. Center	0.32	85	25.9
46-309	Int.	N. Center	0.32	85	25.9
46-309	End	North	0.39	51	15.5
46-317	End	West	0.03	90	27.4
46-317	Int.	W. Center	0.07	127	38.7
46-317	Int.	Center	0.07	192	58.5
46-317	Int.	E. Center	0.11	127	38.7
81-50	End	North	0.67	140	42.7
81-50	Int.	N. Center	0.74	175	53.3
81-50	Int.	N. Center	0.80	175	53.3
81-50	Int.	N. Center	0.72	150	45.7
81-50	Int.	Center	0.64	20	6.1
87-453	End	West	0.19	110	33.5
87-453	Int.	Center	0.10	158	48.2
87-453	End	East	0.51	110	33.5
87-454	End	West	0.57	102	31.1
87-454	Int.	Center	0.54	147	44.8
87-454	End	East	1.21	102	31.1
89-184	End	West	0.99	48	14.6
89-184	Int.	W. Center	0.83	93	28.3

Table A.8: (continued)

Bridge Number	Span Type	Span Location	Crack Density (m/m ²)	Span Length	
				(ft)	(m)
89-184	Int.	E. Center	1.06	70	21.3
89-184	End	East	1.17	50	15.2
89-187	End	West	0.80	45	13.7
89-187	Int.	W. Center	1.00	60	18.3
89-187	Int.	E. Center	0.98	60	18.3
89-187	End	East	1.08	45	13.7
89-206	End	West	0.45	84	25.6
89-206	Int.	W. Center	0.43	116	35.4
89-206	Int.	E. Center	0.42	116	35.4
89-206	End	East	0.40	84	25.6
89-207	End	West	0.31	84	25.6
89-207	Int.	W. Center	0.42	116	35.4
89-207	Int.	E. Center	0.45	116	35.4
89-207	End	East	0.21	84	25.6
89-210	End	South	0.07	65	19.8
89-210	Int.	Center	0.11	82	25.0
89-210	End	North	0.17	65	19.8
89-234	End	West	0.28	73	22.3
89-234	Int.	W. Center	0.26	131	39.9
89-234	Int.	E. Center	0.28	110	33.5
89-234	End	East	0.29	60	18.3
89-235	End	West	0.98	71	21.6
89-235	Int.	W. Center	0.27	131	39.9
89-235	Int.	E. Center	0.15	110	33.5
89-235	End	East	0.32	51	15.5
89-240	End	South	0.31	70	21.3
89-240	Int.	S. Center	0.34	100	30.5
89-240	Int.	N. Center	0.29	100	30.5

Table A.8: (continued)

Bridge Number	Span Type	Span Location	Crack Density (m/m ²)	Span Length	
				(ft)	(m)
89-240	End	North	0.14	60	18.3
89-244	End	South	0.01	96	29.3
89-244	Int.	S. Center	0.01	120	36.6
89-244	Int.	N. Center	0.03	124	37.8
89-244	End	North	0.02	110	33.5
89-245	End	West	0.06	110	33.5
89-245	Int.	W. Center	0.07	170	51.8
89-245	Int.	W. Center	0.09	25	7.6
89-245	Int.	Center	0.03	155	47.2
89-245	Int.	E. Center	0.03	202	61.6
89-245	End	East	0.08	150	45.7
89-246	End	South	0.09	123	37.5
89-246	End	North	0.06	130	39.6
89-247	End	South	0.66	123	37.5
89-247	End	North	0.35	130	39.6
89-248	End	West	0.02	60	18.3
89-248	Int.	Center	0.04	75	22.9
89-248	End	East	0.01	60	18.3

Conventional Overlay Bridges

46-289	End	West	0.68	79	24.1
46-289	Int.	W. Center	0.70	137	41.8
46-289	Int.	E. Center	0.70	137	41.8
46-289	End	East	0.47	79	24.1
46-290	End	West	0.66	79	24.1
46-290	Int.	W. Center	0.63	137	41.8
46-290	Int.	E. Center	0.65	137	41.8
46-290	End	East	0.49	79	24.1
46-299	End	South	0.81	40	12.2
46-299	Int.	S. Center	0.92	64	19.5

Table A.8: (continued)

Bridge Number	Span Type	Span Location	Crack Density (m/m ²)	Span Length	
				(ft)	(m)
46-299	Int.	N. Center	0.79	64	19.5
46-299	End	North	1.03	40	12.2
46-300	End	South	0.75	40	12.2
46-300	Int.	S. Center	0.80	64	19.5
46-300	Int.	N. Center	0.69	64	19.5
46-300	End	North	0.57	40	12.2
46-301	End	West	0.96	55	16.8
46-301	Int.	W. Center	0.69	90	27.4
46-301	Int.	E. Center	0.55	90	27.4
46-301	End	East	0.90	55	16.8
75-1	End	West	0.34	128	39.0
75-1	Int.	Center	0.51	160	48.8
75-1	End	East	0.22	128	39.0
75-49	End	West	0.40	128	39.0
75-49	Int.	Center	0.47	160	48.8
75-49	End	East	0.45	128	39.0
81-49	End	South	0.73	77	23.5
81-49	Int.	Center	0.60	110	33.5
81-49	End	North	0.79	77	23.5
89-183	End	South	0.51	67	20.4
89-183	Int.	S. Center	0.56	88	26.8
89-183	Int.	N. Center	0.48	88	26.8
89-183	End	North	0.45	67	20.4
89-185	End	West	0.63	49	14.9
89-185	Int.	W. Center	0.50	84	25.6
89-185	Int.	E. Center	0.77	71	21.6
89-185	End	East	0.94	51	15.5
89-186	End	West	0.84	45	13.7
89-186	Int.	W. Center	0.67	60	18.3
89-186	Int.	E. Center	0.64	60	18.3
89-186	End	East	0.76	45	13.7
89-196	End	South	0.54	46	14.0
89-196	Int.	Center	0.41	68	20.7

Table A.8: (continued)

Bridge Number	Span Type	Span Location	Crack Density (m/m ²)	Span Length	
				(ft)	(m)
89-196	End	North	0.71	46	14.0
89-198	End	South	0.42	66	20.1
89-198	Int.	S. Center	0.41	97	29.6
89-198	Int.	N. Center	0.38	97	29.6
89-198	End	North	0.30	80	24.4
89-199	End	South	0.54	66	20.1
89-199	Int.	S. Center	0.66	97	29.6
89-199	Int.	N. Center	0.73	97	29.6
89-199	End	North	0.65	80	24.4
89-200	End	South	0.70	84	25.6
89-200	Int.	Center	0.40	150	45.7
89-200	End	North	0.68	84	25.6
89-201	End	South	0.77	84	25.6
89-201	Int.	Center	0.41	150	45.7
89-201	End	North	0.83	84	25.6

Monolithic Bridges

56-148	End	West	0.37	72	21.9
56-148	Int.	Center	0.32	100	30.5
56-148	End	East	0.25	72	21.9
70-107	End	South	0.46	60	18.3
70-107	Int.	Center	0.39	80	24.4
70-107	End	North	0.40	60	18.3
89-204	End	West	0.86	70	21.3
89-204	Int.	Center	0.99	88	26.8
89-204	End	East	0.63	70	21.3
89-208	End	West	0.01	68	20.7
89-208	Int.	W. Center	0.03	106	32.3
89-208	Int.	E. Center	0.04	106	32.3
89-208	End	East	0.02	83	25.3

Table A.9: RCPT and Calculated Diffusion Coefficient Results

Bridge Number	Portion Placed	Date of Placement	Test Result Corrected to 2" (Coulombs)				30 min. x 12 Corrected to 2" (Coulombs)				Surface Conc. kg/m ³	Effective Diff. coeff. mm ² /day
			1	2	3	Avg.	1	2	3	Avg.		
Silica Fume Overlay Bridges												
23-85	East 1/2 SFO	03/29/96	2507	5023	3107	3546	1599	2621	4276	2832	5.08	0.10
23-85	West 1/2 SFO	04/03/96	1619	2414	2668	2234	1173	1531	1893	1532	30.73	0.01
46-302	Lt. 1/2 SFO	04/09/96	1509	1585	1434	1509	1094	1278	1148	1173	1.59	0.18
46-302	Rt. 1/2 SFO	04/11/96	621	---	640	631	528	489	660	559	6.66	0.02
46-309	Rt. 1/2 SFO	10/20/95	1437	761	1001	1066	1199	696	859	918	8.61	0.19
46-309	Lt. 1/2 SFO	10/24/95	2331	1326	876	1511	1618	1102	745	1155	6.57	0.20
46-317	SFO 12'	06/28/96	599	1765	863	1076	515	1253	705	824	5.97	0.06
46-317	SFO 16'	07/01/96	1032	1671	1248	1317	941	1320	1078	1113	5.13	0.23
81-50	SFO Rt. Unit #1	11/15/95	---	---	---	---	---	---	---	---	---	---
81-50	SFO Lt. Unit #1	11/18/95	---	---	---	---	---	---	---	---	---	---
81-50	SFO Rt. Unit #2	11/21/95	2013	1595	1424	1677	1476	1372	670	1173	5.82	0.07
81-50	SFO Lt. Unit #2	11/30/95	1212	678	1187	1026	948	562	934	815	6.83	0.08
87-453	North 22'	06/30/97	2624	5272	6111	4669	2222	2992	3663	2959	6.33	0.25
87-453	South 18'	07/03/97	1875	878	2125	1626	1356	815	1866	1346	7.12	0.10
87-454	Left of CL	09/10/96	1839	2116	6416	3457	1667	1782	3593	2347	5.81	0.16
87-454	Right of CL	10/16/96	1761	1406	3340	2169	1709	1515	1971	1732	6.72	0.15

Table A.9: (continued)

Bridge Number	Portion Placed	Date of Placement	Test Result Corrected to 2" (Coulombs)				30 min. x 12 Corrected to 2" (Coulombs)				Surface Conc. kg/m ³	Effective Diff. coeff. mm ² /day
			1	2	3	Avg.	1	2	3	Avg.		
89-184	Inside	09/26/90	911	681	745	779	729	564	620	638	13.29	0.03
89-184	Outside	09/28/90	385	357	421	388	343	316	381	347	10.88	0.02
89-187	Inside	06/26/90	1544	1373	2214	1710	1178	1142	1680	1333	7.47	0.06
89-187	Outside	06/28/90	1378	1246	923	1182	1080	1010	775	955	6.65	0.05
89-206	Right	10/04/95	934	628	777	780	740	549	645	645	1.23	0.14
89-206	Left	10/10/95	506	333	360	400	439	314	329	361	2.4	0.08
89-207	Left	10/24/95	604	624	603	610	535	549	517	534	1.95	0.11
89-207	Right	04/19/96	1179	383	506	689	992	367	483	614	4.07	0.11
89-210	Right	10/12/95	1113	693	893	900	890	576	684	717	---	---
89-210	Left	10/18/95	706	528	493	576	582	443	439	488	---	---
89-234	SFO South 20'	06/20/96	1473	1389	1347	1403	1318	1241	908	1156	7.81	0.09
89-234	SFO North 18'	06/25/96	1639	1007	1202	1283	1649	939	1122	1237	6.71	0.11
89-234	SFO Center 12'	06/28/96	1068	1573	1643	1428	956	1292	1363	1204	8.06	0.10
89-235	SFO Left 20'	04/29/97	---	---	---	---	---	---	---	---	---	---
89-235	SFO Right 18'	05/01/97	589	350	470	470	513	324	413	417	2.39	0.18
89-235	SFO Center 12'	05/06/97	---	---	---	---	---	---	---	---	---	---
89-240	Rt. 22' SFO	08/05/97	733	737	897	789	633	658	842	711	6.71	0.11
89-240	Lt. 22' SFO	08/07/97	1457	1184	1514	1385	1201	1036	1214	1150	7.63	0.21

Table A.9: (continued)

Bridge Number	Portion Placed	Date of Placement	Test Result Corrected to 2" (Coulombs)				30 min. x 12 Corrected to 2" (Coulombs)				Surface Conc. kg/m ³	Effective Diff. coeff. mm ² /day
			1	2	3	Avg.	1	2	3	Avg.		
89-244	SFO Rt.	10/17/97	929	898	1019	949	810	784	870	821	9.36	0.20
89-244	SFO Lt.	10/21/97	1270	986	1088	1115	1045	853	909	936	11.36	0.21
89-245	Lt. 1/2 Unit 2 SFO	10/20/97	1015	1123	910	1016	845	982	805	877	10.56	0.21
89-245	Lt. 1/2 Unit 1 SFO	10/22/97	1291	1426	1229	1315	1070	1141	1015	1075	6.46	0.25
89-245	Rt. 1/2 Unit 2 SFO	10/23/97	915	1194	1081	1063	813	1010	905	909	8.45	0.30
89-245	Rt. 1/2 Unit 1 SFO	10/24/97	1708	1120	1098	1309	1309	976	959	1081	8.02	0.24
89-246	East 1/2 SFO	09/08/97	1688	1152	1582	1474	1410	993	1279	1227	4.36	0.08
89-246	West 1/2 SFO	09/10/97	1716	1990	1395	1700	1346	1474	1115	1312	2.24	0.28
89-247	Lt. 13' SFO	05/05/97	1122	838	855	938	949	694	709	784	1.03	0.35
89-247	Rt. 26' SFO	05/07/97	857	1435	1343	1212	703	1068	1005	925	1.82	0.22
89-248	Westbound Lane	04/24/98	751	620	798	723	564	521	648	578	0.53	0.11
89-248	Eastbound Lane	05/01/98	1112	863	1186	1054	890	772	936	866	4.28	0.05

Conventional Overlay Bridges

46-289	Inside 24'	09/02/92	2359	1837	2233	2143	1907	1414	1676	1666	10.23	0.05
46-289	Outside 20'	09/11/92	1237	2176	1622	1678	1027	1732	1356	1372	10.58	0.03
46-290	Inside 24'	09/08/92	2702	2133	1371	2069	2099	1588	1111	1599	10.82	0.08
46-290	Outside 10'	09/15/92	---	---	---	---	---	---	---	---	---	---

Table A.9: (continued)

Bridge Number	Portion Placed	Date of Placement	Test Result Corrected to 2" (Coulombs)				30 min. x 12 Corrected to 2" (Coulombs)				Surface Conc. kg/m ³	Effective Diff. coeff. mm ² /day
			1	2	3	Avg.	1	2	3	Avg.		
46-299	Rt. of CL 22'	07/28/94	1203	1800	2289	1764	1030	1411	1737	1393	7.92	0.05
46-299	Lt. of CL 18'	07/30/94	1439	1819	1009	1422	1200	1322	782	1101	5.79	0.19
46-300	BDWS 22' Lt. of CL	08/14/95	2818	2132	2476	2475	2134	1666	1643	1814	6.95	0.21
46-300	BDWS 18' Rt. of CL	08/10/95	1582	2964	3595	2714	1332	2031	2337	1900	7.05	0.21
46-301	BDWS Rt. CL 24'	08/03/94	1354	1482	1672	1503	1150	1232	1285	1222	8.05	0.09
46-301	BDWS Lt. CL 24' to 38'	08/03/94	1380	1791	1912	1694	1057	1287	1380	1241	7.06	0.20
46-301	BDWS Rt. CL 24' to 38'	08/05/94	1800	1150	1381	1444	1397	916	1100	1138	7.46	0.15
46-301	BDWS Lt. CL 24'	08/06/94	998	1633	1640	1424	827	1179	1355	1120	6.71	0.12
75-1	BDWS Lt. of CL	10/17/91	---	1782	3156	2469	---	1322	2044	1683	8.76	0.09
75-1	BDWS Rt. of CL	10/19/91	1502	3680	3924	3035	1294	2344	2584	2074	11.42	0.04
75-49	Eastbound	06/04/91	---	8189	---	8189	---	3687	---	3687	9.44	0.26
75-49	Westbound	06/07/91	2002	4392	2586	2993	1977	2560	1889	2142	7.56	0.17
81-49	BDWS Rt. 22'	04/08/92	2558	1241	1954	1918	1960	1085	1559	1535	5.52	0.03
81-49	BDWS 12' Rt of CL	04/13/92	2121	1807	1226	1718	1681	1407	1084	1391	7.85	0.06
81-49	BDWS Lt. 22'	10/21/92	2118	1125	1921	1721	1636	920	1444	1333	6.73	0.07
81-49	BDWS 12' Lt. of CL	10/23/92	1316	2109	1883	1769	1045	1461	1361	1289	5.88	0.10
89-183	BDWS Rt. Side	09/21/90	3041	2110	6330	3827	2166	1623	3045	2278	7.64	0.09
89-183	BDWS Lt. Side	09/25/90	1981	3626	1797	2468	1503	2216	1351	1690	7.87	0.06

Table A.9: (continued)

Bridge Number	Portion Placed	Date of Placement	Test Result Corrected to 2" (Coulombs)				30 min. x 12 Corrected to 2" (Coulombs)				Surface Conc. kg/m ³	Effective Diff. coeff. mm ² /day
			1	2	3	Avg.	1	2	3	Avg.		
89-185	Outside	06/21/90	2930	1633	7645	4069	1835	1249	3067	2050	7.85	0.12
89-185	Inside	06/23/90	3355	4506	4711	4191	1978	2694	2660	2444	9.41	0.25
89-186	Inside	09/14/90	1311	2378	2245	1978	1064	1609	1638	1437	9.95	0.06
89-186	Outside	09/17/90	1686	2179	1827	1897	1311	1620	1376	1436	8.57	0.09
89-196	BDWS Rt. Side	05/01/92	1929	923	2165	1672	1545	748	1615	1303	6.06	0.07
89-196	BDWS Lt. Side	05/05/92	1752	3398	2659	2603	1360	2199	1754	1771	9.43	0.12
89-198	Left	08/24/91	2063	2187	2271	2174	1756	1590	1702	1683	10.12	0.06
89-198	Right	08/27/91	1825	2074	2219	2039	1597	1771	1895	1754	7.22	0.07
89-199	Left	08/26/91	1765	1812	2046	1874	1375	1396	1585	1452	8.06	0.07
89-199	Right	08/28/91	1870	1952	2245	2022	1464	1463	1658	1528	11.72	0.05
89-200	Right	08/17/91	2922	2326	1957	2402	2227	1846	1529	1867	8.48	0.06
89-200	Left	08/20/91	2707	1944	1702	2118	2120	1557	1269	1649	10.8	0.05
89-201	Right	08/19/91	1618	2253	1649	1840	1233	1705	1306	1415	9.73	0.06
89-201	Left	08/21/91	1911	2162	1672	1915	1461	1607	1308	1459	8.13	0.05
Monolithic Bridges												
56-148	Deck	07/18/91	3884	3440	5024	4116	2430	3975	2607	3004	11.26	0.17
70-107	Deck	10/25/91	3319	5424	3037	3927	2186	2442	3677	2768	11.88	0.20

Table A.9: (continued)

Bridge Number	Portion Placed	Date of Placement	Test Result Corrected to 2" (Coulombs)				30 min. x 12 Corrected to 2" (Coulombs)				Surface Conc. kg/m ³	Effective Diff. coeff. mm ² /day
			1	2	3	Avg.	1	2	3	Avg.		
89-204	Deck	10/03/91	2335	2417	5965	3572	1709	1982	3035	2242	8.81	0.14
89-208	Deck	06/15/95	3670	2455	2181	2769	2301	1685	1452	1813	6.94	0.11

Key

SFO = Silica fume overlay

BDWS = Bridge deck wearing surface, i.e. conventional overlay

CL = centerline

Rt. = Right

Lt. = Left

Table A.10: Chloride Concentration Information

Bridge: 23-85

East Side
 Placement Date 3/29/96
 Survey Date 8/18/98

West Side
 Placement Date 4/3/96
 Survey Date 8/18/98

Off Crack		On Crack		Off Crack		On Crack		Depth (mm)
Sample	kg/m ³	Sample	kg/m ³	Sample	kg/m ³	Sample	kg/m ³	
1A	2.90	2A	3.33	7A	2.85	8A	3.59	9.5
1B	0.26	2B	1.64	7B	0.15	8B	1.77	28.6
1C	0.18	2C	1.15	7C	0.25	8C	1.79	47.6
1D	0.22	2D	0.91	7D	0.45	8D	0.50	66.7
1E	0.22	2E	0.74	7E	0.38	8E	0.17	85.7
3A	2.80	4A	2.53	9A	1.58	10A	3.32	9.5
3B	0.50	4B	1.18	9B	0.24	10B	1.62	28.6
3C	0.20	4C	0.81	9C	0.24	10C	1.07	47.6
3D	0.21	4D	0.76	9D	0.16	10D	0.61	66.7
3E	0.16	4E	0.84	9E	0.17	10E	0.25	85.7
5A	2.22	6A	2.91	11A	1.55	12A	2.01	9.5
5B	0.36	6B	1.44	11B	0.00	12B	1.00	28.6
5C	0.22	6C	0.61	11C	0.17	12C	0.77	47.6
5D	0.21	6D	0.43	11D	0.18	12D	0.48	66.7
5E	0.19	6E	0.51	11E	0.14	12E	0.88	85.7

Table A.10: (continued)

Bridge: 46-289

South Side

Placement Date 9/11/92

Survey Date 8/25/98

North Side

Placement Date 9/2/92

Survey Date 8/25/98

Off Crack		On Crack		Off Crack		On Crack		Depth (mm)
Sample	kg/m ³	Sample	kg/m ³	Sample	kg/m ³	Sample	kg/m ³	
2A	4.58	1A	6.19	8A	5.77	7A	7.32	9.5
2B	0.38	1B	3.58	8B	0.92	7B	4.70	28.6
2C	0.20	1C	3.09	8C	0.24	7C	4.12	47.6
2D	0.18	1D	2.75	8D	0.24	7D	3.82	66.7
2E	0.26	1E	2.49	8E	0.26	7E	3.54	85.7
4A	5.36	3A	6.18	10A	4.31	9A	7.32	9.5
4B	0.45	3B	4.54	10B	0.37	9B	3.91	28.6
4C	0.28	3C	4.01	10C	0.20	9C	3.32	47.6
4D	0.23	3D	3.54	10D	0.25	9D	3.53	66.7
4E	0.24	3E	3.62	10E	0.48	9E	3.16	85.7
6A	4.13	5A	6.01	12A	6.28	11A	7.84	9.5
6B	0.37	5B	3.30	12B	0.95	11B	5.17	28.6
6C	0.23	5C	3.99	12C	0.20	11C	4.00	47.6
6D	0.21	5D	4.16	12D	0.29	11D	3.97	66.7
6E	0.26	5E	3.78	12E	0.30	11E	3.73	85.7

Table A.10: (continued)

Bridge: 46-290

South Side

Placement Date 9/8/92

Survey Date 8/31/98

Off Crack		On Crack		Depth (mm)
Sample	kg/m ³	Sample	kg/m ³	
2A	6.52	1A	LIP	9.5
2B	1.08	1B	3.93	28.6
2C	0.26	1C	3.71	47.6
2D	0.24	1D	2.78	66.7
2E	0.20	1E	2.48	85.7
4A	7.58	3A	8.03	9.5
4B	1.85	3B	4.70	28.6
4C	0.25	3C	3.98	47.6
4D	0.23	3D	4.33	66.7
4E	0.20	3E	4.12	85.7
6A	6.40	5A	7.35	9.5
6B	1.93	5B	3.94	28.6
6C	0.28	5C	3.48	47.6
6D	0.22	5D	3.48	66.7
6E	0.42	5E	2.61	85.7

Table A.10: (continued)
Bridge: 46-299

East Side
 Placement Date 7/28/94
 Survey Date 8/17/98

West Side
 Placement Date 7/30/94
 Survey Date 8/17/98

Off Crack		On Crack		Off Crack		On Crack		Depth (mm)
Sample	kg/m ³	Sample	kg/m ³	Sample	kg/m ³	Sample	kg/m ³	
2A	3.84	1A	4.47	8A	4.15	7A	3.83	9.5
2B	0.17	1B	2.22	8B	0.66	7B	1.81	28.6
2C	0.17	1C	1.29	8C	0.13	7C	0.98	47.6
2D	0.17	1D	0.63	8D	0.18	7D	0.52	66.7
2E	0.14	1E	0.49	8E	0.19	7E	0.35	85.7
4A	3.28	3A	2.38	10A	4.41	9A	4.03	9.5
4B	0.39	3B	4.45	10B	3.42	9B	2.22	28.6
4C	0.13	3C	1.72	10C	1.06	9C	1.84	47.6
4D	0.16	3D	0.71	10D	0.20	9D	1.38	66.7
4E	0.23	3E	0.32	10E	0.16	9E	1.05	85.7
6A	4.21	5A	4.81	12A	3.90	11A	4.97	9.5
6B	0.55	5B	2.40	12B	0.31	11B	2.47	28.6
6C	0.16	5C	2.11	12C	0.13	11C	1.20	47.6
6D	0.22	5D	1.41	12D	0.18	11D	1.15	66.7
6E	0.18	5E	1.00	12E	0.18	11E	0.79	85.7

Table A.10: (continued)

Bridge: 46-300

West Side

Placement Date 8/14/95

Survey Date 8/14/98

East Side

Placement Date 8/10/95

Survey Date 8/14/98

Off Crack		On Crack		Off Crack		On Crack		Depth (mm)
Sample	kg/m ³	Sample	kg/m ³	Sample	kg/m ³	Sample	kg/m ³	
2A	4.72	1A	4.10	8A	4.62	7A	5.44	9.5
2B	1.91	1B	2.40	8B	1.24	7B	2.27	28.6
2C	0.31	1C	1.24	8C	0.17	7C	1.49	47.6
2D	0.15	1D	0.62	8D	0.00	7D	1.07	66.7
2E	0.12	1E	0.50	8E	0.14	7E	0.63	85.7
4A	4.21	3A	3.76	10A	3.99	9A	4.51	9.5
4B	0.91	3B	1.90	10B	0.59	9B	2.41	28.6
4C	0.00	3C	1.18	10C	0.22	9C	1.50	47.6
4D	0.00	3D	0.95	10D	0.19	9D	0.55	66.7
4E	0.00	3E	0.85	10E	0.16	9E	0.22	85.7
6A	4.98	5A	4.43	12A	5.74	11A	5.09	9.5
6B	1.38	5B	2.51	12B	2.62	11B	2.51	28.6
6C	0.00	5C	1.49	12C	0.35	11C	1.96	47.6
6D	0.00	5D	0.79	12D	0.24	11D	1.62	66.7
6E	0.17	5E	0.27	12E	0.16	11E	1.44	85.7

Table A.10: (continued)

Bridge: 46-301

South Side		South of Center Line	
Placement Date	8/5/94	Placement Date	8/3/94
Survey Date	8/20/98	Survey Date	8/20/98

Off Crack		On Crack		Off Crack		On Crack		Depth (mm)
Sample	kg/m ³	Sample	kg/m ³	Sample	kg/m ³	Sample	kg/m ³	
2A	4.57	1A	5.56	8A	5.31	7A	4.76	9.5
2B	1.29	1B	2.96	8B	1.10	7B	2.79	28.6
2C	0.35	1C	2.38	8C	0.40	7C	1.94	47.6
2D	0.37	1D	2.21	8D	0.28	7D	1.36	66.7
2E	0.36	1E	2.62	8E	0.32	7E	1.23	85.7
4A	5.80	3A	5.63	10A	4.65	9A	5.26	9.5
4B	2.39	3B	3.21	10B	0.99	9B	2.33	28.6
4C	0.42	3C	2.47	10C	0.32	9C	1.69	47.6
4D	0.28	3D	2.33	10D	0.30	9D	1.49	66.7
4E	0.41	3E	2.09	10E	0.39	9E	1.24	85.7
6A	5.23	5A	4.30	12A	4.25	11A	4.74	9.5
6B	1.42	5B	2.26	12B	0.61	11B	2.10	28.6
6C	0.38	5C	1.62	12C	0.30	11C	1.68	47.6
6D	0.41	5D	1.70	12D	0.29	11D	1.28	66.7
6E	0.38	5E	2.11	12E	0.32	11E	0.95	85.7

Table A.10: (continued)
Bridge: 46-301 (continued)

North of CL				North Side				
Placement Date		8/6/94		Placement Date		8/3/94		
Survey Date		8/28/98		Survey Date		8/28/98		
Off Crack		On Crack		Off Crack		On Crack		Depth
Sample	kg/m ³	Sample	kg/m ³	Sample	kg/m ³	Sample	kg/m ³	(mm)
14A	2.88	13A	5.61	20A	5.29	19A	4.70	9.5
14B	1.31	13B	3.54	20B	1.48	19B	2.84	28.6
14C	0.39	13C	2.27	20C	0.27	19C	2.35	47.6
14D	0.34	13D	2.70	20D	0.28	19D	2.37	66.7
14E	0.43	13E	1.83	20E	0.33	19E	2.42	85.7
16A	LIP	15A	5.03	22A	4.56	21A	5.58	9.5
16B	0.69	15B	2.38	22B	1.95	21B	2.69	28.6
16C	0.31	15C	1.70	22C	0.45	21C	1.91	47.6
16D	0.24	15D	1.26	22D	0.23	21D	1.57	66.7
16E	0.30	15E	0.93	22E	0.29	21E	1.50	85.7
18A	5.97	17A	5.48	24A	5.63	23A	4.72	9.5
18B	1.58	17B	3.16	24B	2.57	23B	2.12	28.6
18C	0.34	17C	2.57	24C	0.88	23C	1.36	47.6
18D	0.30	17D	2.33	24D	0.24	23D	0.91	66.7
18E	0.37	17E	1.94	24E	0.22	23E	0.65	85.7

Table A.10: (continued)

Bridge: 46-302

West Side

Placement Date 4/9/96

Survey Date 8/11/98

East Side

Placement Date 4/11/96

Survey Date 8/11/98

Off Crack		On Crack		Off Crack		On Crack		Depth (mm)
Sample	kg/m ³	Sample	kg/m ³	Sample	kg/m ³	Sample	kg/m ³	
2A	0.88	1A	2.39	8A	0.41	7A	2.02	9.5
2B	0.15	1B	1.01	8B	0.00	7B	1.35	28.6
2C	0.00	1C	0.92	8C	0.00	7C	1.39	47.6
2D	0.00	1D	1.16	8D	0.00	7D	1.26	66.7
2E	0.00	1E	1.14	8E	0.00	7E	1.15	85.7
4A	1.60	3A	2.06	10A	0.39	9A	2.17	9.5
4B	0.33	3B	1.05	10B	0.00	9B	1.30	28.6
4C	0.18	3C	1.02	10C	0.13	9C	1.47	47.6
4D	0.00	3D	0.94	10D	0.00	9D	1.39	66.7
4E	0.00	3E	0.96	10E	0.00	9E	0.87	85.7
5A	0.38	6A	1.78	12A	0.66	11A	1.52	9.5
5B	0.00	6B	1.20	12B	0.00	11B	1.08	28.6
5C	0.14	6C	1.26	12C	0.27	11C	1.35	47.6
5D	0.00	6D	1.12	12D	0.14	11D	1.47	66.7
5E	0.00	6E	1.05	12E	0.19	11E	1.44	85.7

Table A.10: (continued)
Bridge: 46-309

East Side
 Placement Date 10/20/95
 Survey Date 8/11/98

West Side
 Placement Date 10/24/95
 Survey Date 8/6/98

Off Crack		On Crack		Off Crack		On Crack		Depth (mm)
Sample	kg/m ³	Sample	kg/m ³	Sample	kg/m ³	Sample	kg/m ³	
2A	6.45	1A	5.29	8A	4.28	7A	4.88	9.5
2B	2.32	1B	2.12	8B	1.59	7B	1.81	28.6
2C	0.29	1C	1.66	8C	0.20	7C	1.28	47.6
2D	0.18	1D	1.51	8D	0.22	7D	0.90	66.7
2E	0.21	1E	1.48	8E	0.28	7E	0.63	85.7
4A	5.60	3A	4.87	10A	3.81	9A	4.75	9.5
4B	1.08	3B	1.82	10B	0.62	9B	1.93	28.6
4C	0.16	3C	1.34	10C	0.15	9C	1.83	47.6
4D	0.00	3D	1.32	10D	0.15	9D	1.33	66.7
4E	0.18	3E	0.84	10E	0.00	9E	0.42	85.7
6A	4.78	5A	4.99	12A	4.45	11A	3.46	9.5
6B	1.11	5B	1.65	12B	0.83	11B	1.87	28.6
6C	0.19	5C	1.48	12C	0.18	11C	1.64	47.6
6D	0.16	5D	1.33	12D	0.16	11D	1.36	66.7
6E	0.15	5E	1.05	12E	0.15	11E	1.33	85.7

Table A.10: (continued)

Bridge: 46-317

South Side		North Side	
Placement Date	7/1/96	Placement Date	6/28/96
Survey Date	8/24/98	Survey Date	8/24/98

Off Crack		On Crack		Off Crack		On Crack		Depth (mm)
Sample	kg/m ³	Sample	kg/m ³	Sample	kg/m ³	Sample	kg/m ³	
2A	2.07	1A	3.23	8A	2.14	7A	2.35	9.5
2B	1.60	1B	1.75	8B	0.28	7B	0.96	28.6
2C	0.30	1C	1.54	8C	0.23	7C	1.56	47.6
2D	0.43	1D	0.68	8D	0.20	7D	1.25	66.7
2E	0.64	1E	0.43	8E	0.20	7E	0.72	85.7
4A	4.26	3A	5.27	10A	2.32	9A	5.52	9.5
4B	0.93	3B	2.42	10B	0.20	9B	1.97	28.6
4C	0.26	3C	2.23	10C	0.24	9C	1.65	47.6
4D	0.24	3D	2.42	10D	0.21	9D	1.34	66.7
4E	0.25	3E	2.21	10E	0.22	9E	1.01	85.7
6A	3.90	5A	4.23	12A	2.29	11A	3.34	9.5
6B	0.27	5B	1.83	12B	0.16	11B	1.55	28.6
6C	LIP	5C	2.32	12C	0.20	11C	1.07	47.6
6D	0.19	5D	1.89	12D	0.20	11D	0.58	66.7
6E	0.22	5E	1.77	12E	0.21	11E	0.41	85.7

Table A.10: (continued)

Bridge: 56-148

Placement Date 7/18/91

Survey Date 8/19/98

Off Crack		On Crack		Depth (mm)
Sample	kg/m ³	Sample	kg/m ³	
2A	8.58	1A	7.97	9.5
2B	3.64	1B	4.48	28.6
2C	0.67	1C	3.24	47.6
2D	0.24	1D	1.95	66.7
2E	0.41	1E	0.57	85.7
4A	10.15	3A	9.53	9.5
4B	5.92	3B	5.65	28.6
4C	1.85	3C	3.26	47.6
4D	0.59	3D	1.30	66.7
4E	0.55	3E	0.45	85.7
6A	7.50	5A	6.29	9.5
6B	4.36	5B	2.97	28.6
6C	1.27	5C	2.84	47.6
6D	0.47	5D	1.76	66.7
6E	0.41	5E	0.71	85.7

Table A.10: (continued)

Bridge: 70-107

Placement Date 10/25/91

Survey Date 8/19/98

Off Crack		On Crack		Depth (mm)
Sample	kg/m ³	Sample	kg/m ³	
2A	8.74	1A	2.43	9.5
2B	3.63	1B	9.68	28.6
2C	1.27	1C	2.67	47.6
2D	0.25	1D	0.84	66.7
2E	0.19	1E	0.43	85.7
4A	10.09	3A	9.78	9.5
4B	4.78	3B	5.20	28.6
4C	1.31	3C	3.64	47.6
4D	0.26	3D	1.53	66.7
4E	0.19	3E	0.28	85.7
6A	8.77	5A	8.82	9.5
6B	5.72	5B	4.45	28.6
6C	2.51	5C	2.00	47.6
6D	0.52	5D	0.66	66.7
6E	0.19	5E	0.18	85.7

Table A.10: (continued)

Bridge: 75-1

North Side		South Side	
Placement Date	10/17/91	Placement Date	10/19/91
Survey Date	9/2/98	Survey Date	9/2/98

Off Crack		On Crack		Off Crack		On Crack		Depth (mm)
Sample	kg/m ³	Sample	kg/m ³	Sample	kg/m ³	Sample	kg/m ³	
2A	4.22	1A	6.52	8A	5.85	7A	6.31	9.5
2B	0.52	1B	3.48	8B	0.77	7B	3.67	28.6
2C	0.33	1C	2.79	8C	0.36	7C	2.93	47.6
2D	0.36	1D	2.21	8D	0.29	7D	2.91	66.7
2E	0.34	1E	0.47	8E	0.23	7E	2.70	85.7
4A	4.25	3A	5.50	10A	7.47	9A	6.17	9.5
4B	1.89	3B	3.01	10B	0.75	9B	3.34	28.6
4C	0.63	3C	2.15	10C	0.49	9C	3.24	47.6
4D	0.31	3D	0.75	10D	0.31	9D	2.69	66.7
4E	0.47	3E	0.59	10E	0.40	9E	2.66	85.7
6A	9.94	5A	7.30	12A	5.06	11A	6.81	9.5
6B	3.65	5B	5.63	12B	1.06	11B	4.03	28.6
6C	0.70	5C	3.97	12C	0.51	11C	3.23	47.6
6D	0.26	5D	1.75	12D	0.35	11D	2.09	66.7
6E	0.27	5E	0.64	12E	0.40	11E	1.33	85.7

Table A.10: (continued)

Bridge: 75-49

South Side		North Side	
Placement Date	6/4/91	Placement Date	6/7/91
Survey Date	9/1/98	Survey Date	9/1/98

Off Crack		On Crack		Off Crack		On Crack		Depth (mm)
Sample	kg/m ³	Sample	kg/m ³	Sample	kg/m ³	Sample	kg/m ³	
2A	7.67	1A	5.65	8A	6.02	7A	6.01	9.5
2B	5.26	1B	3.57	8B	3.28	7B	3.41	28.6
2C	2.05	1C	2.97	8C	1.32	7C	2.62	47.6
2D	0.63	1D	2.00	8D	0.34	7D	2.04	66.7
2E	0.21	1E	0.59	8E	0.28	7E	1.64	85.7
4A	7.06	3A	5.90	10A	6.54	9A	7.00	9.5
4B	3.65	3B	LIP	10B	2.64	9B	3.21	28.6
4C	1.07	3C	3.18	10C	0.43	9C	2.54	47.6
4D	0.29	3D	1.85	10D	0.29	9D	2.54	66.7
4E	0.17	3E	0.48	10E	0.24	9E	1.80	85.7
6A	7.74	5A	6.46	12A	5.16	11A	5.25	9.5
6B	5.89	5B	4.86	12B	3.60	11B	4.75	28.6
6C	2.34	5C	2.96	12C	1.11	11C	3.75	47.6
6D	0.72	5D	2.13	12D	0.32	11D	3.09	66.7
6E	0.33	5E	2.51	12E	0.28	11E	2.49	85.7

Table A.10: (continued)

Bridge: 81-49

West Side

Placement Date 10/21/92

Survey Date 8/5/98

West of CL

Placement Date 10/23/92

Survey Date 8/5/98

Off Crack		On Crack		Off Crack		On Crack		Depth (mm)
Sample	kg/m ³	Sample	kg/m ³	Sample	kg/m ³	Sample	kg/m ³	
2A	3.84	1A	5.72	8A	4.02	7A	5.78	9.5
2B	0.88	1B	3.51	8B	1.80	7B	3.86	28.6
2C	0.00	1C	3.16	8C	0.20	7C	2.82	47.6
2D	0.14	1D	2.74	8D	0.14	7D	1.61	66.7
2E	0.12	1E	1.61	8E	0.00	7E	0.76	85.7
4A	4.49	3A	6.21	10A	3.93	9A	5.37	9.5
4B	1.13	3B	3.41	10B	0.84	9B	3.74	28.6
4C	0.13	3C	2.53	10C	0.00	9C	3.37	47.6
4D	0.15	3D	2.28	10D	0.00	9D	2.32	66.7
4E	0.00	3E	1.43	10E	0.12	9E	1.91	85.7
6A	3.73	5A	5.01	12A	3.46	11A	5.17	9.5
6B	0.30	5B	3.14	12B	0.36	11B	2.59	28.6
6C	0.00	5C	3.23	12C	0.00	11C	1.74	47.6
6D	0.00	5D	2.13	12D	0.00	11D	1.02	66.7
6E	0.16	5E	1.04	12E	0.13	11E	0.62	85.7

Table A.10: (continued)

Bridge: 81-49 (continued)

East Side		East of CL	
Placement Date	4/8/92	Placement Date	4/13/92
Survey Date	8/13/98	Survey Date	8/13/98

Off Crack		On Crack		Off Crack		On Crack		Depth (mm)
Sample	kg/m ³	Sample	kg/m ³	Sample	kg/m ³	Sample	kg/m ³	
14A	3.41	13A	2.71	20A	4.90	19A	4.34	9.5
14B	0.21	13B	1.76	20B	0.90	19B	2.14	28.6
14C	0.00	13C	1.49	20C	0.18	19C	1.60	47.6
14D	0.00	13D	1.38	20D	0.12	19D	1.38	66.7
14E	0.15	13E	1.11	20E	0.18	19E	1.03	85.7
16A	1.77	15A	3.73	22A	4.45	21A	5.30	9.5
16B	0.12	15B	1.91	22B	0.64	21B	3.10	28.6
16C	0.00	15C	1.61	22C	0.00	21C	2.05	47.6
16D	LIP	15D	1.60	22D	0.13	21D	1.70	66.7
16E	0.17	15E	1.44	22E	0.00	21E	1.51	85.7
18A	2.49	17A	3.78	24A	4.11	23A	6.38	9.5
18B	0.33	17B	2.04	24B	0.65	23B	3.30	28.6
18C	0.13	17C	1.39	24C	0.15	23C	2.14	47.6
18D	0.16	17D	0.97	24D	0.19	23D	2.53	66.7
18E	0.18	17E	0.81	24E	0.19	23E	2.25	85.7

Table A.10: (continued)

Bridge: 81-50

South Side

Placement Date 11/21/95

Survey Date 8/12/98

North Side

Placement Date 11/30/95

Survey Date 8/12/98

Off Crack		On Crack		Off Crack		On Crack		Depth (mm)
Sample	kg/m ³	Sample	kg/m ³	Sample	kg/m ³	Sample	kg/m ³	
2A	3.64	1A	4.52	8A	3.17	7A	4.09	9.5
2B	0.33	1B	2.00	8B	0.18	7B	1.31	28.6
2C	0.19	1C	1.76	8C	0.00	7C	1.07	47.6
2D	0.14	1D	1.21	8D	0.00	7D	0.17	66.7
2E	0.16	1E	0.78	8E	0.00	7E	0.00	85.7
4A	2.03	3A	3.07	10A	2.80	9A	3.00	9.5
4B	0.14	3B	1.15	10B	0.35	9B	1.52	28.6
4C	0.00	3C	1.57	10C	0.14	9C	1.72	47.6
4D	0.13	3D	1.07	10D	0.00	9D	1.09	66.7
4E	0.12	3E	0.60	10E	0.00	9E	0.50	85.7
6A	1.91	5A	2.71	12A	3.46	11A	3.73	9.5
6B	0.18	5B	1.42	12B	0.17	11B	1.50	28.6
6C	0.14	5C	1.78	12C	0.18	11C	1.54	47.6
6D	0.18	5D	1.63	12D	0.13	11D	1.30	66.7
6E	0.14	5E	0.41	12E	0.15	11E	0.74	85.7

Table A.10: (continued)

Bridge: 87-453

North Side

Placement Date 6/30/97

Survey Date 10/14/98

South Side

Placement Date 7/3/97

Survey Date 10/14/98

Off Crack		On Crack		Off Crack		On Crack		Depth (mm)
Sample	kg/m ³	Sample	kg/m ³	Sample	kg/m ³	Sample	kg/m ³	
2A	2.82	1A	3.11	8A	2.67	7A	2.36	9.5
2B	0.35	1B	1.31	8B	0.24	7B	0.28	28.6
2C	0.27	1C	1.13	8C	0.28	7C	0.35	47.6
2D	0.22	1D	0.83	8D	0.23	7D	0.33	66.7
2E	0.38	1E	0.55	8E	0.29	7E	0.42	85.7
4A	4.24	3A	3.30	10A	2.52	9A	3.31	9.5
4B	0.92	3B	0.83	10B	0.26	9B	1.17	28.6
4C	0.16	3C	0.37	10C	0.30	9C	1.04	47.6
4D	0.23	3D	0.34	10D	0.20	9D	0.96	66.7
4E	0.31	3E	0.80	10E	0.19	9E	0.78	85.7
6A	3.84	5A	3.23	12A	2.57	11A	3.61	9.5
6B	0.69	5B	0.90	12B	0.31	11B	1.46	28.6
6C	0.27	5C	0.48	12C	0.24	11C	1.30	47.6
6D	0.26	5D	0.40	12D	0.24	11D	0.97	66.7
6E	0.23	5E	0.38	12E	0.21	11E	0.72	Depth

Table A.10: (continued)

Bridge: 87-454

South Side

Placement Date 10/16/96

Survey Date 10/13/98

North Side

Placement Date 9/10/96

Survey Date 10/13/98

Off Crack		On Crack		Off Crack		On Crack		Depth (mm)
Sample	kg/m ³	Sample	kg/m ³	Sample	kg/m ³	Sample	kg/m ³	
1A	4.35	2A	3.74	8A	2.49	7A	3.16	9.5
1B	0.82	2B	1.37	8B	0.28	7B	1.25	28.6
1C	0.26	2C	0.78	8C	0.24	7C	0.99	47.6
1D	0.21	2D	0.92	8D	0.21	7D	0.86	66.7
1E	0.19	2E	0.91	8E	0.24	7E	0.77	85.7
3A	3.75	4A	3.55	10A	3.47	9A	3.77	9.5
3B	0.54	4B	0.83	10B	0.49	9B	1.17	28.6
3C	0.29	4C	0.37	10C	0.20	9C	1.02	47.6
3D	0.23	4D	0.24	10D	0.28	9D	0.83	66.7
3E	0.25	4E	0.44	10E	0.32	9E	0.80	85.7
5A	3.15	6A	3.98	12A	4.27	11A	4.12	9.5
5B	0.45	6B	1.23	12B	1.18	11B	1.52	28.6
5C	0.20	6C	0.74	12C	0.28	11C	1.09	47.6
5D	0.26	6D	0.53	12D	0.26	11D	0.95	66.7
5E	0.20	6E	0.39	12E	0.17	11E	0.68	85.7

Table A.10: (continued)
Bridge: 89-183

West Side
 Placement Date 9/25/90
 Survey Date 7/22/98

East Side
 Placement Date 9/21/90
 Survey Date 7/22/98

Off Crack		On Crack		Off Crack		On Crack		Depth (mm)
Sample	kg/m ³	Sample	kg/m ³	Sample	kg/m ³	Sample	kg/m ³	
2A	5.70	1A	4.66	8A	6.22	7A	6.47	9.5
2B	1.50	1B	2.55	8B	1.68	7B	3.58	28.6
2C	0.20	1C	2.25	8C	0.21	7C	3.17	47.6
2D	0.12	1D	1.36	8D	0.14	7D	2.38	66.7
2E	0.16	1E	0.82	8E	0.16	7E	2.54	85.7
4A	3.88	3A	5.00	9A	4.67	10A	5.12	9.5
4B	0.45	3B	2.41	9B	2.07	10B	3.70	28.6
4C	0.00	3C	2.35	9C	0.53	10C	2.40	47.6
4D	0.00	3D	1.64	9D	0.00	10D	1.78	66.7
4E	0.16	3E	0.62	9E	0.16	10E	1.05	85.7
6A	5.10	5A	5.14	11A	5.13	12A	6.67	9.5
6B	1.34	5B	2.95	11B	1.89	12B	3.45	28.6
6C	0.16	5C	2.28	11C	0.23	12C	2.26	47.6
6D	0.24	5D	2.18	11D	0.14	12D	1.68	66.7
6E	0.29	5E	2.23	11E	0.13	12E	1.12	85.7

Table A.10: (continued)

Bridge: 89-184

West Side

Placement Date 9/28/90

Survey Date 7/27/98

East Side

Placement Date 9/26/90

Survey Date 7/27/98

Off Crack		On Crack		Off Crack		On Crack		Depth (mm)
Sample	kg/m ³	Sample	kg/m ³	Sample	kg/m ³	Sample	kg/m ³	
2A	3.78	1A	5.03	8A	6.56	7A	7.72	9.5
2B	0.61	1B	3.61	8B	0.38	7B	3.47	28.6
2C	0.14	1C	3.17	8C	0.19	7C	2.55	47.6
2D	0.17	1D	1.60	8D	0.16	7D	3.52	66.7
2E	0.17	1E	1.50	8E	0.21	7E	2.22	85.7
4A	5.52	3A	7.19	10A	8.02	9A	7.03	9.5
4B	0.17	3B	3.14	10B	1.00	9B	3.27	28.6
4C	0.19	3C	2.95	10C	0.21	9C	2.56	47.6
4D	0.15	3D	2.87	10D	0.22	9D	2.84	66.7
4E	0.20	3E	2.90	10E	0.19	9E	2.62	85.7
6A	4.66	5A	8.36	12A	4.34	11A	6.68	9.5
6B	0.18	5B	4.23	12B	0.22	11B	2.81	28.6
6C	0.16	5C	3.13	12C	0.18	11C	2.50	47.6
6D	0.15	5D	3.91	12D	0.00	11D	3.12	66.7
6E	0.18	5E	3.66	12E	0.15	11E	2.40	85.7

Table A.10: (continued)

Bridge: 89-185

East Side

Placement Date 6/21/90

Survey Date 7/28/98

West Side

Placement Date 6/23/90

Survey Date 7/28/98

Off Crack		On Crack		Off Crack		On Crack		Depth (mm)
Sample	kg/m ³	Sample	kg/m ³	Sample	kg/m ³	Sample	kg/m ³	
2A	6.51	1A	7.20	8A	8.07	7A	7.75	9.5
2B	2.96	1B	4.66	8B	4.92	7B	4.33	28.6
2C	0.80	1C	3.17	8C	2.15	7C	3.29	47.6
2D	0.15	1D	2.49	8D	0.75	7D	3.45	66.7
2E	0.14	1E	1.48	8E	0.18	7E	3.17	85.7
4A	5.20	3A	5.68	10A	8.56	9A	6.87	9.5
4B	1.62	3B	3.67	10B	6.03	9B	3.73	28.6
4C	0.14	3C	2.85	10C	3.29	9C	3.90	47.6
4D	0.13	3D	1.66	10D	1.54	9D	3.08	66.7
4E	0.00	3E	0.60	10E	0.27	9E	1.23	85.7
6A	5.38	5A	5.76	11A	6.37	12A	6.72	9.5
6B	2.46	5B	3.42	11B	3.57	12B	4.85	28.6
6C	0.69	5C	3.08	11C	1.16	12C	3.49	47.6
6D	0.00	5D	2.75	11D	0.22	12D	2.38	66.7
6E	0.00	5E	2.53	11E	0.25	12E	1.54	85.7

Table A.10: (continued)

Bridge: 89-186

South Side

Placement Date 9/17/90

Survey Date 7/27/98

North Side

Placement Date 9/4/90

Survey Date 7/27/98

Off Crack		On Crack		Off Crack		On Crack		Depth (mm)
Sample	kg/m ³	Sample	kg/m ³	Sample	kg/m ³	Sample	kg/m ³	
2A	5.09	1A	7.48	7A	6.02	8A	7.91	9.5
2B	1.69	1B	4.31	7B	1.35	8B	4.14	28.6
2C	0.20	1C	3.19	7C	0.14	8C	2.64	47.6
2D	0.16	1D	2.76	7D	0.15	8D	1.40	66.7
2E	0.23	1E	1.78	7E	0.19	8E	0.80	85.7
4A	5.83	3A	6.59	9A	6.35	10A	5.85	9.5
4B	1.85	3B	3.63	9B	1.72	10B	2.65	28.6
4C	0.22	3C	3.28	9C	0.18	10C	2.46	47.6
4D	0.20	3D	3.49	9D	0.20	10D	2.12	66.7
4E	0.19	3E	1.79	9E	0.18	10E	1.17	85.7
6A	6.91	5A	5.29	11A	6.09	12A	6.34	9.5
6B	2.57	5B	2.98	11B	0.99	12B	3.90	28.6
6C	0.48	5C	2.21	11C	0.14	12C	3.13	47.6
6D	0.24	5D	1.07	11D	0.25	12D	2.32	66.7
6E	0.22	5E	0.43	11E	0.19	12E	1.62	85.7

Table A.10: (continued)

Bridge: 89-187

North Side		South Side	
Placement Date	6/28/90	Placement Date	6/26/90
Survey Date	7/28/98	Survey Date	7/28/98

Off Crack		On Crack		Off Crack		On Crack		Depth (mm)
Sample	kg/m ³	Sample	kg/m ³	Sample	kg/m ³	Sample	kg/m ³	
1A	5.44	2A	6.65	8A	4.60	7A	6.90	9.5
1B	1.52	2B	3.43	8B	0.44	7B	3.81	28.6
1C	0.23	2C	2.80	8C	0.15	7C	2.48	47.6
1D	0.00	2D	2.73	8D	0.17	7D	2.14	66.7
1E	0.00	2E	1.93	8E	0.14	7E	2.19	85.7
3A	2.75	4A	5.44	10A	3.69	9A	6.57	9.5
3B	0.41	4B	2.52	10B	0.28	9B	3.02	28.6
3C	0.00	4C	1.83	10C	0.00	9C	2.66	47.6
3D	0.12	4D	1.71	10D	0.00	9D	2.31	66.7
3E	0.16	4E	0.85	10E	0.00	9E	1.34	85.7
5A	3.68	6A	7.13	12A	5.83	11A	6.47	9.5
5B	0.26	6B	3.31	12B	2.36	11B	3.44	28.6
5C	0.11	6C	2.57	12C	1.01	11C	3.26	47.6
5D	0.00	6D	2.63	12D	0.18	11D	3.67	66.7
5E	0.00	6E	2.61	12E	0.13	11E	2.53	85.7

Table A.10: (continued)

Bridge: 89-196

East Side

Placement Date 5/1/92

Survey Date 8/10/98

West Side

Placement Date 5/5/92

Survey Date 8/10/98

Off Crack		On Crack		Off Crack		On Crack		Depth (mm)
Sample	kg/m ³	Sample	kg/m ³	Sample	kg/m ³	Sample	kg/m ³	
2A	5.60	1A	4.57	8A	LIP	7A	7.15	9.5
2B	1.75	1B	2.87	8B	0.28	7B	5.06	28.6
2C	0.29	1C	1.91	8C	0.18	7C	4.02	47.6
2D	0.23	1D	1.30	8D	0.15	7D	3.14	66.7
2E	0.36	1E	0.58	8E	0.26	7E	2.87	85.7
4A	3.37	3A	6.65	10A	7.75	9A	8.17	9.5
4B	0.75	3B	4.30	10B	4.44	9B	4.37	28.6
4C	0.14	3C	2.83	10C	1.53	9C	3.49	47.6
4D	0.12	3D	2.27	10D	0.27	9D	2.96	66.7
4E	0.17	3E	1.26	10E	0.23	9E	2.26	85.7
6A	2.57	5A	7.45	12A	5.60	11A	8.56	9.5
6B	0.26	5B	4.08	12B	1.73	11B	5.13	28.6
6C	0.13	5C	2.84	12C	0.70	11C	3.63	47.6
6D	0.21	5D	1.93	12D	0.32	11D	2.96	66.7
6E	0.21	5E	1.32	12E	0.32	11E	1.88	85.7

Table A.10: (continued)

Bridge: 89-198

West Side		East Side	
Placement Date	8/27/91	Placement Date	8/24/91
Survey Date	8/4/98	Survey Date	8/4/98

Off Crack		On Crack		Off Crack		On Crack		Depth (mm)
Sample	kg/m ³	Sample	kg/m ³	Sample	kg/m ³	Sample	kg/m ³	
2A	3.97	1A	6.16	8A	5.71	7A	7.04	9.5
2B	0.39	1B	3.93	8B	0.61	7B	3.97	28.6
2C	0.00	1C	3.84	8C	0.17	7C	3.47	47.6
2D	0.15	1D	3.31	8D	0.13	7D	2.71	66.7
2E	0.15	1E	3.19	8E	0.16	7E	2.39	85.7
4A	5.71	3A	5.73	10A	6.37	9A	7.02	9.5
4B	2.21	3B	4.08	10B	1.64	9B	2.94	28.6
4C	0.63	3C	3.36	10C	0.15	9C	1.86	47.6
4D	0.15	3D	2.64	10D	0.13	9D	0.85	66.7
4E	0.15	3E	1.91	10E	0.19	9E	0.23	85.7
6A	3.99	5A	6.28	12A	6.18	11A	6.70	9.5
6B	0.52	5B	3.41	12B	1.34	11B	3.21	28.6
6C	0.00	5C	2.35	12C	0.00	11C	1.82	47.6
6D	0.13	5D	1.38	12D	0.00	11D	1.50	66.7
6E	0.15	5E	0.81	12E	0.00	11E	0.91	85.7

Table A.10: (continued)

Bridge: 89-199

East Side

Placement Date 8/26/91

Survey Date 8/7/98

West Side

Placement Date 8/28/91

Survey Date 8/7/98

Off Crack		On Crack		Off Crack		On Crack		Depth (mm)
Sample	kg/m ³	Sample	kg/m ³	Sample	kg/m ³	Sample	kg/m ³	
2A	5.08	1A	6.28	8A	6.76	7A	7.75	9.5
2B	1.18	1B	3.27	8B	1.14	7B	4.21	28.6
2C	0.16	1C	2.57	8C	0.15	7C	3.23	47.6
2D	0.16	1D	1.84	8D	0.14	7D	2.38	66.7
2E	0.26	1E	0.83	8E	0.18	7E	1.36	85.7
4A	4.60	3A	7.61	10A	6.17	9A	7.46	9.5
4B	0.49	3B	3.61	10B	0.51	9B	3.94	28.6
4C	0.14	3C	2.63	10C	0.16	9C	2.93	47.6
4D	0.17	3D	2.05	10D	0.14	9D	2.83	66.7
4E	0.26	3E	1.53	10E	0.23	9E	2.81	85.7
6A	5.65	5A	5.91	12A	6.18	11A	6.96	9.5
6B	2.00	5B	2.62	12B	0.94	11B	3.26	28.6
6C	0.28	5C	2.51	12C	0.15	11C	2.84	47.6
6D	0.14	5D	2.57	12D	0.19	11D	2.62	66.7
6E	0.24	5E	1.31	12E	0.21	11E	1.59	85.7

Table A.10: (continued)

Bridge: 89-200

West Side

Placement Date 8/17/91

Survey Date 8/4/98

East Side

Placement Date 8/20/91

Survey Date 8/4/98

Off Crack		On Crack		Off Crack		On Crack		Depth (mm)
Sample	kg/m ³	Sample	kg/m ³	Sample	kg/m ³	Sample	kg/m ³	
2A	3.82	1A	4.73	8A	5.23	7A	7.84	9.5
2B	0.96	1B	2.51	8B	0.46	7B	3.49	28.6
2C	0.00	1C	2.52	8C	0.14	7C	2.53	47.6
2D	0.15	1D	2.12	8D	0.00	7D	2.34	66.7
2E	0.17	1E	1.06	8E	0.20	7E	1.57	85.7
4A	6.61	3A	6.00	10A	6.70	9A	7.66	9.5
4B	1.39	3B	2.90	10B	0.76	9B	4.43	28.6
4C	0.16	3C	1.45	10C	0.22	9C	3.69	47.6
4D	0.24	3D	0.62	10D	0.14	9D	3.03	66.7
4E	0.24	3E	0.19	10E	0.35	9E	2.16	85.7
6A	5.26	5A	6.75	12A	5.74	11A	6.11	9.5
6B	1.06	5B	4.10	12B	1.22	11B	4.65	28.6
6C	0.00	5C	3.03	12C	0.14	11C	3.27	47.6
6D	0.18	5D	2.57	12D	0.15	11D	2.99	66.7
6E	0.17	5E	1.47	12E	0.23	11E	3.19	85.7

Table A.10: (continued)
Bridge: 89-201

East Side				West Side				
Placement Date		8/21/91		Placement Date		8/19/91		
Survey Date		8/7/98		Survey Date		8/7/98		
Off Crack		On Crack		Off Crack		On Crack		Depth
Sample	kg/m ³	Sample	kg/m ³	Sample	kg/m ³	Sample	kg/m ³	(mm)
2A	2.82	1A	6.70	8A	4.89	7A	6.80	9.5
2B	0.14	1B	3.31	8B	1.29	7B	3.88	28.6
2C	0.00	1C	2.74	8C	0.17	7C	3.24	47.6
2D	0.00	1D	2.89	8D	0.17	7D	3.14	66.7
2E	0.16	1E	2.88	8E	0.22	7E	3.04	85.7
4A	5.39	3A	3.86	10A	6.70	9A	7.66	9.5
4B	0.62	3B	2.90	10B	0.76	9B	4.43	28.6
4C	0.15	3C	2.37	10C	0.22	9C	3.69	47.6
4D	0.14	3D	2.62	10D	0.14	9D	3.03	66.7
4E	0.13	3E	1.88	10E	0.35	9E	2.16	85.7
6A	5.13	5A	7.59	12A	5.74	11A	6.11	9.5
6B	1.06	5B	3.59	12B	1.22	11B	4.65	28.6
6C	0.18	5C	2.68	12C	0.14	11C	3.27	47.6
6D	0.00	5D	1.84	12D	0.15	11D	2.99	66.7
6E	0.15	5E	1.38	12E	0.23	11E	3.19	85.7

Table A.10: (continued)

Bridge: 89-204

Placement Date 10/3/91
 Survey Date 8/10/98

Off Crack		On Crack		Depth (mm)
Sample	kg/m ³	Sample	kg/m ³	
2A	4.01	1A	5.88	9.5
2B	1.06	1B	3.07	28.6
2C	0.12	1C	2.78	47.6
2D	0.00	1D	2.18	66.7
2E	0.00	1E	1.78	85.7
4A	6.93	3A	8.59	9.5
4B	3.72	3B	6.47	28.6
4C	0.90	3C	4.98	47.6
4D	0.14	3D	3.58	66.7
4E	0.14	3E	4.19	85.7
6A	8.13	5A	8.30	9.5
6B	3.11	5B	5.50	28.6
6C	0.50	5C	4.42	47.6
6D	0.12	5D	2.45	66.7
6E	0.15	5E	1.62	85.7

Table A.10: (continued)

Bridge: 89-206

Left Side

Placement Date 10/10/95

Survey Date 7/14/98

Right Side

Placement Date 10/4/95

Survey Date 7/14/98

Off Crack		On Crack		Off Crack		On Crack		Depth (mm)
Sample	kg/m ³	Sample	kg/m ³	Sample	kg/m ³	Sample	kg/m ³	
2A	1.54	1A	2.26	8A	0.69	7A	0.85	9.5
2B	0.20	1B	1.39	8B	0.00	7B	0.78	28.6
2C	0.00	1C	1.32	8C	0.00	7C	0.63	47.6
2D	0.00	1D	1.23	8D	0.11	7D	0.15	66.7
2E	0.00	1E	1.04	8E	LIP	7E	0.00	85.7
4A	0.85	3A	1.10	10A	0.72	9A	1.50	9.5
4B	0.00	3B	0.64	10B	0.33	9B	1.27	28.6
4C	0.00	3C	0.17	10C	0.00	9C	0.86	47.6
4D	0.00	3D	0.00	10D	0.00	9D	1.06	66.7
4E	0.00	3E	0.17	10E	0.00	9E	1.21	85.7
6A	0.94	5A	1.92	12A	0.72	11A	1.01	9.5
6B	0.00	5B	1.45	12B	0.00	11B	0.69	28.6
6C	0.00	5C	2.82	12C	0.00	11C	0.95	47.6
6D	0.00	5D	0.21	12D	0.00	11D	1.11	66.7
6E	0.00	5E	0.00	12E	0.00	11E	1.06	85.7

Table A.10: (continued)

Bridge: 89-207

Right Side

Placement Date 4/19/96

Survey Date 7/13/98

Left Side

Placement Date 10/24/95

Survey Date 7/13/98

Off Crack		On Crack		Off Crack		On Crack		Depth (mm)
Sample	kg/m ³	Sample	kg/m ³	Sample	kg/m ³	Sample	kg/m ³	
1A	2.67	2A	2.92	7A	0.97	8A	2.74	9.5
1B	0.56	2B	1.17	7B	0.12	8B	1.62	28.6
1C	0.31	2C	1.32	7C	0.14	8C	1.27	47.6
1D	0.17	2D	1.29	7D	0.00	8D	1.00	66.7
1E	0.16	2E	1.07	7E	0.00	8E	1.68	85.7
3A	1.89	4A	1.49	9A	0.81	10A	1.38	9.5
3B	0.23	4B	0.64	9B	0.00	10B	1.39	28.6
3C	0.22	4C	0.33	9C	0.00	10C	1.55	47.6
3D	0.18	4D	0.22	9D	0.00	10D	1.73	66.7
3E	0.19	4E	0.20	9E	0.00	10E	1.55	85.7
5A	1.89	6A	3.22	11A	1.22	12A	0.85	9.5
5B	0.20	6B	1.51	11B	0.15	12B	0.48	28.6
5C	0.20	6C	1.58	11C	0.19	12C	1.45	47.6
5D	0.20	6D	1.22	11D	0.00	12D	1.12	66.7
5E	0.15	6E	1.27	11E	0.00	12E	0.43	85.7

Table A.10: (continued)

Bridge: 89-208

Placement Date 6/15/95
 Survey Date 6/22/98

Off Crack		On Crack		Depth (mm)
Sample	kg/m ³	Sample	kg/m ³	
2A	3.47	1A	2.94	9.5
2B	0.52	1B	0.54	28.6
2C	0.13	1C	0.00	47.6
2D	0.00	1D	0.38	66.7
2E	0.00	1E	0.37	85.7
4A	4.10	3A	3.14	9.5
4B	0.59	3B	0.80	28.6
4C	0.18	3C	0.17	47.6
4D	0.24	3D	0.00	66.7
4E	0.14	3E	0.13	85.7
5A	3.78	6A	2.65	9.5
5B	0.42	6B	0.38	28.6
5C	0.00	6C	0.00	47.6
5D	0.00	6D	0.00	66.7
5E	0.15	6E	0.00	85.7

Table A.10: (continued)

Bridge: 89-210

Left Side

Placement Date 10/18/95

Survey Date 6/24/98

Right Side

Placement Date 10/12/95

Survey Date 6/24/98

Off Crack		On Crack		Off Crack		On Crack		Depth (mm)
Sample	kg/m ³	Sample	kg/m ³	Sample	kg/m ³	Sample	kg/m ³	
2A	0.78	1A	1.75	8A	0.60	7A	1.45	9.5
2B	0.13	1B	0.80	8B	0.23	7B	1.78	28.6
2C	0.20	1C	1.41	8C	0.18	7C	1.86	47.6
2D	0.13	1D	1.38	8D	0.19	7D	1.61	66.7
2E	0.14	1E	1.33	8E	0.27	7E	0.92	85.7
4A	1.01	3A	2.86	9A	0.67	10A	2.20	9.5
4B	0.17	3B	1.59	9B	0.13	10B	1.55	28.6
4C	0.25	3C	1.49	9C	0.15	10C	1.85	47.6
4D	0.13	3D	1.65	9D	0.15	10D	1.79	66.7
4E	0.15	3E	1.91	9E	0.13	10E	0.71	85.7
6A	1.76	5A	1.41	11A	0.60	12A	2.44	9.5
6B	0.14	5B	1.28	11B	0.22	12B	1.22	28.6
6C	0.16	5C	1.50	11C	0.20	12C	0.42	47.6
6D	0.00	5D	1.52	11D	0.13	12D	0.18	66.7
6E	0.00	5E	1.43	11E	0.15	12E	0.20	85.7

Table A.10: (continued)

Bridge: 89-234

South Side		Center	
Placement Date	6/20/96	Placement Date	6/28/96
Survey Date	7/9/98	Survey Date	7/9/98

Off Crack		On Crack		Off Crack		On Crack		Depth (mm)
Sample	kg/m ³	Sample	kg/m ³	Sample	kg/m ³	Sample	kg/m ³	
2A	3.33	1A	4.50	8A	4.72	7A	4.16	9.5
2B	0.17	1B	2.03	8B	0.39	7B	0.85	28.6
2C	0.14	1C	1.91	8C	0.20	7C	0.88	47.6
2D	0.15	1D	0.65	8D	0.12	7D	1.24	66.7
2E	0.12	1E	0.17	8E	0.14	7E	0.87	85.7
4A	3.80	3A	4.22	10A	3.18	9A	4.90	9.5
4B	0.47	3B	1.82	10B	0.23	9B	1.21	28.6
4C	0.16	3C	1.72	10C	0.00	9C	0.51	47.6
4D	0.13	3D	1.75	10D	0.18	9D	0.75	66.7
4E	0.40	3E	1.79	10E	0.12	9E	0.78	85.7
6A	2.96	5A	3.15	12A	2.90	11A	4.69	9.5
6B	0.12	5B	0.96	12B	0.16	11B	3.14	28.6
6C	0.14	5C	0.84	12C	0.00	11C	2.39	47.6
6D	0.16	5D	0.60	12D	0.16	11D	1.95	66.7
6E	0.11	5E	0.77	12E	0.13	11E	2.47	85.7

Table A.10: (continued)

Bridge: 89-234 (continued)

North Side

Placement Date 6/25/96

Survey Date 7/9/98

Off Crack		On Crack		Depth (mm)
Sample	kg/m ³	Sample	kg/m ³	
14A	3.36	13A	3.32	9.5
14B	0.15	13B	1.37	28.6
14C	0.15	13C	1.12	47.6
14D	0.12	13D	0.79	66.7
14E	0.00	13E	0.36	85.7
16A	2.86	15A	3.71	9.5
16B	0.18	15B	1.60	28.6
16C	0.12	15C	1.26	47.6
16D	0.13	15D	1.00	66.7
16E	0.00	15E	0.48	85.7
18A	3.01	17A	3.26	9.5
18B	0.19	17B	1.52	28.6
18C	0.00	17C	1.66	47.6
18D	0.00	17D	1.68	66.7
18E	0.00	17E	0.36	85.7

Table A.10: (continued)
Bridge: 89-235

Placement Date 5/1/97
 Survey Date 7/1/98

Off Crack		On Crack		Depth (mm)
Sample	kg/m ³	Sample	kg/m ³	
2A	1.42	1A	1.53	9.5
2B	0.17	1B	0.97	28.6
2C	0.15	1C	0.61	47.6
2D	0.12	1D	0.49	66.7
2E	0.17	1E	0.25	85.7
4A	0.73	3A	1.56	9.5
4B	0.15	3B	1.36	28.6
4C	0.17	3C	0.87	47.6
4D	0.20	3D	0.68	66.7
4E	0.12	3E	0.14	85.7
6A	1.47	5A	1.62	9.5
6B	0.28	5B	0.64	28.6
6C	0.14	5C	0.18	47.6
6D	0.14	5D	0.15	66.7
6E	0.14	5E	0.21	85.7

Table A.10: (continued)

Bridge: 89-240

West Side

Placement Date 8/7/97

Survey Date 6/29/98

East Side

Placement Date 8/5/97

Survey Date 6/29/98

Off Crack		On Crack		Off Crack		On Crack		Depth (mm)
Sample	kg/m ³	Sample	kg/m ³	Sample	kg/m ³	Sample	kg/m ³	
1A	1.76	2A	2.42	7A	1.78	8A	2.46	9.5
1B	0.19	2B	LIP	7B	0.17	8B	0.38	28.6
1C	0.16	2C	1.07	7C	0.15	8C	0.18	47.6
1D	0.22	2D	0.79	7D	0.19	8D	0.19	66.7
1E	0.19	2E	0.23	7E	0.17	8E	0.17	85.7
3A	3.38	4A	3.67	9A	1.65	10A	2.01	9.5
3B	0.29	4B	0.84	9B	0.16	10B	0.79	28.6
3C	0.23	4C	0.18	9C	0.17	10C	1.05	47.6
3D	0.26	4D	0.18	9D	0.17	10D	0.30	66.7
3E	0.19	4E	0.19	9E	0.16	10E	0.16	85.7
5A	5.04	6A	3.90	11A	2.16	12A	2.53	9.5
5B	0.44	6B	1.06	11B	0.18	12B	0.20	28.6
5C	0.23	6C	0.32	11C	0.18	12C	0.21	47.6
5D	0.28	6D	0.20	11D	0.17	12D	0.20	66.7
5E	0.18	6E	0.17	11E	0.16	12E	0.23	85.7

Table A.10: (continued)

Bridge: 89-244

Left Side

Placement Date 10/21/97

Survey Date 7/6/98

Right Side

Placement Date 10/17/97

Survey Date 7/6/98

Off Crack		On Crack		Off Crack		On Crack		Depth (mm)
Sample	kg/m ³	Sample	kg/m ³	Sample	kg/m ³	Sample	kg/m ³	
1A	4.62	2A	3.63	7A	3.36	8A	5.24	9.5
1B	0.27	2B	0.18	7B	0.21	8B	0.92	28.6
1C	0.24	2C	0.14	7C	0.21	8C	0.55	47.6
1D	0.12	2D	0.14	7D	0.12	8D	0.32	66.7
1E	0.18	2E	0.14	7E	0.13	8E	0.15	85.7
4A	4.16	3A	4.78	10A	3.61	9A	3.93	9.5
4B	0.18	3B	1.29	10B	0.17	9B	0.49	28.6
4C	0.19	3C	0.67	10C	0.13	9C	0.23	47.6
4D	0.15	3D	0.71	10D	0.15	9D	0.17	66.7
4E	0.14	3E	0.69	10E	0.13	9E	0.13	85.7
5A	3.79	6A	3.43	11A	3.18	12A	0.62	9.5
5B	0.17	6B	0.15	11B	0.12	12B	0.16	28.6
5C	0.20	6C	0.19	11C	0.15	12C	0.26	47.6
5D	0.14	6D	0.14	11D	0.15	12D	0.13	66.7
5E	0.13	6E	0.15	11E	0.00	12E	0.00	85.7

Table A.10: (continued)

Bridge: 89-245

Right Side Unit 1

Placement Date 10/24/97

Survey Date 7/16/98

Left Side Unit 1

Placement Date 10/22/97

Survey Date 7/16/98

Off Crack		On Crack		Off Crack		On Crack		Depth (mm)
Sample	kg/m ³	Sample	kg/m ³	Sample	kg/m ³	Sample	kg/m ³	
1A	3.15	2A	3.32	14A	3.09	13A	5.19	9.5
1B	0.18	2B	0.43	14B	0.32	13B	1.41	28.6
1C	0.00	2C	0.18	14C	0.27	13C	1.00	47.6
1D	0.20	2D	0.38	14D	0.16	13D	0.10	66.7
1E	0.00	2E	0.13	14E	0.12	13E	0.46	85.7
4A	3.76	3A	3.50	16A	2.35	15A	2.78	9.5
4B	0.31	3B	0.62	16B	0.12	15B	2.33	28.6
4C	0.19	3C	0.19	16C	0.23	15C	2.19	47.6
4D	0.19	3D	0.48	16D	0.00	15D	1.45	66.7
4E	0.15	3E	0.12	16E	0.12	15E	0.90	85.7
5A	3.09			17A	2.80			9.5
5B	0.13			17B	0.00			28.6
5C	0.17			17C	0.16			47.6
5D	0.32			17D	0.00			66.7
5E	0.00			17E	0.00			85.7

Table A.10: (continued)

Bridge: 89-245

Right Side Unit 1

Placement Date 10/24/97

Survey Date 7/16/98

Left Side Unit 1

Placement Date 10/22/97

Survey Date 7/16/98

Off Crack		On Crack		Off Crack		On Crack		Depth (mm)
Sample	kg/m ³	Sample	kg/m ³	Sample	kg/m ³	Sample	kg/m ³	
6A	4.47			18A	3.31			9.5
6B	0.25			18B	0.20			28.6
6C	0.00			18C	0.23			47.6
6D	0.26			18D	0.16			66.7
6E	0.00			18E	0.15			85.7

Table A.10: (continued)

Bridge: 89-245

Right Side Unit 2

Placement Date 10/23/97

Survey Date 7/16/98

Left Side Unit 2

Placement Date 10/20/97

Survey Date 7/16/98

Off Crack		On Crack		Off Crack		On Crack		Depth (mm)
Sample	kg/m ³	Sample	kg/m ³	Sample	kg/m ³	Sample	kg/m ³	
7A	3.14	8A	2.53	19A	4.53	20A	5.24	9.5
7B	0.00	8B	0.29	19B	0.27	20B	1.88	28.6
7C	0.14	8C	0.19	19C	0.16	20C	1.39	47.6
7D	0.00	8D	0.15	19D	0.15	20D	1.20	66.7
7E	0.00	8E	0.16	19E	0.13	20E	0.60	85.7
9A	3.96	10A	3.12	21A	3.33	22A	4.40	9.5
9B	0.17	10B	0.24	21B	0.15	22B	1.63	28.6
9C	0.23	10C	0.31	21C	0.19	22C	1.46	47.6
9D	0.00	10D	0.17	21D	0.00	22D	1.03	66.7
9E	0.00	10E	0.17	21E	0.00	22E	0.57	85.7
12A	4.36	11A	3.06	24A	4.25	23A	4.31	9.5
12B	0.43	11B	0.25	24B	0.17	23B	1.34	28.6
12C	0.18	11C	0.24	24C	0.17	23C	0.89	47.6
12D	0.19	11D	0.16	24D	0.19	23D	0.55	66.7
12E	0.00	11E	0.22	24E	0.11	23E	0.23	85.7

Table A.10: (continued)

Bridge: 89-246

East Side

Placement Date 9/8/97

Survey Date 7/17/98

West Side

Placement Date 9/10/97

Survey Date 7/17/98

Off Crack		On Crack		Off Crack		On Crack		Depth (mm)
Sample	kg/m ³	Sample	kg/m ³	Sample	kg/m ³	Sample	kg/m ³	
2A	0.96	1A	0.75	7A	0.94	8A	1.48	9.5
2B	0.14	1B	0.11	7B	0.15	8B	0.43	28.6
2C	0.14	1C	0.24	7C	0.17	8C	0.46	47.6
2D	0.14	1D	0.00	7D	0.16	8D	0.30	66.7
2E	0.00	1E	0.00	7E	0.12	8E	0.39	85.7
4A	0.99	3A	1.11	11A	1.16	9A	1.27	9.5
4B	0.11	3B	0.16	11B	0.17	9B	0.44	28.6
4C	0.00	3C	0.12	11C	0.19	9C	0.30	47.6
4D	0.21	3D	0.19	11D	0.00	9D	0.00	66.7
4E	0.13	3E	0.14	11E	0.13	9E	0.13	85.7
6A	0.77	5A	1.15	12A	1.31	10A	1.18	9.5
6B	0.00	5B	0.12	12B	0.15	10B	0.00	28.6
6C	0.15	5C	0.18	12C	0.14	10C	0.18	47.6
6D	0.00	5D	0.18	12D	0.16	10D	0.00	66.7
6E	0.00	5E	0.13	12E	0.11	10E	0.14	85.7

Table A.10: (continued)

Bridge: 89-247

West Side

Placement Date 5/5/97

Survey Date 7/20/98

East Side

Placement Date 5/7/97

Survey Date 7/20/98

Off Crack		On Crack		Off Crack		On Crack		Depth (mm)
Sample	kg/m ³	Sample	kg/m ³	Sample	kg/m ³	Sample	kg/m ³	
1A	0.00	2A	1.04	7A	0.52	8A	1.28	9.5
1B	0.00	2B	0.50	7B	0.00	8B	0.39	28.6
1C	0.00	2C	0.68	7C	0.00	8C	0.25	47.6
1D	0.00	2D	0.64	7D	0.00	8D	0.16	66.7
1E	0.00	2E	0.69	7E	0.00	8E	0.00	85.7
4A	1.11	3A	1.00	9A	1.41	10A	1.18	9.5
4B	0.22	3B	0.81	9B	0.12	10B	0.72	28.6
4C	0.00	3C	0.64	9C	0.00	10C	0.69	47.6
4D	0.00	3D	0.71	9D	0.00	10D	0.47	66.7
4E	0.00	3E	0.86	9E	0.00	10E	0.22	85.7
6A	0.70	5A	0.96	11A	0.76	12A	2.08	9.5
6B	0.10	5B	0.55	11B	0.09	12B	0.74	28.6
6C	0.00	5C	0.58	11C	0.18	12C	0.50	47.6
6D	0.00	5D	0.61	11D	0.13	12D	0.33	66.7
6E	0.00	5E	0.38	11E	0.00	12E	0.24	85.7

Table A.10: (continued)

Bridge: 89-248

New bridge that has not been exposed to deicing chemicals and only seen minimal traffic
Chloride levels are base line levels.

Right Side

Placement Date 5/1/98
Survey Date 8/27/98

Left Side

Placement Date 4/24/98
Survey Date 8/27/98

Off Crack		On Crack		Off Crack		On Crack		Depth (mm)
Sample	kg/m ³	Sample	kg/m ³	Sample	kg/m ³	Sample	kg/m ³	
1A	0.36	2A	0.41	7A	LIP	8A	0.34	9.5
1B	0.29	2B	0.38	7B	0.21	8B	0.21	28.6
1C	0.40	2C	0.41	7C	0.25	8C	0.28	47.6
1D	0.34	2D	0.34	7D	0.00	8D	0.25	66.7
1E	0.43	2E	0.36	7E	0.22	8E	0.24	85.7
3A	0.42	4A	0.37	10A	0.33	9A	0.32	9.5
3B	0.35	4B	0.37	10B	0.23	9B	0.19	28.6
3C	0.40	4C	0.40	10C	0.28	9C	0.21	47.6
3D	0.41	4D	0.39	10D	0.24	9D	0.22	66.7
3E	0.38	4E	0.59	10E	0.31	9E	0.24	85.7
5A	0.39	6A	0.38	11A	0.31	12A	0.36	9.5
5B	0.34	6B	0.32	11B	0.26	12B	0.30	28.6
5C	0.35	6C	0.44	11C	0.32	12C	0.33	47.6
5D	0.39	6D	0.46	11D	0.25	12D	0.38	66.7
5E	0.38	6E	0.52	11E	0.30	12E	0.34	85.7

Table A.11: Pavement Roughness Index

Bridge Number	Location	Avg PRI (mm/km)	Avg PRI (in/mi)
---------------	----------	--------------------	--------------------

Silica Fume Overlay Bridges

23-85	Northbound	612.4	38.8
23-85	Southbound	686.6	43.5
46-302	Southbound	883.8	56
46-302	Northbound	642.4	40.7
46-309	Northbound	834.9	52.9
46-309	Southbound	871.2	55.2
46-317	(Ramp)	920.1	58.3
81-50	Northbound	792.3	50.2
81-50	Southbound	763.9	48.4
87-453	Driving Lane	617.1	39.1
87-453	Passing Lane	542.9	34.4
87-454	Driving Lane	508.2	32.2
87-454	Passing Lane	550.8	34.9
89-184	Driving Lane	667.6	42.3
89-184	Passing Lane	588.7	37.3
89-187	Driving Lane	563.4	35.7
89-187	Passing Lane	629.7	39.9
89-206	Driving Lane	784.4	49.7
89-206	Passing Lane	700.8	44.4
89-207	Passing Lane	656.6	41.6
89-207	Driving Lane	809.7	51.3
89-210	Northbound	683.4	43.3
89-210	Southbound	754.4	47.8
89-234	Driving Lane	732.3	46.4
89-234	Passing Lane	817.6	51.8
89-235	Driving Lane	913.8	57.9
89-235	Passing Lane	675.5	42.8
89-235	Exit Lane	522.4	33.1

Table A.11 (continued)

Bridge Number	Location	Avg PRI (mm/km)	Avg PRI (in/mi)
89-240	Northbound	328.3	20.8
89-240	Southbound	353.5	22.4
89-244	(Ramp)	489.3	31
89-245	(Ramp) Unit 1	804.9	51
89-245	(Ramp) Unit 2	786.0	49.8
89-246	Westbound	632.9	40.1
89-246	Eastbound	533.5	33.8
89-247	Westlane	820.7	52
89-247	Eastlane	863.3	54.7
89-248	Westbound	588.7	37.3
89-248	Eastbound	486.1	30.8
Conventional Overlay Bridges			
46-289	Driving Lane	650.3	41.2
46-289	Passing Lane	830.2	52.6
46-290	Passing Lane	653.4	41.4
46-290	Driving Lane	718.1	45.5
46-299	Passing Lane	817.6	51.8
46-299	Driving Lane	677.1	42.9
46-300	Driving Lane	902.8	57.2
46-300	Passing Lane	749.7	47.5
46-301	Eastbound Driving Lane	729.2	46.2
46-301	Eastbound Passing Lane	730.7	46.3
46-301	Westbound Passing Lane	762.3	48.3
46-301	Westbound Driving Lane	754.4	47.8
75-1	Driving Lane	752.8	47.7
75-1	Passing Lane	591.9	37.5
75-49	Passing Lane	602.9	38.2
75-49	Driving Lane	751.3	47.6
81-49	Southbound Driving Lane	620.3	39.3

Table A.11 (continued)

Bridge Number	Location	Avg PRI (mm/km)	Avg PRI (in/mi)
81-49	Southbound Passing Lane	673.9	42.7
81-49	Northbound Driving Lane	659.7	41.8
81-49	Northbound Passing Lane'	637.6	40.4
89-183	Eastbound	857.0	54.3
89-183	Westbound	1096.9	69.5
89-185	Driving Lane	737.1	46.7
89-185	Passing Lane	808.1	51.2
89-186	Driving Lane	475.1	30.1
89-186	Passing Lane	400.9	25.4
89-196	(Ramp)	956.4	60.6
89-198	Driving Lane	563.4	35.7
89-198	Passing Lane	711.8	45.1
89-199	Passing Lane	----	----
89-199	Driving Lane	648.7	41.1
89-200	Driving Lane	612.4	38.8
89-200	Passing Lane	505.1	32
89-201	Driving Lane	516.1	32.7
89-201	Passing Lane	569.8	36.1
Monolithic Bridges			
56-148	Westbound	631.3	40
56-148	Eastbound	685.0	43.4
70-107	Westbound	617.1	39.1
70-107	Eastbound	752.8	47.7
89-204	(Ramp)	632.9	40.1
89-208	West and Eastbound Average	830.2	52.6





	Edge of Roadway
	Abutment/Pier Centerline
	Survey Boundary
	Crack

Fig. A.1 Legend for Bridge Deck Cracking Patterns

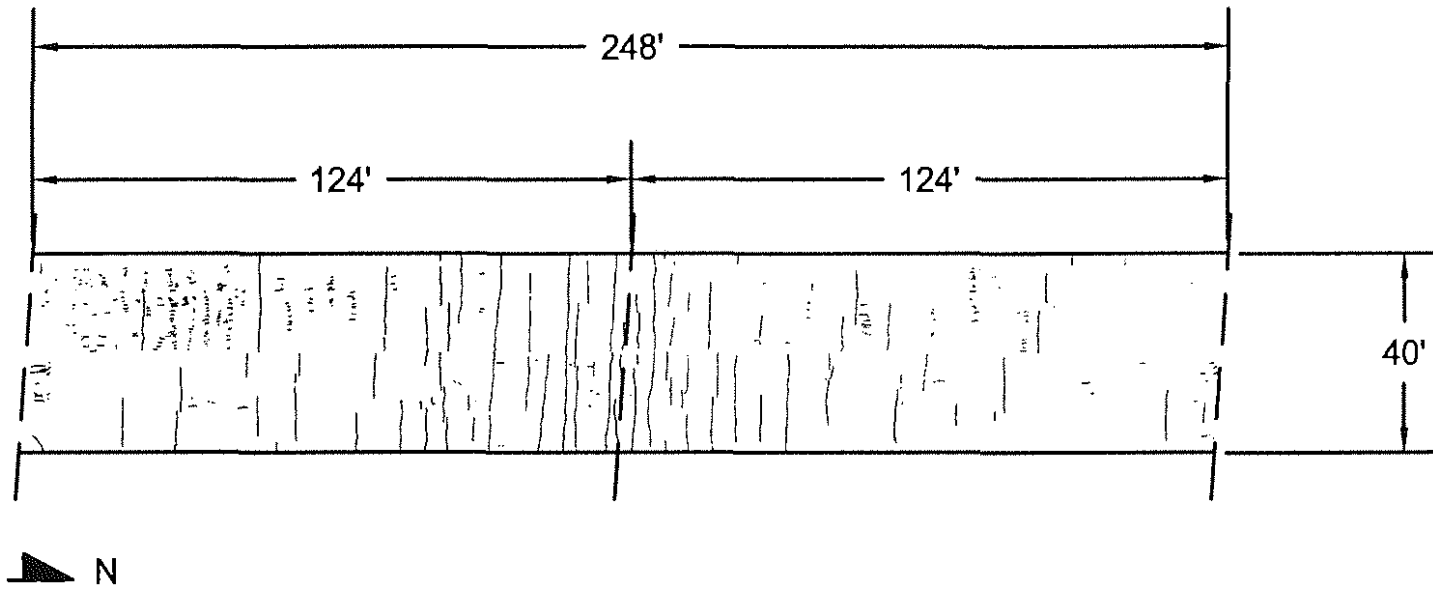


Fig. A.2 Bridge Number 23-85 (Silica Fume Overlay). Scale 1" = 40'-0"

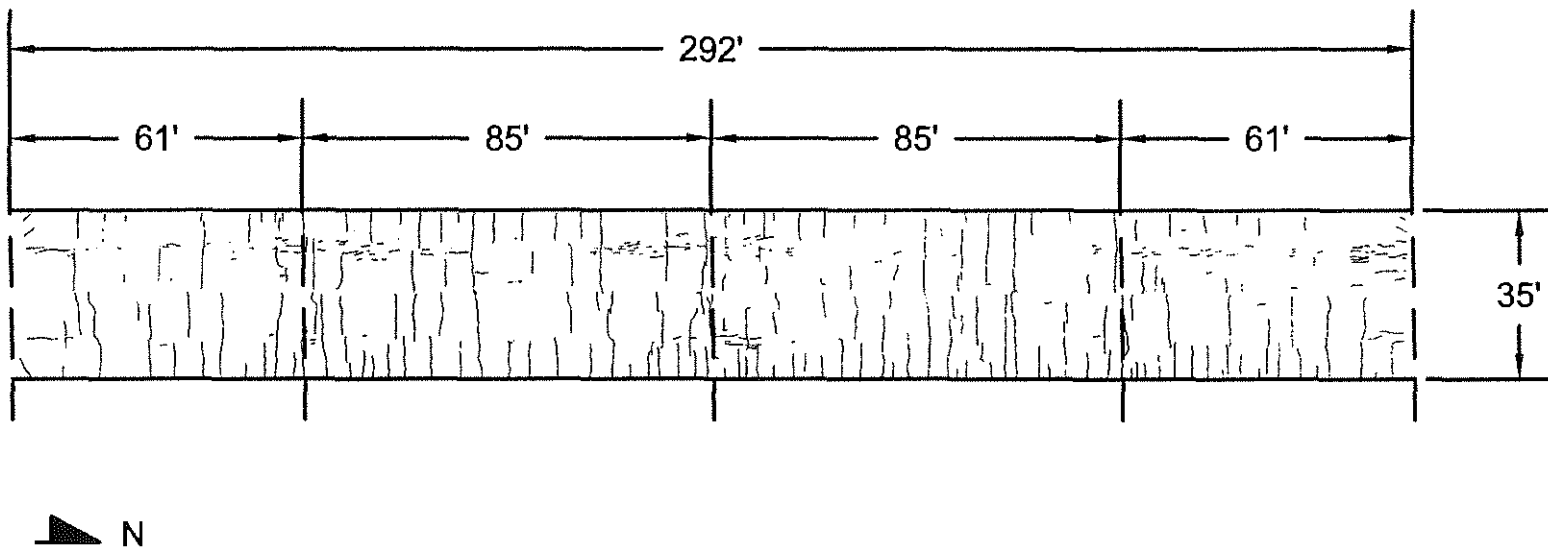


Fig. A.3 Bridge Number 46-302 (Silica Fume Overlay). Scale 1" = 40'-0"

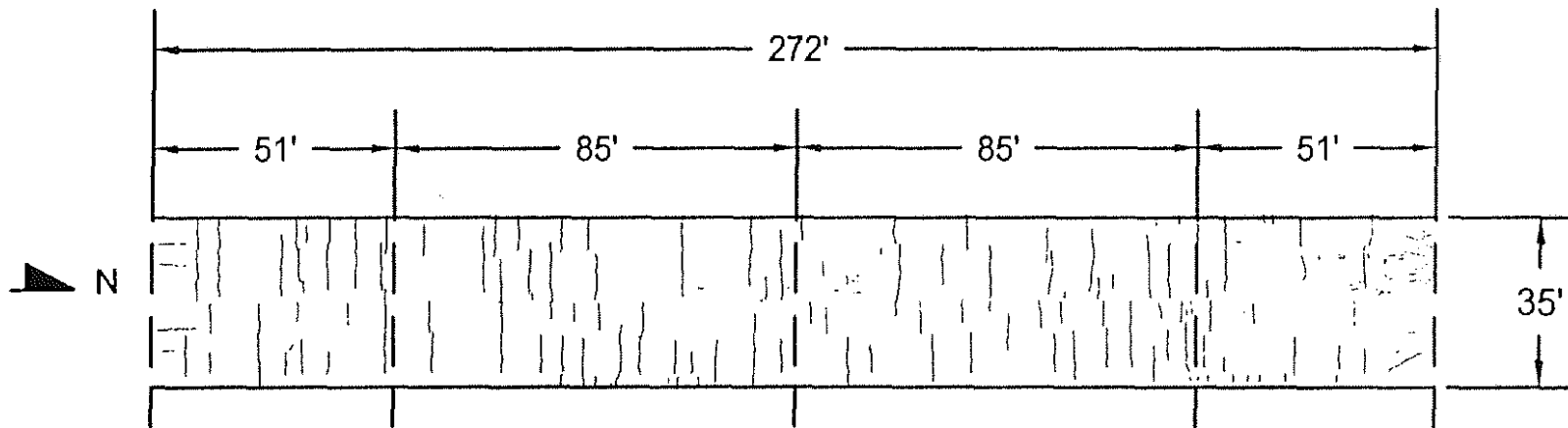


Fig. A.4 Bridge Number 46-309 (Silica Fume Overlay). Scale 1" = 40'-0"

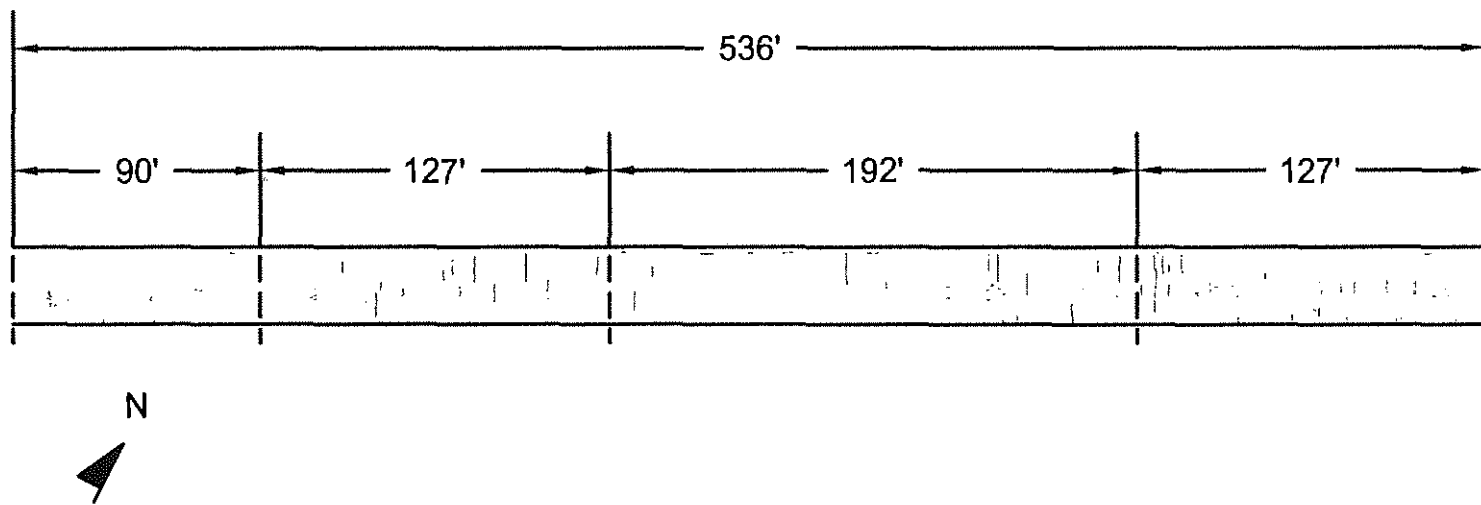


Fig. A.5 Bridge Number 46-317, Unit 1 (Silica Fume Overlay). Scale 1" = 70'-0"

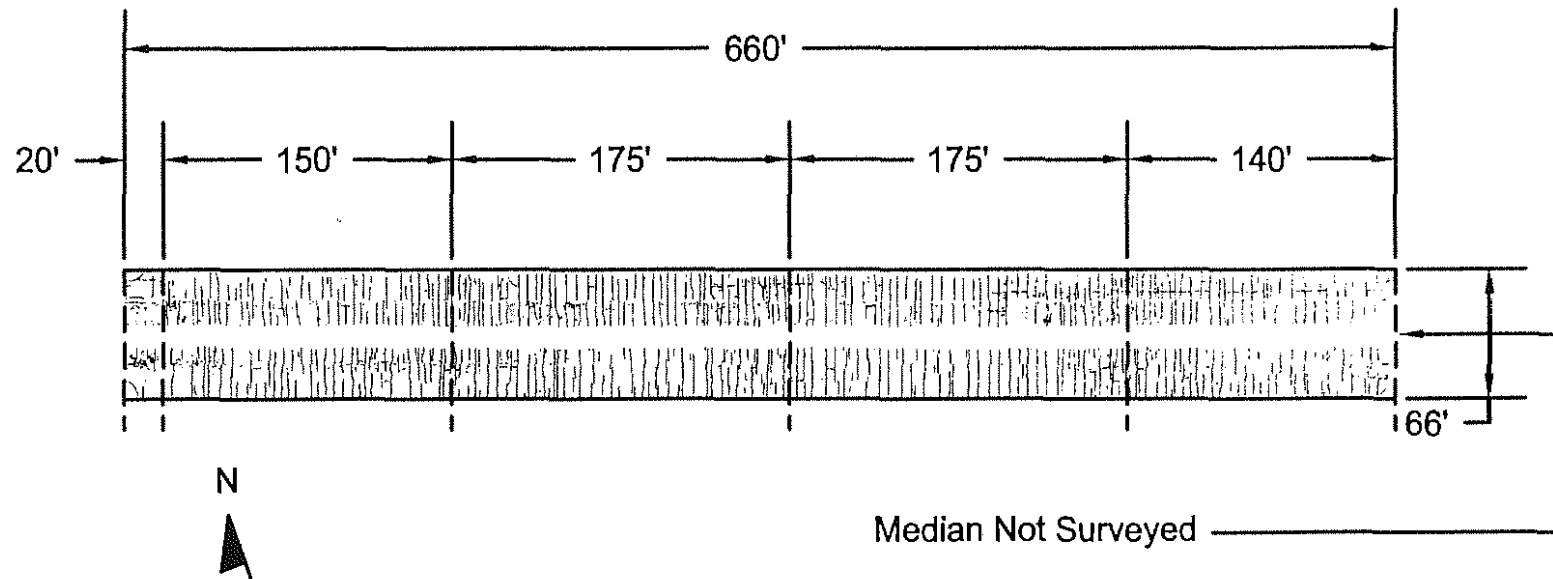


Fig. A.6 Bridge Number 81-50, Unit 2 (Silica Fume Overlay). Scale 1" = 100'-0"

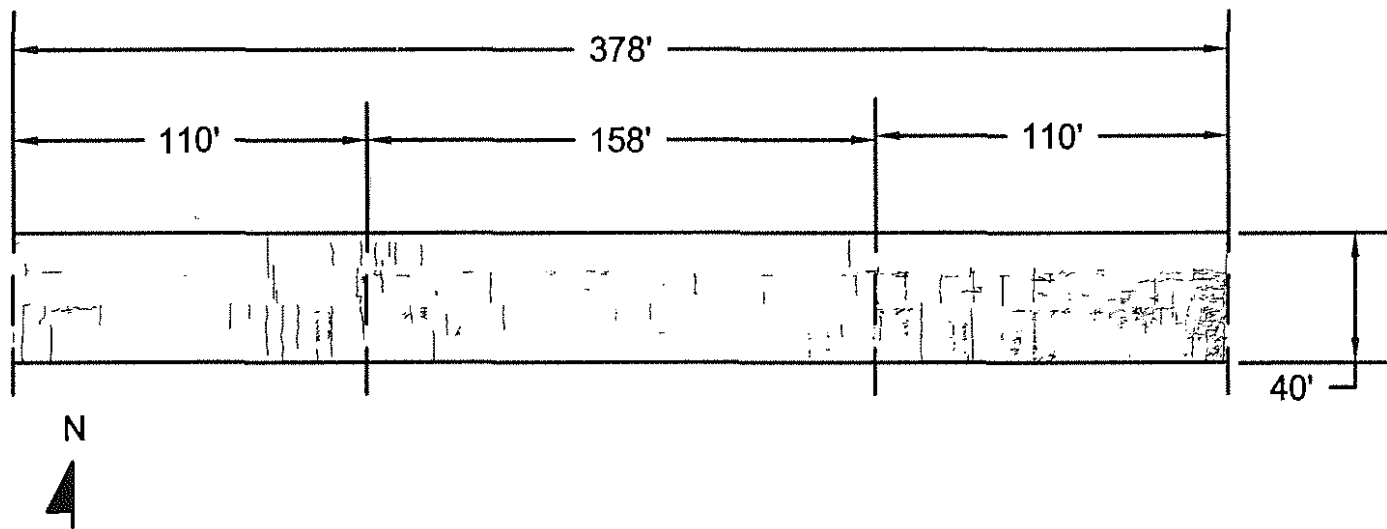


Fig. A.7 Bridge Number 87-453 (Silica Fume Overlay). Scale 1" = 60'-0"

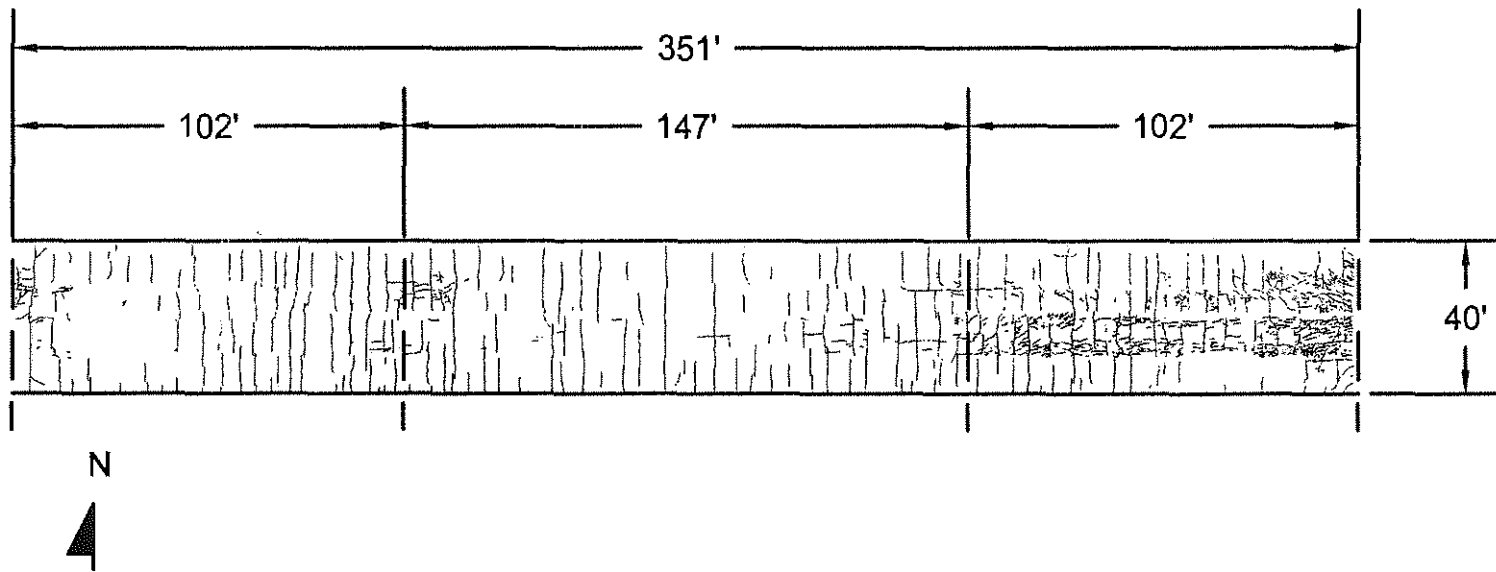


Fig. A.8 Bridge Number 87-454 (Silica Fume Overlay). Scale 1" = 50'-0"

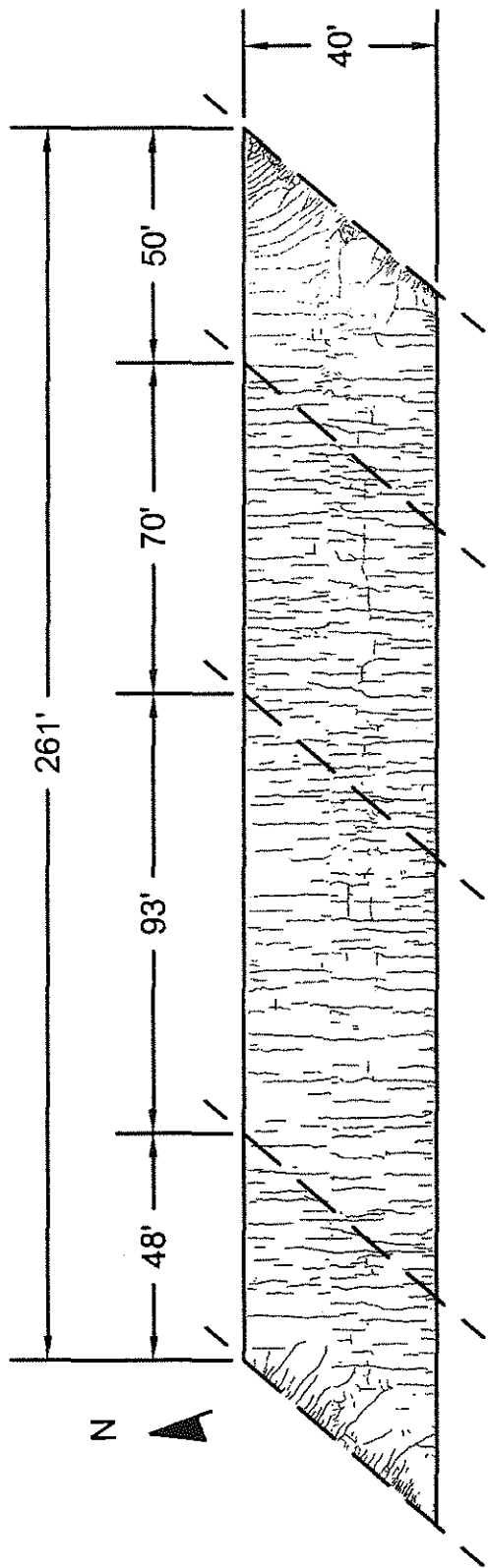


Fig. A.9 Bridge Number 89-184 (Silica Fume Overlay). Scale 1" = 40'

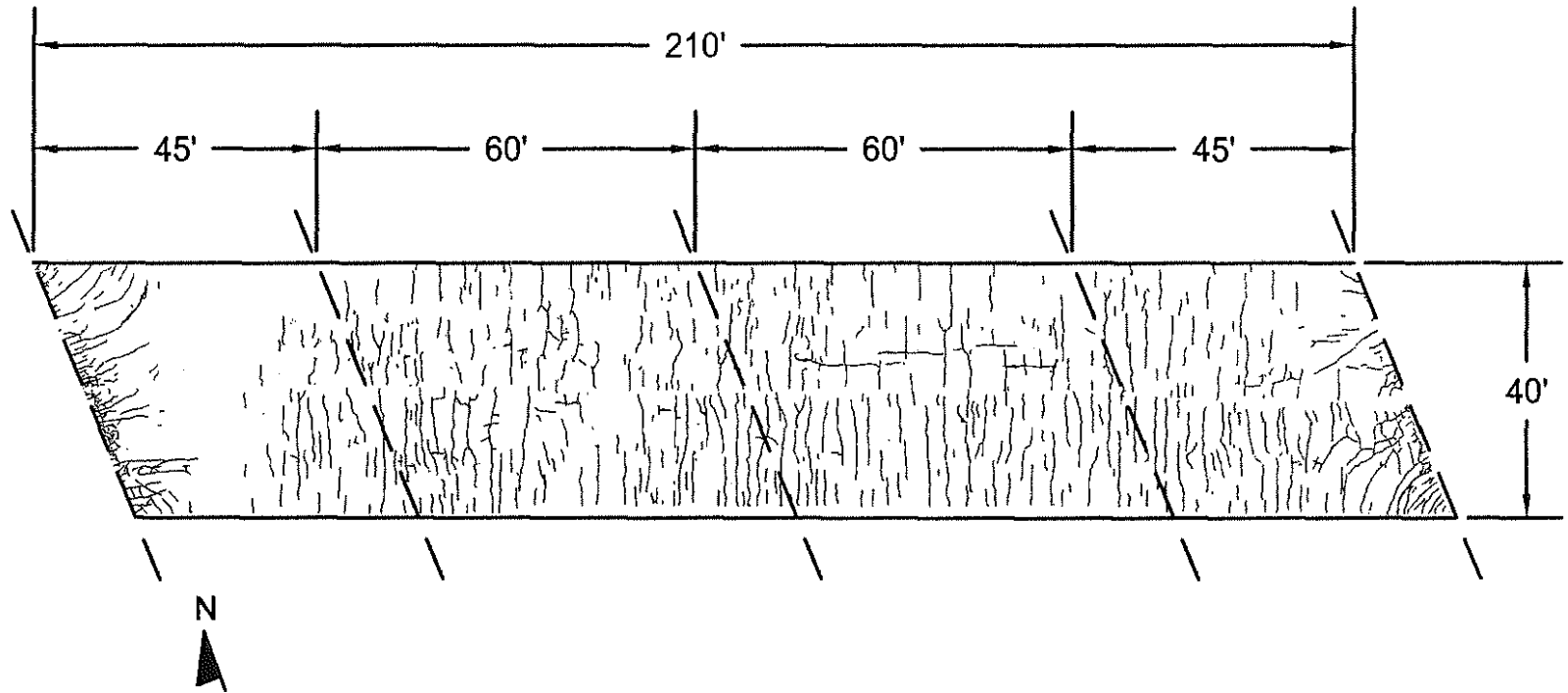


Fig. A. 10 Bridge Number 89-187 (Silica Fume Overlay). Scale 1" = 30'-0"

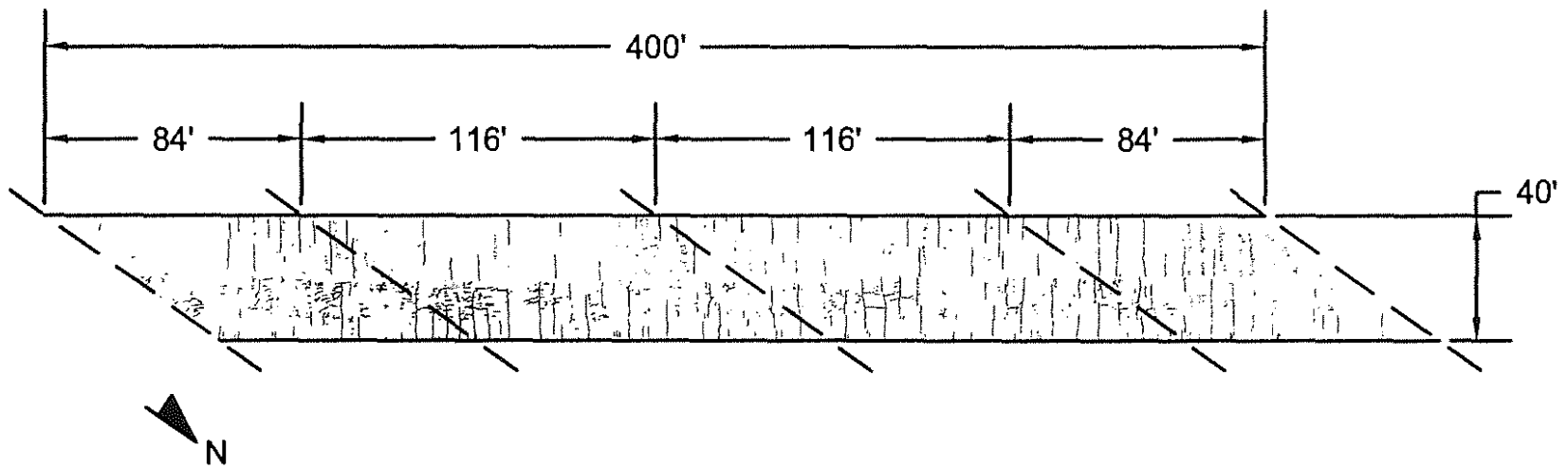


Fig. A.11 Bridge Number 89-206 (Silica Fume Overlay). Scale 1" = 60'-0"

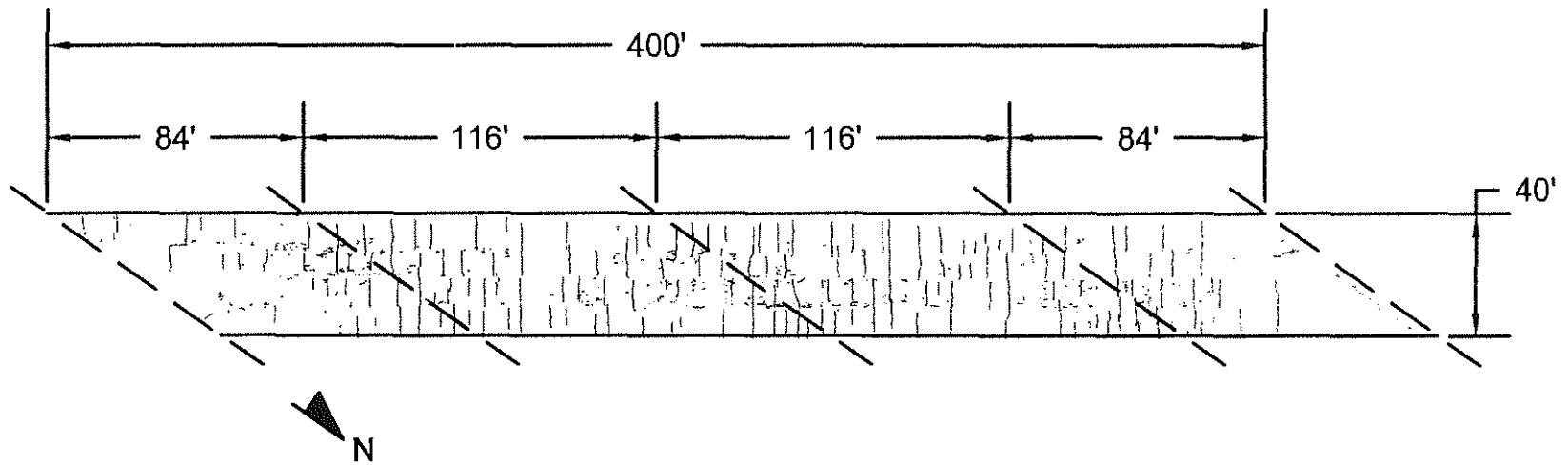


Fig. A.12 Bridge Number 89-207 (Silica Fume Overlay). Scale 1" = 60'-0"

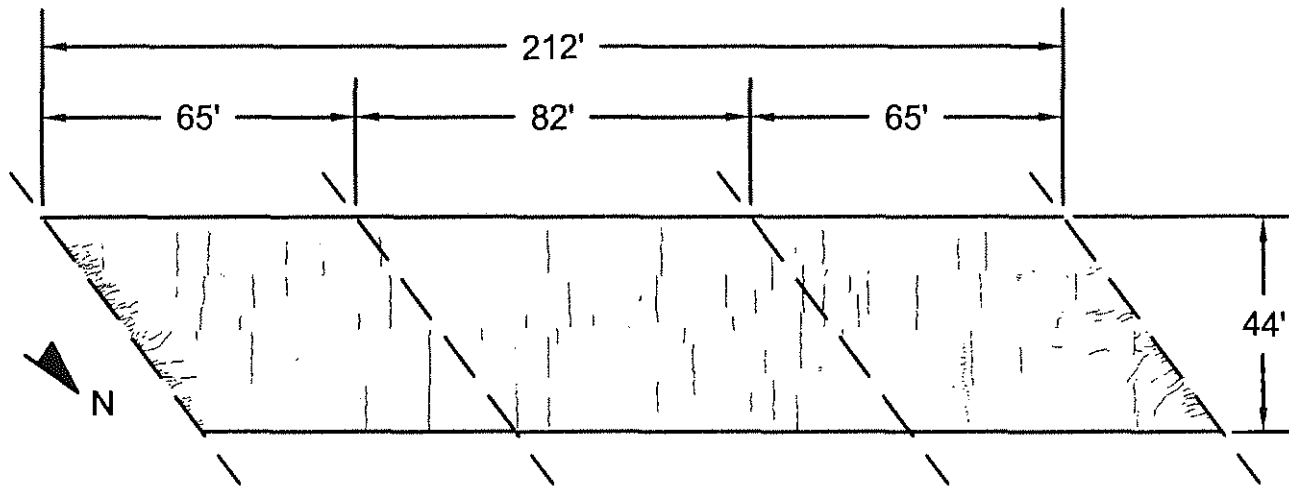
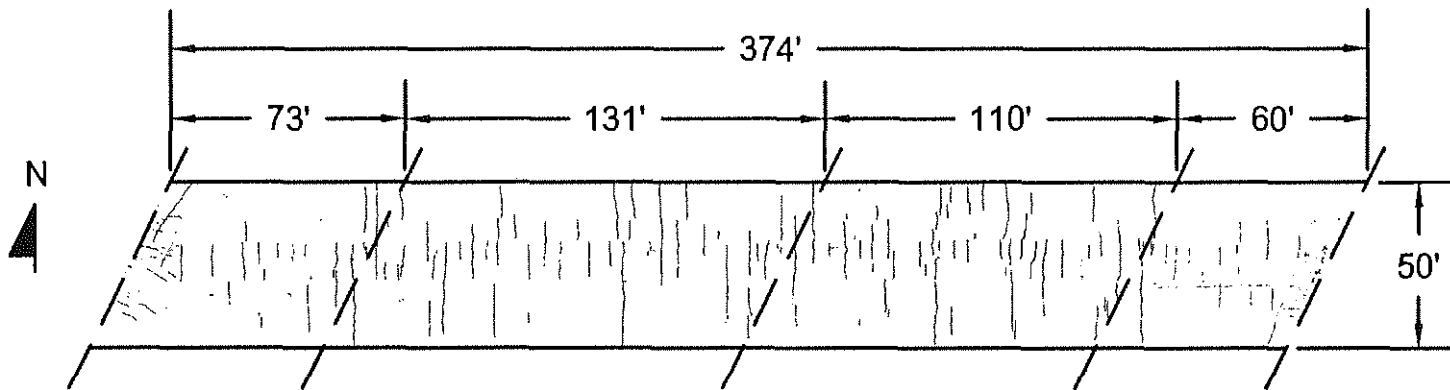


Fig. A.13 Bridge Number 89-210 (Silica Fume Overlay). Scale 1" = 40'-0"



370

Fig. A.14 Bridge Number 89-234 (Silica Fume Overlay). Scale 1" = 60'-0"

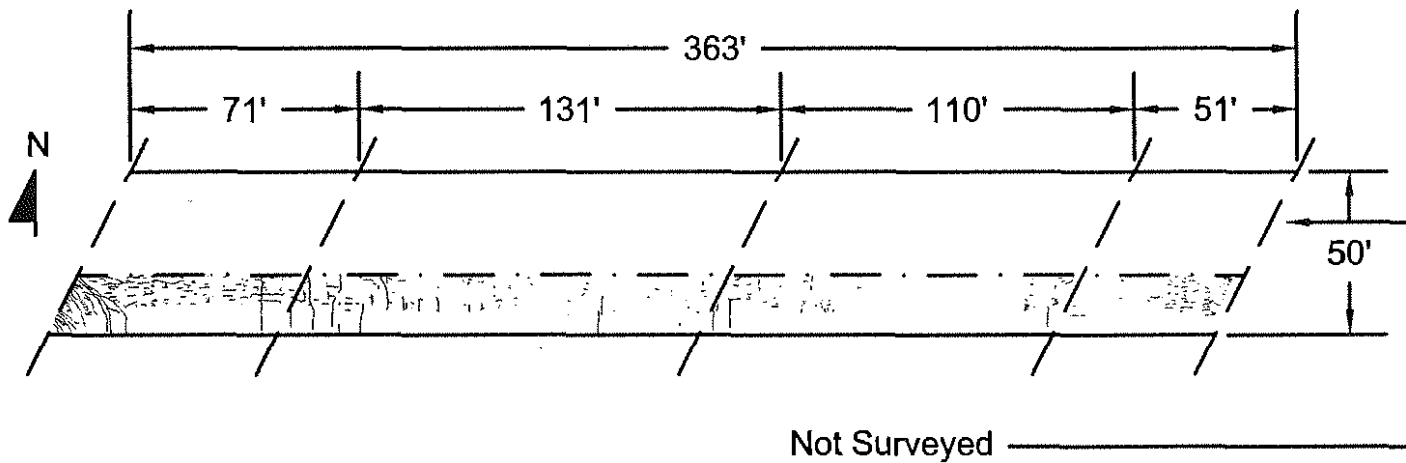


Fig. A.15 Bridge Number 89-235 (Silica Fume Overlay). Scale 1" = 60'-0"

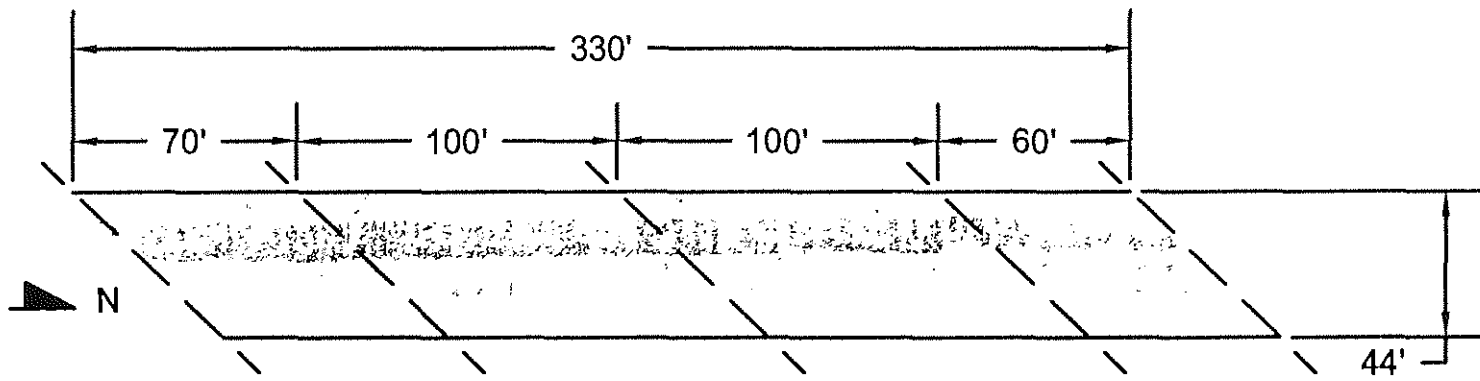


Fig. A.16 Bridge Number 89-240 (Silica Fume Overlay). Scale 1" = 60'-0"

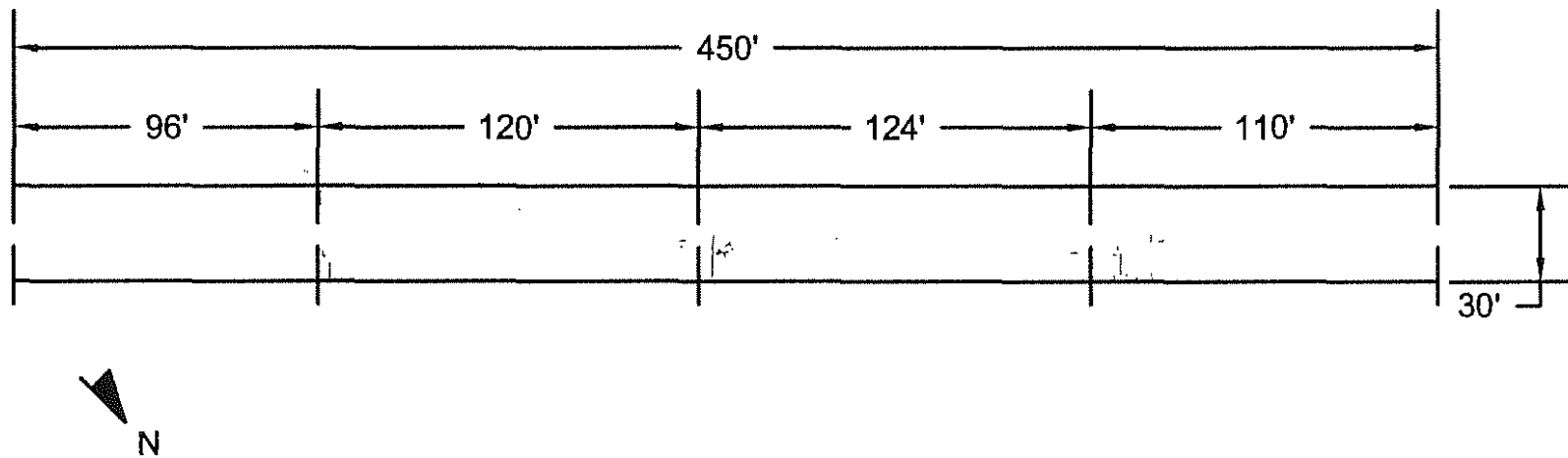


Fig. A.17 Bridge Number 89-244 (Silica Fume Overlay). Scale 1" = 60'-0"

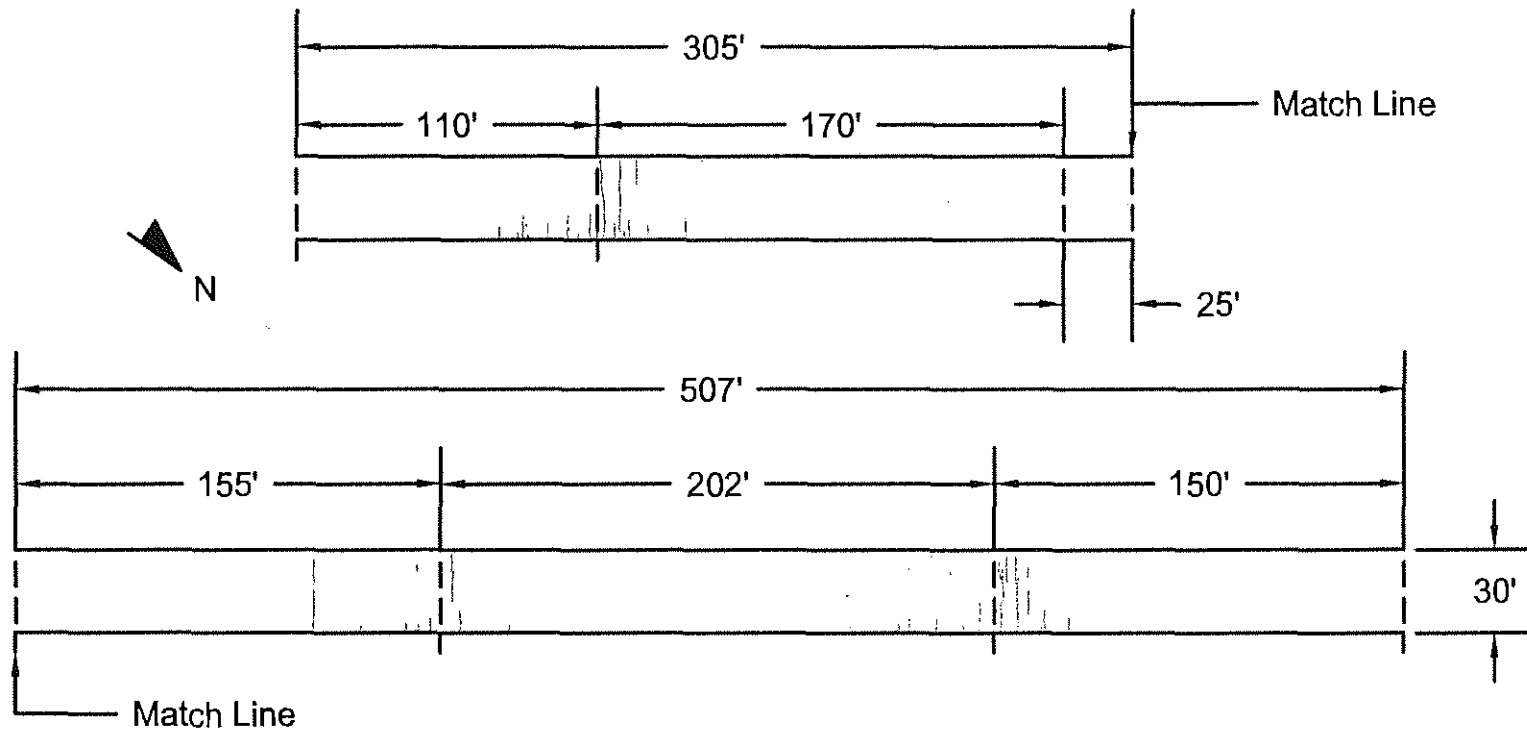


Fig. A.18 Bridge Number 89-245 (Silica Fume Overlay). Scale 1" = 70'-0"

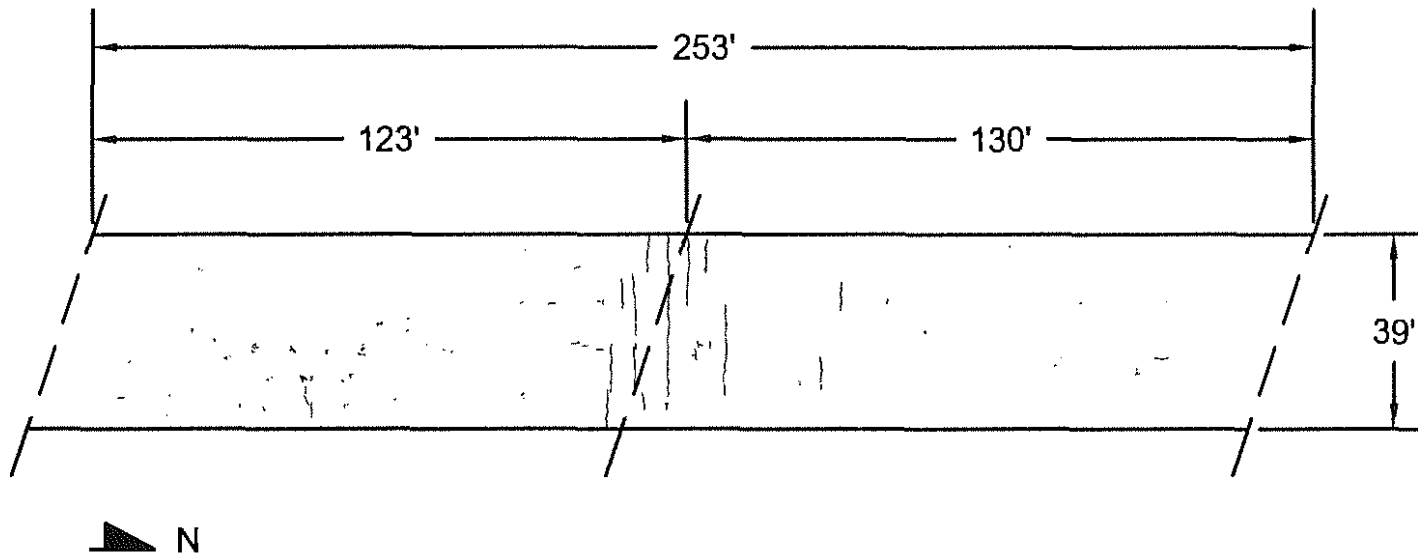


Fig. A.19 Bridge Number 89-246 (Silica Fume Overlay). Scale 1" = 40'-0"

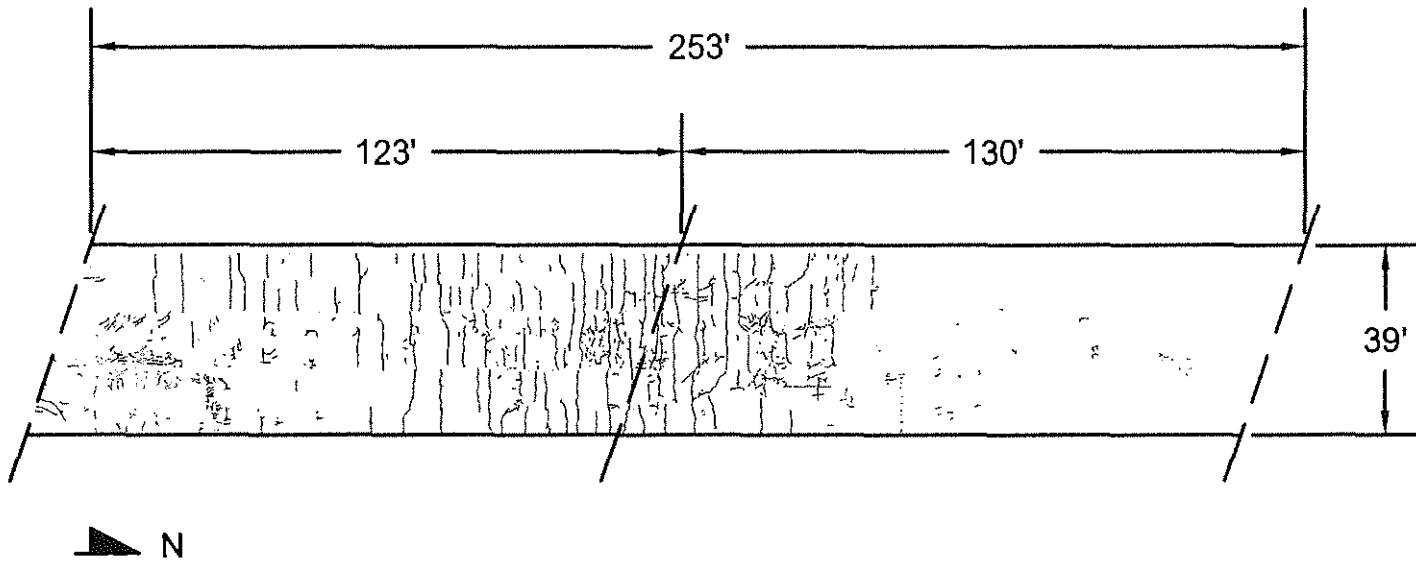


Fig. A.20 Bridge Number 89-247 (Silica Fume Overlay). Scale 1" = 40'-0"

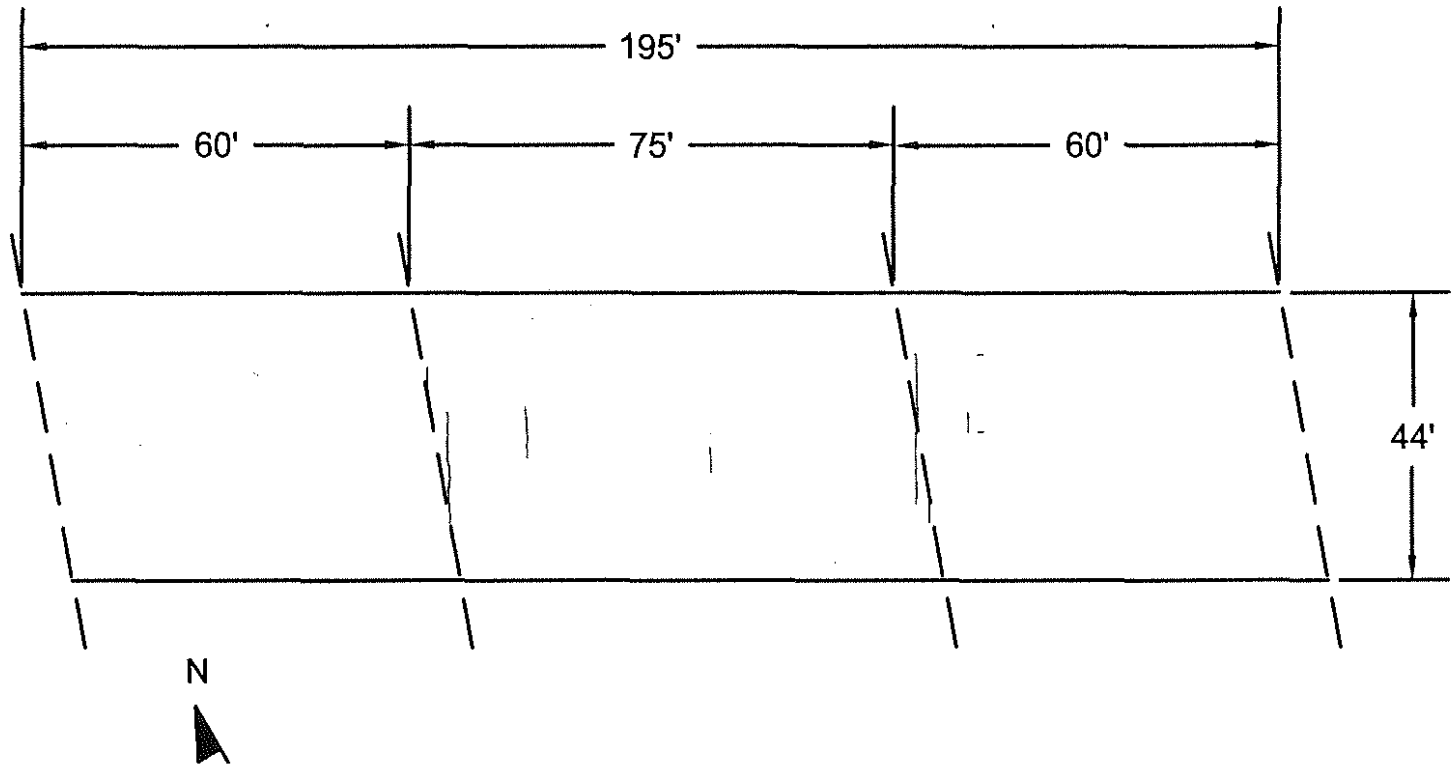


Fig. A.21 Bridge Number 89-248 (Silica Fume Overlay). Scale 1" = 30'-0"

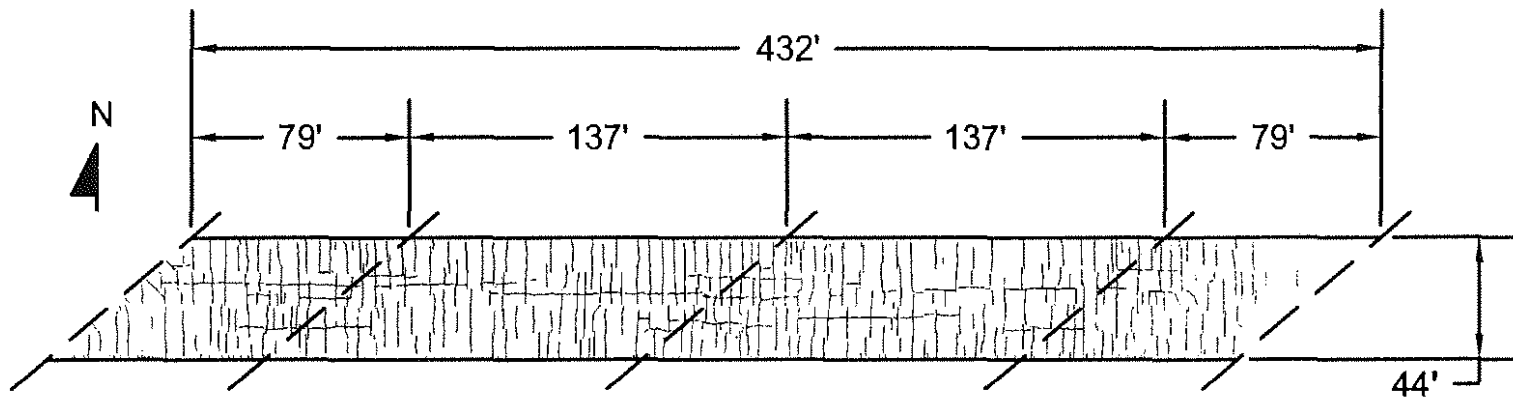


Fig. A.22 Bridge Number 46-289 (Conventional Overlay). Scale 1" = 70'-0"

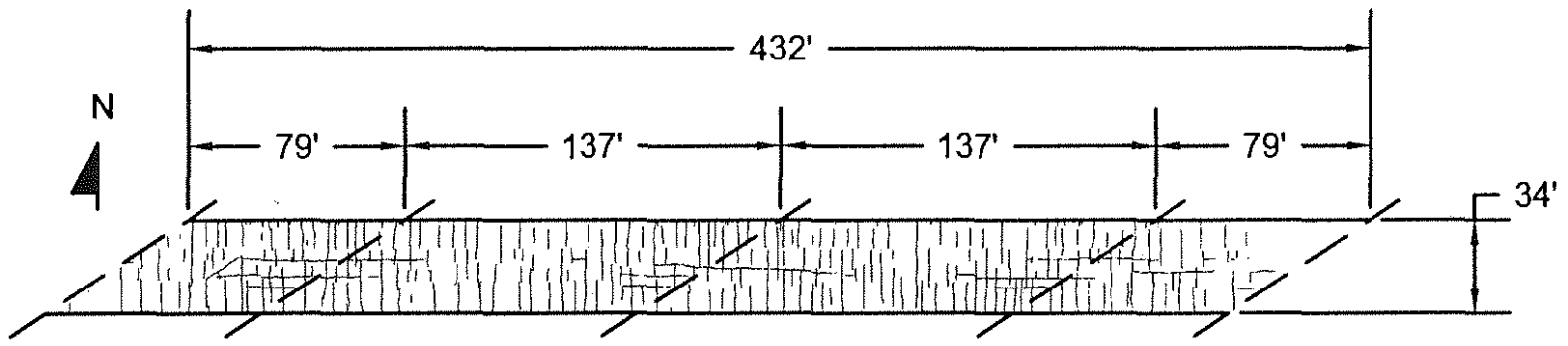


Fig. A.23 Bridge Number 46-290 (Conventional Overlay). Scale 1" = 70'

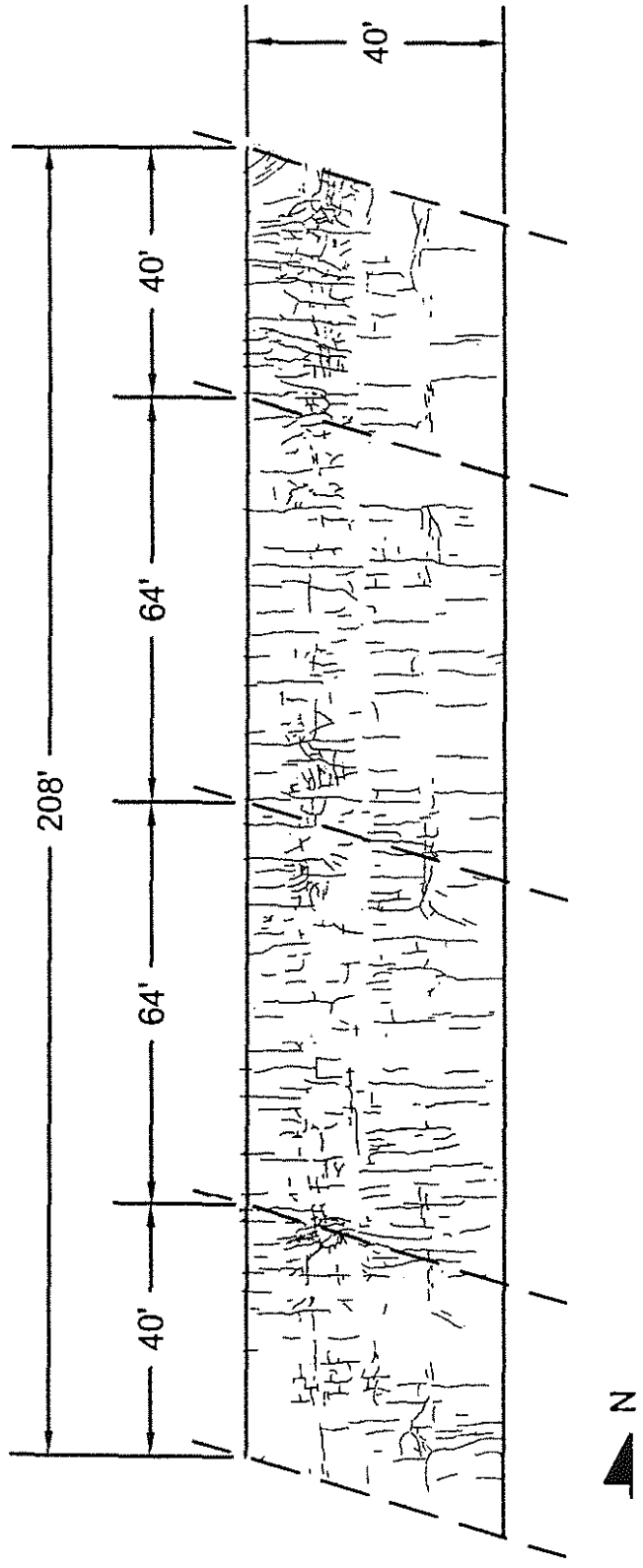


Fig. A.24 Bridge Number 46-299 (Conventional Overlay). Scale 1" = 30'-0"

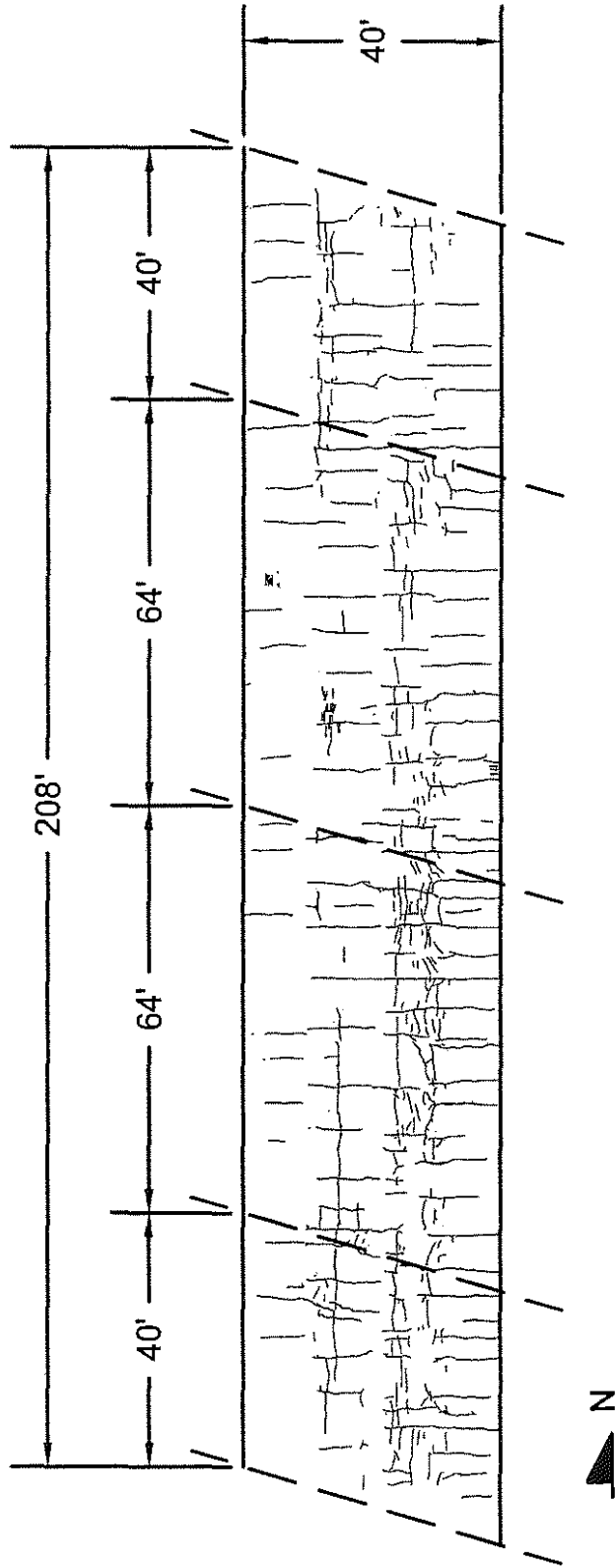


Fig. A.25 Bridge Number 46-300 (Conventional Overlay). Scale 1" = 30'-0"

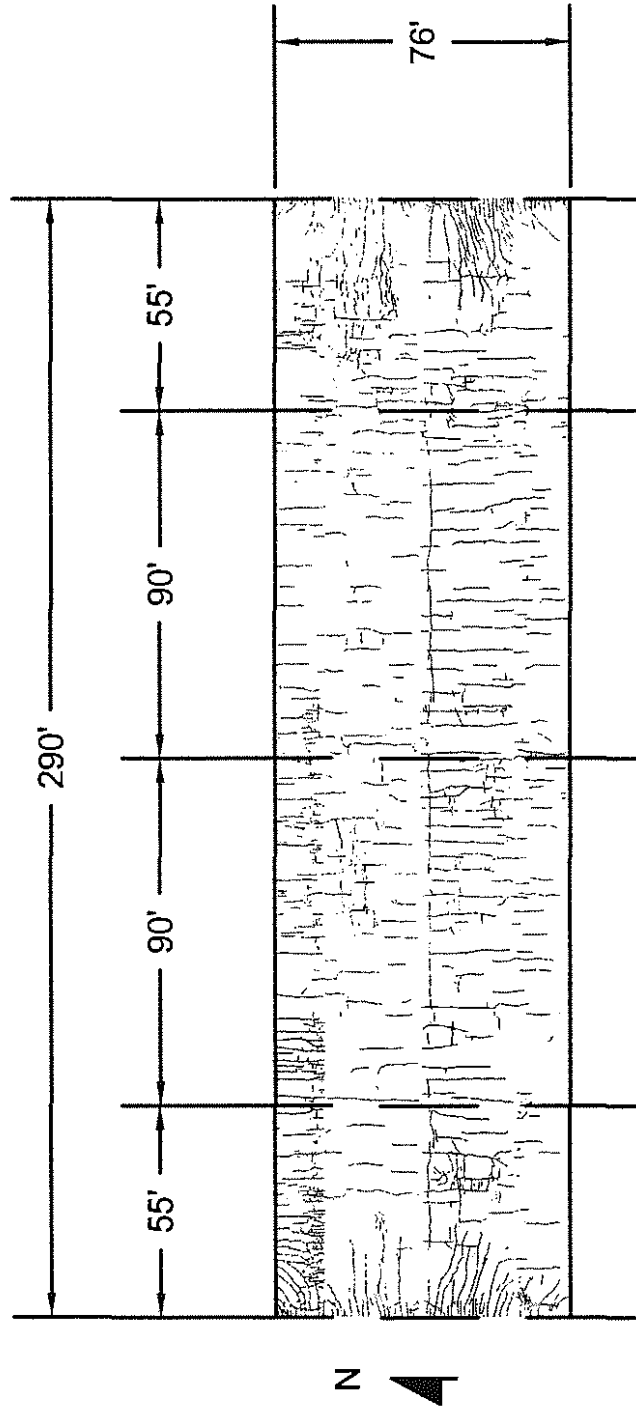


Fig. A.26 Bridge Number 46-301 (Conventional Overlay). Scale 1" = 50'-0"

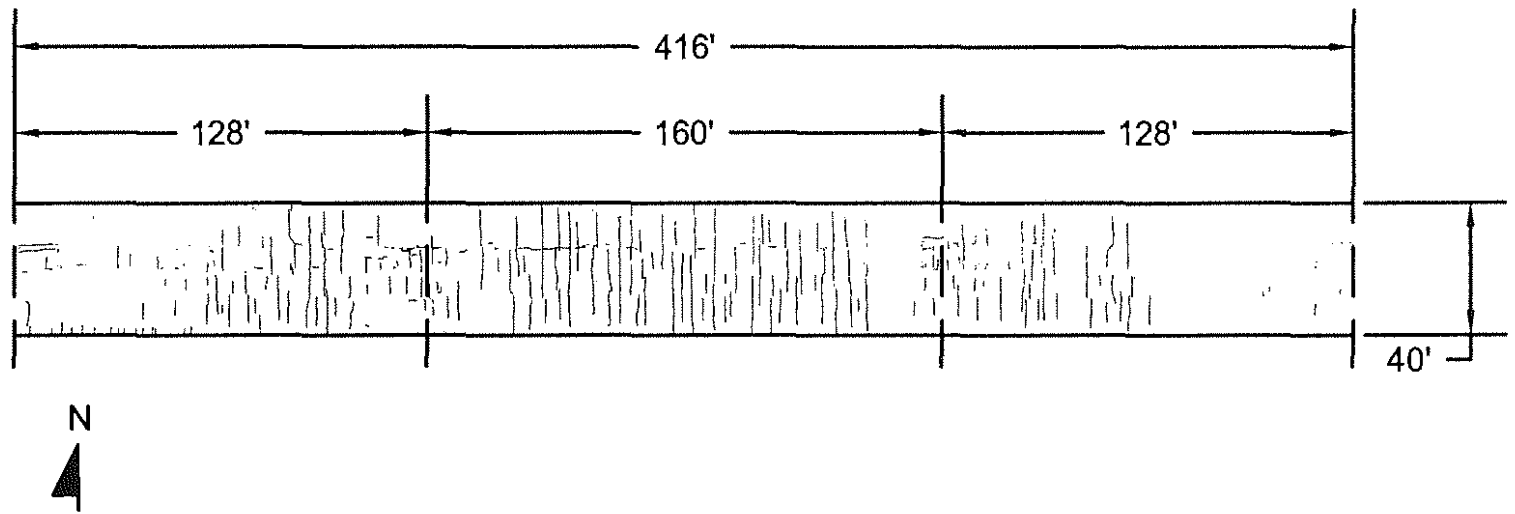


Fig. A.27 Bridge Number 75-01 (Conventional Overlay). Scale 1" = 60'-0"

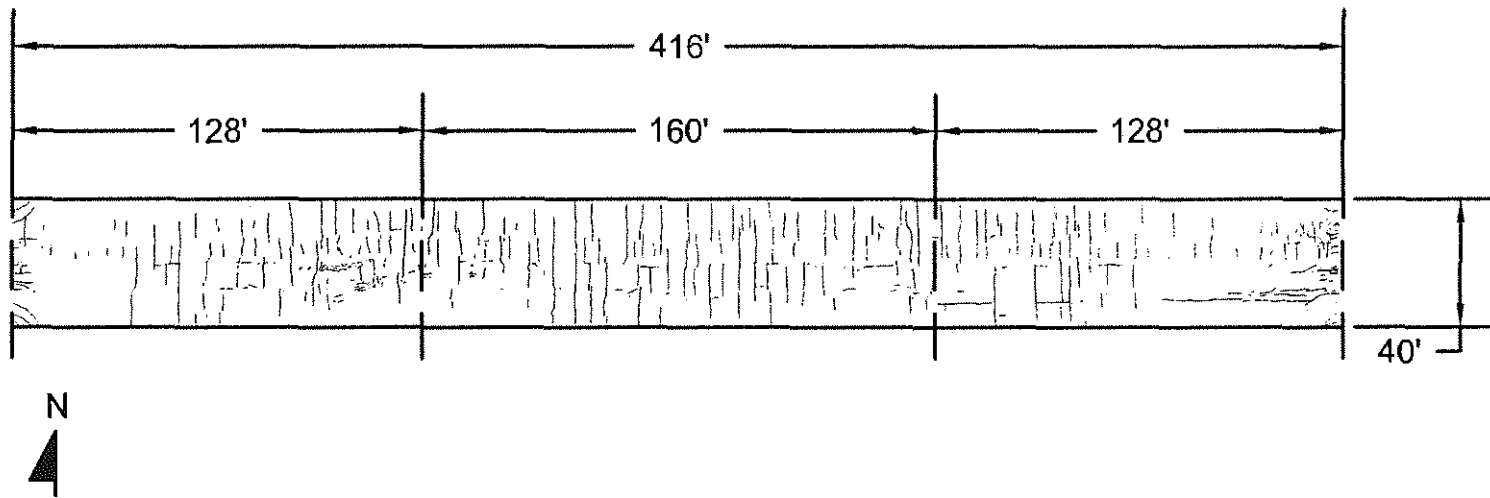


Fig. A.28 Bridge Number 75-49 (Conventional Overlay). Scale 1" = 60'-0"

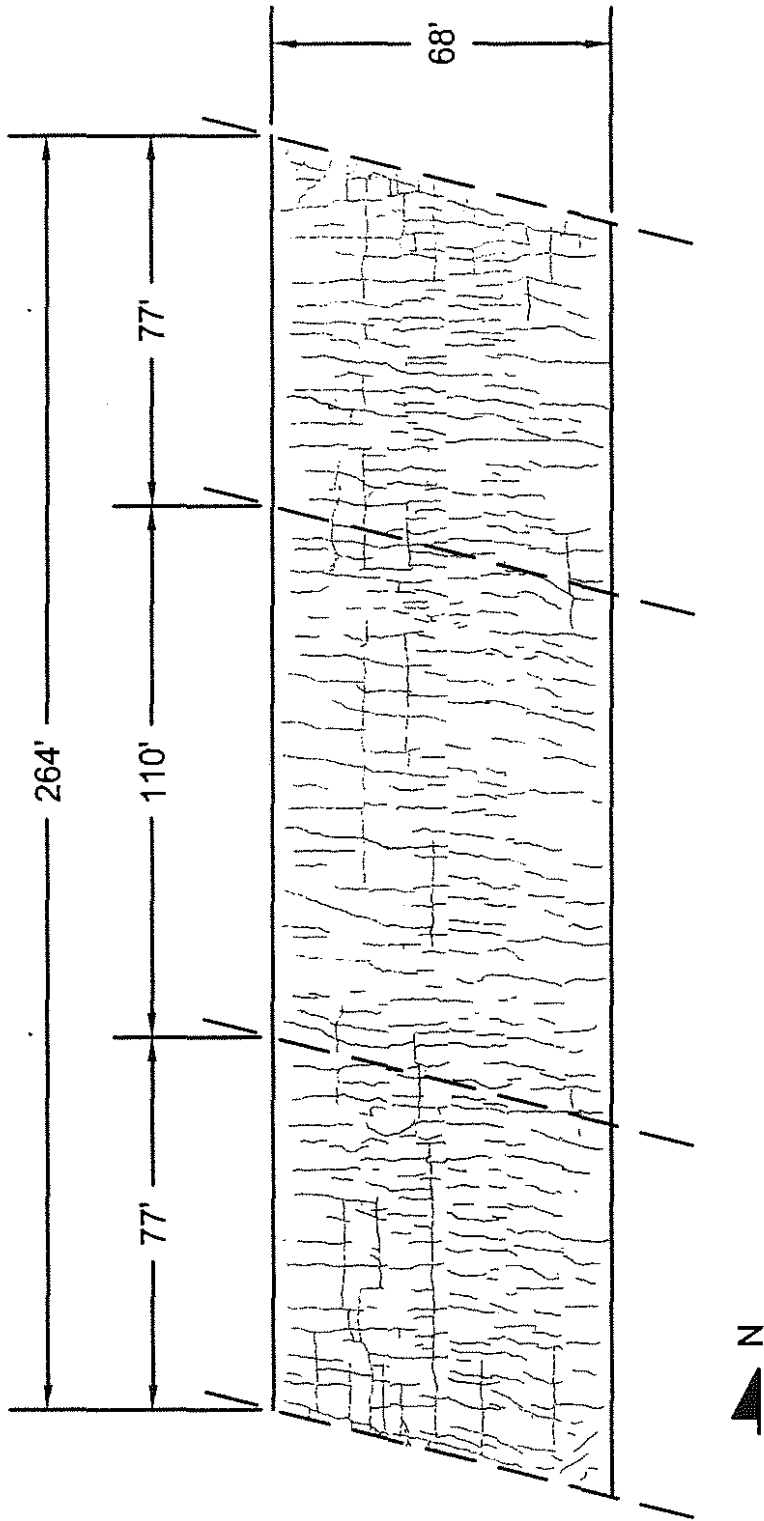


Fig. A.29 Bridge Number 81-49 (Conventional Overlay). Scale 1" = 40'-0"

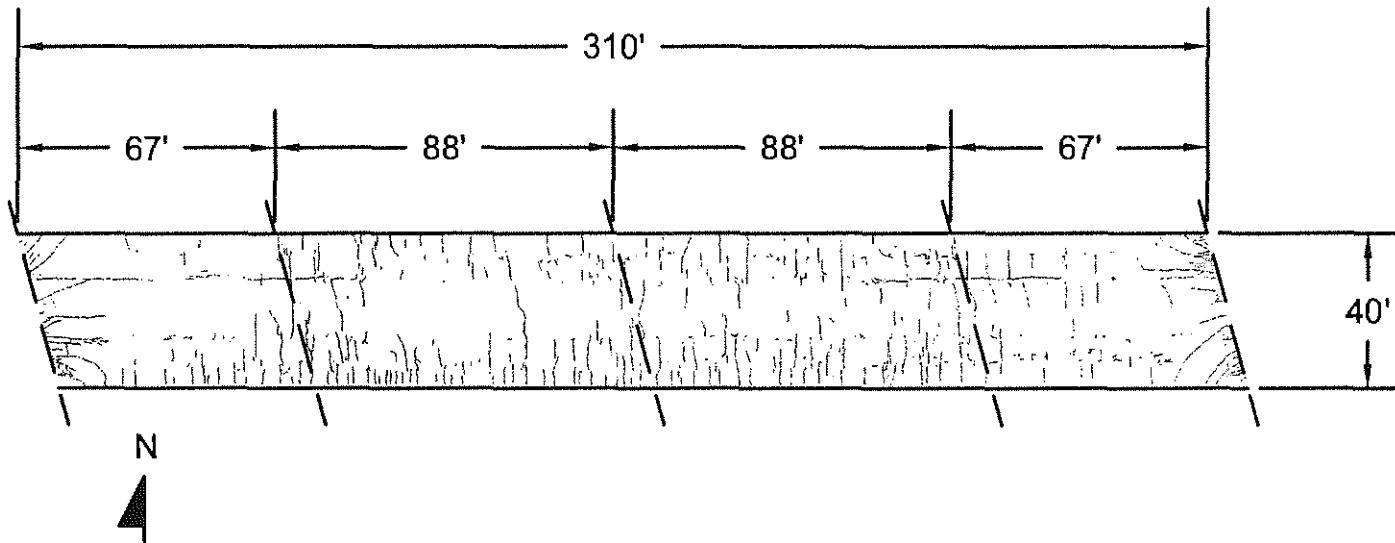


Fig. A.30 Bridge Number 89-183 (Conventional Overlay). Scale 1" = 50'-0"

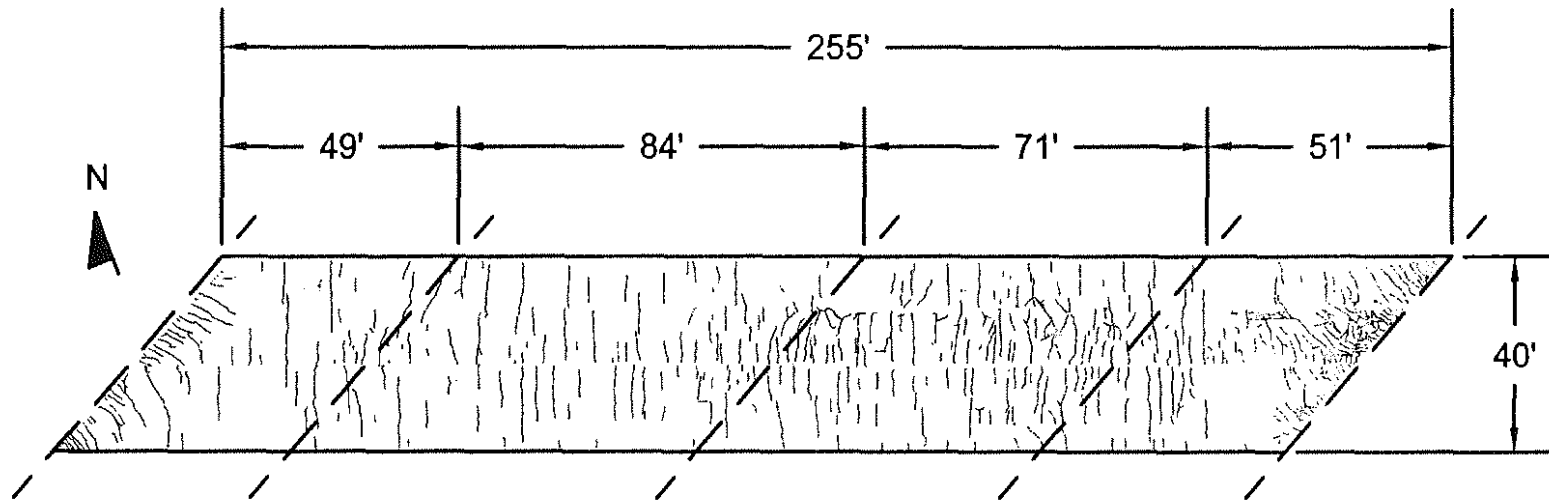


Fig. A.31 Bridge Number 89-185 (Conventional Overlay). Scale 1" = 40'-0"

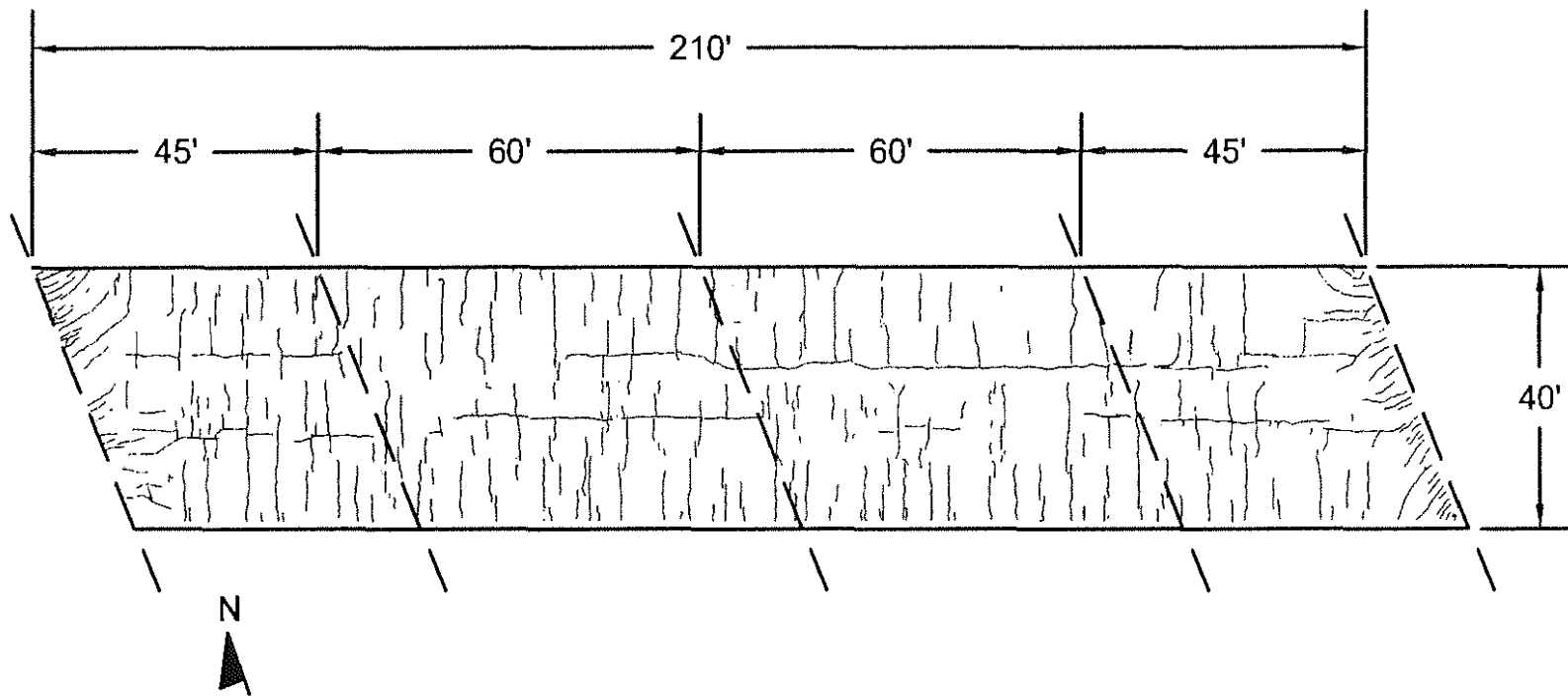


Fig. A.32 Bridge Number 89-186 (Conventional Overlay). Scale 1" = 30'-0"

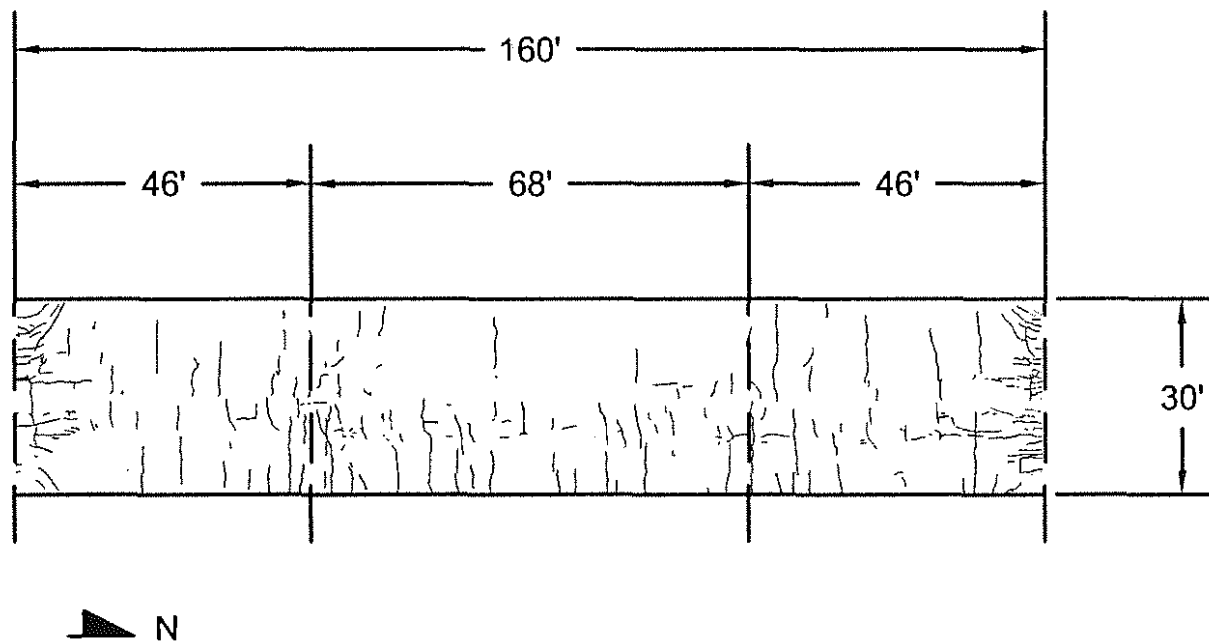


Fig. A.33 Bridge Number 89-196 (Conventional Overlay). Scale 1" = 30'-0"

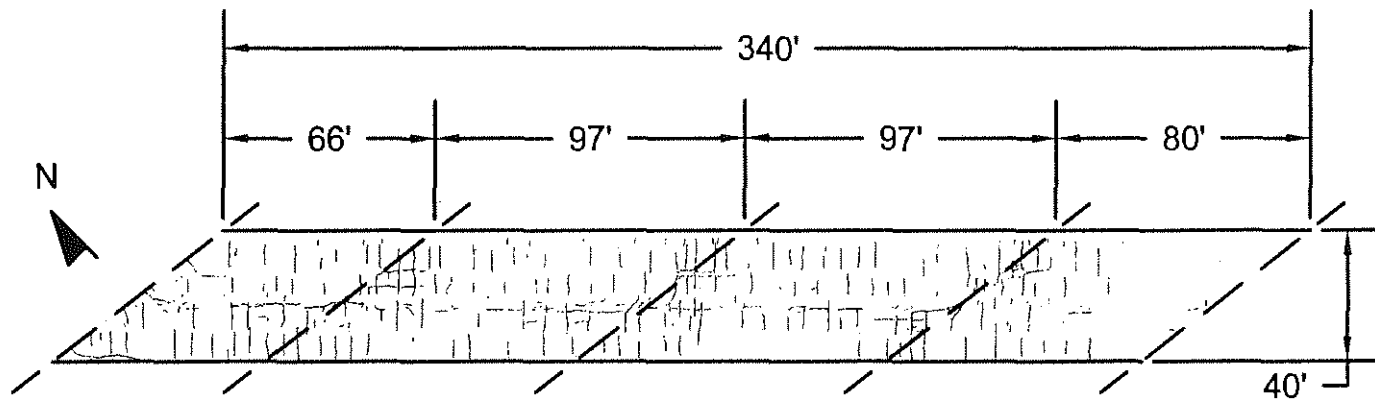


Fig. A.34 Bridge Number 89-198 (Conventional Overlay). Scale 1" = 60'-0"

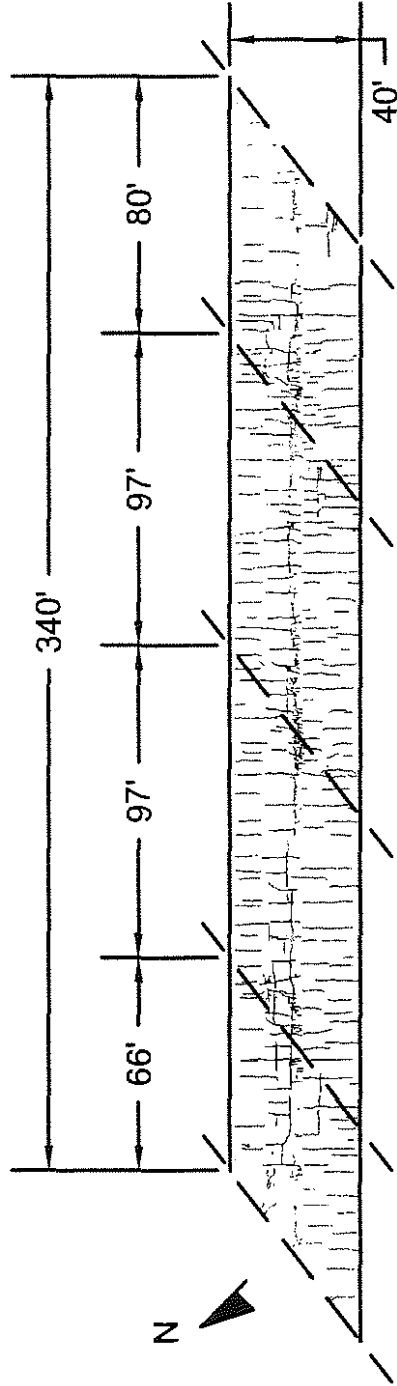


Fig. A.35 Bridge Number 89-199 (Conventional Overlay). Scale 1" = 60'-0"

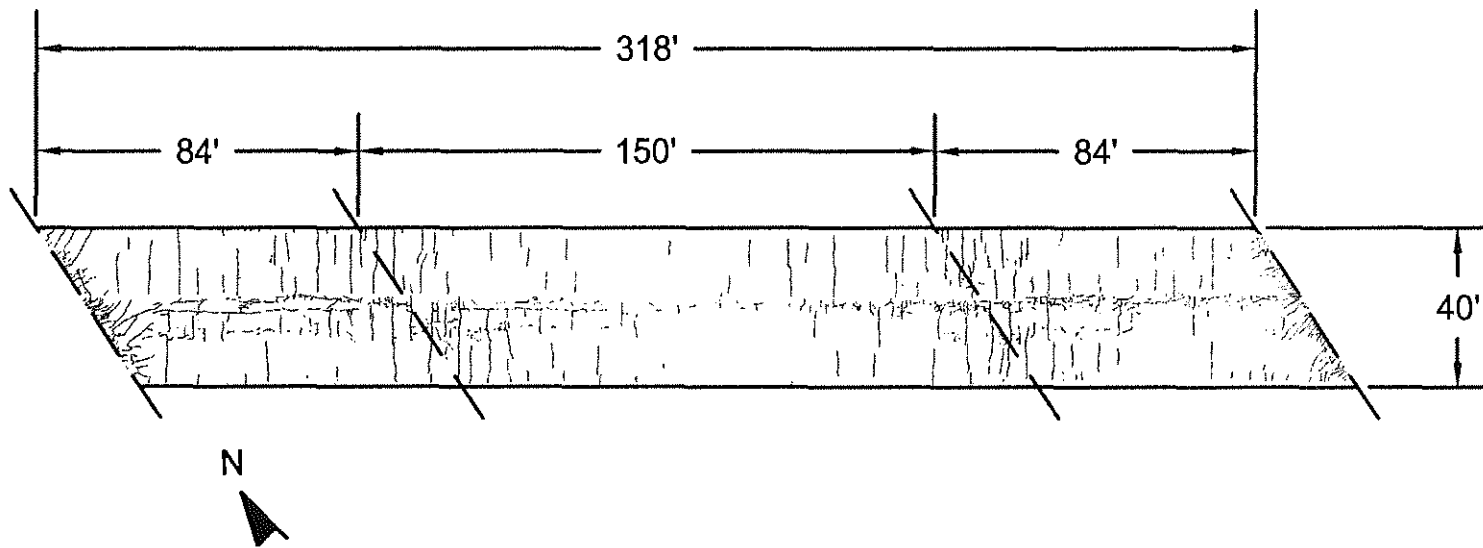


Fig. A.36 Bridge Number 89-200 (Conventional Overlay). Scale 1" = 50'-0"

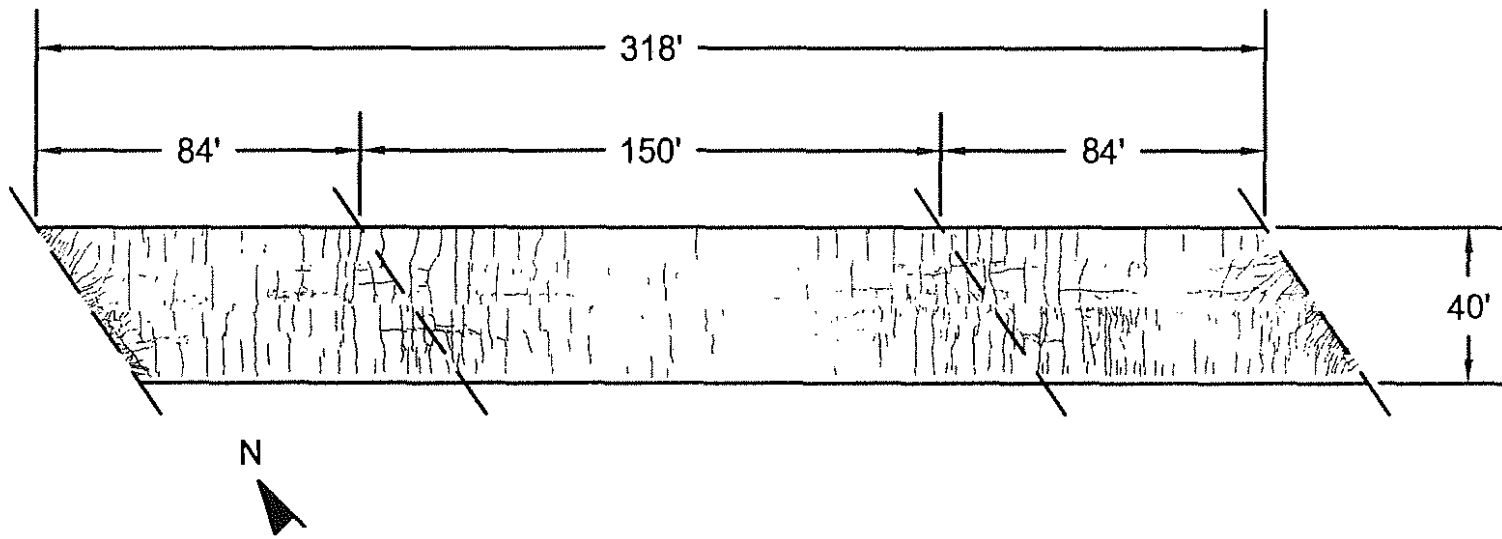


Fig. A.37 Bridge Number 89-201 (Conventional Overlay). Scale 1" = 50'-0"

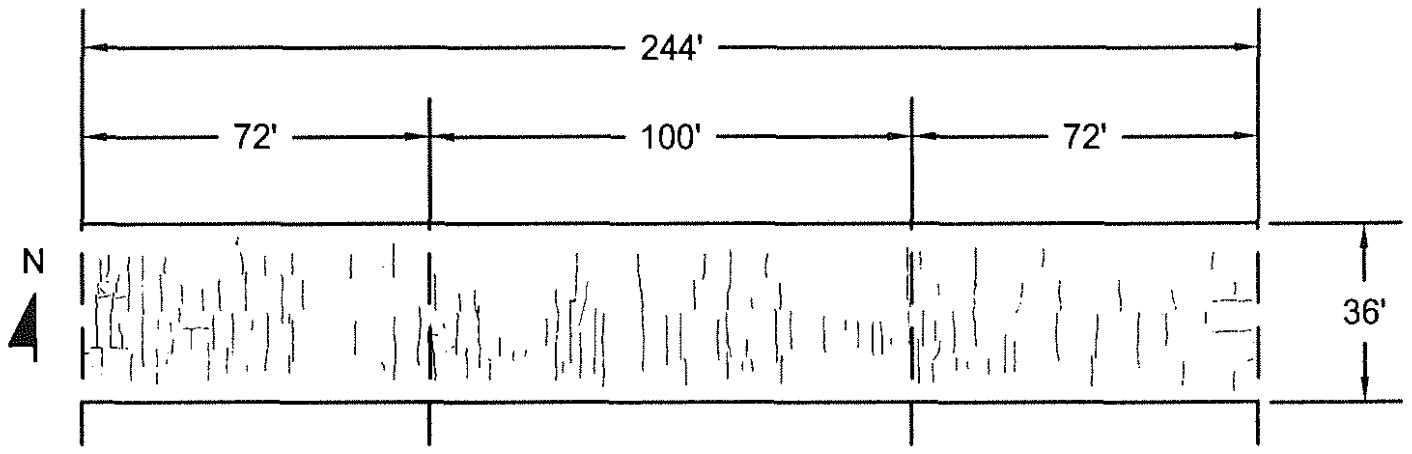


Fig. A.38 Bridge Number 56-148 (Monolithic). Scale 1" = 40'-0"

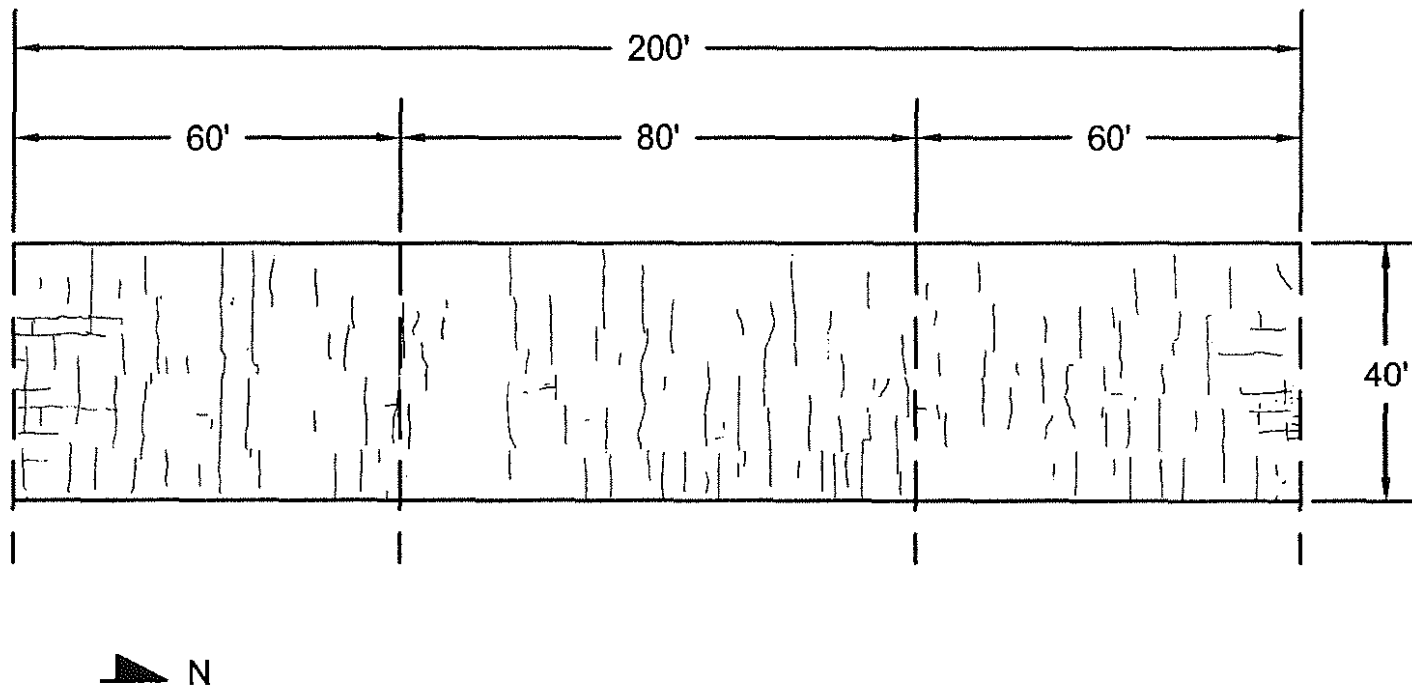


Fig. A.39 Bridge Number 70-107 (Monolithic). Scale 1" = 30'-0"

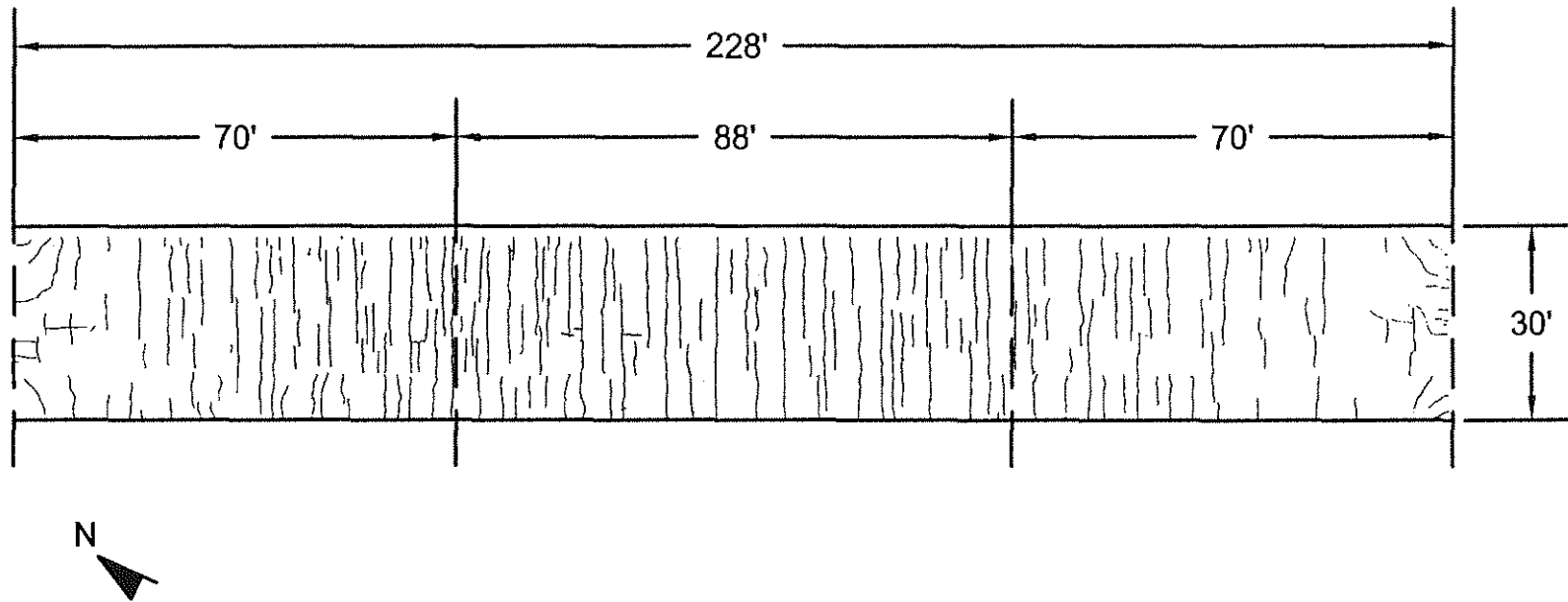


Fig. A.40 Bridge Number 89-204 (Monolithic). Scale 1" = 30'-0"

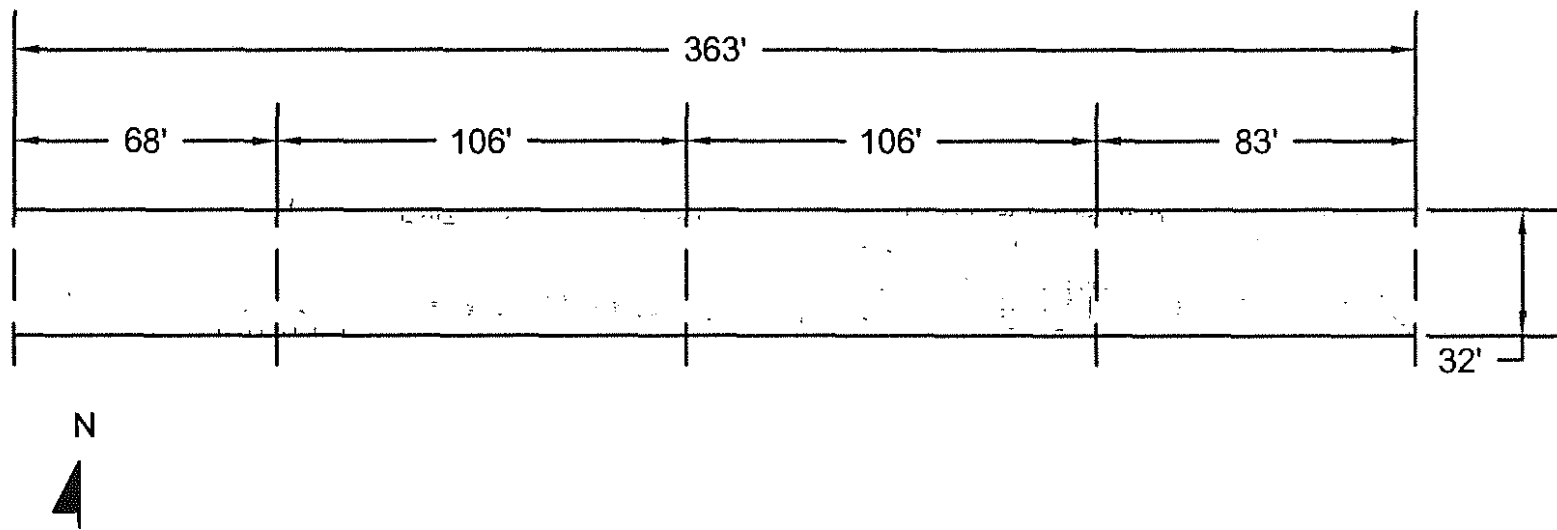


Fig. A.41 Bridge Number 89-208 (Monolithic). Scale 1" = 50'-0"

APPENDIX B
CRACK DENSITY CALCULATION PROGRAM LISTING

```

*
* PROGRAM NAME:  AngLen
*
* VERSION:      3.0  written in Fortran 77
*
* LAST MODIFIED: April 8, 1999
*
* CREATED BY:   Tony R. Schmitt , 1993
*               University of Kansas
*               Department of Civil Engineering
*
* UPDATED BY:  Gerald G. Miller, 1998
*               University of Kansas
*               Department of Civil and Environmental Engineering
*
* FUNCTION:     Takes an ascii file created from a TIFF image file
*               locates pixels that are within a user specified
*               gray level range, groups pixels that are adjacent to
*               one another (these groups represent cracks), and
*               then calculates the length and angle of each crack.
*
*

```

```

*
* INSTRUCTIONS:
*

```

```

*   Step 1:     The a scale drawing is made of the cracks on the bridge.
*               This program is designed to work with a scale of
*               1 inch = 10 feet.
*
*   Step 2:     Photocopy the scale drawing to get a clean copy.
*
*   Step 3:     Scan the drawing into a computer in black and white
*               at 100 dpi and save it as a TIFF image file (uncompressed).
*               Record the image size in pixels for use in the
*               AngLen program.  The width of the bridge is the X
*               coordinate and the length of the bridge is the Y
*               coordinate.
*
*   Step 4:     Remove all lines from the scanned image file that do
*               not represent cracks.  Add a line, one pixel wide,
*               from the top of the page to the top left corner of
*               the bridge (starting point).  The image should be cropped
*               so that both the x and y dimensions are multiples of
*               twenty.
*
*   Step 5:     Use the programs created by Prof. John Gauch at the
*               University of Kansas.  The programs are available at:
*               http://www.ittc.ukans.edu/~jgauch/kuim/source.html
*

```

```

*               The following 2 programs are used as follows:
*

```

```

*               program name [options] infile outfile
*

```

```

*               (1) convert_raw -x Xsize -y Ysize TIFFfilename IMfilename
*

```

* the Y dimension needs to be slightly larger than the
 * actual image to get all the pixel information.
 *
 * (2) *make_raw* -A IMfilename TXTfilename
 *
 * Step 6: The ASCII file created from the TIFF file includes various
 * tags that precede the numbers that represent the gray
 * level of the individual pixels. 0 = black and 255 = white.
 * The AngLen program only needs the gray level of the pixels.
 * Therefore, the ASCII file needs to be opened and the
 * tags need to be removed.
 * The tags can be removed using a text editor. If the image
 * file begins and ends with a row of white pixels, it is
 * possible to identify the end of the tags and the beginning
 * of the image file by looking for a series of 255's in the
 * ASCII file.
 *
 * Step 7: The file containing only the pixel gray level can then be
 * used as an input file for AngLen.

* VARIABLE DEFINITIONS

* REAL VARIABLES:

* ANGLE Angle of crack. Horizontal = 0 degrees.
 * Cracks increasing from left to right are positive.
 * AREA Bridge deck area in square meters.
 * AREAL Bridge deck in square feet.
 * AREAPLAC Area of an individual concrete placement.
 * D Distance between two pixels. This is used to
 * establish the length of a given crack.
 * DENS Crack density of a given deck area.
 * DIVTOTD Total crack density of a bridge division.
 * DIVTOTL Total length of all cracks in a division.
 * DIVTRD Transverse crack density of a bridge division.
 * DIVTRL Total length of all transverse cracks in a division.
 * LENBRG Length of bridge in feet.
 * LENDIV Length of each bridge division.
 * LENGTH Length of an individual crack. This is calculated
 * as the greatest distance between any two pixels
 * in a given crack.
 * LENPLACE Length of an individual concrete placement.
 * RDIVS Number of bridge divisions. (real number format)
 * RDWY Width of roadway in feet.
 * RHIGH Real number variation of integer variable HIGH.
 * RLOW Real number variation of integer variable LOW.
 * RTEMP Real number variation of integer variable ITEMP.
 * SCALE Drawing scale in ft./in. Note that many conversion
 * factors are built into the program and must be
 * modified if the scale of the input image is altered.
 * SKEW Skew of the end of the bridge in degrees.
 * SPANAREA Area of an individual span.
 * SPANG Special angle, in degrees, defined by user to

```

*          investigate angles other than the default angles.
*  SPANLEN  Length of a span.
*  SPDENS   Density of cracks at defined special angle.
*  SPTL     Total length of cracks at defined special angle.
*  TLPG     Total length of cracks in a given angle group.
*  TOL      Tolerance, in degrees, for the special angle.
*  TOTDENS  Total crack density.
*  TOTLEN   Total length of all cracks.
*  WIDPLACE Width of concrete placement.
*  X1       X coordinate of a pixel.
*  X2       X coordinate of a pixel.
*  Y1       Y coordinate of a pixel.
*  Y2       Y coordinate of a pixel.
*
*  INTEGER VARIABLES:
*
*  BOTBND   Bottom bound of bridge section being considered.
*  CHECK    Used in subroutine GROUP to determine when the
*           last of the pixels have been collected into crack
*           groups.
*  CHOICE   Represents "main menu" option.
*  CX       X coordinate of a pixel within graylevel range.
*  CY       Y coordinate of a pixel within graylevel range.
*  DIVTOTC  Total number of cracks in a division
*  DIVTRC   Total number of transverse cracks in a division.
*  HIGH     Used to define angle groups.
*  ITEMP    Used to increment YLOCATOR in division analysis.
*  JUMP     The number of rows in the ascii file that represent
*           one row of pixels in the .tif file.
*  LDPIX    Length of division in units of pixels.
*  LENPIX   Length of an individual placement in units of pixels.
*  LEVEL    Graylevel of a pixel. Takes on a value of 0 (black)
*           to 255 (white)
*  LOW      Used to define angle groups
*  LOWER    Lower graylevel bound.
*  LTBND    Left bound. Used to define the section of bridge
*           being analyzed.
*  N        Total number of pixels in input file.
*  NCL      Limit on number of cracks program will handle.
*  NCPG     Number of cracks per angle group.
*  NUM      Number of additional specified angles (sub. SPECANG)
*  NUMCRCKS Number of cracks.
*  NUMDIVS  Number of divisions.
*  NUMPIX   Number of pixels.
*  NUMPLACE Number of placements.
*  NUMSPANS Number of spans.
*  PCL      Limit on maximum number of pixels allowed in a crack.
*  RDWYPIX  Width of roadway in units of pixels.
*  RES      Resolution in DPI (dots per inch).
*  RTBND    Right bound. Used to define the section of bridge
*           being analyzed.
*  SLPIX    Span Length in units of pixels.
*  SPNC     Number of cracks at the specified angle.
*  TCHECK   Total number of cracks in all angle groups.
*  TOPBND   Top bound. Used in defining a span.
*  TPL      Total pixel limit.
*  UPPER    Upper graylevel bound.

```

```

*   WIDPIX      Width of a placement in units of pixels.
*   X           X coordinate of a pixel.
*   XCOUNT    Counter used to assign proper X coordinate to a
*              selected pixel.
*   XEDGE      X coordinate of line used to locate starting pixel.
*   XLOCATOR    Used to define section of bridge being analyzed.
*   XPERM      Permanent list of X coordinates of pixels within
*              defined graylevel range.
*   XPT2       Used to define section of bridge being analyzed.
*   XSIZE      Number of pixels along X axis in input image.
*   XSTART     X coordinate of starting point pixel.
*   Y           Y coordinate of a pixel.
*   YBOTPT     Used to define section of bridge being analyzed.
*   YCOUNT    Counter used to assign proper Y coordinate to a
*              selected pixel.
*   YLOCATOR    Used to define section of bridge being analyzed.
*   YPERM      Permanent list of Y coordinates of pixels within
*              defined graylevel range.
*   YPT2       Used to define section of bridge being analyzed.
*   YSIZE      Number of pixels along Y axis in input image.
*   YSTART     Y coordinate of starting point pixel.
*   YTOPPT     Used to define section of bridge being analyzed.
*
* CHARACTER VARIABLES:
*
*   INFILE*14   Name of input ascii file.
*   OUTFILE*18  Name of output file.
*   YESNO       See subroutine SPECANG.
*
*****
*   BEGIN
*****
*   PROGRAM MAIN
*   REAL LENGTH, ANGLE, AREA, DENS, TLPG, SCALE, TOTLEN,
+     TOTDENS, SPANG, SPTL, SPDENS, AREA1, SPANLEN, SKEW, RDWY,
+     SPANAREA, LENBRG, WIDPLACE, AREAPLAC, LENPLACE, RTEMP,
+     RDIVS, LENDIV, DIVTRL, DIVTRD, DIVTOTL, DIVTOTD
*   INTEGER X, Y, NUMCRCKS, NUMPIX, CX, CY, NCPG, RES, SPNC,
+     TCHECK, LOWER, UPPER, N, TPL, PCL, NCL, XPERM, YPERM, CHOICE,
+     NUMSPANS, XLOCATOR, YLOCATOR, LTBND, RTBND, BOTBND, TOPBND,
+     XPT2, YPT2, RDWYPIX, SLPIX, YTOPPT, YBOTPT, NUMPLACE, WIDPIX,
+     LENPIX, ITEMP, LDPIX, NUMDIVS, XSTART, YSTART, DIVTRC,
+     DIVTOTC, JOUT
*   CHARACTER INFILE*14, OUTFILE*18
*   DIMENSION X(300000), Y(300000), NUMPIX(1000), CX(3000,1000),
+     CY(3000,1000), LENGTH(1000), ANGLE(1000),
+     NCPG(20), TLPG(20), DENS(20), SPANG(10), SPNC(10),
+     SPTL(10), SPDENS(10), XPERM(300000), YPERM(300000),
+     SPANLEN(12), SLPIX(12), SPANAREA(12), WIDPLACE(8),
+     WIDPIX(8), AREAPLAC(8), LENPLACE(8), LENPIX(8),
+     DIVTRC(50), DIVTRL(50), DIVTRD(50), DIVTOTC(50),
+     DIVTOTL(50), DIVTOTD(50)
*****
*   INPUT INFORMATION SECTION
*
*   RES = 100
*   SCALE = 10.0

```

```

TPL = 300000
PCL = 3000
NCL = 1000
WRITE(6, 1009)
1009 FORMAT (//, 'CURRENT SETTINGS:')
WRITE(6,*) ' '
WRITE(6,*) ' Resolution (DPI).....',RES
WRITE(6,*) ' Drawing Scale (ft./in.).....',SCALE
WRITE(6,*) ' Total Pixel Limit.....',TPL
WRITE(6,*) ' Pixels per Crack Limit.....',PCL
WRITE(6,*) ' Number of Cracks Limit.....',NCL
WRITE(6,*) ' Lower Graylevel Bound (suggested)... 0'
WRITE(6,*) ' Upper Graylevel Bound (suggested)... 200'
WRITE(6,*) ' '
WRITE (6,*) 'ENTER INPUT FILE NAME.'
READ (5,1010) INFILE
1010 FORMAT(A)
WRITE (6,*) 'ENTER LOWER GRAYLEVEL BOUND.'
READ (5,*) LOWER
WRITE (6,*) 'ENTER UPPER GRAYLEVEL BOUND.'
READ (5,*) UPPER
WRITE (6,*) ' '
*
*****
* MAIN SECTION
*
CCC=> The following subroutine scans the ascii file, records the
C coordinates of each pixel within the specified graylevel range,
C and identifies the starting point pixel from which all distances
C are measured (span length, placement width, etc.).
*
CALL COORDS (INFILE,XPERM,YPERM,LOWER,UPPER,N,XSTART,YSTART)
*
CCC=> The following lines represent the program's "main menu". The IF
C statement in line 699 divides the main program into sections
C containing the commands for each menu option.
*
701 WRITE(6,*) ''
WRITE (6,*) 'CRACK DENSITY CALCULATION OPTIONS.'
WRITE(6,*) ' (1) ENTIRE BRIDGE'
WRITE(6,*) ' (2) SPANS'
WRITE(6,*) ' (3) PLACEMENTS'
WRITE(6,*) ' (4) DIVISIONS'
WRITE(6,*) ' (5) FIRST AND LAST DIVISON'
WRITE(6,*) ' (6) QUIT'
WRITE(6,*) ' '
WRITE(6,*) 'ENTER CHOICE.'
700 READ(5,*) CHOICE
IF ((CHOICE.LT.1) .OR. (CHOICE.GT.6)) THEN
WRITE(6,*) 'ENTER 1, 2, 3, 4, 5, OR 6.'
GO TO 700
END IF
*
*****
CCC=>Option 1 -- Entire Bridge.
C This section taken alone is essentially the same as version
C 1.0 of this program.

```



```

*
699  IF (CHOICE .EQ. 1) THEN
      DO 702 I = 1,N
          X(I) = XPERM(I)
          Y(I) = YPERM(I)
702  CONTINUE
      WRITE (6, '(//,A)') 'ENTER OUTPUT FILE NAME.'
      READ (5,1010) OUTFILE
      OPEN (13, FILE = OUTFILE, STATUS = 'UNKNOWN')
      WRITE (6, '(//,A)') 'ENTER BRIDGE DECK AREA (ft.^2).'
      READ (5,*) AREA
      AREA1 = AREA
      AREA = AREA*(0.09290304)
*
      WRITE(13, *) OUTFILE
      WRITE(13,*) ''
      WRITE (13,*) 'OPTION 1: ENTIRE BRIDGE'
      WRITE(13,*) ''
      WRITE(13,*) 'AREA = ',AREA1,' (ft^2)'
      WRITE(13,*) 'AREA = ',AREA,' (m^2)'
      WRITE(13,*) ''
*
      CALL GROUP (N, X, Y, NUMCRCKS, NUMPIX, CX, CY)
      CALL CALCS (NUMCRCKS, NUMPIX, ANGLE, LENGTH, CX, CY)
      CALL OUTINFO (NUMCRCKS, ANGLE, LENGTH, AREA, NCPG, TLPG,TOTLEN,
+          TOTDENS, TCHECK, DENS)
      CALL OUTPUT (NCPG, TLPG, DENS, TCHECK, AREA, AREA1, NUMCRCKS,
+          TOTLEN, TOTDENS, OUTFILE)
      CALL SPECANG (AREA, NUMCRCKS, ANGLE, LENGTH, SPANG, SPNC,
+          SPTL, SPDENS)
*
      CLOSE(13)
      GO TO 701
*
*****
CCC=>Option 2 -- Spans.
*
      ELSEIF (CHOICE .EQ. 2) THEN
          WRITE(6,*) 'ENTER OUTPUT FILE NAME.'
          READ(5, 1010) OUTFILE
          OPEN(13, FILE = OUTFILE, STATUS = 'UNKNOWN')
          WRITE(6, '(//,A)') 'ENTER WIDTH OF ROADWAY. (ft.)'
          READ(5,*) RDWY
          RDWYPIX = NINT(RDWY*10)
          WRITE(6, '(//,A)') 'ENTER NUMBER OF SPANS.'
          READ(5, *) NUMSPANS
          DO 710 I = 1, NUMSPANS
              WRITE(6,*) 'ENTER LENGTH OF SPAN',I,'. (ft.)'
              WRITE(6,*) '(NOTE: Span 1 is at the top of the TIFF image.)'
              READ(5,*) SPANLEN(I)
              SLPIX(I) = NINT(SPANLEN(I)*10)
              SPANAREA(I) = SPANLEN(I) *RDWY
              SPANAREA(I) = SPANAREA(I)*(0.09290304)
710  CONTINUE
          WRITE(6, '(//,A)') 'ENTER SKEW. [(+) OP. (-) DEGREES]'
          READ(5,*) SKEW
          XLOCATOR = XSTART

```

```

YLOCATOR = YSTART
LTBND = XSTART
RTBND = LTBND + RDWYPIX
DO 712 I = 1, NUMSPANS
  AREA = SPANAREA(I)
  AREA1 = AREA/0.09290304
  IF (SKEW .EQ. 0) THEN
    BOTBND = YLOCATOR + SLPIX(I)
    TOPBND = YLOCATOR
    DO 714 J = 1, N
      IF ((XPERM(J).LT.LTBND).OR.(XPERM(J).GT.RTBND)) THEN
        X(J) = 0
        Y(J) = 0
      ELSEIF ((YPERM(J).LT.TOPBND).OR.(YPERM(J).GT.BOTBND)) THEN
        X(J) = 0
        Y(J) = 0
      ELSE
        X(J) = XPERM(J)
        Y(J) = YPERM(J)
      END IF
714 CONTINUE
    ELSE
      YPT2 = YLOCATOR - NINT(TAND(SKEW)*RDWY*10)
      XPT2 = RTBND
      DO 716 J = 1, N
        IF ((XPERM(J).LT.LTBND).OR.(XPERM(J).GT.RTBND)) THEN
          X(J) = 0
          Y(J) = 0
        ELSE
          YTOPPT = YLOCATOR + ( (-XPERM(J) +XLOCATOR) *
+             (YLOCATOR-YPT2) ) /RDWYPIX
          YBOTPT = YTOPPT + SLPIX(I)
          IF( (YPERM(J).LT.YTOPPT).OR.(YPERM(J).GT.YBOTPT) ) THEN
            X(J) = 0
            Y(J) = 0
          ELSE
            X(J) = XPERM(J)
            Y(J) = YPERM(J)
          ENDIF
716 CONTINUE
        ENDIF
      ENDIF
    CONTINUE
  ENDIF
  WRITE(13, *) 'OUTFILE'
  WRITE(13, *) ' '
  WRITE (13, *) 'OPTION 2: SPANS'
  WRITE(13, *) ' '
  WRITE(13, *) 'AREA = ', AREA1, ' (ft^2)'
  WRITE(13, *) 'AREA = ', AREA, ' (m^2)'
  WRITE(13, *) ' '
  WRITE(13, *) 'SPAN #:', I
  WRITE(13, *) 'SPAN LENGTH (ft):', SPANLEN(I)
  WRITE(13, *) ' '
  CALL GROUP (N, X, Y, NUMCRCKS, NUMPIX, CX, CY)
  CALL CALCS (NUMCRCKS, NUMPIX, ANGLE, LENGTH, CX, CY)
  CALL OUTINFO (NUMCRCKS, ANGLE, LENGTH, AREA, NCPG, TLPG, TOTLEN,

```

```

+           TOTDENS, TCHECK, DENS)
CALL OUTPUT (NCPG, TLPG, DENS, TCHECK, AREA, AREA1, NUMCRCKS,
+           TOTLEN, TOTDENS, OUTFILE)
CALL SPECANG (AREA, NUMCRCKS, ANGLE, LENGTH, SPANG, SPNC,
+           SPTL, SPDENS)
YLOCATOR = YLOCATOR + SLPIX(I)
*
712  CONTINUE
      CLOSE (13)
      GO TO 701
*
*****
CCC=>Option 3 -- Placements.
*
      ELSEIF (CHOICE .EQ. 3) THEN
        WRITE(6,*)'ENTER OUTPUT FILE NAME.'
        READ(5, 1010) OUTFILE
        OPEN(13, FILE = OUTFILE, STATUS = 'UNKNOWN')
        WRITE(6, '(//,A)')'ENTER SKEW. [(+) OR (-) DEGREES]'
        READ(5,*) SKEW
        WRITE(6, '(//,A)')'PLACEMENTS ARE . . .'
        WRITE(6,*)' (1) FULL LENGTH/PARTIAL WIDTH'
        WRITE(6,*)' (2) PARTIAL LENGTH/FULL WIDTH'
        WRITE(6,*)' '
        WRITE(6,*) 'ENTER CHOICE.'
720  READ(5,*) CHOICE
        IF ((CHOICE.NE.1) .AND. (CHOICE.NE.2)) THEN
          WRITE(6,*)'ENTER 1 OR 2.'
          GO TO 720
        ENDIF
        IF (CHOICE .EQ. 1) THEN
          WRITE(6, '(//,A)')'ENTER LENGTH OF BRIDGE. (ft.)'
          READ(5,*) LENBRG
          WRITE(6, '(//,A)')'ENTER NUMBER OF PLACEMENTS.'
          READ(5,*) NUMPLACE
          DO 722 I = 1, NUMPLACE
            WRITE(6,*)'ENTER WIDTH OF PLACEMENT' ,I, '. (ft.)'
            READ(5,*) WIDPLACE(I)
            WIDPIX(I) = NINT(WIDPLACE(I)*10)
            AREAPLAC(I) = LENBRG * WIDPLACE(I)*0.09290304
722  CONTINUE
          XLOCATOR = XSTART
          DO 724 I = 1, NUMPLACE
            LTBND = XLOCATOR
            RTBND = LTBND + WIDPIX(I)
            AREA = AREAPLAC (I)
            AREA1 = AREA/0.09290304
            DO 726 J = 1, N
              IF ((XPERM(J) .LT. LTBND) .OR. (XPERM(J) .GT. RTBND)) THEN
                X(J) = 0
                Y(J) = 0
              ELSE
                X(J) = XPERM(J)
                Y(J) = YPERM(J)
              ENDIF
            ENDIF
726  CONTINUE
*

```

```

WRITE(13, *) OUTFILE
WRITE(13, *) ''
WRITE (13, *) 'OPTION 3: PLACEMENTS'
WRITE(13, *) ''
WRITE(13, *) 'AREA = ', AREA1, ' (ft^2)'
WRITE(13, *) 'AREA = ', AREA, ' (m^2)'
WRITE(13, *) ''
WRITE(13, *) 'FULL LENGTH / PARTIAL WIDTH'
WRITE(13, *) 'PLACEMENT #:', I
WRITE(13, *) 'WIDTH OF PLACEMENT (ft):', WIDPLACE(I)
WRITE(13, *) ''
*
CALL GROUP (N, X, Y, NUMCRCKS, NUMPIX, CX, CY)
CALL CALCS (NUMCRCKS, NUMPIX, ANGLE, LENGTH, CX, CY)
CALL OUTINFO (NUMCRCKS, ANGLE, LENGTH, AREA, NCPG, TLPG, TOTLEN,
+           TOTDENS, TCHECK, DENS)
CALL OUTPUT (NCPG, TLPG, DENS, TCHECK, AREA, AREA1, NUMCRCKS,
+           TOTLEN, TOTDENS, OUTFILE)
CALL SPECANG (AREA, NUMCRCKS, ANGLE, LENGTH, SPANG, SPNC,
+           SPTL, SPDENS)
*
XLOCATOR = RTBND
724 CONTINUE
ELSE
WRITE(6, *) 'ENTER NUMBER OF PLACEMENTS.'
READ(5, *) NUMPLACE
WRITE(6, *) 'ENTER WIDTH OF ROADWAY. (ft.^2).'
READ(5, *) RDWY
RDWYPIX = NINT(RDWY*10)
DO 730 I = 1, NUMPLACE
WRITE(6, *) 'ENTER LENGTH OF PLACEMENT', I, '. (ft.).'
READ(5, *) LENPLACE(I)
LENPIX(I) = NINT(LENPLACE(I)*10)
AREAPLAC(I) = RDWY * LENPLACE(I) * 0.09290304
730 CONTINUE
XLOCATOR = XSTART
YLOCATOR = YSTART
LTBND = XSTART
RTBND = LTBND + RDWYPIX
DO 732 I = 1, NUMPLACE
AREA = AREAPLAC(I)
AREA1 = AREA/0.09290304
IF (SKEW .EQ. 0) THEN
BOTBND = YLOCATOR + LENPIX(I)
TOPBND = YLOCATOR
DO 734 J = 1, N
IF ((XPERM(J) .LT. LTBND) .OR. (XPERM(J) .GT. RTBND)) THEN
X(J) = 0
Y(J) = 0
ELSEIF( (YPERM(J) .LT. TOPBND) .OR. (YPERM(J) .GT. BOTBND) )
+ THEN
X(J) = 0
Y(J) = 0
ELSE
X(J) = XPERM(J)
Y(J) = YPERM(J)
END IF

```

```

734      CONTINUE
      ELSE
      YPT2 = YLOCATOR - NINT(TAND(SKEW)*RDWY*10)
      XPT2 = RTBND
      DO 736 J = 1,N
        IF ((XPERM(J) .LT. LTBND) .OR. (XPERM(J) .GT. RTBND)) THEN
          X(J) = 0
          Y(J) = 0
        ELSE
          YTOPPT = YLOCATOR + ( (-XPERM(J) + XLOCATOR) *
+             (YLOCATOR-YPT2) ) /RDWYPIX
          YBOTPT = YTOPPT + LENPIX(I)
          IF( (YPERM(J) .LT. YTOPPT) .OR. (YPERM(J) .GT. YBOTPT) ) THEN
            X(J) = 0
            Y(J) = 0
          ELSE
            X(J) = XPERM(J)
            Y(J) = YPERM(J)
          END IF
        ENDIF
      CONTINUE
736    ENDIF
*
      WRITE(13, *) OUTFILE
      WRITE(13, *) ''
      WRITE (13,*) 'OPTION 3: PLACEMENTS'
      WRITE(13, *) ''
      WRITE(13,*) 'AREA = ',AREA1,' (ft^2)'
      WRITE(13,*) 'AREA = ',AREA,' (m^2)'
      WRITE(13,*) ''
      WRITE(13,*) 'PARTIAL LENGTH / FULL WIDTH'
      WRITE(13,*) 'PLACEMENT #:',I
      WRITE(13,*) 'LENGHT OF PLACEMENT (ft):',LENPLACE(I)
      WRITE(13,*) ''
*
      CALL GROUP (N, X, Y, NUMCRCKS, NUMPIX, CX, CY)
      CALL CALCS (NUMCRCKS, NUMPIX, ANGLE, LENGTH, CX, CY)
      CALL OUTINFO (NUMCRCKS, ANGLE, LENGTH, AREA, NCPG, TLPG, TOTLEN,
+        TODDENS, TCHECK, DENS)
      CALL OUTPUT (NCPG, TLPG, DENS, TCHECK, AREA, AREA1, NUMCRCKS,
+        TOTLEN, TODDENS, OUTFILE)
      CALL SPECANG (AREA, NUMCRCKS, ANGLE, LENGTH, SPANG, SPNC,
+        SPTL, SPDENS)
*
      YLOCATOR = YLOCATOR + LENPIX(I)
732    CONTINUE
      ENDIF
      CLOSE(13)
      GO TO 701
*
*****
CCC=>Option 4 -- Divisions.
*
      ELSEIF (CHOICE .EQ. 4) THEN
      WRITE(6,*) 'ENTER OUTPUT FILE NAME.'
      READ(5, 1010)OUTFILE
      OPEN(13, FILE=OUTFILE, STATUS='UNKNOWN')

```

```

WRITE(6,*) 'ENTER WIDTH OF ROADWAY. (ft.)'
READ(5,*) RDWY
RDWYPIX = NINT(RDWY*10)
WRITE(6,*) 'ENTER LENGTH OF BRIDGE. (ft.)'
READ(5,*) LENBRG
*
* THE FOLLOWING LINES WERE CHANGED SO THAT THE LENGTH OF DIVISION
* COULD BE CHOSEN INSTEAD OF THE NUMBER OF DIVISIONS
* WRITE(6,*) 'ENTER NUMBER OF DIVISIONS.'
* READ(5,*) NUMDIVS
* RDIVS = REAL(NUMDIVS)
* LENDIV = LENBRG/RDIVS
* LDPIX = NINT(LENDIV*10)
*
* THE CHANGES START HERE
WRITE(6,*) 'NOTE!!!!!!'
WRITE(6,*) 'THE LAST DIVISION WILL NOT NECESSARILY BE THE CHOSEN
LENGTH'
WRITE(6,*) 'IF THE BRIDGE LENGTH IS NOT EVENLY DIVISIBLE BY THE
DIVISION LENGTH'
WRITE(6,*)
WRITE(6,*) 'ENTER LENGTH OF DIVISIONS (ft.)'
READ(5,*) LENDIV
LDPIX = NINT(LENDIV*10)
RDIVS = LENBRG/LENDIV
NUMDIVS = (INT(RDIVS)+1)
*
* END OF CHANGES
*
AREA = LENDIV*RDWY* 0.09290304
AREA1 = AREA/0.09290304
WRITE(6,*) 'ENTER SKEW. [(+) OR (-) DEGREES]'
READ(5,*) SKEW
XLOCATOR = XSTART
YLOCATOR = YSTART
LTBND = XLOCATOR
RTBND = LTBND + RDWYPIX
DO 742 I = 1,NUMDIVS
  IF (SKEW .EQ. 0) THEN
    BOTBND = YLOCATOR + LDPIX
    TOPBND = YLOCATOR
    DO 744 J = 1,N
      IF ((XPERM(J).LT. LTBND) .OR. (XPERM(J).GT. RTBND)) THEN
        X(J) = 0
        Y(J) = 0
      ELSEIF((YPERM(J).LT.TOPBND).OR.(YPERM(J).GT.BOTBND)) THEN
        X(J) = 0
        Y(J) = 0
      ELSE
        X(J) = XPERM(J)
        Y(J) = YPERM(J)
      ENDIF
    CONTINUE
  ELSE
    YPT2 = YLOCATOR - NINT(TAND(SKEW)*RDWY*10)
    XPT2 = RTBND
    DO 746 J = 1,N
      IF ((XPERM(J).LT.LTBND).OR.(XPERM(J).GT.RTBND)) THEN

```

```

      X(J) = 0
      Y(J) = 0
    ELSE
      YTOPPT = YLOCATOR + ((-XPERM(J) + XLOCATOR) *
+         (YLOCATOR-YPT2)) / RDWYPIX
      YBOTPT = YTOPPT + LDPIX
      IF((YPERM(J).LT.YTOPPT).OR.(YPERM(J).GT.YBOTPT)) THEN
        X(J) = 0
        Y(J) = 0
      ELSE
        X(J) = XPERM(J)
        Y(J) = YPERM(J)
      ENDIF
    ENDIF
746   CONTINUE
      END IF
*
      CALL GROUP (N, X, Y, NUMCRCKS, NUMPIX, CX, CY)
      CALL CALCS (NUMCRCKS, NUMPIX, ANGLE, LENGTH, CX, CY)
      CALL OUTINFO (NUMCRCKS, ANGLE, LENGTH, AREA, NCPG, TLPG, TOTLEN,
+         TODDENS, TCHECK, DENS)
*
      DIVTRC(I) = NCPG(1)
      DIVTRL(I) = TLPG(1)
      DIVTRD(I) = DENS(1)
      DIVTOTC(I) = TCHECK
      DIVTOTL(I) = TOTLEN
      DIVTOTD(I) = TODDENS
      RTEMP = I*LENDIV*10
      ITEMP = NINT(RTEMP)
      YLOCATOR = YSTART + ITEMP
742   CONTINUE
      DO 747 J = 1,2
        IF (J .EQ. 1) THEN
          JOUT = 6
        ELSE
          JOUT = 13
        ENDIF
        WRITE (JOUT, *) OUTFILE
        WRITE(JOUT,*) ' '
        WRITE (JOUT,*) 'OPTION 4: DIVISIONS'
        WRITE(JOUT,*)
        WRITE(JOUT,*) 'DIVISION LENGTH =',LENDIV,' (ft.)'
        WRITE(JOUT,*) '          =',LENDIV*0.3048,' (m)'
        WRITE(JOUT,*) ' '
        WRITE(JOUT,*) 'NUMBER OF DIVISIONS',NUMDIVS
        WRITE(JOUT,*) ' '
        WRITE(JOUT,*) 'DIVISION AREA =',AREA1,' (ft.^2)'
        WRITE(JOUT,*) '          =',AREA,' (m^2)'
        WRITE(JOUT,*) ' '
        WRITE (JOUT,1730)
        WRITE (JOUT,1732)
        WRITE (JOUT,1734)
        WRITE (JOUT,1736)
        DO 745 I = 1,NUMDIVS
          WRITE (JOUT,1745) I, DIVTRC(I), DIVTRL(I), DIVTRD(I),
+             DIVTOTC(I), DIVTOTL(I), DIVTOTD(I)

```

```

745     CONTINUE
747     CONTINUE
      WRITE(JOUT,*) ''
1730  FORMAT (7X, '-----TRANSVERSE-----', 2X,
+         '-----TOTAL-----')
1732  FORMAT ('DIV.', 3X, '#CRACKS', 2X, 'LENGTH', 2X, 'DENSITY', 2X,
+         '#CRACKS', 2X, 'LENGTH', 2X, 'DENSITY')
1734  FORMAT (18X, '(m)', 3X, '(m/m^2)', 13X, '(m)', 3X, '(m/m^2)')
1736  FORMAT ('----', 3X, '-----', 1X, '-----', 1X, '-----', 2X,
+         '-----', 1X, '-----', 1X, '-----')
1745  FORMAT(2X, I2, 5X, I3, 4X, F6.2, 3X, F5.3, 5X, I3, 4X, F6.2, 3X, F5.3)
      CLOSE(13)
      GO TO 701
*
*****
CCC=>Option 5 - First and Last 10 ft (or other length) of bridge deck
*
      ELSEIF (CHOICE .EQ. 5) THEN
        WRITE(6,*) 'ENTER OUTPUT FILE NAME.'
        READ(5, 1010)OUTFILE
        OPEN(13, FILE=OUTFILE, STATUS='UNKNOWN')
        WRITE(6,*) 'ENTER WIDTH OF ROADWAY. (ft.)'
        READ(5,*) RDWY
        RDWYPIX = NINT(RDWY*10)
        WRITE(6,*) 'ENTER LENGTH OF BRIDGE. (ft.)'
        READ(5,*) LENBRG
        WRITE(6,*) 'ENTER LENGTH OF FIRST AND LAST DIVISIONS. (ft.) (10)''
        READ(5,*) LENDIV
*      LENDIV is now the length in feet of the first and last division
        RDIVS = LENBRG/LENDIV
        LDPIX = NINT(LENDIV*10)
*      10 pixels per foot for a 100 dpi image
*      LDPIX is the number of pixels for the length of the division
        AREA = LENDIV*RDWY* 0.09290304
*      1 square ft = 0.0929304 square meters
*      AREA is area of the div in square meters
        AREA1 = AREA/0.09290304
*      AREA1 is the area of the div in square ft.
        WRITE(6,*) 'ENTER SKEW. [(+) OR (-) DEGREES]''
        READ(5,*) SKEW
        XLOCATOR = XSTART
        YLOCATOR = YSTART
        LTBND = XLOCATOR
        RTBND = LTBND + RDWYPIX
*
        DO 2742 I = 1,2
          IF (SKEW .EQ. 0) THEN
            BOTBND = YLOCATOR + LDPIX
            TOPBND = YLOCATOR
            DO 2744 J = 1,N
              IF ((XPERM(J).LT. LTBND) .OR. (XPERM(J).GT. RTBND)) THEN
                X(J) = 0
                Y(J) = 0
              ELSEIF((YPERM(J).LT.TOPBND) .OR. (YPERM(J).GT.BOTBND)) THEN
                X(J) = 0
                Y(J) = 0
              ELSE

```



```

        X(J) = XPERM(J)
        Y(J) = YPERM(J)
    ENDIF
2744    CONTINUE
    ELSE
        YPT2 = YLOCATOR - NINT(TAND(SKEW)*RDWY*10)
        XPT2 = RTBND
        DO 2746 J = 1,N
            IF ((XPERM(J).LT.LTBND).OR.(XPERM(J).GT.RTBND)) THEN
                X(J) = 0
                Y(J) = 0
            ELSE
                YTOPPT = YLOCATOR + ((-XPERM(J) + XLOCATOR) *
+                 (YLOCATOR-YPT2)) / RDWYPIX
                YBOTPT = YTOPPT + LDPIX
                IF((YPERM(J).LT.YTOPPT).OR.(YPERM(J).GT.YBOTPT)) THEN
                    X(J) = 0
                    Y(J) = 0
                ELSE
                    X(J) = XPERM(J)
                    Y(J) = YPERM(J)
                ENDIF
            ENDIF
        ENDIF
2746    CONTINUE
    END IF
*
    CALL GROUP (N, X, Y, NUMCRCKS, NUMPIX, CX, CY)
    CALL CALCS (NUMCRCKS, NUMPIX, ANGLE, LENGTH, CX, CY)
    CALL OUTINFO (NUMCRCKS, ANGLE, LENGTH, AREA, NCPG, TLPG, TOTLEN,
+    TOTDENS, TCHECK, DENS)
*
    WRITE (13, *) OUTFILE
    WRITE(13,*) ' '
    WRITE (13,*) 'OPTION 5: FIRST AND LAST DIVISION'
    WRITE (13,*)
    WRITE (13,*) 'DIVISION NUMBER ',I
    WRITE(13,*)
    WRITE(13,*) 'DIVISION LENGTH =',LENDIV,' (ft.)'
    WRITE(13,*) '          =',LENDIV*0.3048,' (m)'
    WRITE(13,*) 'DIVISION AREA =',AREA1,' (ft.^2)'
    WRITE(13,*) '          =',AREA,' (m^2)'
    WRITE(13,*) ' '
    WRITE (13,*) 'DIVISON 1 IS THE FIRST ',LENDIV,' (ft.)OF THE BRIDGE
DECK'
    WRITE (13,*) 'DIVISON 2 IS THE LAST ',LENDIV,' (ft.)OF THE BRIDGE
DECK'
    WRITE(13,*) ' '
*
    CALL OUTPUT (NCPG, TLPG, DENS, TCHECK, AREA, AREA1, NUMCRCKS,
+    TOTLEN, TOTDENS, OUTFILE)
*
*
    Cracks between -5 and 5 degrees are considered transverse
    DIVTRC(I) = NCPG(1)
    DIVTRL(I) = TLPG(1)
    DIVTRD(I) = DENS(1)
    DIVTOTC(I) = TCHECK

```

```

      DIVTOTL(I) = TOTLEN
      DIVTOTD(I) = TOTDENS
*
*      Set YLOCATOR to a distance LENDIV or LDPIX from the far end of
*      the bridge
      RTEMP = (LENBRG - LENDIV)*10
      ITEMP = NINT(RTEMP)
      YLOCATOR = YSTART + ITEMP
2742  CONTINUE
*
      DO 2747 J = 1,2
        IF (J .EQ. 1) THEN
          JOUT = 6
        ELSE
          JOUT = 13
        ENDIF
        WRITE (JOUT, *) OUTFILE
        WRITE(JOUT,*) ''
        WRITE (JOUT,*) 'OPTION 5: FIRST AND LAST DIVISION'
        WRITE(JOUT,*)
        WRITE(JOUT,*) 'DIVISION LENGTH =',LENDIV, ' (ft.)'
        WRITE(JOUT,*) '                        =',LENDIV*0.3048, ' (m)'
        WRITE(JOUT,*) 'DIVISION AREA =',AREAL, ' (ft.^2)'
        WRITE(JOUT,*) '                        =',AREA, ' (m^2)'
        WRITE(JOUT,*) ' '
        WRITE (JOUT,*) 'DIVISON 1 IS THE FIRST ',LENDIV, ' (ft.)OF THE
+          BRIDGE DECK'
        WRITE (JOUT,*) 'DIVISON 2 IS THE LAST ',LENDIV, ' (ft.)OF THE BRIDGE
+          DECK'
        WRITE(JOUT,*) ' '
        WRITE (JOUT,3730)
        WRITE (JOUT,3732)
        WRITE (JOUT,3734)
        WRITE (JOUT,3736)
        DO 2745 I = 1,2
          WRITE (JOUT,3745) I, DIVTRC(I), DIVTRL(I), DIVTRD(I),
+            DIVTOTC(I), DIVTOTL(I), DIVTOTD(I)
2745  CONTINUE
2747  CONTINUE
      WRITE(JOUT,*) ''
3730  FORMAT (7X, '-----TRANSVERSE-----', 2X,
+         '-----TOTAL-----')
3732  FORMAT ('DIV.', 3X, '#CRACKS', 2X, 'LENGTH', 2X, 'DENSITY', 2X,
+         '#CRACKS', 2X, 'LENGTH', 2X, 'DENSITY')
3734  FORMAT (18X, ' (m) ', 3X, ' (π/m^2) ', 13X, ' (m) ', 3X, ' (m/m^2) ')
3736  FORMAT ('----', 3X, '-----', 1X, '-----', 1X, '-----', 2X,
+         '-----', 1X, '-----', 1X, '-----')
3745  FORMAT(2X, I2, 5X, I3, 4X, F6.2, 3X, F5.3, 5X, I3, 4X, F6.2, 3X, F5.3)
      CLOSE(13)
      GO TO 701
*
*****
CCC=>Option 6 -- Quit.
*
      ELSE
        WRITE(6,*) 'END!'
      ENDIF

```

```

END
*
*****
*   SUBROUTINE GROUP
*****
*   DIVIDES PIXELS INTO CRACK GROUPS
*   NUMCRCKS = TOTAL NUMBER OF CRACKS IN SECTION CONSIDERED
*   NUMPIX(K) = TOTAL NUMBER OF PIXELS IN A GIVEN CRACK K
*   N = TOTAL NUMBER OF PIXELS IN THE INPUT FILE
*
SUBROUTINE GROUP (N,X,Y,NUMCRCKS,NUMPIX,CX,CY)
INTEGER N,X,Y,NUMCRCKS,NUMPIX,CX,CY,CHECK,H
DIMENSION X(300000),Y(300000),NUMPIX(1000),CX(3000,1000),
+           CY(3000,1000)
*
*
DO 24 I = 1,1000
  DO 23 J = 1,3000
    CX(J,I) = 0
    CY(J,I) = 0
23  CONTINUE
24  CONTINUE
NUMCRCKS = 0
H = 0
DO 50 K = 1,1000
  H=H + 1
  WRITE(6,*)'K = ',K
  WRITE(6,*)'H = ',H
  CHECK = 0
  DO 25 M = 1,N
    CHECK = CHECK + X(M)
25  CONTINUE
    WRITE(6,*)'check = ',CHECK
    IF (CHECK .EQ. 0) THEN
      GO TO 60
    ELSE
      NUMPIX(H) = 1
      DO 5 L = 1,N
        IF (X(L) .NE. 0) THEN
          CX(1,H) = X(L)
          CY(1,H) = Y(L)
          X(L) = 0
          Y(L) = 0
          GO TO 8
        ENDIF
      CONTINUE
5      CONTINUE
8      DO 40 J = 1,3000
        IF (CX(J,H) .NE. 0) THEN
          DO 30 I = 1,N
            IF (X(I) .NE. 0) THEN
              IF (((X(I) .EQ. CX(J,H)) .OR. (X(I) .EQ. (CX(J,H)+1)) .OR.
+                (X(I) .EQ. (CX(J,H)-1)))
+                .AND.
+                ((Y(I) .EQ. CY(J,H)) .OR. (Y(I) .EQ. (CY(J,H)+1)) .OR.
+                (Y(I) .EQ. (CY(J,H)-1)))) THEN
                NUMPIX(H) = NUMPIX(H) + 1
                CX(NUMPIX(H),H) = X(I)

```

```

        CY(NUMPIX(H),H) = Y(I)
        X(I) = 0
        Y(I) = 0
    ENDIF
ENDIF
30    CONTINUE
*
    IF (NUMPIX(H).EQ.1) THEN
        NUMCRCKS = NUMCRCKS-1
        H=H-1
    ENDIF
    ELSE
        GO TO 45
    ENDIF
40    CONTINUE
45    CONTINUE
        NUMCRCKS = NUMCRCKS + 1
    END IF
50    CONTINUE
60    CONTINUE
    WRITE(6,*)'numcrcks = ',NUMCRCKS
    RETURN
END
*
*****
* SUBROUTINE CALCS
*****
* CALCULATES LENGTH AND ANGLE OF EVERY CRACK
*   K = CRACK NUMBER
*   J = FIXED (BASE) PIXEL FROM WHICH DISTANCES ARE MEASURED
*   I = VARIABLE (ENDPOINT) PIXEL
*
    SUBROUTINE CALCS (NUMCRCKS, NUMPIX, ANGLE, LENGTH, CX, CY)
    REAL ANGLE,LENGTH,D,X1,Y1,X2,Y2
    INTEGER NUMCRCKS, NUMPIX, CX, CY
    DIMENSION ANGLE(1000),LENGTH(1000),NUMPIX(1000),CX(3000,1000),
+       CY(3000,1000) ,D(1000)
*
*
    DO 78 I = 1,1000
        ANGLE(I) = 0
78    CONTINUE
    DO 90 K = 1,NUMCRCKS
        LENGTH(K) = 0
        DO 80 J = 1,NUMPIX(K)
            X1 = REAL(CX(J,K))
            Y1 = REAL(CY(J,K))
            DO 70 I = 1,NUMPIX(K)
                X2 = REAL(CX(I,K))
                Y2 = REAL(CY(I,K))
*
                D calculates the distance between two pixels
                D(K)=SQRT(((X1-X2)**2)+((Y1-Y2)**2))
                IF (D(K) .GT. LENGTH(K)) THEN
                    LENGTH(K) = D(K)
                    IF (X1 .EQ. X2) THEN
                        ANGLE(K) = 90
                    ELSEIF (Y1 .EQ. Y2) THEN

```

```

        ANGLE(K) = 0
        ELSE
*       Angle is the angle in degrees between the first pixel in the crack
*       and the last pixel in the crack.
            ANGLE(K)=(ATAN((Y1-Y2)/(X1-X2)))*(-180/3.14159265)
            ENDIF
        END IF
70      CONTINUE
80      CONTINUE
90      CONTINUE
*
CCC=> THE FOLLOWING LINES CONVERT THE LENGTHS FROM PIXELS TO METERS.
CCC=> IF THE RESOLUTION OR DRAWING SCALE CHANGES, THE CONVERSION FACTOR
CCC=> MUST CHANGE ACCORDINGLY.
CCC=> (1 in./100 pix)*(10 feet/1 in.)*(0.3048m/foot) = 0.03048m/pix
*
        DO 95 K = 1,NUMCRCKS
            LENGTH(K) = LENGTH(K) * (0.03048)
95      CONTINUE
        RETURN
        END
*
*****
*   SUBROUTINE OUTINFO
*****
*   CREATES INFORMATION FOR OUTPUT
*   NCPG = NUMBER OF CRACKS PER GROUP
*   TLPG = TOTAL LENGTH PER GROUP
*   DENS = CRACK DENSITY PER GROUP (LIN. m/m^2)
*
*
        SUBROUTINE OUTINFO (NUMCRCKS,ANGLE,LENGTH,AREA,NCPG,TLPG,TOTLEN,
+       TOTDENS, TCHECK, DENS)
        REAL ANGLE, LENGTH, AREA, TLPG, TOTLEN, TOTDENS, DENS
        INTEGER NUMCRCKS , NCPG, TCHECK, LOW, HIGH
        DIMENSION ANGLE(1000),LENGTH(1000),NCPG(20),TLPG(20),DENS(20)
*
*
        DO 110 L = 1,19
            NCPG(L) = 0
            TLPG(L) = 0
            DENS(L) = 0
110      CONTINUE
        DO 130 K = 1,NUMCRCKS
            LOW = -5
            HIGH = 5
            DO 120 L = 1,9
                IF ((ANGLE(K).GE. LOW) .AND. (ANGLE(K).LT. HIGH)) THEN
                    NCPG(L) = NCPG(L) + 1
                    TLPG(L) = TLPG(L) + LENGTH(K)
                    GO TO 130
                ENDIF
                LOW = LOW + 10
                HIGH = HIGH + 10
120      CONTINUE
            IF ((ANGLE(K).GE.85).AND.(ANGLE(K).LE.90)) .OR.
+           ((ANGLE(K).LT.-85).AND.(ANGLE(K).GT.-90))) THEN

```

```

      NCPG(10) = NCPG(10) + 1
      TLPG(10) = TLPG(10) + LENGTH(K)
    END IF
    LOW = -15
    HIGH = -5
    DO 125 L = 11,18
      IF ((ANGLE(K) .GE. LOW) .AND. (ANGLE(K) .LT. HIGH)) THEN
        NCPG(L) = NCPG(L) + 1
        TLPG(L) = TLPG(L) + LENGTH(K)
        GO TO 130
      ENDIF
      LOW = LOW - 10
      HIGH = HIGH - 10
125   CONTINUE
130   CONTINUE
      DO 140 L = 1,18
        DENS(L) = TLPG(L)/AREA
140   CONTINUE
      TOTLEN = 0
      DO 145 K = 1,NUMCRCKS
        TOTLEN = TOTLEN + LENGTH(K)
145   CONTINUE
      TOTDENS = TOTLEN/AREA
      TCHECK = 0
      DO 147 I = 1,18
        TCHECK = TCHECK + NCPG(I)
147   CONTINUE
      RETURN
    END

*
*****
* SUBROUTINE OUTPUT
*****
* WRITES RESULTS TO THE SCREEN AND TO AN OUTPUT FILE
*
      SUBROUTINE OUTPUT (NCPG,TLPG,DENS,TCHECK,AREA,AREA1,NUMCRCKS,
+      TOTLEN,TOTDENS,OUTFILE)
      REAL TLPG, DENS, AREA, AREA1, TOTLEN, TOTDENS
      INTEGER NCPG, TCHECK, NUMCRCKS, LOW, HIGH
      CHARACTER OUTFILE*18
      DIMENSION NCPG(20),TLPG(20),DENS(20)

*
*
      WRITE(6,*) ''
      WRITE(6,1012)
      WRITE(6,1014)
      WRITE(6,1016)
      WRITE(6,1018)
      LOW = -5
      HIGH = 5
1012  FORMAT(15X,'# OF',6X,'TOTAL',8X,'CRACK')
1014  FORMAT(4X,'ANGLE',5X,'CRACKS',4X,'LENGTH',7X,'DENSITY')
1016  FORMAT(4X,'(deg)',17X,'(m)',6X,'(Lin. m/m^2)')
1018  FORMAT('-----',4X,'---',5X,'-----',5X,'-----')
1020  FORMAT(1X,'(,I3,')-(,I3,')',4X,I3,3X,F8.2,8X,F9.7)
      DO 150 I = 1,10
        WRITE(6,1020) LOW, HIGH, NCPG(I),TLPG(I),DENS(I)

```

```

        LOW = LOW + 10
        HIGH = HIGH + 10
150  CONTINUE
        LOW = -5
        HIGH = -15
        DO 160 I = 11,18
            WRITE(6,1020)LOW, HIGH, NCPG(I),TLPG(I),DENS(I)
            LOW = LOW - 10
            HIGH = HIGH - 10
160  CONTINUE
        WRITE(6,1030) 'TOTAL' ,NUMCRCKS, TOTLEN, TOTDENS
        WRITE(6, 1037) 'CHECK' ,TCHECK
        WRITE(6,*) ''
1030  FORMAT (4X,A5,7X,I3,3X,F8.2,8X,F9.7)
*
        WRITE(13,1012)
        WRITE(13,1014)
        WRITE(13,1016)
        WRITE(13,1018)
        LOW = -5
        HIGH = 5
        DO 170 I = 1,10
            WRITE(13,1020)LOW, HIGH, NCPG(I),TLPG(I),DENS(I)
            LOW = LOW + 10
            HIGH = HIGH + 10
170  CONTINUE
        LOW = -5
        HIGH = -15
        DO 180 I = 11,18
            WRITE(13,1020)LOW, HIGH, NCPG(I),TLPG(I),DENS(I)
            LOW = LOW - 10
            HIGH = HIGH - 10
180  CONTINUE
        WRITE(13,1030) 'TOTAL' ,NUMCRCKS, TOTLEN, TOTDENS
        WRITE(13,1037) 'CHECK', TCHECK
        WRITE(13,*) ''
        WRITE(13,*) ''
1037  FORMAT (4X,A5,7X,I3)
        RETURN
        END
*
*****
*  SUBROUTINE SPECANG
*****
*  SPECIFIED ANGLE SECTION
*
        SUBROUTINE SPECANG (AREA, NUMCRCKS, ANGLE, LENGTH, SPANG, SPNC,
+          SPTL, SPDENS)
        REAL AREA, ANGLE, LENGTH, SPANG, SPTL, SPDENS, RLOW, RHIGH, TOL
        INTEGER NUMCRCKS, SPNC, NUM
        CHARACTER YESNO
        DIMENSION ANGLE(20),LENGTH(20),SPANG(10),SPNC(10),SPTL(10),
+          SPDENS (10)
*
*
        WRITE(6, 1050)
1050  FORMAT(//,//,' DO YOU WISH TO SEE INFORMATION FOR ANGLES OTHER')

```

```

WRITE(6,*)'THAN THOSE LISTED?'
1051 FORMAT (A1)
READ(5,1051) YESNO
IF (YESNO .EQ. 'Y' .OR. YESNO .EQ. 'y') THEN
  WRITE(6,*)'ENTER THE NO. OF ADDITIONAL ANGLES DESIRED.'
  READ(5,*)NUM
  WRITE(6,*)'ENTER TOLERANCE FOR EACH ANGLE (+/- ___deg.).'
  READ(5,*) TOL
  DO 190 I = 1,NUM
    WRITE(6,*)'ENTER ANGLE',I,'(deg.).'
    READ(5,*) SPANG(I)
190  CONTINUE
    DO 195 I = 1,10
      SPNC(I) = 0
      SPTL(I) = 0
      SPDENS(I) = 0
195  CONTINUE
    DO 200 K = 1,NUMCRCKS
      DO 198 I = 1,NUM
        IF((ANGLE(K).GT.(SPANG(I)-TOL)) .AND.
+         (ANGLE(K).LT.(SPANG(I)+TOL))) THEN
          SPNC(I) = SPNC(I) + 1
          SPTL(I) = SPTL(I) + LENGTH(K)
        ENDIF
198  CONTINUE
200  CONTINUE
      DO 210 I = 1,NUM
        SPDENS(I) = SPTL(I)/AREA
210  CONTINUE
      WRITE(6,1052)
1052 FORMAT(//, 'SPECIFIED ANGLES:')
*   See the end of the Subroutine for the format statements
      WRITE(6,*)' '
      WRITE(6,1062)
      WRITE(6,1064)
      WRITE(6,1066)
      WRITE(6,1068)
      WRITE(13,1052)
      WRITE(13,*)' '
      WRITE(13,1062)
      WRITE(13,1064)
      WRITE(13,1066)
      WRITE(13,1068)
      DO 220 I = 1,NUM
        RLOW = SPANG(I) - TOL
        RHIGH = SPANG(I) + TOL
        WRITE(6,1060)RLOW, RHIGH, SPNC(I),SPTL(I),SPDENS(I)
        WRITE(13,1060)RLOW, RHIGH, SPNC(I),SPTL(I),SPDENS(I)
220  CONTINUE
      END IF
1060 FORMAT(1X, '(' ,F5.1') - (' ,F5.1, ')', 4X, I3, 3X, F6.2, 8X, F9.7)
1062 FORMAT(19X, '# OF', 4X, 'TOTAL', 8X, 'CRACK')
1064 FORMAT(6X, 'ANGLE', 7X, 'CRACKS', 2X, 'LENGTH', 7X, 'DENSITY')
1066 FORMAT(6X, '(deg)', 17X, '(m)', 6X, '(Lin. m/m^2)')
1068 FORMAT('-----', 4X, '---', 3X, '-----', 5X, '-----')
      WRITE(13,*)' '
      WRITE(13,*)' '

```



```

RETURN
END
*
*****
*   SUBROUTINE COORDS
*****
*   SELECTS ALL "DARK" PIXELS FROM ASCII FILE AND WRITES THEIR
*   COORDINATES TO FILE coords.dat
*
SUBROUTINE COORDS (INFILE,XPERM,YPERM,LOWER,UPPER,N,XSTART,
+   YSTART)
INTEGER LEVEL, XCOUNT, YCOUNT, XPERM, YPERM, LOWER, UPPER, N,
+   XSIZE, YSIZE, CHOICE, JUMP, XEDGE, XSTART, YSTART
*
INTEGER SHIFT,CHECK
*
CHARACTER INFILE*14
DIMENSION LEVEL(20),XPERM(300000),YPERM(300000)
*
*
XSIZE = 600
YSIZE = 4200
WRITE(6,*)'DEFAULT IMAGE SIZE:      ',XSIZE,' x ',YSIZE
WRITE(6,*)' (1) USE DEFAULT'
WRITE(6,*)' (2) SPECIFY NEW SIZE'
WRITE(6,*)' '
WRITE(6,*) 'ENTER CHOICE'
600 READ(5,*)CHOICE
IF ((CHOICE .NE. 1) .AND. (CHOICE .NE. 2)) THEN
WRITE(6,*)'ENTER 1 OR 2.'
GO TO 600
ENDIF
IF (CHOICE .EQ. 2) THEN
WRITE(6,*)
WRITE(6,*)
WRITE(6,*)'BOTH X AND Y DIMENSIONS MUST BE MULTIPLES OF 20'
WRITE(6,*)'FOR THE PROGRAM TO FUNCTION CORRECTLY!!!'
WRITE(6,*)
WRITE(6,*)
601 WRITE(6,*)'ENTER X-DIMENSION.'
READ(5,*)XSIZE
WRITE(6,*) 'ENTER Y-DIMENSION.'
READ(5,*)YSIZE
WRITE(6,*)'NEW IMAGE SIZE: ',XSIZE,' x ',YSIZE
WRITE(6,*)' (1) ACCEPT'
WRITE(6,*)' (2) MODIFY'
WRITE(6,*)' '
WRITE(6,*) 'ENTER CHOICE'
602 READ(5,*)CHOICE
IF ((CHOICE .NE. 1) .AND. (CHOICE .NE. 2)) THEN
WRITE(6,*)'ENTER 1 OR 2.'
GO TO 602
END IF
IF (CHOICE .EQ. 2) THEN
GO TO 601
ENDIF
ENDIF
ENDIF

```

```

*
*   20 is the number of columns of data in the ASCII file.
*   JUMP is the number of rows of the ASCII file that make up one row
*   of the TIFF image.
*   JUMP = XSIZE/20
*   WRITE(6,*)'SCANNING ASCII FILE . . .'
1002  FORMAT (20(I3,1X))
*****
*   Starting test process here!!!!
*   This group of lines opens the data file and reads in the first line
*   so that the program can determine in which column the data starts.
*   SHIFT represents the number of empty columns before the first data
*   point
*   REWIND should tell the program to go back to the beginning of the
*   data file
*   SHIFT = 0
*   CHECK = 0
*   OPEN (11,FILE=INFILE,STATUS='OLD')
*   READ (11,1002) (LEVEL(I), I=1,20)
*   DO 300 I = 1,20
*       IF (LEVEL(I).NE.0) THEN
*           CHECK = 1
*       ENDIF
*       IF ((LEVEL(I).EQ.0).AND.(CHECK.EQ.0)) THEN
*           SHIFT = SHIFT + 1
*       ENDIF
300  CONTINUE
*   REWIND (11)
*****
*   OPEN (11,FILE=INFILE,STATUS='OLD')
*
*   The first read statement reads only the first row.
*   The first row requires an additional if then so that XCOUNT
*   starts at 1 in the correct column.
*
*   N = 0
*   YCOUNT = 1
*   XCOUNT=0
*   IF (SHIFT.EQ.0) THEN
*       GO TO 320
*   ENDIF
*   READ (11,1002) (LEVEL(I), I=1,SHIFT)
*   DO 310 I = 1,20
*       IF (I.GT.SHIFT) THEN -
*           XCOUNT = XCOUNT + 1
*           IF ((LEVEL(I).GE.LOWER).AND.(LEVEL(I).LE.UPPER)) THEN
*               N = N + 1
*               XPERM(N) = XCOUNT
*               YPERM(N) = YCOUNT
*           END IF
*       ENDIF
310  CONTINUE
*
*   The following lines examine the remaining rows
*   This is where the program begins if SHIFT = 0

```

```

320 DO 3 K = 1, YSIZE
      DO 2 J = 1, JUMP
        READ (11, 1002) (LEVEL(I), I=1, 20)
        DO 1 I = 1, 20
*       if XCOUNT = XSIZE then the end of a row has been reached and
*       the next row needs to be started
          IF ((XCOUNT.EQ.XSIZE).AND.(YCOUNT.EQ.YSIZE)) THEN
            GO TO 330
          ENDIF
          IF (XCOUNT.EQ.XSIZE) THEN
            XCOUNT = 0
            YCOUNT = YCOUNT + 1
          ENDIF
          XCOUNT = XCOUNT + 1
          IF ((LEVEL(I).GE.LOWER).AND.(LEVEL(I).LE.UPPER)) THEN
            N = N + 1
            XPERM(N) = XCOUNT
            YPERM(N) = YCOUNT
          END IF
1         CONTINUE
2         CONTINUE
3         CONTINUE
*
330 CLOSE (11)
*
*****
CCC=>The following lines locate the starting point pixel.
      IF (YPERM(1).NE.1) THEN
        WRITE(6,*) 'ERROR!! CHECK TIFF FILE.'
        STOP
      ENDIF
      XEDGE = XPERM(1)
      J= 1
      DO 610 I = 1, N
        IF ((XPERM(I).EQ. XEDGE) .AND. (YPERM(I).EQ. J)) THEN
          XSTART = XPERM(I)
          YSTART = YPERM(I)
          J=J+1
          XPERM(I) = 0
          YPERM(I) = 0
        END IF
610     CONTINUE
CCC=>
      OPEN (12, FILE='coords.dat', STATUS='UNKNOWN')
*
      WRITE (12,*) 'SHIFT:', SHIFT, ' CHECK:', CHECK
      WRITE (12,*) 'XSIZE:', XSIZE, ' YSIZE:', YSIZE
*
1003  FORMAT (3X, I3, 4X, I4)
      DO 4 I = 1, N
        IF (XPERM(I).NE.0) THEN
          WRITE (12, 1003) XPERM(I), YPERM(I)
        ENDIF
4     CONTINUE
      CLOSE (12)
*
      WRITE(6,*) 'TOTAL NUMBER OF "DARK" PIXELS =', N, '.'

```

RETURN
END